FINAL REPORT

Hydrogeology and Documentation of the Northern Trinity and Woodbine Aquifer System Groundwater Availability Model (NTGAM)

Prepared For: North Texas GCD and Groundwater Management Area 8

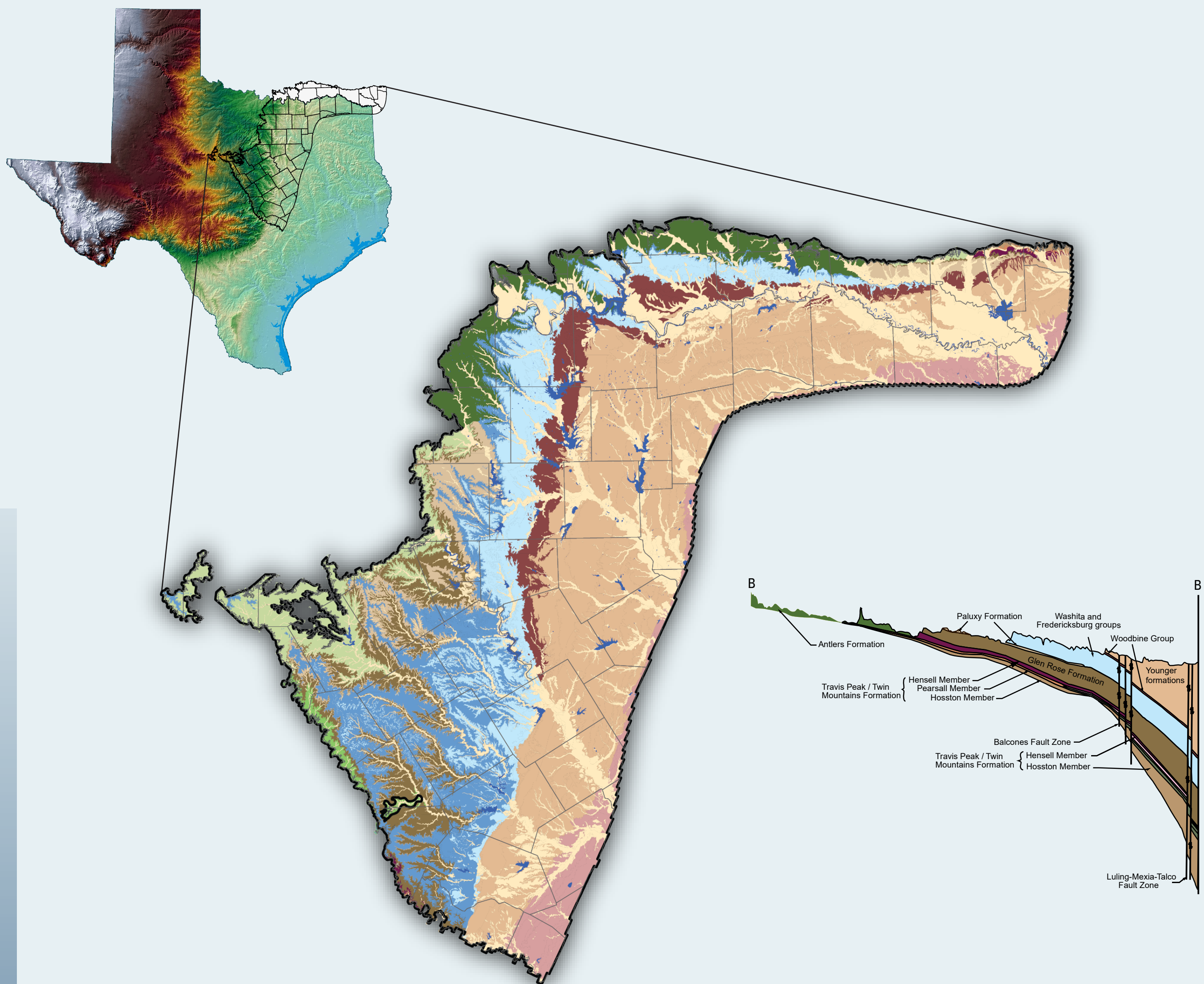

Prepared By:

INTERA Incorporated
9600 Great Hills Trail, Suite 300W
Austin, Texas 78759

December 2025

FINAL REPORT

HYDROGEOLOGY AND DOCUMENTATION OF THE NORTHERN TRINITY AND WOODBINE AQUIFER SYSTEM GROUNDWATER AVAILABILITY MODEL (NTGAM)

Prepared for the North Texas Groundwater Conservation District and Groundwater Management Area 8

Prepared by:

John Ellis, P.G.

Andres Prieto-Estrada, Ph.D., P.E.

Andrew Osborne

Neil Deeds, Ph.D., P.E., P.G.

Jeremy White, Ph.D.

Mike Keester, P.G.

Contributors:

Coco Liu

Marisa Earll

INTERA

Professional Engineer / Geoscientist Seal(s)

The following registered professionals are responsible for this report:

John H. Ellis, PG (Texas No. 15291)
Mr. Ellis was the Project Manager for this contract and responsible for oversight of the project.

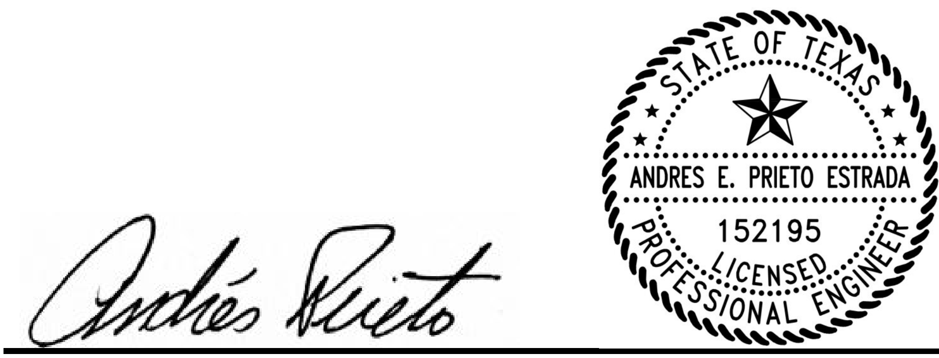

Andres Prieto Estrada, PE (Texas No. 152195)
Mr. Prieto-Estrada was the lead modeler for the project.

Michael Keester, PG (Texas No. 10331)
Mr. Keester was responsible for development of the recharge package for the model.

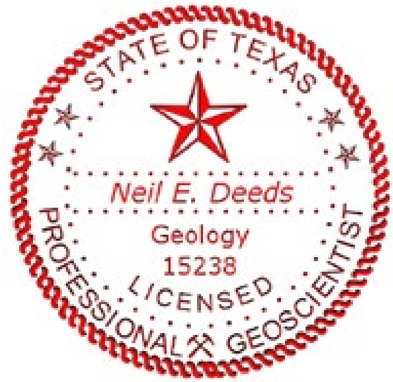

Neil E. Deeds, PG (Texas No. 15238)
Mr. Deeds was responsible for assisting with development and calibration of the groundwater flow model.

Table of Contents

List of Figures

List of Tables

Acronyms and Abbreviations

1:1	one-to-one
AFY	acre-feet per year
BFZ	Balcones Fault Zone
CTGCD	Central Texas Groundwater Conservation District
CUWCD	Clearwater Underground Water Conservation District
DEM	digital elevation model
DFCs	Desired Future Conditions
ET	evapotranspiration
FINAL	final pumping volume
FRAC	fraction
ft	feet
ft/d	foot per day
ft^2/d	square feet per day
GAM	Groundwater Availability Model
GCDs	groundwater conservation districts
GHS	geo-hydrostratigraphic
GMA 8	Groundwater Management Area 8
GPCD	gallons per day per capita
GWDB	Groundwater Database
GWDB/SDR	Groundwater Database/Submitted Driller's Report Database
GWF	Groundwater Flow
IES	iterative ensemble smoother
IMS	iterative model solution
MAE	mean absolute error
MAG	Modeled Available Groundwater
MAW	multi-aquifer well
mg/L	milligrams per liter
NRCS	National Resources Conservation Service
NTGAM	updated GAM
NWT	MODFLOW 6 with the Newton-Raphson formulation
PGMA	Priority Groundwater Management Area
PWS	public supply well
RIV	River Package on MODFLOW-6
SWB	Soil Water Balance
SWN	state well number
TCEQ	Texas Commission on Environmental Quality

TDS	total dissolved solids
TWDB	Texas Water Development Board
USDA	United States Department of Agriculture
USGS	United States Geological Survey
UWCD	Underground Water Conservation District
WUS	Water Use Survey

Executive Summary

As a part of the Texas Water Development Board (TWDB) groundwater availability modeling program, INTERA Incorporated (INTERA) developed the northern Trinity and Woodbine aquifer Groundwater Availability Model (NTGAM) and ensemble to simulate groundwater flow (GWF) in the northern part of the Trinity and Woodbine aquifer system (the study area) in Texas. Since the publication of a previous groundwater model for the northern Trinity and Woodbine aquifer system in 2014 (NTWGAM; Kelley and others, 2014), there have been changes to the distribution of groundwater withdrawals and advances in modeling tools. To reflect these changes and to simulate more recent conditions, the NTGAM was developed in cooperation with the North Texas Groundwater Conservation District and Groundwater Management Area 8 (GMA 8) to provide an updated Groundwater Availability Model (GAM).

The Trinity Aquifer is a major aquifer in Texas (George and others, 2011), and the northern portion is a major water resource for a large portion of north-central Texas and growing population centers along the Interstate 35 corridor from the Dallas-Fort Worth Metropolitan Area to Austin. There are five distinct aquifers/formations within the northern Trinity Aquifer from youngest to oldest: the Paluxy Aquifer, the Glen Rose Formation, the Hensell Aquifer, the Pearsall Aquifer, and the Hosston Aquifer. These aquifers are comprised of interbedded sands and shales, and potable water quality can be found in most of the study area except for the Paluxy Aquifer. The Washita/Fredericksburg groups are located between the northern Trinity Aquifer and the Woodbine Aquifer and constitute what is generally considered a confining unit but can produce potable groundwater. The Woodbine Aquifer is the youngest aquifer included in this model and is predominantly a sandstone with interbedded shale. The Woodbine Group is an aquifer from the Texas-Oklahoma state line in the north to northernmost McLennan County in the south where it thins and becomes predominantly shale.

Pumping was estimated for the northern Trinity and Woodbine aquifers in Texas from 1890 through 2020. A variety of sources and methods were used to estimate pumping in the period prior to 1980. Flowing wells, which were an important source of aquifer discharge generally prior to the 1930s, were retained from the NTWGAM model. After 1980, pumping was estimated using water use survey data from the TWDB and metered data made available by Groundwater Conservation Districts (GCDs) in the study area. Groundwater production increased significantly from the late 1930s through the 1980s and is still increasing in some areas but at a slower rate than that prior to 1980.

Transient water-level data with at least five measurements over a period of many years were selected as long-term hydrographs for comparison to model results. These hydrographs indicate that drawdown began occurring prior to 1910 before the most reliable pumping estimates are available from the TWDB water use survey data. Rapid declines in many areas persisted across the duration of the study period, although conversions to surface water resources in some areas lead to a stabilization or recovery of groundwater levels.

This study reviewed the relevant literature discussing water quality of the northern Trinity and Woodbine aquifers and developed maps of total dissolved solids (TDS), chloride, and hydrogeochemical facies to better describe and understand the hydrodynamics of the aquifers. The hydrogeochemical

facies analysis suggested that the outcrop areas of the northern Trinity and Woodbine aquifers are an active recharge zone with a strong similarity in groundwater chemistry (calcium-magnesium facies) across aquifers and formations suggesting a well- connected shallow groundwater system. The extent of TDS concentration less than or equal to 1,000 mg/L was mapped for each of the aquifers. It is important to note that the model includes significant portions of the northern Trinity and Woodbine aquifers that would be classified as brackish groundwater (greater than 1,000 mg/L and less than 10,000 mg/L).

In a generalized conceptual model of the northern Trinity and Woodbine aquifer system, water enters the groundwater system in topographically high outcrops of the hydrogeologic units in the western part of the aquifer system. Groundwater that does not discharge to streams flows to deeper zones of the aquifer system eastward of the outcrop areas, where it is discharged by wells and by upward leakage in topographically low areas. The uppermost parts of the aquifer system, which include outcrop areas, are under unconfined conditions. As depth increases in the aquifer system, water-table conditions evolve into confined conditions where groundwater is under pressure.

The NTGAM was developed using the groundwater simulation code MODFLOW6 and simulates the aquifer system using eight layers—one for each of the seven hydrogeologic units and a top layer that simulates the shallow surficial flow system as well as the younger formations overlying the Woodbine and Washita/Fredericksburg groups east of the Woodbine Aquifer and Washita/Fredericksburg groups outcrops. An initial steady-state stress period (1889) was configured to represent predevelopment mean annual inflows and outflows. The steady-state model represents a period of long-term equilibrium between aquifer recharge and aquifer discharge. Transient GWF was simulated from predevelopment (1890) through 2020.

History matching targets included water-level measurements, water-level difference measurements, which track transient water-level trends over time, stream baseflow measurements, and transmissivity. There were 16,510 water-level measurements distributed across 1,428 wells in the history matching period. Wells used to determine long-term water level trends in the aquifer system were also used to compare observed and simulated water levels. The model baseflow was compared to time-averaged flux measurements from twenty-nine stream gages.

A Bayesian framework was used to represent uncertainty in modeled parameters and simulated outputs of interest. History matching and uncertainty quantification were performed by using a Monte Carlo approach enabled through iterative ensemble smoother (IES) software to produce an ensemble of models fit to historical data. The IES substantially reduced the computational demand of parameter estimation by approximating the first-order relation between model inputs and outputs, thereby allowing 133,644 adjustable parameters to be used for history matching at a relatively low computational and time cost.

The adjusted mean absolute error (MAE) (MAE divided by the range in observed hydraulic heads) for the transient period is less than four percent, and the MAE for all layers is less than nine percent. The mean error for the transient period is -54 ft, and the mean error for all layers is between -14 ft and -76 ft. On average, the model oversimulates the observed water levels in each layer during the transient period. However, the long-term water level trends across more than 100 years are reasonably reproduced, particularly given the more than 1,000 ft of water level declines in some areas.

The calibrated average recharge to the northern Trinity and Woodbine aquifers totals 3,135,337 acre-ft per year (AFY), which is approximately 5.1 percent of precipitation (61,628,647 AFY) model-wide. Water discharges from the northern Trinity and Woodbine aquifers primarily through ephemeral streams (55 percent of net outflow), perennial streams (40 percent of net outflow), groundwater use (3.5 percent of net outflows), and evapotranspiration (ET) (1.5 percent). Analysis of the transient water budget provides insight into the current conditions within the deep, confined portions of the northern Trinity and Woodbine Aquifer. As pumping rapidly increased from 1940 through 1990 in the deeper confined portions of the aquifer, the amount of groundwater flowing to the deep aquifer greatly increased. Early on, a large fraction of deep pumping is supplied by aquifer storage. However, by the 1980s, capture from the updip portions of the northern Trinity and Woodbine aquifer supplies the majority of the groundwater pumped at depth.

This study provides a model that has been calibrated across the entire period of record through 2020, which is a benefit to GCDs, GMA 8, and stakeholders. The updated GAM and the information collected and interpreted to support the study provide GCDs with the best available science to inform final rule-making, groundwater management within GCD boundaries, and joint planning. The data collected and made public from this study provides a wealth of knowledge to support GCDs in local-scale hydraulic calculations with analytic tools to address such issues as well spacing.

1.0 Introduction

The Texas Water Development Board (TWDB) has identified the major and minor aquifers in Texas based on the regional extent and amount of water produced. The major and minor aquifers are shown in Figures 1-1 and 1-2, respectively. Major aquifers are those that supply large quantities of water over large areas of the state, and minor aquifers are those that supply relatively small quantities of water over large areas of the state or large quantities of water over small areas of the state. A general discussion of the major and minor aquifers in Texas is found in George and others (2011).

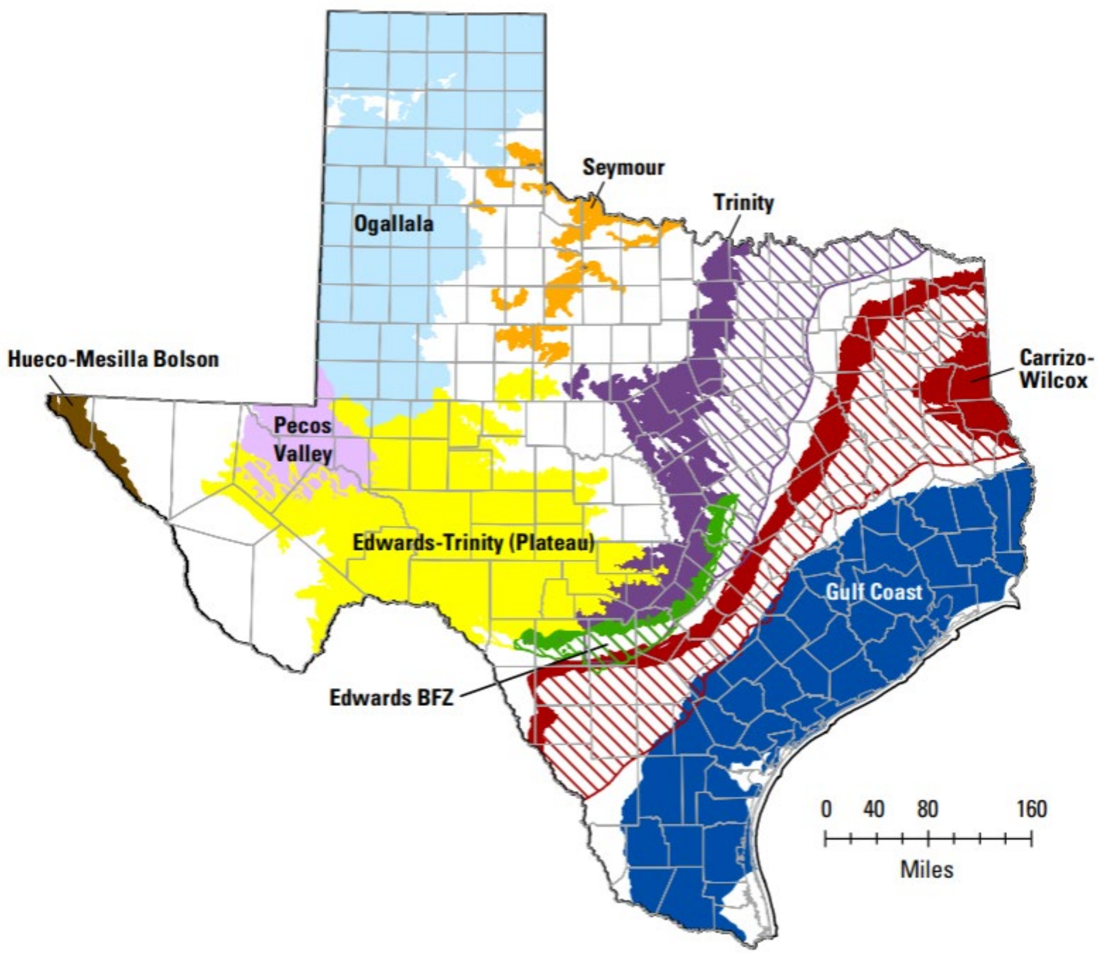

Figure 1-1. Locations of major aquifers in Texas.

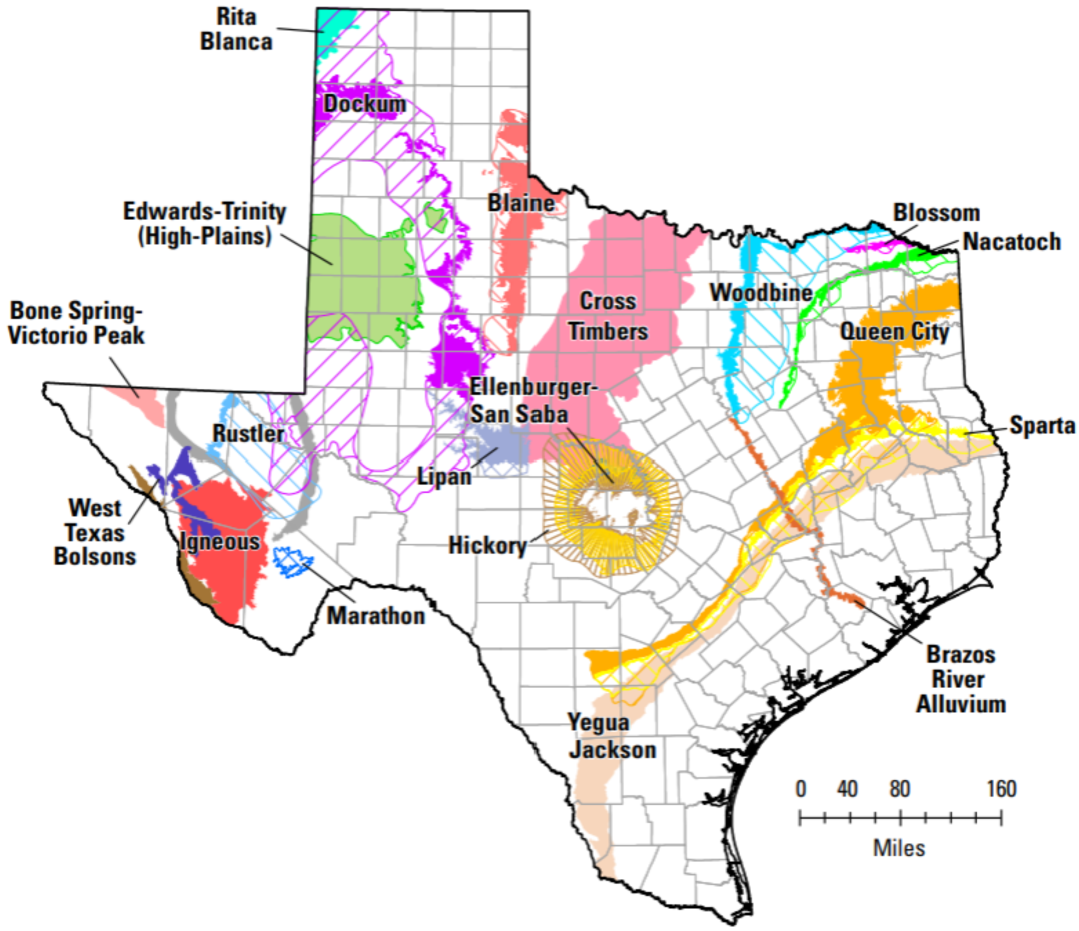

Figure 1-2. Locations of minor aquifers in Texas.

The northern portion of the Trinity and Woodbine aquifer system (the "study area") (Figure 1-3) is a major water resource for a large portion of north-central Texas and growing population centers along the Interstate 35 corridor from the Dallas-Fort Worth Metroplex to Austin. The northern Trinity Aquifer generally coincides with the portion of the Trinity Group north of the Colorado River. The northern Trinity Aquifer outcrops in Texas along its western extent. North of the Brazos River, the northern Trinity Aquifer is overlain by the Woodbine Aquifer, defined as a minor aquifer in Texas by the TWDB (see Figure 1-4). The Woodbine Aquifer is named for the Cretaceous-age Woodbine Group (George and others, 2011). In Texas, this aquifer generally outcrops in a band parallel to and east of the northern Trinity Aquifer outcrop and is an aquifer from the Texas-Oklahoma border to northern McLennan County. South of northern McLennan County, the Woodbine Group is predominantly shale and not an aquifer.

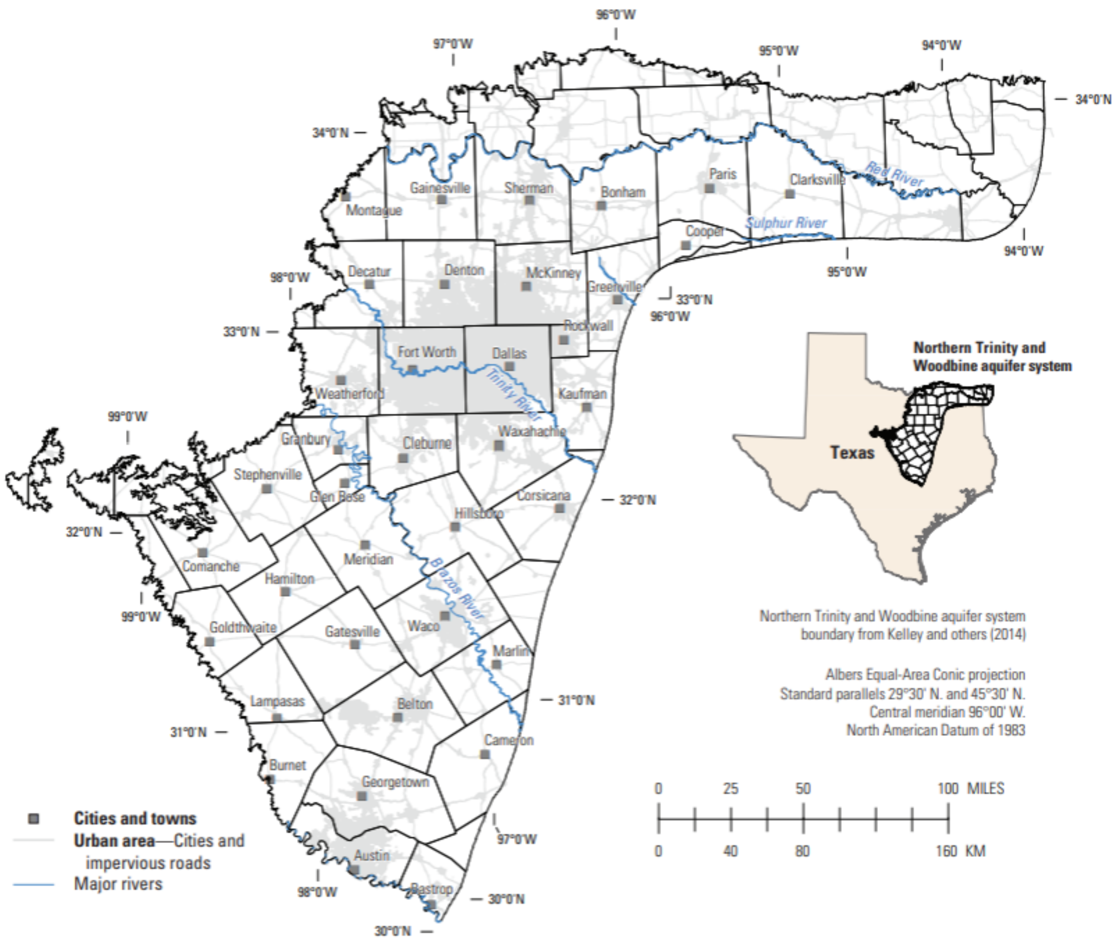

Figure 1-3. Roads and selected rivers and cities and towns in the northern Trinity and Woodbine Aquifers study area.

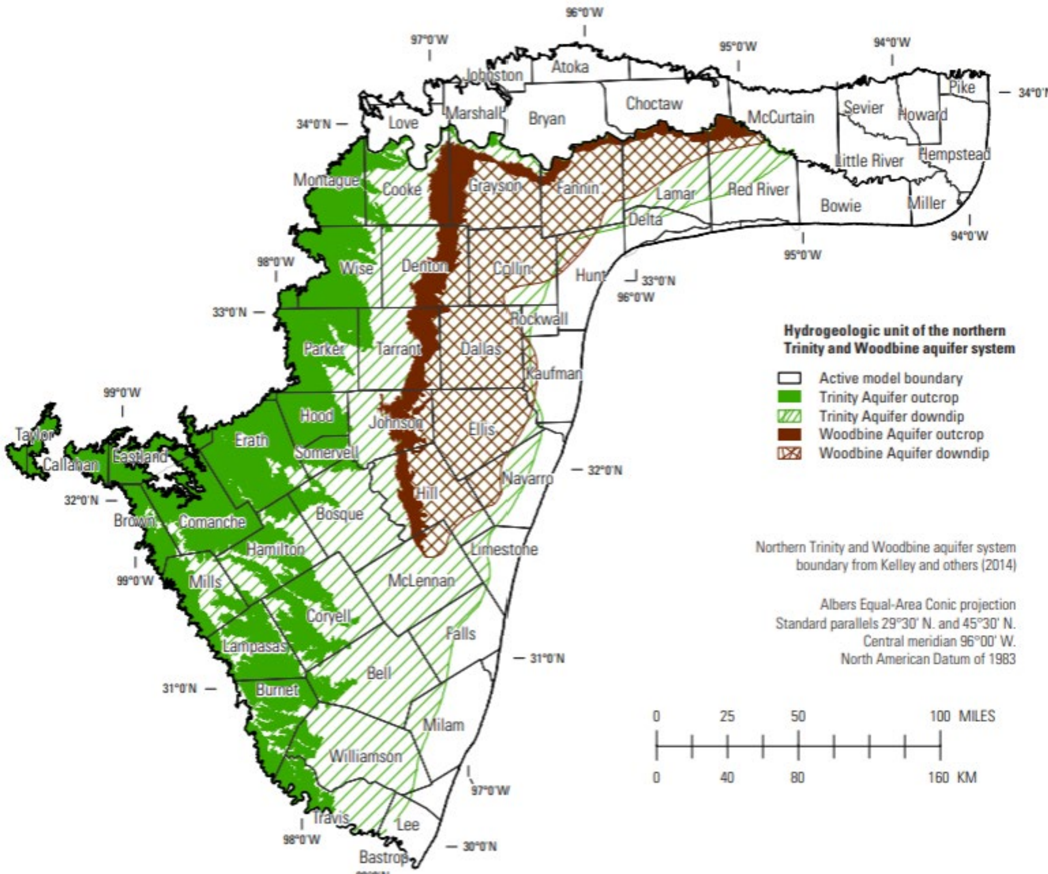

Figure 1-4. Boundary of the northern Trinity and Woodbine Aquifer in Texas, Oklahoma, and Arkansas.

Significant groundwater use in the northern Trinity and Woodbine aquifers started in the late 1800s with the construction of deep (termed “artesian” in the literature because they flowed at the surface) flowing wells in the Waco and Fort Worth areas. Hill (1901) documented many flowing wells in both the northern Trinity and Woodbine aquifers in north-central Texas. While some of these wells or “springs” continue to flow today, most ceased flowing by about 1950 in Waco and by about 1914 in Fort Worth (Leggat, 1957). With the advent of modern pumping technology and significant population growth in the late 1940s and 1950s, groundwater use within the region increased dramatically. As a result, water levels declined significantly (George and others, 2011) in the northern Trinity and Woodbine aquifers. In some areas, water levels have declined by as much as 800 feet (ft) locally in the northern Trinity Aquifer and as much as 400 ft locally in the Woodbine Aquifer. While there has been a conscious effort to move to surface water as the region’s population has increased, expanded growth in near-urban areas continues to put pressure on the area’s aquifers with trends of increasing groundwater pumping in some counties.

The northern portion of the Trinity Aquifer and the Woodbine Aquifer are in GMA 8 (Figure 1-5). The first round of joint planning within GMA 8 employed the 2004 northern Trinity and Woodbine aquifers

GAM developed by Bené and others (2004) to determine the Modeled Available Groundwater (MAG, then termed Managed Available Groundwater) based upon GMA 8 developed Desired Future Conditions (DFCs). Many of the new GCDs formed after the designation by Texas Commission on Environmental Quality (TCEQ) of the Central Texas–Trinity Aquifer Priority Groundwater Management Area (PGMA) and the North-Central Texas–Trinity and Woodbine Aquifers PGMA were created during or after the first GMA 8 joint-planning cycle, which ended in September of 2010.

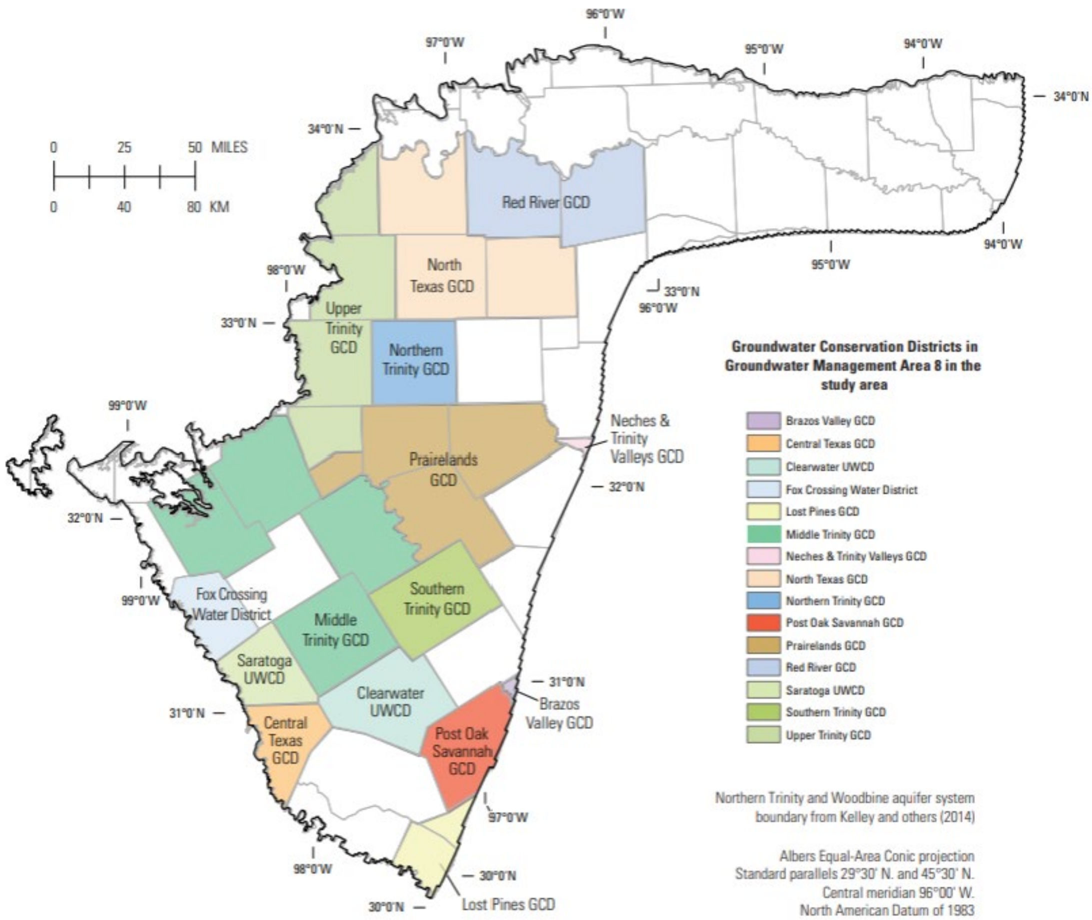

Figure 1-5. **Groundwater Conservation Districts in the northern Trinity and Woodbine aquifer system area**

The updated GAM (NTGAM) for the northern Trinity and Woodbine aquifers documented in this report offers improvements to the 2014 GAM (NTWGAM; Kelley and others, 2014), including (1) an extension of the model through 2020 to better reflect more recent conditions, (2) additional groundwater level measurements used for model history matching from the end date of the previous model (2014) through 2020; (3) the incorporation of spatially-distributed recharge; (4) an update to the model structure based on the incorporation of additional geophysical log data, and (5) the use of a newer and more robust groundwater code. The updated GAM and the information collected and interpreted to support the study provide the GCDs in GMA 8 with the best available science to inform final rule-making, groundwater management within GCD boundaries, and joint planning.

1.1 Objective and Scope

The primary objective of this study was to develop an updated GAM for the northern Trinity and Woodbine aquifers. This model update utilizes the conceptual model and hydrogeologic framework from the previous study (Kelley and others, 2014). Since 1999, the TWDB has been tasked with developing GAMs of the aquifers in Texas through the groundwater availability modeling program. The GAMs and associated reports include extensive documentation on the aquifer hydrogeologic and hydraulic properties; such properties are surface and subsurface geology, aquifer conceptualization including inflows (such as recharge, lateral flow, seepage from streams) and outflows (such as seepage to streams, groundwater use), the hydrogeologic framework (hydrogeologic unit geospatial extent, bed orientation, unit thickness), construction, and calibration (or "history matching") of the GAM. Pursuant to Texas Water Code §36.1132, the TWDB uses the GAMs to estimate the modeled available groundwater. Results from the groundwater availability modeling program are intended to be a tool that water-resource managers can use to address future groundwater availability issues.

1.2 Study Area

The location of the study area, as defined by the active model boundary, for the update of the northern Trinity and Woodbine aquifers GAM is shown in Figure 1-3. This area includes a large portion of central and north-central Texas, a narrow band in southeastern Oklahoma, and a small portion of southwestern Arkansas. Similar to the NTWGAM, the spatial extent of the aquifers has been extended beyond the official TWDB boundaries into Oklahoma and Arkansas based on surface geology and estimated downdip extents (Figure 1-4). The active model boundary is defined on the west and north as the contact between northern Trinity Group formations and the underlying Paleozoic-age strata, on the south by the Colorado River, and on the east by the approximate center line of the Mexia-Talco Fault Zone. The eastern boundary in Arkansas connects the eastern extent of the northern Trinity Group with the center line of the Mexia-Talco Fault Zone.

In Texas, the northern Trinity Aquifer extends across much of the central and north-central portions of the state (Figure 1-4). The Trinity Aquifer outcrop consists of a north-south trending band from Montague County in the north to Travis County in the south. The outcrop width varies across this band, which exists in parts of 26 counties in Texas and is widest in the area of Callahan, Eastland, Comanche, Erath, and Somervell counties. The outcrop extends into Oklahoma and Arkansas as a narrow, trending east-west band. The downdip portion of the northern Trinity Aquifer lies to the east and south of the outcrop area and exists in 39 counties. The Woodbine Aquifer is located in the north-central portion of the State and outcrops in a north-south trending band from Cooke and Grayson counties in the north to McLennan County in the south and as a narrow, east-west trending band from Grayson County in the west to Red River County in the east. The aquifer outcrops in parts of 11 Texas counties. The downdip portion of the Woodbine Aquifer lies to the east and south of the outcrop area and exists in 13 Texas counties.

Roadways, cities, and towns located in the study area are shown in Figure 1-3. The largest urban area in the study area is the Dallas-Fort Worth Metroplex. In general, urban areas lie along the Interstate 35 corridor in Texas from Austin to the Dallas-Fort Worth Metroplex, along U.S. 82 in the northern part of Texas, and U.S. 75 from Dallas north to Sherman and Denison, Texas. Numerous small streams and rivers are located in the study area as well as five major rivers, which, from north to south, are the Red, Sabine, Trinity, Brazos, and Colorado rivers. Numerous large and small lakes/reservoirs are also located in the study area.

While the study area is large enough to encompass a wide range of ecological settings, the majority of the study area is comprised of two ecological landscapes, Piney Woods and Texas Black Land Prairie (Griffith and others, 2007). These landscapes can broadly be classified as fertile pastureland with varying amounts of woods and cropland. The outcrop area of these aquifers falls under the Subtropical category (Larkin and Bomar, 1983), with the eastern portion of the study area being subclassified as Humid and the western portion of the model being Subhumid.

Figure 1-6 shows the topography in the study area. In general, the ground surface elevation decreases from west to east. The maximum elevation of about 2,300 ft is observed in Taylor County, and the lowest elevations are observed along the stream valleys in southwest Arkansas and northeast Texas. The drainage features of the major rivers can be seen in the topographic gradients in much of the study area, although the drainage patterns are somewhat muted as the terrain flattens to the east.

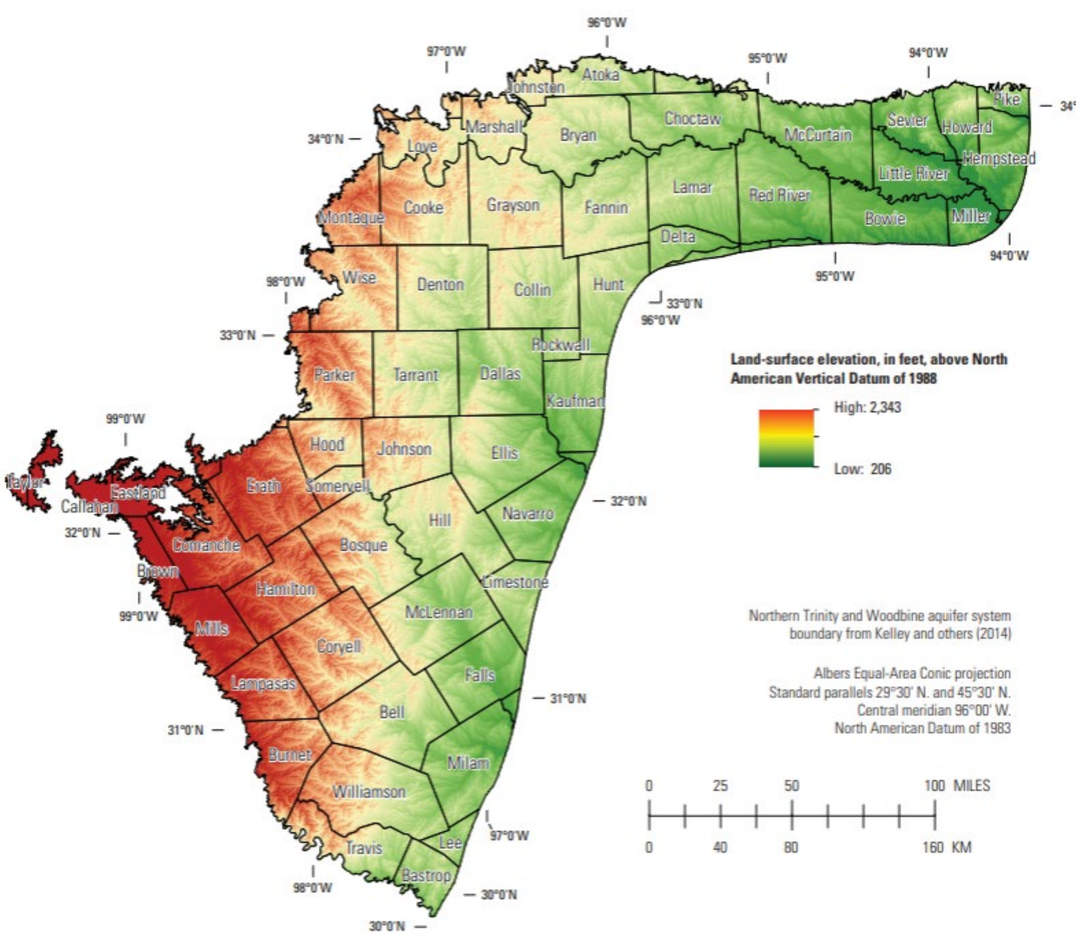

Figure 1-6. Elevation of the land surface in the northern Trinity and Woodbine Aquifers.

The climate in the study area is classified as Subtropical or Modified Marine climate, as defined in Larkin and Bomar (1983). The onshore flow of air from the Gulf of Mexico causes the marine climate. Distinctions in the climate occur based on the moisture content of the maritime air. Air from the Gulf of Mexico decreases in moisture content from east to west as it travels across the State. The intrusion of continental air into the maritime air occurs seasonally and also affects the moisture content of the air. In the study area, the Subtropical classification is subdivided based on this moisture content into Humid and Subhumid regions. The Woodbine Aquifer outcrop is located in the transition zone between the Humid and Subhumid classifications, so the eastern part of the study area is Humid, and the western part is Subhumid. Subtropical Humid climate is most noted for warm summers, and Subtropical Subhumid climate is characterized by hot summers and dry winters.

Precipitation data are available from the PRISM climate group (PRISM, 2023) within the study area (Figure 1-7), which was used to characterize the long-term climate of the northern Trinity and Woodbine aquifer system study area. Mean annual precipitation for 1890-2020 was 31 inches (Figure 1-7). A substantial period of above-mean annual precipitation occurred generally after about 1980, whereas substantial periods of below-mean annual precipitation occurred between about 1890 and 1960.

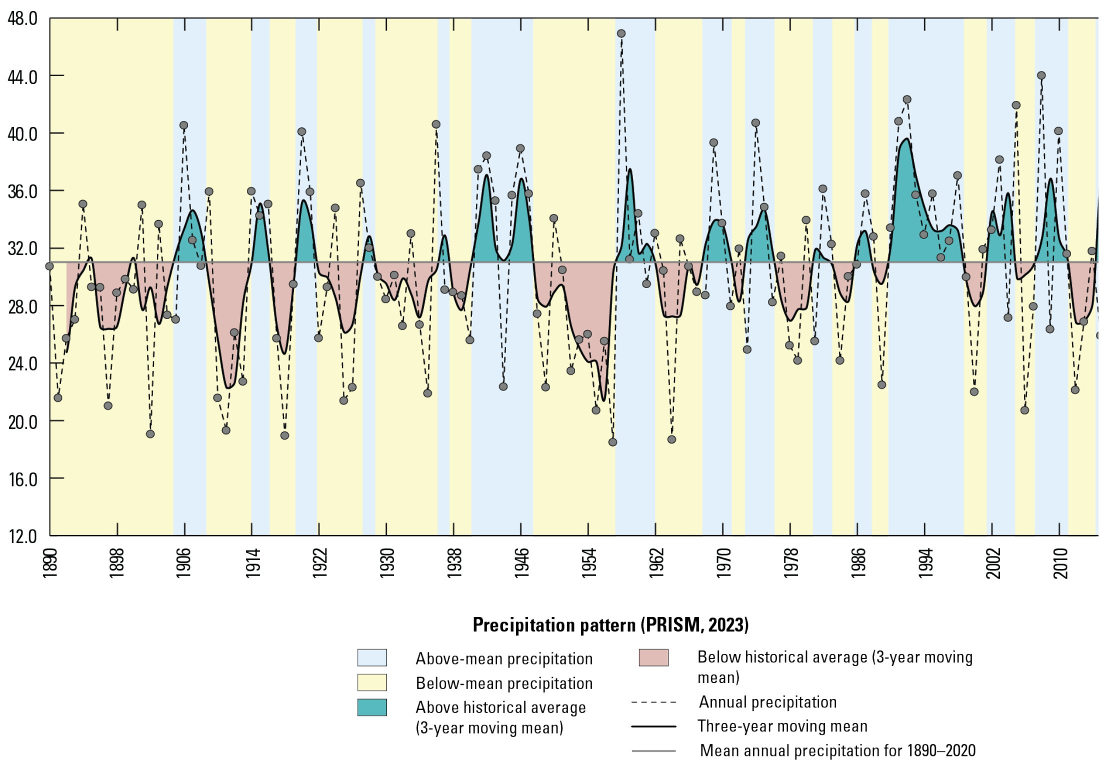

Figure 1-7. Precipitation and climate characteristics for the northern Trinity and Woodbine aquifer system

Land-cover data for the study area for 2023 were obtained from the CropScape database (National Agricultural Statistics Service, 2025) (Figure 1-8). This database included land-cover characteristics at a 30-meter resolution for land overlying the northern Trinty and Woodbine aquifer systems. Land cover and crop data were used for the 2023 season. During this period, the land cover (3.6 million acres) was primarily grass/pasture (39.3 percent), forest (23.5 percent), developed (12.3 percent), shrubland (10.4 percent), wetlands (3.5 percent), open water (2.5 percent), and cropland (8.7 percent).

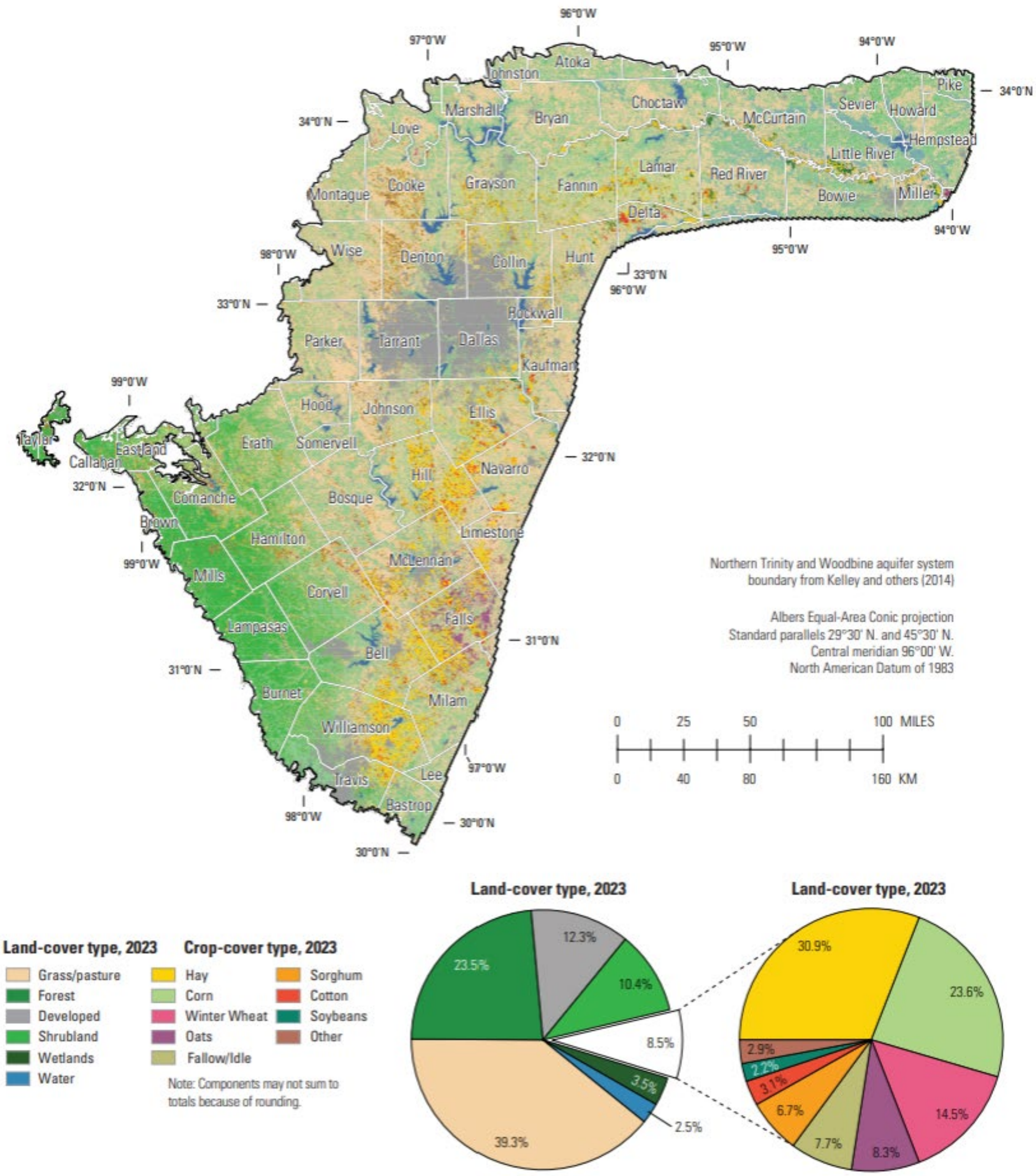

Figure 1-8. Land Use/Land Cover for the surface area of the northern Trinity and Woodbine aquifer system.

Hay, which accounted for 30.9 percent of cropland by area, was the dominant crop type in the study area. Corn (23.6 percent), winter wheat (14.5 percent), oats (8.3 percent), and sorghum (6.7 percent) were the only other crop types accounting for at least 5 percent of cropland by area (Figure 1-8). About 8 percent of cropland by area was fallow or idle. Although crop types could change depending on economic conditions and hydrologic factors such as flooding or drought conditions, the percentages of total cropland cover and individual crop types did not change substantially during 2023.

2.0 Hydrogeology

This section details the data compilation and analyses used to support the development of the conceptual model for the northern Trinity and Woodbine aquifers. This information, in total, defines the hydrogeologic setting, and it includes a discussion of the geologic and hydrogeologic units, structure, hydraulic properties, groundwater use, groundwater levels, water quality, and recharge. This study uses the comprehensive analysis of the northern Trinity and Woodbine aquifer system hydrogeologic framework presented in Kelley and others (2014) and incorporates re-completed groundwater level and groundwater use data, reformulated spatially distributed recharge, and more recent structural data to characterize the aquifer system.

2.1 Geologic and Hydrogeologic Units

The northern Trinity and Woodbine aquifers represent an important water resource in north-central Texas, offering essential supplies to various industries, municipalities, and agricultural activities. These aquifers, originating from Cretaceous-aged deposits, consist of interbedded sandstones, limestones, and shales, reflecting their complex depositional and structural history. Their functionality and regional importance are shaped by the stratigraphy, structural geology, depositional environments, and groundwater quality.

2.1.1 Geologic Units

The rocks and sediments that comprise the northern Trinity and Woodbine aquifers are contained in the northern Trinity and Woodbine groups deposited during the Cretaceous Period (Table 2-1), which lasted from about 145 to 65 million years ago. Cretaceous-age strata are exposed at the surface across broad areas of Texas. The geologic units that make up the northern Trinity and Woodbine groups extend from the Colorado River near Austin north to southern Oklahoma and into far southwestern Arkansas. Cretaceous-age stratigraphic units in north and central Texas lie on the northwestern margin of the Gulf of Mexico Basin. Through geologic time, the Gulf of Mexico Basin has progressively filled from the margins toward the center until achieving the shoreline configuration that exists today. Cretaceous-age strata are the oldest part of the Gulf of Mexico Basin fill that is still exposed at the surface.

Table 2-1. Stratigraphic column for the study area.

<table>
<tr><th rowspan="2">Period</th><th rowspan="2">Group</th><th>North and West</th><th colspan="2">Central</th><th colspan="2">South</th><th rowspan="2" colspan="2">Hydrogeologic Unit (Figures 2-3, 3-1, 3-2)[1]</th></tr>
<tr><th>Formation</th><th colspan="2">Formation | Member</th><th colspan="2">Formation | Member</th></tr>
<tr><td>Quaternary</td><td rowspan="2" colspan="6">Differentiation not necessary for this study</td><td colspan="2">Alluvium</td></tr>
<tr><td>Tertiary</td><td colspan="2">N/A</td></tr>
<tr><td rowspan="13">Cretaceous</td><td>Navarro</td><td rowspan="4" colspan="5">Differentiation not necessary for this study</td><td rowspan="4" colspan="2">Younger Formations</td></tr>
<tr><td>Taylor</td></tr>
<tr><td>Austin</td></tr>
<tr><td>Eagle Ford</td></tr>
<tr><td rowspan="2">Woodbine</td><td>Lewisville</td><td colspan="2">Lewisville</td><td rowspan="2" colspan="2">Pepper Shale</td><td rowspan="2" colspan="2">Woodbine Aquifer</td></tr>
<tr><td>Dexter</td><td colspan="2">Dexter</td></tr>
<tr><td rowspan="3">Washita</td><td>Grayson Marl</td><td colspan="2">Buda, Del Rio</td><td colspan="2">Buda, Del Rio</td><td rowspan="7" colspan="2">Washita/Fredericksburg Groups</td></tr>
<tr><td>Mainstreet, Pawpaw, Weno, Denton</td><td rowspan="2" colspan="2">Georgetown</td><td rowspan="2" colspan="2">Georgetown</td></tr>
<tr><td>Fort Worth, Duck Creek</td></tr>
<tr><td rowspan="4">Fredericksburg</td><td>Kiamichi</td><td colspan="2">Kiamichi</td><td colspan="2">Kiamichi</td></tr>
<tr><td rowspan="2">Goodland</td><td colspan="2">Edwards</td><td colspan="2">Edwards</td></tr>
<tr><td colspan="2">Comanche Peak</td><td colspan="2">Comanche Peak</td></tr>
<tr><td>Walnut Clay</td><td colspan="2">Walnut Clay</td><td colspan="2">Walnut Clay</td></tr>
<tr><td rowspan="3">Cretaceous (continued)</td><td rowspan="3">Trinity</td><td rowspan="3">Antlers</td><td colspan="2">Paluxy</td><td colspan="2">Paluxy</td><td rowspan="3">Trinity Aquifer</td><td>Paluxy Aquifer</td></tr>
<tr><td colspan="2">Glen Rose</td><td colspan="2">Glen Rose</td><td>Glen Rose Formation</td></tr>
<tr><td>Twin Mou</td><td>Hensell</td><td>Travis</td><td>Hensell</td><td>Hensell Aquifer</td></tr>
</table>

<table>
<tr><th rowspan="2">Period</th><th rowspan="2">Group</th><th>North and West</th><th colspan="2">Central</th><th colspan="2">South</th><th colspan="2" rowspan="2">Hydrogeologic Unit (Figures 2-3, 3-1, 3-2)[1]</th></tr>
<tr><th>Formation</th><th colspan="2">Formation | Member</th><th colspan="2">Formation | Member</th></tr>
<tr><td rowspan="2"></td><td rowspan="2"></td><td rowspan="2"></td><td rowspan="2"></td><td>Pearsall</td><td rowspan="2"></td><td>Pearsall/ Hammett/ Cow Creek</td><td rowspan="2"></td><td>Pearsall Formation</td></tr>
<tr><td>Hosston</td><td>Sycamore /Hosston/ Sligo</td><td>Hosston Aquifer</td></tr>
<tr><td rowspan="2">Permian</td><td>Wichita</td><td colspan="5">Differentiation not necessary for this study</td><td colspan="2" rowspan="5">N/A</td></tr>
<tr><td>Bowie</td><td colspan="5">Differentiation not necessary for this study</td></tr>
<tr><td rowspan="3">Pennsylvanian</td><td>Cisco</td><td colspan="5">Differentiation not necessary for this study</td></tr>
<tr><td>Canyon</td><td colspan="5">Differentiation not necessary for this study</td></tr>
<tr><td>Strawn</td><td colspan="5">Differentiation not necessary for this study</td></tr>
</table>

[1]Note that the seven hydrogeologic units do not occur individually in all parts of the study area. For example, in the northern part there are only two or three contrasting layers; the sandstones of the Antlers Formation, the shale and limestone of the Washita/Fredericksburg groups, and the sandstone of the Woodbine Group, where present.

The Cretaceous-age sediments were deposited unconformably upon an erosional surface of Paleozoic-age strata. These older strata primarily date to the Permian and Pennsylvanian periods and consist of diverse sedimentary units that dip and thicken toward the East Texas Basin. The depositional history of the Cretaceous sediments indicates that the East Texas Basin was undergoing subsidence during this time, creating accommodation space for the extensive sedimentary deposits. These sediments are subdivided into stratigraphic groups in descending order: Navarro, Taylor, Austin, Eagle Ford, Woodbine, Washita, Fredericksburg, and Trinity groups (Table 2-1) (Hill, 1901). However, the current study focuses on the Woodbine through Trinity groups, which are important to the structure and function of the aquifers under consideration.

The Cretaceous sediments reflect deposition in varied terrestrial and marine environments, including fluvial plains, interfluves, deltaic shorelines, and marine shelves. This diversity resulted in stratigraphic units with significant lithological variability, from systems dominated by sands and gravels to formations characterized by shales and offshore limestones. This inherent variability contributes to the intricate geologic nomenclature and stratigraphic relationships evident in these formations, as summarized in Table 2-1.

Figure 2-1 illustrates the generalized surface geology of the study area, and Figure 2-2 provides structural cross-sections of the stratigraphic units. These figures, along with Table 2-1, help contextualize the terminology and stratigraphic relationships described in the text (George and others, 2011; Bené and others, 2004; Nordstrom, 1982; Klemt and others, 1975). The Paleozoic-age sediments underlying the northern Trinity Group represent the eastern shelf deposits of the Permian Basin. These strata are composed, from youngest to oldest, of the Wichita, Bowie, Cisco, Canyon, and Strawn groups (Table 2-1). Each of these groups reflects distinct depositional environments. The Wichita Group is a heterogeneous mix of sand, gravel, and shale, while the Bowie Group, predominantly continental in origin, includes coarse-grained sediments. The Cisco Group exhibits a mix of fluvial-deltaic and marine deposits, characterized by poorly mapped sandstone units and extensive limestone formations (Brown and others, 1990). The Strawn and Canyon groups primarily consist of fluvial-deltaic deposits, with the Canyon Group also containing limestones indicative of lower energy environments. The overall dip of the Paleozoic sediments is to the west, contrasting with the east-southeast dip of the overlying Cretaceous sediments.

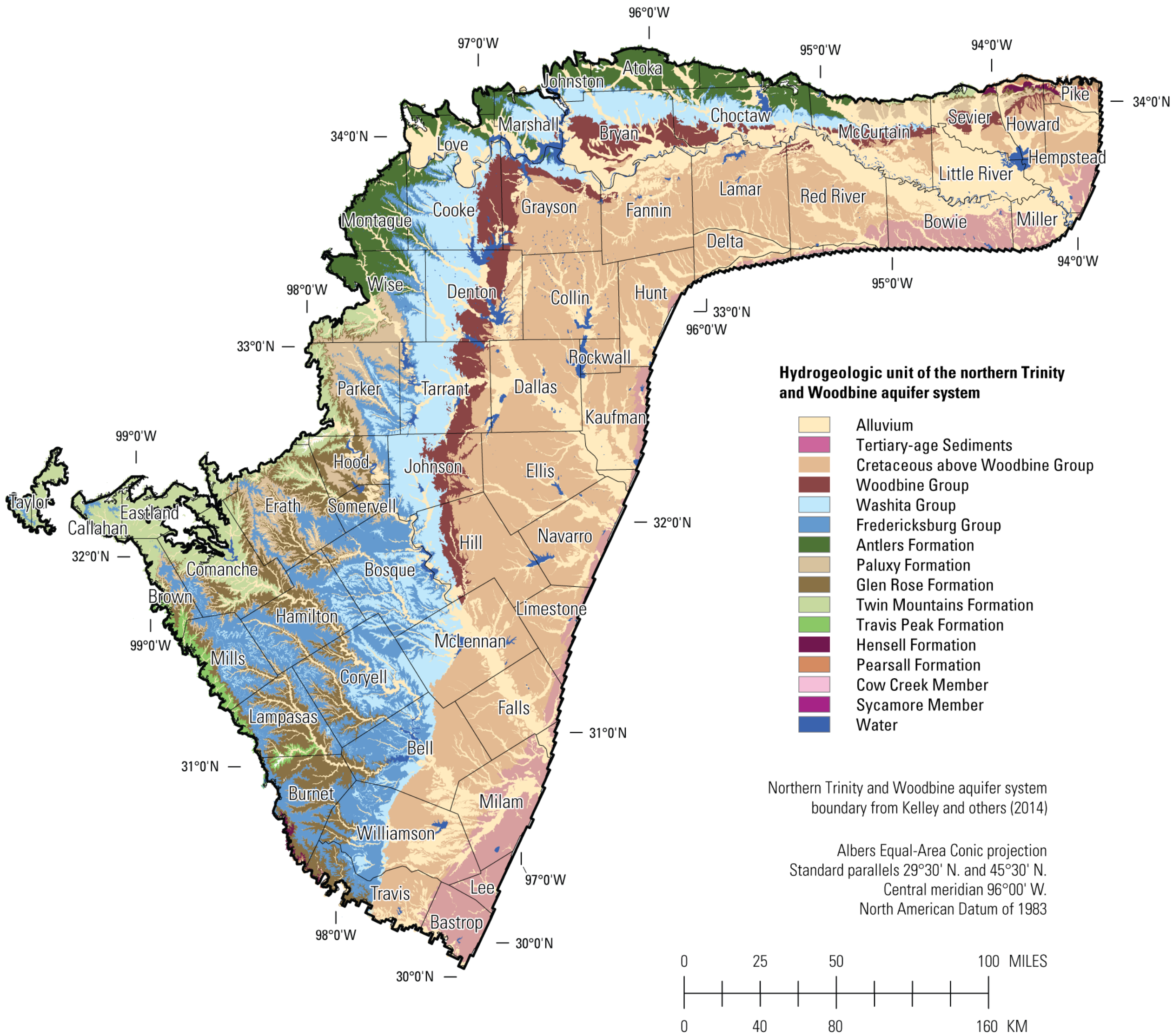

Figure 2-1. Generalized surface geology for the northern Trinity and Woodbine aquifer system.

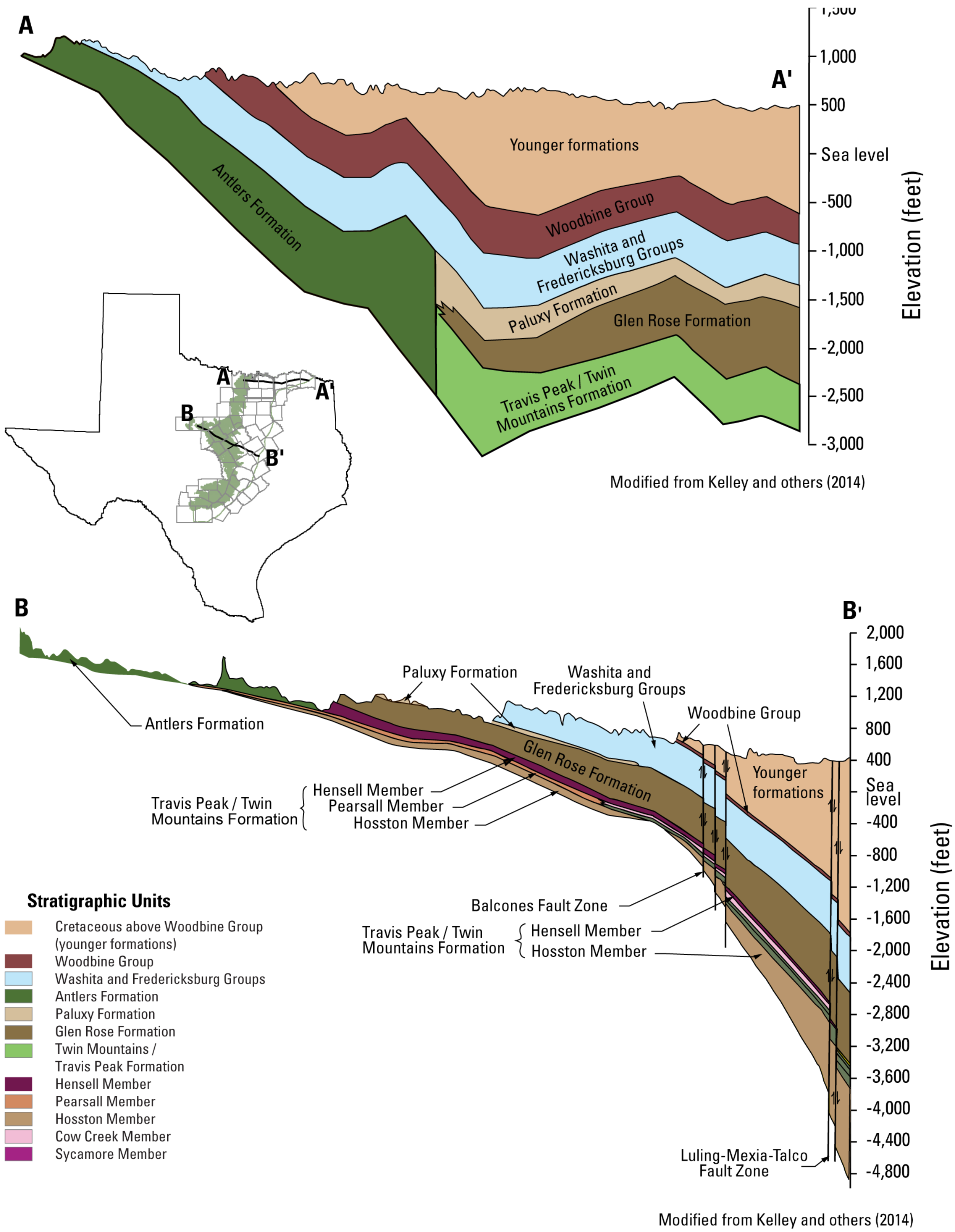

Figure 2-2. **Cross sections of the stratigraphic units of the northern Trinity and Woodbine aquifer system.**

The northern Trinity Group is defined by regional variations in nomenclature and stratigraphic composition (Figure 2-2, Table 2-1). In the northern and western portions of the study area, this group is primarily represented by the undifferentiated Antlers Formation. Nordstrom (1982 and 1987) describes the Antlers Formation as comprising an upper section dominated by sand and sandstone, a middle section characterized by sandy clay with interbedded sandstone and siltstone, and a lower section consisting of conglomerate and gravel with occasional clay lenses. In the central and southern parts of the study area, the northern Trinity Group is divided into several formations, including the Paluxy, Glen Rose, and Twin Mountains formations, the latter of which is also known as the Travis Peak formation.

The Travis Peak Formation exemplifies the northern Trinity Group’s stratigraphic complexity and contains several distinct members: the Hensell, Pearsall/Cow Creek/Hammet, and Hosston/Sligo members. The Hensell Member, composed largely of sandstone, differs from other Cretaceous sandstone units due to its relatively consistent thickness across the region, irrespective of its proximity to the East Texas Basin (Hill, 1901; Klemt and others, 1975; Bené and others, 2004). The Pearsall Member, positioned stratigraphically above these units, represents a transitional environment between marine shelf and deltaic systems. Its composition varies geographically, with more clastic sediments in the north and more carbonate-rich facies in the south. The Hosston Member, a predominantly sandstone unit, was deposited in fluvial coastal plain environments and exhibits a high percentage of sand content across its extent. In contrast, the Sligo Member reflects finer-grained offshore deposits. The Twin Mountains Formation, which corresponds to the Travis Peak Formation in the northern parts of the study area, is similarly dominated by sand-rich deposits.

Overlying the Twin Mountains and Travis Peak formations is the Glen Rose Formation, a limestone unit deposited on an expansive shallow marine shelf. This formation is characterized by dense, finely crystalline limestone interbedded with shale, sandy shale, and anhydrite. The Paluxy Formation, positioned above the Glen Rose Formation, transitions from a coastal plain depositional environment in the north and west to deltaic and marine shelf environments in the central and southern portions of the study area. Its lithology reflects this transition, with thick, friable quartz sands dominating in the north and an absence of significant sand units in the southernmost areas (Klemt and others, 1975).

The Washita and Fredericksburg groups (collectively the “Washita/Fredericksburg”) are composed of limestone and shale across the entire study area. The Washita/Fredericksburg groups are exposed at the surface in between the northern Trinity and Woodbine group outcrops. The Washita/Fredericksburg groups thicken downdip from about 400 ft near the outcrop to 800 ft along the downdip boundary of the study area. The thickness of the Washita/Fredericksburg groups is relatively constant from north to south (Figure 2-2). The deposition of the Washita/Fredericksburg groups records a major marine transgression similar to the Glen Rose Formation but even more extensive. There were no significant sources of sand during the Washita/Fredericksburg depositional episode; shallow marine conditions prevailed across the area.

The Woodbine Group, deposited during the Late Cretaceous, includes both sand and shale facies. The sand facies, prominent in the northern and northeastern regions, consist of sand and sandstone with interbedded shale and clay. It is subdivided into the Dexter and Lewisville members, which were deposited in deltaic shoreline environments. South of Hill County, the shale facies, known as the Pepper Shale, become dominant. The Woodbine Group is unconformably overlain by the Eagle Ford Group.

2.1.1.1 Previous Geologic Investigations

Investigations of Cretaceous-age rocks in Texas began as early as the mid-1800s. Some of these early reports include Shumard (1860), which describes observations on the Cretaceous-age strata of Texas, and Taff (1892), which reports on Cretaceous-age strata located north of the Colorado River. The first comprehensive description of the Cretaceous-age rocks in central and north-central Texas is provided in Hill (1901), which documents investigations conducted by Hill independently or with others beginning in 1882. Hill (1901) presents a discussion of defects of earlier classifications of these formations and provides a refinement of the nomenclature. This refinement includes dividing the Cretaceous-age rocks into a lower Comanche Series and an upper Gulf Series, identifying groups within each series, and naming formations based on several local stratigraphic sections. Many of his formation names, as well as group and series divisions and names, are still in use. Hill (1901) also provides detailed descriptions of the formations.

Numerous county-specific geologic investigations have been conducted for counties in the study area. For Texas counties, these reports, in general, describe the topography, physiography, stratigraphy, structure, and mineral resources/economic geology of the county. Some reports provide additional information such as petroleum development (e.g., Cooke County), paleontology (e.g., Bell and Tarrant counties), and well data (e.g., Bell and McLennan counties). The Oklahoma Geological Survey published a series of bulletins on the geology and groundwater resources of various counties in that state. These include Bullard (1925) for Love County, Bullard (1926) for Marshall County, Davis (1960) for McCurtain County, Huffman and others (1975) for Choctaw County, Huffman and others (1978) for Bryan County, and Huffman and others (1987) as an update to Bullard (1926) for Marshall County. In Arkansas, hydrogeological assessments have been performed and documented for most of the counties in the study area, including Hempstead, Lafayette, Little River, Miller, and Nevada counties (Ludwig, 1973) and Pike and Howard counties (Thornton, 1992). The available geological and groundwater resource reports for counties in the study area are provided in Table 3.1.1.

In addition, numerous geologic and stratigraphic investigations involving Cretaceous-age rocks in the study area have been conducted. Examples include but are not limited to, studies of the upper Cretaceous-age formations of southwestern Arkansas (Dane, 1929); the Mesozoic Systems in Texas (Adkins, 1933); the stratigraphy of the Woodbine Group (Dodge, 1952; Adkins and Lozo, 1951; Bryan, 1951; Price, 1951; Lee, 1958; Hamman, 2001), the lower Cretaceous-age Paluxy Sand in central Texas (Atlee, 1962), the northern Trinity Group deposits of central Texas (Boone, 1968; Stricklin and others, 1971), rocks of the Comanchean series of central Texas (Hayward and Brown, 1967), the Glen Rose Limestone in Texas (Rodgers, 1967), the Cretaceous-age and pre-Cretaceous-age strata in north-central Texas (Bain, 1973), the Comanchean Series in east central Texas (Mosteller, 1970), and the Paluxy sand in north-central Texas (Owen, 1979).

As a result of historical use of confusing—and sometimes inappropriate geologic nomenclature—Fisher and Rodda (1966) developed a revised nomenclature for the basal Cretaceous-age rocks in the area between the Red and Colorado rivers and on the Callahan Divide in Texas. They divide these units geographically into three distinctive lithologic outcrop sequences corresponding to north-central Texas, north and west-central Texas, and central Texas, and one subsurface sequence in north-central Texas. The stratigraphic nomenclature applied by Fisher and Rodda (1966) is summarized in Table 3.1.2. They present the addition of a new formation, named the Twin Mountains Formation, in north-central Texas because the basal Cretaceous-age rocks in that area have facies distinct from that of the Travis Peak Formation in central Texas. Their nomenclature has been adopted by most modern groundwater availability studies in the study area.

The depositional systems in the Woodbine Group and Glen Rose Formation in northeast Texas are presented in Oliver (1971) and Davis (1974), respectively. Investigation of the depositional systems in the Paluxy Formation for application to oil, gas, and groundwater resources is presented in Caughey (1977). Hall (1976) presents the depositional systems and facies in lower Cretaceous-age sandstones in north-central Texas and discusses their hydrogeological significance. Numerous other reports discuss the depositional systems of the Cretaceous-age strata in central and north-central Texas.

2.1.1.2 Hydrostratigraphy

The hydrostratigraphy of the northern Trinity and Woodbine aquifers is defined by interbedded sandstones, shales, and limestones that formed during the Cretaceous Period. These formations are part of the Gulf of Mexico Basin fill and exhibit significant variability in thickness, lithology, and hydraulic conductivity. The Woodbine Group, separated from the Trinity Group by the Washita/Fredericksburg groups, contains sandstones primarily deposited in deltaic shoreline environments. These formations are thickest in the northeast and thinnest toward the south, reflecting their depositional history and the influence of structural features such as fault zones. The sand-dominated aquifers of the Trinity Group include the Paluxy, Hensell, and Hosston formations, while the Woodbine Group contains additional sandstone aquifers separated from the Trinity by the limestone and shale layers of the Washita/Fredericksburg Group. The Trinity Group formations represent major aquifers characterized by high hydraulic conductivity and groundwater productivity. The Paluxy Aquifer, located higher in the stratigraphic sequence, rivals the Hosston in productivity in certain regions but exhibits significant regional variability in thickness and lithologic composition. The Hensell Aquifer is sand-dominated but exhibits thinning and a transition to shale downdip. The Hosston Aquifer, the basal unit of the Trinity Group, is the most widespread and hydraulically significant, with thick sandstones providing extensive groundwater resources.

Hydrostratigraphic characteristics vary across the GCDs within the study area. The Upper Trinity GCD features sand-dominated aquifers in outcrop regions, with the Hosston and Hensell units providing significant groundwater resources. In the North Texas GCD, thick sandstone sequences in both the northern Trinity and Woodbine aquifers support extensive water use, with low-salinity groundwater extending to substantial depths. The Northern Trinity GCD contains well-developed sandstones in the Paluxy, Hensell, and Hosston aquifers. These formations provide high-quality groundwater, although well-to-well variability is high due to the influence of fluvial depositional systems. In the Prairielands GCD, sandstone development is highly variable, with the Hosston Aquifer offering the most consistent groundwater resources.

2.1.1.3 Structural Features

Structural geology plays a pivotal role in shaping the behavior of the northern Trinity and Woodbine aquifers. The Cretaceous formations were tilted southeastward due to the subsidence of the Gulf of Mexico Basin, creating a structural dip that enhanced downward GWF. This dip varies across the study area, ranging from gentle inclinations in outcrop regions to steeper dips near the East Texas Basin. Faulting affects the aquifers significantly, introducing vertical discontinuities that influence groundwater movement. The Balcones Fault Zone, characterized by displacements of 100 to 400 ft, creates vertical offsets that can isolate aquifers or facilitate vertical flow. The Mexia-Talco Fault Zone (Figure 2-2) marks the eastern boundary of freshwater occurrence in the aquifers, with displacements reaching up to 700 ft. Smaller localized faults and fractures are abundant within the Cretaceous formations and contribute to localized variability in aquifer connectivity and water quality.

2.1.1.4 Depositional Environment

The depositional history of the northern Trinity and Woodbine aquifers reflects the dynamic paleogeography of the Cretaceous Period. Fluctuating sea levels during this time resulted in alternating episodes of fluvial sedimentation and marine transgression, creating the interbedded sandstone, limestone, and shale sequences characteristic of the aquifers. Fluvial systems deposited broad sand belts in the lower portions of the aquifers, particularly the Hosston and Hensell units. These environments, dominated by river channels and deltas, contributed to the high sandstone concentration and hydraulic conductivity observed in these formations. The Paluxy Aquifer, formed by converging fluvial systems, exhibits elongated sand trends that reflect its depositional history. Marine transgressions during the Cretaceous Period deposited extensive limestone and shale layers, such as those in the Glen Rose Formation and Washita/Fredericksburg groups. These units act as confining layers, restricting vertical GWF and compartmentalizing the aquifer system. The Woodbine Aquifer, representing the final phase of sandy depositional systems, was deposited in deltaic shoreline environments and exhibits significant variability in thickness and quality across the study area.

2.1.2 Hydrogeologic Units

For this study, the Woodbine, Washita/Fredericksburg, and northern Trinity groups in the study area were divided into the seven hydrogeologic units as with Kelley and others (2014) based on significant differences in geologic properties. These are the Woodbine Aquifer, Washita/Fredericksburg groups, Paluxy Aquifer, Glen Rose Formation, Hensell Aquifer, Pearsall Formation, and Hosston Aquifer. Figure 2-3 shows the generalized surface expression of these hydrogeologic units. Generally, the layering differentiates between sandstone-dominated layers that are aquifers and shale- and limestone-dominated layers that are typically confining units. Shales have low hydraulic conductivities and include soluble mineral salts that decrease groundwater quality. Most limestones in the study area possess similar properties. Sand and sandstone, in contrast, typically have high hydraulic conductivities and are composed of relatively insoluble quartz and feldspar grains.

The presence of seven contrasting layers does not occur in all parts of the study area. For example, in the northern part, there are only two or three contrasting layers: the sandstones of the Antlers Formation, the shale and limestone of the Washita/Fredericksburg groups, and the sandstone of the Woodbine Group, where present. In fact, all seven contrasting layers are present together only in portions of the central part of the study area. Vertically adjacent hydrogeologic units can have similar hydraulic properties, and subdividing a thick sandstone sequence, such as the Antlers Formation, adds resolution to the conceptual and groundwater models.

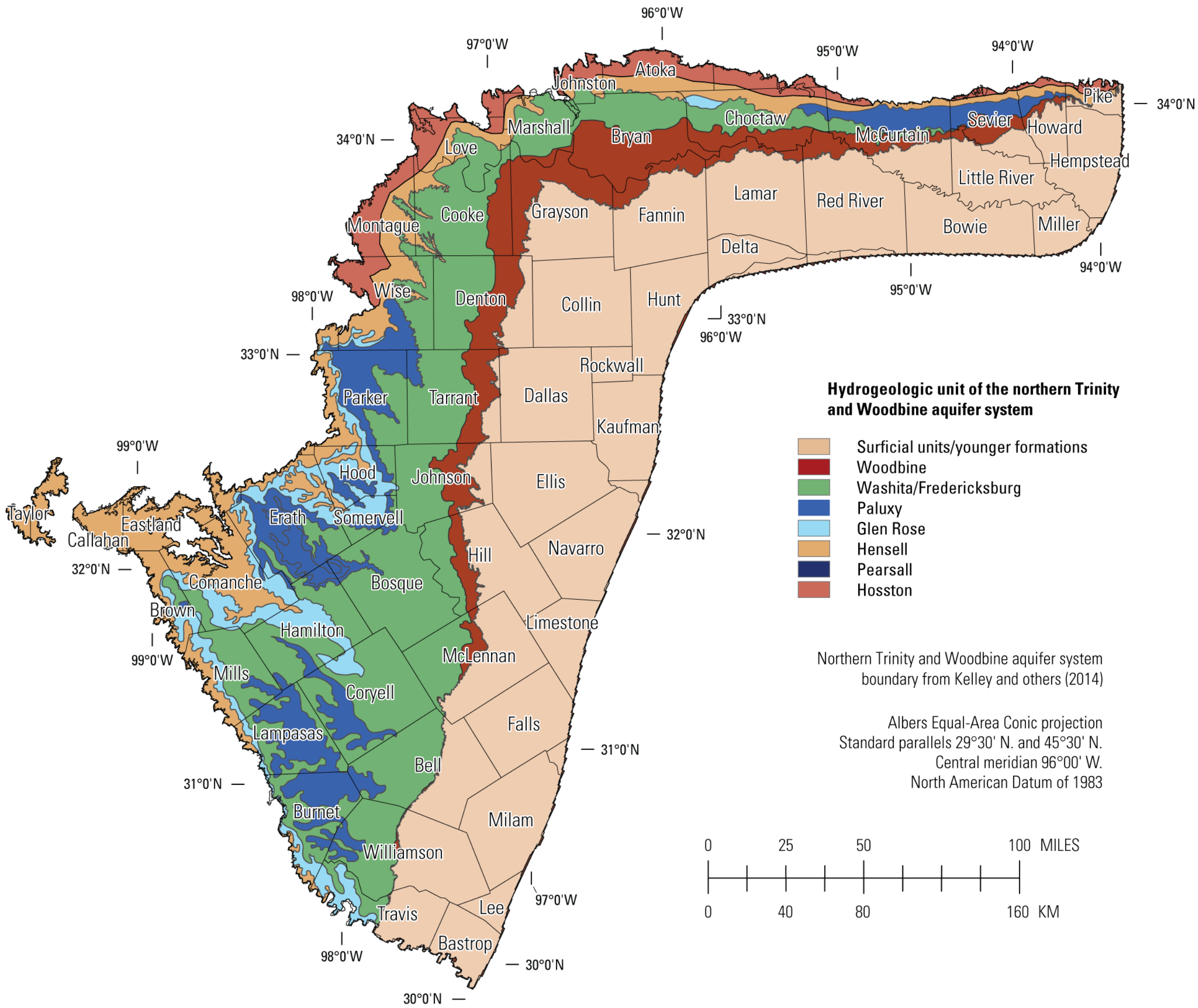

Figure 2-3. **Generalized surface expression of the hydrogeologic units of the northern Trinity and Woodbine aquifer system.**

The areas where the northern Trinity and Woodbine aquifers exist include three regions of large-scale faulting and structural deformation. The Balcones Fault Zone (BFZ) extends into the model area from the south through Travis, Bell, McLennan, and Hill counties. Displacements on faults in this zone range from 100 to 400 ft, which are sufficient to completely disconnect some layers (Klemt and others, 1975). The Mexia-Talco Fault Zone is a complex zone of interweaving faults that extends along the entire length of the downdip boundary of the study area. Individual faults in the Mexia-Talco Fault Zone have as much as 700 ft of displacement. Fresh groundwater in the northern Trinity and Woodbine aquifers does not extend beyond the Mexia-Talco Fault Zone. An area of faulted and folded strata occurs in Cooke and Grayson counties and extends northwest into Oklahoma. This structurally deformed area is commonly known as the Sherman Syncline and Preston Anticline.

Of the seven aquifers or formations defined in this study, the Woodbine, Paluxy, Hensell, and Hosston aquifers are considered to be aquifers because of their lithologic character (sand dominated over large portions of the study area). The Woodbine Aquifer is sand-dominated in north-central Texas but loses significant sand content in the far eastern portions of Texas and Oklahoma and south of McLennan County, where the Woodbine Group is no longer considered an aquifer. The Paluxy Aquifer, also predominantly sand over most of the study area, was deposited in a coastal plain and deltaic environment in all areas except the far southern portion of the study area, where it is predominantly a shale unit. The Hensell Aquifer is also predominantly a sand unit, being deposited in a coastal plain and deltaic environment over most of the study area. The Hosston Aquifer is a sand-dominated unit over most of the study area owing to it being deposited in a coastal fluvial plain depositional environment.

2.1.2.1 Previous Hydrogeological Investigations

The earliest systematic investigation of groundwater in the study area is documented in Hill (1901). As discussed previously in Section 2.1, Hill (1901) provides detailed descriptions of the geology of the Cretaceous-age rocks in the study area. In addition, he conducted detailed investigations of the artesian waters in these rocks. Earlier wells drilled into the Paluxy Formation and the northern Trinity Group encountered artesian conditions and, in many instances, pressures were sufficient to cause wells to flow at the surface. Hill (1901) set forth in his study to identify the formations from which artesian waters could be obtained, the depths of those waters, and the height to which water in those formations would rise in an effort to provide information useful for future well development. He provides descriptions of the northern Trinity and Woodbine aquifers, existing knowledge of the chemistry of the groundwater in these aquifers, and estimated locations where the pressure in the aquifers was sufficient to result in flowing wells. He also includes well schedules for selected wells and some information on aquifer yield and surface flow rates.

In response to the concern of residents regarding the cessation of flowing conditions in wells, Fiedler (1934) conducted an investigation of artesian water in Somervell County, Texas. His investigation "comprised a study of the use and waste of artesian water, the safe yield of artesian reservoirs, underground leakage of wells, methods of constructing wells, and other related features necessary for the formulation of a conservation program." County- or multicounty-based studies of geology and groundwater resources have been conducted for several counties in the study area by past and present Texas state agencies responsible for water resources. In general, the main objective of those investigations was the assessment of groundwater resources in the county.

During 1942 and 1943, several local investigations were conducted to evaluate groundwater availability and estimate the impact of future pumping in association with war efforts related to selecting locations for military facilities or providing water for war-related industries. Sundstrom and Barnes (1942) report on groundwater resources in the vicinity of Gatesville, Texas. Livingston and Hastings (1942) report on a test well drilled at a proposed army camp southeast of Gatesville, Texas; and Guyton and George (1943) and Rose (1943) present results of pumping tests conducted in wells at Camp Hood and the Tank Destroyer Center, respectively, located near Gatesville, Texas. Investigations of groundwater resources in the vicinity of Belton, Texas, and McGregor, Texas, made at the request of the military, are documented in Bennett (1942) and Livingston and Bennett (1942), respectively. The evaluation of groundwater resources for the military in selected areas in Erath, Hood, and Hamilton counties are summarized in Rose and George (1942), and in the vicinity of Burnet, Texas, and Bertram, Texas, are summarized in George (1942). In anticipation of an influx of workers for war industries, an investigation of groundwater resources in Fort Worth and its vicinity was conducted by George and Rose (1942). Additional reports related to groundwater supplies for war or post-war purposes include the results of aquifer pumping tests conducted on wells in Waco, Texas (George and Barnes, 1945), groundwater resources at Sherman, Texas (Livingston, 1945), and results of aquifer pumping tests on city wells at Waxahachie, Texas (Sundstrom, 1948). An investigation conducted for the city of Burnet, Texas, in response to well failures during the drought of the early 1950s is discussed in Mount (1962).

Winslow and Kister (1956) report on the saline water resources of Texas, which includes a discussion of the northern Trinity and Woodbine aquifer. The purpose of their report was "to outline the occurrence, quantity, and quality of saline water available in Texas; to discuss and identify aquifers containing saline water, with emphasis on those capable of yielding large quantities; and to delineate areas in which a considerable amount of saline surface water is available." As part of a statewide program to assess groundwater supplies and availability, reconnaissance investigations of principal aquifers were conducted in the Sabine River basin (Baker and others, 1963a), the Red River, Sulphur River, and Cypress Creek basins (Baker and others, 1963b); the Trinity River basin (Peckham and others, 1963); and the Brazos River basin (Cronin and others, 1973). These investigations were conducted on the basis of river basins because the approach to state water planning at that time was by river basins. Two studies of groundwater availability were conducted by the TWDB or a predecessor agency at the request of city officials for Whitney, Texas (Mount, 1963) and Commerce, Texas (Baker, 1971). Both of these investigations focused on the possibility of producing water from the northern Trinity Aquifer.

Leggat (1957), in his investigation of groundwater in Tarrant County, estimated that Lake Worth recharges the Paluxy Formation at a rate of about 650 AFY and that recharge from Eagle Mountain Lake is likely similar. Based on comparisons of levels in Lake Grapevine and groundwater elevations in the Woodbine Group, Leggat (1957) indicates that the recharge of the group by the lake is likely small. Baker (1960) suggests that, prior to development, natural discharge occurred from the Antler Formation along the crest and southern flank of the Preston Anticline and along the Red River in Grayson County. He suggests that groundwater movement in the Antlers Formation in the county was towards the Red River prior to significant development and the impoundment of Lake Texoma. Afterward, he suggests that the Preston Anticline became a recharge area for the Antlers Formation. Cross-formational flow is also given as a natural discharge mechanism in the downdip portions of the Antlers Formation and the Woodbine Group in Grayson County by Baker (1960).

Regional studies of groundwater resources of the northern Trinity and Woodbine aquifers are documented in Klemt and others (1975) and Nordstrom (1982 and 1987). Klemt and others (1975) studied the Antlers and Travis Peak formations in portions of central Texas. The counties included in their investigation, either wholly or partially, are Bell, Bosque, Brown, Burnet, Callahan, Comanche, Coryell, Eastland, Erath, Falls, Hamilton, Hill, Lampasas, Limestone, McLennan, Milam, Mills, Somervell, Travis, and Williamson. The portions of their report that discuss groundwater movement are summarized here.

Klemt and others (1975) suggest that the movement of groundwater downdip from the outcrop areas may be significantly restricted by the BFZ and Mexia-Talco Fault Zone. Groundwater movement may also be restricted in the vicinity of McGregor High, located in Coryell County, due to thinning of the lower Cretaceous-age sediments. They suggest that the impact of this high is likely most significant for the

Hosston Member of the Travis Peak Formation. They also estimate that groundwater movement in the Antlers and Travis Peak formations is impacted by thicker accumulations of sand in valleys of the pre-Cretaceous Period surface and thinner accumulations on the ridges.

Klemt and others (1975) state that the basal sediments in the Travis Peak and Antlers formations are hydraulically connected, having the same potentiometric surface and water quality. They state that the most important aquifers in the study area are, first, the Hosston Member of the Travis Peak Formation and, second, the Hensell Member of the Travis Peak Formation. The Hensell Member is the source for most domestic wells in the study area of Klemt and others (1975). The Glen Rose Formation provides small quantities of water to predominately domestic and stock wells in localized areas on and adjacent to its outcrop. Downdip, the groundwater in the Glen Rose Formation becomes highly mineralized. Small to moderate amounts of groundwater are supplied by the Paluxy Formation in the northern and central areas of Klemt and others (1975) investigation. In their study area, the Woodbine Group is an important source of groundwater only in the northeast, in Hill County. The Woodbine Group provides groundwater for many domestic and stock wells and several small towns and industries.

The sources of recharge to the Travis Peak and Antlers formations are precipitation in the outcrop areas, seepage from some lakes, particularly Proctor Lake and Lake Travis, some streams, particularly the Lampasas, Leon, and Sabine rivers, seepage from ponds, and irrigation return flow (Klemt and others, 1975). They estimate that recharge to the Travis Peak Formation through the infiltration of precipitation is less in Burnet, Lampasas, Mills, and Brown counties due to tight soils in the outcrops and well-cemented sediments in the subsurface. Due to interbedded sands and shales in the outcrop areas of the Travis Peak and Antlers formations, perched water locally occurs in these two formations. Before the development of groundwater in the Travis Peak Formation, the pressure in the formation was sufficient to drive water to the ground surface in wells drilled in topographic lows downdip of the outcrop area. Klemt and others (1975) indicate that groundwater in the Travis Peak and Antlers formations moved downdip from the recharge area in the outcrops prior to development. They report that natural discharge from these two formations occurs in the outcrops through seeps, springs, and ET and in the downdip areas along faults and through cross-formational flow.

Recharge to the Woodbine Group occurs through infiltration of precipitation in the outcrop and seepage from streams (Klemt and others, 1975). The movement of groundwater in this group is from the outcrop area to the downdip area. They indicate that natural discharge from the Woodbine Group is through seeps, springs, and ET in the outcrop area and cross-formation flow in the downdip area. One of the main objectives of the Klemt and others (1975) investigation was numerical simulation of predicted future water-level declines. That modeling is discussed in Section 3.1.

Nordstrom (1982) discusses groundwater resources in the Cretaceous-age strata of north-central Texas. His report includes a discussion of the geology of the study area as it relates to the occurrence of groundwater; the stratigraphy of the water-bearing formations; the groundwater chemistry as related to use; the occurrence and development of groundwater resources, including hydraulic characteristics and historical water-level declines; the availability of groundwater, and well construction. His study included all or parts of Collin, Cook, Dallas, Delta, Denton, Ellis, Fannin, Grayson, Hood, Hunt, Johnson, Kaufman, Lamar, Montague, Navarro, Parker, Red River, Rockwall, Tarrant, and Wise counties. The most prolific aquifers in his study area are the Antlers, Twin Mountains, and Paluxy aquifers. Groundwater is also provided by the Woodbine Group in the eastern portion of his study area. Although well yields in the Twin Mountains and Antlers formations are higher than those in the shallower Paluxy Formation, the area over which development has occurred is greater for the Paluxy Formation. In Nordstrom's (1982) study area, the Twin Mountains Formation is the most prolific aquifer, and the Woodbine Group is the most important in large parts of the area. He reports that the basal portions of the Twin Mountains and Antlers formations are hydraulically connected. Production from the upper portion of the Antlers Formation is less than that from the lower portion. In the Twin Mountains Formation, well yields are lower in the outcrop area and increase downdip, and are generally lower in the southern portion of his study area and increase to the north (Nordstrom, 1982). Well yields in the Paluxy Formation also show a greater downdip than in the outcrop area. Large yields can be obtained from the Woodbine Group in portions of both the outcrop and downdip areas.

Nordstrom (1987) discusses the groundwater resources in the outcrop areas of the Antlers and Travis Peak formations in north-central Texas. His study included all or parts of Brown, Callahan, Comanche, Eastland, Erath, and Hamilton counties. He states that the primary sources of groundwater in this area are the formations of the northern Trinity Group. The Paluxy Formation provides small quantities of water to domestic and stock wells, predominantly along the edge of the outcrop. Although the Glen Rose Formation can supply small quantities of water, some of the water from this formation is of poor quality. Beyond this information, Nordstrom (1987) does not discuss these two formations but rather focuses on the Travis Peak and Antlers formations, which are the principal sources of groundwater in his study area. Like Klemt and others (1975), Nordstrom (1987) indicates that the potentiometric surface of the lower sediments in the Antlers Formation is equivalent to that in the Hosston Member of the Travis Peak Formation. He also states that the Hensell Member of the Travis Peak Formation is hydraulically separate from the lower Hosston Member based on both water levels and water chemistry. The principal source of groundwater in his study area is the Hosston Member, and the second most important is the Hensell Member. Nordstrom (1987) also indicates that the Hensell Member is tapped by most of the small-capacity wells in his study area.

Nordstrom (1987) reports that groundwater in the Travis Peak and Antlers formations is recharged through the infiltration of precipitation on the outcrops, stream loss, and irrigation return flow. The predevelopment movement of groundwater in these two formations is in the downdip direction. Natural discharge in the outcrop area of the Twin Mountains and Antlers formations occurs through seeps, springs, and ET. This description is consistent with that given by Klemt and others (1975). Through an evaluation of transient water-level data, Nordstrom (1987) concluded that, in general, recharge in the outcrops is sufficient for the formations to recover from the summer pumping conducted for irrigation purposes.

Duffin and Musick (1991) report on their evaluation of groundwater resources in Bell, Burnet, Travis, Williamson, and parts of adjacent counties. Structural features impacting groundwater are the erosional pre-Cretaceous Period surface, which resulted in thicker sediments in valleys and thinner sediments on ridges, and the BFZ and Mexia-Talco Fault Zone, across which groundwater movement might be blocked or restricted. They proposed that these fault systems could also be conduits of groundwater from deeper formations. Duffin and Musick (1991) indicate that in their study area, the northern Trinity Group produces water from the Hosston Member, small amounts from the Cow Creek Member in or near its outcrop, and the Hensell Member of the Travis Peak Formation, and from the Glen Rose

Formation in localized areas on or adjacent to its outcrop. The aquifers of the Hosston and Hensell members of the Travis Peak Formation are separated by the Hammett Shale Member. The Paluxy Formation is present only in the eastern and northeastern portions of Burnet County and is not tapped by any wells. The Edwards Formation and associated limestone are the principal aquifers in their area, and they are referred to as the Edwards BFZ Aquifer. In some portions of the area studied by Duffin and Musick (1991), they found that the pressure in the Hosston Member was sufficient to cause the groundwater to flow at the surface. Wells completed into the Hensell Member were also observed to flow in some areas, such as along Lake Austin and in the city of Austin. Duffin and Musck (1991) indicate that, where it is present, the Paluxy Formation is hydraulically connected to the upper portion of the underlying Glen Rose Formation. They found no evidence of springs issuing from the northern Trinity Group.

Dutton and others (1996) present the results of numerical modeling of the Twin Mountains and Paluxy formations and the Woodbine Group in north-central Texas. That modeling is described in Section 3.1. In addition, they provide discussions on the regional hydrogeological setting, the stratigraphy and depositional systems of the formations, and the hydrogeological framework of the formations, including historical conditions, hydraulic heads, detailed investigation of hydraulic properties, recharge, discharge, and groundwater velocity.

In response to the passage of House Bill 2 by the Texas Legislation in 1985, which required the "identification and study of critical ground-water areas in the State," the hydrogeological conditions of the northern Trinity Aquifer and other aquifers in part of central Texas are presented in Baker and others (1990a) and in part of north-central Texas in Baker and others (1990b). The purpose of these investigations was the identification of "problems related to pumping over-drafts and contamination of ground water as they exist or are expected to occur." Updated investigations conducted by the TWDB evaluating changes in groundwater conditions, demands, and availability in the northern Trinity and Woodbine aquifers are provided in Bradley (1999) for portions of central Texas and for the northern Trinity, Woodbine, and other aquifers are provided in Langley (1999) for portions of north-central Texas.

The geology and hydrology of the Antlers Formation in Oklahoma are presented in two hydrologic atlases prepared cooperatively by the Oklahoma Geological Survey and the USGS. Hart (1974) covers the Ardmore and Sherman quadrangles, covering approximately the western half of the Antlers Aquifer in Oklahoma, and Marcher and Bergman (1983) cover the McAlester and Texarkana quadrangles, covering the eastern half of the Antlers Aquifer in Oklahoma. Davis and Hart (1978) was the first major study focusing entirely on the Antlers Aquifer in Oklahoma, and they documented hydrological data for the aquifer, including well characteristics, water quality, several springs, and low-flow discharge from area streams.

2.1.2.2 Structure Update

One of the objectives of this study was to update the hydrogeologic structure of the existing northern Trinity and Woodbine aquifer system using structural datasets collected since the publication of the NTWGAM (Kelley and others, 2014). A variety of structural data from GCDs were obtained, including electronic copies of resistivity logs, datasets with borehole coordinates and aquifer depths, and spatial locations of aquifer depth point locations.

All uninterpreted logs of satisfactory quality with adequate supporting metadata were analyzed and integrated with pre-interpreted stratigraphic picks. The existing dataset of stratigraphic picks from the NTWGAM was also considered during this study. Electronic copies of logs and metadata were received from Northern Trinity GCD, Prairielands GCD, and Upper Trinity GCD. Twelve additional logs in Milam County were used in the update. Coordinates with aquifer stratigraphic picks were received from Central Texas GCD, and shapefiles of aquifer tops and bottoms were received from Middle Trinity GCD and Clearwater GCD. The raster surfaces from the latest Edwards BFZ Aquifer GAM (Jones, 2023) were also considered during the structure update. The updated surface of the top of the Paluxy Aquifer is similar to the surface of the top of the Trinity Aquifer in the Edwards BFZ Aquifer GAM. Figure 2-4 shows the locations of the data used in the northern Trinity and Woodbine aquifer system structure update.

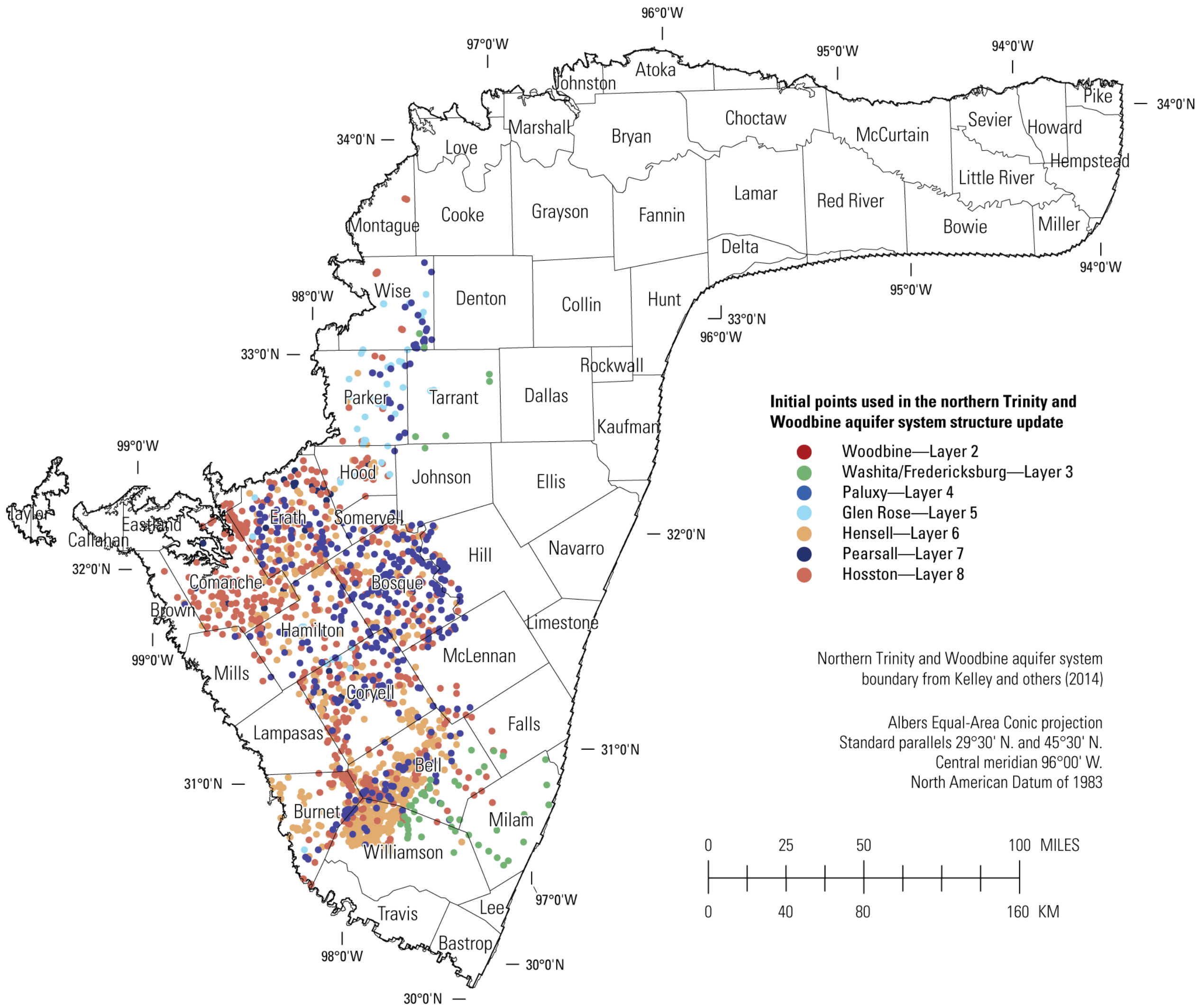

Figure 2-4. Initial points used in the Northern Trinity and Woodbine aquifer system structure update.

The update of the hydrogeologic structure was completed with the goal of preserving the extensive work performed as a part of Kelley and others (2014). As such, the aquifer surfaces were updated primarily where new data was available. The aquifer surface stratigraphic picks used to create the structure in the original NTWGAM (Figure 2-5) were used as a buffer. New aquifer surface stratigraphic picks within two miles of the original data were not used in the structure update on a per-hydrogeologic unit basis. To eliminate unreasonable values in the datasets received, the stratigraphic picks were filtered based on the difference from the existing surfaces. For each hydrogeologic unit, differences between the new stratigraphic picks and existing aquifer surfaces were calculated and recorded. Stratigraphic picks with an associated difference from the existing surface that was higher than the 95th percentile were then discarded from the updated structure dataset. This filtering resulted in a threshold of maximum difference from the existing surface that varied between 110 ft and 187 ft, depending on the hydrogeologic unit.

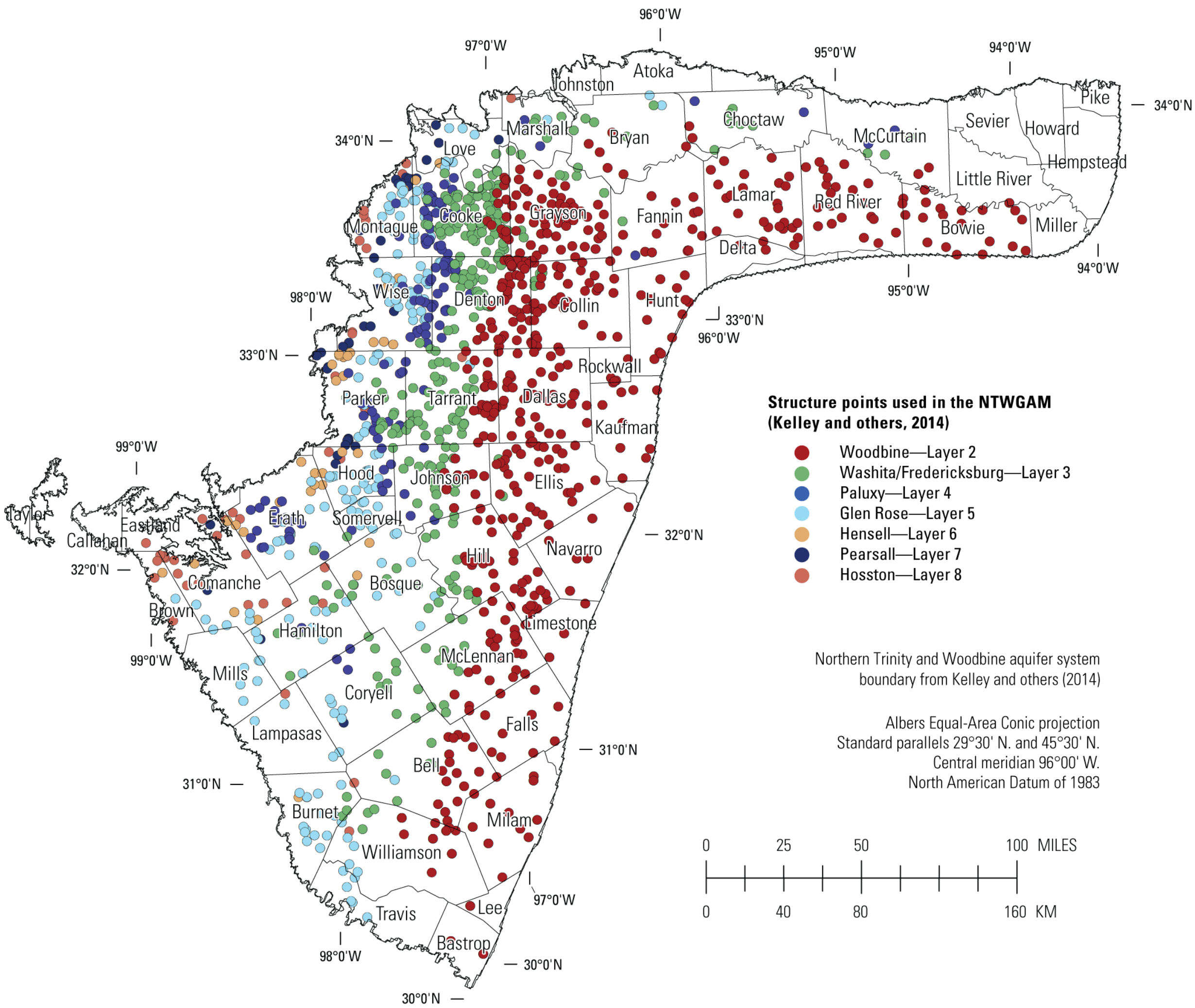

Figure 2-5. Structure points used in the NTWGAM (Kelley and others, 2014).

New hydrogeologic unit surfaces were then generated using the existing model grid and the filtered dataset of new stratigraphic picks. For each hydrogeologic unit, the centroid of each layer grid cell was calculated and merged with the filtered, new stratigraphic picks to create a point shapefile. Then, all centroids within two miles of a new stratigraphic pick were discarded, except those centroids, which comprised the edges of the model grid. Using Topo-to-Raster, new surfaces were interpolated using the combined, filtered new stratigraphic picks and filtered centroids. The new surfaces were resampled at the locations of the centroids within two miles of the new stratigraphic picks. A minimum thickness of 30 ft was enforced for each hydrogeologic unit, following the convention set by the original NTWGAM.

Structural changes in the layer 2 surface (Woodbine equivalent) were limited to Milam, Bell, and Williamson counties (Figure 2-6), as new log coverage in this area was limited. Changes to the top of the Paluxy Aquifer (Figure 2-7) were more widespread and most concentrated in Bosque and western Hill County. In Bosque, a majority of the updates resulted in the rise of the upper surface of the Paluxy Aquifer. This update did not necessarily result in an increase in thickness; however, many of the surfaces in a single column of the aquifer system may have been changed because of the update. For example, several of the same cells that demonstrated a rise in the Paluxy's top surface elevation in Figure 2-7 also show a rise in the Hensell and Hosston top surface elevations in Figures 2-8 and 2-9. Note that the model structure of the NTWGAM, which was created for MODFLOW-NWT, contained one-foot-thick "passthrough" cells corresponding to pinched-out layers. These cells were effectively removed from the NTMGAM structure by reducing their thickness down to zero and inactivating them in MODFLOW 6.

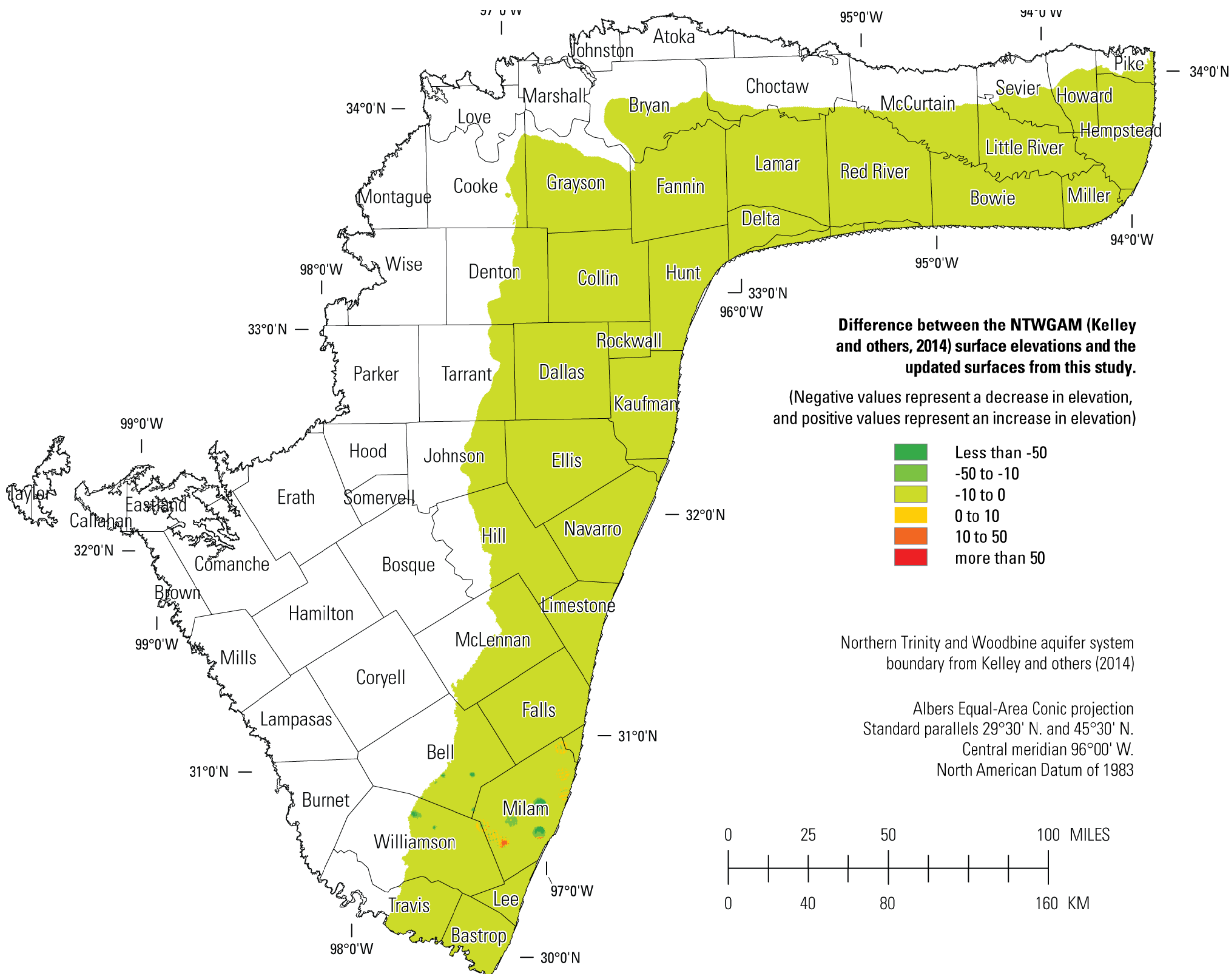

Figure 2-6. Difference between the NTWGAM (Kelley and others, 2014) surface elevation and the surface elevation of the updated surfaces for the Woodbine aquifer.

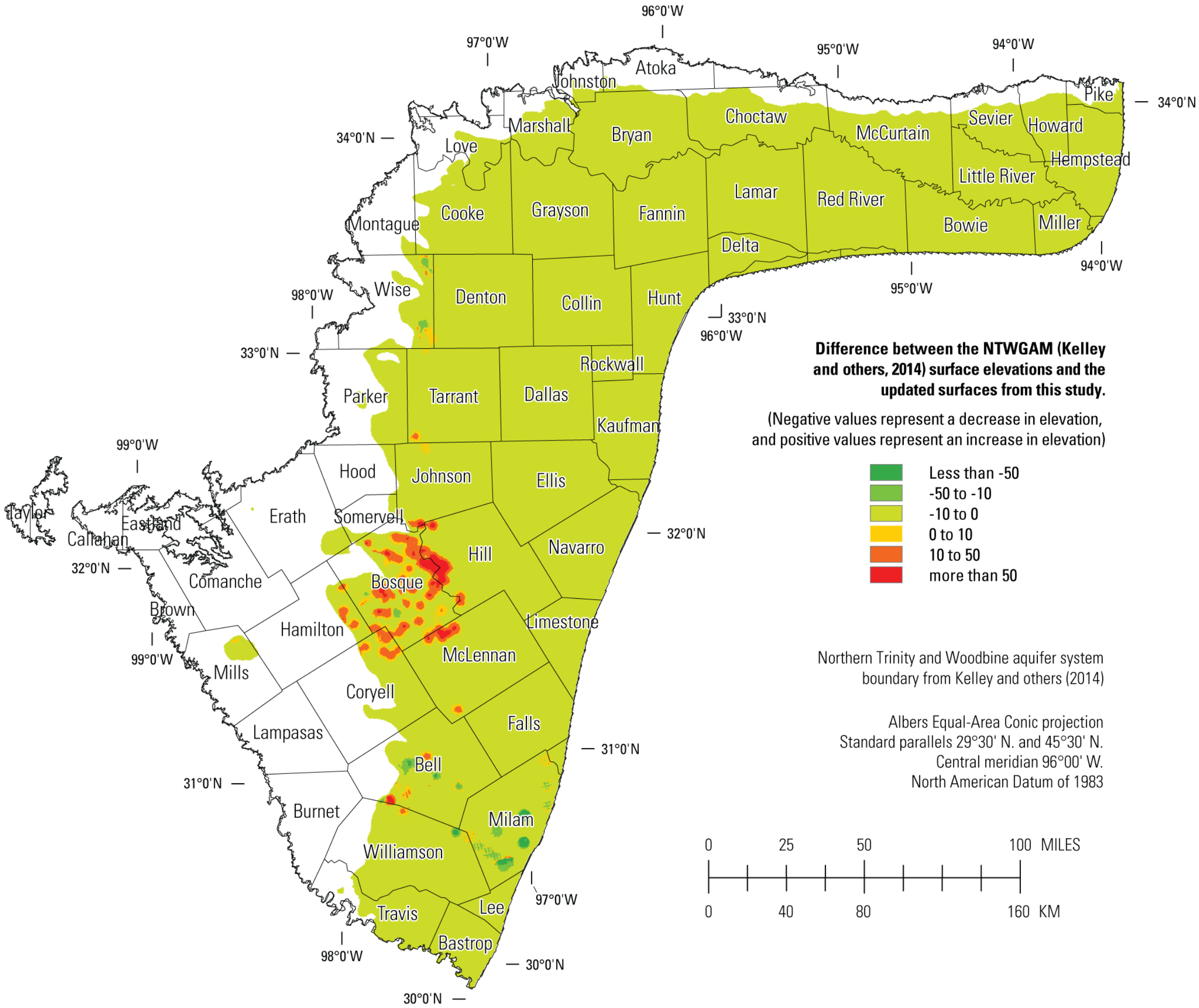

Figure 2-7. Difference between the NTWGAM (Kelley and others, 2014) surface elevation and the surface elevation of the updated surfaces for the Paluxy aquifer.

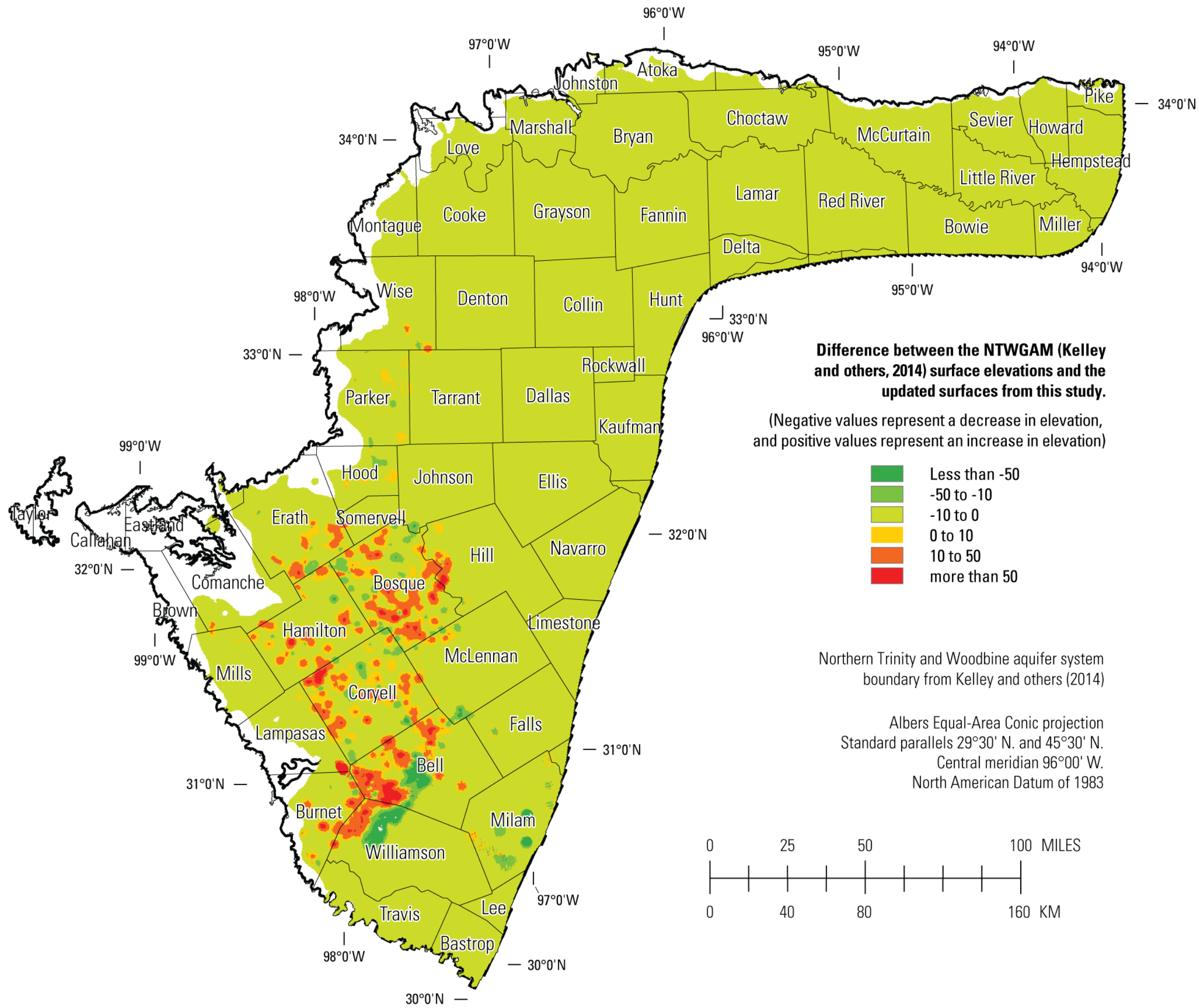

Figure 2-8. Difference between the NTWGAM (Kelley and others, 2014) surface elevation and the surface elevation of the updated surfaces for the Hensell aquifer.

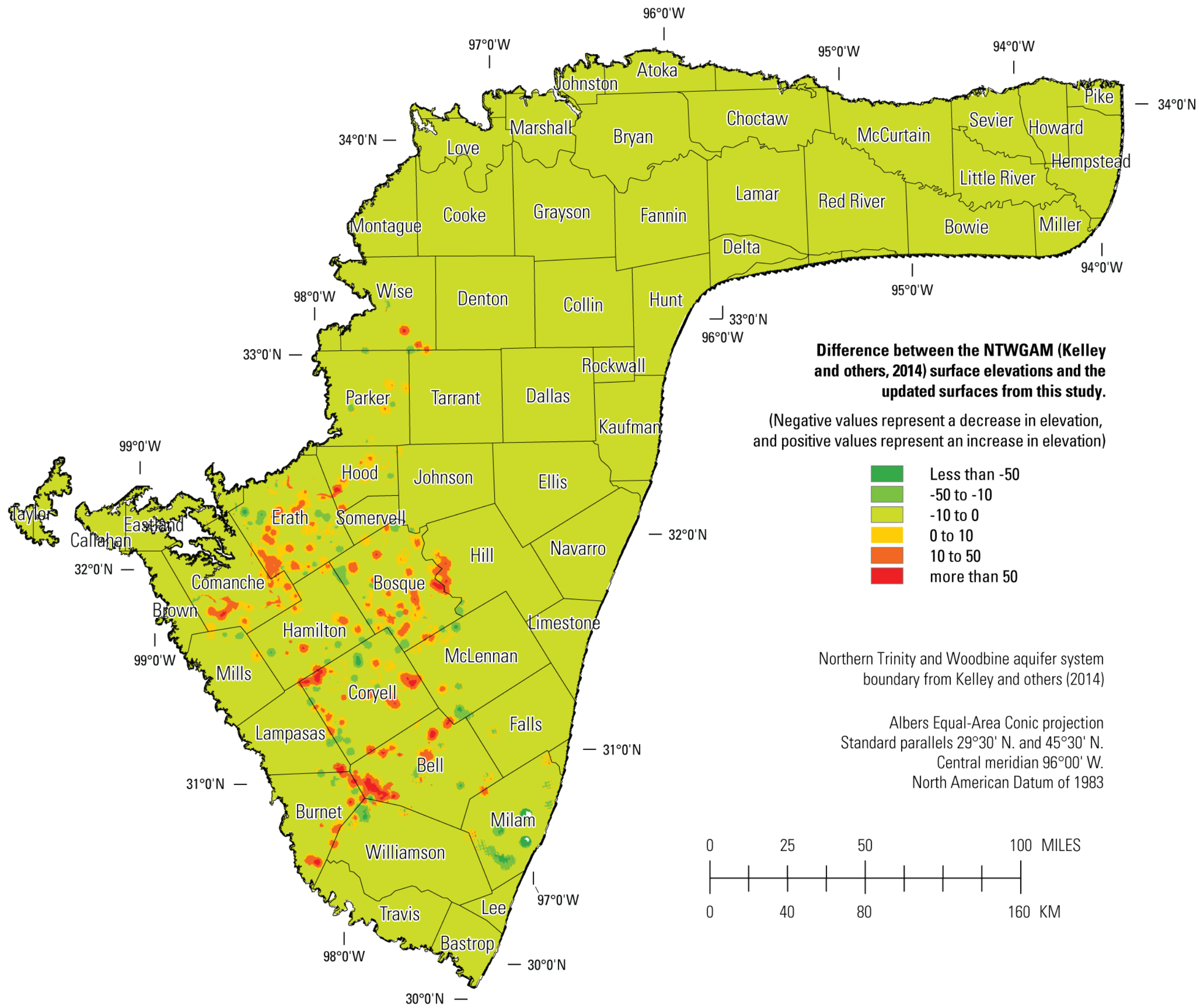

Figure 2-9. Difference between the NTWGAM (Kelley and others, 2014) surface elevation and the surface elevation of the updated surfaces for the Hosston aquifer.

2.1.2.3 Hydraulic Properties

Recent datasets of hydraulic properties were used to update the existing northern Trinity and Woodbine GAM. A variety of hydraulic property data was received, including point locations with transmissivity by aquifer from Central Texas GCD and Clearwater UWCD, as well as electronic copies of uninterpreted pumping tests with associated metadata from Upper Trinity GCD. Interpreted pumping test data from the TWDB groundwater database, various Groundwater Availability Certifications from Johnson County, and pumping test data from an aquifer storage and recovery study performed in Bell County (Kelley and others, 2023) were also used. Additionally, the 500 pumping tests used in the creation of the NTWGAM (Kelley and others, 2014) were added to the dataset.

Five 48-hour pumping tests were sourced from Groundwater Availability Certifications from Prairielands GCD. These tests were all in the Woodbine Aquifer. Time-drawdown data and well construction information were supplied for 14 middle- and lower-Trinity pumping tests in Upper Trinity GCD with test lengths that ranged from 24 to 38 hours. Eight of the tests were determined to have comprehensive and adequate quality data, and transmissivity was calculated from these tests using the Cooper-Jacobs straight-line method (Cooper and Jacob, 1946). Transmissivity data from aquifer tests in Clearwater Underground Water Conservation District (UWCD) were compiled from a variety of sources, which included Meyers (1969), Klemt and others (1975), Yelderman and others (2018), and several hydrogeologic reports prepared for Clearwater UWCD by independent consultants. Aquifer tests from Clearwater UWCD were of various lengths, with a maximum of 30 days. Central Texas GCD provided a shapefile of transmissivity data and well construction information from 72 aquifer tests compiled from various hydrogeologic reports submitted to their District. Data from the 500 pumping tests provided in the geodatabase of the NTWGAM were also utilized in this study. These tests are comprised of pumping tests from all model layers and 31 different counties. Details on the specific data sources of these tests can be found in Kelley and others (2014).

2.2 Groundwater Use

Since the late 1800s, most of the groundwater withdrawals in the study area have been primarily from the hydrogeologic units that compose the northern Trinity and Woodbine aquifer system—the Woodbine, Washita/Fredericksburg, Paluxy, Glen Rose, Hensell, Pearsall, and Hosston units. Withdrawals from these units are used for a variety of purposes, including municipal, domestic, commercial, industrial, irrigation, livestock, and other purposes.

Estimated historical pumping and discharge from flowing wells in the northern Trinity and Woodbine aquifers were obtained from the literature and calculated for the time period from 1890 through 1979. Water use survey data provided by the TWDB, in tandem with data received by the GMA 8 member GCD's were used to obtain estimated historical 1980 through 2020 pumping for the following use types: municipal, manufacturing, mining, power, irrigation, and livestock. Note that the "mining" category includes oil and gas use. Census block data were used to estimate rural domestic pumping during this same time period.

In Texas, the Edwards BFZ Aquifer is a major aquifer within the study area. It has a state-approved GAM (Jones, 2003 and 2023), and the updated northern Trinity and Woodbine Aquifers GAM was not developed to replace or revise it. However, because pumping from the Edwards BFZ Aquifer can impact hydraulic conditions in portions of the northern Trinity Aquifer, estimated pumping for the Edwards BFZ Aquifer was also developed and integrated into the pumping database for this study. In Oklahoma and Arkansas, estimated historical pumping from the northern Trinity Aquifer equivalent, the Antlers Aquifer, was based on historical data and the methodology developed for a model of the Antlers Aquifer in Oklahoma by Oliver and others (2013).

For this study, groundwater development is separated into two periods based on the reliability and availability of production estimates from each time period: predevelopment to developed conditions, from about 1890 to 1979, and post-developed conditions, from 1980 to present (2024). It should be noted that as this is an update of the existing NTGAM, pumping estimated for the predevelopment –

1979 period was carried over from the previous investigation. A brief overview of the data sources used in the original model is included in Section 2.2.1, though a more detailed description can be found in Kelley and others (2014). The combined time series of groundwater use by county is shown in Figures 2-10 through 2-16 and in Table 2-2.

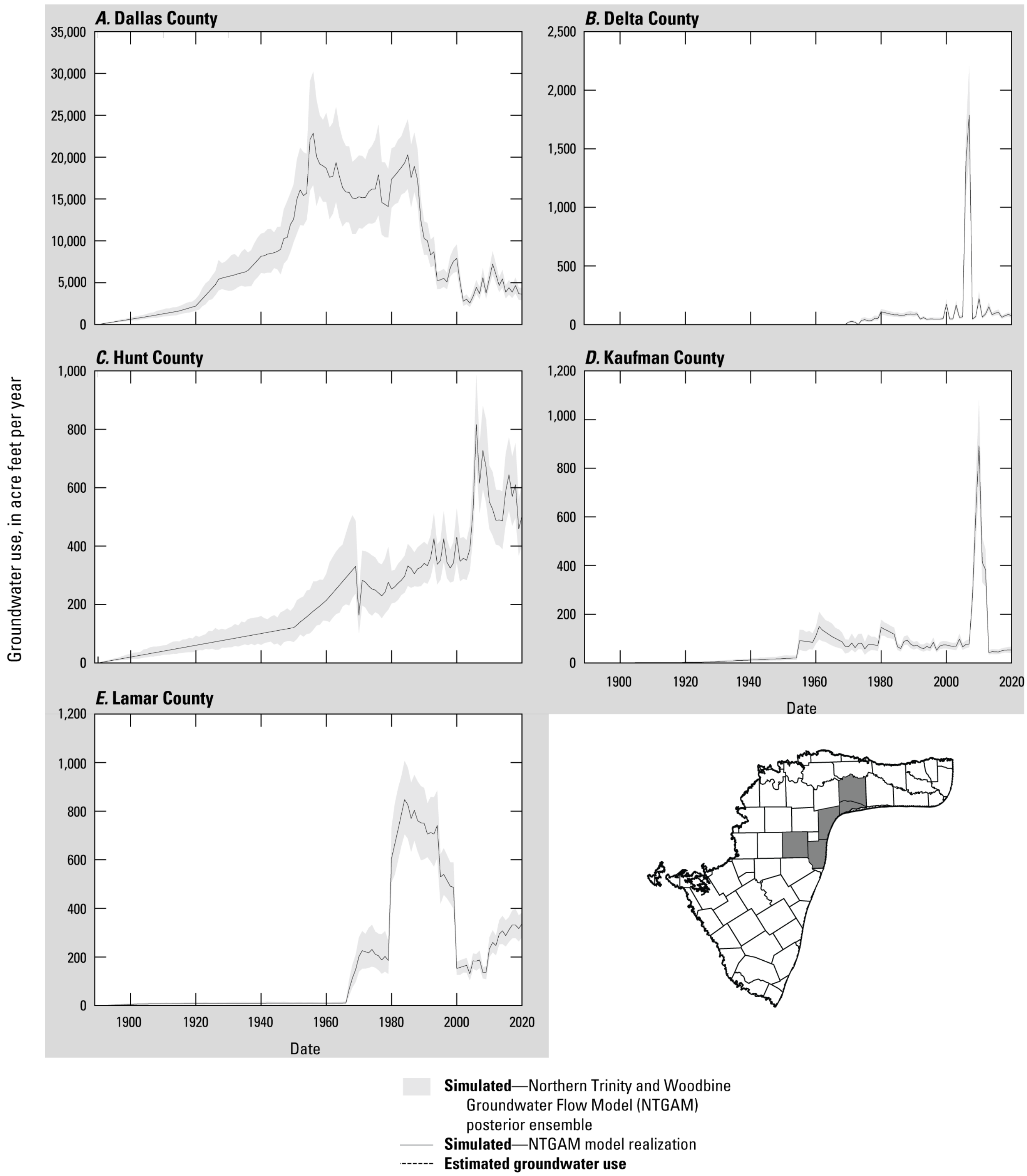

Figure 2-10. Temporal distribution of groundwater use by county for the northwestern part of the northern Trinity and Woodbine aquifer system.

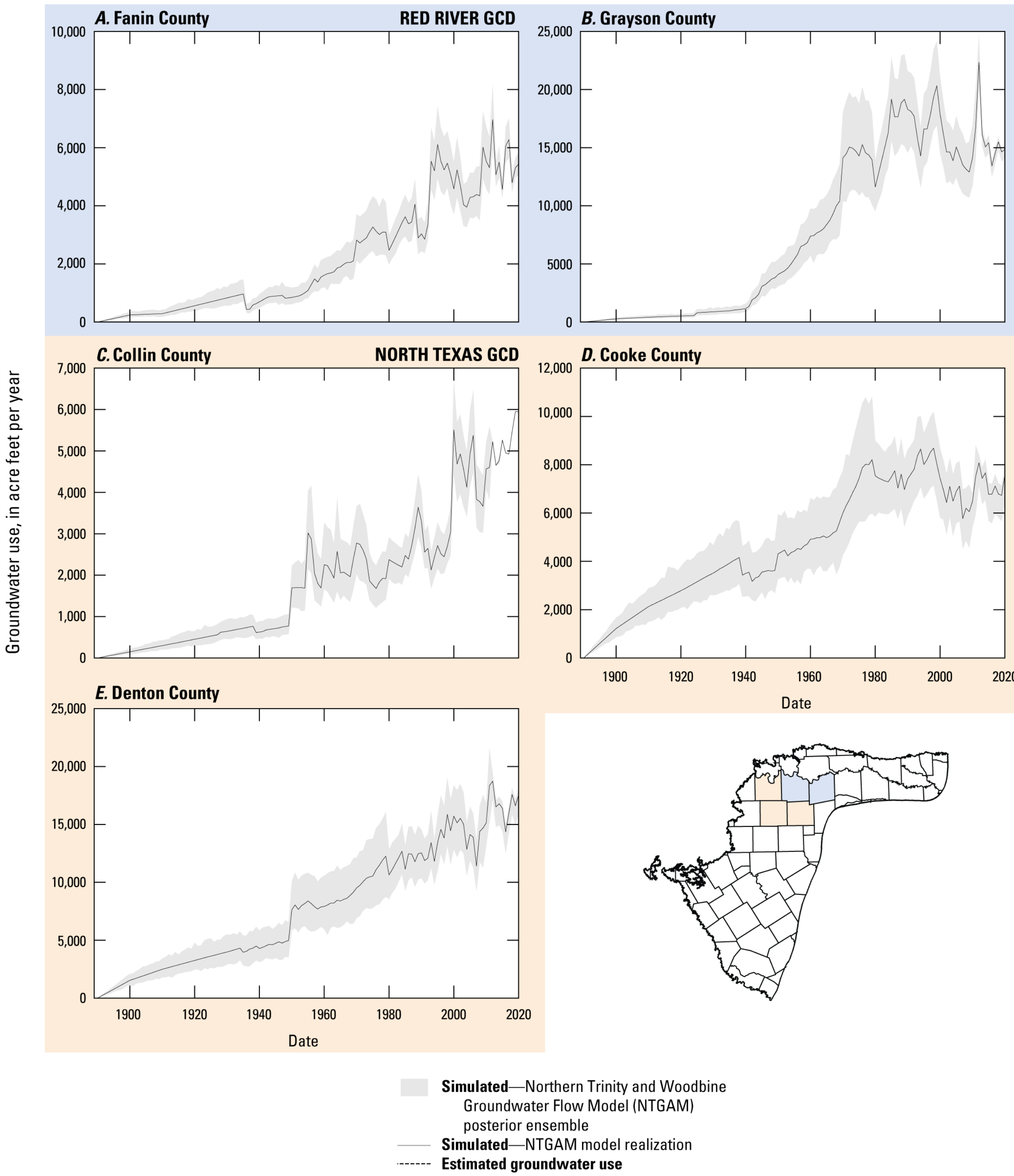

Figure 2-11. Temporal distribution of groundwater use by county for the Red River GCD and North Texas GCD.

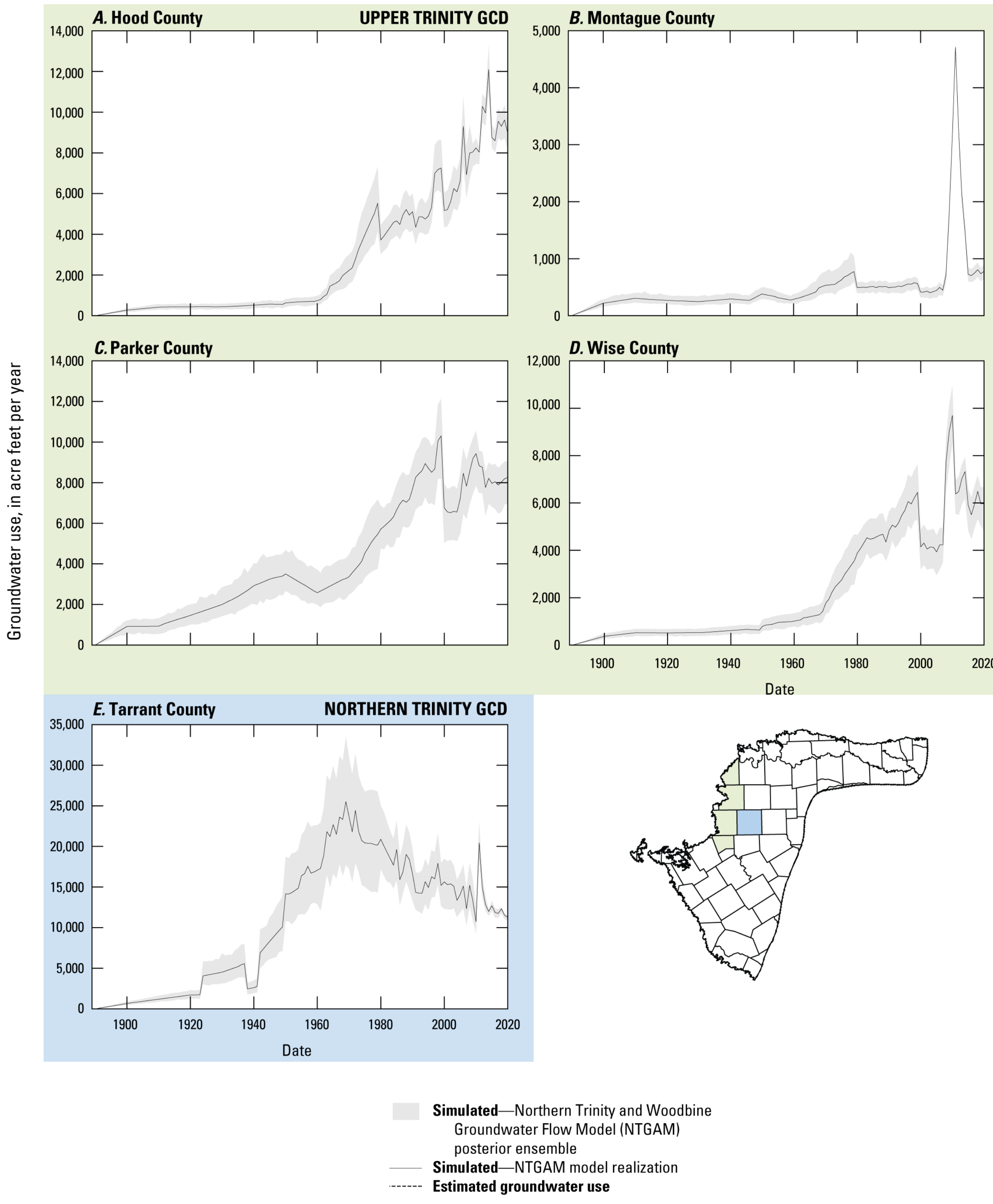

Figure 2-12. Temporal distribution of groundwater use by county for the Upper Trinity GCD and Northern Trinity GCD.

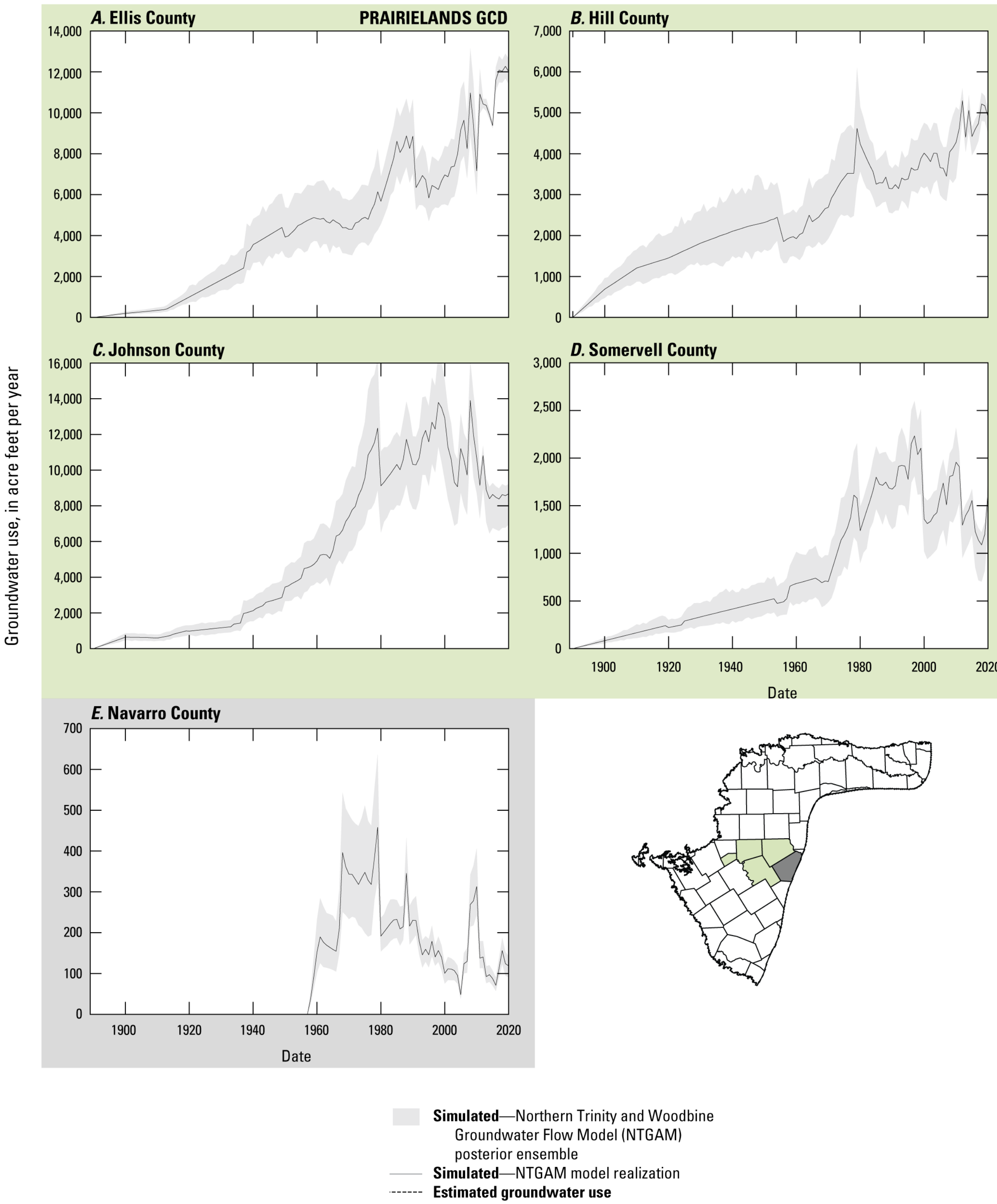

Figure 2-13. Temporal distribution of groundwater use by county for the Prairielands GCD and Navarro County.

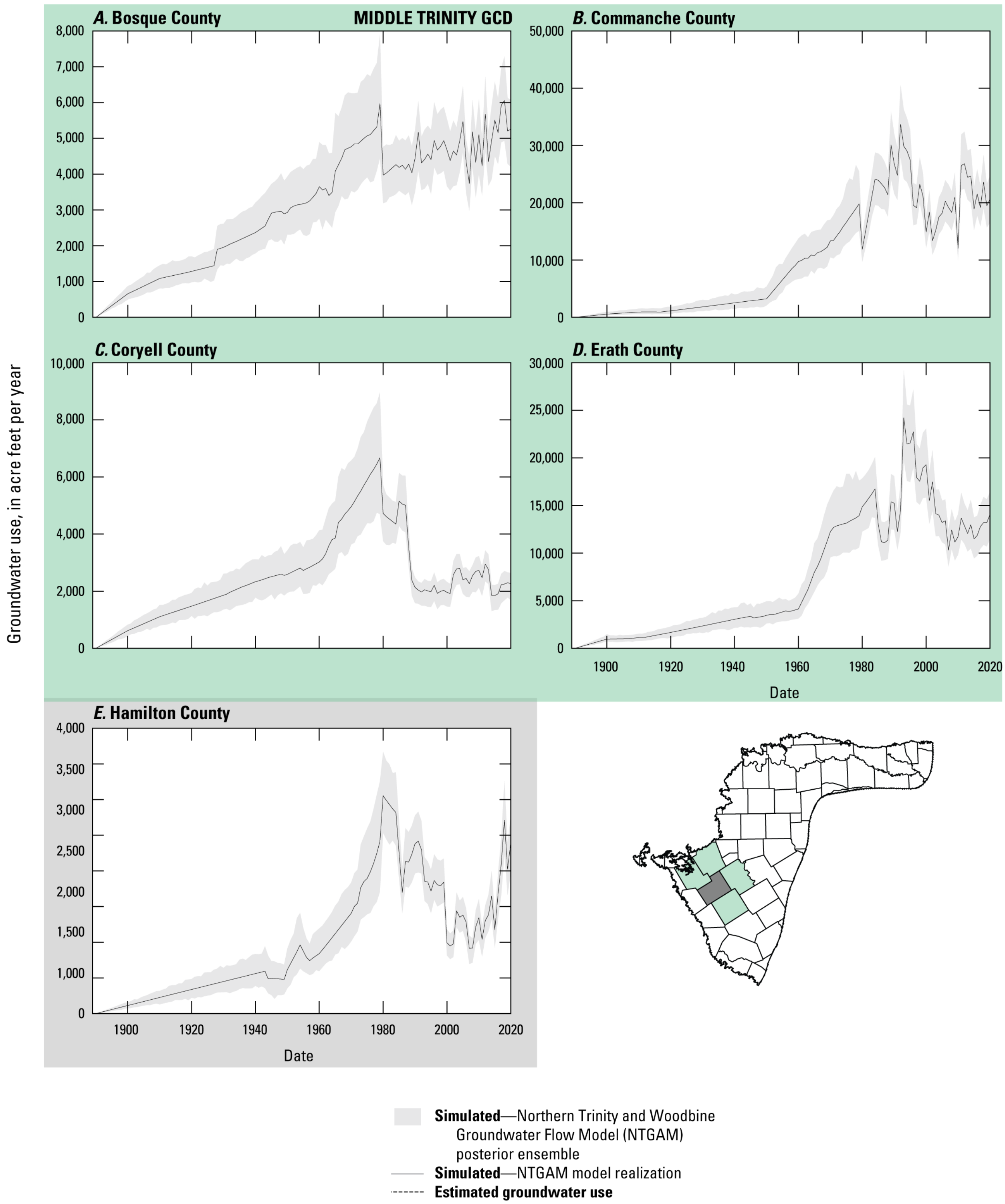

Figure 2-14. Temporal distribution of groundwater use by county for the Middle Trinity GCD and Hamilton County.

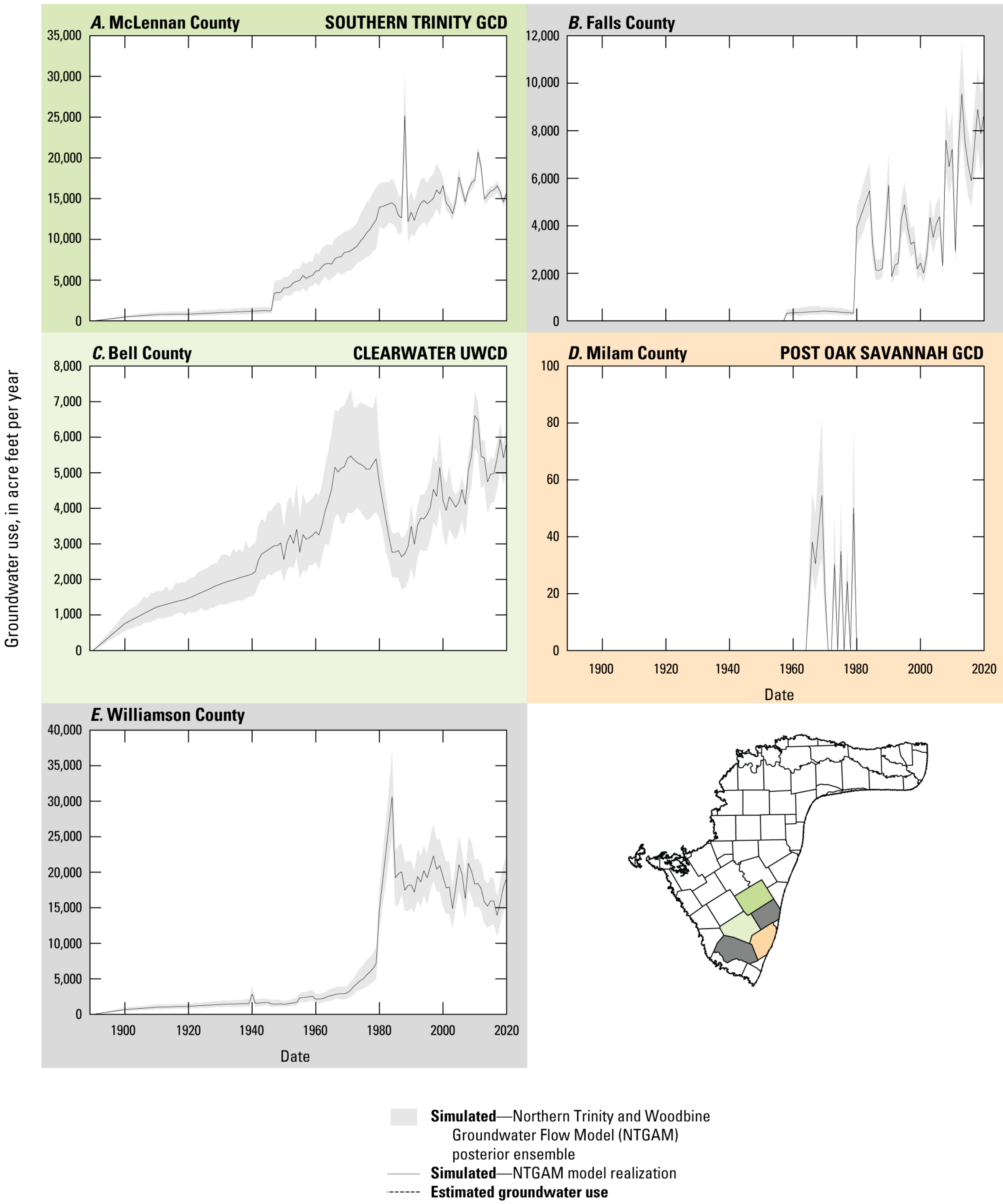

Figure 2-15. Temporal distribution of groundwater use by county for the Saratoga GCD, Clearwater UWCD, Post Oak Savannah GCD, Falls County, and Williamson County.

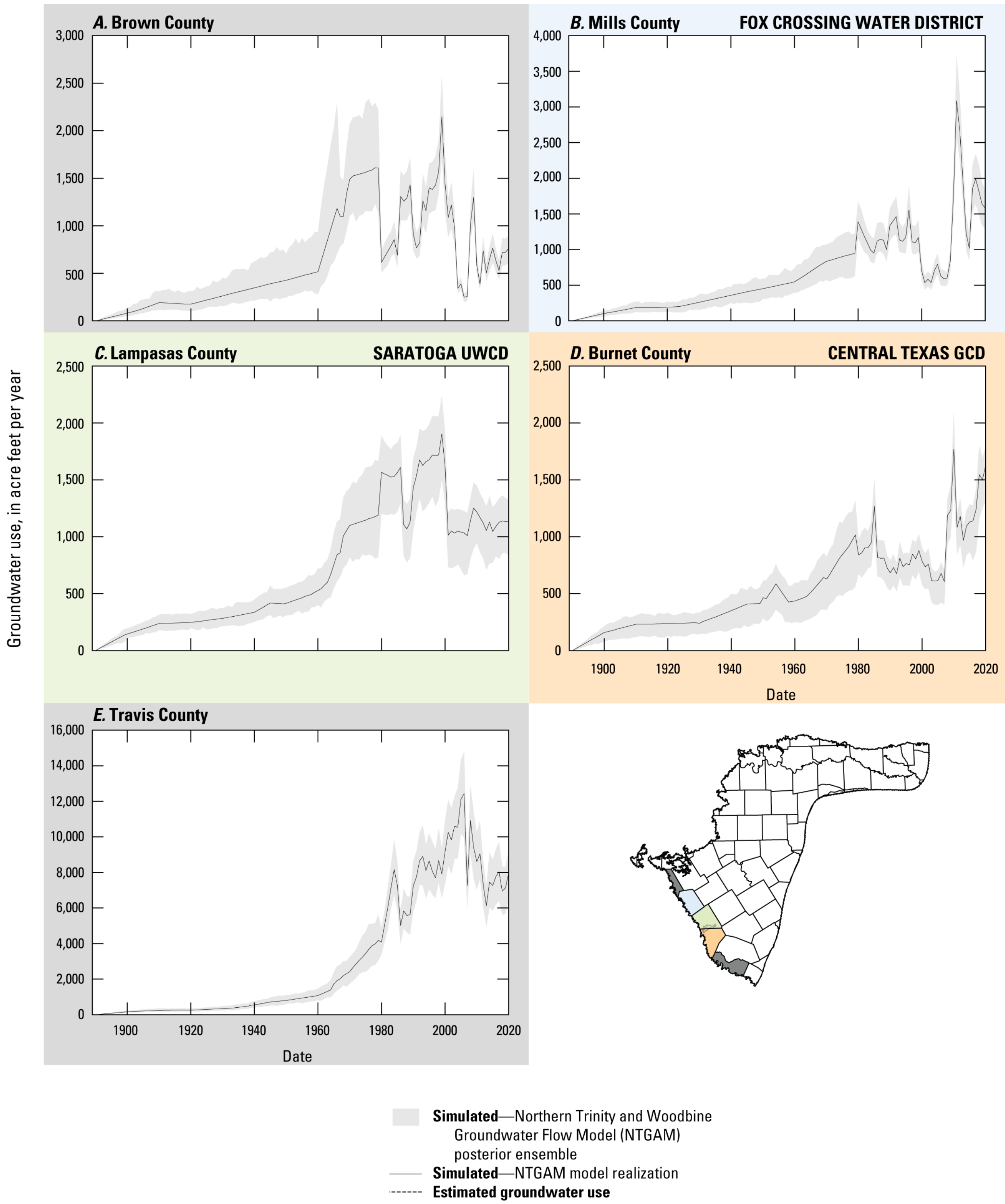

Figure 2-16. Temporal distribution of groundwater use by county for the Fox Crossing Water District, Saratoga UWCD, Central Texas GCD, Brown County, and Travis County

Table 2-2. Groundwater use by Groundwater Conservation District and county for the northern Trinity and Woodbine aquifer system.

GCD[1]	County	Groundwater use by decade (Acre-feet)[2]											
		1910	1920	1930	1940	1950	1960	1970	1980	1990	2000	2010	2020
Northwestern (figure 2-10)	Dallas	1,260	2,200	5,740	8,120	12,580	18,620	15,260	17,310	10,270	7,870	5,520	3,610
	Delta	0	0	0	0	0	0	20	110	90	170	220	80
	Hunt	40	60	80	100	120	210	160	250	340	430	550	500
	Kaufman	0	0	10	10	20	110	70	150	70	70	890	50
	Lamar	10	10	10	10	10	10	200	600	750	150	230	340
Red River (Figure 2-11)	Fannin	290	560	830	690	850	1,610	2,820	2,460	3,040	4,580	5,540	5,430
	Grayson	420	520	870	1,150	4,160	7,480	14,360	11,590	18,290	17,850	14,100	14,830
North Texas GCD (Figure 2-11)	Collin	300	450	640	630	1,700	2,250	2,780	2,370	3,300	5,490	4,570	5,930
	Cooke	2,130	2,780	3,520	3,490	4,310	4,910	6,000	7,520	7,410	7,420	6,480	7,570
	Denton	2,490	3,250	3,980	4,270	7,630	7,890	9,520	10,610	12,540	15,670	15,130	17,490
Upper Trinity GCD (Figure 2-12)	Hood	430	440	440	510	630	740	2,220	3,710	5,110	5,150	8,250	8,940
	Montague	310	270	250	290	380	290	530	490	490	410	3,140	780
	Parker	930	1,460	2,000	2,920	3,500	2,570	3,370	5,700	7,690	6,740	9,430	8,240
	Wise	520	510	520	610	790	1,010	1,770	3,880	4,830	4,130	9,700	5,960
Northern Trinity GCD (Figure 2-12)	Tarrant	1,200	1,700	4,510	2,590	14,150	17,030	23,720	20,830	16,630	15,590	10,740	11,240
Prairielands GCD (Figure 2-13)	Ellis	340	1,000	1,830	3,550	3,930	4,820	4,300	5,660	8,850	6,950	7,170	11,990
	Hill	1,210	1,450	1,810	2,100	2,320	1,920	2,690	4,230	3,150	4,010	4,280	4,890
	Johnson	590	980	1,160	2,120	3,450	4,890	7,380	9,100	10,320	12,890	10,690	8,650
	Somervell	170	220	330	420	500	680	700	1,240	1,680	1,360	1,960	1,630
Middle Trinity GCD (Figure 2-14)	Bosque	1,090	1,280	1,960	2,360	2,930	3,640	4,770	3,960	4,440	4,660	5,100	5,240
	Comanche	950	1,130	1,810	2,520	3,220	9,700	13,340	11,830	26,820	14,830	12,000	20,600
	Coryell	1,110	1,470	1,860	2,330	2,590	3,010	4,960	4,710	2,130	1,950	2,730	2,260
	Erath	1,130	1,660	2,340	3,060	3,460	4,120	12,250	14,830	15,230	19,240	11,720	14,040
Southern Trinity GCD (Figure 2-15)	Mclennan	790	820	1,010	1,170	4,050	6,090	8,460	13,910	13,340	16,540	17,250	15,690

GCD[1]	County	Groundwater use by decade (Acre-feet)[2]											
		1910	1920	1930	1940	1950	1960	1970	1980	1990	2000	2010	2020
Clearwater UWCD (Figure 2-15)	Bell	1,220	1,470	1,870	2,150	2,560	3,330	5,400	4,700	3,490	4,210	6,600	5,830
Post Oak Savannah GCD (Figure 2-15)	Milam	0	0	0	0	0	0	21	0	0	0	0	0
Fox Crossing Water District (Figure 2-16)	Mills	190	190	260	360	450	550	830	1,390	1,340	700	1,750	1,580
Saratoga UWCD (Figure 2-16)	Lampasas	240	250	280	340	420	530	1,100	1,560	1,430	1,620	1,220	1,130
Central Texas GCD (Figure 2-16)	Burnet	230	240	240	350	460	430	630	840	680	780	1,770	1,620
GCD[1]	County	Groundwater use by decade (Acre-feet)[2]											
		1910	1920	1930	1940	1950	1960	1970	1980	1990	2000	2010	2020
Other counties in the Northern Trinity and Woodbine aquifer system	Brown	190	180	260	350	430	520	1,490	610	910	1,440	580	760
	Callahan	150	140	180	370	660	810	960	1,780	1,600	1,220	1,540	1,180
	Eastland	280	410	310	370	310	330	7,880	9,960	8,520	12,050	4,790	3,250
	Falls	0	0	0	0	0	330	420	3,930	5,710	2,430	7,230	8,690
	Hamilton	230	340	450	560	620	840	1,410	3,050	2,380	990	1,340	2,400
	Jack	0	0	0	0	10	10	10	30	40	10	170	20
	Navarro	0	0	0	0	0	150	340	190	230	100	310	120
	Palo Pinto	0	0	0	0	0	0	0	0	0	0	100	30
	Red River	30	40	40	70	100	330	460	1,810	830	430	450	1,220
	Taylor	0	0	0	0	0	0	0	50	30	30	40	50
	Travis	250	250	340	540	800	1,080	2,420	4,080	7,250	9,140	8,620	7,910
	Williamson	1,000	1,120	1,400	2,840	1,420	2,110	3,060	14,670	18,230	19,300	18,340	19,060
	OK & AR[3]	3,160	3,900	4,740	5,730	6,520	7,280	7,100	8,810	7,060	8,820	10,020	4,860

[1]Groundwater Conservation District

[2]All groundwater use values are rounded to the nearest tenth

[3]Oklahoma and Arkansas groundwater use

2.2.1 Groundwater Use Sources

Sources reviewed for historical estimates of pumping between predevelopment and 1979 from the northern Trinity and Woodbine aquifers in Texas include reports by the TWDB and its predecessor agencies, the USGS, the University of Texas at Austin Bureau of Economic Geologic, and the Baylor Geological Society. The types of historical reports include regional hydrogeologic studies, studies of groundwater resources in individual counties, summaries of historical municipal water use, investigations conducted during World War II related to water supplies, and water supply investigations conducted at the request of municipalities. Also included in the sources of historical data from the literature is a report related to a groundwater model of the northern Trinity and Woodbine aquifers as part of the investigation of the Super Conducting Super Collider site (Dutton and others, 1996) and the Hill (1901) report on artesian waters in the Black and Grande prairies of Texas.

Pumpage for the period from 1980 to the end of the model's history matching period (2020) is comprised of a combination of TWDB Water Use Survey estimates, reported pumping from GCDs, and census-based estimates of rural domestic usage. INTERA received reported production values from eight GCDs: Central Texas GCD, Clearwater Underwater Conservation District, North Texas GCD, Northern Trinity GCD, Prairielands GCD, Red River GCD, Southern Trinity GCD, and Upper Trinity GCD. Data received included individual well construction data, permitting info, and production data by year (or 6-month period). INTERA supplemented relevant missing information using the TWDB's GWDB when possible. Production from 2000-2009 was sourced from the datasets sent to INTERA during the development of the NTGAM in 2012-2014. Any production data received for this study was used in lieu of production data supplied to INTERA during the last NTGAM update, except for 2010. The total 2010 volumes for production data received during the development of the NTGAM do not always match the 2010 volumes received in any county for any GCD. Thus, for 2010, the rates from the dataset with higher total production for each county were used.

INTERA used the TWDB Water Use Survey (WUS) (TWDB, 2024) in combination with the GCD estimates. For the years 1980 and 1984-2020, WUS data were obtained for each county within the active model area. Estimates for the years 1981-1983 were interpolated linearly for each use type/county/aquifer combination. Pumping estimates for the following aquifers were considered when distributing pumping: "TRINITY AQUIFER," "BRAZOS RIVER ALLUVIUM AQUIFER," "WOODBINE AQUIFER," "EDWARDS-BFZ AQUIFER," "UNKNOWN," and "OTHER AQUIFER." Pumping listed as "OTHER AQUIFER" was conditionally considered to be an estimate for the Trinty Aquifer when deemed appropriate based on the other major and minor aquifers in the county. Pumping assigned to an "UNKNOWN" aquifer was assigned to all other listed aquifers for each county and year in proportion to the amount already estimated. Any county that did not have significant Trinity production in the NTWGAM was not assigned TWBD pumping in this update. For the years 2000-2020, the data downloaded from the TWDB is more detailed, as it is listed by entity. The specific entity was not considered when distributing pumping, except for "Municipal" pumping with a listed Entity of "NON-SURVEYED ESTIMATE." Estimated volumes for this type are the TWDB's estimate for rural domestic use. These totals were removed from the dataset, as INTERA calculated rural domestic pumping separately.

Rural and domestic pumping estimates for this study (1980-2020) were derived from U.S. Census Bureau population data at the block and county levels. Block-level data, offering the finest resolution, were available for the 1990, 2000, 2010, and 2020 census years. For interim years, county-level annual population estimates were downscaled to block-level resolution using linearly interpolated spatial distributions based on the decadal block data. In areas where the study region partially overlapped a county, the block-level data were used to calculate a representative proportion of the county population. These proportions were also linearly interpolated for interim years. The 1990 block distribution was assumed for years before 1990, and the 2020 distribution was applied to years after 2020. Census tracts, representing an intermediate resolution between blocks and counties, were not used in this analysis. These spatial distributions, combined with annual county-level population estimates, provided refined temporal and spatial population inputs for the model. These population estimates were then converted into groundwater use volumes using an average gallons-per-capita use rate. This process is explained in greater detail in Section 3.4.4.

Pumping estimates from outside of Texas were sourced differently depending on the state and were only updated after the 2010 stress periods. Pumping estimated for Oklahoma was received by INTERA from the Oklahoma Water Resources Board (OWRB, 2023) as production volumes associated with specific permits on specific parcels of land. Production for cells in Arkansas was estimated using a modified version of the method from (Oliver and others, 2013), which utilizes census data (US Census Bureau, 2010 and 2020) and an average gallons per day per capita (GPCD). The population of each Arkansas county in the model area was obtained from the 2010 and 2020 censuses and linearly interpolated for the years 2011-2019. Starting with the total pumping in the existing model in the 2010 stress period, the volumetric estimates for each grid cell in these counties was scaled proportionally to the total population of the county.

2.2.2 Groundwater Usage Trends (Predevelopment–1950)

The development of groundwater resources in the northern Trinity and Woodbine aquifer system began in the late 19th and early 20th centuries. In the late 1800s, settlers in north-central Texas, particularly in Tarrant County, initially relied on shallow wells tapping into surface water and alluvial deposits (Leggat, 1957). Flowing wells (where the potentiometric surface is above land surface) were common in much of the study area and led to substantial development of groundwater resources.

Among the first artesian flowing wells in the Trinity aquifer was discovered in Fort Worth in 1882, and a significant number of wells were installed subsequently, as pressure was sufficient for these wells to flow continuously (Hill, 1901; Dutton and others, 1996). In McLennan County, the first artesian (flowing) well was drilled in 1886 into the Glen Rose Formation in Waco, Texas (Hill, 1901; Adkins, 1923; Dutton and others, 1996). In the City of Sherman in Grayson County, the first well was drilled in 1889 in the Paluxy Aquifer (Livingston, 1945). In 1890, the City of Fort Worth drilled a successful test well below the Paluxy Aquifer and had 13 wells drilled into the Travis Peak Formation two years later (Leggat, 1957). Five years later, there were between 150 to 160 wells in the Fort Worth area and likely many others in Tarrant County (Hill, 1901). In 1904, the City of Waco purchased the first wells drilled in the Travis Peak Formation and used 11 artesian (flowing) wells (Livingston and Bennett (1942). A year later, the City of Fort Worth drilled a second wellfield in the Travis Peak Formation.

Hill (1901) documented the number of wells present in the northern Trinity and Woodbine aquifer system in 1900. Greater than 150 wells produced water from the Woodbine Aquifer, including 43 in

Dallas County (also noted in Schuler [1918]), more than 33 in Ellis County, and 25 in Grayson County (Bené, 2004). There were also more than 160 wells producing from the Paluxy aquifer, including 46 in Tarrant County, 45 in Denton County, and 37 in Cooke County. In the Trinity Aquifer, there were listed more than 600 wells as follows: nearly 300 in Somervell County, 67 in Bosque County, and more than 20 wells in Bell, Coryell, Erath, Hamilton, Hood, McLennan, Parker, and Williamson Counties.

Common practice by early well owners was to allow water to freely discharge from flowing wells, resulting in large amounts of groundwater loss and reduction in hydraulic heads in the northern Trinity and Woodbine aquifer system. Hill (1901) and Sundstrom and others (1947) estimated total discharge from the northern Trinity Aquifer in 1900 through flowing wells in Waco of 10,500 and 11,200 AFY, respectively. Additionally, expanding urban populations and agricultural industries increased groundwater extraction significantly from both the Trinity and Woodbine aquifers, resulting in the loss of artesian pressure and conversion to surface water in some areas. However, in other areas, pumps were installed, and groundwater development continued. All counties experienced increased groundwater usage, with some, such as Tarrant and Dallas counties, experiencing annual groundwater usage increases of over 40% each year until 1950.

Between 1900 and the early 1950s, groundwater use rapidly increased across the northern Trinity and Woodbine aquifer systems. Across the aquifer system, average annual water usage by county increased by 12.5%. Total average groundwater usage increased from approximately 14,000 AFY to over 85,000 acre-ft per year. Although the City of Fort Worth had abandoned its well field by 1914 and converted to surface water supplies, commerce and industrial uses rapidly expanded, particularly after 1941 (Figure 2-12).

By 1950, the average county in the region had a groundwater usage of 2,135 acre-ft per year, with a maximum of approximately 14,000 acre-ft used by Tarrant County. The largest increases in groundwater usage over that period were in the high-demand counties of Dallas and Tarrant, with both increasing their annual usage by more than 10,000 acre-ft by 1950.

2.2.3 Groundwater Usage Trends (1950–Present)

The northern Trinity and Woodbine aquifers experienced significant trends in groundwater use from 1950 onward, largely driven by agricultural demands and urban expansion. In the early decades, particularly from 1950 to the 1970s, groundwater extraction steadily increased as agricultural activities expanded and urban areas expanded.

Overall, groundwater usage of the Trinity aquifer system increased as development continued up to the present. Annual usage increased from 85,000 AFY in 1950 to 230,000 AFY in 2020. In 2020, the average county used 5,700 acre-ft per year, and the maximum usage was over 20,000 acre-ft used in Commanche County. By the 1980s, awareness of the potential for aquifer depletion led to increased regulatory oversight. The creation of GCDs in Texas, under the authority of the Texas Legislature, began to moderate the rate of groundwater extraction through various management strategies, including permitting and usage caps.

Average groundwater use growth generally slowed by the 1980s in the northern part of the aquifer system, although some areas continued to experience increases in use (Figures 2-10 to 2-12). One notable exception in this pattern was the 2011-2012 drought, which saw the highest groundwater usage year, with maximum groundwater use occurring in 2012 in some areas.

Broadly, the counties in the study area fall under two categories: those that have increased groundwater production on average each year since 1900 and those that peaked in the 1970-1990 period and have declined since then. 17 of 40 counties have decreased pumping since 1990, with the remainder either increasing or sustaining similar amount of use. Generally, these counties are located near Fort Worth or are located along the western section of the aquifer and the majority of them use between 5,000 and 15,000 AFY in 2020.

All but three counties have generally continued to increase groundwater usage since 1950, with only Coryell, Dallas, and Tarrant showing decreased usage by 2020. These counties undertook the construction of large reservoirs in the 1950s-1970s: Cedar Creek Reservoir in Tarrant County, Lake Ray Hubbard in Dallas County, and Belton Lake in Coryell, amongst others. These improved surface water supplies drove much of the reduction in usage of groundwater from 1970 on, varying by county. These three counties have reduced their annual groundwater usage by as much as 75% in the case of Dallas, with the other two reducing their annual use by closer to 20%.

The total groundwater usage from the Woodbine and Trinity aquifers was approximately 230,000 acre-ft in 1990, and 230,000 acre-ft in 2020. The general trend was for counties without improvements in surface water supplies to continue to increase groundwater usage, while those counties that undertook construction and development of additional surface water resources saw declines in this period.

2.3 Groundwater-Level Measurements

Groundwater levels in the study area have been measured by the TWDB (or predecessor agencies), USGS, and other entities periodically since the early 1900s and more frequently since the 1960s. For the purposes of this report, the term "groundwater level" is synonymous with a groundwater elevation measured in ft above a vertical datum (North American Vertical Datum of 1988) and applies to wells screened in either (1) an unconfined aquifer, where the upper water surface (water table) is at atmospheric pressure, or (2) a confined aquifer, where fine-grained units above (and below) the aquifer result in pressurized conditions so that the groundwater level in a well penetrating the aquifer will rise above the top of the aquifer.

Note that the water levels are presented as a depth below land surface in Section 2.3.3 to show the large early time decreases in the northern Trinity and Woodbine aquifer system. The presentation of these groundwater levels as a depth below land surface precludes direct comparisons of measurements between hydrographs. However, a discussion of the overall pattern of water level changes is the primary purpose for the inclusion of the hydrographs in this section. Through the assimilation of groups of hydrographs for each region of the aquifer, the reader gains a generalized understanding of the stress history of the aquifer system.

Figures 2-17 to 2-42 show selected hydrographs based on several criteria. First, a review of all hydrographs was conducted in order to select those that show early water-level declines (Figures 2-17 to 2-22) or a long-term record of data generally spanning at least 40 years with at least five groundwater-level measurements (Figures 2-22 to 2-42). Second, hydrographs were selected based on spatial location in an effort to show a variety of groundwater conditions across the study area in each of the hydrogeologic units. Third, the hydrographs selected generally contain the greatest number of water level measurements across the longest time interval in the study area to best define hydraulic head trends. In the discussions below, the hydrograph for specific wells mentioned in the text is shown in the cited figures. The following sections describe the study area groundwater levels from predevelopment through 2020 using these hydrographs and information obtained from numerous historical reports and databases.

2.3.1 Data Sources

In Texas, groundwater level data for the study area were obtained from historical groundwater reports, the TWDB groundwater database, and GCD data. In Oklahoma, data were obtained from the Oklahoma Water Resources Board online database as well as the USGS NWIS database (USGS, 2023a). In Arkansas, data were obtained from the USGS NWIS database (USGS, 2023a).

Water-level measurements given in historical reports published by the TWDB and predecessor agencies were collected and digitized for selected counties in the Texas portion of the study area. The reports reviewed were those whose data had not already been entered into the TWDB groundwater database, which is an electronic database maintained by the TWDB containing well, water-level, and water quality data for selected wells in the State (TWDB, 2023). The criteria used to select water-level data from historical reports were measurements made prior to 1950 for counties with few measurements during that time from other sources. Historical water-level measurements were digitized from Fielder (1934), Leggat (1957), Rayner (1959), Baker (1960), and Taylor (1976). Additionally, well screens and total depth were digitized from these reports and the TWDB groundwater database.

2.3.2 Modern Data Sources and Aquifer Assignments

The TWDB GWDB (TWDB, 2023) was queried to obtain water-level data for the counties in the study area. An effort was made to collect all available water-level data and evaluate those data for use in the updated NTGAM. The data were evaluated and selected based on the following criteria: (1) water-level measurements in the GWDB with a “Publishable” flag were generally used, (2) water levels from wells without a reported total depth were not used, and (3) when identified, anomalous data for a well were not used based an analysis of water level data from each well.

The water-level data obtained from the GWDB ranges in date from 1902 through 2020, and the majority of observations have measurement dates after 1950. This database is the most significant source of water-level data available. The GWDB contains coordinates for each well. Therefore, the well locations from these data were considered to have a high degree of certainty, with the understanding that older wells may be based on public land surveys that determined well locations accurate only to a quarter section.

Water-level data was received from several of the GCDs in the study area to supplement data from the GWDB. Only observations from wells with associated TWDB State Well Numbers were retained in the history-matching dataset. Data for dates ranging from 2008 to 2023 were obtained from the Central Texas GCD, from 1950 to 2023 from the Clearwater UWCD, from 2017 to 2020 from the Northern Trinity GCD, from 2014 to 2020 from the Prairielands GCD, from 1926 to 2023 from the Southern Trinity GCD, and from 1945 to 2023 from the Upper Trinity GCD. Wells from the GWDB were often duplicates of those from the composite GCD databases. As a result, the combined final datasets contained duplicate wells with different sets of water level measurements. Water levels that were duplicated (measured on the same day, month, and year) between multiple sources were removed, with preference given to the GWDB measurements if there was a discrepancy. A total of 387 wells had the same water level measurement(s) in two or more datasets. Water level data from Oklahoma were obtained from the Oklahoma Water Resources Board online database as well as the USGS NWIS database (USGS, 2023a) and ranged from 1956 through 2020.

The method of measurement of water-level observations was also considered. Observations that were measured using an airline, a measurement procedure that involves using the pressure in a downhole tube to estimate the water level in a well, were considered to be less certain than observations measured using other methods. These other methods of water level measurements include steel tape, pressure transducers, and sonic devices.

Using completion data from the TWDB (or provided by the GCDs), the aquifers or formations across which the wells were completed was estimated by comparing the completion interval to the structure data. Completion information consists of the depth to the top and bottom of each screen in the well. The number of screens in a well varies from one to as many as twenty, and the majority of the wells have one or two screened intervals. 1,403 out of the 2,286 wells with water level observations (61%) had completion information supplied either by the TWDB or a GCD. The remaining wells had only total depth.

Water level observations were assigned to model layers based on either the associated screened intervals or total depth for the well (when screened interval data was absent). Water level observations from wells without a listed total depth were removed from the history-matching dataset. Aquifer assignments for water levels were predicated on the percentage of screened thickness in each model layer. Therefore, many of the water-level observations were associated with multiple model layers. If a well's screen was completely beneath the bottom of model layer eight or entirely within model layer 1, the well was removed from the history matching dataset. Wells assigned to multiple aquifers, and the impacts of these multi-layer assignments to calibration, are discussed in Section 3.5.1.1.

If screened interval data was not available, the total depth was used to estimate the screened intervals of the wells. If the total depth was not available or listed as zero and the well did not have any associated screened intervals, the well and its observations were removed from the history matching dataset. Any well with a total depth that did not extend below the bottom of model layer 1, whether it be an outcrop or not, was assigned to model layer 1. If the well was designated as being a public water supply (PWS) well and completed below model layer 1, the well was assigned to all existing model layers above and in which the total depth was completed. If the well was not a PWS well and the total depth was completed below the bottom of model layer 1, the well was assigned to a single layer 50 ft above the total depth and was marked as "uncertain." Non-PWS wells with a total depth of less than 70 ft were assigned to the layer in which the well was completed.

2.3.3 Water-Level Trends (Predevelopment–1950)

From the early 1900s until about 1930, periodic measurements of groundwater levels were documented in the northern Trinity and Woodbine aquifer system. Hill (1901) surveyed early data on water levels in a wide area of the aquifer system and compiled the measurements. Groundwater-level data became somewhat more available in the 1930s as various entities began to investigate the rapid development of groundwater resources and associated sizeable water level declines. Selected groundwater levels from these surveys and the locations of each well are presented in Figures 2-17 to 2-21 and in Table 2-3. Although the hydrographs in these figures represent groundwater levels for a relatively small number of wells, they are representative of the larger trends in each area where the hydrographs are shown.

Table 2-3. Early wells with long-term groundwater-level measurements in the northern Trinity and Woodbine aquifer system.

Groundwater-well groups	TWDB state well number	Map ID (figs. 2-17 to 2-21)	County	Hydrogeologic unit (Figure 2-3)	Period of record (may contain gaps) (M/Y)[1]		Well depth, in feet below land surface[2]
					Begin	End	
Tarrant County north (figure 2-17)	3214402	A	Tarrant	Hosston	1/1924	3/1954	1,060
	3214401	B	Tarrant	Hosston	1/1912	3/1958	1,053
	3214404	C	Tarrant	Pearsall and Hosston	1/1921	12/1953	1,060
	3214405	D	Tarrant	Pearsall and Hosston	12/1921	11/1954	1,055
	3214606	E	Tarrant	Paluxy	5/1943	4/1984	482
	3214704	F	Tarrant	Hensell	1/1902	2/1954	728
	3214722	G	Tarrant	Pearsall and Hosston	1/1911	6/1944	938
Tarrant County south (figure 2-18)	3213902	H	Tarrant	Pearsall and Hosston	5/1946	1/1958	834
	3214701	I	Tarrant	Pearsall and Hosston	1/1912	8/1954	964
	3214802	J	Tarrant	Pearsall	4/1942	2/1957	1,000
	3222205	K	Tarrant	Hosston	1/1932	2/1955	1,095
	3222204	L	Tarrant	Hosston	1/1937	5/1954	1,080
	3223103	N	Tarrant	Pearsall and Hosston	1/1914	8/1969	1,432
	3222401	O	Tarrant	Pearsall	1/1917	5/1964	1,083
Northern Model Area (figure 2-19)	1817902	A	Grayson	Hensell and Pearsall	1/1935	9/1977	1,518
	1829301	B	Grayson	Woodbine	1/1936	2/2022	709
	1830102	C	Fannin	Woodbine	1/1936	3/1982	528
	1725301	D	Fannin	Woodbine and Washita	1/1921	5/1947	1,673
	1829901	E	Grayson	Woodbine	1/1938	3/2023	1,160
	1845603	F	Collin	Woodbine	1/1939	11/1977	1,853
Central Texas area (figure 2-20)	3250202	A	Somervell	Hosston	11/1929	1/1997	297
	3250308	B	Somervell	Glen Rose	1/1929	5/1962	140
	3243703	C	Somervell	Middle-Lower Trinity	1/1904	2/1989	374
	3260701	D	Bosque	Hensell	2/1943	3/1984	675
	3255902	E	Hill	Hosston	1/1939	3/1977	1,835

Groundwater-well groups	TWDB state well number	Map ID (figs. 2-17 to 2-21)	County	Hydrogeologic unit (Figure 2-3)	Period of record (may contain gaps) (M/Y)[1]		Well depth, in feet below land surface[2]
					Begin	End	
	3263910	F	Hill	Paluxy and Glen Rose	11/1941	3/1979	845
	3357601	G	Hill	Woodbine	8/1930	3/1980	832
	3359302	H	Navarro	Woodbine	9/1917	11/1976	1,721
Southern Model Area (figure 2-21)	4035401	A	Coryell	Middle-Lower Trinity	1/1951	7/1964	680
	4031102	B	McLennan	Middle-Lower Trinity	9/1942	3/1985	1,540
	4016401	C	McLennan	Glen Rose and Hensell	2/1932	9/1970	2,010
	4056301	D	Falls	Pearsall and Hosston	1/1940	3/1977	3,300
	4061104	E	Bell	Middle-Lower Trinity	1/1942	11/1969	1,186
	5829602	F	Williamson	Pearsall and Hosston	1/1934	3/1976	3,308

[1]Well end dates are current as of December 2024.

[2]The hydrogeologic unit assigned to each well is based on the well screened interval (reported or estimated); therefore, the well depth is listed to provide general information on well construction.

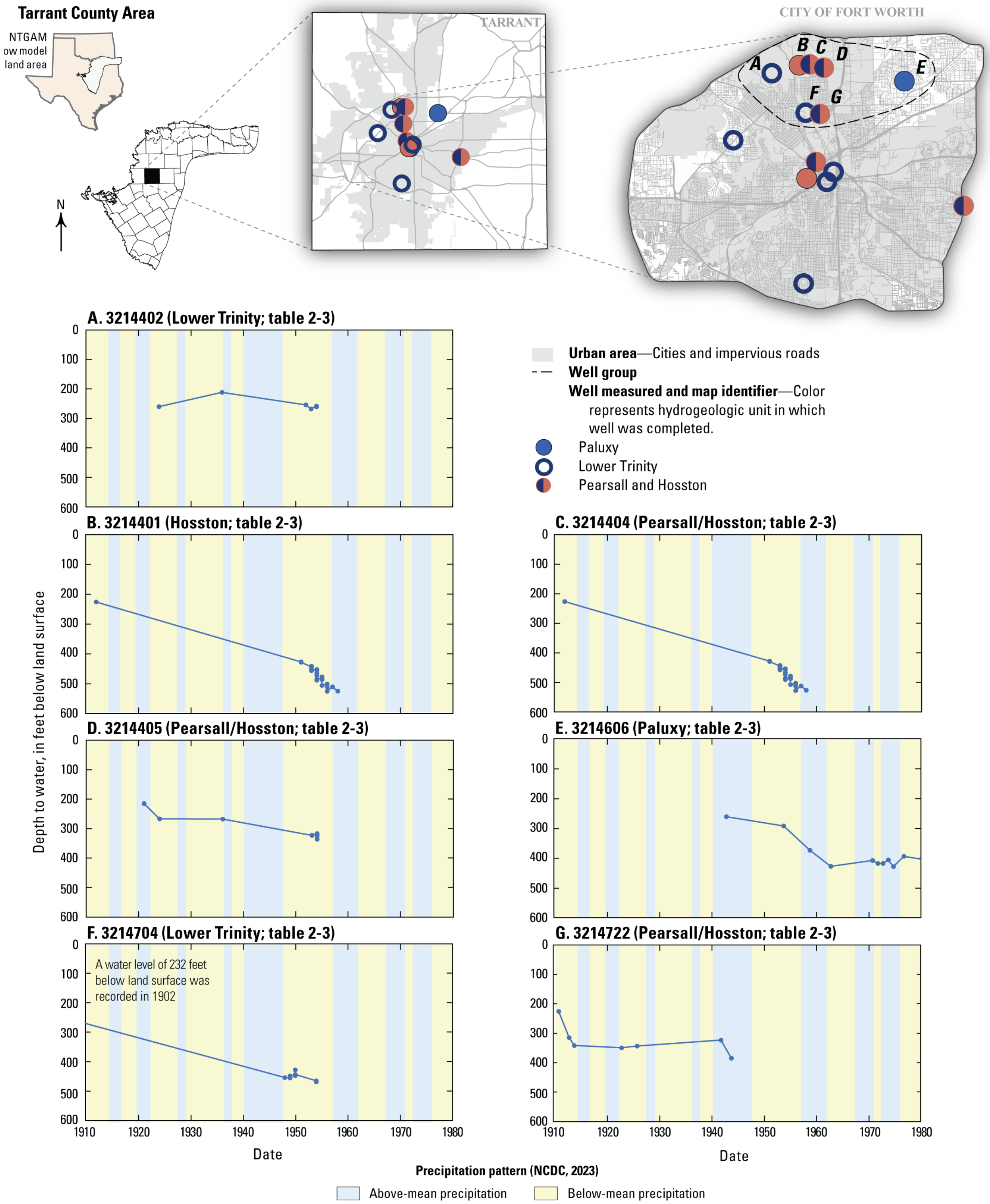

Figure 2-17. Locations and hydrographs of groundwater levels for selected wells in the northern part of the City of Fort Worth in Tarrant County from 1910 to 1980.

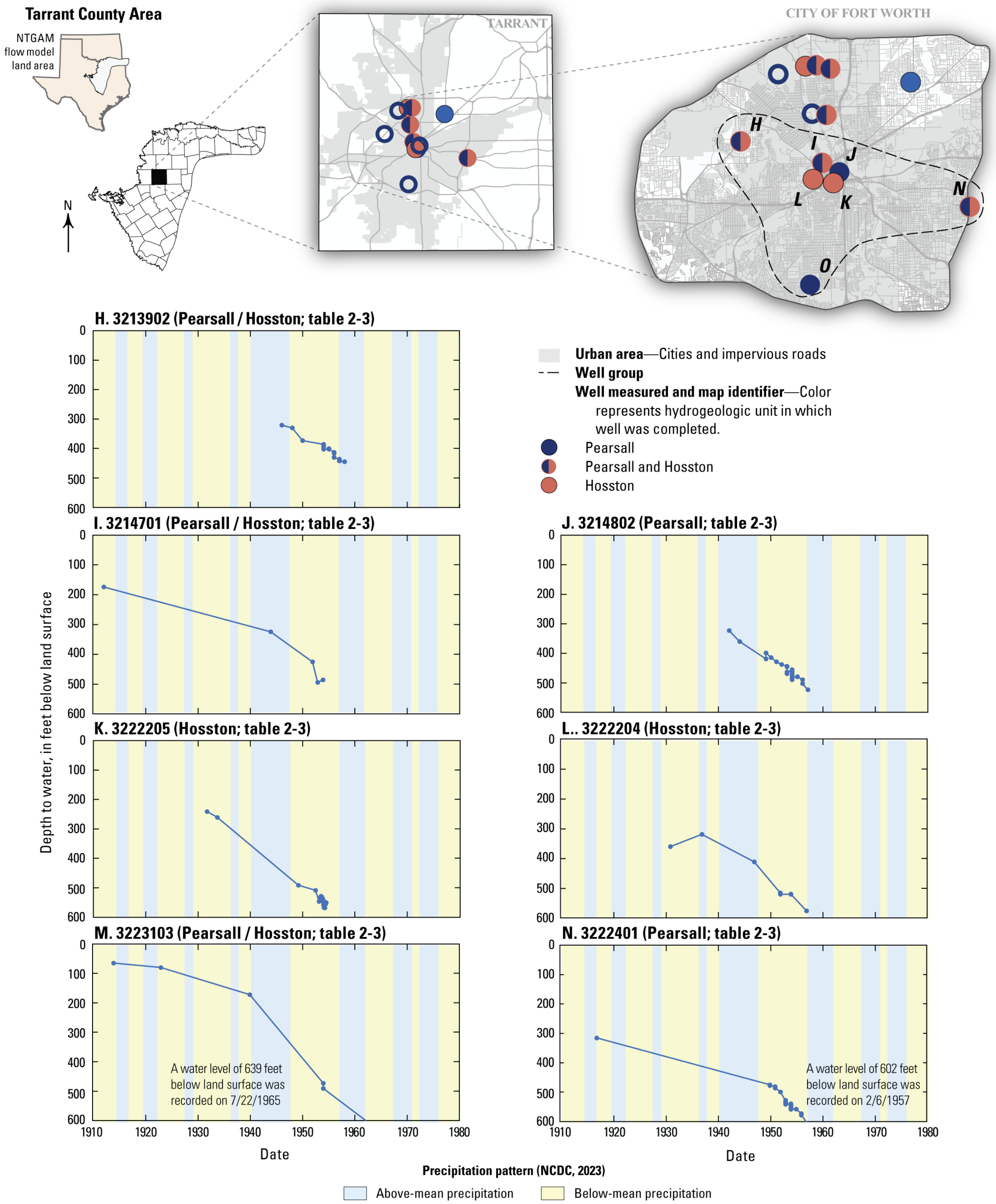

Figure 2-18. Locations and hydrographs of groundwater levels for selected wells in the southern part of the City of Fort Worth in Tarrant County from 1910 to 1980.

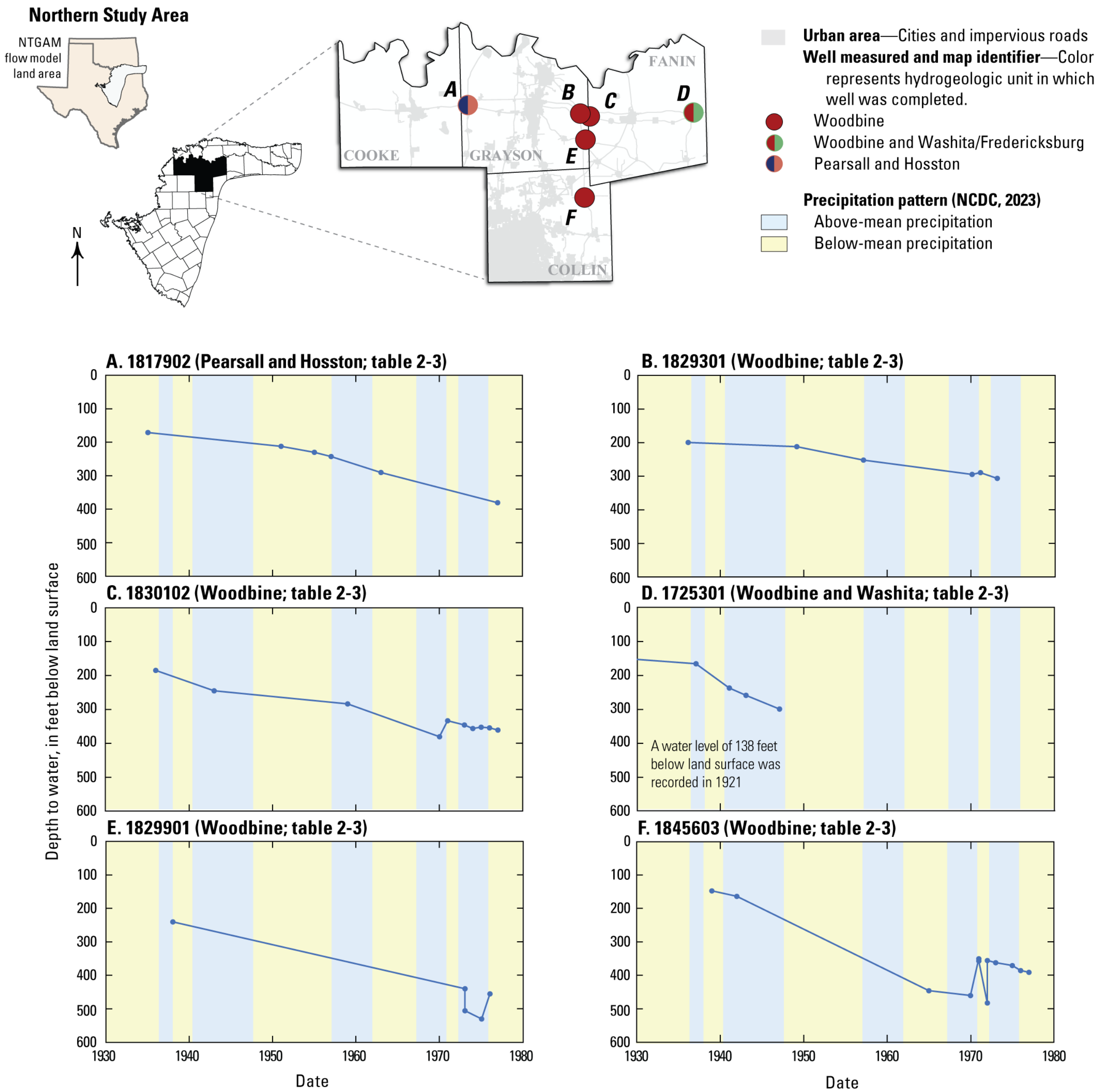

Figure 2-19. Locations and hydrographs of groundwater levels for selected wells in Collin, Cooke, Fanin, and Grayson Counties from 1930 to 1980.

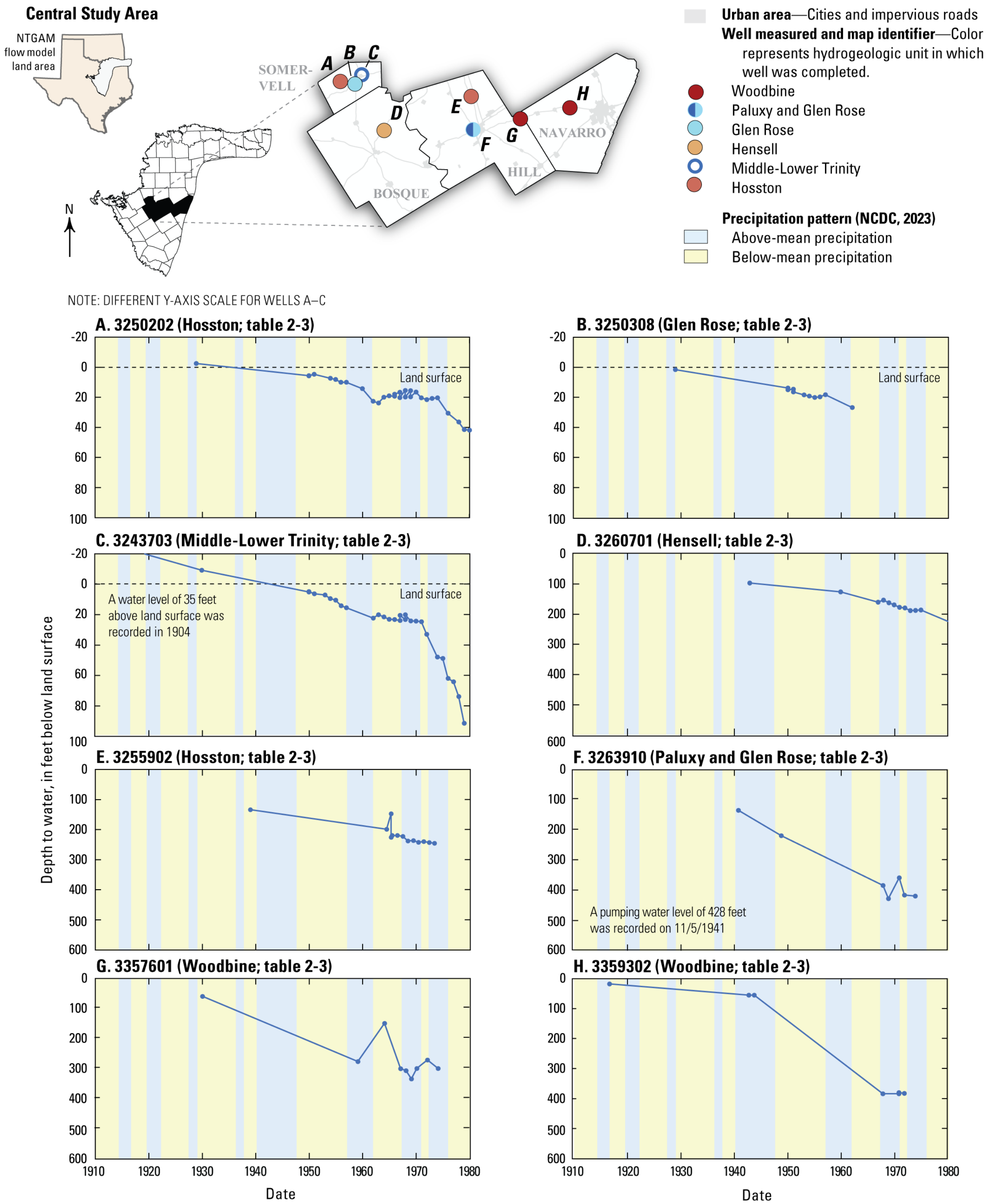

Figure 2-20. Locations and hydrographs of groundwater levels for selected wells in Bosque, Hill, Navarro, and Somervell Counties from 1910 to 1980.

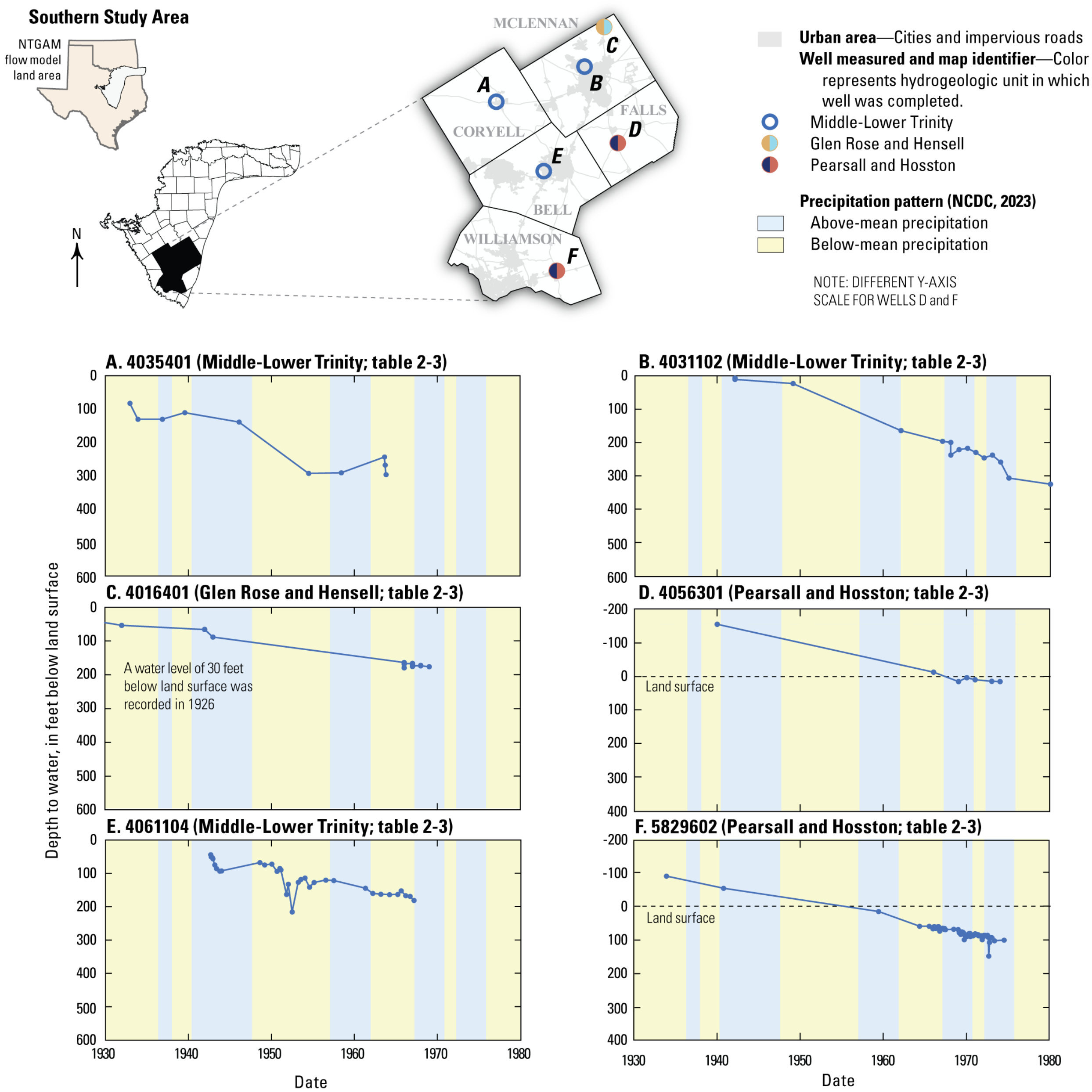

Figure 2-21. Locations and hydrographs of groundwater levels for selected wells in Bell, Coryell, Falls, McLennan, and Williamson Counties from 1930 to 1980.

2.3.3.1 Loss of Artesian Pressure

The artesian pressure during the late 1800s was substantial in the northern Trinity and Woodbine aquifer system. A Trinity aquifer well drilled in 1890 in Fort Worth had a reported water level of 90 to 100 ft above land surface (Mace, 1994). In other areas, artesian conditions were also present, whereby flowing wells were discharged at rates between 1 and 694 gallons per minute (Hill, 1901). In McLennan County, the artesian pressure in the first flowing well drilled in 1886 in Waco, Texas in the Glen Rose Formation was estimated to be as much as 184 ft above the land surface in 1912 (Livingston and Bennett, 1942). By 1891, there were 11 flowing wells, and by 1897, there were a total of 27 flowing wells in McLennan County. These wells lead to the nickname of “Geyser City” for the City of Waco, located in this county. In Somervell County, the first flowing well was likely drilled around 1880 and was followed by another 80 flowing wells between 1888 and 1897 (Fielder, 1934). By 1900, there were nearly 200 flowing wells between depths of 30 and 300 ft (Hill, 1901), where flowing conditions persisted for many years in Somervell County (Fielder, 1934). In Dallas County, the first artesian well was drilled in 1890 (the “Dallas Geyser”). The first Trinity Aquifer flowing well was drilled in Hill County sometime in the late 1800s (Mount, 1963). In Cooke County, Bybee and Bullard (1927) note the existence of over 100 shallow flowing wells and a few flowing wells from the Trinity aquifer in Gainesville (Figure 1-3). Similarly, in Ellis County, many flowing wells were noted by Hill (1901).

Expanding urban populations and agricultural industries increased groundwater extraction significantly from both the Trinity and Woodbine aquifers. By 1891, decreased flow was observed with multiple wells in Dallas County, and by 1905, wells completed in the Woodbine Aquifer had ceased to flow. By 1894, some wells in Fort Worth had ceased to flow. By 1914, the City of Fort Worth had abandoned their wellfields for surface water supplies due to the loss of artesian pressure from a large amount of concentrated water use (Leggat, 1957), whereby water levels in some locations were more than 200 ft below land surface (Figures 2-17 and 2-18). Of the six initially flowing wells in Cleburne (Johnson County, Figure 1-3), only one still flowed by 1922 (Winton and Scott, 1922). Similarly, by the early 1920s, the artesian wells in Waco no longer flowed freely (Well C, Figure 2-21) (Adkins, 1923). In 1930, after the completion of a reservoir, the City of Waco largely changed to surface water supplies for its water needs (George and Barnes, 1945), and a general recovery of water levels was observed. However, other uses continued drawing from the Trinity Aquifer for public supply and industrial uses (George and Barnes, 1945).

By 1929, the groundwater level in Somervell County in several long-term wells was at or somewhat above land surface (wells A-C; Figure 2-20) and reported in Fielder (1934) to be between about 20 ft above land surface to about 80 ft below land surface in wells completed in different aquifer units. Water level measurements prior to 1929 are infrequent; however, based on Fielder (1934), water level declines since the early 1900s were likely in the 70-to-75-foot range. Wells by 1929 in Somervell County were reported to flow only in a relatively small part of the county due to the water level declines (Fielder, 1934). In Cooke County, the earliest reported water level measurement of 74 ft below land surface was taken in 1931 (Harden, 1960). In other wells in nearby Grayson, Fannin, and Collin counties, the water level in the late 1930s was between about 150 and 225 ft below land surface (Figure 2-19).

2.3.3.2 Trends by Region

In Tarrant County, the rapid increase in groundwater use, particularly after 1930, resulted in substantial groundwater level declines through 1950 (Figures 2-17 and 2-18). In the Fort Worth area, water level declines were between 460 ft from 1892 to 1942 (well G, Figure 2-17) to 389 ft during the same period (well I, Figure 2-18) (Leggat, 1957). Water level declines were particularly substantial during and after wartime conditions between 1942 and the early 1950s, with declines of up to 30 ft per year in some locations (wells J–M, Figure 2-18) (Leggat, 1957). These declines were due to the substantial groundwater use in both Fort Worth and Dallas, which resulted in a large cone of depression extending over an extensive area (Leggat, 1957, Mace and others, 1994).

In the northern part of the study area (Figure 2-19), declines through 1950 were present but less pronounced than in the Tarrant County area, due to distance from the large amounts of pumping around Fort Worth. Declines from first measurements generally ranged from less than 50 feet in the Pearsall and Hosston in Grayson County (well A, Figure 2-19)) to about 150 feet in the Woodbine and Washita in eastern Fannin County (Well D, Figure 2-19).

In the central part of the study area (Figure 2-20), declines were modest prior to 1950, although the lack of many early measurements makes it difficult to assess the amount of water level decline prior to the first measurements at some of the wells. In general, where early measurements are available, the decline appears to be in the range of 20 to 40 feet prior to 1950.

In the southern part of the study area (Figure 2-21), declines also appear to be modest prior to 1950, although the lack of multiple early measurements across the early time period makes interpretation difficult. In Coryell County (Well A), the water level decreases slightly but is relatively steady across the early time period. A similar trend is shown in Bell County (Well E) where there is some variation but not a clear downward trend prior to 1950. McLennan County has a hydrograph (Well C) that does show a clear decline of about 50 feet or more prior to 1950.

2.3.4 Water-Level Trends (1950–2024)

Selected northern Trinity and Woodbine groundwater levels from 1950 through 2024 are shown in Figures 2-22 through 2-42. The hydrograph plots shown in Figures 2-22 through 2-42 include a label indicating the TWDB state well number, and the completion depth for the well is provided on Table 2-4. Substantial groundwater level declines had already taken place by 1950 in many areas of the aquifer system; therefore, the declines shown in these figures do not represent the full extent of the water level drawdown.

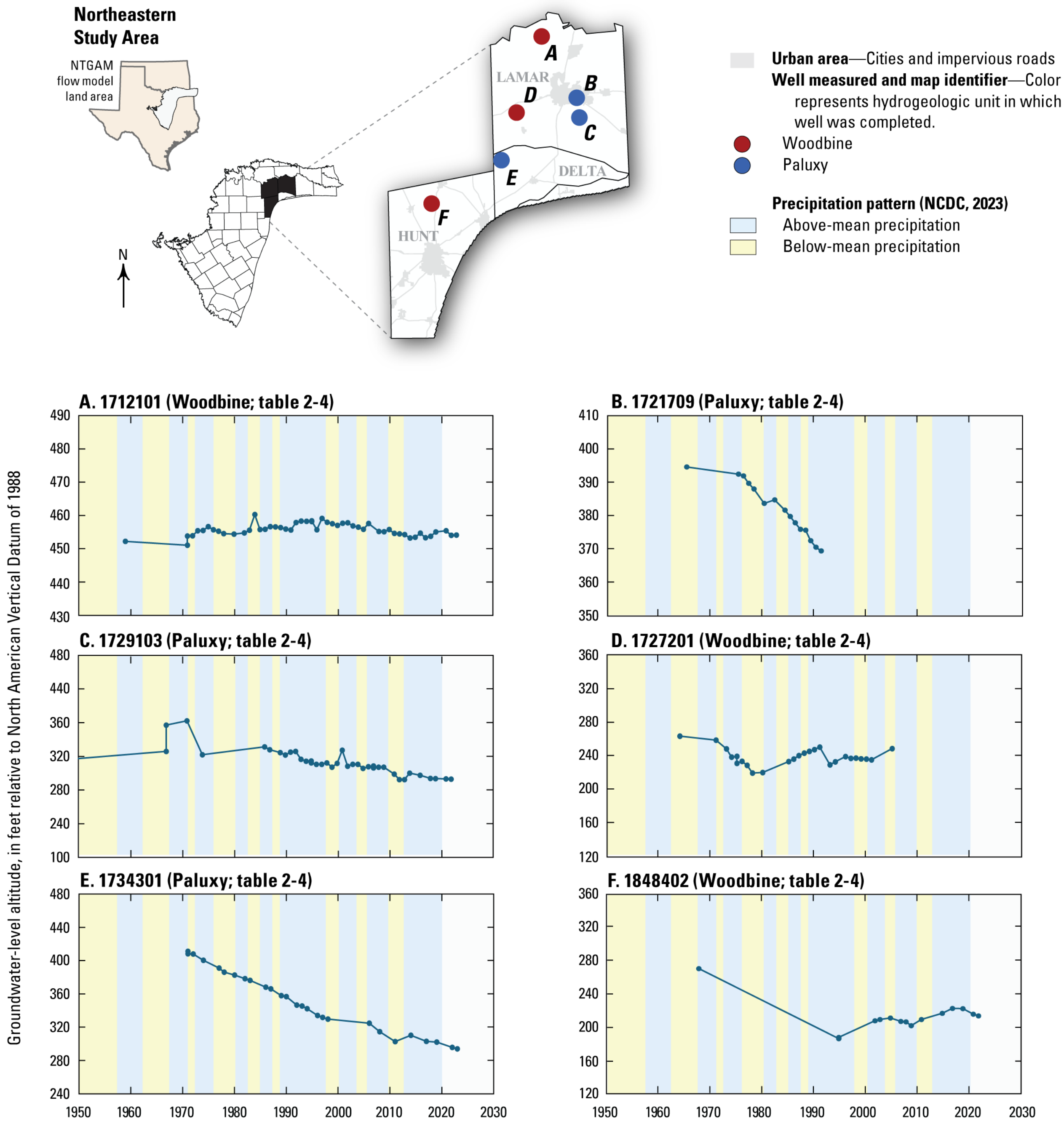

Figure 2-22. Locations and hydrographs of groundwater levels for selected wells in the northeastern part of the Northern Trinity and Woodbine aquifer system from 1950 to 2024.

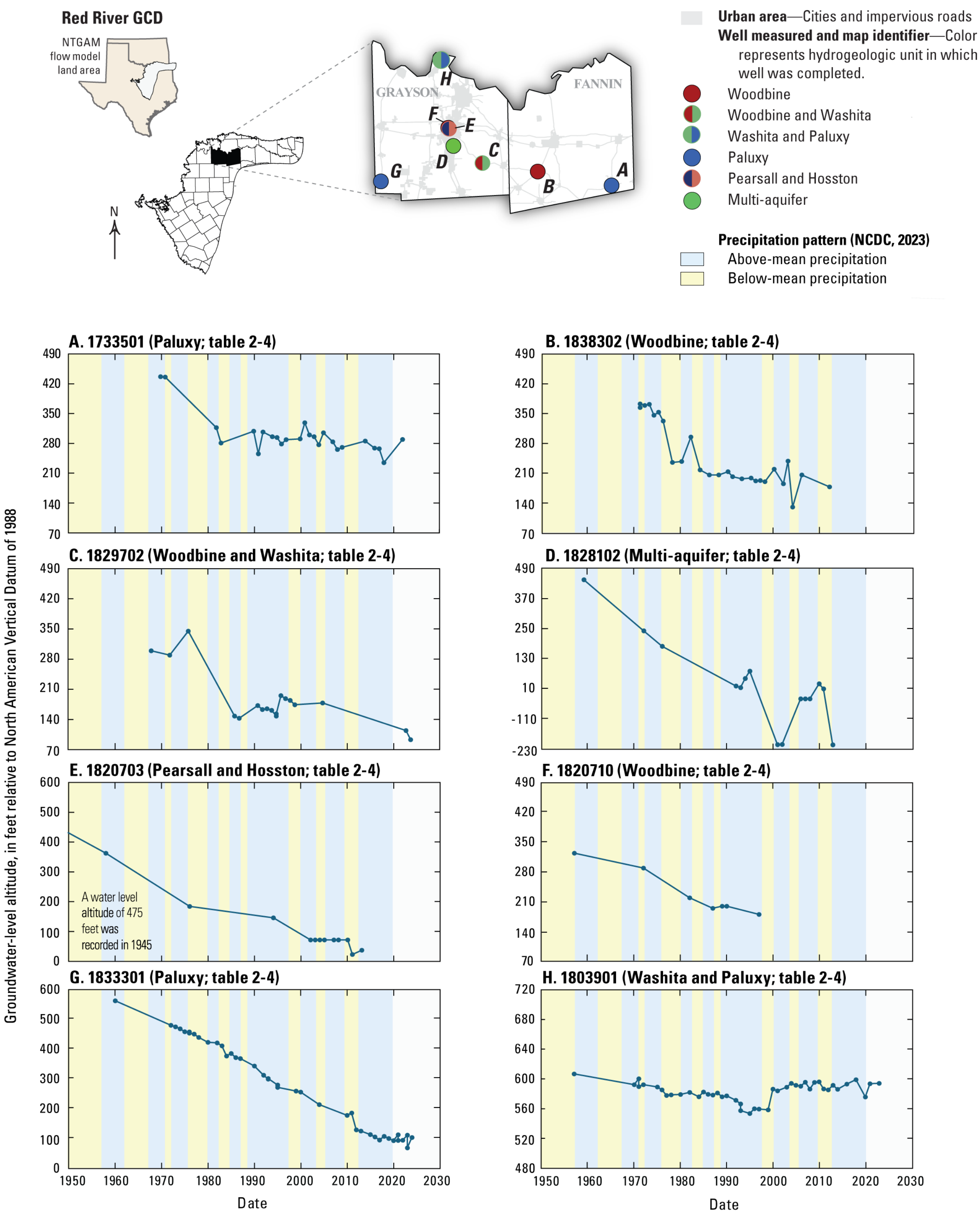

Figure 2-23. Locations and hydrographs of groundwater levels for selected wells in the Red River Groundwater Conservation District from 1950 to 2024.

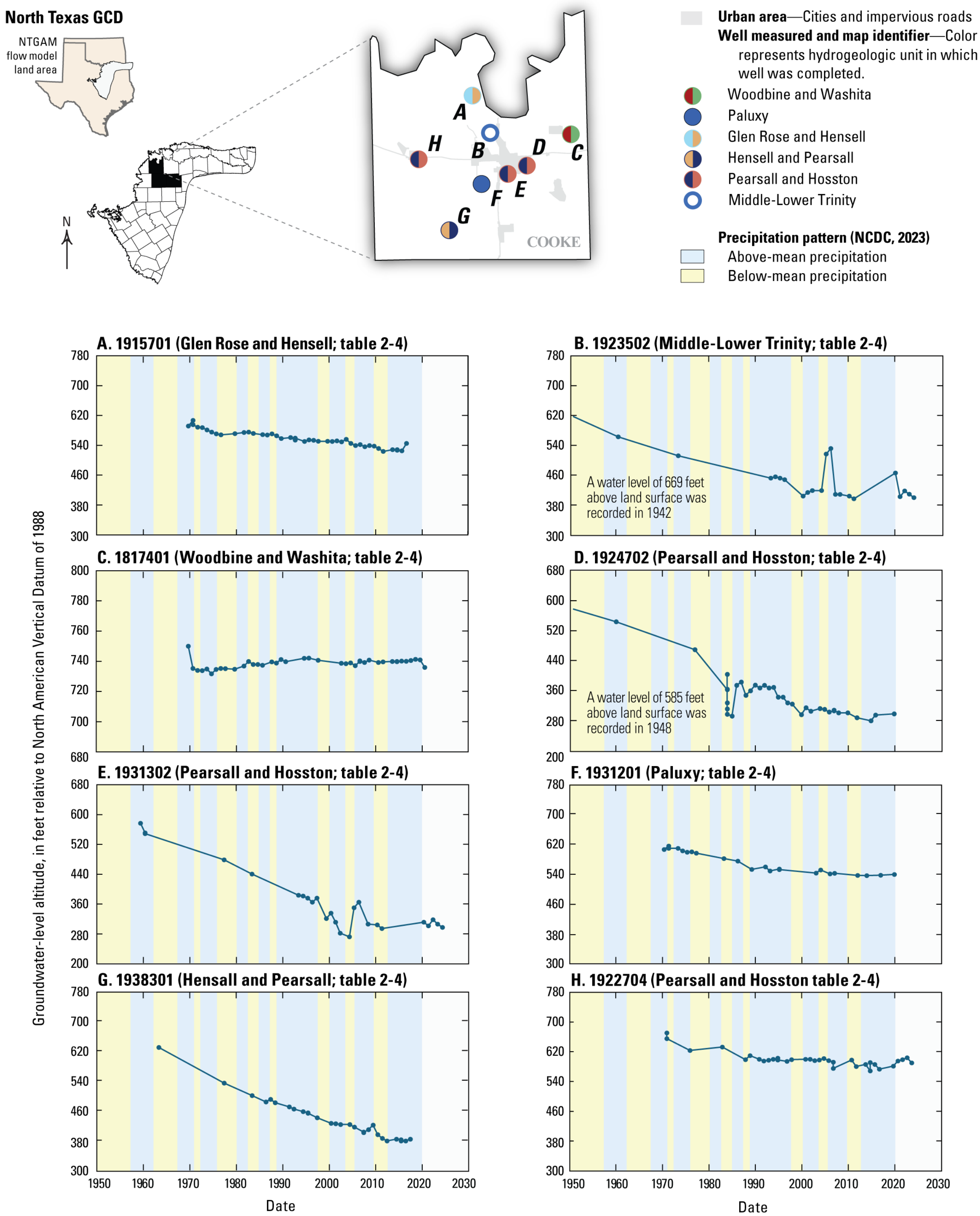

Figure 2-24. Locations and hydrographs of groundwater levels for selected wells in the North Texas Groundwater Conservation District in Cooke County from 1950 to 2024.

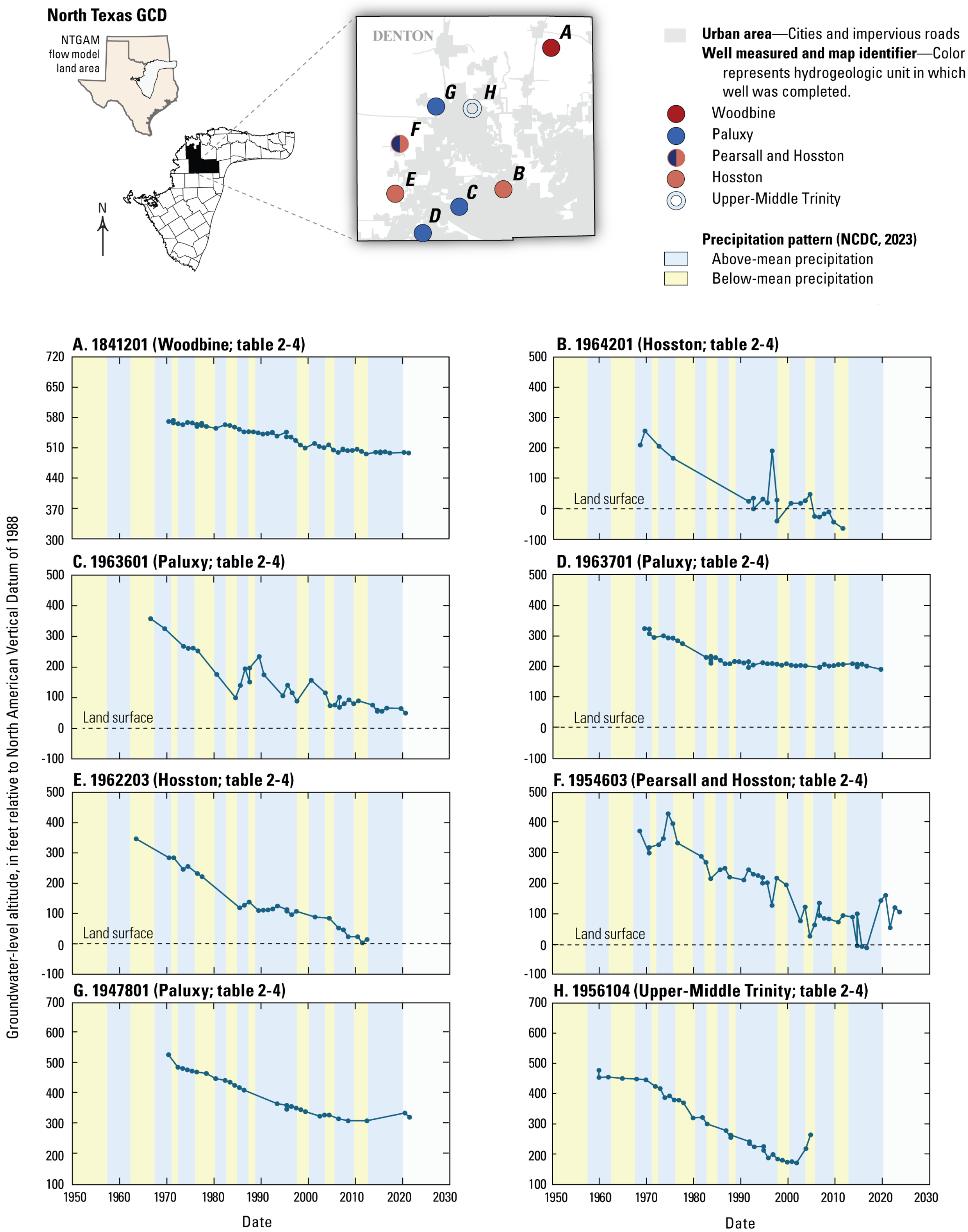

Figure 2-25. Locations and hydrographs of groundwater levels for selected wells in the North Texas Groundwater Conservation District in Denton County from 1950 to 2024.

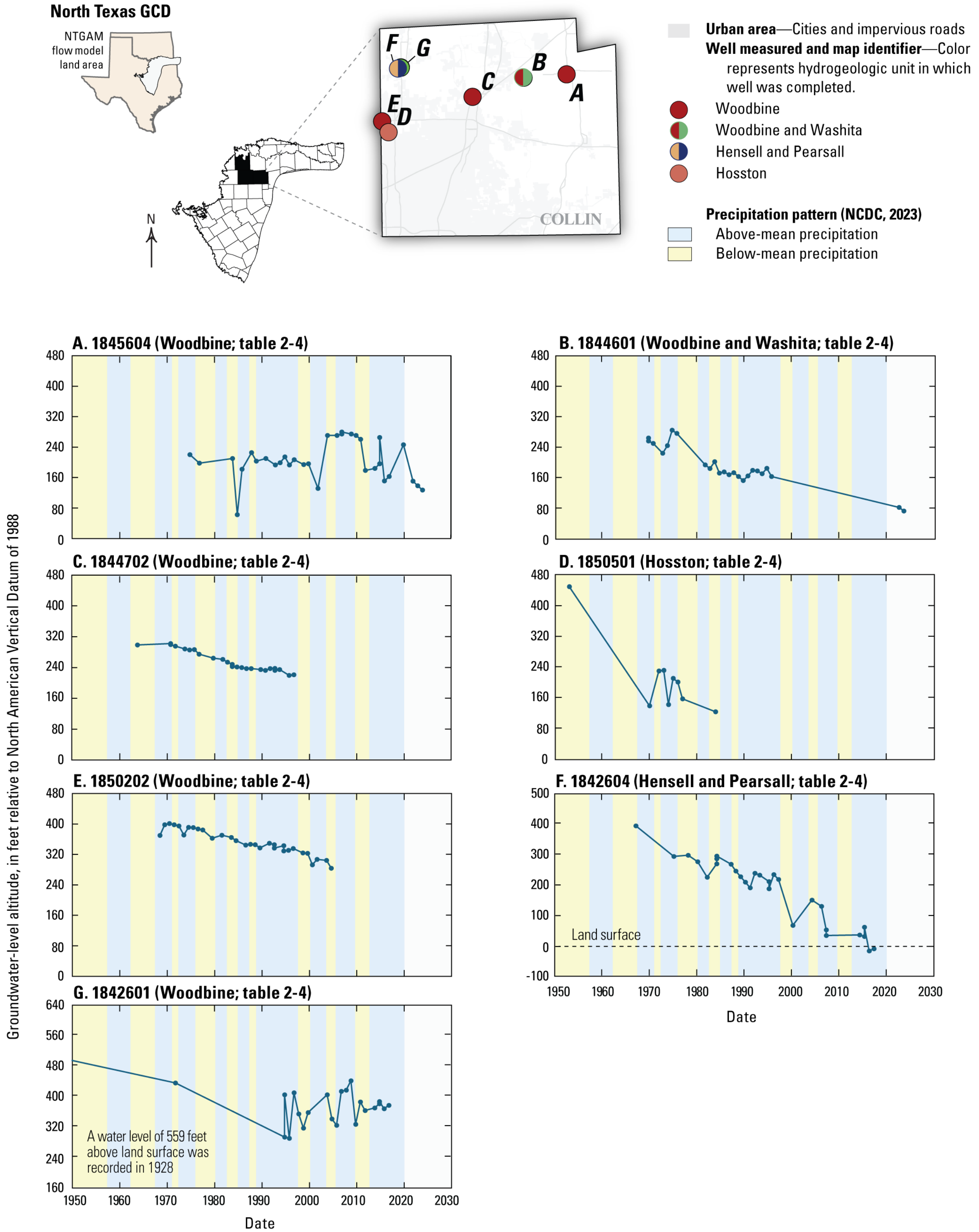

Figure 2-26. Locations and hydrographs of groundwater levels for selected wells in the North Texas Groundwater Conservation District in Collin County from 1950 to 2024.

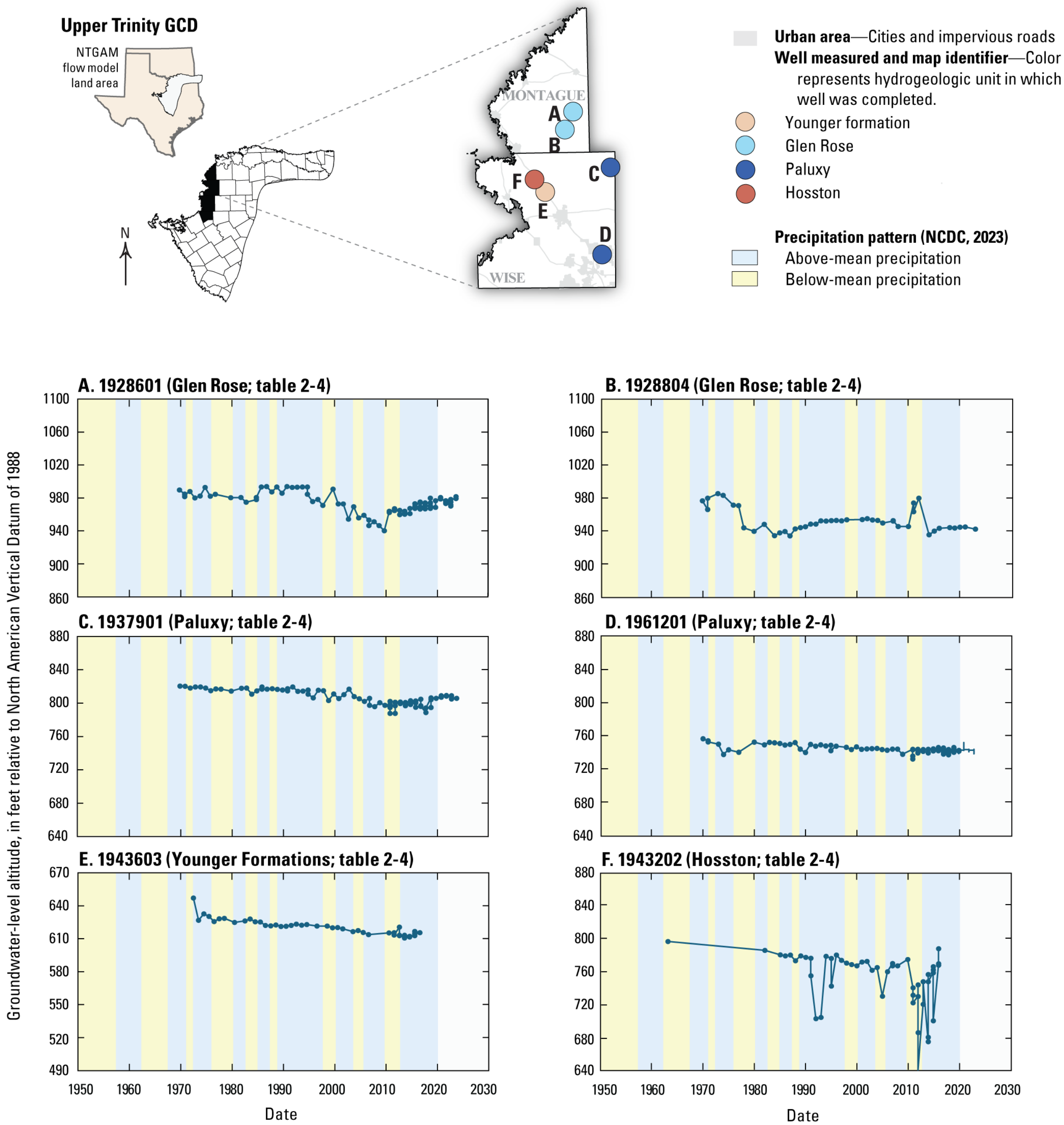

Figure 2-27. Locations and hydrographs of groundwater levels for selected wells in the Upper Trinity Groundwater Conservation District in Montague and Wise Counties from 1950 to 2024.

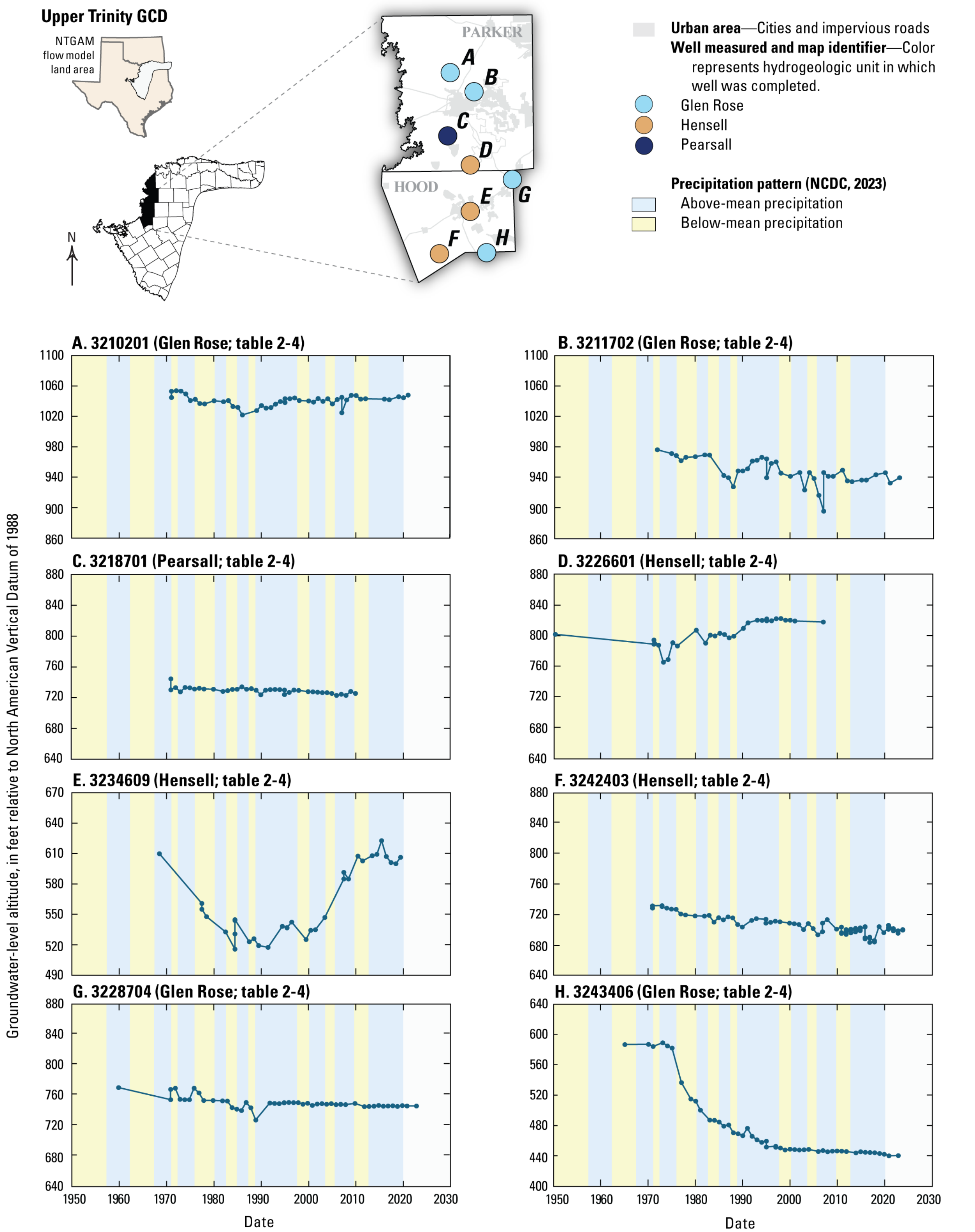

Figure 2-28. Locations and hydrographs of groundwater levels for selected wells in the Upper Trinity Groundwater Conservation District in Parker and Hood Counties from 1950 to 2024.

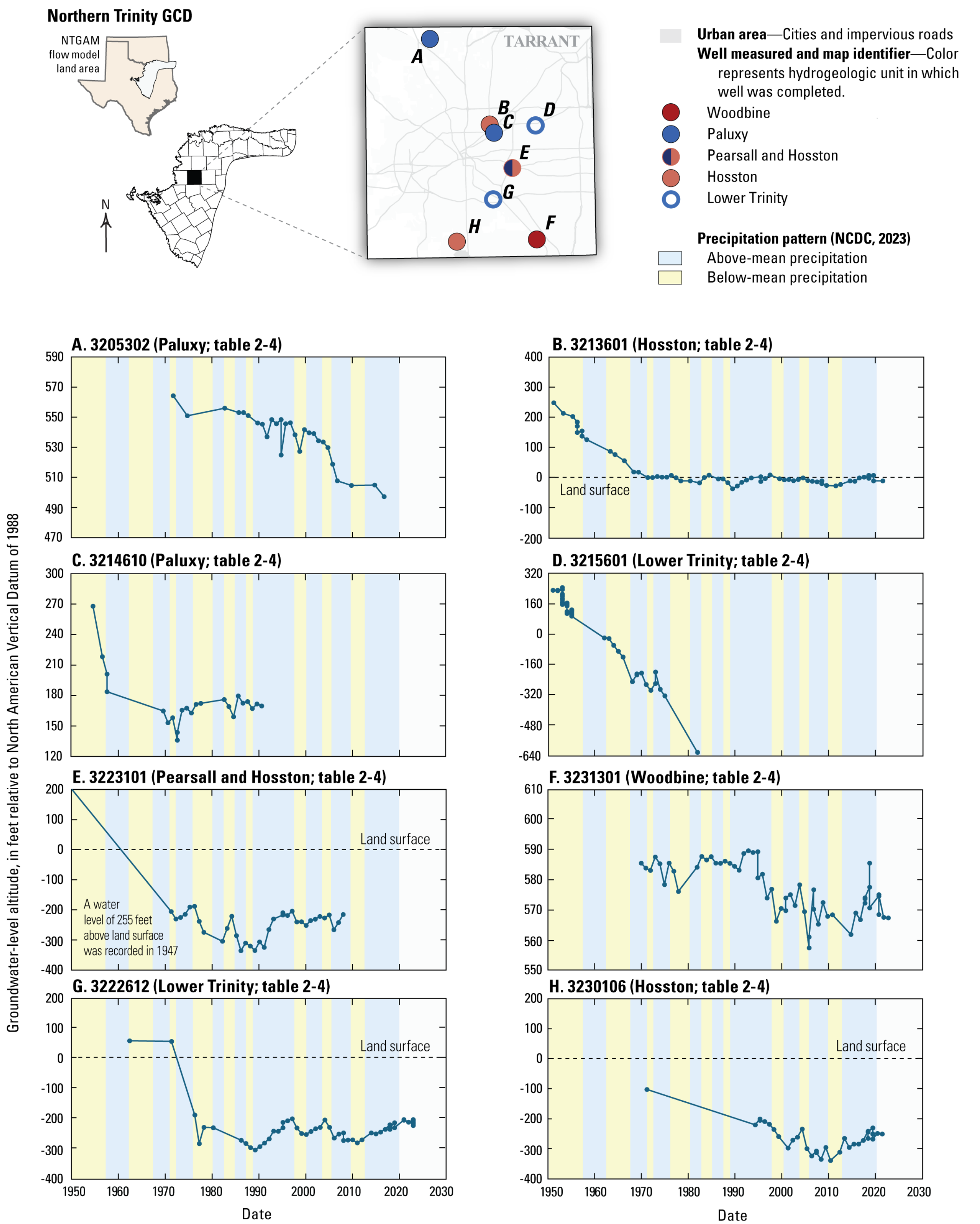

Figure 2-29. Locations and hydrographs of groundwater levels for selected wells in the Northern Trinity Groundwater Conservation District from 1950 to 2024.

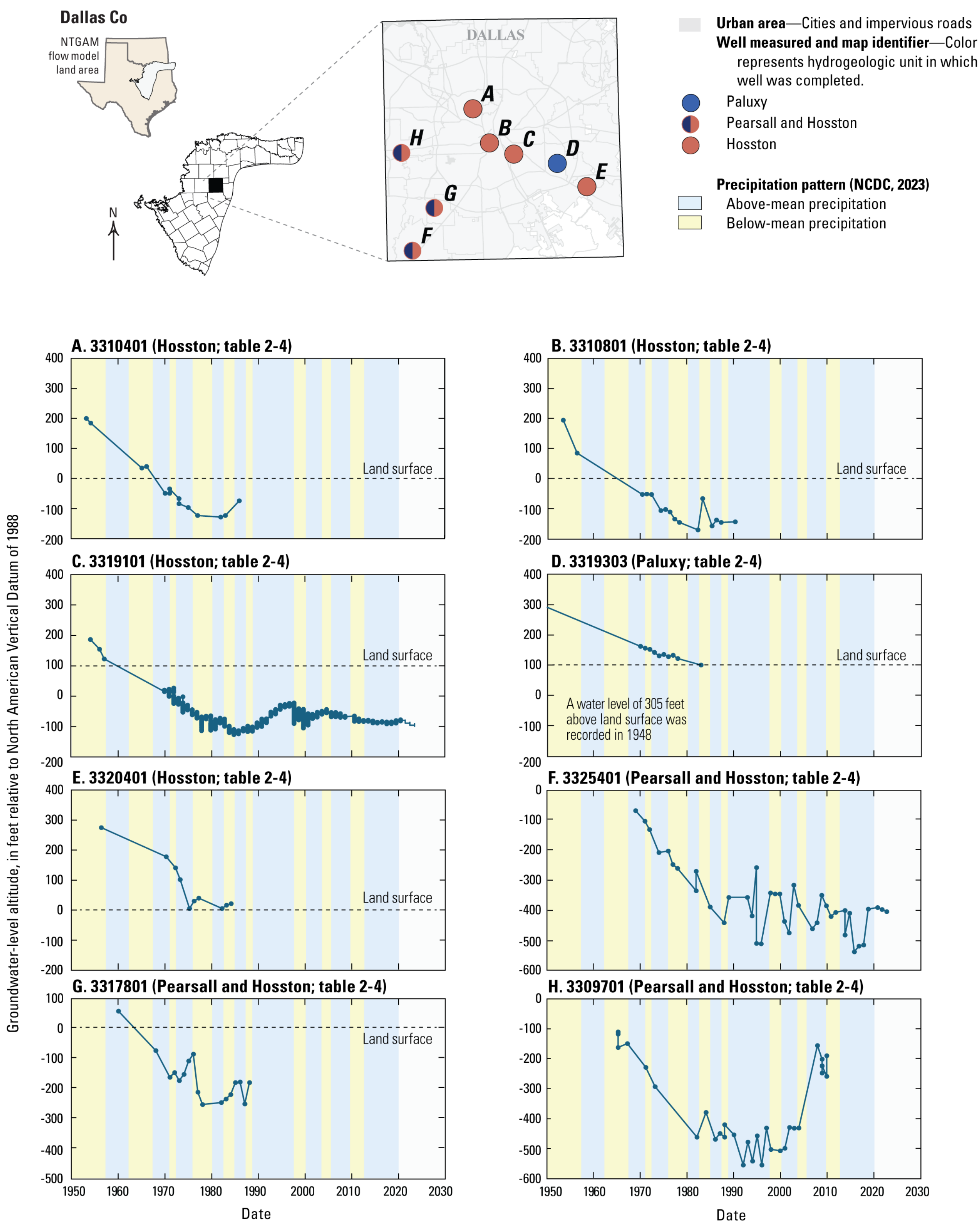

Figure 2-30. Locations and hydrographs of groundwater levels for selected wells in Dallas County from 1950 to 2024.

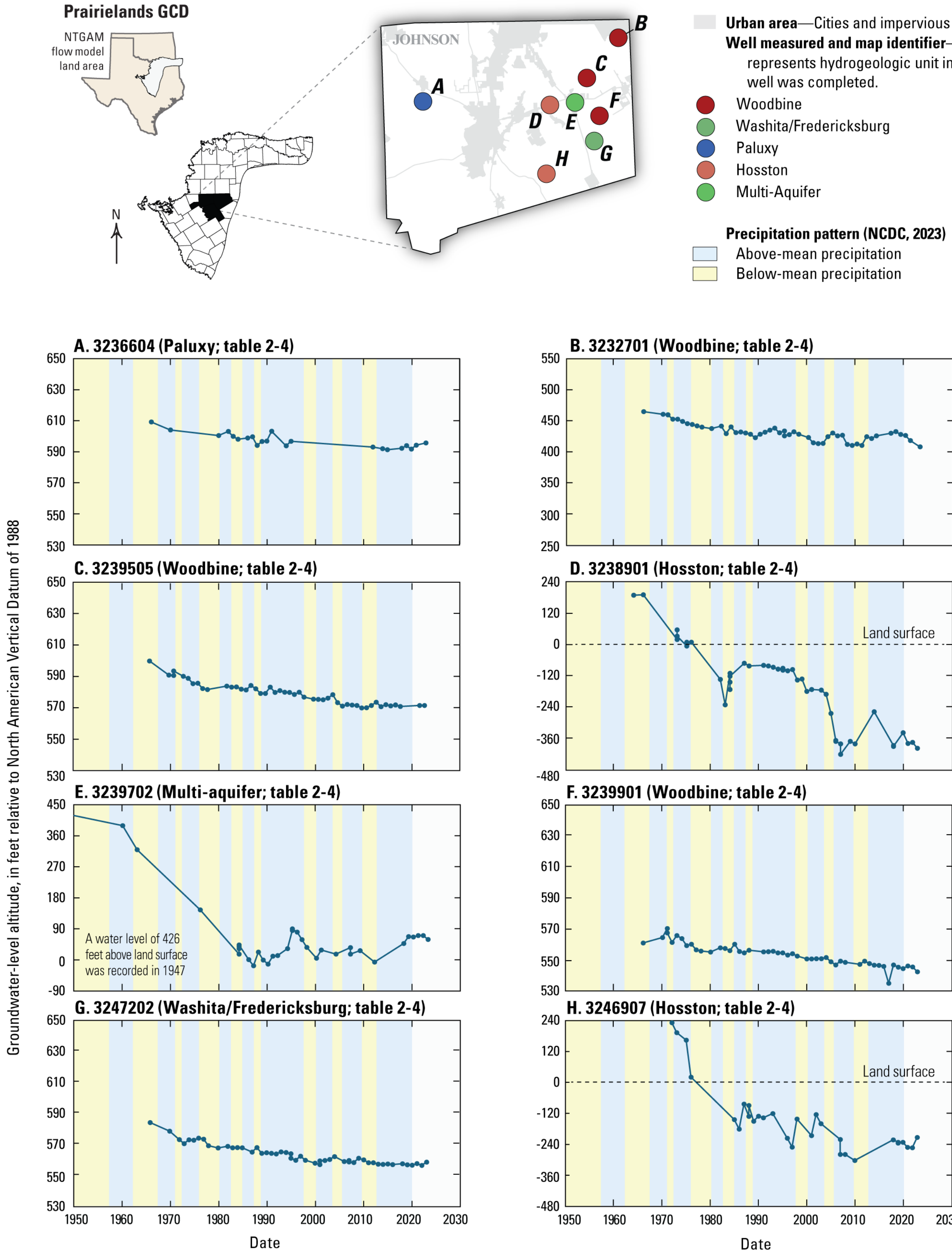

Figure 2-31. Locations and hydrographs of groundwater levels for selected wells in the Prairielands Groundwater Conservation District in Johnson County from 1950 to 2024.

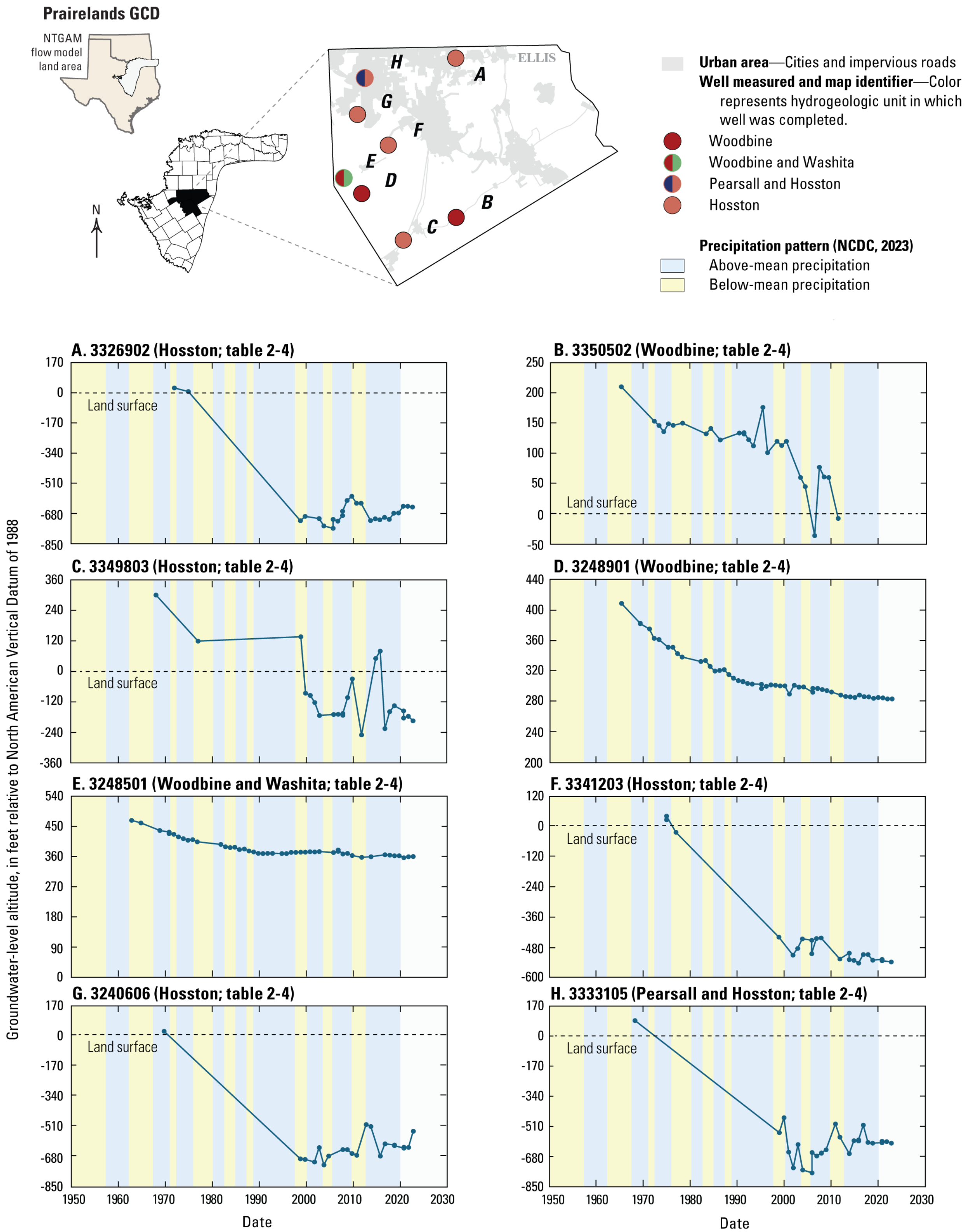

Figure 2-32. Locations and hydrographs of groundwater levels for selected wells in the Prairielands Groundwater Conservation District in Ellis County from 1950 to 2024.

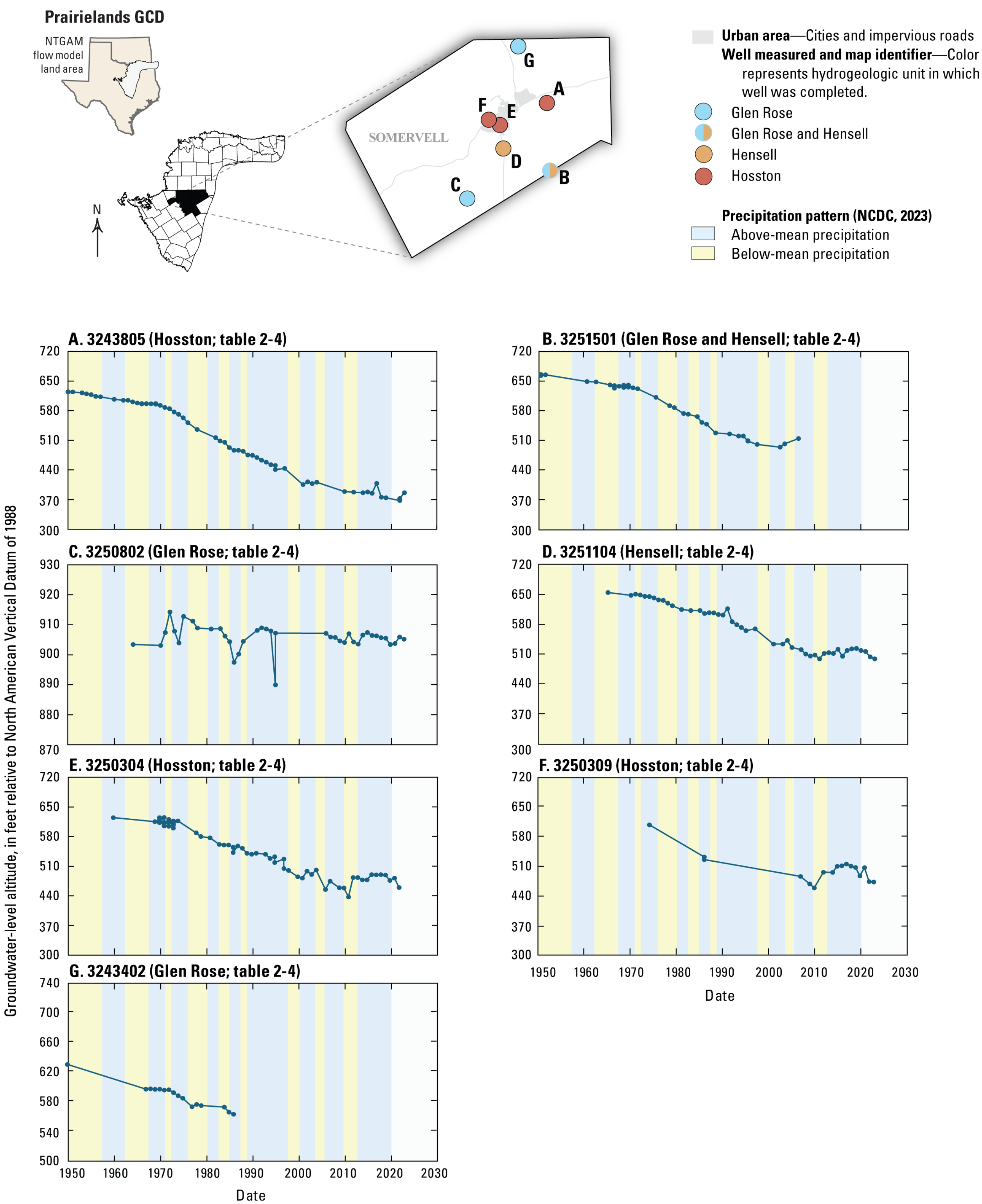

Figure 2-33. Locations and hydrographs of groundwater levels for selected wells in the Prairielands Groundwater Conservation District in Somervell County from 1950 to 2024.

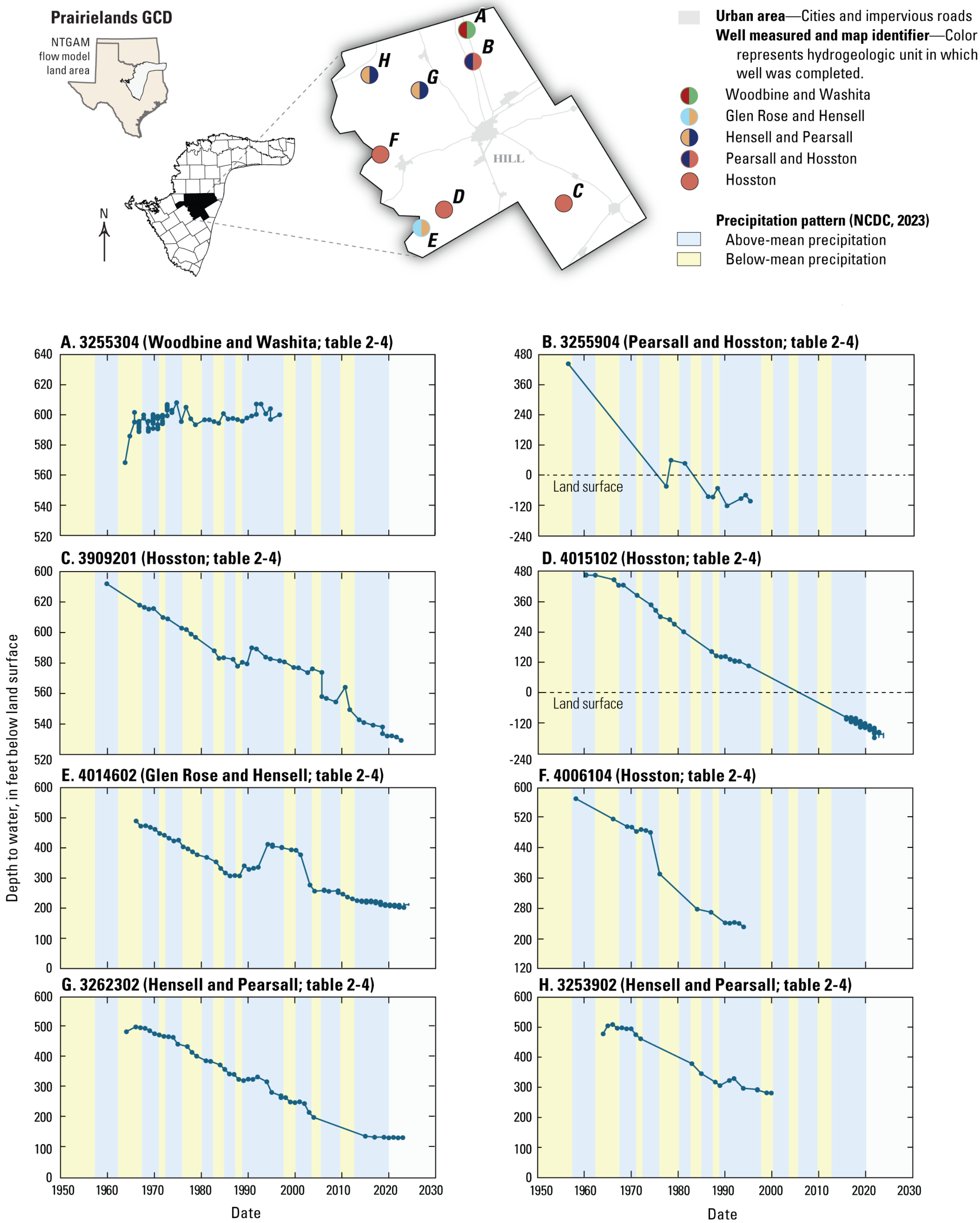

Figure 2-34. Locations and hydrographs of groundwater levels for selected wells in the Prairielands Groundwater Conservation District in Hill County from 1950 to 2024.

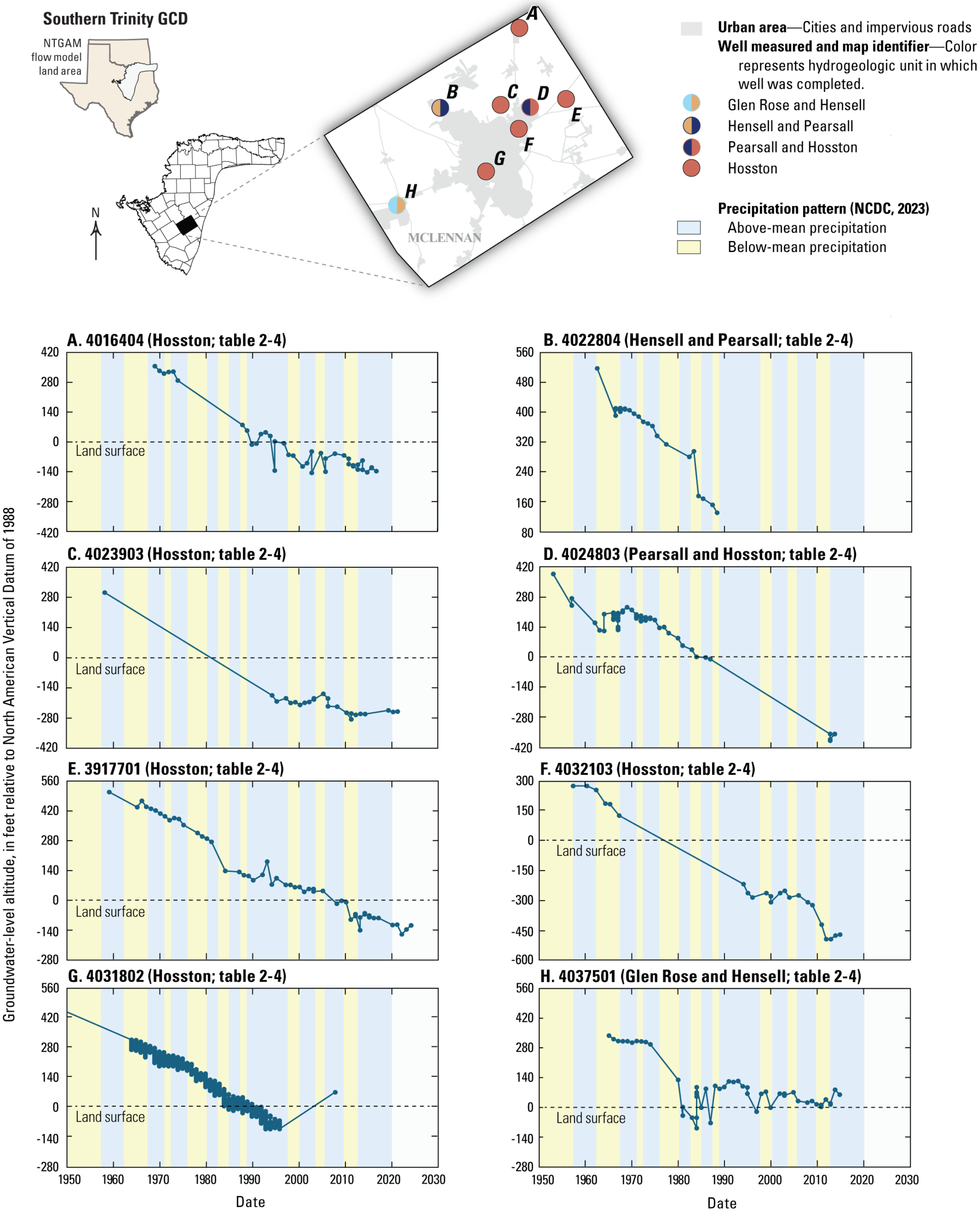

Figure 2-35. Locations and hydrographs of groundwater levels for selected wells in the Southern Trinity Groundwater Conservation District from 1950 to 2024.

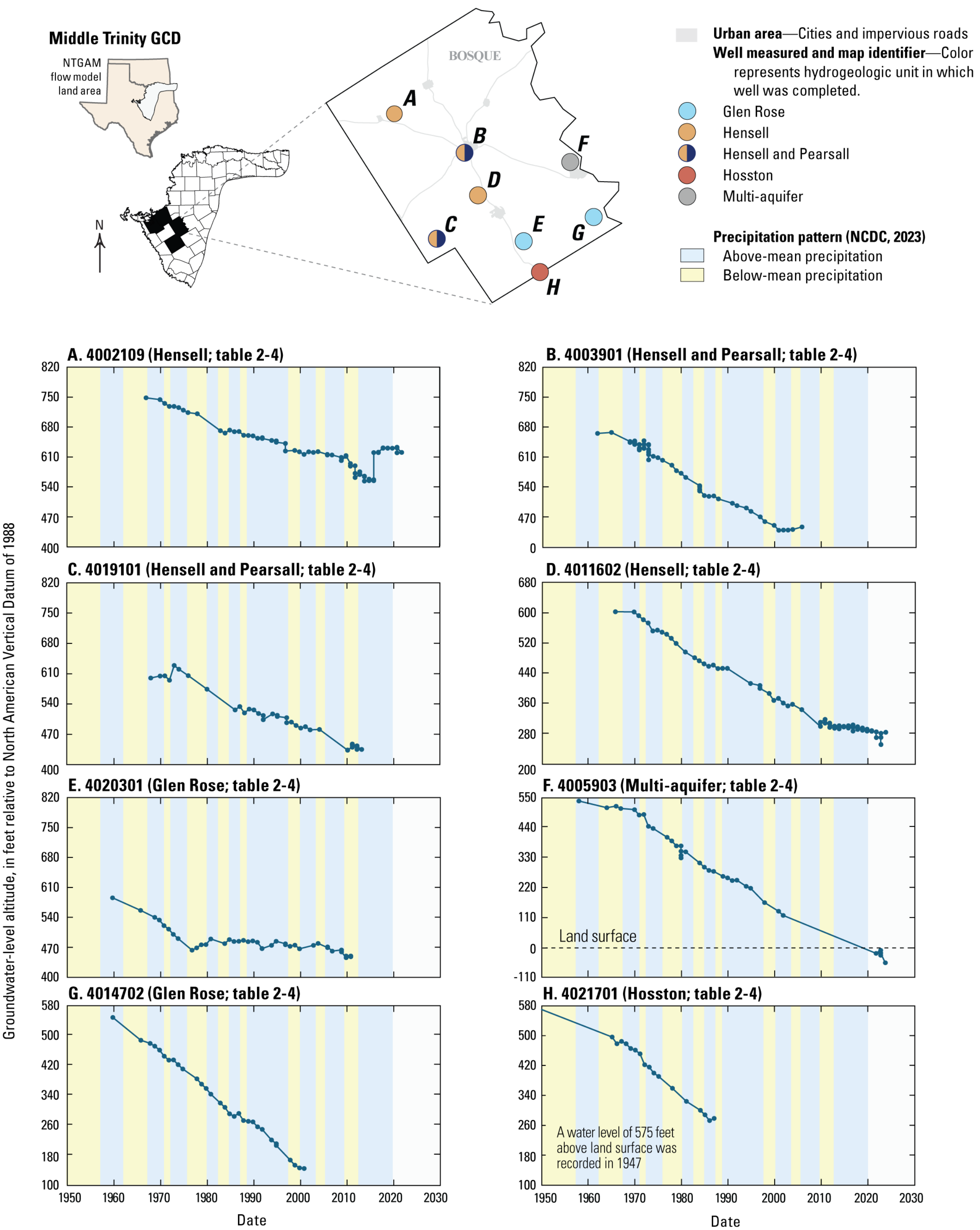

Figure 2-36. Locations and hydrographs of groundwater levels for selected wells in the Middle Trinity Groundwater Conservation District in Bosque County from 1950 to 2024.

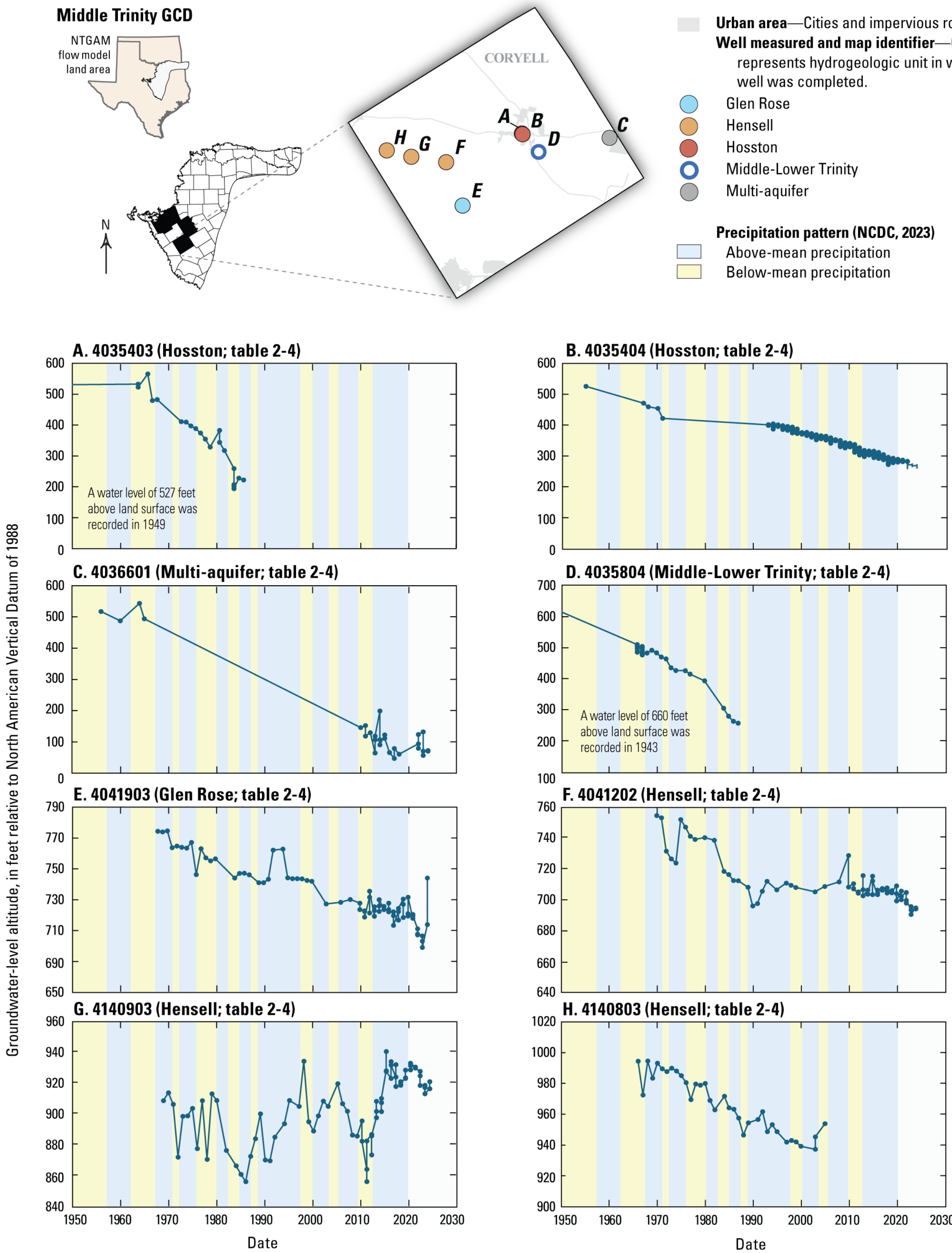

Figure 2-37. Locations and hydrographs of groundwater levels for selected wells in the Middle Trinity Groundwater Conservation District in Coryell County from 1950 to 2024.

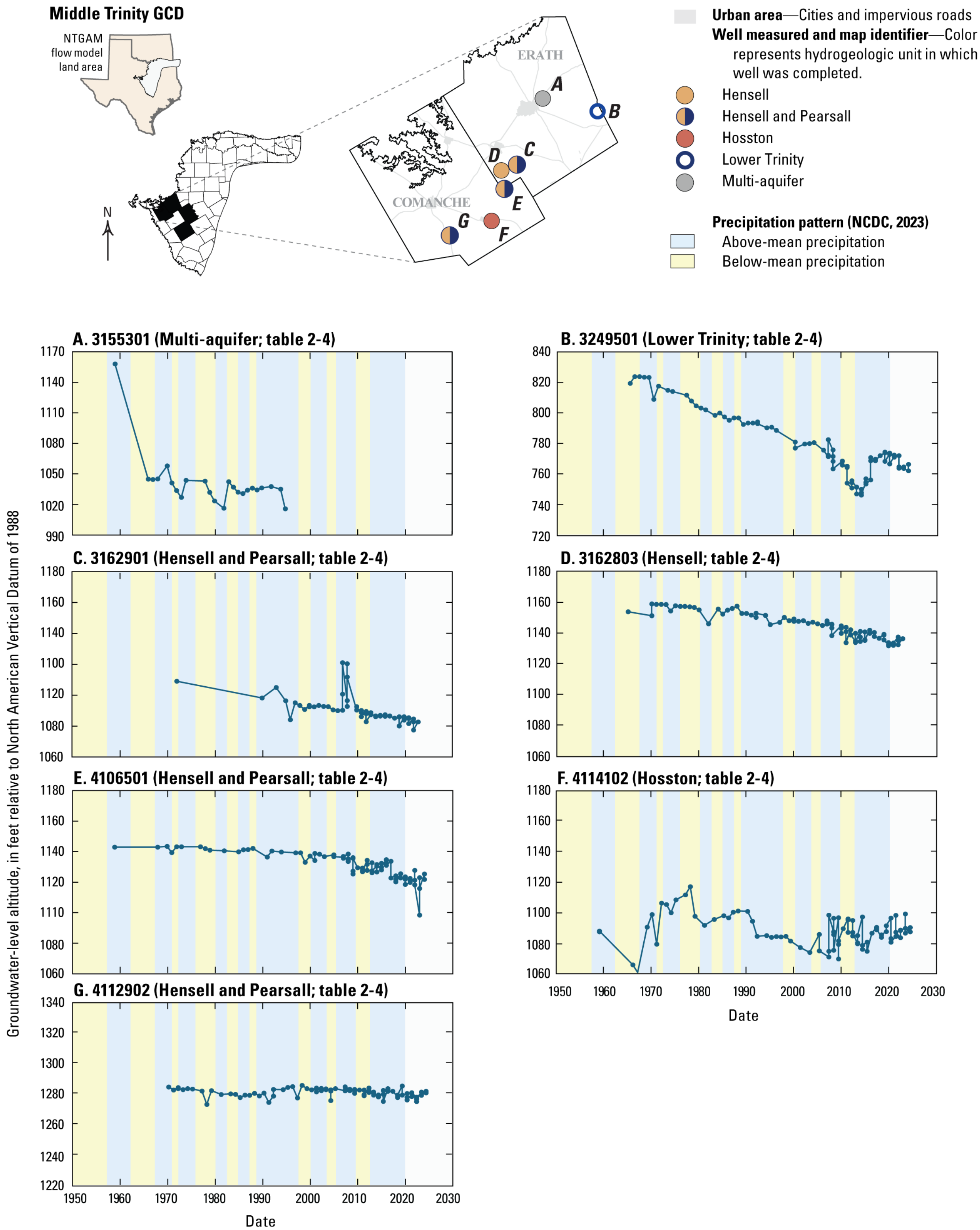

Figure 2-38. Locations and hydrographs of groundwater levels for selected wells in the Middle Trinity Groundwater Conservation District in Erath and Commanche Counties from 1950 to 2024.

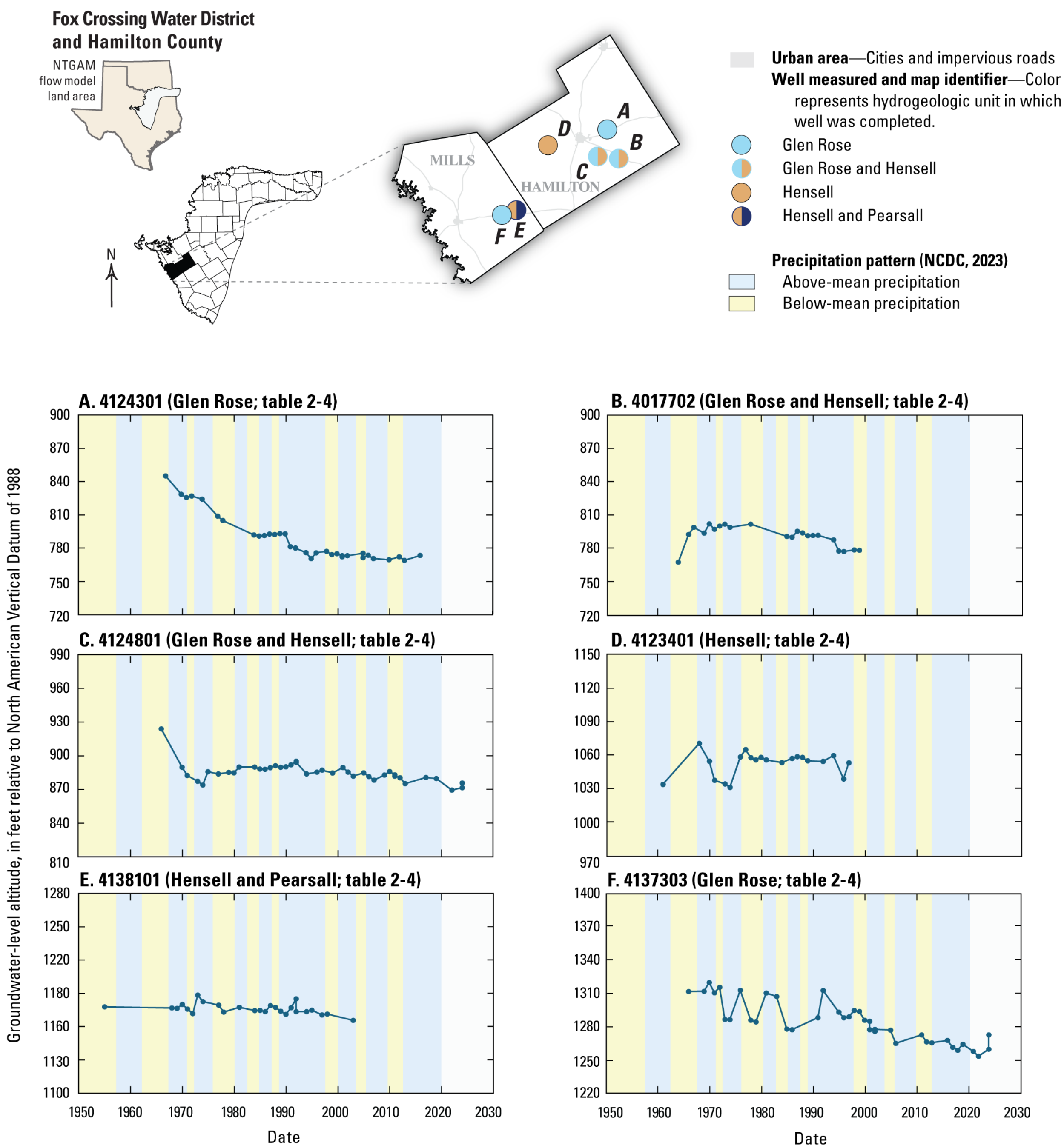

Figure 2-39. Locations and hydrographs of groundwater levels for selected wells in Mills and Hamilton Counties from 1950 to 2024.

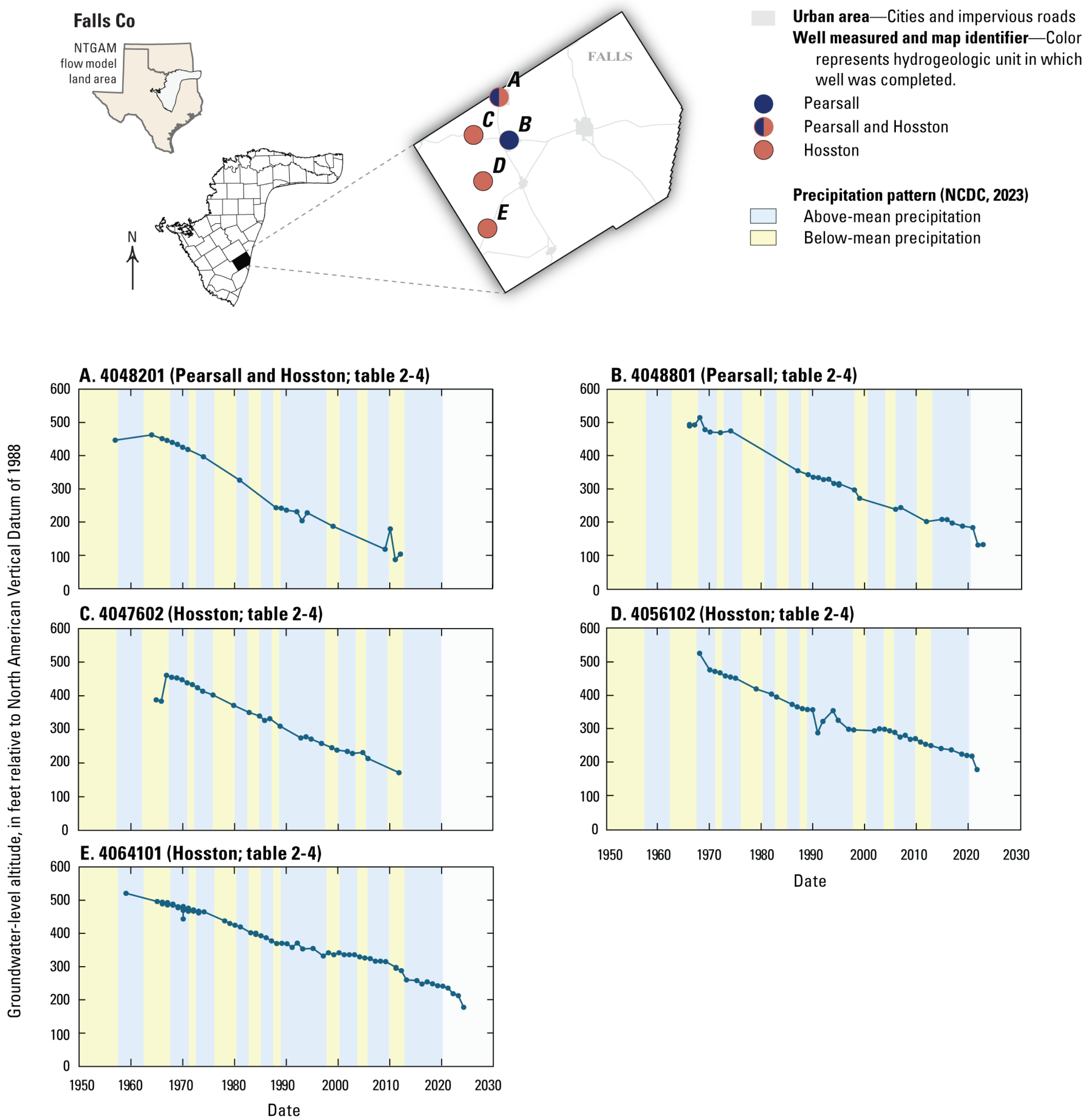

Figure 2-40. Locations and hydrographs of groundwater levels for selected wells in Falls County from 1950 to 2024.

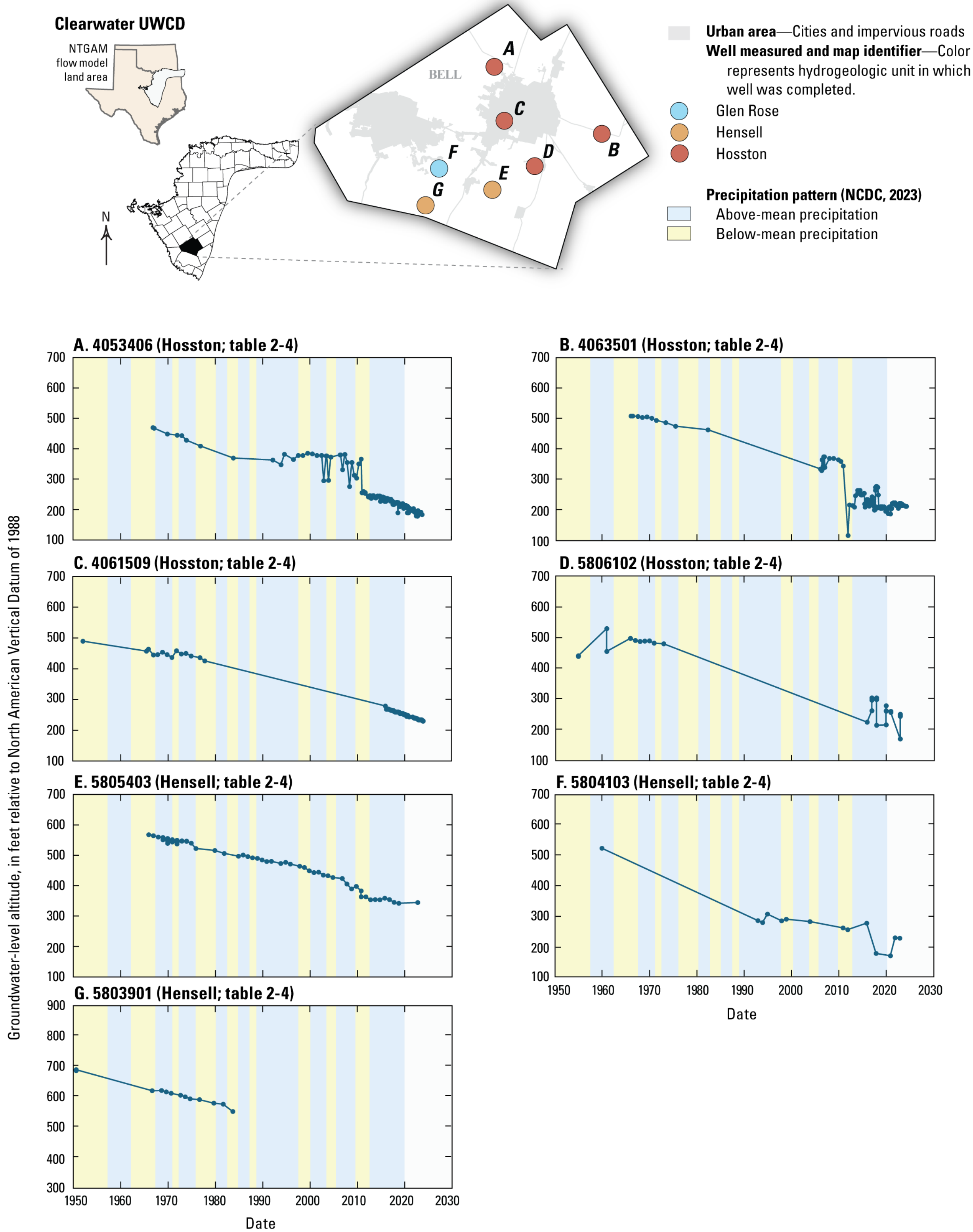

Figure 2-41. Locations and hydrographs of groundwater levels for selected wells in the Clearwater Underground Water Conservation District from 1950 to 2024.

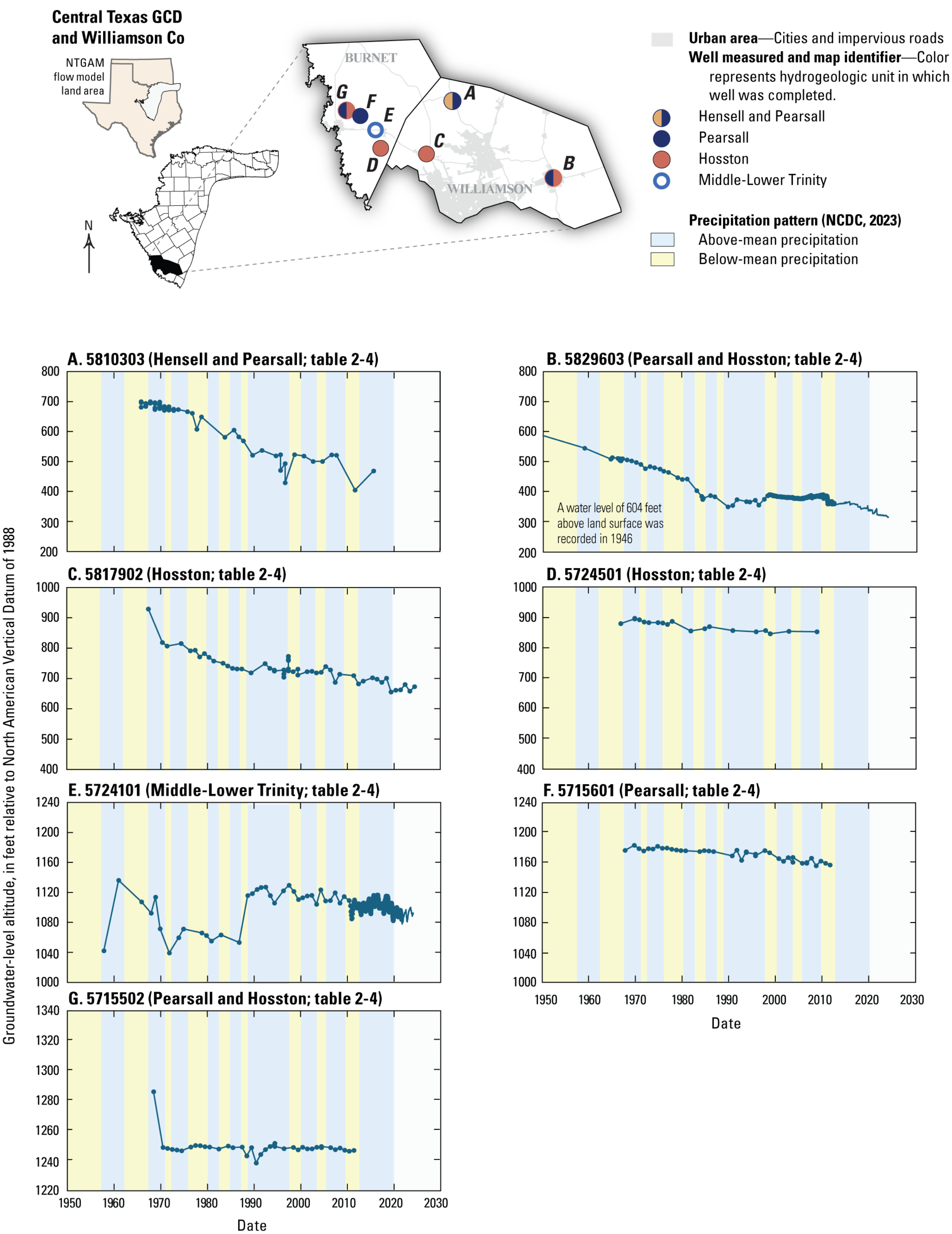

Figure 2-42. Locations and hydrographs of groundwater levels for selected wells in the Central Texas Groundwater Conservation District and Williamson County from 1950 to 2024.

Table 2-4. Wells with long-term groundwater-level measurements within the northern Trinity and Woodbine aquifer system.

Groundwater-well groups	TWDB State Well Number	Map ID (figures 2-22 to 2-42)	County	Hydrogeologic unit (Figure 2-3)[1]	Period of record (may contain gaps) (M/Y)[2]		Well depth, in feet below land surface[3]
					Begin	End	
Northeastern area (figure 2-22)	1712101	A	Lamar	Woodbine	10-1959	11-2023	165
	1721709	B	Lamar	Paluxy	03-1965	01-1991	2,145
	1729103	C	Lamar	Paluxy	02-1967	11-2023	2,563
	1727201	D	Lamar	Woodbine	09-1964	12-2005	1,610
	1734301	E	Delta	Paluxy	05-1971	11-2023	3,333
	1848402	F	Hunt	Woodbine	10-1968	11-2022	2,388
Red River GCD (figure 2-23)	1733501	A	Fannin	Paluxy	12-1970	11-2022	3,366
	1838302	B	Fannin	Woodbine	07-1971	11-2012	1,297
	1829702	C	Grayson	Woodbine and Washita	05-1968	03-2024	1,475
	1828102	D	Grayson	Multi-aquifer	01-1959	04-2013	2,460
	1820703	E	Grayson	Pearsall and Hosston	11-1945	04-2013	2,136
	1820710	F	Grayson	Woodbine	08-1957	11-1997	789
	1833301	G	Grayson	Paluxy	01-1960	01-2024	923
	1803901	H	Grayson	Washita and Paluxy	09-1957	12-2023	290
North Texas GCD (figures 2-24, 2-25, 2-26)	1915701	A	Cooke	Glen Rose and Hensell	09-1970	10-2017	348
	1923502	B	Cooke	Middle-Lower Trinity	08-1942	01-2024	938
	1817401	C	Cooke	Woodbine and Washita	09-1970	11-2021	235
	1924702	D	Cooke	Pearsall and Hosston	03-1948	02-2020	1,238
	1931302	E	Cooke	Pearsall and Hosston	03-1959	01-2024	997
	1931201	F	Cooke	Paluxy	09-1970	11-2020	350
	1938301	G	Cooke	Hensell and Pearsall	08-1963	10-2017	794
	1922704	H	Cooke	Pearsall and Hosston	05-1971	01-2024	660
	1841201	A	Denton	Woodbine	09-1970	03-2021	210
	1964201	B	Denton	Hosston	08-1969	10-2012	1,747
	1963601	C	Denton	Paluxy	12-1967	04-2021	856
	1963701	D	Denton	Paluxy	10-1970	03-2020	626
	1962203	E	Denton	Hosston	08-1963	11-2012	1,003
	1954603	F	Denton	Pearsall and Hosston	07-1969	02-2024	980
	1947801	G	Denton	Paluxy	09-1970	03-2021	615
	1956104	H	Denton	Upper-Middle Trinity	05-1957	11-2005	1,200

	1845604	A	Collin	Woodbine	02-1975	02-2024	1,900
	1844601	B	Collin	Woodbine and Washita	01-1970	02-2024	1,783
	1844702	C	Collin	Woodbine	08-1964	11-1997	1,136
	1850501	D	Collin	Hosston	09-1953	01-1984	2,694
	1850202	E	Collin	Woodbine	07-1969	12-2005	640
	1842604	F	Collin	Hensell and Pearsall	08-1967	10-2017	2,300
	1842601	G	Collin	Woodbine	03-1928	10-2017	700
Upper Trinity GCD (figures 2-27, 2-28)	1928601	A	Montague	Glen Rose	09-1970	06-2024	200
	1928804	B	Montague	Glen Rose	09-1970	12-2023	250
	1937901	C	Wise	Paluxy	10-1970	06-2024	335
	1961201	D	Wise	Paluxy	10-1970	06-2024	360
	1943603	E	Wise	Younger Formation	11-1972	04-2016	180
	1943202	F	Wise	Hosston	01-1963	12-2016	381
	3210201	A	Parker	Glen Rose	06-1971	11-2021	165
	3211702	B	Parker	Glen Rose	08-1972	12-2023	220
	3218701	C	Parker	Pearsall	02-1971	06-2011	204
	3226601	D	Parker	Hensell	03-1950	02-2007	310
	3234609	E	Hood	Hensell	07-1968	11-2019	222
	3242403	F	Hood	Hensell	06-1971	07-2024	355
	3228704	G	Hood	Glen Rose	10-1960	12-2023	353
	3243406	H	Hood	Glen Rose	03-1965	12-2023	212
Northern Trinity GCD (figure 2-29)	3205302	A	Tarrant	Paluxy	03-1972	11-2017	419
	3213601	B	Tarrant	Hosston	04-1951	11-2021	967
	3214610	C	Tarrant	Paluxy	01-1955	02-1991	425
	3215601	D	Tarrant	Lower Trinity	11-1951	03-1982	1,483
	3223101	E	Tarrant	Pearsall and Hosston	12-1947	01-2008	1,363
	3231301	F	Tarrant	Woodbine	11-1970	08-2023	171
	3222612	G	Tarrant	Lower Trinity	07-1962	12-2023	1,352
	3230106	H	Tarrant	Hosston	11-1971	11-2021	1,220
Dallas Co (figure 2-30)	3310401	A	Dallas	Hosston	07-1953	03-1986	2,689
	3310801	B	Dallas	Hosston	05-1953	01-1990	2,797
	3319101	C	Dallas	Hosston	05-1954	12-2024	3,076
	3319303	D	Dallas	Paluxy	07-1948	04-1983	2,297
	3320401	E	Dallas	Hosston	05-1956	03-1984	4,110
	3325401	F	Dallas	Pearsall and Hosston	07-1969	11-2023	2,430
	3317801	G	Dallas	Pearsall and Hosston	05-1960	01-1988	2,614
	3309701	H	Dallas	Pearsall and Hosston	05-1965	06-2010	2,049
	3236604	A	Johnson	Paluxy	10-1966	02-2023	500
	3232701	B	Johnson	Woodbine	10-1966	10-2023	240

Prairielands GCD (figures 2-31, 2-32, 2-33, 2-34)	3239505	C	Johnson	Woodbine	10-1966	10-2023	210
	3238901	D	Johnson	Hosston	10-1964	11-2023	1,630
	3239702	E	Johnson	Multi-aquifer	05-1947	11-2023	1,656
	3239901	F	Johnson	Woodbine	10-1966	10-2023	220
	3247202	G	Johnson	Washita/Fredericksburg	08-1966	10-2023	216
	3246907	H	Johnson	Hosston	04-1972	11-2023	1,560
	3326902	A	Ellis	Hosston	02-1972	11-2023	3,178
	3350502	B	Ellis	Woodbine	06-1965	11-2011	1,238
	3349803	C	Ellis	Hosston	05-1968	12-2023	2,700
	3248901	D	Ellis	Woodbine	06-1965	10-2023	384
	3248501	E	Ellis	Woodbine and Washita	07-1963	10-2023	367
	3341203	F	Ellis	Hosston	01-1975	01-2023	2,564
	3240606	G	Ellis	Hosston	11-1970	12-2023	2,411
	3333105	H	Ellis	Pearsall and Hosston	07-1968	11-2023	2,354
	3243805	A	Somervell	Hosston	08-1950	10-2023	464
	3251501	B	Somervell	Glen Rose and Hensell	09-1950	07-2006	370
	3250802	C	Somervell	Glen Rose	10-1964	11-2023	321
	3251104	D	Somervell	Hensell	05-1965	10-2023	376
	3250304	E	Somervell	Hosston	09-1960	11-2022	352
	3250309	F	Somervell	Hosston	09-1974	11-2023	472
	3243402	G	Somervell	Glen Rose	09-1950	03-1986	200
	3255304	A	Hill	Woodbine and Washita	07-1964	01-1997	273
	3255904	B	Hill	Pearsall and Hosston	06-1956	11-1995	1,856
	3909201	C	Hill	Hosston	05-1960	11-2023	3,138
	4015102	D	Hill	Hosston	01-1960	12-2024	1,485
	4014602	E	Hill	Glen Rose and Hensell	03-1966	12-2024	1,102
	4006104	F	Hill	Hosston	07-1958	02-1994	1,166
	3262302	G	Hill	Hensell and Pearsall	01-1964	10-2023	1,213
	3253902	H	Hill	Hensell and Pearsall	09-1964	11-2000	934
Southern Trinity GCD (figure 2-35)	4016404	A	McLennan	Hosston	04-1969	10-2017	1,982
	4022804	B	McLennan	Hensell and Pearsall	07-1962	04-1988	1,150
	4023903	C	McLennan	Hosston	09-1958	10-2021	2,114
	4024803	D	McLennan	Pearsall and Hosston	02-1953	01-2014	2,494
	3917701	E	McLennan	Hosston	04-1959	10-2024	3,129
	4032103	F	McLennan	Hosston	05-1957	12-2015	2,396
	4031802	G	McLennan	Hosston	08-1947	04-2008	2,040
	4037501	H	McLennan	Glen Rose and Hensell	04-1965	12-2015	1,050
	4002109	A	Bosque	Hensell	03-1967	04-2022	364
	4003901	B	Bosque	Hensell and Pearsall	07-1962	01-2006	570

Middle Trinity GCD (figure 2-36, 2-37, 2-38)	4019101	C	Bosque	Hensell and Pearsall	11-1968	04-2013	540
	4011602	D	Bosque	Hensell	08-1966	04-2024	631
	4020301	E	Bosque	Glen Rose	05-1960	12-2011	650
	4005903	F	Bosque	Multi-aquifer	02-1958	04-2024	1,135
	4014702	G	Bosque	Glen Rose	04-1960	12-2001	1,010
	4021701	H	Bosque	Hosston	03-1949	03-1987	962
	4035403	A	Coryell	Hosston	07-1949	04-1986	828
	4035404	B	Coryell	Hosston	07-1955	12-2024	755
	4036601	C	Coryell	Multi-aquifer	04-1956	07-2024	1,170
	4035804	D	Coryell	Middle-Lower Trinity	01-1943	04-1987	745
	4041903	E	Coryell	Glen Rose	10-1968	07-2024	271
	4041202	F	Coryell	Hensell	03-1970	07-2024	420
	4140903	G	Coryell	Hensell	01-1969	07-2024	440
	4140803	H	Coryell	Hensell	04-1966	01-2005	372
	3155301	A	Erath	Multi-aquifer	12-1959	02-1995	520
	3249501	B	Erath	Lower Trinity	10-1965	05-2024	512
	3162901	C	Erath	Hensell and Pearsall	08-1972	05-2023	333
	3162803	D	Erath	Hensell	10-1965	01-2023	265
	4106501	E	Commanche	Hensell and Pearsall	10-1959	06-2024	250
	4114102	F	Commanche	Hosston	10-1959	06-2024	179
	4112902	G	Commanche	Hensell and Pearsall	03-1970	06-2024	112
Mills and Hamilton Co (figure 2-39)	4124301	A	Hamilton	Glen Rose	04-1967	10-2016	177
	4017702	B	Hamilton	Glen Rose and Hensell	09-1964	01-1999	327
	4124801	C	Hamilton	Glen Rose and Hensell	05-1966	10-2024	432
	4123401	D	Hamilton	Hensell	08-1961	01-1997	362
	4138101	E	Mills	Hensell and Pearsall	06-1955	12-2003	325
	4137303	F	Mills	Glen Rose	04-1966	10-2024	213
Falls Co (figure 2-40)	4048201	A	Falls	Pearsall and Hosston	06-1957	10-2012	2,640
	4048801	B	Falls	Pearsall	03-1966	10-2023	2,874
	4047602	C	Falls	Hosston	08-1965	10-2012	2,609
	4056102	D	Falls	Hosston	02-1968	10-2022	2,765
	4064101	E	Falls	Hosston	05-1959	10-2024	3,060
Clearwater UWCD (figure 2-41)	4053406	A	Bell	Hosston	01-1967	06-2024	1,192
	4063501	B	Bell	Hosston	10-1965	06-2024	3,200
	4061509	C	Bell	Hosston	03-1952	12-2024	1,261
	5806102	D	Bell	Hosston	07-1955	12-2023	2,210
	5805403	E	Bell	Hensell	03-1966	10-2023	1,630
	5804103	F	Bell	Glen Rose	07-1960	10-2023	767
	5803901	G	Bell	Hensell	06-1951	03-1984	857

Central Texas GCD and Williamson Co (figure 2-42)	5810303	A	Williamson	Hensell and Pearsall	08-1966	10-2016	728
	5829603	B	Williamson	Pearsall and Hosston	08-1946	12-2024	3,335
	5817902	C	Williamson	Hosston	10-1967	10-2024	740
	5724501	D	Burnet	Hosston	04-1967	02-2009	460
	5724101	E	Burnet	Middle-Lower Trinity	01-1958	12-2024	480
	5715601	F	Burnet	Pearsall	12-1968	02-2012	205
	5715502	G	Burnet	Pearsall and Hosston	10-1968	02-2011	205

[1]The "Washita" listed here is a shortened form of "Washita/Fredericksburg". Note that the "Lower Trinity" designation is synonymous with the Twin Mountains and Travis Peak Formations.

[2]Well end dates are current as of December 2024.

[3]The hydrogeologic unit assigned to each well is based on the well screened interval (reported or estimated); therefore, the well depth is listed to provide general information on well construction.

2.3.4.1 Trends through 1960

By the mid-1950s, water levels in wells in Dallas County were rapidly declining (Figure 2-30) (Gard, 1957) due to substantial increases in groundwater use (Figure 2-10). Previous declines in Dallas County were as much as 450 ft from the early 1900s through the early 1940s (Kelley and others, 2014). The water level in Tarrant County in the Trinity Aquifer had also declined to a similar level, Figure 2-29) by the 1950s due to large increases in groundwater use (Figure 2-12).

By the late 1950s, wells in Grayson County had declined somewhat (Wells B and E, Figure 2-19), although Baker (1960) reports substantial declines of at least 180 feet in Sherman due to the substantial groundwater use in Sherman and Gainesville. Substantial declines were also noted in the Woodbine Aquifer in the Sherman area; however, declines in areas outside of the centers of heavy pumping in the county were less substantial (Wells B and E, Figure 2-19) (Baker, 1960). A Woodbine Aquifer well nearby in Collin County also shows a similar but greater decline (Well F, Figure 2-19). By 1960, the average water level decline in Cooke County was between about 55 and 80 ft since 1931 (Harden, 1960; Peckham, 1963).

By 1960, water levels in Hill County had declined substantially since the late 1800s, particularly after 1940, based on the available water level data (Wells E–G, Figure 2-20) (Mount, 1963). Similarly, water levels in Ellis County also experienced large declines between 1915 and the mid-1960s due to large increases in groundwater use in Ellis County and, more likely, in Dallas County (Thompson, 1967). In the Woodbine and Hosston aquifers, the decline in Ellis County during this period was 114 ft and 263 ft, respectively (Thompson, 1967). In Johnson County, a similar decline was observed in Trinity wells, whereby water levels in a well in the Trinity Aquifer declined by 254 ft (Thompson, 1969). In Navarro County to the east, water level declines of up to 420 feet since the early 1900s had occurred (Well H, Figure 2-20) (Thompson, 1972).

2.3.4.2 1960–1980

Regionally, in the 1960 to 1980 period, many locations experienced changes in the rate of decline of their water levels. In some portions of the aquifer system, water levels leveled off or recovered, while in others, the rate of decline decreased somewhat. In general, between 1960 and 1980, large areas of substantial water level declines included the Dallas-Fort Worth Metroplex and surrounding area and the central part of the study area including the City of Waco (McLennan County) and surrounding counties.

In the center of Tarrant County, extensive Trinity Aquifer water level declines from 1960 to 1980 were recorded (Figures 2-29, 2-30). Groundwater levels in this area were as low as -277 and -233 ft above mean sea level (amsl) in 1978 (Wells E and G, Figure 2-29), and a groundwater level of -622 ft amsl was measured in 1982 (Well D, Figure 2-29). A peak in groundwater use occurred generally between about 1960 and the early 1970s (Figure 2-12). As a result, by the early 1980s the water level declines had generally leveled off across the county as access to surface water supplies had improved and groundwater use decreased. In Dallas County, there was an initial peak in groundwater use during the late 1950s, whereby use decreased by about a third through 1980 (Figure 2-10). However, substantial groundwater level declines continued through this period similar to Tarrant County before largely ceasing by the 1980s. In the northern part of the Dallas-Fort Worth Metroplex in Collin and Denton Counties, water level declines continued through this period, although declines were modest in central and eastern Collin County (Figures 2-25, 2-26). In western Collin County and across Denton County, water level declines were substantial, averaging about 9 feet per year due to successive annual increases in groundwater use during this period (Figure 2-11).

To the north of the Dallas-Fort Worth Metroplex, water level declines were also substantial in Cooke and Grayson Counties between 1960 and 1980 (Figures 2-23, 2-24) due to annually increasing groundwater use during this period (Figure 2-11). In Grayson County, the Trinity Aquifer experienced declines of between 7 and 15 feet per year during this period, whereas Trinity Aquifer declines in Cooke County were smaller—between 4 and 7 feet per year. To the northeast of the Dallas-Fort Worth Metroplex, groundwater level changes were moderate, with some wells showing increases in the water level, and others decreases (Figure 2-22).

To the south of the Dallas-Fort Worth Metroplex, large groundwater level declines were observed in the Trinity Aquifer between 1960 and 1980 in Johnson and Ellis Counties (Figures 2-31, 2-32) due to steadily increasing groundwater use in both counties between 1960 and 1980 (Figure 2-13). In eastern Johnson County, annual declines in the Trinity Aquifer were more than 15 feet per year. In central and western Ellis County, interpolated declines of between 21 and 28 feet per year were recorded, although little data is available during most of this period.

Extensive groundwater declines also occurred between 1960 and 1980 in the central part of the study area centered on McLennan County. In McLennan County, Trinity Aquifer groundwater level declines were substantial, averaging about 215 feet between 1960 and 1980 (Figure 2-35). This was due to the steadily increasing annual groundwater use rates in McLennan County during this period (Figure 2-15). Trinity Aquifer water levels were as low as 88 ft amsl by 1980 in the county, and annual water level declines in the Trinity Aquifer were between about 8 and 15 feet per year between 1960 and 1980. To the north in Hill County, water level decline rates in the Trinity Aquifer were similar to McLennan County, between about 6 and 16 feet per year (Figure 2-34), due to increasing groundwater use rates during this period (Figure 2-13). To the west in Bosque County, annual groundwater level declines in the Trinity Aquifer were fairly steady (Figure 2-36), due to increasing groundwater use during this period (Figure 2-14). Annual groundwater level decline rates in Bosque County were between about 5 and 11 feet per year—also similar to McLennan County, but at a somewhat lower rate. In Coryell County, Trinity Aquifer declines in the eastern part of the County were similar to McLennan County (Wells A, C, and D, Figure 2-37), although at a rate of about 8 to 10 feet per year. To the southeast in Falls County, annual Trinity Aquifer declines in the western part of the county were between about 5 and 9 feet per year (Figure 2-40). To the south in Bell County, annual groundwater level declines were smaller—between about 2 and 6 feet per year (Figure 2-41) between 1960 and 1980.

2.3.4.3 1980–2000

During the period from 1980 to 2000, water level change rates varied across the study area. Some of the water level trends from the 1960 to 1980 period persisted; however, the decrease in groundwater use (and increase in surface water use) in some areas resulted in smaller water level declines to slight recoveries compared to prior years. In general, (1) the substantial water level declines in the immediate Dallas-Fort Worth Metroplex during the previous eighty years lessened considerably, (2) the ongoing water level declines to the north of the metroplex and in the center of the study area from prior years continued.

In the Dallas-Fort Worth Metroplex, the 1980-2000 timeframe marks a transition from the large continual groundwater level declines prior to 1980 to a period largely absent of these declines in 2000–2020. In Tarrant County, Trinity Aquifer water level changes were between about 50 ft of recovery and 14 ft of decline between 1980 and 2000 (Figure 2-29) due to decreases in groundwater use (Figure 2-12). This period marks the first time that Trinity Aquifer water levels across Tarrant County were generally not experiencing regular large decreases. Historical water level minimums were generally reached in the county beginning in the mid-1970s—coincident with the maximum groundwater use period—although this minimum level did not occur in some wells until around 2010 (Well H, Figure 2-29). Similarly, in Dallas County, water level changes were between about 20 feet of recovery and 45 feet of decline between 1980 and 2000 (Figure 2-30). A second peak in Dallas County groundwater use occurred in the mid-1980s, followed by a sharp subsequent decline in use (Figure 2-10). In Johnson County, water levels began to stabilize in the 1980s (Figure 2-31) following an initial peak of groundwater use in the late 1970s (Figure 2-13). However, in Ellis County, water levels declined throughout this period at a rate of generally 19 to 31 feet per year until reaching historical minimums in the early to mid-2000s (Figure 2-32). This was due to groundwater use that rapidly increased between 1980 and 1985 and remained at a (nearly) historical maximum for the following five years until decreasing to the 1983 level by 2000 (Figure 2-13). In Denton County, water levels declined steadily at a rate of generally 5 to 7 feet per year from 1980 to 2000 (Figure 2-25) due to annual increases in groundwater use during this period (Figure 2-11).

Water level declines in Grayson and Cooke Counties between 1980 and 2000 followed similar trends from the prior period (Figures 2-23, 2-24) due to groundwater use remaining near a historical peak (Figure 2-11). In Grayson County, the Trinity Aquifer experienced declines of between 4 and 8 feet per year during this period, whereas Trinity Aquifer declines in Cooke County were smaller—between 1 and 7 feet per year. To the northeast of the Dallas-Fort Worth Metroplex, Paluxy Aquifer groundwater level changes were between 1 to 3 feet per year (Figure 2-22).

In McLennan County, Trinity Aquifer the average groundwater level decline was about 250 feet (Wells A, D, E, G; Figure 2-35) due to regular increases in groundwater use during this period (Figure 2-15).

Average groundwater level decline rates were between 12 and 16 feet per year (Wells A, D, E, G; Figure 2-35). In Hill County, water level decline rates in the Trinity Aquifer were between about 6 and 10 feet per year (Figure 2-34), due to increasing groundwater use rates during this period (Figure 2-13). In Bosque County, annual groundwater level declines in the Trinity Aquifer were fairly steady (Figure 2-36), averaging between 4 and 11 feet per year, due to increasing groundwater use during this period (Figure 2-14). In Falls County, annual Trinity Aquifer declines in the western part of the county were similar to the 1960-1980 period—between about 5 and 9 feet per year (Figure 2-40). In Bell County, annual groundwater level declines were likely similar to 1960-1980, although decline rates for some wells decreased (Wells A and G, Figure 2-41) and several wells do not have water level measurements during this period (Wells E and H, Figure 2-41).

2.3.4.4 2000–2024

During the period from 2000 to 2024, water level change rates continued to vary across the study area. In general, the substantial water level declines across much of the central and northern parts of the study area from prior years had largely begun to attenuate during this period, whereas water level declines in the central to southern part of the study area continued, if at a somewhat reduced rate. The 2000 to 2024 period includes the formation of several GCDs in the study area, and continued regulation of groundwater in previously established GCDs.

In the central to northern part of the study area, historical water level minimums were reached in most wells in Cooke, Grayson, Denton, and Collin Counties (Figures 2-23 through 2-26). Water level changes between 2000 and 2024 were generally less than 30 feet for many wells in Cooke, Grayson, and Denton Counties, although two wells in Cooke County (Wells E and G, Figure 2-24) had declines of about 40 ft, and two wells in Grayson County (Wells C and G, Figure 2-23) had declines between 80 and 153 ft. The smaller groundwater level changes were due to the stabilization of the large continual growth in groundwater use in these counties year over year generally prior to 2000. In Tarrant, Dallas, Johnson, and Ellis Counties, water levels were largely static or recoveries occurred in most wells where data is available (Figures 2-29 through 2-32) due to the large decreases in groundwater use that had begun in the 1970s and 1980s in Tarrant and Dallas Counties (Figures 2-10, 2-12) and in Johnson County beginning in the mid-2000s (Figure 2-13). In Ellis County, water levels did not appreciably decrease even though groundwater use increased between 2000 and 2020. However, the substantial groundwater use declines in Dallas County to the north likely accounted for the minor changes in water levels in Ellis County.

In the central to southern part of the study area, groundwater level declines continue similar to prior years. In McLennan County, declines ranged from 30 to about 200 feet, although the water level in one well recovered by about 60 feet (Figure 2-35). Groundwater use generally increased during this period; however, a decline in use occurred from about 2013 onward (Figure 2-15), which is reflected in lower rates of water level decline (and some recovery) from 2013 to 2024. In Hill County, declines ranged from about 115 ft to 288 ft (Figure 2-34), due to continued increases in groundwater use during this period (Figure 2-13). In Bosque County, groundwater level declines in the Trinity Aquifer were between 84 and 193 ft (Wells D and F, Figure 2-36), although a Hensell well recovered by about 2 ft during this period (Well A, Figure 2-36). In Coryell County, Trinity Aquifer declines in the eastern part of the County were about 105 to 151 ft (Wells B and C, Figure 2-37), although water level changes varied across the rest of the county. In Falls County, Trinity Aquifer declines in the western part of the county were about 60 to 170 ft between 2000 and 2024 (Figure 2-40). In Bell County, groundwater level declines were between about 60 to 200 ft (Figure 2-41).

2.3.4.5 Outcrop Area

In general, hydraulic heads in the outcrop area show less water level change than the downdip areas. In Montague, Wise, and Parker Counties, the only appreciable water level change from the hydrographs is in a Hosston well in Wise County (Well F, Figure 2-27) where drawdowns due to pumping were captured when water level measurements were taken at this well. In Hood County, Well E (Figure 2-28) shows variations in water levels of about 100 ft, but the starting and ending water level is similar, whereas Well H has a water level decline of about 150 feet between 1965 and 2023 (Figure 2-28). In Erath and Commanche Counties, water levels were relatively stable other than Well A (Figure 2-38) which may be an errant first-water measurement from when the well was drilled. Water levels in Hamilton and Mills Counties (Figure 2-39) are also relatively stable through time. Water levels were likewise stable in Burnet County (Figure 2-42) through time.

2.4 Groundwater Quality

The groundwater quality of the northern Trinity and Woodbine aquifers has been studied extensively and new data from this model update was limited. This section provides a short review of key studies, followed a summary of Kelley and others (2014) focusing on hydrochemical facies, total dissolved solids (TDS) and chloride, and how these inform regional flow as well as recharge and discharge.

2.4.1 Previous Studies

Groundwater quality in these aquifers has been the subject of numerous investigations, starting with early work by Hill (1901). County reports across the region provide a wealth of water quality data, supplemented by regional studies conducted by organizations such as the TWDB and its predecessor agencies. Important contributions include analyses by Klemt and colleagues (1975), Nordstrom (1982 and 1987), and more recent works by Chaudhuri and Ale (2013).

Groundwater quality in the aquifers is shaped by natural geochemical processes as water moves along flow paths from recharge to discharge areas. Groundwater typically becomes more mineralized with increased residence time. For example, lignite deposits in the Woodbine Aquifer in southern Tarrant and Johnson counties contribute to higher sulfate concentrations (Bradley, 1999). Geological features such as the Mexia-Talco Fault Zone and the BFZ also influence groundwater quality by facilitating cross-formational flow. Anthropogenic activities, including oil field brine disposal and agricultural runoff, have further affected water quality in some areas, particularly near outcrops.

Studies have highlighted the role of cross-formational flow in degrading water quality. Excessive drawdown in the northern Trinity Aquifer has exacerbated this issue, with multi-completed wells allowing for mixing between different stratigraphic units. Ambrose (1990) linked high TDS water in the Hosston Aquifer near Dallas to drawdown-induced flow from the Glen Rose Formation. These findings underscore the interconnection of aquifers in the system and the need for careful management.

More recent studies have documented changes in groundwater quality over time. Diehl (2011) reported increasing TDS with depth in McLennan County, with steeper gradients in the Hensell Aquifer compared to the Hosston Aquifer. Chaudhuri and Ale (2013) observed an overall improvement in water quality in outcrop areas, which they attributed to better regulation of oil field brine disposal. However, groundwater levels in the region have continued to decline, reflecting ongoing challenges in balancing water use and conservation.

Kelly and others (2014), which is the primary reference for this section, provides a comprehensive evaluation of groundwater quality trends and hydrogeochemical processes in North-Central Texas. Drawing on historical and recent data, the study highlights the dominant influence of geochemical evolution, structural features, and cross-formational flow on water quality. It emphasizes increasing TDS and sulfate concentrations downdip, with calcium-bicarbonate facies marking recharge zones and sodium-chloride facies indicating older, more mineralized water. Notably, vertical leakage from overlying units such as the Glen Rose Formation contributes significantly to confined aquifer recharge, while fault zones facilitate both recharge and discharge through cross-formational mixing. The study also maps the spatial extent of freshwater, identifying key limitations due to lithology and anthropogenic impacts, and supports conceptual models of regional flow using hydrochemical facies and TDS-chloride gradients.

Robinson, Deeds, and Lupton (2019) conducted a focused assessment of brackish groundwater within the Northern Trinity Aquifer system as part of the Texas Water Development Board's efforts to support brackish water development under House Bill 30. Their technical note synthesizes hydrogeologic data, geophysical well logs, and groundwater quality measurements to delineate zones with total dissolved solids (TDS) between 1,000 and 10,000 mg/L—commonly referred to as "brackish" groundwater. The authors identified and mapped potential production zones within multiple stratigraphic units of the aquifer system, including the Hosston, Pearsall, Hensell, Glen Rose, and Paluxy formations. These zones were evaluated based on depth, thickness, salinity, and proximity to known production areas. The study also flagged areas with limited data or geologic constraints and provided guidance for future development and monitoring.

2.4.2 Geochemical Evidence of Regional Flow

The chemical composition of groundwater provides important clues about regional flow systems. As recharge water infiltrates the surface and migrates through aquifers, it undergoes a series of chemical transformations driven by interactions with soil and rock. Chebotarev's classic 1955 model describes an evolutionary sequence for anions that generally progresses from bicarbonate-dominated waters in recharge areas to sulfate- and chloride-dominated waters in older, deeper, and more sluggish flow zones. This framework has been validated in other studies, including those by Ophori and Toth (1989) in Alberta and Back (1966) in the Atlantic Coastal Plain. These studies found that recharge areas are characterized by low TDS, high calcium-to-magnesium ratios, and bicarbonate dominance, while discharge areas tend to have high TDS, lower calcium-to-magnesium ratios, and elevated sulfate and chloride levels.

The Northern Trinity and Woodbine aquifers display similar patterns. Geochemical zoning reflects residence time, depth, and proximity to recharge sources. These transitions in water chemistry reflect changes in flow direction, aquifer connectivity, and the effects of geological layering and faulting.

2.4.3 Hydrogeochemical Facies

Hydrogeochemical facies are shown for each aquifer and formation in Kelley and others (2014), Figures 4.4.2 to 4.4.8. A hydrogeochemical facies is defined as a zone where groundwater chemistry is dominated by particular ions—such as calcium, magnesium, sodium, bicarbonate, sulfate, or chloride. These facies were constructed using chemical data converted from concentrations (mg/L) to milliequivalents per liter, a measure that standardizes for ion charge. The resulting facies maps reveal spatial patterns that align with both recharge zones and structural or depositional boundaries.

Recharge zones were consistently marked by calcium and calcium-magnesium facies, while more distal regions showed increased presence of sodium and chloride, reflecting ion exchange and evaporite dissolution. In the Paluxy, Glen Rose, Hensell, Pearsall, and Hosston formations, calcium and calcium-magnesium facies were widespread in outcrop areas, strongly suggesting active recharge. The presence of similar facies across multiple formations supports the conclusion that cross-formational flow is occurring, likely aided by high pumping rates, multi-completed wells, and vertical conduits such as fractures and faults.

In the Woodbine and Washita/Fredericksburg units, recharge signals (e.g., calcium-magnesium facies) were evident but more limited, possibly due to fewer data points or more restricted recharge conditions. The Glen Rose Formation's facies patterns varied with depositional environment: marginal marine sandstone areas exhibited different chemistries than marine shelf limestone zones, which had more prevalent sulfate facies due to evaporite minerals like gypsum and anhydrite. Similarly, sodium-chloride facies in the Hosston Aquifer were observed in several counties, potentially due to upwelling of deeper brines or saltwater migration along faults.

Some facies transitions also align with mapped depositional systems, suggesting that changes in sediment composition influence groundwater chemistry. In areas where calcium-bicarbonate waters give way to sulfate or chloride dominance, the underlying lithology often shifts from clean sandstone to clay-rich or evaporitic deposits.

2.4.4 TDS and Chloride Distribution and Freshwater Limits

Maps of TDS and chloride concentrations are shown for each aquifer and formation in Kelley and others (2014), Figures 4.4.9 to 4.4.22. These maps delineate the extent of usable freshwater and also help to interpret hydrochemical processes. TDS thresholds are a common basis for water classification: fresh water contains less than 1,000 mg/L, brackish water between 1,000 and 10,000 mg/L, and saline water exceeds 10,000 mg/L. Chloride standards are similarly defined, with secondary drinking water standards set at 250–300 mg/L.

In the Hosston Aquifer, freshwater extends over 100 miles downdip in areas like Falls County, an unusually long reach attributed to high sand connectivity and possible deep discharge mechanisms. In contrast, the Woodbine Aquifer loses freshwater character within 5–20 miles of the outcrop, likely due to the presence of sulfate-bearing materials like lignite and gypsum. In some regions, elevated chloride and TDS values appear to be the result of anthropogenic impacts such as oilfield brine pits or leaking well casings, while in other locations they reflect natural upwelling of deeper saline water, especially near faults or where Paleozoic rocks underlie the aquifers.

Across many formations, abrupt transitions in TDS and chloride concentrations coincide with known fault zones or regions of reduced transmissivity. However, the data suggest that faults with offsets less than 100 feet generally do not form significant barriers to flow. Instead, these structures may actually enhance vertical mixing, particularly where hydraulic gradients are strong or well densities are high.

2.4.5 Implications for Recharge and Discharge Boundaries

Hydrochemical mapping strongly supports the conclusion that outcrop zones of all seven studied formations are active recharge areas. The presence of calcium and calcium-magnesium facies, often near the surface or in areas of high precipitation and permeable soils, aligns well with mapped outcrops. Furthermore, recharge is not confined to direct infiltration through the outcrop; vertical leakage through overlying units such as the Glen Rose and Fredericksburg groups also plays a major role.

Rapp (1988) estimated that up to 80 percent of the effective recharge to the confined Trinity units originates from vertical leakage. This mechanism significantly enlarges the effective recharge area beyond the narrow outcrop belt, extending the reach of modern water input into deeper and more confined zones of the aquifer system.

The maps of TDS and chloride concentrations also inform the conceptual model of groundwater discharge. The presence of freshwater in the downdip reaches of the Hosston, Pearsall, and Hensell aquifers suggests that water must be discharging beyond these zones, likely east of Falls County. The primary discharge mechanism is interpreted to be cross-formational flow into adjacent formations, facilitated by fault zones like the Mexia-Talco system. Localized discharge through vertical flow paths created by faults or poorly completed wells is a secondary, though still important, process.

Predevelopment conditions likely featured a vertical gradient from the Hosston upward to the Hensell, allowing discharge through faults and sandy formations. The Glen Rose Formation, acting as a semi-confining unit, allowed only limited upward flow, but its capacity for leakage appears to be greater in areas where overlying aquifers have sandy rather than shaley lithologies. Where the Hensell transitions from sand to shale (e.g., in Bell and Coryell counties), discharge appears to decline, and flow may even reverse due to pumping, resulting in downward movement of degraded water into deeper units.

In areas with multi-aquifer well completions, mixing among formations is likely. The absence of freshwater in parts of Bell and Coryell counties may be attributed to structural barriers, decreased transmissivity, or induced downward gradients that draw in more mineralized water from overlying units.

2.5 Recharge and Groundwater Flow

Recharge is defined in this study as the downward flow of water reaching the water table and increasing groundwater storage (Healy, 2010). Recharge represents the primary inflow to the aquifer, which constrains the water balance of the aquifer system under predevelopment conditions (prior to pumping). Recharge is generally considered a rate or flux, with units of length over time similar to precipitation, and is generally reported in inches per year. The following subsections describe the conceptual understanding of recharge as it pertains to the study area, review recharge estimates from previous studies that include the study area, and present recharge estimates using the Soil-Water-Balance code.

2.5.1 Conceptual Framework

In the northern Trinity and Woodbine aquifer system, groundwater recharge occurs in the outcrop zone of the aquifer system (Figure 1-4), and groundwater discharge occurs at streams through base flow and as ET by riparian vegetation along streams. Groundwater recharge, in this report, is defined as water that infiltrates from the land surface through the unsaturated zone to the top of the water table (saturated zone) in the shallow system. Most of the water that recharges the northern Trinity and Woodbine aquifer system infiltrates downward to the topographically controlled shallow saturated zone and flows to nearby streams, where the water is discharged as base flow. Recharge to local flow systems occurs in topographically high areas, and discharge occurs in nearby, topographically low areas. In this way, much of the recharge enters and exits the shallow groundwater system within relatively localized sections of the aquifer system; however, some fraction of recharge may penetrate deeper into the confined portion of the aquifer in the outcrop area before discharging to surficial features. An even smaller fraction of recharge moves deeper into the confined portion of the aquifer located downdip of the outcrop area and regionally discharges through younger overlying sediments or through structural features such as faults.

The northern Trinity Aquifer has a large outcrop area (7,634 square miles), while the Woodbine Aquifer has a smaller outcrop area (1,726 square miles). The Washita/Fredericksburg groups crop out between the northern Trinity and Woodbine aquifers with an area of 7,869 square miles. While the Washita/Fredericksburg groups are considered a confining unit over much of the study area, recharge does occur in this unit. Recharge rates are considered to be lower than for the more permeable outcrops of the northern Trinity and Woodbine aquifers. A potential exception is the Edwards BFZ Aquifer.

2.5.2 Previous Investigations

Information on measured recharge rates in the northern Trinity and Woodbine aquifers is limited. Recharge rates were compiled by Scanlon and others (2002a) for major aquifers in Texas. That report, however, referenced only two modeled estimates of recharge in the northern Trinity and Woodbine aquifer system, with rates ranging from 0.02 to 4.4 inches per year, both of which are given in Dutton and others (1996). Other recharge references in the northern Trinity and Woodbine aquifer system generally assumed a specific rate (e.g., less than 1 inch per year in Nordstrom [1982] and 0.5 inches per year in Thompson [1969] for sandy portions of the aquifer in Johnson County). Others assumed recharge as a percentage of mean annual precipitation (i.e., 3 percent of mean annual precipitation in Klemt and others [1975], 1.5 percent of mean annual precipitation in Muller and Price [1979], and Duffin and Musick [1991]). Klemt and others (1975) also report an estimated regional recharge to the confined portion of the Paluxy Aquifer of 0.13 inches per year (0.3 percent of precipitation) and to the confined portion of the Woodbine Aquifer of 0.3 inches per year (0.75 percent precipitation).

Rapp (1988) studied recharge processes in the northern Trinity and Woodbine aquifer system in central Texas in the Leon, Lampasas, and Paluxy River basins. This study suggests that approximately 20 percent of recharge (5,000 AFY or 0.12 inches per year) to the northern Trinity and Woodbine aquifer system is derived from sandy parts of the outcrop area, representing about 25 percent of the aquifer outcrop area. He attributed the remaining 80 percent (20,000 AFY or 0.16 inches per year) of recharge to cross-formational flow through the overlying Glen Rose Formation and Washita/Fredericksburg Groups based on groundwater head data and chemistry data.

In Oklahoma, where the northern Trinity Aquifer is termed the Antlers Aquifer, several investigators have estimated recharge through low-flow studies. Hart and Davis (1981) used low-flow discharge from Davis and Hart (1978), Westfall and Cummings (1963), and Laine and Cummings (1963) to estimate that it would require recharge of approximately 3.2 inches per year to account for the observed flows in creeks draining portions of the Antlers Aquifer outcrop. They then increased that value to account for ET and cross-formational flow, resulting in a total recharge value of 6 inches per year for the Antlers Aquifer outcrop in Oklahoma and western Arkansas.

Many estimates of recharge in the northern Trinity and Woodbine aquifers have been determined through history matching of groundwater models. When considering estimates of recharge from modeling studies, it is important to recognize what Johnston (1997) calls “the scale problem.” As a general rule, for properly constrained groundwater models, the scale of the horizontal model grid and the scale and number of model layers impact the estimate of recharge that a model may predict. The model grid size is the model spatial integration scale, and if it is very large, the possibility of properly modeling recharge and discharge processes becomes problematic. As a result, very large models typically have calibrated recharge estimates that are smaller than those of finer-scale models. This is particularly true if a hydrologic system consists of substantial near-surface flow components, such as areas with large topographic variability and multiple small ephemeral streams and seeps. As a rule, Johnson (1997) found that the larger the model grid, the more likely that recharge would be underestimated through model history matching.

Klemt and others (1975) performed a study of the groundwater resources of a 20-county area of central Texas. As part of that study, they present an early digital groundwater model of the Hensell and Hosston aquifers. The applied recharge in the model was approximately 3 percent of precipitation. Although they did not model these aquifers, they also reported an estimated recharge rate for the Paluxy and Woodbine aquifers of 0.13 and 0.3 inches per year, respectively. Klemt and others (1975) assumed that their recharge estimates were more representative of recharge to the confined portions of the aquifer and were not representative of total recharge.

Morton (1992) developed a groundwater model of the Antlers Aquifer (northern Trinity Aquifer equivalent) in Oklahoma and Arkansas. Calibrated recharge rates ranged from 0.32 to 0.96 inches per year. Dutton and others (1996) developed two models of the northern Trinity Aquifer near the Superconducting Super Collider site in north-central Texas. The two models focused on the Twin Mountains, Paluxy, and Woodbine aquifers. Dutton and others (1996) first developed a two-dimensional cross-section model that included the aquifers and the confining layers. The purpose of this model was to “evaluate model boundary conditions and the vertical hydrologic properties of the confining layers” (Dutton and others, 1996). The range in simulated recharge from the cross-sectional model was 0.02 to 0.5 inches per year. Because this model effectively cut out the outcrop and shallow confined portions of the aquifer, the recharge estimates would be representative of recharge to the confined portions of the aquifer downdip of the outcrop. They then developed a three-dimensional model of the aquifers using results and insights gained from the cross-sectional model. The recharge range for that model was 2.7 to 4.4 inches per year. However, in the steady-state model, the effective recharge to the confined section downdip of the outcrop was only 0.04 inches per year.

Bené and others (2004) developed the original state GAM for the northern Trinity and Woodbine aquifers. The simulated recharge rates from the calibrated model range from 0.21 to 3.5 inches per year. Ninety-six percent of the recharge in the model discharges through groundwater ET (which was simulated to represent groundwater ET and shallow mechanisms of discharge, such as small streams and springs). Approximately 4 percent of recharge in the model discharges through simulated streams and rivers, and nearly zero recharge moves to the deep confined portion of the aquifer downdip of the outcrop in predevelopment conditions. The recharge numbers used by Bené and others (2004) appear reasonable, given the literature.

Keese and others (2005) estimated recharge for Parker County using one-dimensional unsaturated flow modeling. Their best estimate of recharge rate assuming a vegetated, texturally variable soil profile was 1.1 inches per year. The modeling analysis in their study showed the importance of soil texture and vegetation in reducing recharge because recharge as a function of precipitation alone (mean annual precipitation of 34 inches per year in the model) in bare sandy soils was as high as 16.7 inches per year. The impact of vegetation alone resulted in a recharge rate of 7.6 inches per year for vegetated sandy soils. Therefore, finer textured soils, soil textural layering, and vegetation have a large impact on actual recharge rates.

Kelley and others (2014) performed stream hydrograph separation analysis (referred to as base flow analysis) on 36 stream gages and associated watersheds intersecting the outcrop of the northern Trinity and Woodbine aquifer system. Aquifer discharge to streams, or base flow, is considered to be a lower bound estimate of aquifer recharge because aquifer recharge discharges through other processes, including groundwater ET, spring discharge, cross-formational flow in the regional confined section downdip of the outcrop, and pumping capture. An estimate of the amount of recharge required to sustain the base flow of a stream was calculated by dividing the average volumetric base flow by the drainage area to obtain base flow in inches per year. Recharge estimates ranged from 0.2 to 2.9 inches per year. In Texas, these values compare favorably to those of Scanlon and others (2002a), which places average recharge to the northern Trinity Aquifer at 0.1 to 2 inches per year based on a compilation of past studies in the Texas portion of the study area.

2.5.3 Soil-Water-Balance Code

Spatially distributed recharge to the Gulf Coast aquifer system was computed for each month of the study period by using the U.S. Geological Survey Soil Water Balance (SWB) code (Westenbroek and others 2010). As described by Westenbroek and others (2010), the SWB code uses a modified Thornthwaite-Mather SWB approach (Thornthwaite and Mather, 1957) to calculate components of the water balance equation at a daily timestep. The code allows users to quickly and easily calculate spatial and temporal estimates of net infiltration out of the root zone based on climate, topography, land use, and soil data. In a GWF model, modelers may choose to simulate recharge using MODFLOW's Unsaturated Zone Flow Package (Niswonger and others, 2006; Langevin and others, 2017) or to calibrate recharge as a multiplier on the net infiltration. This discussion reflects the requirements and options associated with version 1 of the SWB code described by Westenbroek and others (2010) or at the code repository (Westenbroek, 2023).

The SWB code combines gridded and tabular input data to calculate potential groundwater recharge separately for each grid cell within a specified SWB model domain. It evaluates the sources and sinks of water within each grid cell at and near the land surface and then calculates net infiltration as the difference between the change in soil moisture along with the sources and sinks. Sources of water in the SWB include precipitation, snowmelt, and inflow (surface runoff from an adjacent grid cell), while sinks include interception (rainfall trapped and used by vegetation and evaporated or transpired from plant surfaces), and outflow (surface runoff to an adjacent grid cell), and ET. Westenbroek and others (2010) describe the calculation as:

$$R = (P + S + R_i) - (Int + R_o + P_{et}) - \Delta Sm \qquad \text{(Equation 2-1)}$$

where

R is recharge,

P is precipitation,

S is snowmelt,

Ri is surface runoff inflow,

Int is plant interception,

Ro is surface runoff outflow,

Pet is potential ET, and

ΔSm is the change in soil moisture.

Several input parameters are required to calculate ET and the change in soil moisture. Figure 2-43 illustrates the input parameters used in the SWB model calculations.

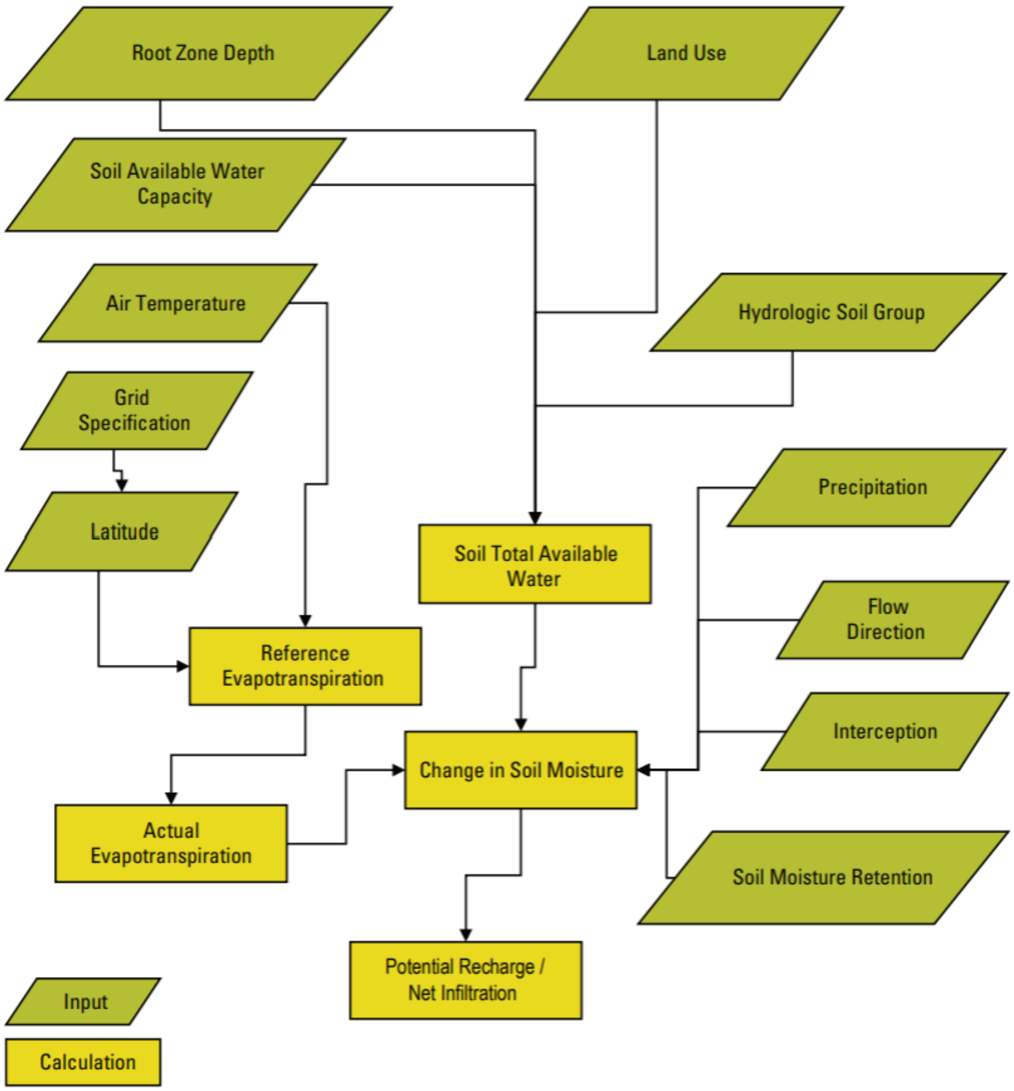

Figure 2-43. Input parameters used in the Soil Water Balance model calculations.

2.5.3.1 Climate

PRISM Climate Group (PRISM, 2023) data was utilized for the climate data inputs. Specifically, the gridded datasets for precipitation, minimum temperatures, and maximum temperatures were collected for each day from January 1, 1981, through December 31, 2022, and for each month from 1895 through 1980. Each gridded PRISM dataset covers the conterminous United States with a resolution of approximately four kilometers. After clipping each grid to the model domain, a bilinear interpolation was used to resample the grid to the model grid resolution (1,320 ft x 1,320 ft cells). In addition, the precipitation units were converted from millimeters to inches, and the temperature units were converted from Celsius to Fahrenheit, as required by the SWB model. Mean annual precipitation for the northern Trinity and Woodbine aquifer system is shown in Figure 2-44.

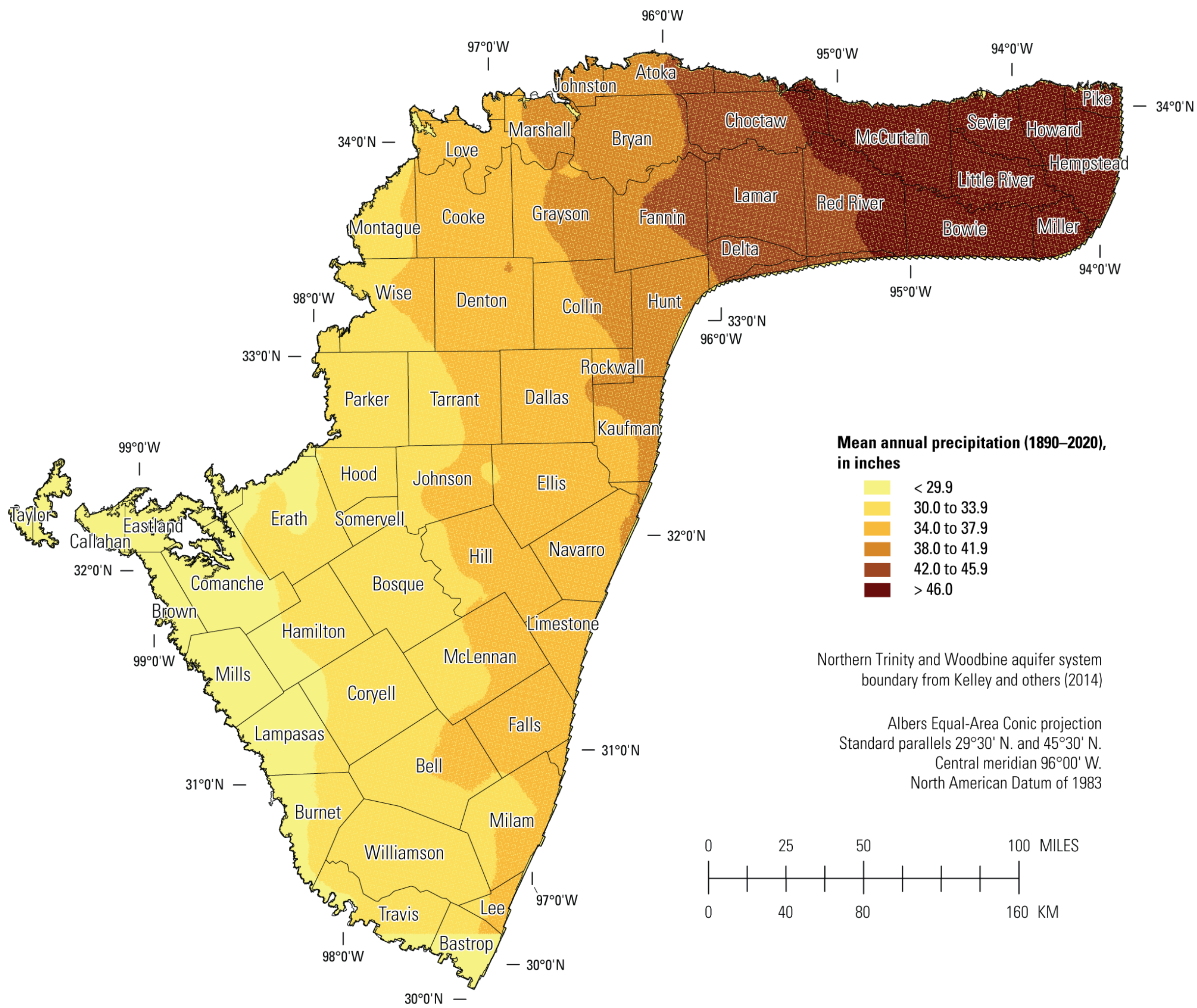

Figure 2-44. Average annual precipitation to the northern Trinity and Woodbine aquifer system.

The SWB model requires daily climate data. For data from 1890 through 1980, the "method of fragments" discussed by Westenbroek and others (2018) was applied. To apply the approach, the fragment (that is, percent) of total monthly precipitation or average monthly temperature that occurred each day of the month for the period from 1981 through 2022 was first calculated. To create daily climate grids for the period from 1895 through 1980, a year between 1981 and 2022, inclusive, was randomly selected, and the calculated fragments to the monthly data for that year were applied. For the period from 1890 through 1894, a year from 1895 through 1925, inclusive, was randomly selected to apply for the year of interest. For the steady state period (conditions prior to 1890), the average of the calculated daily values from 1895 through 1925, inclusive, was used.

2.5.3.2 Land Use, Soils, and Topography

The hydrologic soil group, along with the land use, defines how precipitation may run off or how water may be stored in the soil zone. For the SWB model, the hydrogeologic soil group and soil available water capacity data from datasets available from the Natural Resources Conservation Service (USDA-NRCS, 2022) were used. The model grid dimensions were used to calculate the area of each cell that intersected a defined hydrogeologic soil group and the group covering the most area of the cell as the single cell integer value was assigned. The same process was used to assign the soil available water capacity values as a real number to create a gridded dataset. Figure 2-45 illustrates the available water capacity for each SWB model cell, and Figure 2-46 illustrates the hydrologic soil group designations.

The physics of overland flow are determined by topography. To account for overland flow, the SWB model uses the overland flow direction at each grid cell as a model input. The overland flow direction at each grid cell is derived from a digital elevation model (DEM) for the model domain. For the SWB model, flow direction from one grid cell to another was derived by clipping a DEM to the model domain and then resampling the land surface elevation values using bilinear interpolation to create a topography grid. To fill any sinks in the gridded topography input, geoprocessing tools available within ArcGIS® were used. The flow direction using the geoprocessing tool within ArcGIS® was then calculated. The flow direction grid uses integer values to define which direction flow would occur from a cell. These integer values allow the SWB model code to route flow across the land surface. If precipitation is greater than the amount that the soil can absorb or can be captured by ET, then the flow direction value designates the direction in which outflow or runoff from the cell will occur. This runoff becomes a source of potential infiltration for the cell to which it flows.

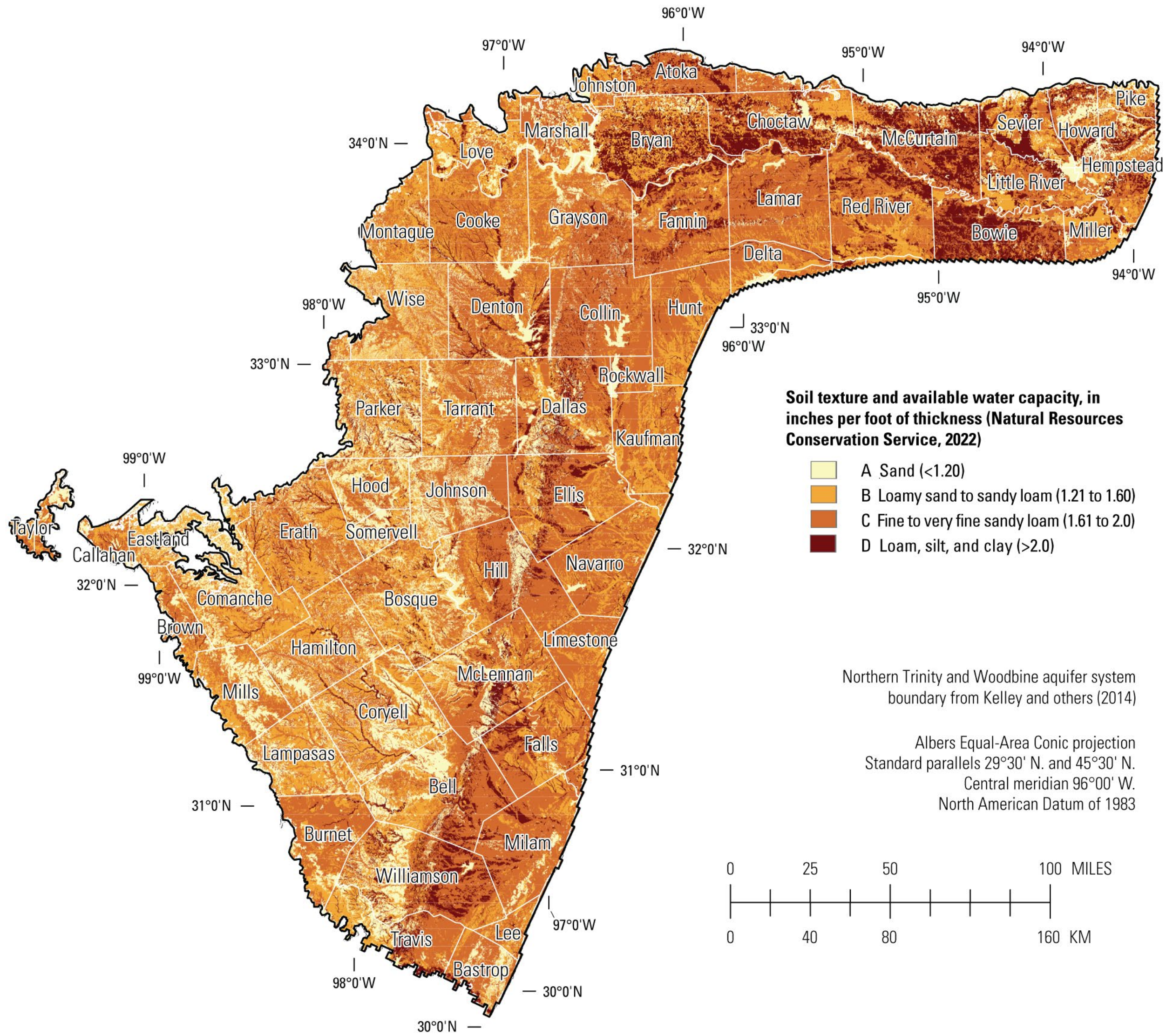

Figure 2-45. Spatial distribution of soil texture and available water capacity.

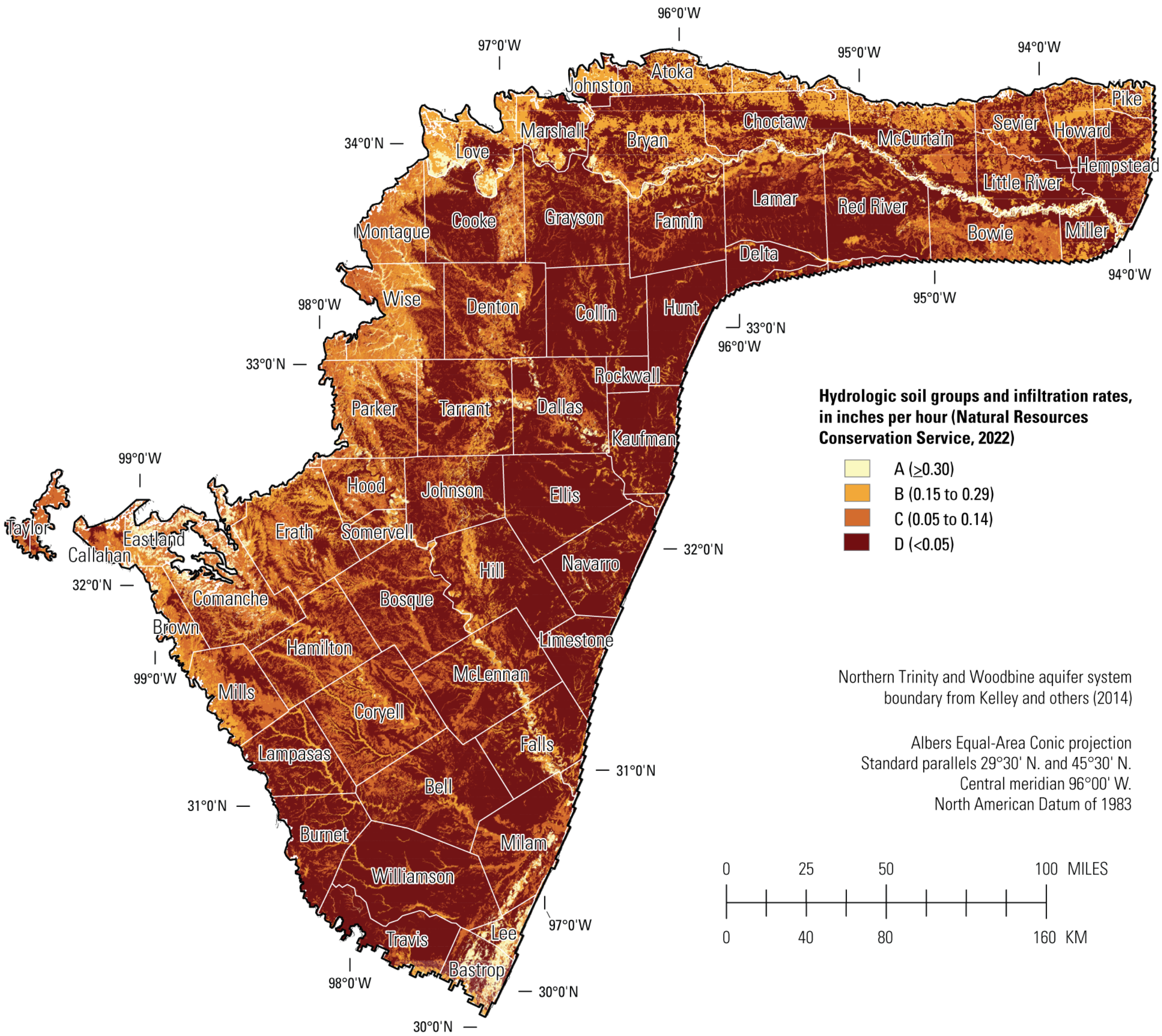

Figure 2-46. Spatial distribution of hydrologic soil groups and infiltration rates.

2.5.3.3 Tabular Input

The tabular input includes information regarding the Natural Resources Conservation Service (NRCS) curve number, rooting depth, and maximum daily recharge specific to a land use classification and hydrologic soil group. Interception values during the growing and non-growing seasons are also included in the lookup table. In addition, the SWB model code can use a soil moisture retention table for the calculations, which does not require any user modification.

Table 2-5 lists the tabular input values used for the SWB model. For these input values, values developed as part of the recharge modeling for the Edwards-Trinity (Plateau) Aquifer (Sen and others, 2022) were used. Initial values in the SWB model for the Edwards-Trinity (Plateau) Aquifer were based on published sources, which were then adjusted during model history matching. Initial curve number values were assigned based on the NRCS publication "Urban Hydrology for Small Watersheds" (USDA-NRCS, 1986). Initial growing season interception values of 0.08 inches per day for forests, 0.05 inches per day for shrubland, and 0.03 inches per day for grassland, cropland, and hay/pasture were based on estimates developed by Horton (1919) with a value of zero for the non-growing season. Initial rooting depth values were based on work by Foxx and others (1984) and Fan and others (2016). We assigned the maximum recharge rate per soil group as 2.00, 0.60, 0.24, and 0.12 inches per day for hydrologic soil groups A, B, C, and D, respectively, based on example SWB model code input values (Westenbroek and others, 2010).

Table 2-5. Soil Water Balance model land use lookup table.

Land Use Code	Land Use Description	Runoff Curve Number per Soil Group				Root Zone Depth per Soil Group, in feet			
		A	B	C	D	A	B	C	D
1	Water	100	100	100	100	0	0	0	0
2	Developed	52	73	83	88	0.58	0.44	0.26	0.21
3, 4, 5	Mechanically Disturbed (3 = National Forests, 4 = Other Public Lands, 5 = Private)	52	73	83	88	0.58	0.44	0.26	0.21
6	Mining	75	85	91	93	0.4	0.3	0.18	0.14
7	Barren	75	85	91	93	0.4	0.3	0.18	0.14
8	Deciduous Forest	30	56	71	78	54.37	40.76	24.72	19.3
9	Evergreen Forest	30	56	71	78	54.37	40.76	24.72	19.3
10	Mixed Forest	30	56	71	78	54.37	40.76	24.72	19.3
11	Grassland	28	55	67	74	0.45	2.84	0.2	0.16
12	Shrubland	37	60	75	82	1.38	1.03	0.63	0.49
13	Cropland	28	55	67	74	0.45	2.84	0.2	0.16
14	Hay/Pasture land	28	55	67	74	0.45	2.84	0.2	0.16
15	Herbaceous Wetland	28	55	67	74	2.8	2.1	1.27	0.99
16	Woody Wetland	30	49	66	69	2.8	2.1	1.27	0.99

2.5.3.4 Mesonet Climate Data

As indicated by equation 1, the change in soil moisture is an important parameter for the estimation of recharge. TexMesonet began collecting data in May 2016 (TWDB, 2023) and currently operates several stations that collect soil moisture measurements within the study area. In addition, hundreds of stations operated by other entities collect climate parameter measurements across the study area, and these data are available through Synoptic (2023). Figure 2-47 illustrates the location of the mesonet stations for which data was obtained for reference ET calculations or soil moisture estimates. There are multiple soil moisture measurements per day available for each station. The measurements are provided as the percent soil moisture at a specified depth. To develop a comparison dataset, the average percent soil moisture for each day at the deepest interval (typically 50 centimeters or about 20 inches) was calculated.

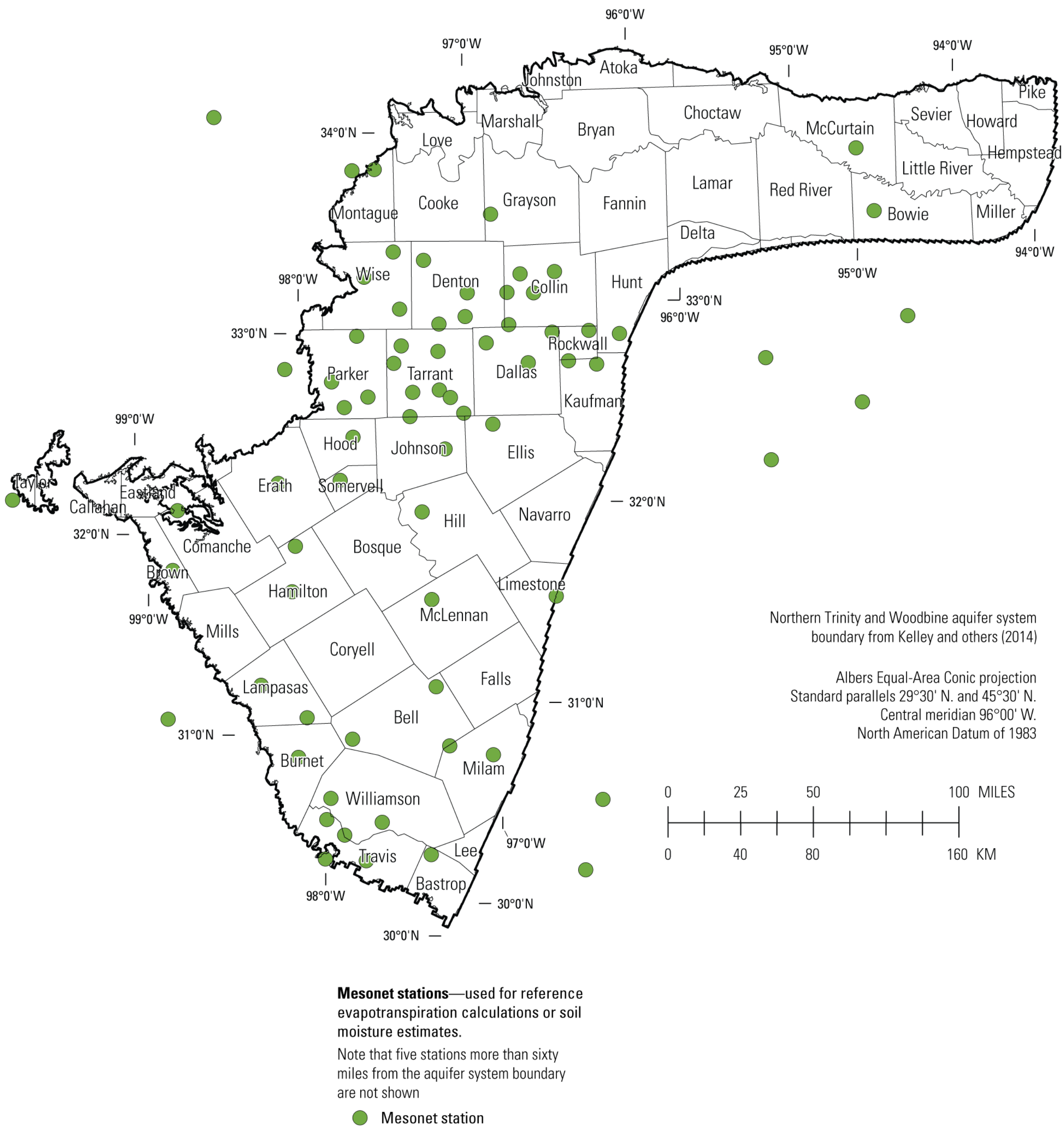

Figure 2-47. **Spatial distribution of Mesonet climate stations in and near the northern Trinity and Woodbine aquifer system**

The daily reference ET was also calculated using the Penman-Monteith equation (Allen and others, 1998). These calculations were performed using data collected at the Mesonet stations and the ET Python package (Roehrig and Villegas, 2021). Data necessary to calculate the reference ET are the station elevation and latitude, measurement date, daily minimum and maximum temperature, average wind speed, minimum and maximum relative humidity, and solar radiation. If the solar radiation data were missing, or those data were not collected at a station, the Astral Python package (Kennedy, 2022) was used to estimate the solar radiation at the station location.

2.5.3.5 Control File

The SWB model requires a control file that identifies the required input data files and parameters used in the calculations. This file also identifies the results the user desires and the time period of the simulation. In addition to the input data discussed above, the following section discusses other input values required in the control file.

For the plant growing season, the period from March 15 through October 15 of each year was used. The growing season defines whether the code will apply growing season or non-growing season interception amounts to a grid cell. Precipitation amounts must exceed the interception amount before the code uses precipitation as an input to the soil moisture calculation.

The Hargreaves-Samani (1985) equation for estimating ET with a southern latitude of 30.2835°N and a northern latitude of 34.5468°N was used. These bounding latitude values are used within the code to estimate extraterrestrial radiation. Equation 2 is the Hargreaves-Samani (1985) equation as implemented in the SWB model code.

$$\boldsymbol{ET_0} = \frac{\boldsymbol{a \times R_a \times (T_{avg} + b) \times (T_{max} - T_{min})^c}}{\boldsymbol{25.4}} \qquad \text{(Equation 2-21)}$$

Where:

$ET_0 = reference\ evapotranspiration, inches$

$R_a = extraterrestrial\ radiation, millimeters\ per\ day$

$T_{avg} = average\ air\ temperature, °C$

$T_{max} = maximum\ air\ temperature, °C$

$T_{min} = minimum\ air\ temperature, °C$

$a, b, \&\ c = empirical\ coefficients\ (default =\ 0.0023, 17.8, and\ 0.5, respectively)$

Work on the SWB model for the Edwards-Trinity (Plateau) Aquifer found that the empirical coefficient values of 0.00138, 24.49, and 0.685 for *a*, *b*, and *c*, respectively, in Equation 2 compared better with calculations using the Penman-Monteith equation. As discussed by Sen and others (2022), these modified coefficients can improve the estimate of reference ET. As such, these coefficient values using undocumented features of the SWB code (Westenbroek, 2023) were applied.

The initial soil moisture was set at a constant value of 50 percent to use in the first year of the simulation, which is a “warm-up” period for the model. For subsequent years of the simulation, initial soil moisture was set equal to the ending soil moisture of the previous year. Not including the warm-up period, the total simulation time was from January 1, 1890, through December 31, 2022.

2.5.3.6 Results

SWB output includes 1,572 two-dimensional arrays of simulated monthly recharge from January 1890 through December 2020. To aid the model simulation, and remove unrealistic large values of simulated recharge, each SWB output array was processed with a low-pass filter. The filter's upper cutoff limit was calculated separately for each month of the year as the 97.5th-percentile value (corresponding to two standard deviations [2-sigma] above the mean) of an empirical cumulative distribution function, approximately corresponding to the upper limit of a 2-sigma probability distribution. The empirical cumulative distribution function was formed for each month by combining and sorting the SWB-simulated recharge rates in active model cells from all arrays representing a given month.

Table 2-6 summarizes the average calculated recharge and reference ET per outcrop area for the northern Trinity and Woodbine aquifer system. Characteristics of the Woodbine Aquifer result in the highest simulated recharge in the model area with the lowest average rate of potential ET. The calibrated average recharge to the northern Trinity and Woodbine aquifers totals 3,657,550 AFY, which is approximately 5.9 percent of precipitation (61,628,647 AFY) model wide.

The SWB-computed recharge was determined for the spatial extent of the study area and was computed without relation to the location or depth of the water table (or potentiometric surface) for the hydrogeologic units of the northern Trinity and Woodbine aquifer system. The minimum annual mean recharge for the study period was 1.02 inches in 1964, coincident with the smallest annual amount of precipitation for the period of record (Figure 2-48). The maximum annual mean recharge was 6.98 inches in 2016, which coincides with the largest annual amount of annual precipitation for the period of record (Figure 2-48).

Table 2-6. Soil Water Balance average recharge and evapotranspiration for 1890 through 2020 to the northern Trinity and Woodbine aquifer system outcrop area.

Aquifer	Average recharge, in in/yr	Average recharge, in acre-ft/yr	Average reference evapotranspiration, in in/yr	Average evapotranspiration, in acre-ft/yr
Woodbine	4.2	428,666	62.6	6,389,165
Washita/Fredericksburg	3.1	1,044,235	64.3	21,659,455
Paluxy	3.3	326,139	64	6,325,120
Glen Rose	3.0	725,380	65.8	15,910,001
Hensell	3.2	430,133	65.3	8,777,408
Pearsall	3.5	127,832	65.8	2,403,235
Hosston	3.7	575,165	66.3	10,306,335

In general, higher recharge rates are estimated in the northern/northeastern and far western portions of the study area and lower recharge rates in the southwest and southern portion (Figure 2-49). Note that the SWB-derived recharge is representative of recharge to the shallow groundwater system, most of which would flow quickly to nearby rivers and streams and be discharged as baseflow. Only a small amount of this recharge would be expected to infiltrate downdip into the deeper portions of the aquifer system. The recharge that flows into the deeper system is described in Section 3.5.3.3.

Simulated reference ET generally increases from east to west across the model domain, with the highest values in the southwest corner of the study area. These higher reference ET values allow more water to be captured prior to infiltrating into deeper parts of the formations. The combination of higher reference ET along with less favorable soil characteristics for infiltration in the southern part of the study area results in generally lower rates of recharge in the south compared to the northeastern area.

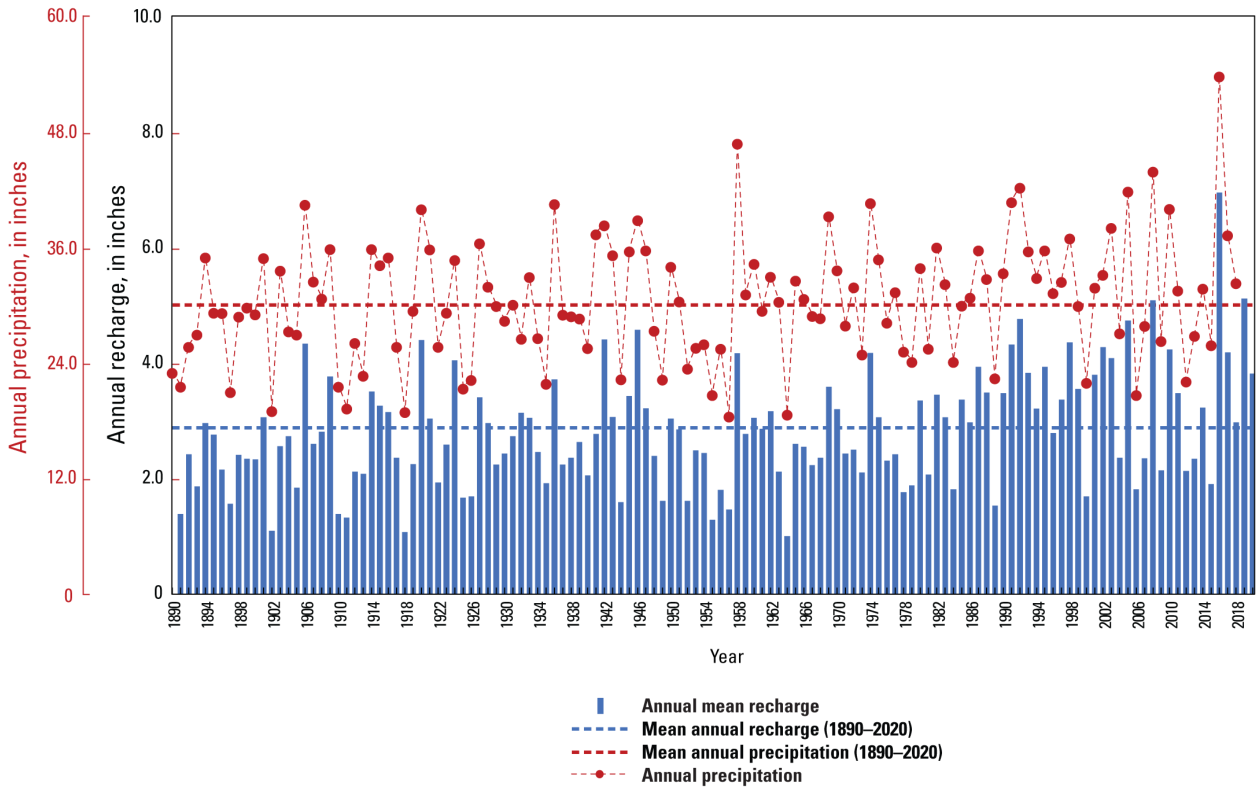

Figure 2-48. **Annual recharge and precipitation using the Soil-Water-Balance code for the northern Trinity and Woodbine aquifer system.**

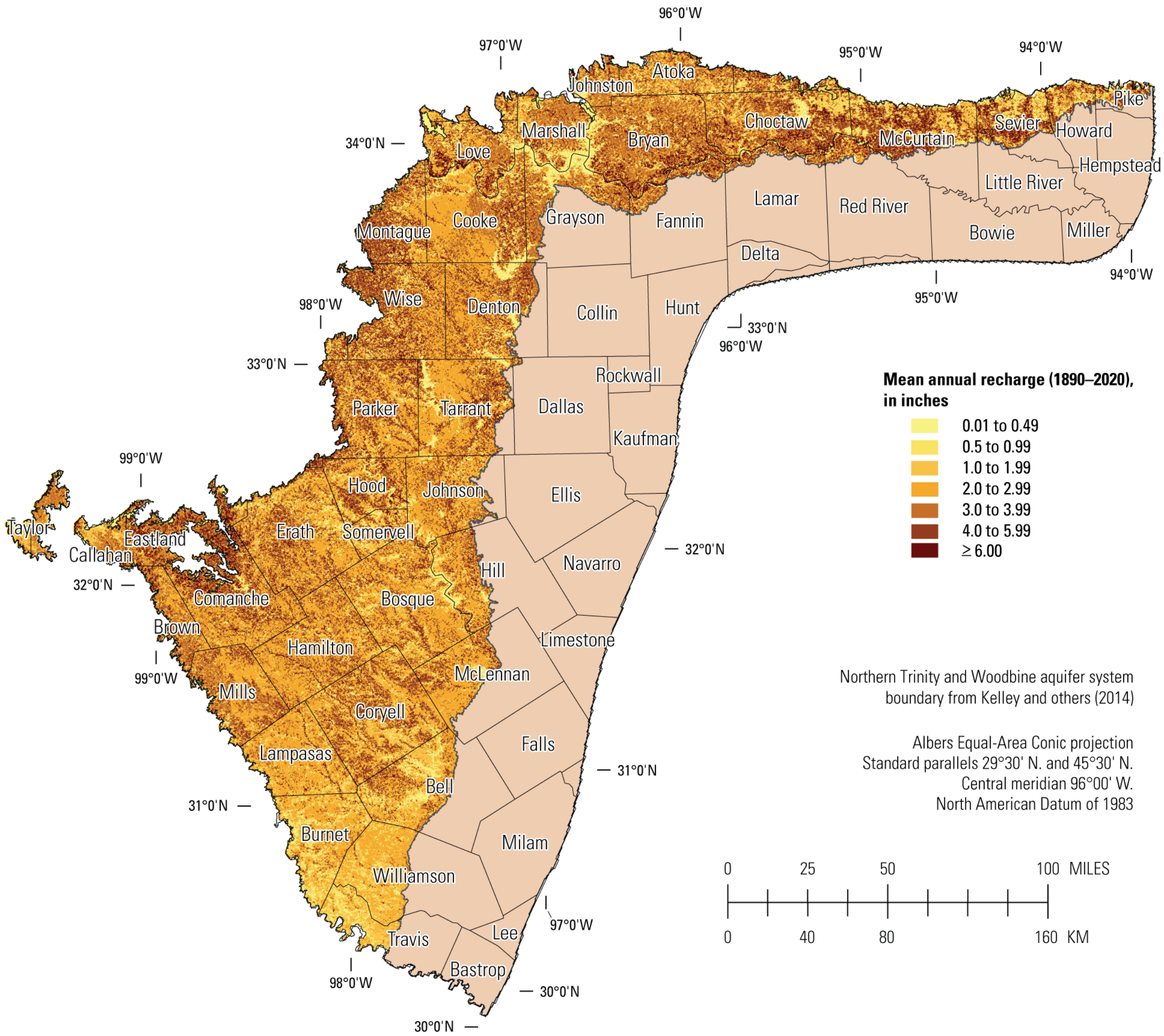

Figure 2-49. **Mean annual recharge using the Soil-Water-Balance code for the northern Trinity and Woodbine aquifer system.**

3.0 Simulation of Groundwater Flow

Groundwater flow in the NTGAM and ensemble were simulated by using MODFLOW 6 (Langevin and others, 2021) with the Newton-Raphson formulation, which facilitates the improved solution of problems involving drying and rewetting of model cells. In the modular design of MODFLOW 6, each hydrologic boundary, such as stream seepage, recharge, or groundwater use, is included as a package that, when activated, adds new inflow and outflow terms to the groundwater-flow equation being solved. Model space is discretized into cells, and the cell size is the finest resolution at which spatially changing properties can be represented and varied. Model time is discretized into time steps within stress periods. The stress period length is the finest resolution at which temporally varying inflows and outflows could be represented and varied, and the time step length is the finest length of time for which model outputs could be written.

3.1 Previous Numerical Modeling Studies

Five previous modeling studies have been conducted in the study area. The first modeling study was performed in the early 1970s for the TWDB and modeled the Travis Peak Formation over a large part of central Texas (Klemt and others, 1975). The second model simulated GWF in the Antlers Aquifer in southeastern Oklahoma and northeastern Texas (Morton, 1992). The third was performed in association with the investigation of the Superconducting Super Collider Site and considered the regional aquifers in north-central Texas (Dutton and others, 1996). The fourth was a GAM of the northern Trinity and Woodbine aquifers performed for the TWDB (Bené and others, 2004).

The model documented by Klemt and others (1975) considered the Travis Peak Formation over a large part of central Texas. The purpose of the modeling was to simulate future drawdown in the Travis Peak Formation due to estimated projected pumping to provide a mechanism for evaluating the aquifer's ability to meet anticipated future groundwater demands. The model consisted of 584 nodes, with half simulating conditions in the Hensell Aquifer and the other half simulating conditions in the Hosston Aquifer. The two members were connected using a vertical leakage value designed to represent the Pearsall Member or the Hammett and Cow Creek members of the Travis Peak Formation. The BFZ was assumed to be a barrier to flow and given lower transmissivity values than in the rest of the model. Recharge in the outcrop area was estimated to be about 3 percent of the annual precipitation.

The modeling study consisted of three parts. First, the model was calibrated to drawdowns calculated by subtracting observed water levels in the spring of 1967 from estimated 1900 water levels. Second, predicted water-level declines for the periods' spring 1967 to 1975, spring 1967 to 1990, and spring 1967 to 2020 were simulated for both the Hensell and Hosston aquifers using estimated projected pumping. Third, simulations were conducted to estimate the annual pumping required to lower the water level in the Hensell and Hosston aquifers to between 400 and 500 ft below land surface or to the top of the water-bearing sand in 2020. This reduction in water levels was considered to occur only in the portions of the aquifers between the outcrop and the downdip limit of fresh to saline water. The model results indicated tremendous water-level declines in heavily pumped areas, including one area with predicted dewatering of the Hosston Aquifer, and provided a means for estimating the available groundwater from downdip areas of the aquifers.

Conclusions from model predictions documented in Klemt and others (1975) include (1) tremendous water-level declines would occur in areas of the model with heavy pumping based on pumping projections obtained from resource planning studies. These areas include the vicinity of Belton, Gatesville, Hillsboro, McGregor, Stephenville, and Waco, (2) dewatering of the Hosston Aquifer is possible by 2020 in the area of Stephenville, and (3) water-level declines in excess of 1,000 ft by 2020 are possible in the area of Waco.

Morton (1992) developed a two-dimensional model of the Antlers Aquifer in southeastern Oklahoma and northeastern Texas. The purposes of the modeling were to predict the effects of increased pumping through 2040 on water levels and well yields and to gain an improved understanding of the aquifer, including hydraulic properties, recharge, flow, and connectivity to overlying confining units. The model, developed using MODFLOW, consisted of grid blocks with a dimension of 2 miles in the north-south direction and 3 miles in the east-west direction across the northern 85 percent of the modeled region. In the southern 15 percent of the modeled region, the size of the grid blocks was incrementally increased in the north-south direction. The model encompassed an area of about 10,000 square miles. In the confined portion of the aquifer, the overlying confining units were modeled using a specified-head boundary representing the water table. Constant-head boundaries were used to represent selected lakes and head-dependent flux boundaries were used to represent selected larger streams.

At the time the model was developed, there was little pumping from the aquifer and historical water levels indicate little to no long-term change. Therefore, a steady-state history matching was conducted using observed heads from 1970. The calibrated model had recharge of 0.32 inches per year on about the western two-thirds of the outcrop and 0.96 inches per year on about the eastern one-third of the outcrop, a hydraulic conductivity of 5.74 ft per day in the northern two-thirds of the model and 0.57 ft per day in the southern one-third of the model, and a uniform hydraulic conductivity of 2.07×10^{-4} ft per day for the overlying confining unit. The preceding values for hydraulic conductivity were taken from the text in the main body of the report. However, different values are given in the summary and conclusions section of the report. The summary section indicates that aquifer hydraulic conductivity ranged from 0.87 to 3.75 ft per year and that the vertical hydraulic conductivity of the confining units was 1.5 x 10-4 ft per day.

Morton (1992) conducted a sensitivity analysis on the calibrated model to evaluate the sensitivity of model results to the history matching parameters, which were recharge, aquifer hydraulic conductivity, and vertical conductivity of the overlying confining units. Projection simulations were conducted using estimated future pumping to predict drawdown by decade from 1990 to 2040. The predictive simulations used an average storage coefficient of 0.0005 for the confined portion of the aquifer and a specific yield of 0.17 for the aquifer outcrop.

Conclusions reported by Morton (1992) include: (1) the simulated results are consistent with the conclusion that that Antlers Aquifer is in steady state as indicated by groundwater hydrologic data, (2) because a transient history matching was not performed due to minimal pumping in the Antlers Aquifer, the head changes predicted by the projection simulations are estimates only, and (3) the projection simulations show little change in storage in the aquifer for the assumed future pumping volumes.

Dutton and others (1996) document modeling conducted near the Superconducting Super Collider site in north-central Texas. They constructed two models that focused on the Twin Mountains, Paluxy, and Woodbine aquifers. Dutton and others (1996) first developed a two- dimensional cross-section model that included the aquifers and the confining layers. The purpose of this model was to “evaluate model boundary conditions and the vertical hydrologic properties of the confining layers” (Dutton and others, 1996). They then developed a three-dimensional model of the aquifers using results and insights gained from the cross-sectional model. The primary purpose of the three-dimensional model was prediction of the effects of future groundwater production. Dutton and others (1996) indicate that the two models “developed in this study were used as tools to estimate amounts of recharge and discharge, evaluate uncertain hydrologic characteristics of confining layers and aquifer boundaries, and quantitatively estimate how water levels will respond to future pumping rates.”

For use in their models, Dutton and others (1996) developed formation structure using about 1,200 geophysical logs. Hydraulic conductivity for the aquifers was assigned based on results of aquifer pumping test and specific capacity tests and sandstone distributions. The transmissivity distributions for the Woodbine, Paluxy, and Twin Mountains aquifers indicate lower values near the center of the aquifers, as a result of less sandstone in those areas, and higher values in and near the outcrop and along the Mexia-Talco Fault Zone. Vertical hydraulic conductivity in the aquifer units was assumed to be a factor of ten lower than the horizontal hydraulic conductivity. The horizontal hydraulic conductivity for the confining units was developed based on results of aquifer pumping tests or literature values and estimated sand/shale percentages. A single value was used for the confining units. The vertical hydraulic conductivity in the confining units was assumed to be a factor of 100 less than the horizontal value. Dutton and others (1996) state that “storativity initially was assigned as a covarying function of depth and transmissivity and constrained by the mean and range of values determined from aquifer tests.”

Dutton and others (1996) used over 22,000 water-level measurements for history matching. They used information from numerous historical reports to estimate historical pumping from 1891 to 2000 on a county basis. This pumping was distributed in the counties on a random basis at the start of each 10-year stress period using “a binomial probability density function controlled by the number of blocks per county and total pumping in the county” (Dutton and others, 1996). The projected future pumping for 2000 to 2050 was obtained from the TWDB. MODFLOW was used for both the cross-sectional and three-dimensional models.

The cross-sectional model of Dutton and others (1996) included the aquifers of the Twin Mountains and Paluxy formations and the Woodbine Group, as well as the confining units of the Glen Rose Formation and the Fredericksburg, Washita, Eagle Ford, Austin, Taylor, and Navarro groups. The model consists of 54 columns extending a distance of 111 miles and 10 layers that extend from ground surface to the base of the Twin Mountains Formation. A steady-state history matching of the model to water-level measurements reported in Hill (1901) was conducted by adjusting hydraulic properties. A general head boundary condition was applied at the top surface of the model and a no-flow boundary was applied to the bottom surface of the model. Several different types of boundary conditions were applied at the downdip limit of the model, which corresponded to the Mexia-Talco Fault Zone, to evaluate the nature of this boundary. The boundary condition types evaluated were no-flow, specified head assuming hydrostatic conditions, and no-flow with a column of high vertical hydraulic conductivity.

The best model history matching for the cross-sectional model was obtained using the specified head boundary condition at the fault zone. The results of the model suggest that “ground water exits the aquifers through the Mexia-Talco Fault Zone” and “cross-formational flow between the aquifers is not an important control on ground-water movement compared to the discharge through the fault zone”

(Dutton and others, 1996). The initial horizontal hydraulic conductivities were adjusted during model history matching. The resultant hydraulic conductivities indicate increasing values in the downdip direction in all three aquifers. The cross-sectional model predicted recharge rates of 0.11 inches per year for the Twin Mountains Aquifer, 0.25 inches per year for the Paluxy Aquifer, and 0.017 inches per year for the Woodbine Aquifer (Dutton and others, 1996).

The three-dimensional model of Dutton and others (1996) was developed based on insights gained from the cross-sectional model. This model included three layers representing the Twin Mountains, Paluxy, and Woodbine aquifers and vertical conductance factors representing the confining units. Uniform grid-block dimensions of 2 miles by 2 miles were used over the 30,600 square mile modeled region. A head-dependent boundary condition was assigned to the top of the model to represent recharge and discharge in the outcrop area and vertical leakage in the confined area. A no-flow boundary was assigned at the bottom of the model. After trying several boundary conditions at the Mexia- Talco Fault Zone, the final one used was the Drain Module of MODFLOW to simulate vertical discharge from the aquifers at the location of the fault zone. The hydraulic conductivity distributions were not adjusted during model history matching.

The calibrated model overestimated heads as compared to those given in Hill (1901) for all three aquifer units. The overestimates were considered to be acceptable considering the fact that the water levels in Hill (1901) reflected the effects of pumping and free-flowing wells in the late 1800s. The three-dimensional steady-state model predicted recharge rates of 2.7 inches per year for the Woodbine Aquifer and approximately 4.4 inches per year for the Twin Mountains and Paluxy aquifers. Almost all of this recharge exited head boundaries within the outcrop, representing stream, spring, and groundwater ET losses. In a steady state, the model predicted an effective (deep recharge to the confined section) recharge rate of 0.04 inches per year.

The calibrated model was then used to simulate historical conditions from 1891 to 2000 and projected future conditions from 2001 through 2050. The transient model results were compared to selected historical hydrographs and potentiometric surfaces from 1900 and 1990 for all three aquifers, but the transient model was not calibrated. They also present predicted potentiometric surfaces in 2050 based on the assumed projected future pumping in the model. Effective recharge increased from 0.04 inches per year in the steady-state simulation to 0.3 inches per year by 1990 as a result of pumping. The authors questioned whether this induced increase in effective recharge was realistic or an artifact of the boundary conditions employed and suggested further study towards that point.

Conclusions reached by Dutton and others (1996) include: (1) net sand distributions provide an excellent guide for interpreting regional patterns of transmissivity and storativity, (2) predevelopment water levels were very high in the outcrop areas (at or near surface) and were above surface in many areas of the confined portions of the aquifers, (3) the free discharge of groundwater from flowing wells in the early twentieth century depressurized large portions of the aquifer and removed significant quantities of water from storage. Discharge rates from flowing wells declined as the hydraulic head was lowered until approximately the 1940s when pumping accelerated, (4) most water recharged in the aquifer outcrop exits through surficial discharge mechanisms. They estimated that the confined aquifer system recharge was approximately 25,000 AFY, which they noted was far less than annual groundwater production.

Bené and others (2004) present the first GAM developed for the northern Trinity and Woodbine aquifers under the TWDB GAM program. The model was developed to evaluate the availability of groundwater in the aquifers over a 50-year planning period and evaluate aquifer response to projected future pumping and a potential drought. The model was built using the MODFLOW-96 code and structured into seven layers that included both aquifer and confining units, specifically the Woodbine, Paluxy, Hensell, and Hosston aquifers, as well as confining units such as the Fredericksburg/Washita, Glen Rose, and Pearsall/Cow Creek/Hammett formations. The model domain extended from the outcrop boundaries of the aquifers to the downdip Mexia-Talco Fault Zone and south to the Colorado River. Using 1-mile grid spacing, the model incorporated over 694,000 grid blocks, with more than 220,000 considered active.

Development of the model's structural framework relied on over 1,000 geophysical logs, which were also used to determine net sand thicknesses in the aquifers. Hydraulic conductivity distributions were derived through a multi-step process involving statistical correlations between transmissivity and net sand thickness, followed by refinement during calibration. Adjustments were made to horizontal and vertical hydraulic conductivity values as well as to storage coefficients, particularly in the downdip portions of aquifers. Recharge in the outcrop areas was simulated as a function of precipitation, soil properties, land use, and aquifer characteristics. However, nearly all of this recharge was assumed to discharge through streams and ET processes, meaning very little actually reached the confined portions of the aquifer system.

Boundary conditions for the model included MODFLOW’s River, ET, Streamflow-Routing, and General Head Boundary packages. Faulting in the Mexia-Talco Fault Zone was represented using the Horizontal Flow Barrier (HFB) Package, and a no-flow boundary was assigned at the model base. The modeling process included a steady-state/transitional model that first ran a quasi-steady-state simulation (over 100,000 years) with no pumping to establish initial heads. These results then served as initial conditions for a transitional model simulating 1880-1980 with gradually increasing pumping and constant recharge based on mid-20th-century precipitation. The transitional model’s results informed the transient calibration/verification model, which simulated 1980-2000 conditions and was calibrated to 1990 and verified against 2000 water-level and baseflow data. Calibration efforts focused on adjusting storage, conductivities, and boundary parameters.

A sensitivity analysis conducted on the calibrated model explored 12 parameters, identifying horizontal and vertical hydraulic conductivities, storativity, and pumping as the most influential on model outcomes. The model was then used to project aquifer conditions through 2050, assuming steady recharge and increasing groundwater demand. Additionally, five simulation scenarios incorporated a projected drought of record using historical drought data from 1954-1956. These simulations demonstrated the model's capability to evaluate future conditions and stress scenarios, including reduced recharge in the final years of each simulation.

Bené and colleagues drew several key conclusions from their modeling efforts. They noted historical drawdowns of 800 to 1,000 ft in major pumping areas such as Tarrant, Dallas, and McLennan counties. Despite these significant drawdowns in confined sections, water levels in the outcrop areas had remained stable over five decades, implying stable aquifer storage. The model suggested that nearly all recharge in predevelopment times was rejected—i.e., discharged at the surface—highlighting the limited penetration of recharge into confined aquifer zones. Importantly, aquifer water levels appeared relatively insensitive to recharge rates, indicating a degree of resilience to drought. Finally, the model predicted the potential recovery of artesian water levels in response to reduced pumping, though this outcome was uncertain due to anticipated population growth and water demand increases along the I-35 corridor.

Overall, the Bené and others (2004) GAM established a foundational understanding of the northern Trinity and Woodbine aquifers and provided a robust tool for simulating GWF and availability under varying future conditions. It demonstrated the complexities of modeling multi-layered aquifer systems with significant spatial variability in geologic and hydrologic properties and laid the groundwork for subsequent model updates that incorporated more advanced data and methods.

The Northern Trinity and Woodbine Aquifer GAM (Kelly and others, 2014) provided a comprehensive evaluation of groundwater conditions across a significant portion of north-central Texas. This study updates the Bené and others (2004) model to reflect improved geological, hydrological, and technical data, utilizing advanced modeling approaches to support local GCDs and regional planning entities. The Northern Trinity Aquifer, a key water supply source for urban centers along the I-35 corridor from Dallas-Fort Worth to Austin, and the overlying Woodbine Aquifer are the focus of this work. These aquifers, along with the confining Washita/Fredericksburg units, were mapped in detail, capturing their lithological variability and complex depositional history, which spans both terrestrial and marine environments. Five distinct aquifers within the Trinity Group—Hosston, Pearsall, Hensell, Glen Rose, and Paluxy—were characterized in the study, with special emphasis on variations in water quality and aquifer properties.

This model redevelopment employed MODFLOW-NWT, a robust three-dimensional numerical modeling code. It features a finely spaced grid (0.25-mile cells) covering over 12 million cells across eight layers representing key aquifer and confining units. Extensive data collection efforts supported the development of a detailed conceptual model, including over 1,300 geophysical logs and more than 30,000 aquifer tests (specific capacity and long-term pumping). These datasets helped establish hydraulic properties such as conductivity and transmissivity through a conceptual geo-hydrostratigraphic (GHS) model, which integrated lithological and test-derived parameters. Recharge estimation incorporated multiple methodologies, including chloride mass balance and stream hydrograph separation, yielding spatially variable recharge values ranging from 0.25 to 7.2 inches per year, with a model-wide average of 1.6 inches per year. Recharge patterns also considered the effects of urbanization and historical climate.

A key contribution of the study is its detailed water quality analysis, which includes maps of TDS, chloride concentrations, and hydrogeochemical facies. The findings confirm the presence of active recharge zones in the outcrop areas, where shallow groundwater systems are strongly interconnected. While much of the water is potable, substantial portions of the aquifers exhibit brackish conditions (TDS >1,000 =mg/L). The model simulates groundwater conditions from 1890 through 2012, accounting for historical and modern pumping patterns. Estimates show that pumping increased rapidly from the 1930s to 1980 and continued to rise at a slower pace thereafter, with a total of approximately 260,000 acre per ft pumped in 2012. This historical perspective is especially valuable given the role of flowing wells in early aquifer discharge, which has now largely diminished.

Model calibration was performed for both steady-state and transient conditions, with the steady-state model representing predevelopment conditions and the transient model extending through 2012. Calibration incorporated over 27,000 water-level observations and nearly 700 long-term hydrographs, successfully replicating historical trends and regional drawdown patterns. Statistical performance met or exceeded TWDB standards, with mean absolute errors generally below 10% of the observed head range. Key insights from transient modeling highlight how intensive deep pumping depletes aquifer storage and increasingly relies on capture from shallower zones—a process that is inefficient due to low vertical conductivity and storage coefficients. This underscores the challenge of recovering water levels even when pumping stabilizes.

The model's development was uniquely led and funded by four GCDs in GMA 8—North Texas, Northern Trinity, Prairielands, and Upper Trinity—under an interlocal agreement. Conducted in a transparent, public process mirroring TWDB practices, the model included input from a Technical Advisory Committee comprising representatives from GCDs, TWDB, and the United States Geological Survey (USGS). The updated GAM is designed to bridge the gap between regional and local-scale planning tools and includes predictive scenarios to support joint planning, as documented by Kelley and Ewing (2014). This study represents a significant advancement in both the scientific understanding and practical management of two critical aquifers in Texas, offering GCDs a calibrated, flexible tool grounded in the most current data and methodologies.

3.2 Model Conversion

An initial conversion of the NTWGAM to MODFLOW 6 was obtained by running the program Mf5to6 on the NTWGAM, which uses MODFLOW-NWT (Niswonger and others, 2011). The resulting MODFLOW 6 version was compared against the NWT model to ensure that all properties were accurately preserved. Model inputs not accurately converted by Mf5to6 from multiple stress packages were programmatically re-written from NWT to MODFLOW6 using the python-based package FloPy (Bakker and others, 2016). A number of River cells in the inactive model domain (where IDOMAIN = 0) were removed from the RIV6 package (RIV equivalent in MODFLOW 6) to allow the MODFLOW 6 executable to run. Likewise, several RIV6 cells with river bottoms specified below cell bottoms and/or with river stages specified below river bottoms, were all reset to 5 ft above cell and river bottoms, respectively. Duplicate cells in the RIV6 package were also removed while keeping unique cells with the lowest river stage. In addition to performing logical, programmatic verification of model property conversions between the NWT and MODFLOW 6 models, a comparative water balance for all model sources and sinks was found to be less than 1% using the USGS software GW Chart (Winston, 2020).

Conduit cells, defined in the IBOUND array of the NWT version, were designated as inactive cells using the IDOMAIN flag of -1 in MODFLOW 6. A number of HFB cells in the inactive model domain (IDOMAIN = 0 and IDOMAIN = -1) were removed from the package to allow MODFLOW 6 to run. The temporal discretization was extended from 2012 through 2020 for a total of 132 model stress periods defined in the MODFLOW 6 TDIS package. The "NEWTON" option was activated in the MODFLOW 6 name file, and the option auto_flow_reduce = 0.25 was defined in the WEL6 package, equivalent to the variable phiramp in the NWT Well package. For ease of model property identification and parameterization, the converted RIV6, DRN6, and WEL6 packages were split into multiple packages. The packages are titled as the following: "riv" (perennial streams), "res" (reservoirs), and "young" (younger formations) RIV6 packages; "drn" (ephemeral streams), "et" (evapotranspiration), "flow" (flowing wells) DRN6 packages; and "wel_a," "wel_b," "wel_c," "wel_0," "wel_1," "wel_2" WEL6 packages. These packages are further described in Section 3.4.

3.3 Spatial and Temporal Discretization

The NTGAM uses the NTWGAM rectangular model grid that is spatially discretized into 1,124 rows and 1,412 columns containing 1,320-ft by 1,320-ft cells that are rotated at a 25-degree angle clockwise of north-south. This configuration results in the NTGAM grid overlying the NTWGAM model grid and the 2004 northern Trinity and Woodbine aquifers GAM developed by Bené and others (2004). In this way, the grid is oriented with the principal direction of flow in Texas, which is southeast, and multiple models can be compared more easily. The updip limit of the northern Trinity Aquifer defines the western and northern extents of the active model domain. The downdip extent (southeast) of the active model domain is defined by the Mexia-Talco Fault Zone. The southern boundary of the active model domain is defined by the Colorado River. The eastern extent of the northern Trinity aquifer is treated as a distance boundary to the developed portions of the aquifer.

For modeling purposes, the NTGAM is divided into eight layers–one for each hydrogeologic unit and an additional top layer that represents younger sediments and the surficial portion of each hydrogeologic unit (Figures 3-1, 3-2). This approach is similar to that taken in the NTWGAM. The hydrogeologic units are discussed in Section 2.1.2. The model layers have areas where the thickness differs compared to the NTWGAM based on updates to the stratigraphic contacts made as a part of this investigation.

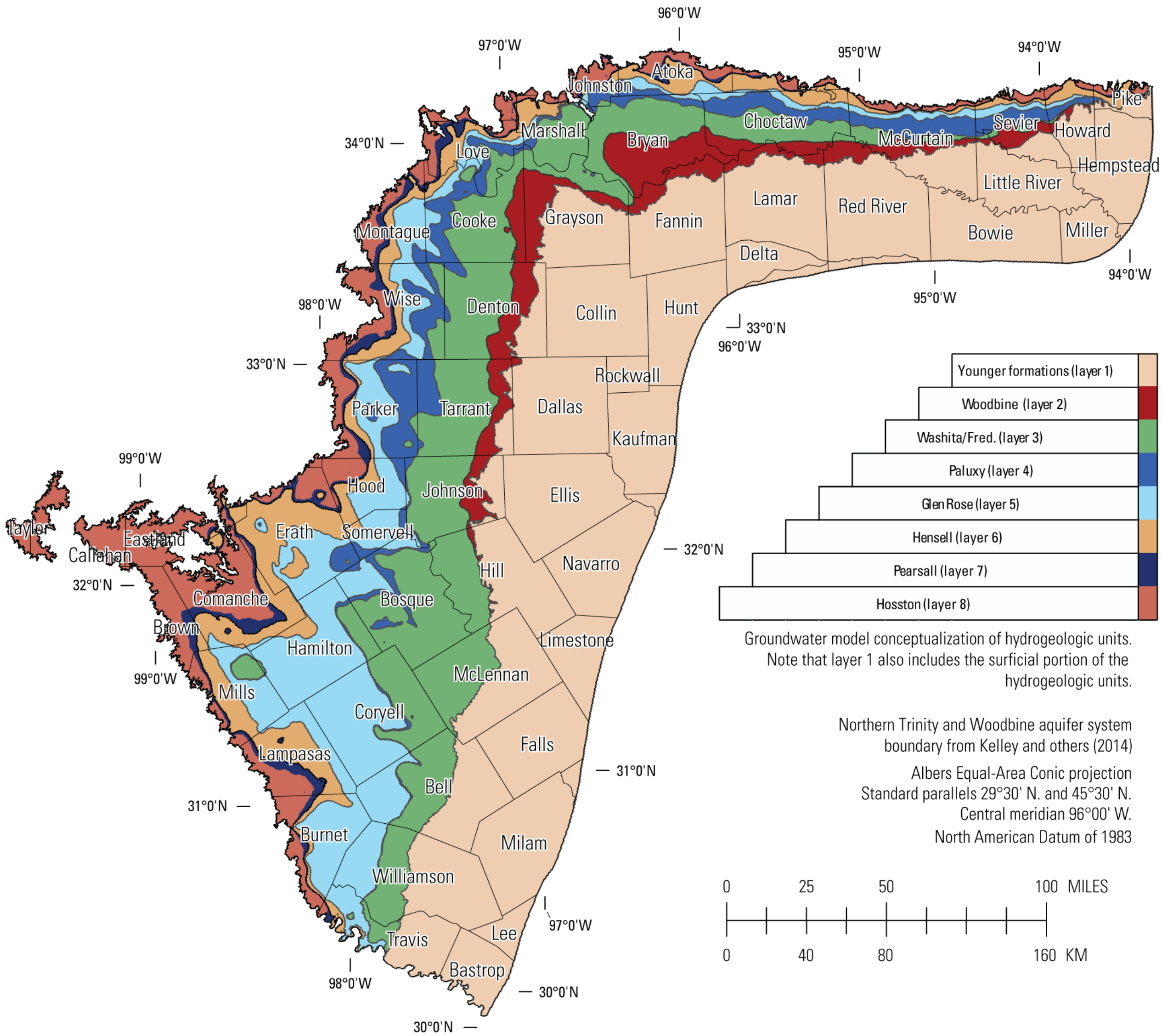

Figure 3-1. **Hydrogeologic units in layers 2–8 of the Northern Trinity and Woodbine aquifer system.**

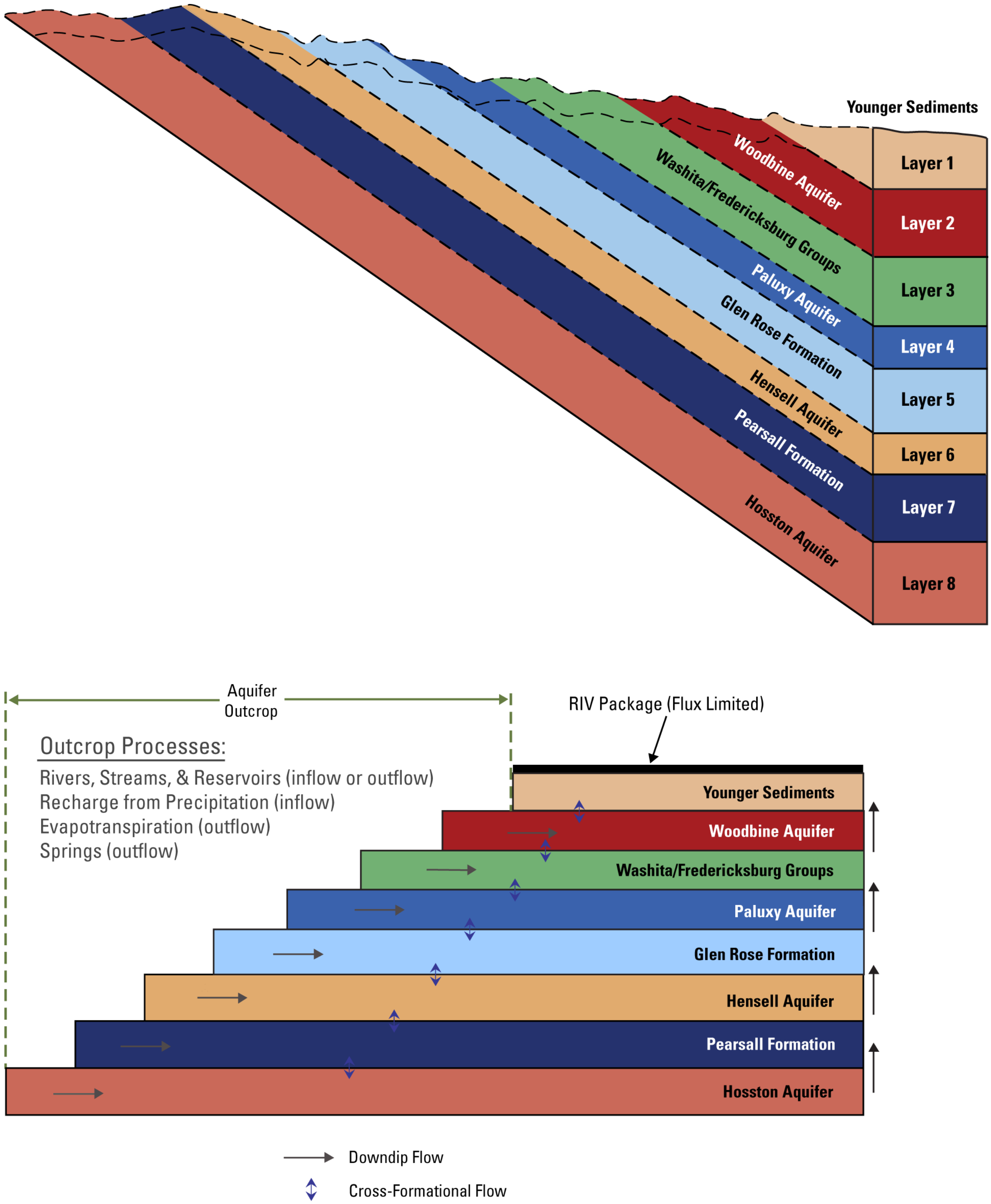

Figure 3-2. Conceptual groundwater model implementation for the northern Trinity and Woodbine aquifer system.

Layer 1 is used to represent the shallow flow system that is dominated by inflow from recharge and outflow to surface water boundaries (rivers, streams), where it overlies the outcrop of each layer. In the remainder of the model area, Layer 1 represents the younger formations that overly the downdip portions of the Woodbine Aquifer and Washita/Fredericksburg groups. However, the inclusion of this portion of the upper layer is intended only to provide a first-order representation of the overlying younger formations as a boundary condition. Specifically, all recharge, pumping, and surface water interaction that occurs within the younger formations are aggregated into the river boundary condition applied to this portion of Layer 1. The land surface elevation of Layer 1 was estimated from a 10-meter DEM averaged to the grid cells. Where Layer 1 represents the shallow flow system, the base is set 50 ft below the one-mile average of the estimated predevelopment water level, in order to keep the cells in the layer mostly wet/active. Where it represents the younger formations overlying the Woodbine Aquifer, the base of Layer 1 is defined by the top of the Woodbine Aquifer.

Model layers 2 through 8 represent the portions of the aquifers/formations underlying and downdip of the surficial outcrop area (Figure 3-2). The Woodbine Aquifer is represented by model Layer 2. Model Layer 3 represents the Washita/Fredericksburg groups, which includes a portion of the Edwards BFZ Aquifer at the southern extent of the model domain. The Paluxy Aquifer is represented by model Layer 4. Model Layer 5 represents the Glen Rose Formation. The Hensell Aquifer is represented by model Layer 6. Model Layer 7 represents the Pearsall Formation. The Hosston Aquifer is represented by model Layer 8. All layers are simulated as convertible between unconfined and confined conditions. A minimum layer thickness of 30 ft was enforced, whereby layer basal elevations were lowered if necessary to maintain the minimum thickness.

MODFLOW 6 has the capability to connect non-adjacent layers. In previous versions of MODFLOW, “pass-through” cells would be used to connect non-adjacent model layers that represented adjacent formations. For example, where Layer 1, representing the shallow system, overlies Layer 8, representing the Hosston Aquifer, there are six numerical grid layers in between. The previous NTWGAM used “pass-through” cells with a thickness of 1 foot in these six numerical layers and flagged those cells in the IBOUND array for clarity.

In the updated MODFLOW 6 version, the IBOUND flags of these pass-through cells were all set to a value of -1 in the IDOMAIN array (designating them as inactive and creating a direct connection between the grid cells above and below) with a cell thickness reduced from 1 ft to 0 ft. This improves computational efficiency and accuracy of vertical, intra-formational flow representation.

In a MODFLOW 6 simulation, the periods during which applied stresses (such as pumping) remain constant are known as stress periods. The groundwater model simulation period was temporally discretized into 132 annual stress periods with 1 time step each, representing the period from 1889 to 2020 (Appendix 7.1). This annual stress period approach was similar to the NTWGAM but extended the calibration period by 10 years from 2010 to 2020. The first stress period (1889) is considered steady-state, representing long-term average predevelopment conditions in the aquifer before 1890, which marked the beginning of a period of significant development. Although historical data indicate some development prior to 1890, water level records suggest that the aquifer remained largely in its natural, predevelopment state in many locations outside of the present-day metropolitan areas.

3.4 Hydrologic Boundaries

Hydrologic boundaries in the groundwater model represent the locations where the inflow or outflow of water may occur (Figure 3-3) and characterize the interaction between the active model domain and the surrounding environment. For a specified-flux boundary, a user-specified discharge rate governs groundwater exchange at that boundary. Recharge and pumping discharge are specified flux boundaries. Specified no-flow boundary conditions (a special form of the specified flux boundary) were assigned to the lateral boundaries where the adjoining units are not expected to yield water. A no-flow boundary was also used at the bottom of Layer 8 (the Hosston Aquifer). It was assumed that Paleozoic-age sands that directly underlie portions of the Hosston Aquifer primarily act as additional saturated thickness and, thereby, additional transmissivity and storativity rather than a source of hydraulic head support. Therefore, the hydraulic connection between the northern Trinity Aquifer and the Paleozoic-age strata was not explicitly included in the model. A head-dependent boundary simulates flow based on the difference between a user-specified groundwater level and the groundwater level in model cells. Head-dependent boundaries were assigned to cells representing perennial streams (river package) and ephemeral streams, springs, and riparian ET (drain package) in Layer 1.

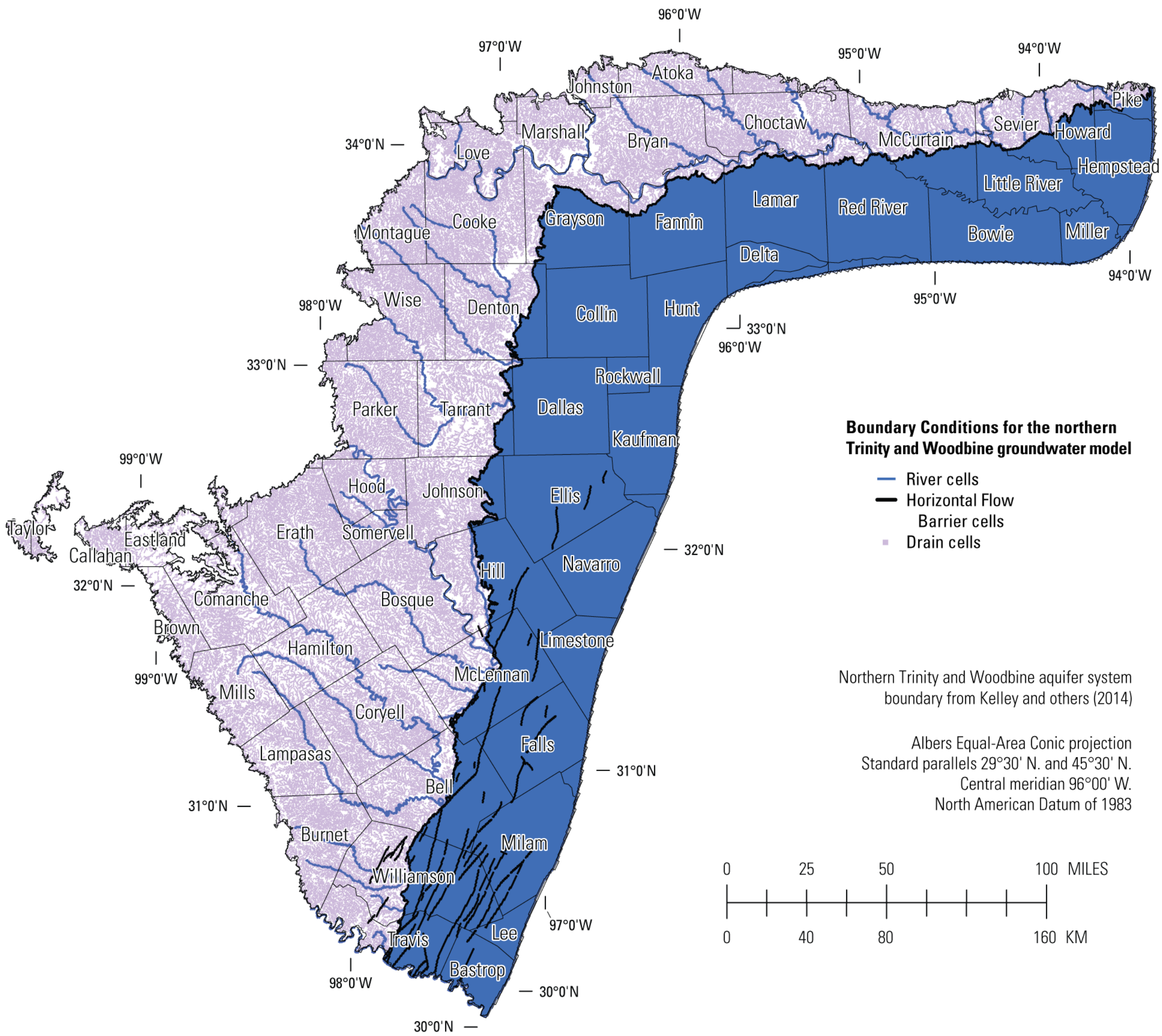

Figure 3-3. Subset of boundary conditions of the northern Trinity and Woodbine aquifer system

Additionally, the model uses a head-dependent flow boundary in Layer 1 where it represents the younger formations that overly the Woodbine Aquifer. This boundary represents the diffuse regional (primarily) outflow discharge from the northern Trinity and Woodbine aquifers into the younger overlying formations. The NTGAM uses the river package to represent this boundary (rather than a general head boundary) to limit the magnitude of simulated inflow from this boundary under increasing vertical gradient conditions. The hydraulic conductance in the river package represents the composite vertical conductance of the younger formations. The difference between the hydraulic heads in the northern Trinity and Woodbine aquifers (heads in the cell) and the younger formations (reference stage in the river package) sets the gradient that, along with the composite vertical conductivity, governs the amount of outflow from the northern Trinity and Woodbine aquifers to the younger formations. Any flow from the younger formations to the Woodbine Aquifer is not based on the difference in hydraulic heads but is limited by a unit gradient because the stages are set one foot above the river bottom. In this way, the river package limits the downward gradient while also limiting flow via the conductance. This approach avoids the unlimited flow that could otherwise occur due to increased gradients from significant pumping and drawdown occurring in the underlying aquifers.

3.4.1 Recharge

Areally distributed recharge derived from the SWB code (described in Section 2.5) was simulated using the recharge package (Langevin and others, 2021) in the NTGAM. MODFLOW 6 computes the volume of water added to the model for each stress period as the product of the specified recharge rate at each node and the cell area. Recharge is applied to the highest active cell in the numerical grid. Transient recharge used in each stress period was filtered to remove some extreme recharge values (Section 2.5.3.6). Some spatial and temporal adjustments of recharge also occurred during history matching.

3.4.2 Lateral Flow

The lateral model boundaries were developed to comply with structural or otherwise natural hydrologic boundaries to the best degree possible as defined by the extent of the northern Trinity and Woodbine aquifers. Beyond the extent of the aquifers, grid cells were set as inactive, creating a no-flow boundary along the intersection of the active and inactive cells.

The updip limit of the northern Trinity Aquifer outcrop defines the western and northern extents of the active model domain, which is a natural lateral no-flow boundary. The southeastern extent of the active model domain is defined by the Mexia-Talco Fault Zone, where the fault offsets are significant enough to assume to represent a lateral no-flow boundary. The southern boundary of the active model domain is defined by the Colorado River, which is a regional discharge boundary assumed to be adequately represented by a lateral no-flow boundary. The eastern extent of the northern Trinity aquifer is treated as a distance boundary to the developed portions of the aquifer and is implemented as a lateral no-flow boundary.

3.4.3 Discharge (Rivers, Streams, Evapotranspiration [ET], & Flowing Wells)

Surface-water/groundwater interaction was simulated using the river package (Langevin and others, 2021) to represent perennial rivers, reservoirs, and younger formations (Figure 3-3). The river package allows for stream-related discharge during gaining conditions and for recharge from the stream during losing conditions. For perennial rivers, the river stage was set to the minimum DEM value in each grid cell, and the river bottom was set five ft below the river stage. If the river stage was below the base of Layer 1, the stage was set five ft above the layer bottom, and the river bottom was reset to five ft below the river stage. The river conductance for perennial rivers was calculated based on an assumed riverbed conductivity of 1 foot per day (ft/d), an assumed river width of 40 ft, and the length of the river within a given model grid cell. Where reservoirs exist, the river stage was set to the time-varying reservoir stage after impoundment, and the areal extent of the river cells was defined by the reservoir coverage. Prior to reservoir impoundment, the river stage was set to estimate the river channel elevation and river boundary conditions were only applied to the river channel. Reservoir bed conductivities were uniformly set to 1×10^{-4} ft/d for all reservoirs, and the conductance was calculated as the product of the bed conductivity and the area of the reservoir within a given model grid cell divided by an assumed bed thickness of five ft.

The drain package (Langevin and others, 2021) was used to represent ephemeral streams, springs, and ET. To represent ephemeral streams, the drain package was applied within ephemeral stream channels as described by the National Hydrography Dataset (USGS, 2023b). The drain elevations for ephemeral streams were set 10 ft below the top of the model, and the drain conductances were uniformly set to 1,000 square ft per day (ft^2/d). The drain elevations for springs were set 10 ft below the top of the model, and the drain conductances were uniformly set to 1,000 ft^2/d. The drain package was also used to simulate ET in riparian cells neighboring perennial streams in the surficial outcrop area of model Layer 1 (Figure 3-3). The drain elevation was set to 10 ft below the top of the model, and the drain conductance was uniformly set to 1,000 ft^2/d.

As described in Section 2.2, a number of wells in the northern Trinity and Woodbine aquifers were artesian and produced a substantial amount of water when initially completed in the late 1800s and early 1900s. To account for discharge from these wells, drain cells were implemented in the model at the well locations. The drain elevation for each flowing well was set to the average land surface elevation for the well's model cell. The drain conductance was uniformly set to the relatively large value of 1,000 ft^2/d for all flowing wells. This results in the discharge rate from the flowing wells, which is governed primarily by the properties of the formation.

3.4.4 Groundwater Use

The withdrawal of groundwater was simulated using the Well package (Langevin and others, 2021). INTERA separated pumping estimates into six groups based on the amount of supporting information and corresponding uncertainty of the underlying data used in the estimates. These groups manifest as six individual Well packages. Packages A and B represent Irrigation and Non-Irrigation production from the Predevelopment-1979 stress periods, respectively. This pumping was compiled from the NTWGAM and is described in that report and summarized in Section 3.4.4.2. Package C represents all pumping from outside Texas. Package zero represents the reported pumping received from the GCDs. This pumping was considered correct and was also not modified during calibration. Package 1 represents a portion of the Water Usage Survey from the TWDB. Package 2 represents INTERA's census-based estimates for rural domestic pumping inside Texas. Discretization methods for all Well packages are described in the sections below.

3.4.4.1 Aquifer Assignments for Production Wells

Data on wells and their corresponding construction information were received either from GCDs or compiled using the TWDB Groundwater Database/Submitted Driller's Report Database (GWDB/SDR). Wells with associated information about their screened intervals were assigned to all model layers over which the screen crossed, provided that the fraction of total screen in a model layer was greater than 1/(total layers screened). This prevents production from being applied to layers with very small amounts of screen and preferentially applies pumping to layers with the most screened thickness. Wells screened entirely below the bottom of model Layer 8 were removed from the dataset.

Wells that did not have associated screened intervals were assigned to model layers based on total depth. GWDB/SDR wells that did not have either screened intervals or total depth were removed from the dataset. GWDB/SDR wells which had total depths less than 20 ft were also removed from the dataset. Some GCDs included estimated aquifers with their production wells. For GCD wells that did not have either screened intervals or total depth, the well was assigned to the model layers associated with the estimated aquifer. If there was no total depth, screened intervals, or an estimated aquifer, the total depth was estimated using the average total depth of GWDB/SDR wells within 0.5 miles and of the same listed use type. All wells with a reported or estimated total depth were then assigned to the model layer 50 ft above the total depth. If the total depth of a GCD well without screened intervals could not be estimated, the well (and its associated production) was removed from the dataset.

Note that wells assigned by the GCDs to both the Fredericksburg Washita and the Paluxy were assumed to be assigned only to the Paluxy. If wells were reported by a GCD to be assigned to the Cross Timbers Aquifer (such as in Upper Trinity GCD) or to the Ellenberger San Saba (such as in Central Texas GCD), the production well was removed from the dataset and was not applied to the model. Use types for wells were synthesized using the substitutions in Table 3-1.

Table 3-1. Use types reported by Groundwater Conservation Districts or the Texas Water Development Board and the use type assumed during processing.

Original Use Type	Final Use Type
Ag/Irrigation	Irrigation
Irrigation (or Irrigation + another use type)	Irrigation
Stock	Livestock
Livestock/Poultry	Livestock
Livestock (or Livestock + another use type)	Livestock
Aquaculture	Livestock
Poultry	Livestock
Industrial	Manufacturing
De-watering	Manufacturing
Industrial (cooling)	Manufacturing
Air Conditioning	Manufacturing
Bottling	Manufacturing
Rig Supply	Mining
Fracking Supply	Mining
Oil	Mining
Public Supply	Municipal
Commercial	Municipal
Institution	Municipal
Public Water Supply (or PWS + another use type)	Municipal
Recreation	Municipal
Fire	Municipal
Medicinal	Domestic
Plugged or Destroyed	Other

Original Use Type	Final Use Type
Unused	Other
Not Used	Other
Monitoring	Other
Unknown	Unknown
No listed use type	Unknown

3.4.4.2 Well Packages (Prior to 1980, Non-Texas Use)

Packages A and B comprise all pumping in the model within Texas before the 1980 stress period and were compiled directly from the well file of the NTWGAM. The methods for distributing pumping before 1980 within Texas can be found in detail in Kelley and others (2014).

Package C is comprised of estimated pumping from Oklahoma and Arkansas overall stress periods. Before the 2011 stress period, Package C was compiled directly from the well file of the NTWGAM (Kelley and others, 2014). The methods for distributing pumping outside of Texas can be found in detail in Kelley and others (2014). Beginning in 2011, estimates from Oklahoma were received as production rates from specific parcels of land. These parcels were intersected with the model grid, and production volumes were applied equally among those grid cells with which it intersected, as well as equally among the layers representing the Antlers Aquifer in that region (layers 4-8). Production estimated for Arkansas was scaled proportionally to the county population totals, as referenced in Section 2.2.2. The distribution of Arkansas pumping from the 2010 stress period was retained through the end of the history matching period. The volume in each cell was scaled proportionally to the total linearly interpolated population of the county containing the centroid of the grid cell for each stress period. Vertical distributions of production rates in the 2010 stress period were also retained through the end of the history matching period.

3.4.4.3 Well Packages (GCD, TWDB, and Rural Domestic)

Package 0 is comprised of reported pumping estimates from GCDs. These pumping volumes were applied to the grid cells where the wells associated with the production or production permit were located. For wells associated with two or more aquifers, pumping for each well was split evenly among each associated aquifer.

Package 1 is comprised of pumping estimates from the TWDB's WUS, which are reported on a county-wide basis. In order to discretize these estimates to grid cells and aquifer layers, WUS and GCD reported volumes were first totaled by county and year. If the GCD reported volumes for a certain year and the county exceeded the WUS estimates, no production would be assigned to the model from Package 1 for that county in the associated stress period.

For each county and year where the estimated total TWDB pumping exceeded the estimated total GCD pumping, the difference (DIFF) between the WUS and GCD reported volumes was calculated and totaled for all aquifers. All existing wells (drilled and not yet plugged for the associated stress period) from the GWDB/SDR in that county were compiled. The fraction (FRAC) of these existing wells within the active model area with adequate construction information was recorded. The DIFF was multiplied by the FRAC to obtain the final pumping volume (FINAL) applied to each county in addition to the GCD estimates. FINAL, a modified volume representative of the WUS from all aquifers, was then further divided into individual aquifer estimates based on the ratio of production volumes estimated in the WUS. For each aquifer, that volume was distributed equally into the existing, non-domestic GWDB/SDR wells screened within that aquifer within the county. The per-well volume was split equally among all model layers in which the well was assigned.

Package 2 is comprised of INTERA's rural domestic production estimates. Beginning with the spatial distribution of people per census block derived from methods detailed in Section 2.2.2, this data was integrated into the model grid to estimate the number of people per model cell. Each model cell in the NTGAM represents 0.0625 square miles. To convert population data into groundwater pumping estimates, the population density for each cell was calculated based on the distribution of people within the corresponding census blocks. The United States Department of Agriculture (USDA) defines rural areas as open countryside with population densities of less than 500 people per square mile. INTERA examined the distribution of rural-domestic wells and compared it to the resulting distributions of pumping using a variety of population densities lower than 500 people per square mile. We decided on a threshold value of 200 people per square mile, finding it to be the most realistic distribution of rural population when overlain with the distribution of rural domestic wells. A threshold value of 200 people per square mile was therefore used to distinguish rural from urban areas, ensuring accurate attribution of rural domestic water use. Additionally, a lower end-member threshold of 0.1 people per square mile was enforced to remove unrealistically low pumping estimates from the dataset.

Next, per capita water use rates were applied to the population estimates to calculate annual pumping volumes. Per capita use rates were estimated to be a constant 100 gallons per person per day. The pumping estimates were generated using the assumption that all rural domestic water use is supplied by groundwater from the aquifer outcropping in each location. This methodology allowed for detailed calculation of rural domestic groundwater use on a cell-by-cell basis, incorporating both population growth and changes in water demand over the model period. The total annual groundwater pumping for rural domestic use was thus derived for each year from 1980 to 2020, reflecting spatial and temporal variations in water use across the model domain. All pumping associated with Package 2 was applied to model layer 1 where the grid cell represented the outcrop of a lower layer. In grid cells where model layer 1 represented the Younger Formations, no rural domestic pumping was assumed.

3.5 History Matching and Uncertainty Quantification

To aid decision-making purposes underlying the use of the NTGAM, a Bayesian framework (Tarantola, 2005; Doherty and Simmons, 2013; Doherty, 2015; Hemmings and others, 2020) was used to represent uncertainty in model parameters and simulated outputs of interest. History matching is the process of changing model stresses and parameters to acceptably fit historical information such as hydraulic-head observations and baseflow estimates. It is also performed to allow the model to better address a range of hydrologic problems. The term "history matching" is used to describe reservoir modeling in the petroleum industry and avoids the implication of parameterization finality. The history-matching approach used in this study incorporates a Monte Carlo approach for determining the parameter values and avoids the implications of a traditional "calibrated" model having arrived at a finalized dataset of exactly known parameter values given that there are any number of differing parameter value datasets that could potentially be used (Doherty and Simmons, 2013). Model history matching and uncertainty quantification were performed by using the IES PESTPP-IES (White, 2018), included in the PEST++

software suite (Welter and others, 2015; White and others, 2020a), in conjunction with the open-source Python packages FloPy (Bakker and others, 2016) and pyEMU (White and others, 2016a and b). The combination of these software tools allows much of the history matching and uncertainty quantification workflow to be performed programmatically, which provides transparency and reproducibility (White and others, 2020a and b; Fienen and others, 2021).

The IES algorithm is available through the open-source PEST++ software suite (White and others, 2020a). IES provides two important advantages over the more frequently used deterministic parameter estimation algorithms: reduced computational demand for highly parameterized models and an accessible way to estimate the uncertainty of forecasts that depend on a high number of parameters (White and others, 2020a and b).

The IES algorithm substantially reduces the computational demand of parameter estimation for highly parameterized models by using a Monte Carlo approach to approximate the first-order relation between model inputs (parameters) and outputs (simulated equivalents of historical observations and forecasted conditions). This approximation allows the number of model runs required in each iteration of the IES process to be substantially fewer than the number of adjustable parameters (White, 2018). The initial NTGAM ensemble was comprised of 540 sets of possible random parameter values (or “realizations” of parameter values), including 133,644 adjustable input parameters.

The IES approach also provides the benefit of a built-in uncertainty analysis. The result of the IES algorithm is an ensemble of realizations (the “posterior parameter ensemble”) that show similar success in simulating historical conditions using different combinations of parameter values. This represents a level of nonuniqueness in aquifer properties and system stresses that exist after assimilating historical observations of groundwater levels, baseflow, and transmissivity estimates. This posterior ensemble is used to estimate uncertainty in future aquifer-system conditions by evaluating scenarios of future water use.

3.5.1 Model Observations

The model is designed to simulate the groundwater-level response to stress patterns in a temporally meaningful way and is primarily focused on simulating long-term changes in these quantities at regional to subregional spatial scales. Historical observations of groundwater levels and stream baseflow, and transmissivity estimates were used for history matching. Temporal differences in groundwater levels were also calculated with respect to every observation period in each monitoring well, providing an additional set of history-matching observations.

Because of the inherent noise associated with the different types of observation datasets, a complex grouping strategy was designed to formulate the history-matching objective function (Φ), summarized in Table 3-2. Groundwater levels were grouped by model layer, long-term versus non-long-term well (described in 3.5.1.1), type of model layer assignment (on the basis of well screen information availability or not), and measurement method. Groundwater-level temporal differences were grouped by measurement method only. Transmissivity observations were grouped by data source, and baseflow observations were grouped by stream-gage station. In addition to assigning observation weights reflecting the level of certainty given to various observation groups, a standard deviation of measurement noise (σ_ε) was assigned to each group, as indicated in Table 3-2. The σ_ε values were used to generate realizations of uncorrelated observation noise that were coupled to parameter realizations by the PEST++iES algorithm. This Bayesian parameter estimation approach was implemented to reduce the likelihood of parameter bias by coupling the uncertainty of model observations to parameter uncertainty in the history-matching process.

Table 3-2. Observation groups and subgroups comprising the objective function (Φ).

Group	Group contribution to Φ (%)	Subgroup	Subgroup contribution to Group (%)	Observation by layer	Subgroup σ_ε
Water Levels	60	Long-term, certain, non-airline[1]	70	Yes	15 ft
		Long-term, certain, airline	4	Yes	40 ft
		Long-term, uncertain, non-airline[1]	2	Yes	45 ft
		Long-term, uncertain, airline	1.4	Yes	60 ft
		Non-long-term, certain, non-airline[1]	20	Yes	20 ft
		Non-long-term, certain, airline	1.4	Yes	40 ft
		Non-long-term, uncertain, non-airline[1]	0.8	Yes	45 ft
		Non-long-term, uncertain, airline	0.4	Yes	80 ft
Water-Level Differences	5	Non-airline measurement type[1]	80	Yes	0.2 x measured
		Other (unknown)	15	Yes	0.3 x measured
		Airline	5	Yes	0.4 x measured
Transmissivity	30	CUWCD	76	No	0.1 x measured
		Other GCDs	5	No	0.2 x measured
		NTWGAM[2]	4	No	0.2 x measured
		CTGCD[3]	15	No	0.3 x measured
Baseflow	5	Streamgage Stations	100	No	0.2 x measured

[1]Non-airline: measured by any method other than both airline and unknown.,
[2]NTWGAM (Kelley and others, 2014) database

Group	Group contribution to Φ (%)	Subgroup	Subgroup contribution to Group (%)	Observation by layer	Subgroup
					σ_ε

[3]Uncertain: no screen information available for aquifer assignment.

3.5.1.1 Groundwater Levels

Groundwater-level observations for NTGAM (Figures 3-4 to 3-6, Table 3-3) were obtained from the USGS NWIS database (USGS, 2023a), the TWDB GWDB (TWDB, 2020b), and study area GCDs (Figure 1-5). An initial observation filtering process was performed, followed by a spatial and temporal observation declustering process to ensure that disparate groundwater levels did not occur in an area with spatially dense observations and that all model areas were represented during model history matching (Table 3-3, Figure 3-7). The remaining groundwater levels were then smoothed temporally (described below), and target observations were created from the smoothed observation values nearest the end of each stress period ("Model observations," Table 3-3 and Figure 3-7). In this way, much of the high-frequency noise associated with these observations was removed, but the important patterns expected to be matched by the model, such as longer-term changes in groundwater levels, were retained.

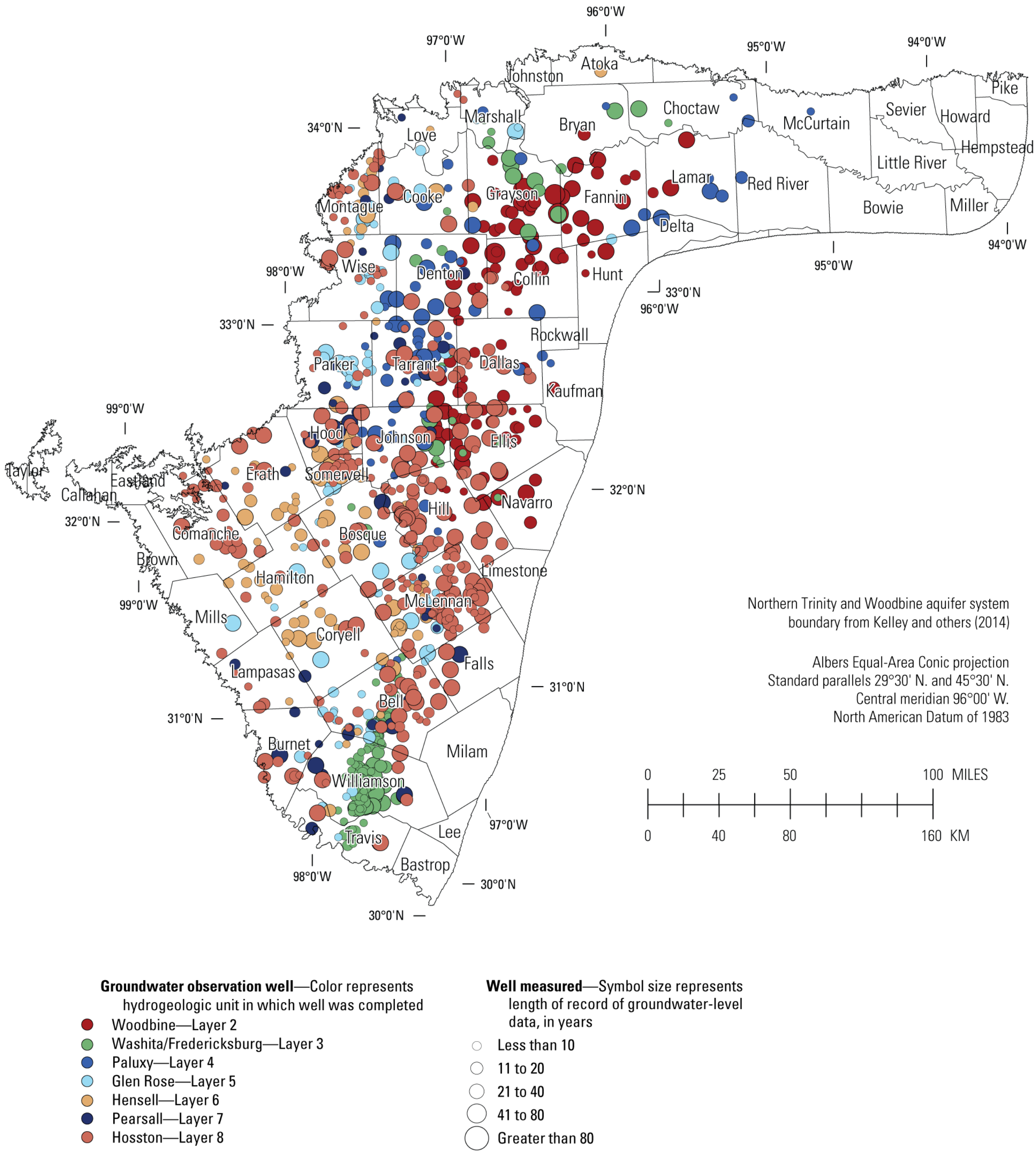

Figure 3-4. Spatial distribution of groundwater-level observations for observation wells screened in one hydrogeologic unit in the northern Trinity and Woodbine aquifer system.

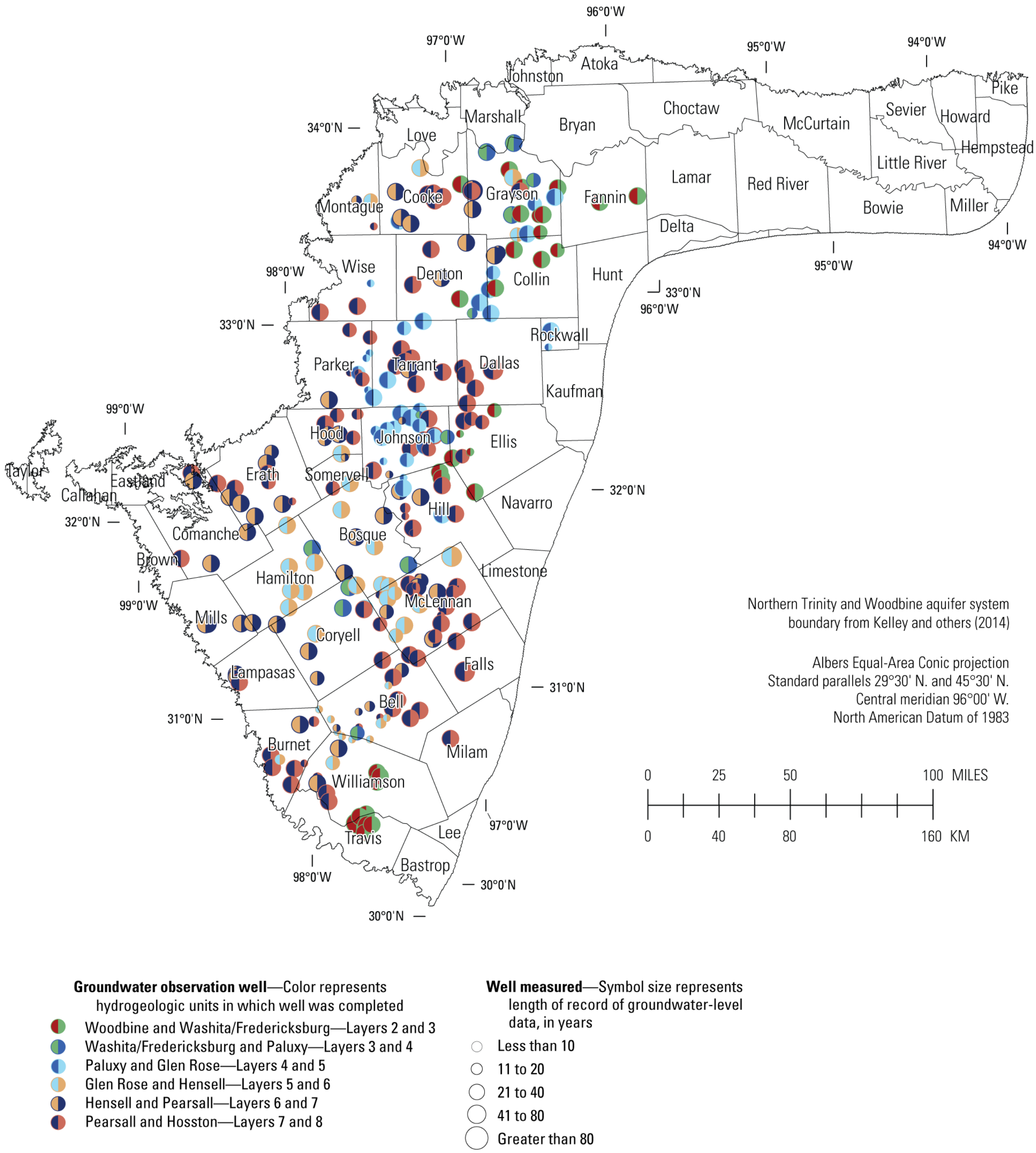

Figure 3-5. **Spatial distribution of groundwater-level observations for observation wells screened in two hydrogeologic units in the northern Trinity and Woodbine aquifer system.**

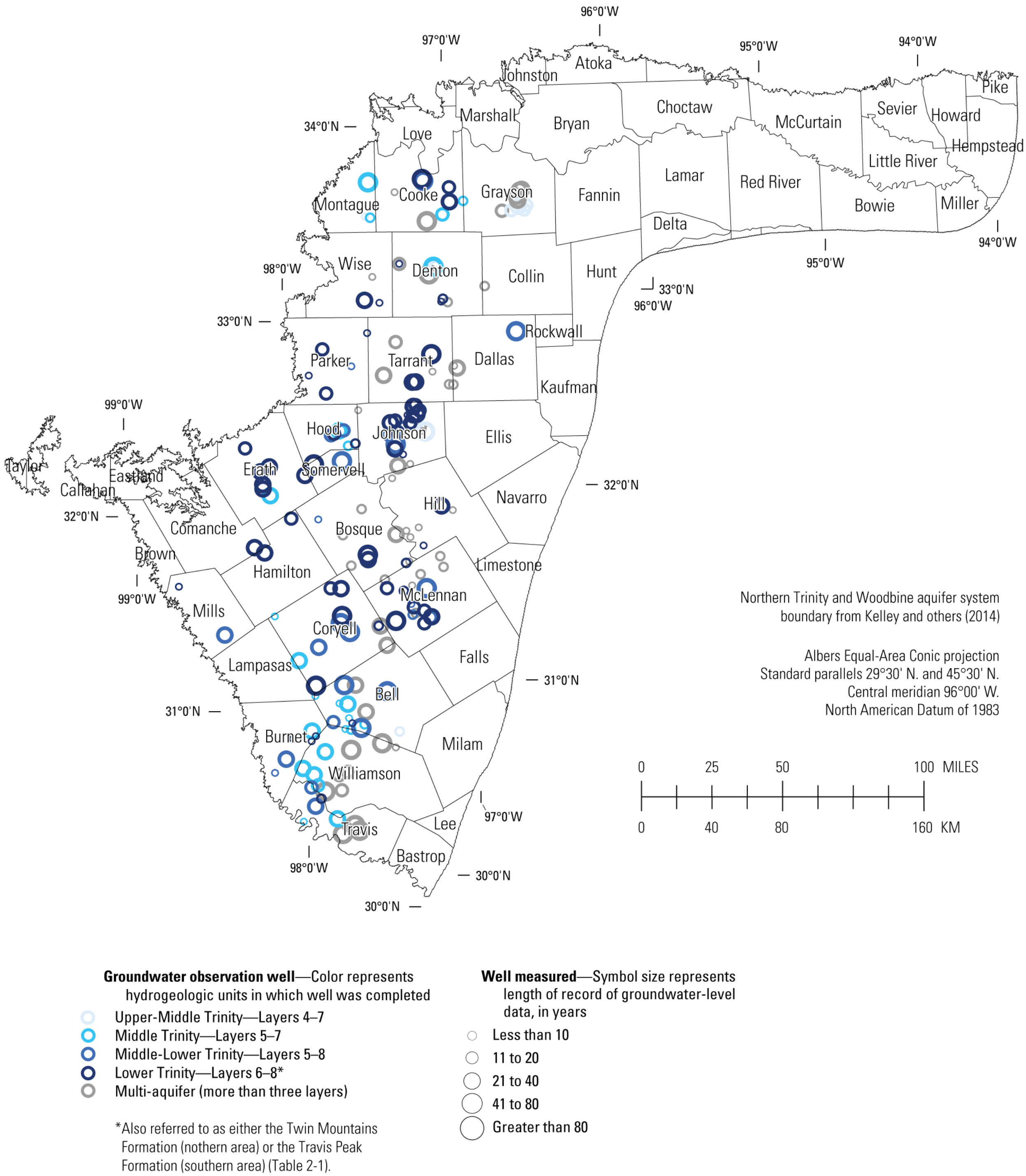

Figure 3-6. Spatial distribution of groundwater-level observations for observation wells screened in three or more hydrogeologic units in the northern Trinity and Woodbine aquifer system.

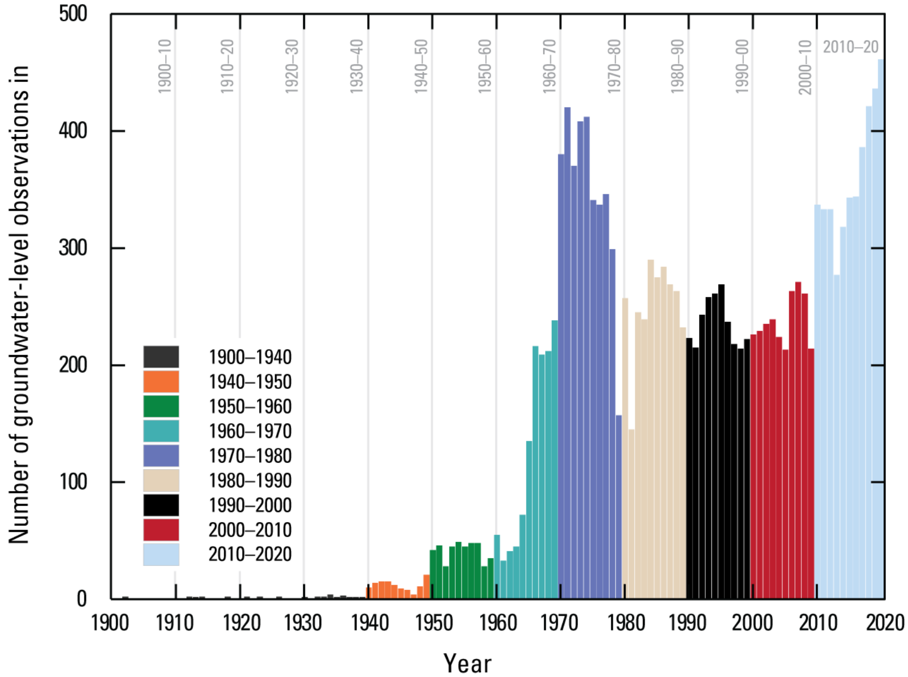

Figure 3-7. **Number of groundwater-level observations in model stress periods for the northern Trinity and Woodbine model.**

Table 3-3. Listing of observations in selected stress period for the northern Trinity and Woodbine Groundwater-Flow model.

Stress period[1]	Start date	End date	Total observations[1]	Model observations[2]	Stress period[1]	Start date	End date	Total observations[1]	Model observations[2]
14	1/1/1902	12/31/1902	1	1	84	1/1/1972	12/31/1972	1,657	370
24	1/1/1912	12/31/1912	2	1	85	1/1/1973	12/31/1973	1,618	408
25	1/1/1913	12/31/1913	2	2	86	1/1/1974	12/31/1974	1,219	412
26	1/1/1914	12/31/1914	1	1	87	1/1/1975	12/31/1975	1,186	341
30	1/1/1918	12/31/1918	1	1	88	1/1/1976	12/31/1976	1,057	337
33	1/1/1921	12/31/1921	2	1	89	1/1/1977	12/31/1977	1,024	346
35	1/1/1923	12/31/1923	1	1	90	1/1/1978	12/31/1978	1,082	299
38	1/1/1926	12/31/1926	2	1	91	1/1/1979	12/31/1979	908	157
42	1/1/1930	12/31/1930	2	2	92	1/1/1980	12/31/1980	1,192	257
44	1/1/1932	12/31/1932	2	1	93	1/1/1981	12/31/1981	1,048	145
45	1/1/1933	12/31/1933	1	1	94	1/1/1982	12/31/1982	1,039	245
46	1/1/1934	12/31/1934	5	4	95	1/1/1983	12/31/1983	820	239
47	1/1/1935	12/31/1935	2	2	96	1/1/1984	12/31/1984	1,515	290
48	1/1/1936	12/31/1936	4	3	97	1/1/1985	12/31/1985	1,143	275
49	1/1/1937	12/31/1937	8	2	98	1/1/1986	12/31/1986	787	284
50	1/1/1938	12/31/1938	4	2	99	1/1/1987	12/31/1987	735	269
51	1/1/1939	12/31/1939	10	2	100	1/1/1988	12/31/1988	658	263
52	1/1/1940	12/31/1940	39	10	101	1/1/1989	12/31/1989	607	232
53	1/1/1941	12/31/1941	65	14	102	1/1/1990	12/31/1990	565	223
54	1/1/1942	12/31/1942	114	15	103	1/1/1991	12/31/1991	662	215
55	1/1/1943	12/31/1943	88	15	104	1/1/1992	12/31/1992	740	243
56	1/1/1944	12/31/1944	57	12	105	1/1/1993	12/31/1993	854	258
57	1/1/1945	12/31/1945	35	9	106	1/1/1994	12/31/1994	963	261
58	1/1/1946	12/31/1946	36	8	107	1/1/1995	12/31/1995	1,044	269
59	1/1/1947	12/31/1947	10	4	108	1/1/1996	12/31/1996	889	237
60	1/1/1948	12/31/1948	32	11	109	1/1/1997	12/31/1997	867	218
61	1/1/1949	12/31/1949	112	21	110	1/1/1998	12/31/1998	749	214
62	1/1/1950	12/31/1950	209	42	111	1/1/1999	12/31/1999	796	222
63	1/1/1951	12/31/1951	222	46	112	1/1/2000	12/31/2000	906	226

64	1/1/1952	12/31/1952	223	28	113	1/1/2001	12/31/2001	995	229
65	1/1/1953	12/31/1953	254	45	114	1/1/2002	12/31/2002	1,160	235
66	1/1/1954	12/31/1954	392	49	115	1/1/2003	12/31/2003	1,566	239
67	1/1/1955	12/31/1955	241	45	116	1/1/2004	12/31/2004	1,446	224
68	1/1/1956	12/31/1956	217	48	117	1/1/2005	12/31/2005	1,341	213
69	1/1/1957	12/31/1957	296	48	118	1/1/2006	12/31/2006	1,568	263
70	1/1/1958	12/31/1958	249	28	119	1/1/2007	12/31/2007	1,707	271
71	1/1/1959	12/31/1959	222	35	120	1/1/2008	12/31/2008	1,736	261
72	1/1/1960	12/31/1960	258	55	121	1/1/2009	12/31/2009	3,846	214
73	1/1/1961	12/31/1961	288	33	122	1/1/2010	12/31/2010	5,566	337
74	1/1/1962	12/31/1962	245	41	123	1/1/2011	12/31/2011	5,789	333
75	1/1/1963	12/31/1963	446	45	124	1/1/2012	12/31/2012	6,419	333
76	1/1/1964	12/31/1964	402	72	125	1/1/2013	12/31/2013	6,875	277
77	1/1/1965	12/31/1965	466	135	126	1/1/2014	12/31/2014	7,523	318
78	1/1/1966	12/31/1966	950	216	127	1/1/2015	12/31/2015	9,651	343
79	1/1/1967	12/31/1967	1,085	209	128	1/1/2016	12/31/2016	10,620	344
80	1/1/1968	12/31/1968	578	212	129	1/1/2017	12/31/2017	14,459	386
81	1/1/1969	12/31/1969	729	238	130	1/1/2018	12/31/2018	17,839	421
82	1/1/1970	12/31/1970	1,359	380	131	1/1/2019	12/31/2019	18,289	436
83	1/1/1971	12/31/1971	1,800	420	132	1/1/2020	12/31/2020	19,668	461

[1]Total observations refers to the number of groundwater-level observations available from the Texas Water Development Board, the U.S. Geological Survey, Groundwater Conservation Districts, and others. These observations are then temporally declustered into each model stress period.

[2]Model observations refers to the number of groundwater-level observations used for model history matching produced from the spatial and temporal observation declustering process described in Section 3.5.1.1.

Single-layer monitoring wells (Figure 3-4) were assigned to unique model grid cells. As shown in Figure 3-4, the majority of single-layer wells are screened within the Hosston Aquifer, encompassing the largest areal distribution within the state of Texas with respect to other single-layer wells. Observations wells screened within The Glen Rose Formation, and Washita/Fredericksburg Groups are also ubiquitous throughout the model, while Paluxy and Woodbine wells are mostly in the middle and northern sections of the domain. In turn, most Pearsall and Hensell wells are located throughout the southern and southwestern portions of the model domain (Figure 3-4). Furthermore, Figure 3-5 shows observation wells screened across two model layers. Most of these wells are screened within the Hosston and Pearsall aquifers, encompassing a large area in the western portion of the model domain. Most wells screened both in the Glen Rose and Hensell units are located in the southern section, while those in both the Woodbine and Washita/Fredricksburg units are in the middle and northern sections of Texas. Lastly, wells screened in more than two layers are shown in Figure 3-6, with the majority of wells screened in the Lower Trinity aquifer and those designated as multi-aquifer wells screened across more than three layers.

The initial groundwater-level dataset, including model layer assignments of monitoring wells described in section 2.3.3, consisted of 2,289 wells with a state well number (SWN) available in the TWDB groundwater database. Wells that were completely screened below the Hosston aquifer (layer 8) or only in layer 1 (outcrop, alluvium, and/or younger formations) were removed from the history-matching dataset. Wells with data beginning after 2020, wells with only a single measurement with no screen information, or wells located along the southwestern edge of the active model domain (likely screened in another aquifer system other than the northern Trinity and Woodbine) were also excluded from history matching. This filtering reduced the initial number of wells to 1,692 assigned to 2,517 grid cells, out of which 172 were non-uniquely assigned to the same lateral (row, column) location. Clusters of two and three wells assigned to the same spatial location were programmatically de-clustered by keeping wells with unique layer assignments where possible while selecting wells with longer records in cases where multiple SWNs were assigned to the same cell (layer, row, column), resulting in 1,428 SWNs uniquely assigned to 2,514 grid cells.

Groundwater level measurements were aligned with the NTGAM temporal discretization. Data collected during winter months (between November and February) were preferred for history-matching, as these measurements are less likely to be affected by pumping. However, if winter data was not available for a well in a given year, measurements from other months were considered. The median water level of the first winter months in each hydrograph was generally selected as the first annual measurement. For subsequent consecutive years, the data point with the smallest difference with respect to the previous year was selected as the annual measurement. If no data was available for a consecutive year, the same criterion was applied to select the first annual measurement for a subsequent non-consecutive year. Upon generating an annual dataset, an outlier analysis was performed to remove measurements using the time-series Z-score metric:

$$\boldsymbol{z} = \frac{x-\mu}{\sigma} \quad \text{Equation 3-1}$$

Where *x* is a data point, μ is the moving average within the full temporal span of each hydrograph, and σ is the moving standard deviation. Measurements with -2 < Z-score < 2 were eliminated from the history-matching dataset.

A programmatic algorithm was also developed to reduce the number of history-matching wells to capture regional gradients. Clusters comprised of multiple wells within a mile of each other were identified, wherein wells assigned to model layers by screen information and with the longest historical records were preferred for history matching. Wells with water level records spanning a timeline before and/or after preferred wells, as well as all multi-aquifer wells were also kept. Furthermore, the following method was used to obtain single simulated hydrographs at monitoring wells crossing multiple model layers:

$$H_{tw} = \frac{\sum_{ijk}^{ijn} H_{ijk} \times HK_{ijk} \times b_{ijk}}{\sum_{ijk}^{ijn} HK_{ijk} \times b_{ijk}} = \frac{\sum_{ijk}^{ijn} H_{ijk} \times T_{ijk}}{\sum_{ijk}^{ijn} T_{ijk}} \qquad \text{Equation 3-2}$$

Where H_{tw} = transmissivity-weighted hydrograph, H_{ikj} = simulated hydrograph at cell *ijk* (layer, row, column), b_{ikj} = thickness of cell *ijk*, HK_{ijk} = hydraulic conductivity of cell *ijk*, T = transmissivity of cell *ijk*. Finally, a moving average with a 5-year window was applied to smooth the annual groundwater-level dataset, facilitating the assimilation of regional trends through history matching. The resulting groundwater-level dataset consisted of 16,510 measurements (Table 3-3) distributed in 1,428 wells, out of which 972 were single-layer wells with 11,176 measurements, and 456 were multi-layer wells with 5,334 measurements.

3.5.1.2 Transmissivity Estimates

Transmissivity estimates described in Section 2.1.2.3 were incorporated into the NTGAM history-matching dataset. Transmissivity targets were eliminated from model cells where the well screen encompassed less than 30% of the model layer thickness. In situations where multiple estimates were assigned to the same model cell, the arithmetic mean of all coincident transmissivity values was used as the history-matching target, resulting in unique cell assignments of prior transmissivity estimates. Given the multi-scale nature of transmissivity estimates, prior values that resulted in model hydraulic conductivity values greater than 40 ft/day were discarded. Model transmissivity was calculated as:

$$T = \sum_{ijk}^{ijn} HK_{ijk} \times b_{ijk} \qquad \text{Equation 3-3}$$

Where *b* is the layer thickness, and *HK* is the hydraulic conductivity of model cell *ijk*.

3.5.1.3 Stream Baseflow Measurements

Time-averaged flux measurements from 29 USGS stream gage stations were used as history-matching targets. These targets represented groundwater contributions to stream base flow, simulated through RIV and DRN cells representing perennial streams. Simulated fluxes were aggregated from all appropriate RIV and DRN cells within each drainage basin and evaluated against the corresponding stream-gage data.

3.5.2 Prior Parameter Distribution

A multivariate Gaussian (normal) distribution of model parameters is the primary assumption underlying the Bayesian data-assimilation process implemented in this work. Except for the SWB-based recharge arrays, the NTWGAM (Kelley and others, 2014) parameters were used as mean values of the prior (pre-history matching) probability distribution of the updated model. This was expressed by generating sets of adjustable multipliers encompassing the plausible variability of model parameters as percentage ranges (Table 3-4). These ranges were further constrained by lower and upper bounds representing minimum and maximum acceptable parameter values, respectively. As indicated in Table 3-4, a combination of grid-scale, pilot-point, and constant multipliers was implemented to perturb parameter values at multiple spatiotemporal scales, comprising a total of 133,644 adjustable parameters. Specifically, constant multipliers were implemented to represent domain-scale parameter variability, pilot points represented broad-scale heterogeneity, and grid-scale multipliers represented localized variability. Both grid-scale and pilot-point multipliers were assigned spatial or temporal correlations through geostatistical variograms using the pyEMU library, defining the prior parameter covariance.

Table 3-4. Aquifer parameters and mean prior parameter distribution multiplier range.

Aquifer property	Multiplier parameter					
	Domain scale multiplier	Pilot point multiplier	Individual cell (Grid scale) multiplier	Temporal variation	Lower and upper limits for each multiplier	Absolute upper and lower limit
Horizontal Hydraulic Conductivity (Alluvium Zone in Layer 1)[1]	X	X	--	--	0.1–10	1–300 [ft/d]
Vertical Hydraulic Conductivity (Alluvium Zone in Layer 1)[1]	X	X	--	--	0.1–10	0.1–30 [ft/d]
Vertical Hydraulic Conductivity (Outcrop Zone in Layer 1)	X	X	--	--	0.1–1.9	10^{-7}–30 [ft/d]
Horizontal Hydraulic Conductivity (Layer 2)	X	X	--	--	0.01–100	10^{-3}–40 [ft/d]
Horizontal Hydraulic Conductivity (Layer 3)	X	X	--	--	0.01–100	10^{-3}–40 [ft/d]
Horizontal Hydraulic Conductivity (Layer 4)	X	X	--	--	0.01–100	10^{-3}–40 [ft/d]
Horizontal Hydraulic Conductivity (Layer 5)	X	X	--	--	0.01–100	10^{-3}–40 [ft/d]
Horizontal Hydraulic Conductivity (Layer 6)	X	X	--	--	0.01–100	10^{-3}–40 [ft/d]
Horizontal Hydraulic Conductivity (Layer 7)	X	X	--	--	0.01–100	10^{-3}–40 [ft/d]
Horizontal Hydraulic Conductivity (Layer 8)	X	X	--	--	0.01–100	10^{-3}–40 [ft/d]
Vertical Hydraulic Conductivity (Layer 2)	X	X	--	--	0.01–100	10^{-8}–10 [ft/d]
Vertical Hydraulic Conductivity (Layer 3)	X	X	--	--	0.01–100	10^{-8}–10 [ft/d]
Vertical Hydraulic Conductivity (Layer 4)	X	X	--	--	0.01–100	10^{-8}–10 [ft/d]
Vertical Hydraulic Conductivity (Layer 5)	X	X	--	--	0.01–100	10^{-8}–10 [ft/d]
Vertical Hydraulic Conductivity (Layer 6)	X	X	--	--	0.01–100	10^{-8}–10 [ft/d]
Vertical Hydraulic Conductivity (Layer 7)	X	X	--	--	0.01–100	10^{-8}–10 [ft/d]
Vertical Hydraulic Conductivity (Layer 8)	X	X	--	--	0.01–100	10^{-8}–10 [ft/d]
Specific Storage (Layer 2)	X	X	--	--	0.01–100	10^{-8}–10^{-4} [ft–1]
Specific Storage (Layer 3)	X	X	--	--	0.01–100	10^{-8}–10^{-4} [ft–1]

Aquifer property	Multiplier parameter					
	Domain scale multiplier	Pilot point multiplier	Individual cell (Grid scale) multiplier	Temporal variation	Lower and upper limits for each multiplier	Absolute upper and lower limit
Specific Storage (Layer 4)	X	X	--	--	0.01–100	10^{-8}–10^{-4} [ft–1]
Specific Storage (Layer 5)	X	X	--	--	0.01–100	10^{-8}–10^{-4} [ft–1]
Specific Storage (Layer 6)	X	X	--	--	0.01–100	10^{-8}–10^{-4} [ft–1]
Specific Storage (Layer 7)	X	X	--	--	0.01–100	10^{-8}–10^{-4} [ft–1]
Specific Storage (Layer 8)	X	X	--	--	0.01–100	10^{-8}–10^{-4} [ft–1]
Perennial Rivers, Conductance (RIV)	--	--	X	--	0.01–100	10^{-2}–10^{6} [ft^2 d–1]
Reservoir Conductance (RIV)	X	--	--	--	0.01–100	10^{-4}–500 [ft^2 d–1]
Younger Formations Conductance (RIV)	X	--	--	--	0.01–100	1–1,000 [ft^2 d-1]
Ephemeral Streams Conductance (DRN)	X	--	--	--	0.01–100	10^{2}–10^{5} [ft^2 d-1]
Riparian Evapotranspiration Conductance (DRN)	--	--	X	--	0.01–100	10^{2}–10^{5} [ft^2 d-1]
Flowing Wells Conductance (DRN)	X	--	--	--	0.01–100	10^{2}–10^{5} [ft^2 d-1]
Springs Conductance (DRN)	X	--	--	--	0.01–100	10^{2}–10^{5} [ft^2 d-1]
Groundwater Use (pre-1980 irrigation)	--	--	X	X	0.4–1.6	--
Groundwater Use (pre-1980 all other uses)	--	--	X	X	0.7–1.3	--
Groundwater Use (pre-1980 outside Texas)	--	--	X	X	0.6–1.4	--
Groundwater Use (post-1980 TWDB)	--	--	X	X	0.8–1.2	--
Groundwater Use (post-1980 rural/domestic)	--	--	--	X	0.6–1.2	--
Recharge	X	X	--	X	0.9–1.1	--

[1]The alluvium zone represents alluvial sediment adjacent to major rivers represented in the model using the River package.

3.5.3 History Matching with PEST++iES

A stochastic data assimilation approach was implemented by generating a prior parameter ensemble of 600 realizations. The prior "base" model realization, corresponding to the converted MODFLOW 6 NTWGAM version, was upgraded along with all ensemble members that reduced model-to-measurement misfit throughout multiple optimization iterations (Figures 3-8, 3-9). The Φ evolution resulted in a posterior ensemble centered around the base realization after two optimization iterations, with subsequent iterations incurring data noise overfitting. Re-inflating the ensemble variance after four iterations to prevent an ensemble collapse from noise overfitting did not improve the optimization outcome. Hence, 522 model realizations comprising the iteration 2 ensemble were used as the posterior parameter ensemble.

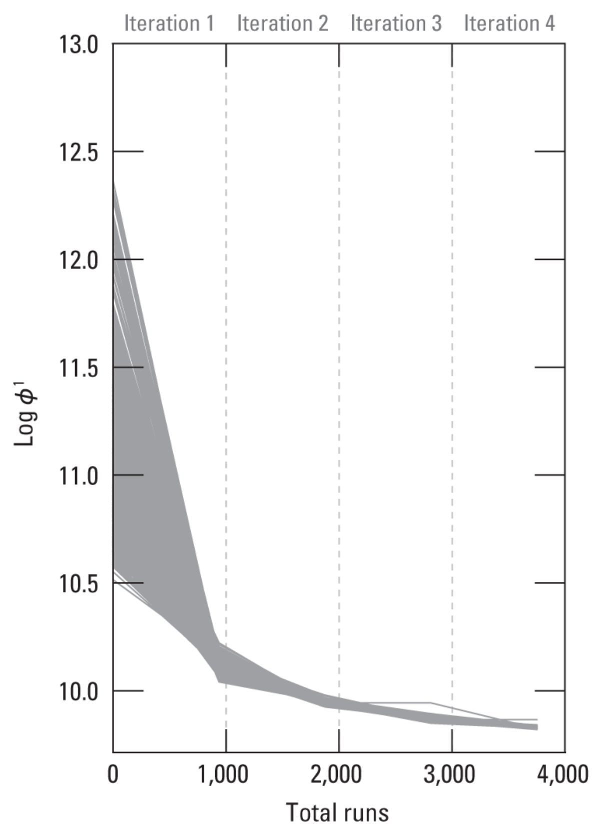

[1]The objective function (ϕ) is the sum of squared weighted residuals.

Figure 3-8. Objective function reduction over four iterations.

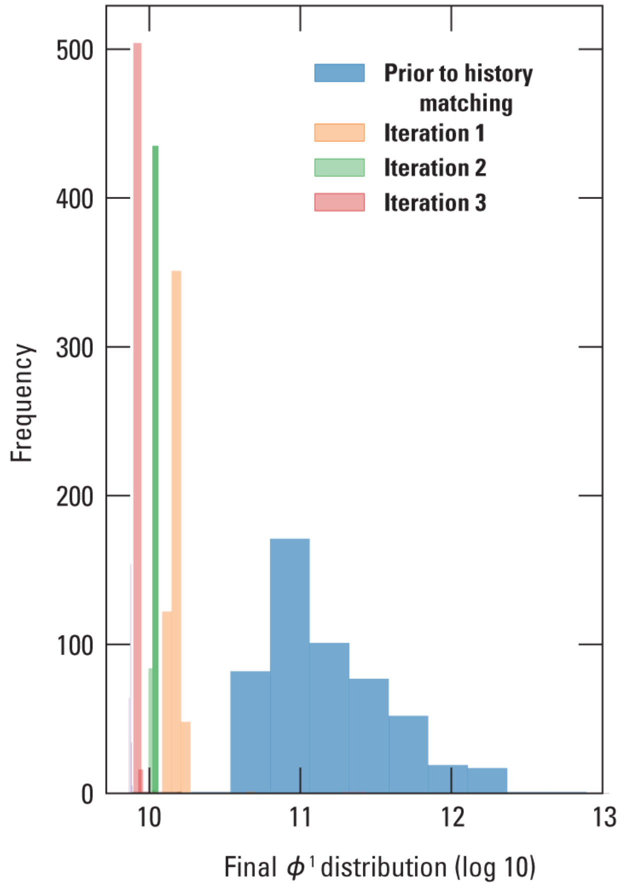

[1]The objective function (ϕ) is the sum of squared weighted residuals.

Figure 3-9. Histograms of the objective function reduction over four iterations.

Results from the second PEST++iES optimization iteration comprise the posterior parameter ensemble. In general, parameter values in the posterior ensemble were constrained within the prior ensemble variance, while most values of the posterior base realization were constrained within the parameter values of the previous MODFLOW-NWT NTWGAM version. However, a noteworthy deviation from the NWT version increased values of hydraulic conductivity driven by transmissivity targets and increased the values of streambed conductance in perennial and ephemeral streams, driven by baseflow targets and SWB-derived recharge, respectively. Despite these adjustments, the parameter distribution of the posterior ensemble indicated that the conceptual understanding of the Northern Trinity and Woodbine aquifer system was not modified via history matching.

A single realization (which is “the” NTGAM) was selected from the Posterior, which represents the maximum a priori realization. That is, this realization represents the mean of the Prior and, therefore, is also near the Posterior mean. Conceptually, this realization represents the model inputs with minimum prior heterogeneity and is also the closest ensemble method equivalent to the minimum error variance solution (Moore and Doherty, 2005; Doherty, 2015). This single realization can be used as the history-matched NTGAM model when a single realization is preferred.

3.5.3.1 Hydraulic Conductivity and Storage Parameters

Figures 3-10 through 3-12 include violin plots displaying the prior and posterior ensemble distribution of aquifer hydraulic parameters. The frequency and range of numerical values are represented by the width and the length of the violin plots, respectively. As shown in Figures 3-10 through 3-12, the encapsulation of the posterior ensemble within prior uncertainty bounds indicates that history matching resulted in a stochastic distribution of aquifer hydraulic properties with physical plausibility in a regional scale context. Likewise, the posterior ensemble did not show a tendency for numerical hydraulic properties to collapse near physical parameter bounds, represented by the vertical extent of each violin plot. This indicates minimal statistical bias in the resulting property distributions. A few noteworthy exceptions to this observation include the horizontal hydraulic conductivity of the alluvium zone of layer 1 and the vertical hydraulic conductivity of the outcrop zone of layer 1, with 21% and 15% of the ensemble realizations distributed near upper parameter bounds, respectively. The former was likely driven by groundwater outflow towards perennial streams in the alluvium zone, whereas the latter was primarily attributed to recharge flux towards deeper confined units, including the Hosston aquifer (layer 8). This was further evidenced by 7% of the posterior ensemble of vertical hydraulic conductivity of layer 8 near its upper bound (Figure 3-11), coinciding with the highest values in the base realization.

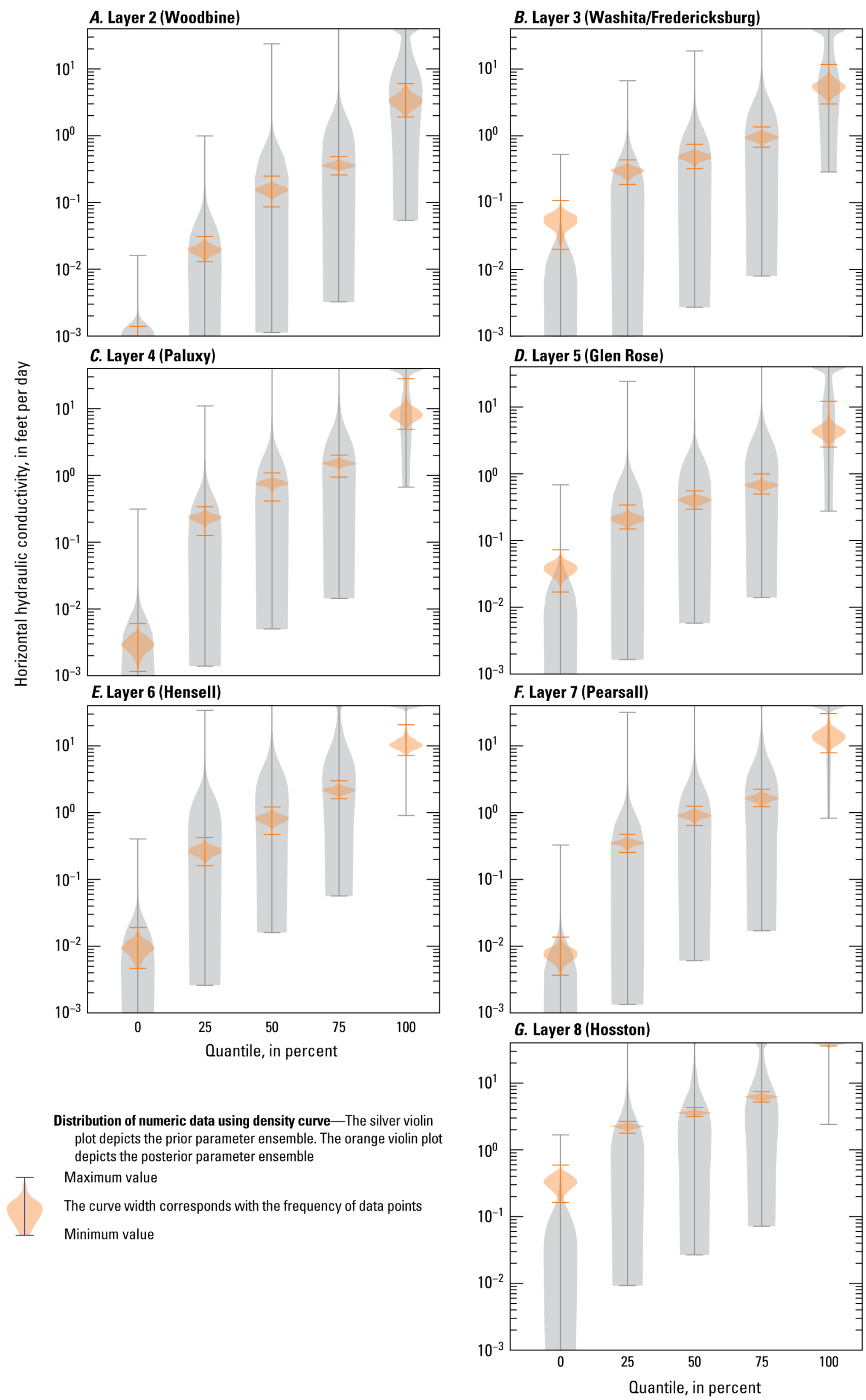

Figure 3-10. Violin plots showing the prior and posterior parameter ensemble horizontal hydraulic conductivity.

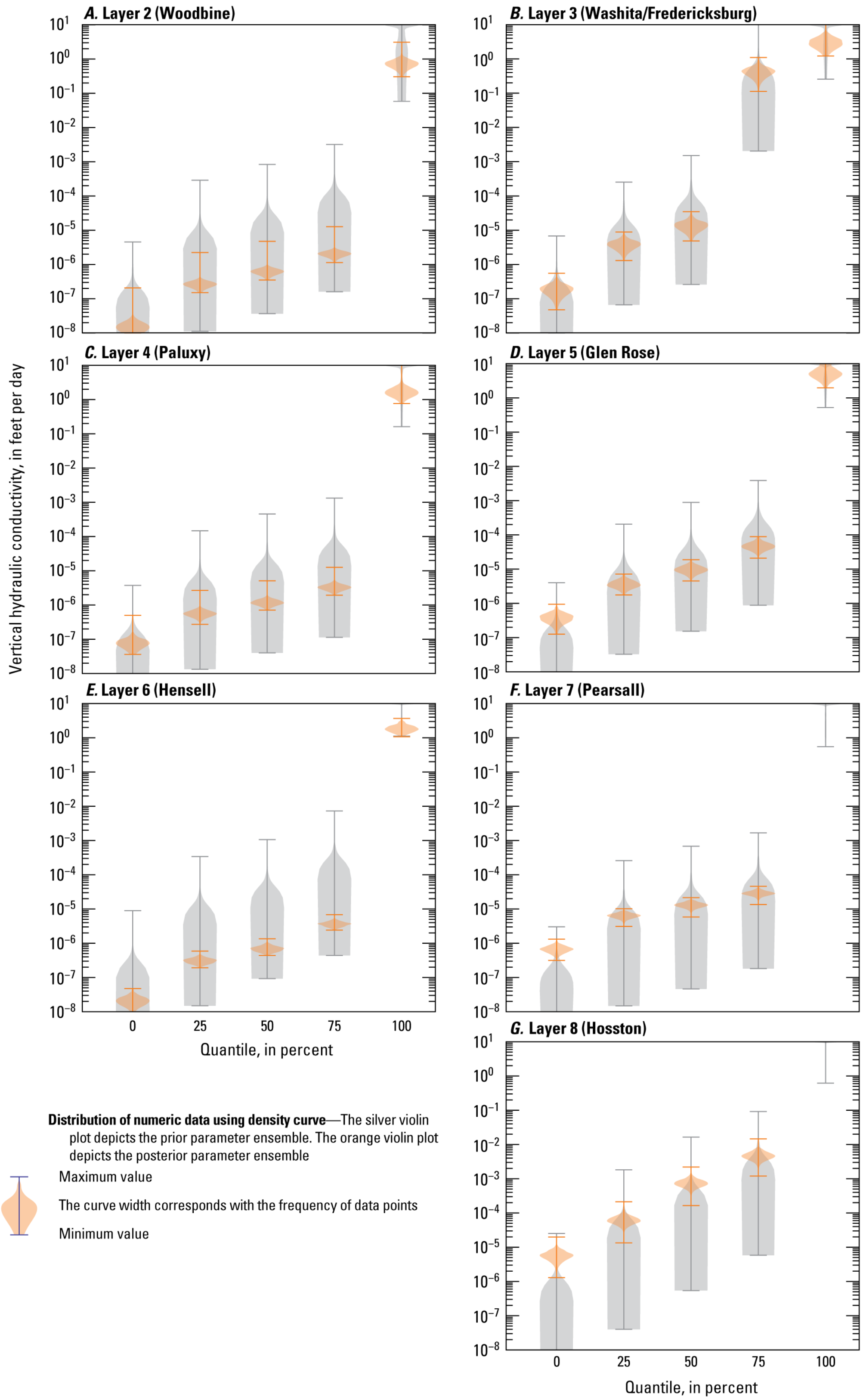

Figure 3-11. Violin plots showing the prior and posterior parameter ensemble vertical hydraulic conductivity.

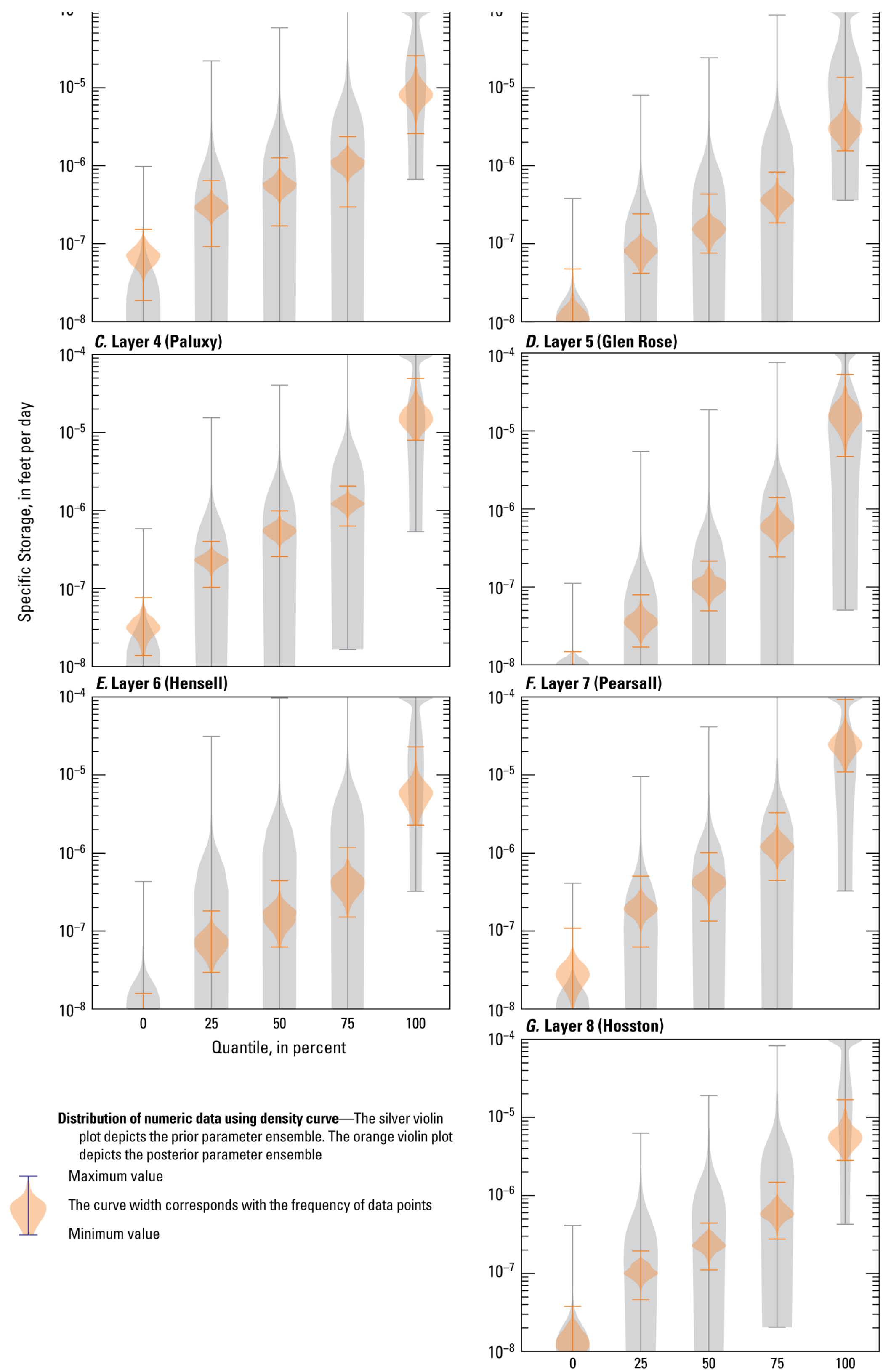

Figure 3-12. Violin plots showing the prior and posterior parameter ensemble specific storage.

Figures 3-13 through 3-36 show the history-matched aquifer hydraulic properties in all model layers, which are also summarized in Table 3-5. As shown in Figures 3-13 and 3-21, both the horizontal and vertical hydraulic conductivity values are higher in the up-dip outcrop areas of layer 1, which includes the highly transmissive alluvial sediments. Likewise, all confined layers (Figures 3-12 through 3-20) tend to have higher values of hydraulic conductivity and specific storage in the up-dip areas, with values decreasing towards the eastern model boundary. Localized deviations from this trend are only present in the southern portion of the Hosston aquifer (Figure 3-20), where relatively higher values of horizontal hydraulic conductivity were constrained by transmissivity values estimated from aquifer hydraulic tests. Furthermore, all confined layers in Figures 3-22 through 3-28 show a fringe of higher values of vertical hydraulic conductivity, allowing water to flow through the BFZ and discharge to the Younger Formations in layer 1. Although this flow mechanism is uncertain, i.e., not well constrained by hydrogeological characterization data, it is consistent with the original conceptual understanding of NTWGAM.

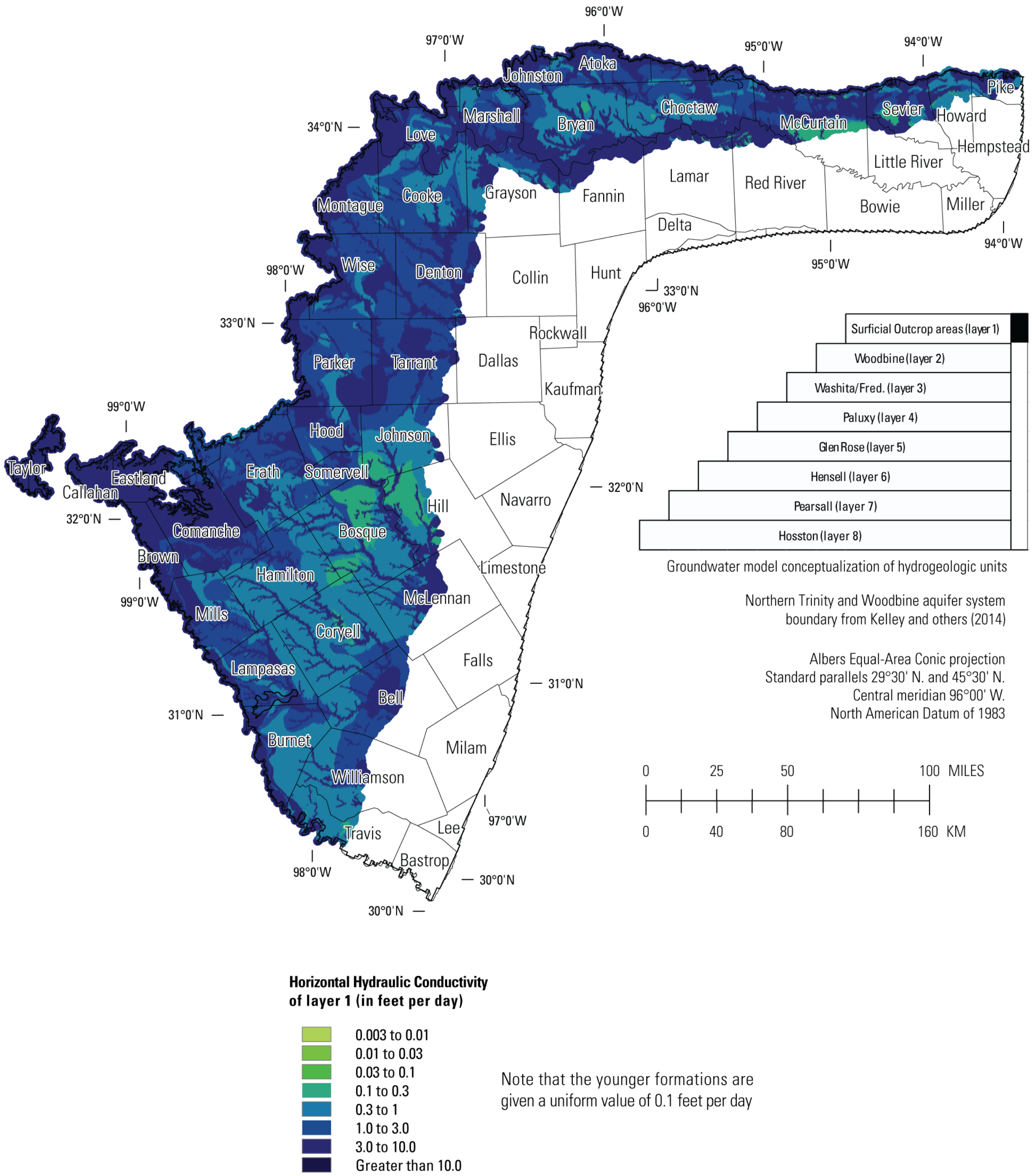

Figure 3-13. History-matched horizontal hydraulic conductivity for the surficial outcrop area of layer 1

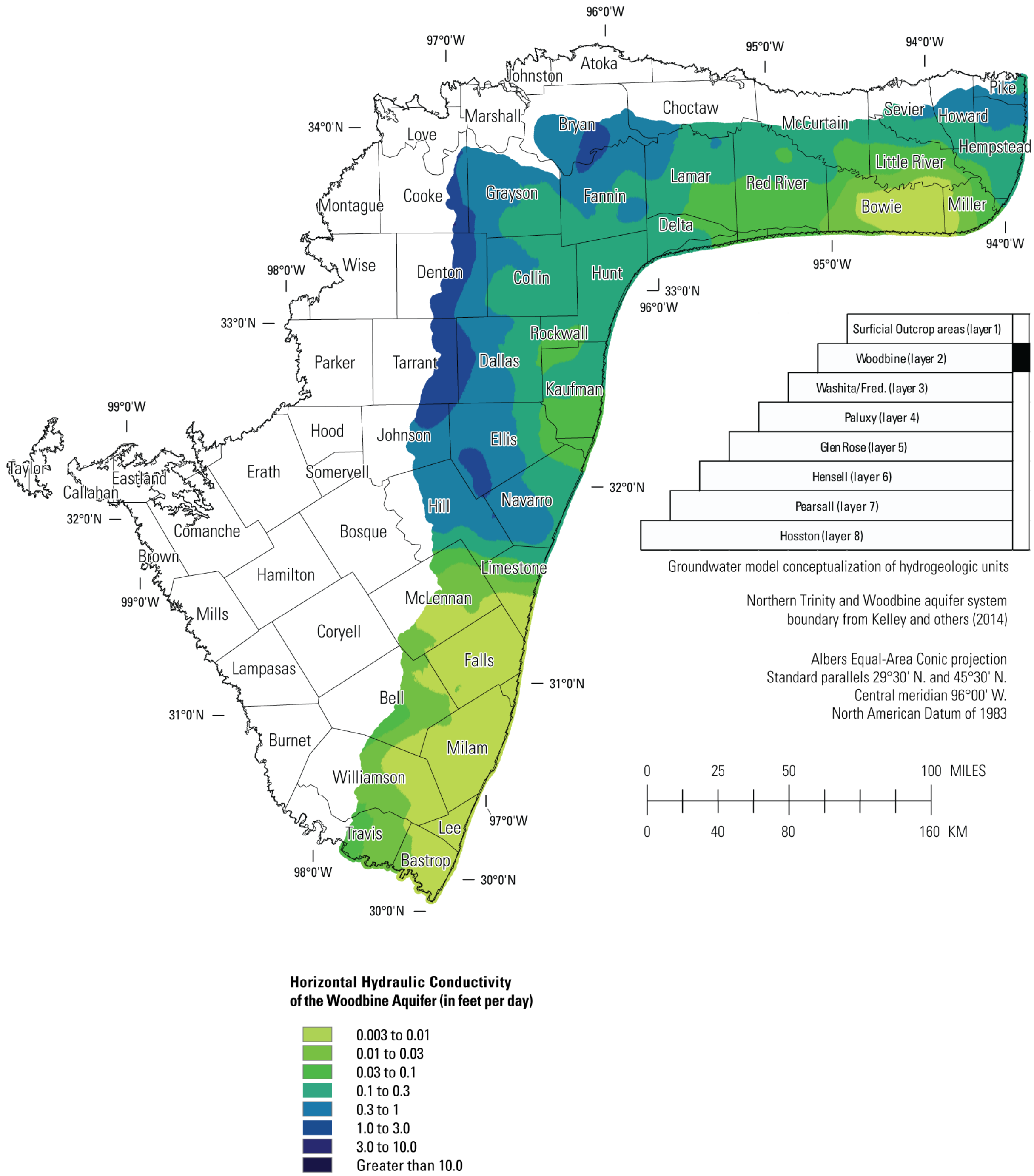

Figure 3-14. History-matched horizontal hydraulic conductivity for the Woodbine Aquifer (layer 2).

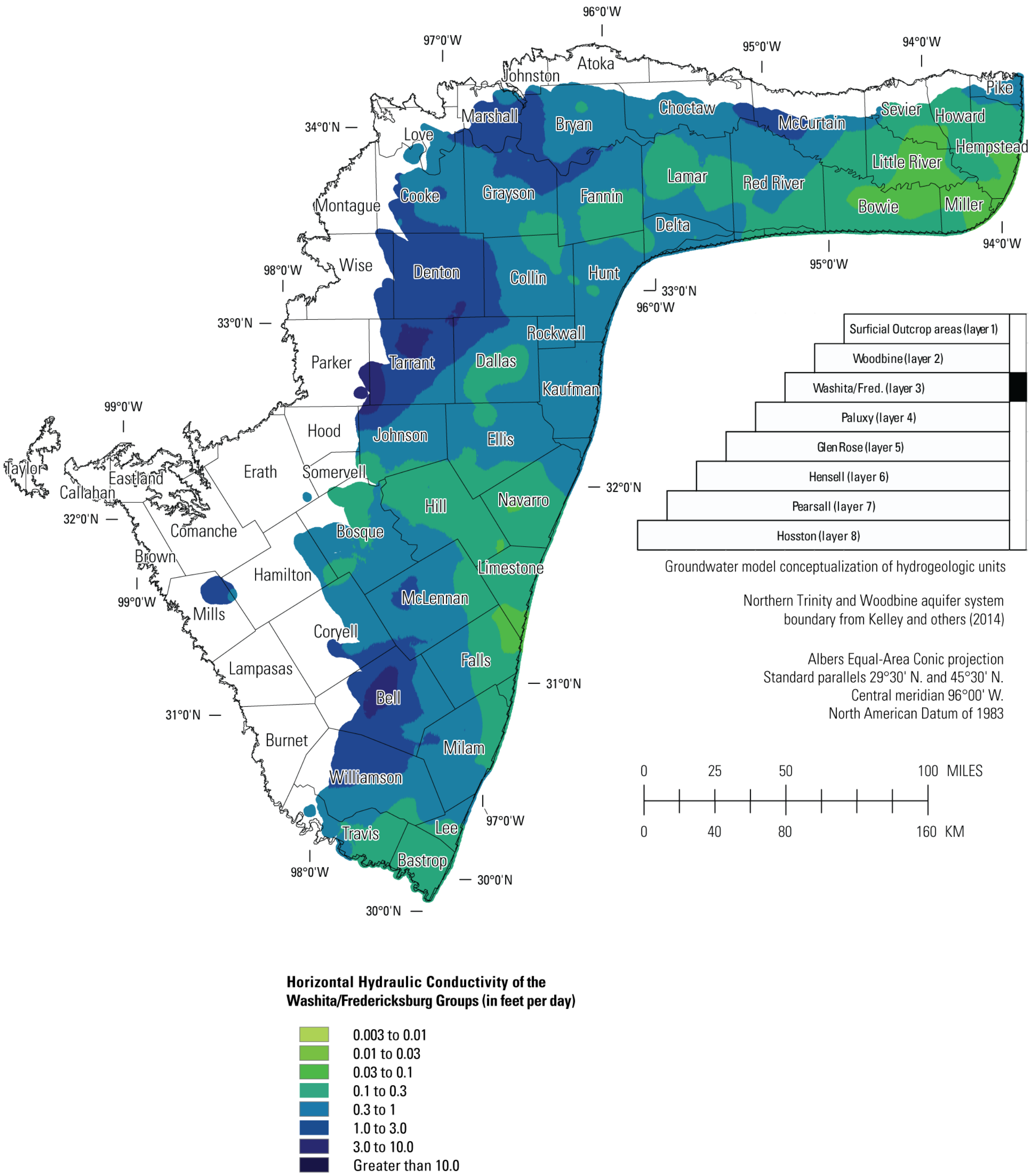

Figure 3-15. History-matched horizontal hydraulic conductivity for the Washita/Fredericksburg Groups (layer 3).

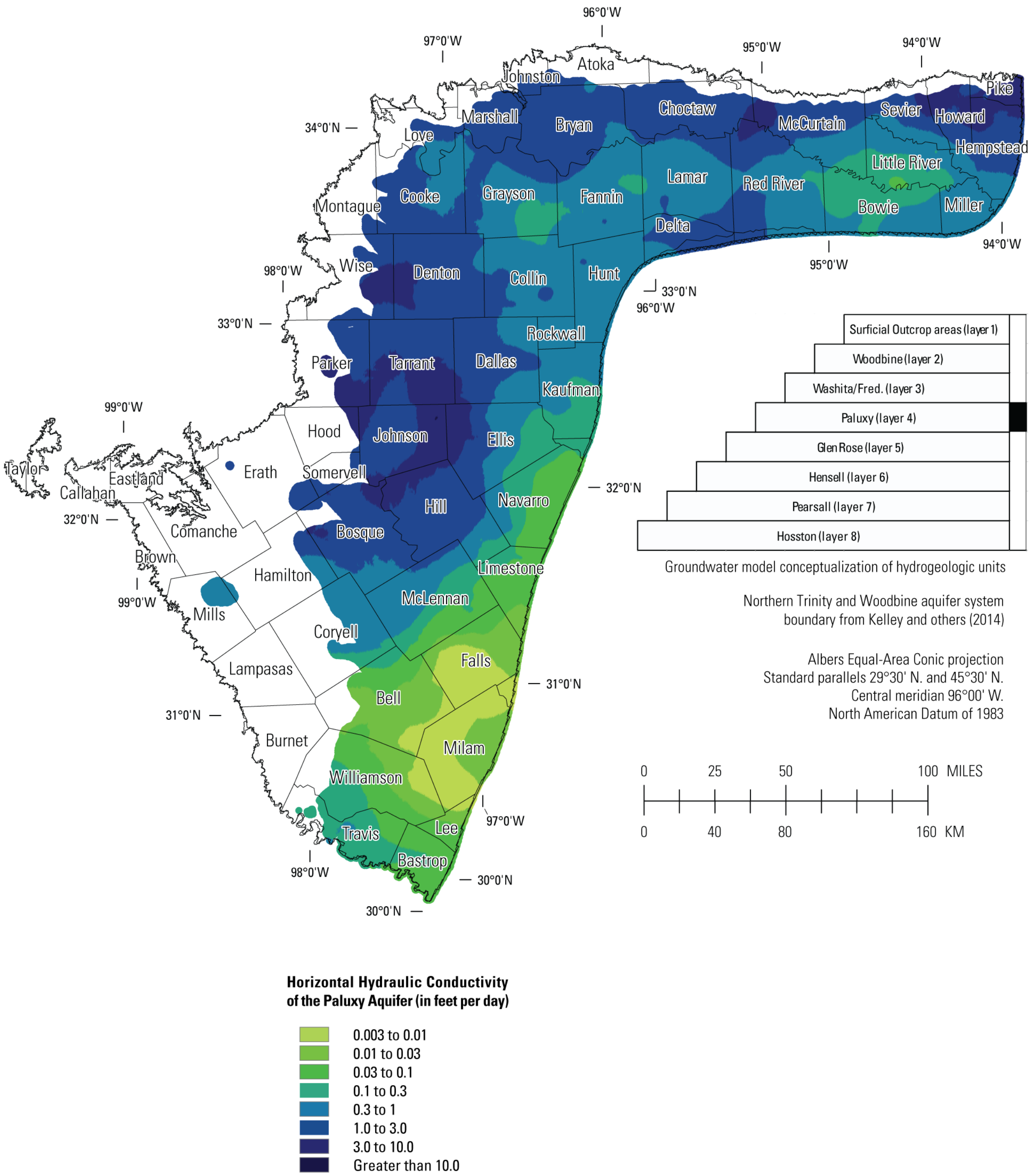

Figure 3-16. History-matched horizontal hydraulic conductivity for the Paluxy Aquifer (layer 4).

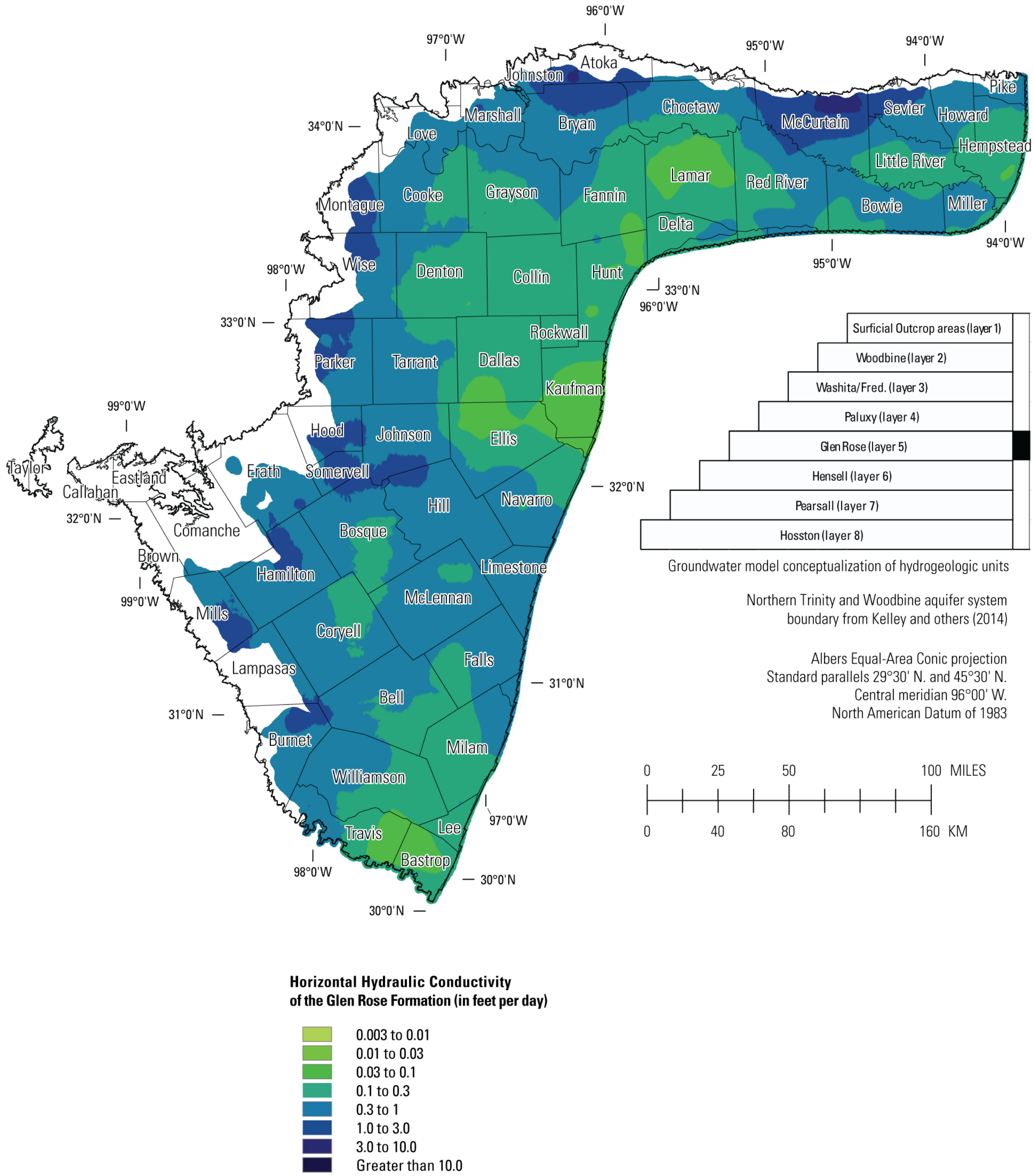

Figure 3-17. History-matched horizontal hydraulic conductivity for the Glen Rose Formation (layer 5).

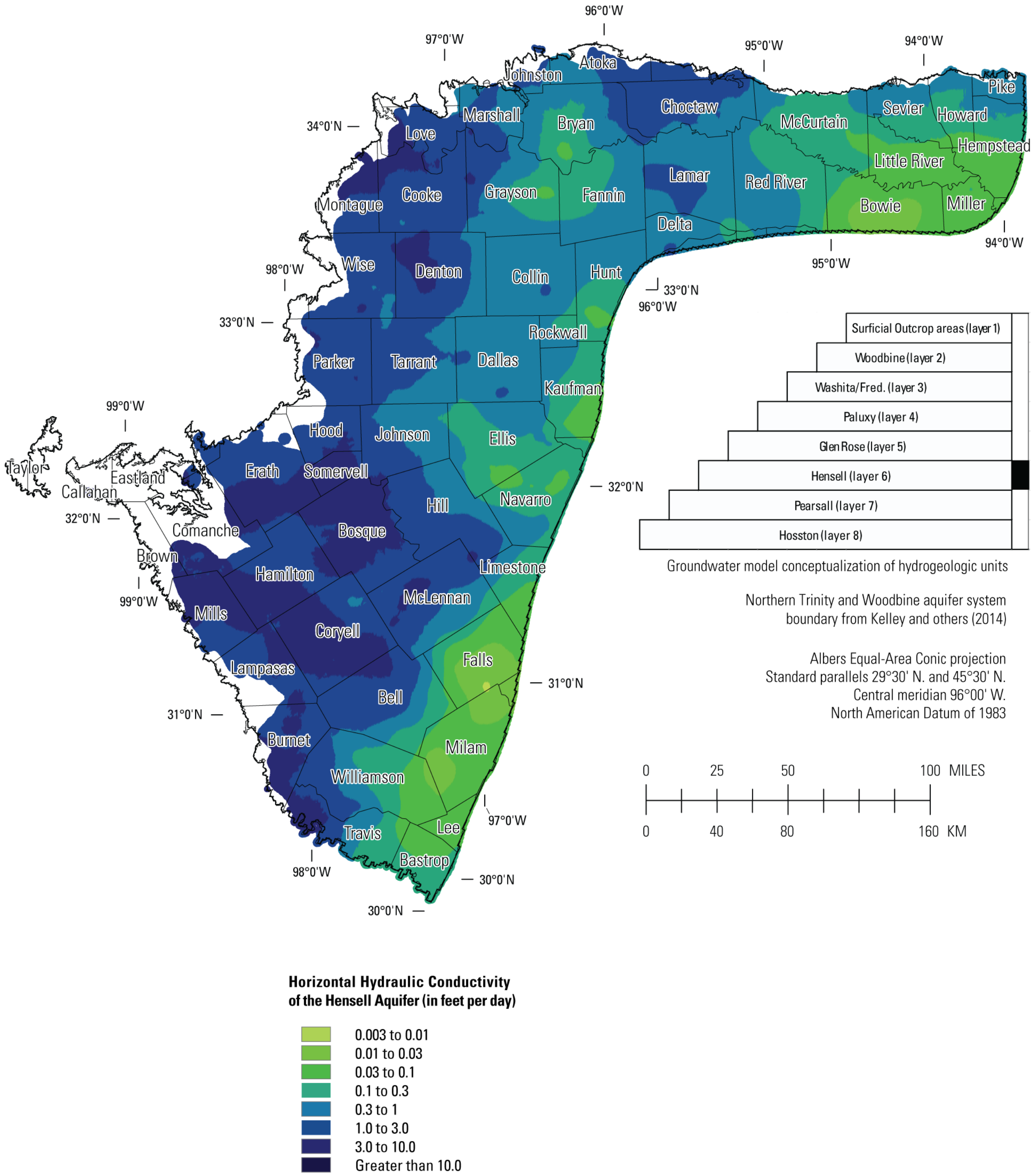

Figure 3-18. History-matched horizontal hydraulic conductivity for the Hensell Aquifer (layer 6).

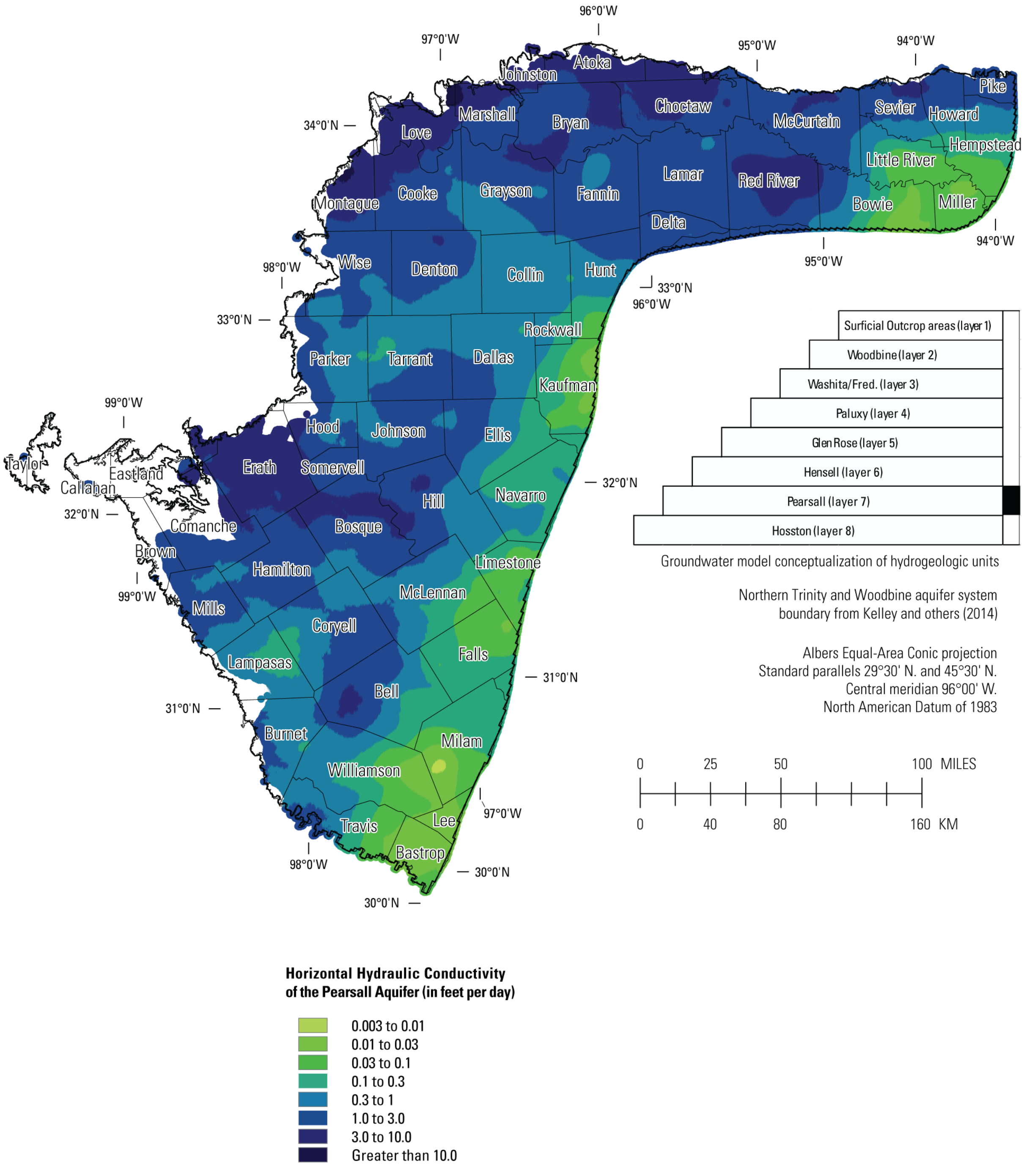

Figure 3-19. History-matched horizontal hydraulic conductivity for the Pearsall Formation (layer 7).

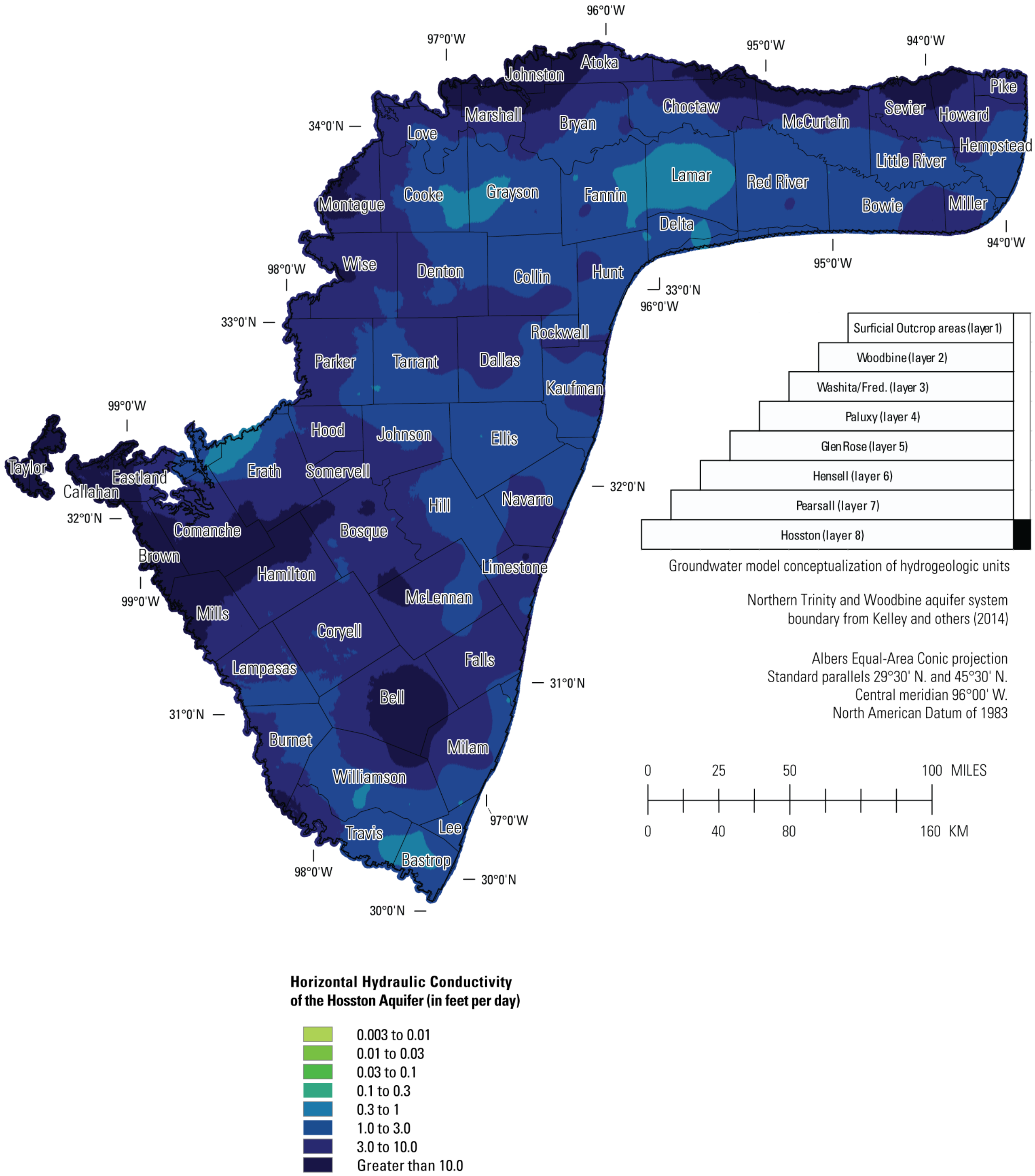

Figure 3-20. **History-matched horizontal hydraulic conductivity for the Hosston Aquifer (layer 8).**

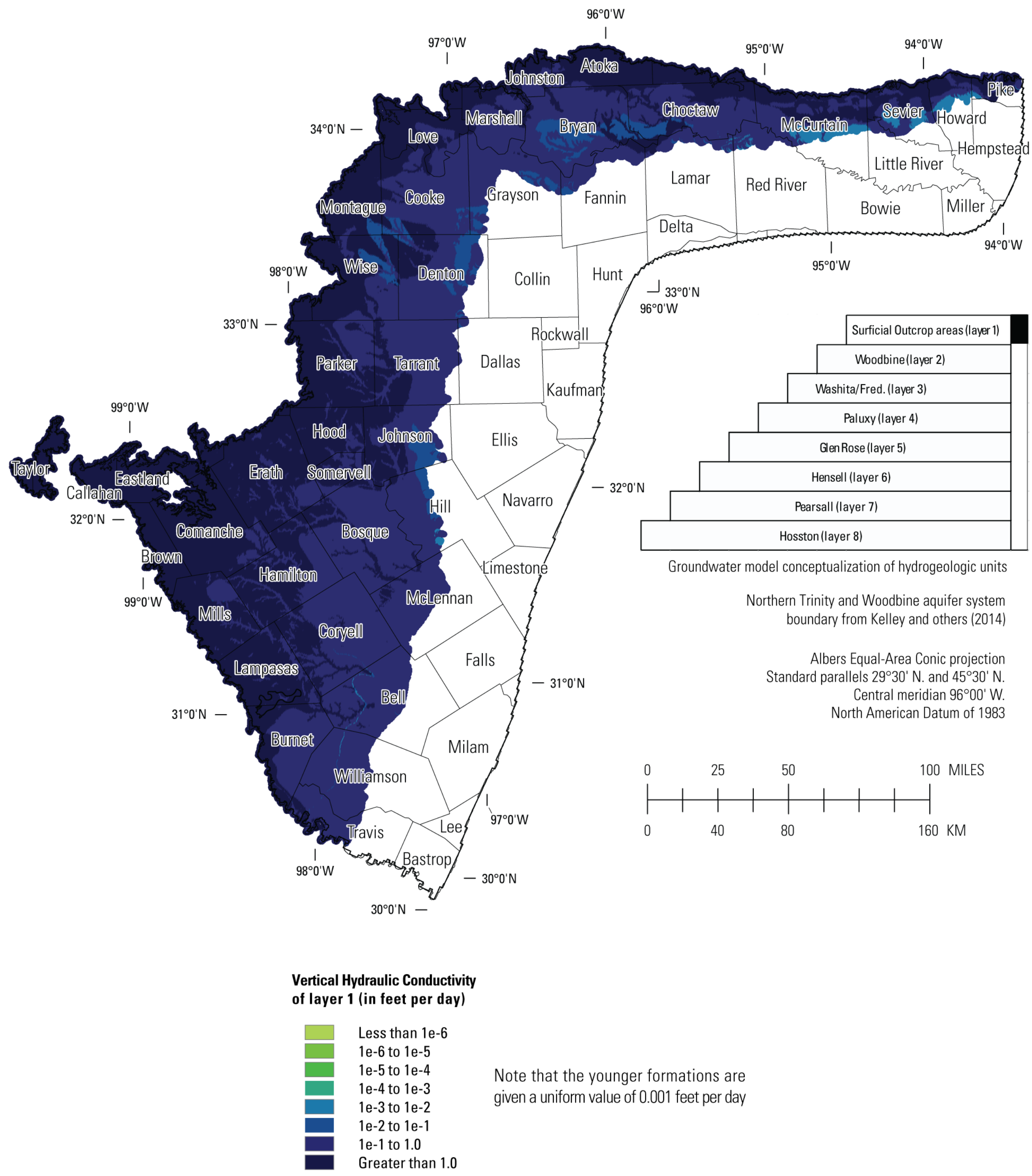

Figure 3-21. History-matched vertical hydraulic conductivity for the surficial outcrop area of layer 1

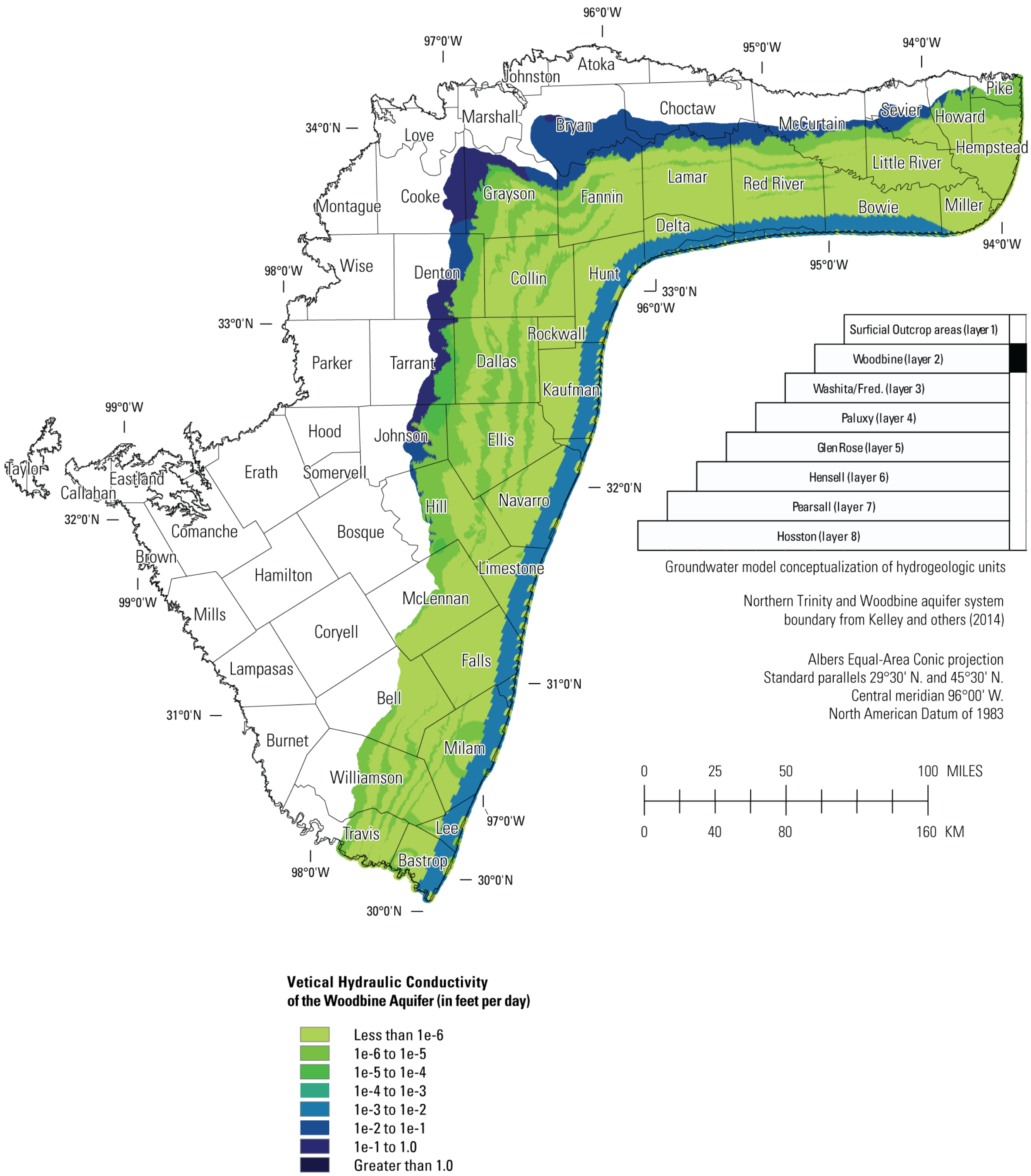

Figure 3-22. History-matched vertical hydraulic conductivity for the Woodbine Aquifer (layer 2).

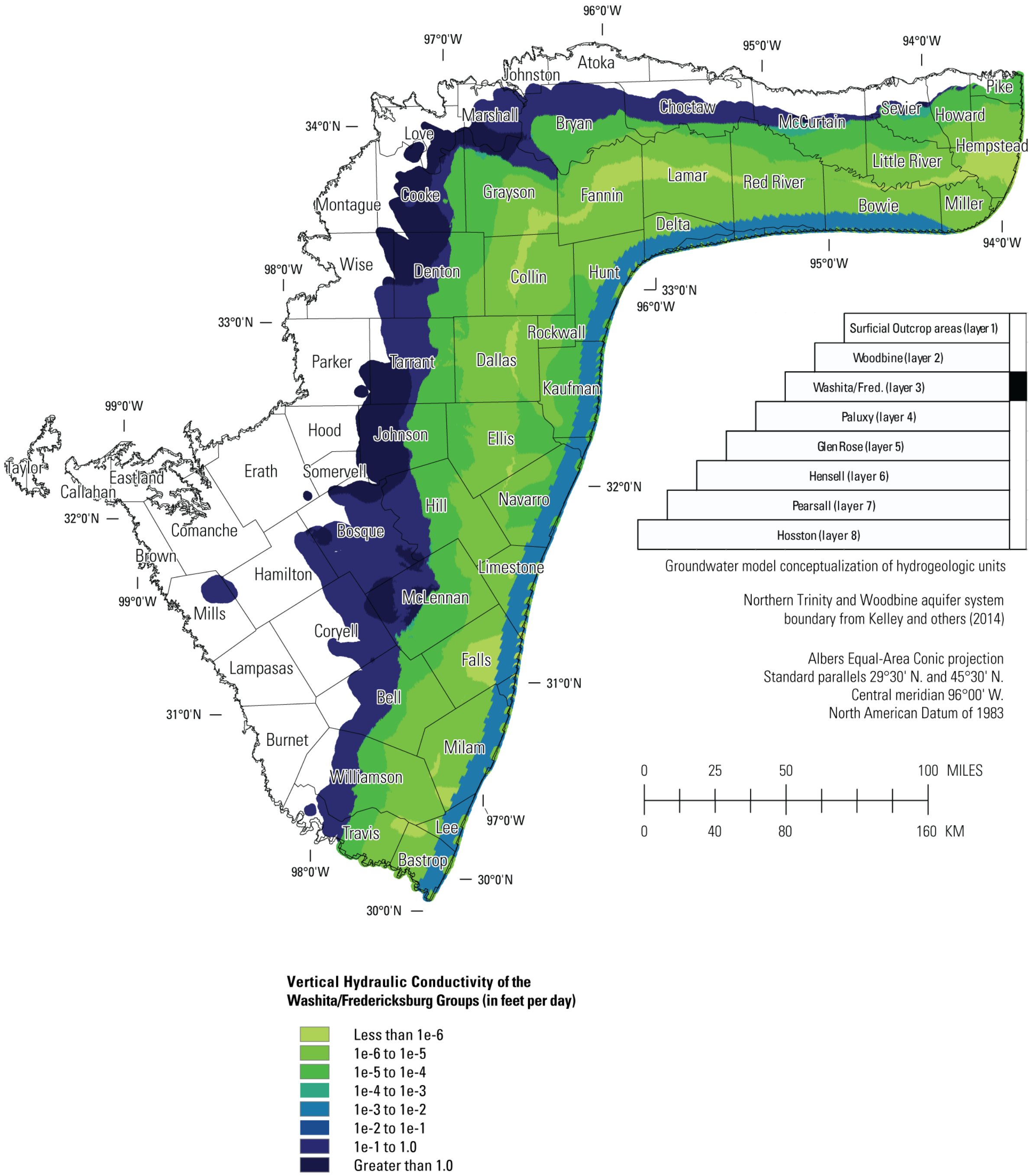

Figure 3-23. **History-matched vertical hydraulic conductivity for the Washita/Fredericksburg Groups (layer 3).**

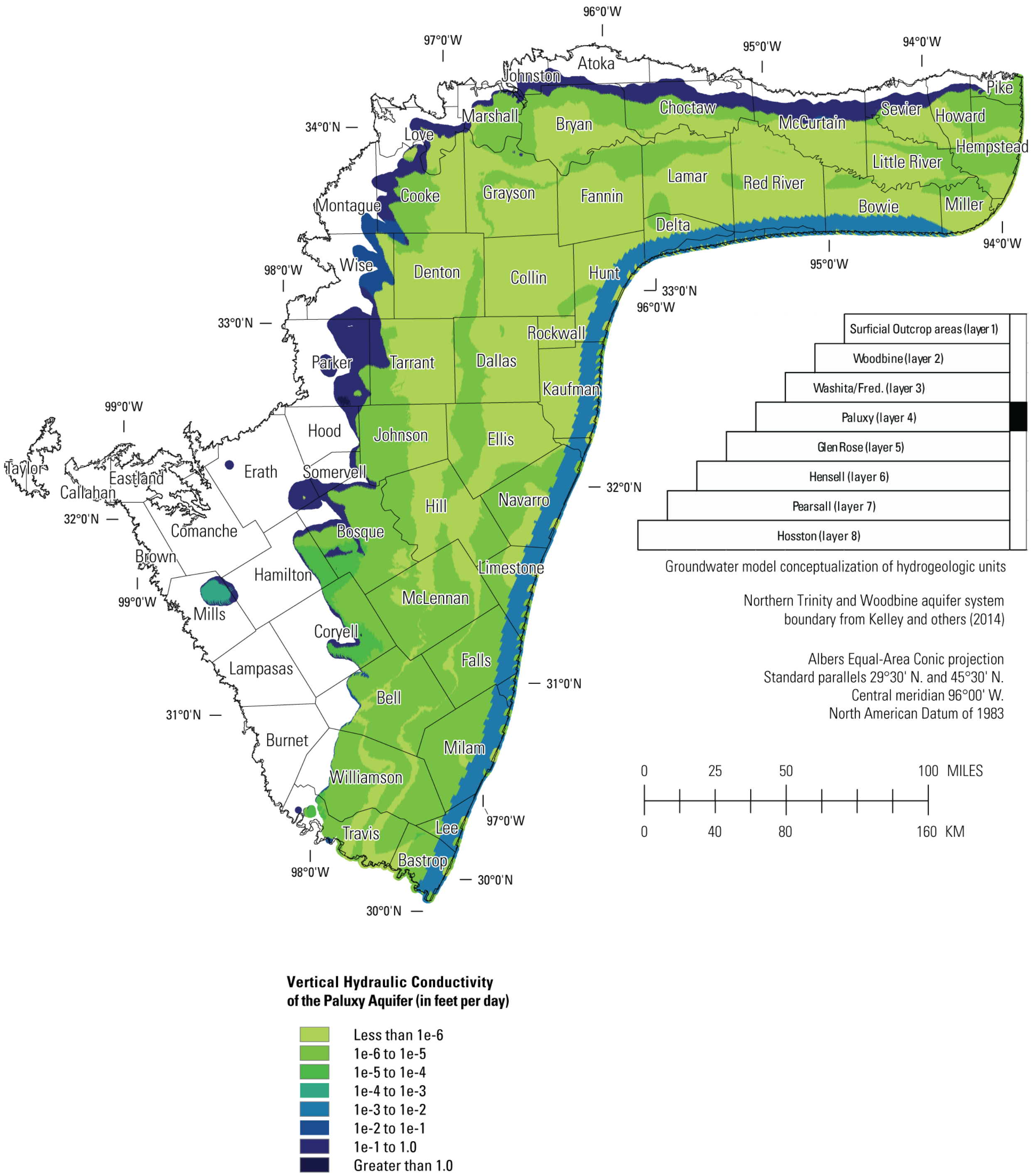

Figure 3-24. History-matched vertical hydraulic conductivity for the Paluxy Aquifer (layer 4).

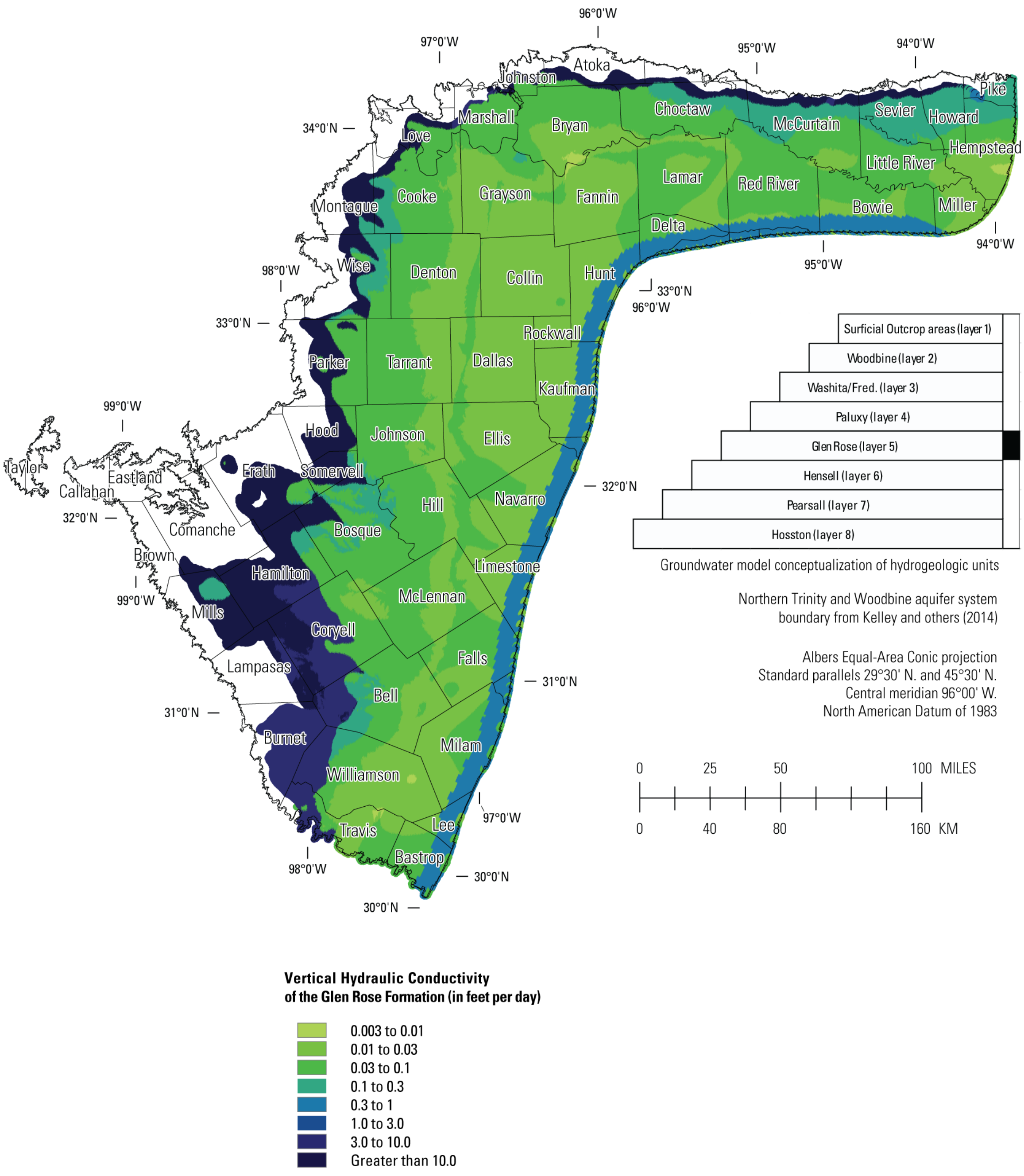

Figure 3-25. History-matched vertical hydraulic conductivity for the Glen Rose Formation (layer 5).

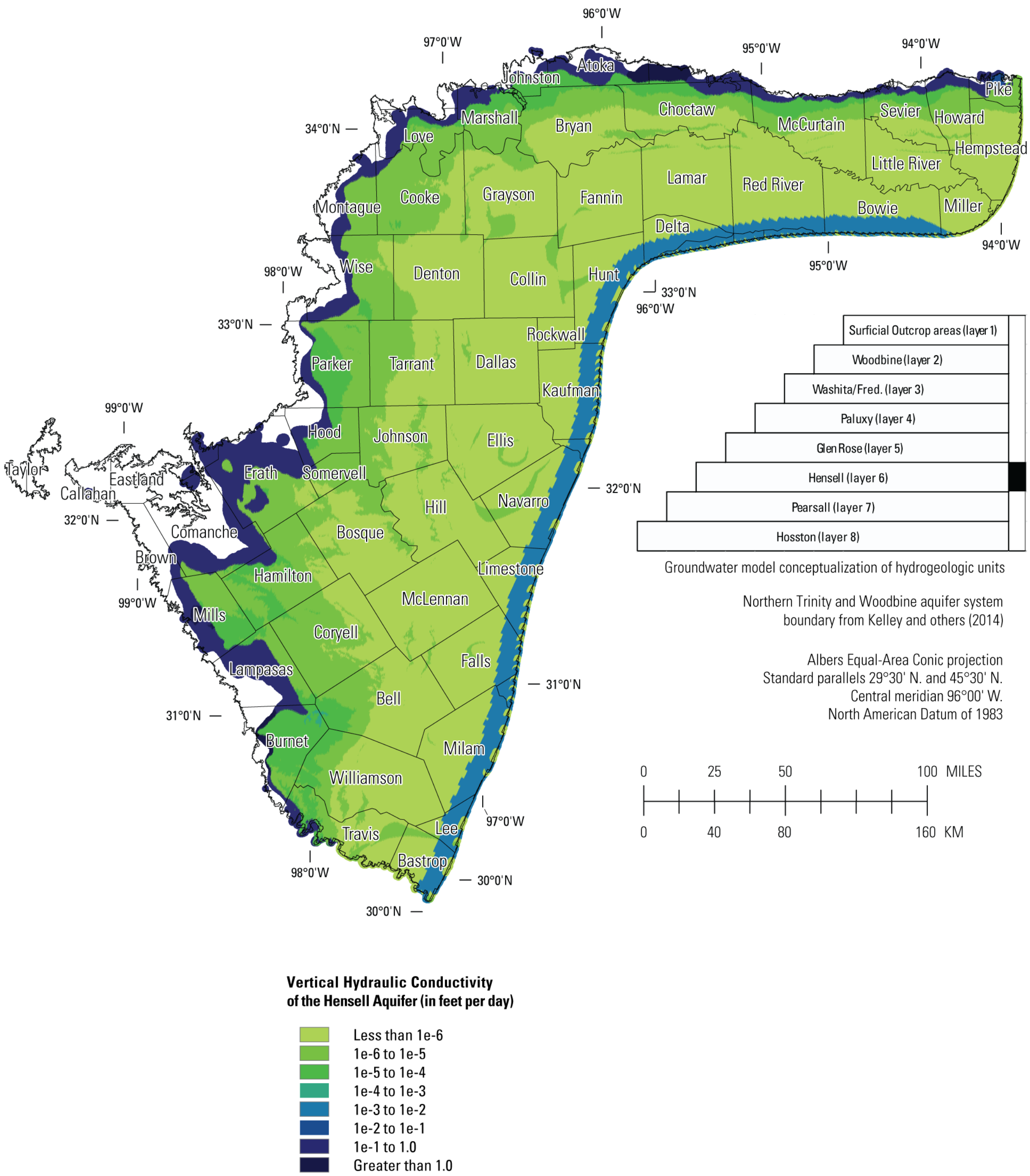

Figure 3-26. **History-matched vertical hydraulic conductivity for the Hensell Aquifer (layer 6).**

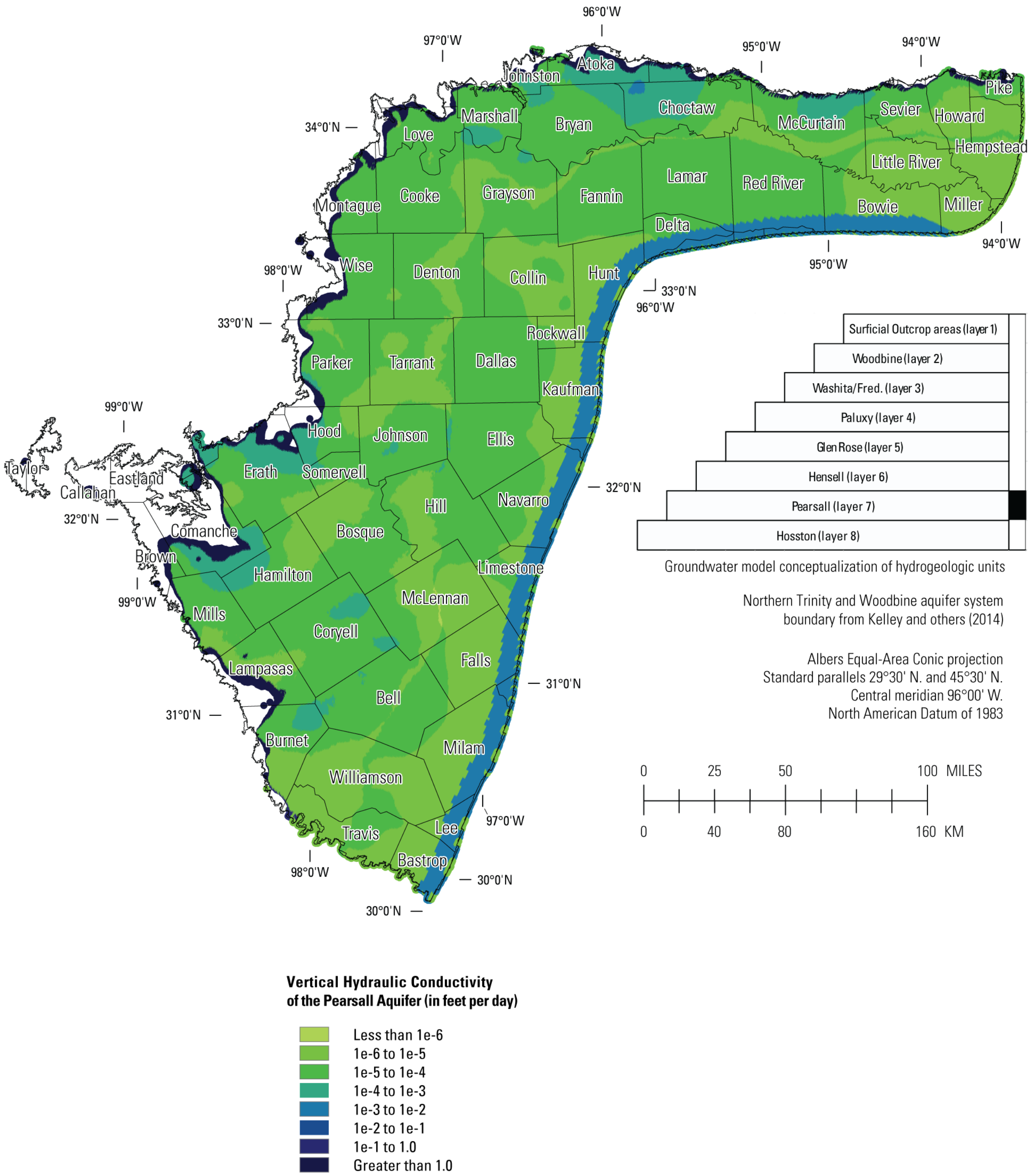

Figure 3-27. History-matched vertical hydraulic conductivity for the Pearsall Formation (layer 7).

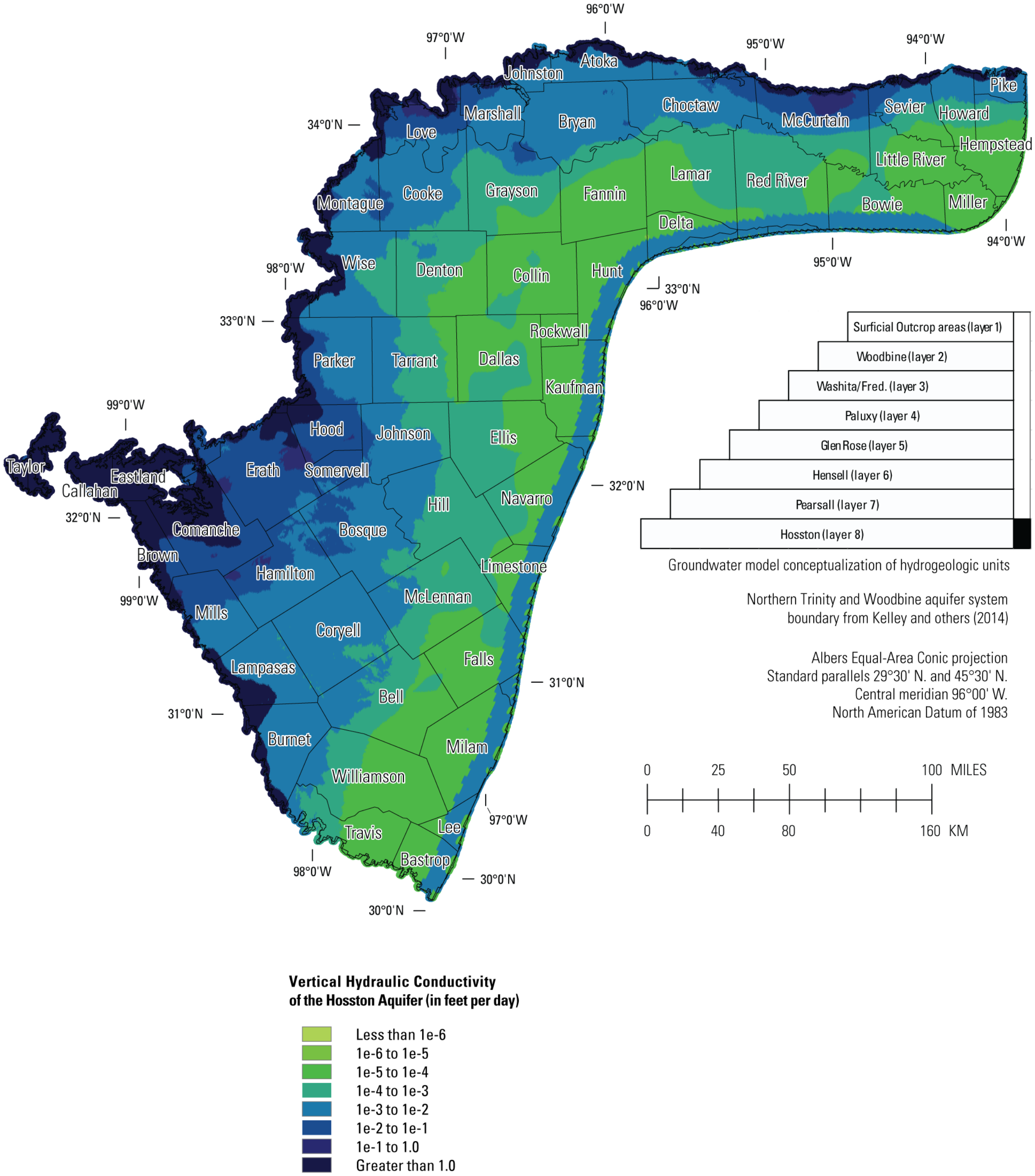

Figure 3-28. History-matched vertical hydraulic conductivity for the Hosston Aquifer (layer 8).

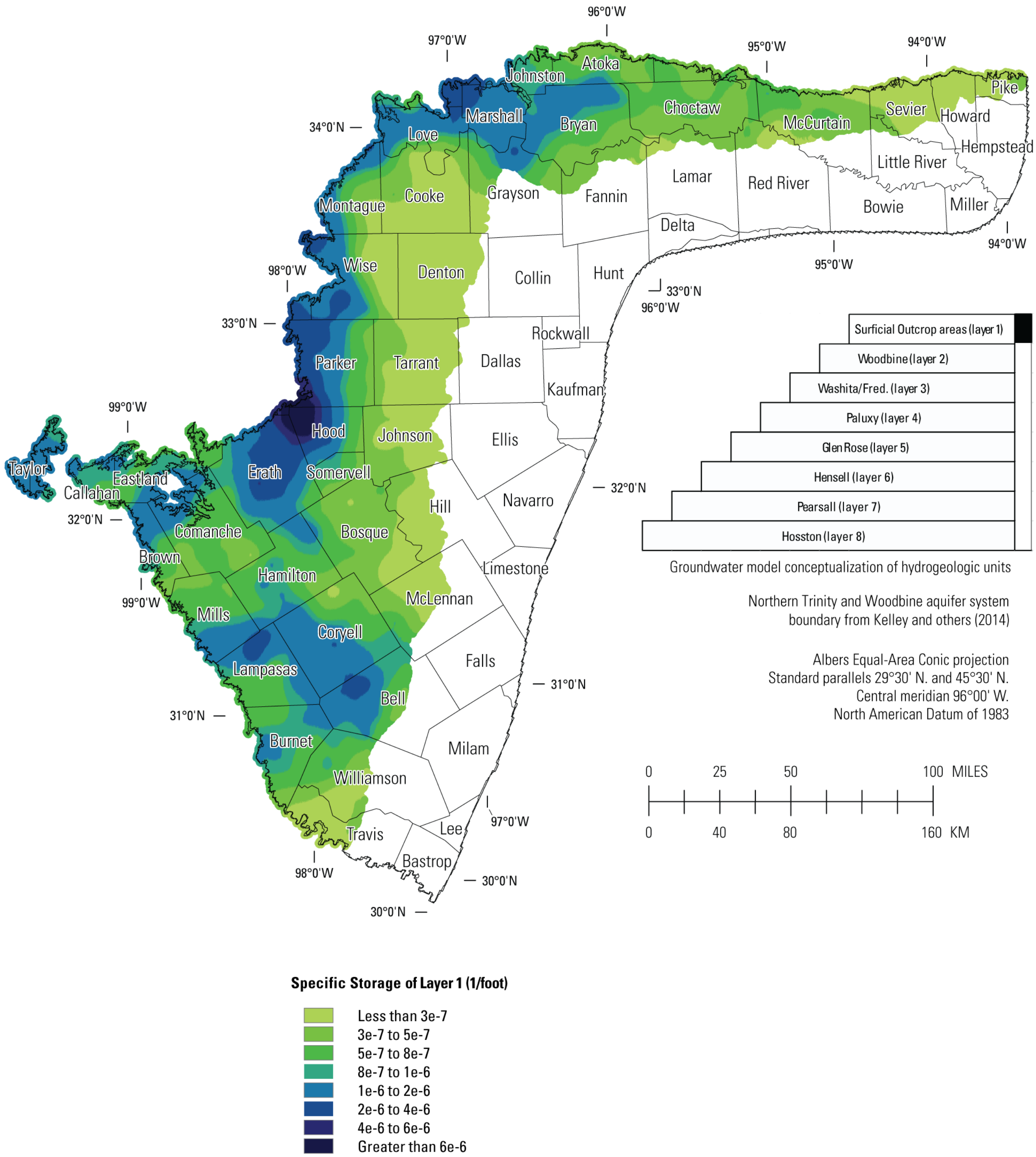

Figure 3-29. History-matched specific storage for the surficial outcrop area of layer 1.

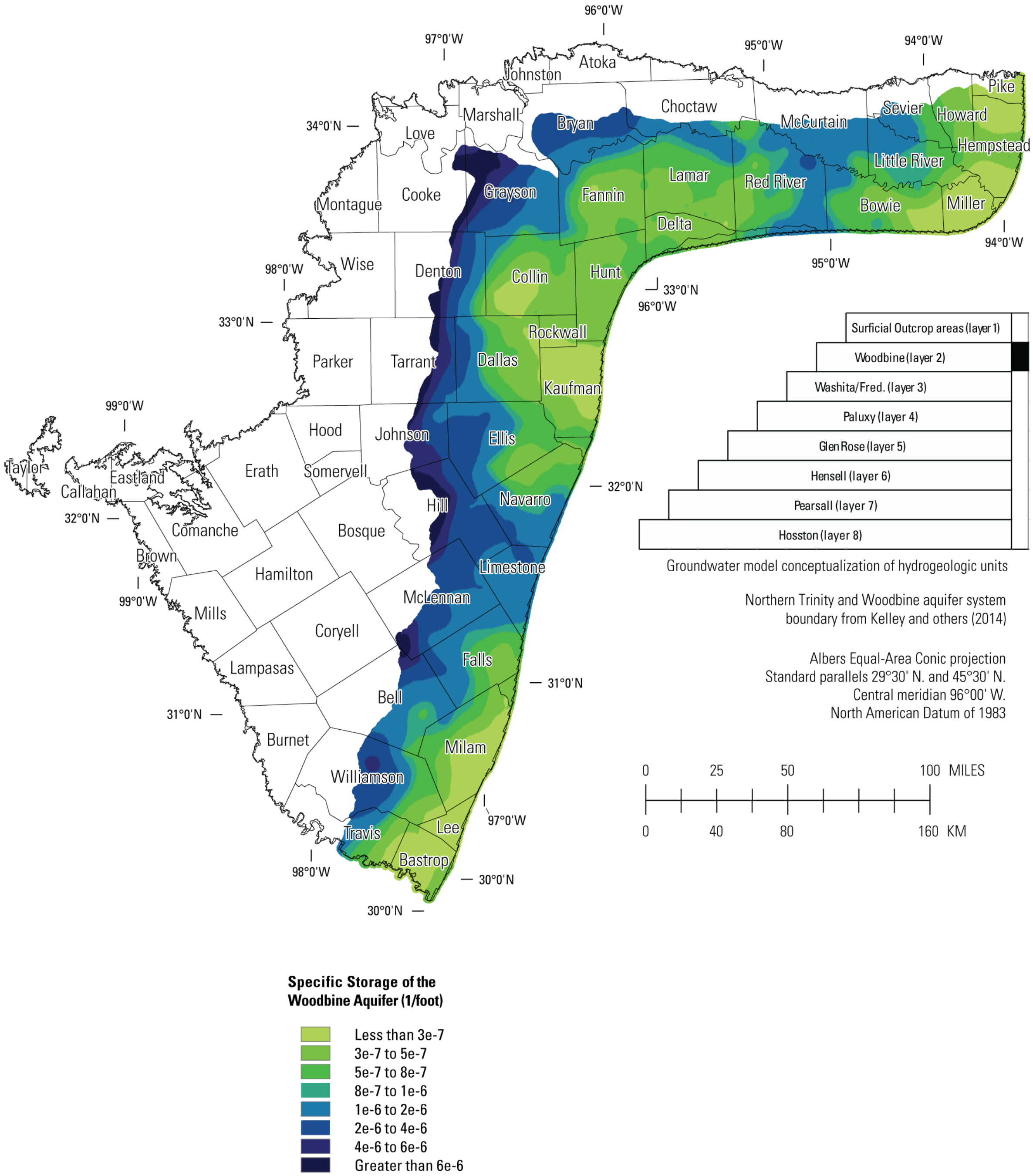

Figure 3-30. History-matched specific storage for the Woodbine Aquifer (layer 2).

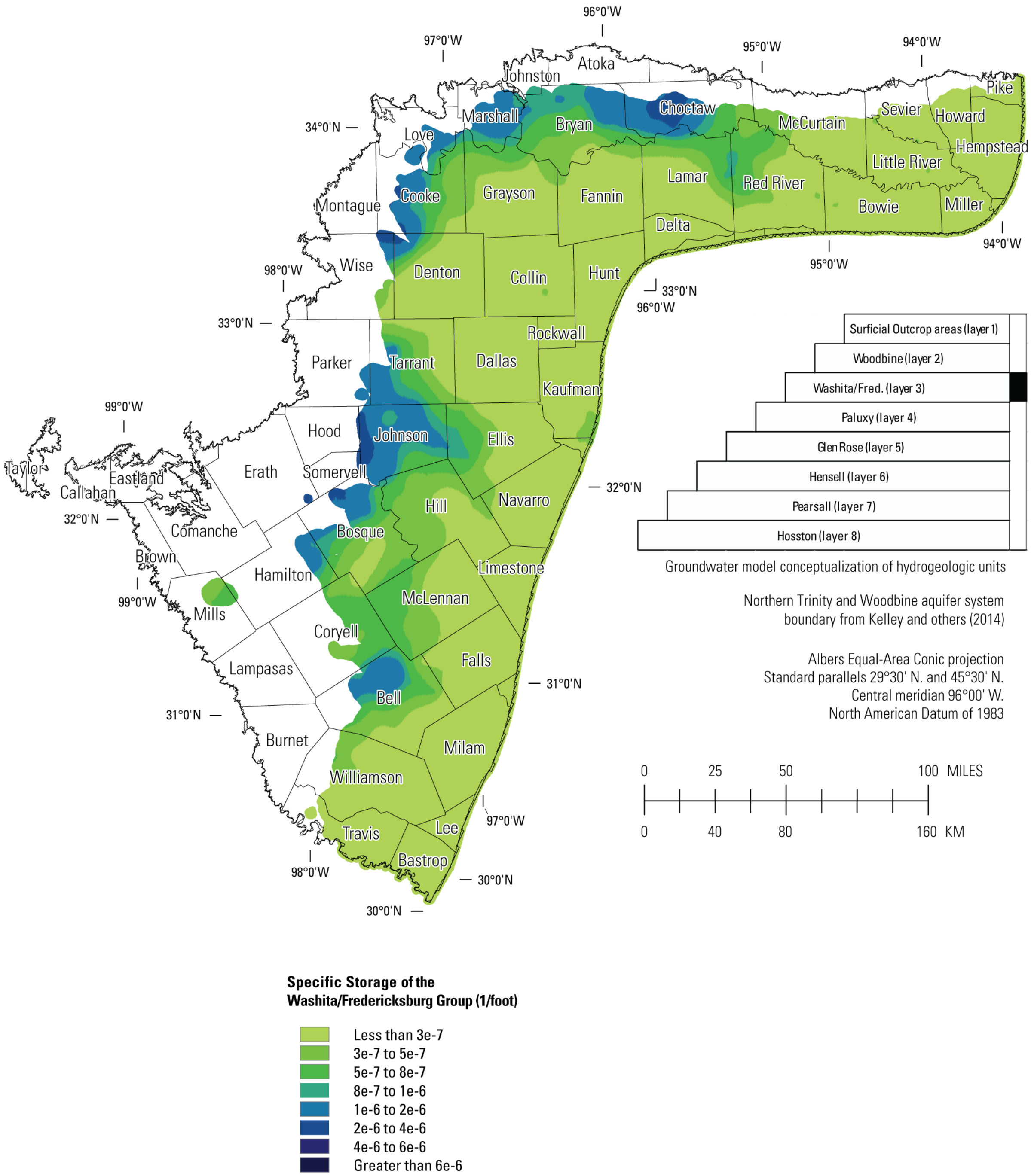

Figure 3-31. History-matched specific storage for the Washita/Fredericksburg Groups (layer 3).

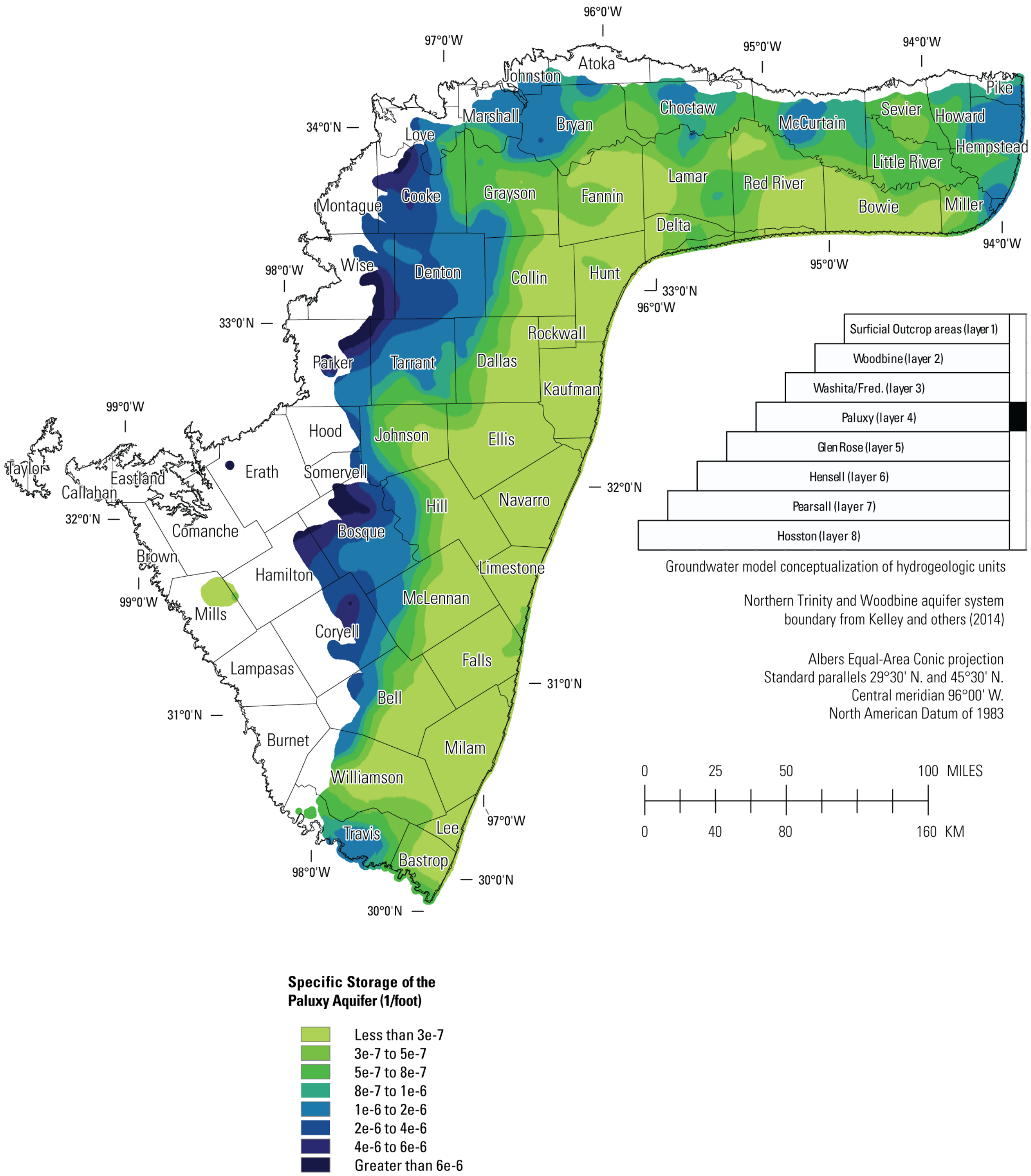

Figure 3-32. **History-matched specific storage for the Paluxy Aquifer (layer 4).**

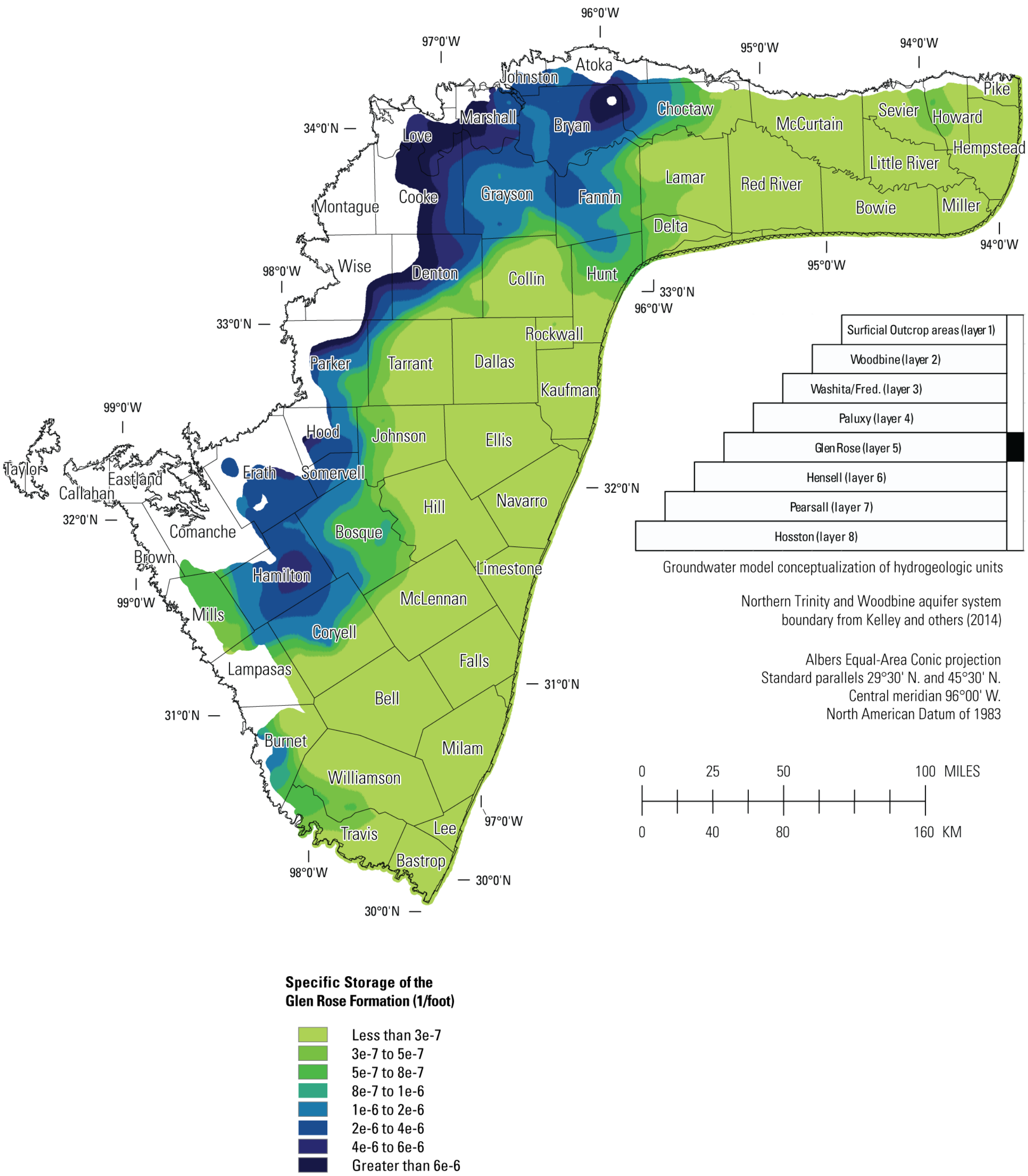

Figure 3-33. History-matched specific storage for the Glen Rose Formation (layer 5).

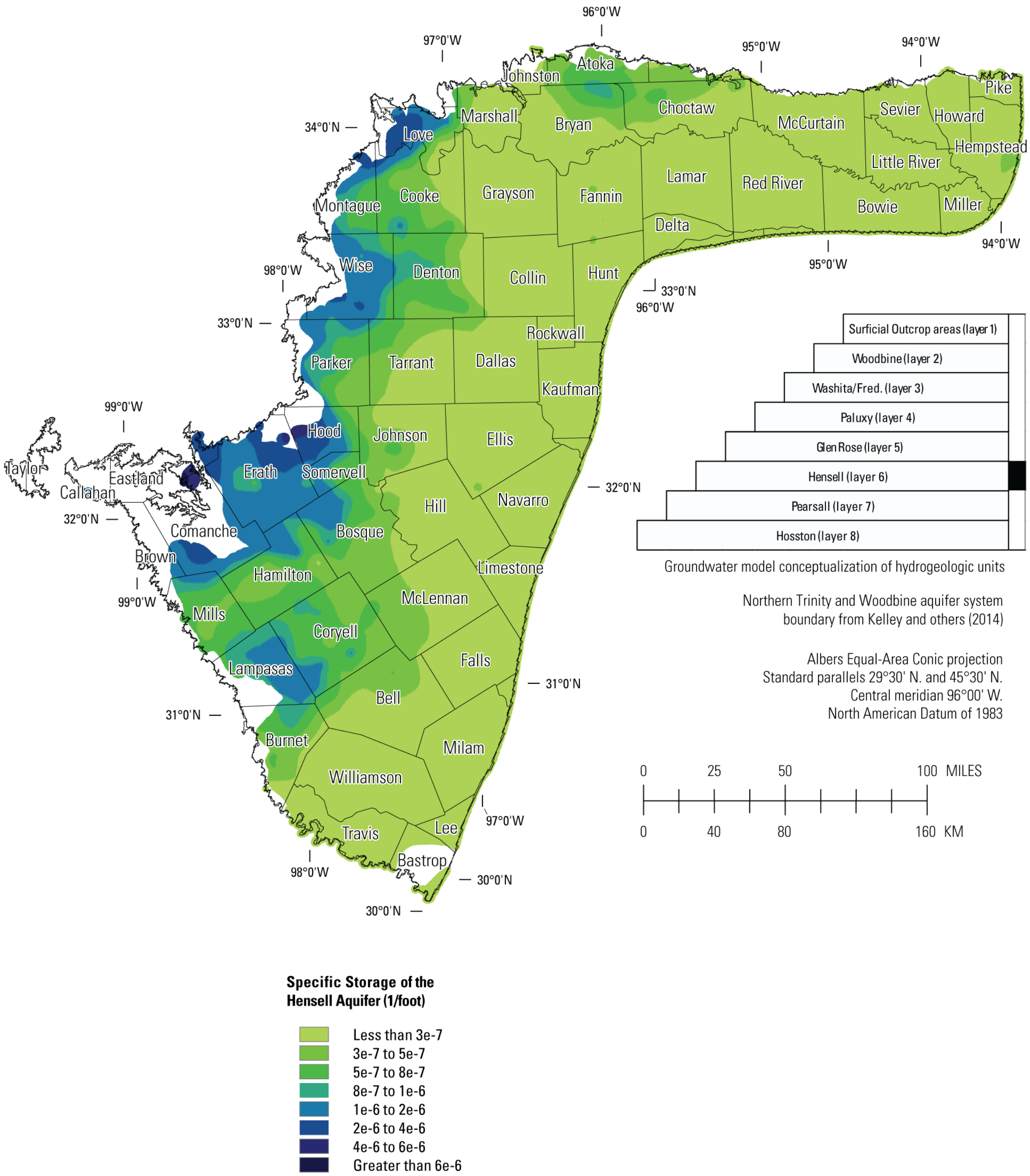

Figure 3-34. **History-matched specific storage for the Hensell Aquifer (layer 6).**

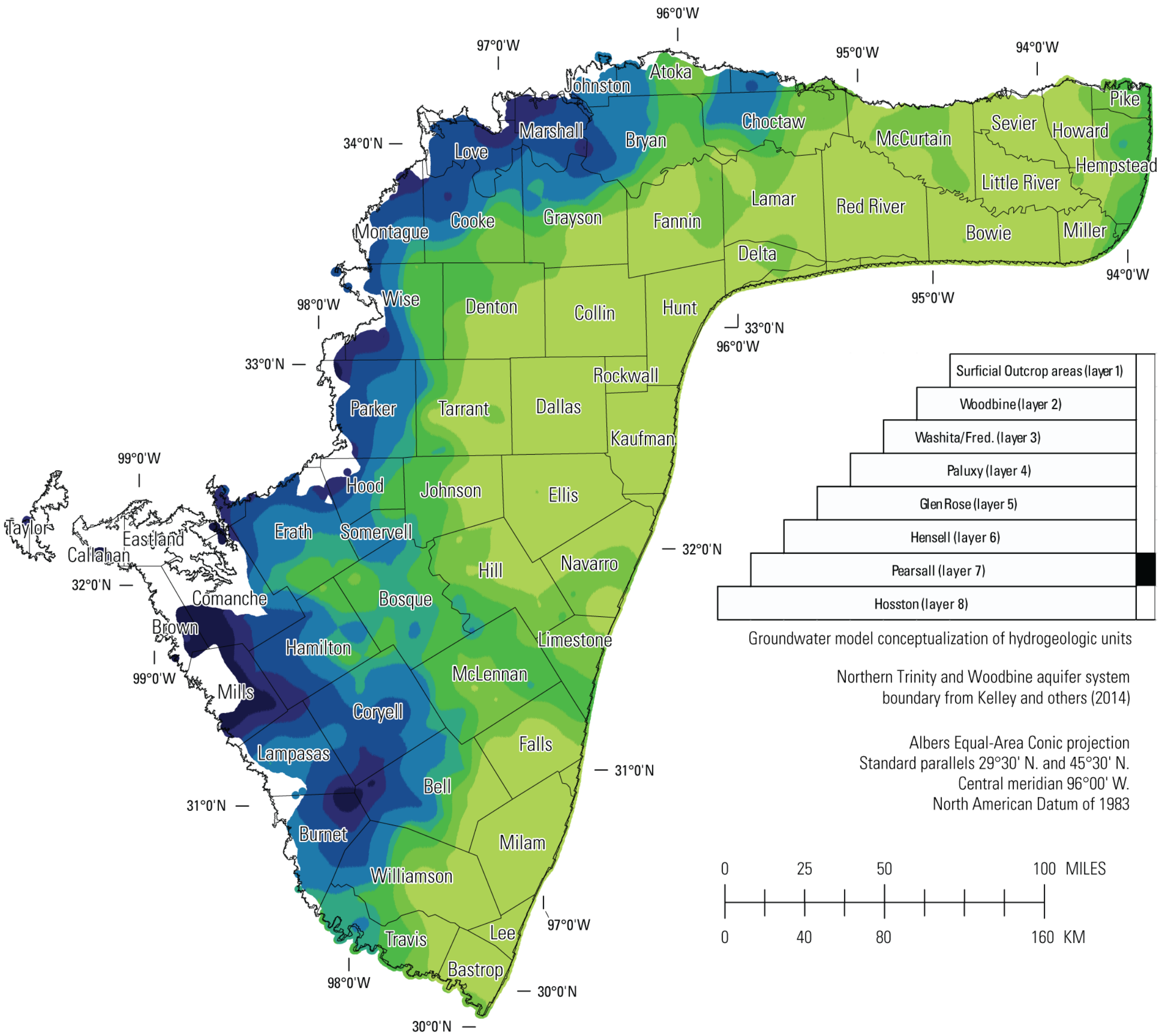

Specific Storage of the Pearsall Aquifer (1/foot)

- Less than 3e-7
- 3e-7 to 5e-7
- 5e-7 to 8e-7
- 8e-7 to 1e-6
- 1e-6 to 2e-6
- 2e-6 to 4e-6
- 4e-6 to 6e-6
- Greater than 6e-6

Figure 3-35. History-matched specific storage for the Pearsall Formation (layer 7).

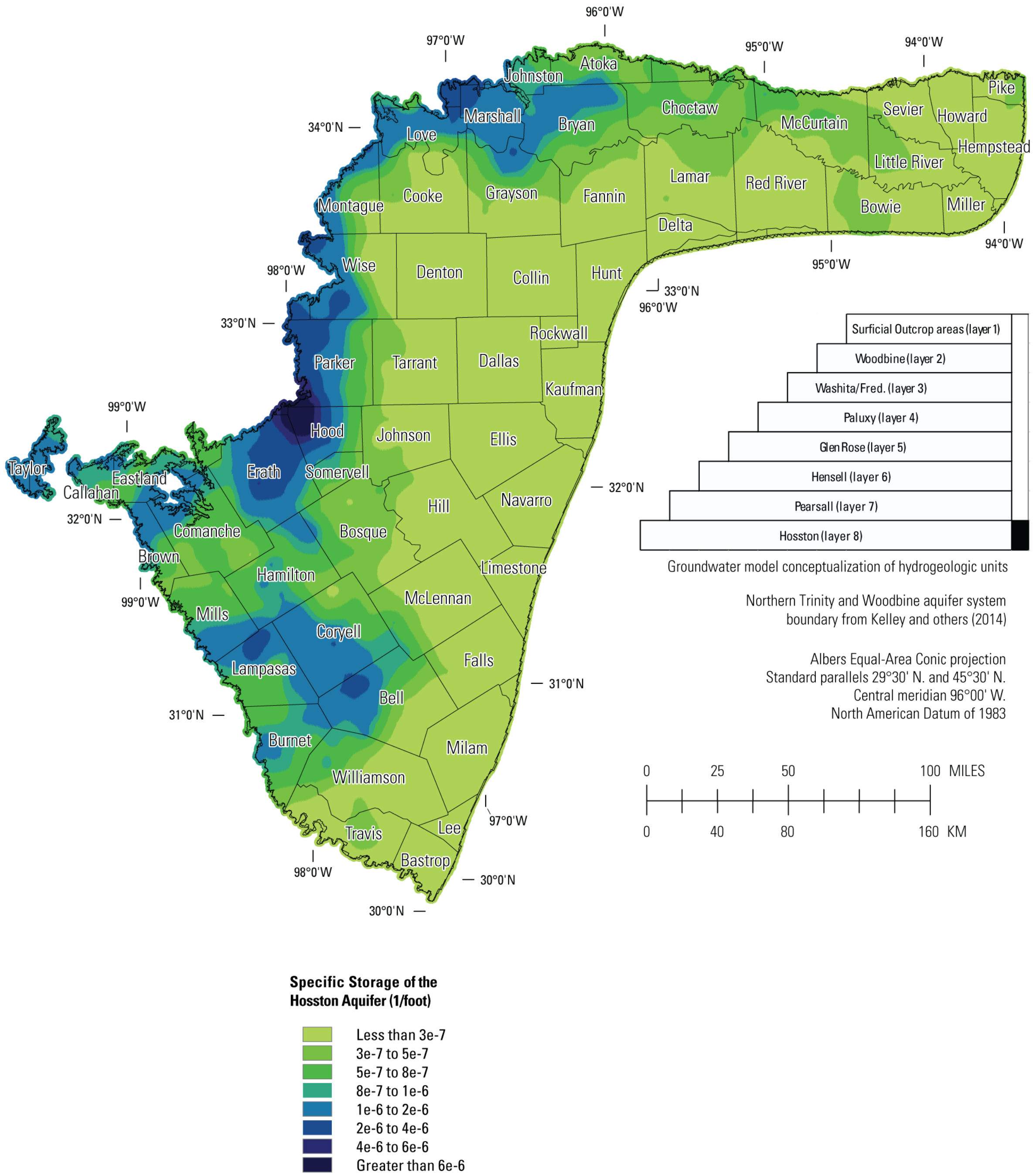

Figure 3-36. History-matched specific storage for the Hosston Aquifer (layer 8).

Table 3-5. Hydraulic conductivity and storage parameter values.

Aquifer property	Hydrogeologic Unit	Layer	Layer Zone	NTGAM Mean	NTGAM 5th quantile	NTGAM 95th quantile
Horizontal hydraulic conductivity (ft/d) (Figures 3-13 to 3-20)	Surficial	1	Alluvium	195	119	300
	Surficial	1	Outcrop	2.7	0.31	11.8
	Younger Formations	1	Younger Formations	0.1	0.1	0.1
	Woodbine Aquifer	2	Layer	0.27	0.002	1.08
	Washita/Fredericksburg Groups	3	Layer	0.7	0.10	2.1
	Paluxy Aquifer	4	Layer	1.1	0.01	3.3
	Glen Rose Formation	5	Layer	0.5	0.10	1.2
	Hensell Aquifer	6	Layer	1.3	0.05	4.0
	Pearsall Formation	7	Layer	1.4	0.04	4.3
	Hosston Aquifer	8	Layer	5.0	1.06	14.7
Vertical hydraulic conductivity (ft/d) (Figures 3-21 to 3-28)	Surficial	1	Alluvium	1.9	0.41	6.2
	Surficial	1	Outcrop	6.0	0.10	30
	Younger Formations	1	Younger Formations	0.0001	0.0001	0.0001
	Woodbine Aquifer	2	Layer	0.01	9.91E-08	0.07
	Washita/Fredericksburg Groups	3	Layer	0.23	1.02E-06	1.2
	Paluxy Aquifer	4	Layer	0.02	1.89E-07	0.16
	Glen Rose Formation	5	Layer	0.26	2.50E-06	2.2
	Hensell Aquifer	6	Layer	0.04	1.35E-07	0.24
	Pearsall Formation	7	Layer	0.12	3.19E-06	0.01
	Hosston Aquifer	8	Layer wide	0.78	3.32E-05	10
	Surficial	1	Alluvium	1.52E-02	6.55E-03	2.70E-02
	Surficial	1	Outcrop	1.06E-02	4.12E-03	2.18E-02

Aquifer property	Hydrogeologic Unit	Layer	Layer Zone	NTGAM Mean	NTGAM 5th quantile	NTGAM 95th quantile
Specific storage (ft^{-1}) (Figures 3-29 to 3-36)	Younger Formations	1	Younger Formations	2.49E-03	3.34E-04	1.13E-02
	Woodbine Aquifer	2	Layer	1.40E-06	2.15E-07	4.80E-06
	Washita/Fredericksburg Groups	3	Layer	3.44E-07	3.74E-08	1.16E-06
	Paluxy Aquifer	4	Layer	9.32E-07	7.61E-08	3.35E-06
	Glen Rose Formation	5	Layer	1.41E-06	2.95E-08	6.95E-06
	Hensell Aquifer	6	Layer	3.64E-07	3.12E-08	1.25E-06
	Pearsall Formation	7	Layer	1.00E-06	7.05E-08	3.87E-06
	Hosston Aquifer	8	Layer	5.35E-07	4.88E-08	1.76E-06

3.5.3.2 Groundwater Use

Adjustment of well rates during history-matching resulted in minimal differences between the posterior ensemble and prior estimates of groundwater use. Figures 2-11 to 2-16 show the temporal variability of total groundwater use within each county in the model area. The minimal variance of the posterior groundwater use ensemble suggested minimal sensitivity of parameterized model well packages with respect to observations including groundwater-level targets. However, the relatively low model sensitivity with respect to prior groundwater use estimates did not consider either the spatiotemporal uncertainty of GCD-derived estimates nor the spatial uncertainty of post-1980 rural/domestic production estimates (described in section 2.2.2). While the former honored the groundwater production values supplied by GCDs, the latter was computationally limited by the grid resolution and pumping allocation to all model cells on a county basis (section 2.2.2).

3.5.3.3 Net Groundwater Flow

Layer 1 in the NTGAM was used to simulate the shallow groundwater system; therefore, net GWF between layer 1 and the underlying layers is described as “net GWF.” This “net GWF” is also similar to the “deep recharge” described in some published reports. Figure 3-37 shows rates of net GWF between layer 1 and confined aquifer units considering the outcrop footprint of each layer. The outcrop footprint of each layer in NTGAM is defined in the IDOMAIN array of layer 1 (IBOUND array of layer 1 in NTWGAM). The net flow between the outcrop footprint of each aquifer in layer 1 and the same footprint in the corresponding confined layer was divided by the area of each outcrop footprint to produce the flux units shown in Figure 3-37. Because the dashed line corresponds to zero net flow, the negative flux rate in the Hosston aquifer indicates an upward flow from the confined layer 8 to the unconfined layer 1 within the outcrop area. This upward flux suggests a natural tendency for the Hosston aquifer to support surface water flows in the outcrop area, which is comprised of the highest values of vertical hydraulic conductivity (Figure 3-21) and the thinnest confined cells, as compared to thicker aquifer portions with lower vertical hydraulic conductivity in the down-dip area.

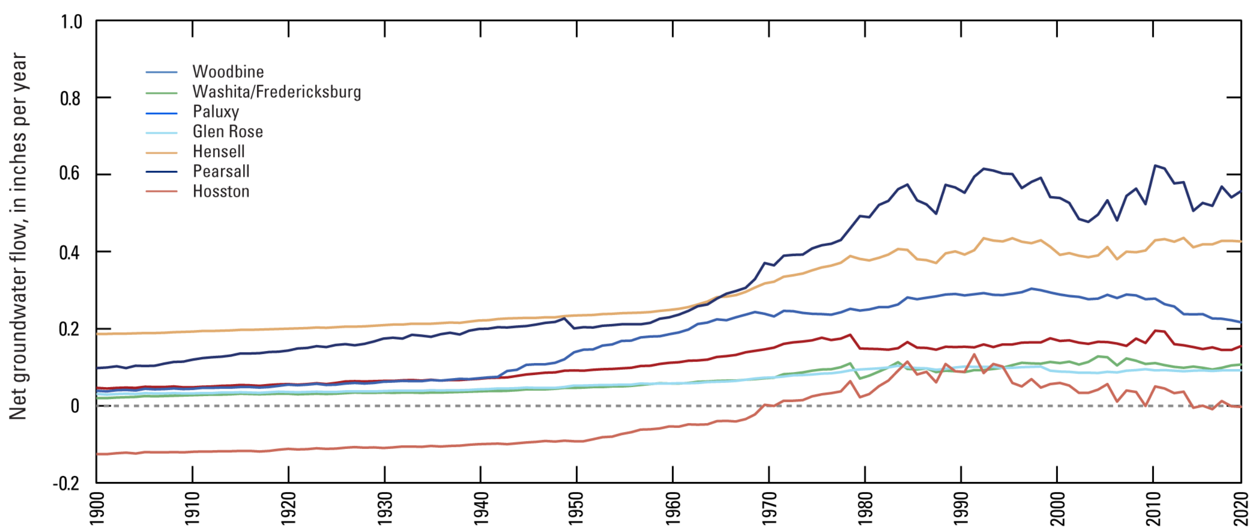

Figure 3-37 Net groundwater flow from layer 1 to the underlying layers.

Despite differences in net fluxes, all aquifer units showed an overall trend of increasing rates from predevelopment through approximately the year 1980, with relatively stable rates from that point onward. These trends are likely driven by total groundwater use throughout the simulation period, as described in section 3.5.6 below. In general, Figure 3-37 also shows that the Pearsall Formation and Hensell Aquifer consistently received the greatest recharge flux stemming from their outcrop footprints in layer 1. Because the Pearsall Formation has a relatively small outcrop area (demarcated by the highest vertical hydraulic conductivity region in Figure 3-37, the relatively high rates of recharge flux suggest a flow divergence towards down-dip areas driven by groundwater use and towards the outcrop region of the underlying Hosston Aquifer. The highest rates in the Pearsall Formation and early-time upward flux in the Hosston outcrop region are consistent with results from the NTWGAM. Likewise, the SWB-derived recharge in NTGAM increased the net downward flux towards the Hensell Aquifer in comparison to the NTWGAM. This net flow analysis indicated that, on average, only between 0.9 and 1.5 percent of SWB recharge reaches the confined aquifers downdip of the outcrop.

3.5.3.4 Model Fit to Observations

The history-matched NTGAM and ensemble fit to observations were evaluated based on the reduction of residuals between historical observations and the simulated equivalents. When plotting simulated and observed (or estimated) groundwater levels, transmissivity, or stream baseflow, all the points would plot on the one-to-one (1:1) correlation line if the simulated results perfectly matched the measured data. Similarly, when plotting the residuals against the simulated groundwater levels, the residual between the measured data and simulated results would be zero if the simulated results matched the measured data perfectly. Additionally, when the simulated results are evaluated based on calculated mean residuals, a mean residual closest to zero indicates less model bias. Residuals were calculated as observed minus simulated values; positive residuals indicate lower simulated than observed values (undersimulated), and negative residuals indicate higher simulated than observed values (oversimulated). Note that the 1:1 correlation and residual distribution plots refer only to the NTGAM model, whereas the observed and simulated plots present both the NTGAM model and Posterior results.

3.5.3.4.1 Groundwater Levels

Figures 3-38 through 3-41 show residuals between measured and simulated observations, including 1:1 correlation plots and histograms for the history-matched NTGAM. In Figure 3-38, parts A and B show a reasonable fit to all groundwater-level measurements, with a mean residual value of -54 ft, indicating an average tendency for over-simulating groundwater levels. Parts C and D correspond to groundwater-level residuals from wells with long-term measurements and screen information. History matching using these wells resulted in a lower mean residual of -41 ft, reflecting the increased confidence in the greater representativeness of the long-term time series of data versus the entire water level dataset (parts A and B). In contrast, parts E and F represent residuals from airline measurements of groundwater levels, which carried the lowest weight during history matching because of their high level of uncertainty. This uncertainty is reflected in the large mean groundwater-level residual of -100 ft. As shown in Figure 3-38 (all parts), the normal Gaussian distribution of overall residuals indicates an unbiased distribution of model-to-measurement misfit, suggesting a reasonable representation of groundwater-level spatiotemporal trends.

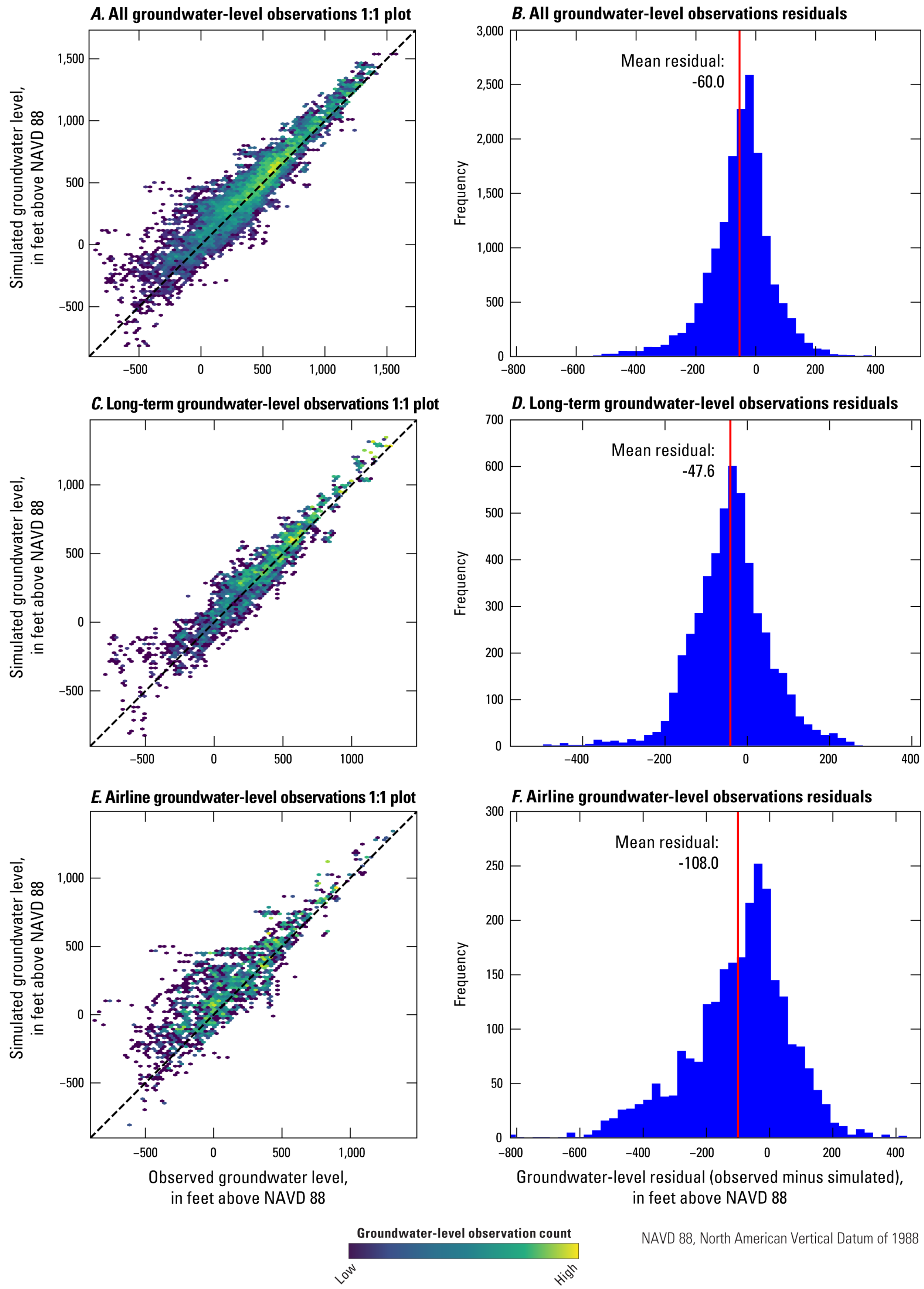

Figure 3-38. Observed and simulated groundwater levels and groundwater level residual distributions for all aquifer units, for long-term groundwater-level observations, and for airline observations.

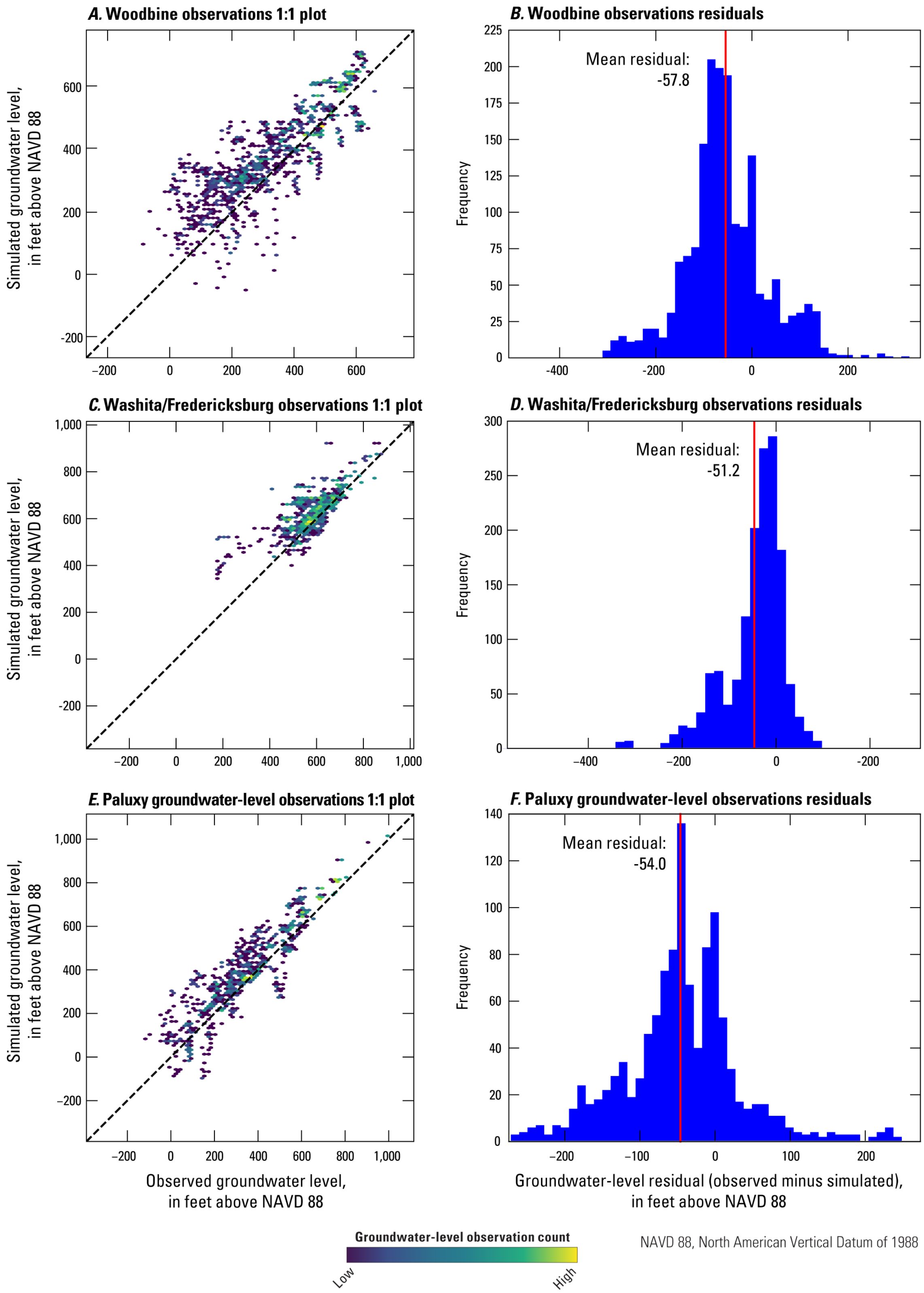

Figure 3-39. Observed and simulated groundwater levels and groundwater level residual distributions for the Woodbine Aquifer, Washita/Fredericksburg Groups, and Paluxy Aquifer.

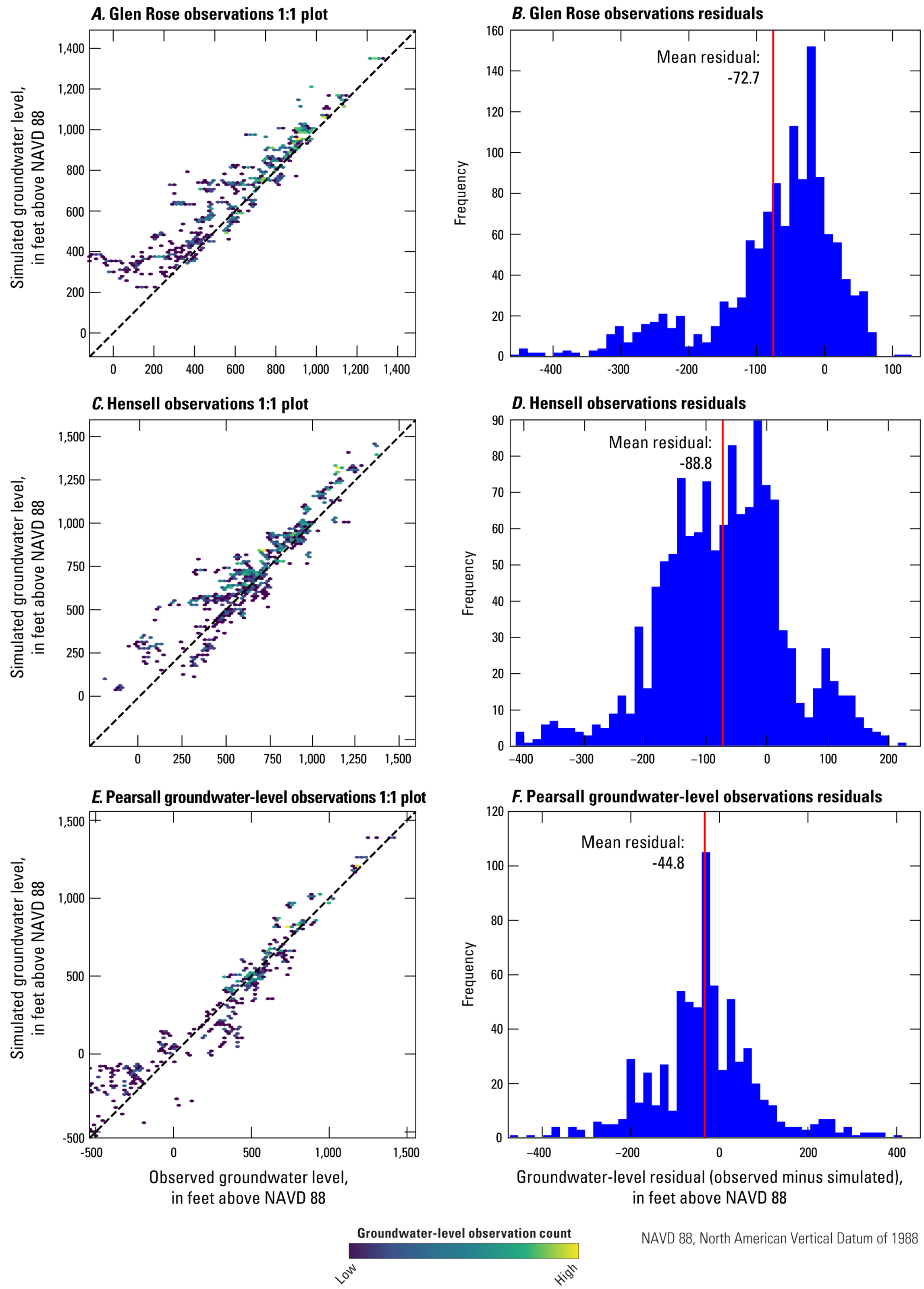

Figure 3-40. Observed and simulated groundwater levels and groundwater level residual distributions for the Glen Rose Formation, Hensell Aquifer, and Pearsall Aquifer.

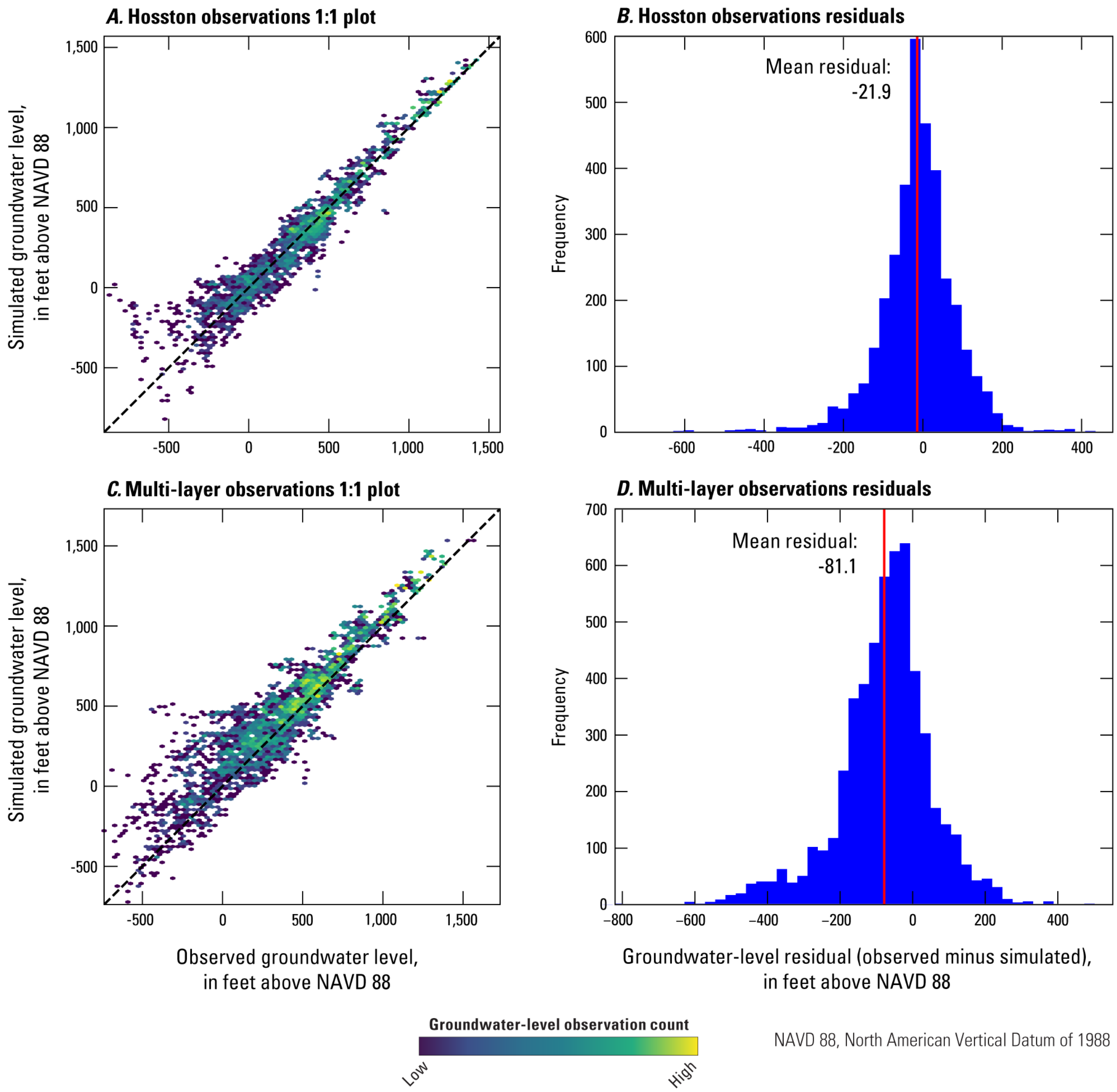

Figure 3-41. Observed and simulated groundwater levels and groundwater level residual distributions for the Hosston Aquifer, and multi-layer observations.

Groundwater-level residuals are also summarized on a layer basis in Figures 3-38 through 3-41. The lowest mean residuals of -14 ft were attained in the Hosston aquifer (Figure 3-41A and 3-41B), whereas the highest residuals of -78 ft correspond to multi-layer aquifers (Figure 3-41C and 3-41D). However, residuals in both the Hosston and multi-layer observations are reasonably distributed (Figure 3-41A through 3-41D), whereas residuals in the Washita/Fredericksburg and Glen Rose units exhibit a negatively skewed distribution (Figures 3-39C and 3-40A). The particularly pronounced negative skewness in the Glen Rose Formation and 1:1 plot (Figure 3-40A and 3-40B) suggests localized trends for over-simulating groundwater levels driven by the quality of the history-matching data. Long-term wells with screen information (certain), given the highest priority in Φ, represented only 5% and 6% of all wells available for history matching in the Washita/Fredericksburg and Glen Rose confining units, respectively. This contrasts with 15% in both the Paluxy and Hosston aquifers, 16% in Woodbine, and 18% in multi-aquifer wells. Because the extreme residual values in all model layers were attributed to the degree of uncertainty in the groundwater-level data, encapsulated in Φ weights and noise, the majority of residuals clustering near the 1:1 line (Figures 3-39 through 3-41) emphasize a good agreement between observed and simulated groundwater levels.

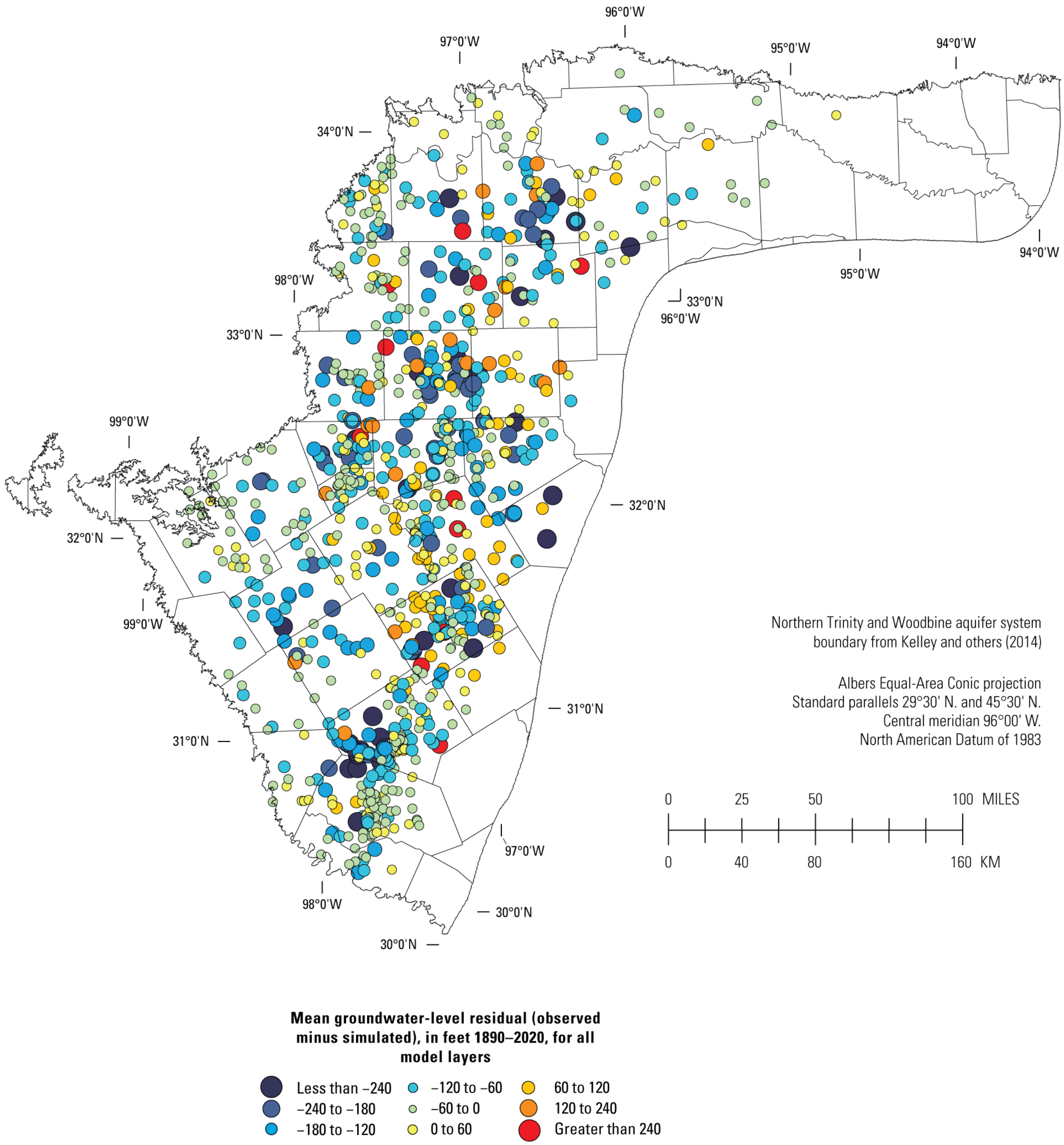

Figure 3-42. Spatial distribution of mean groundwater-level residuals for all model layers.

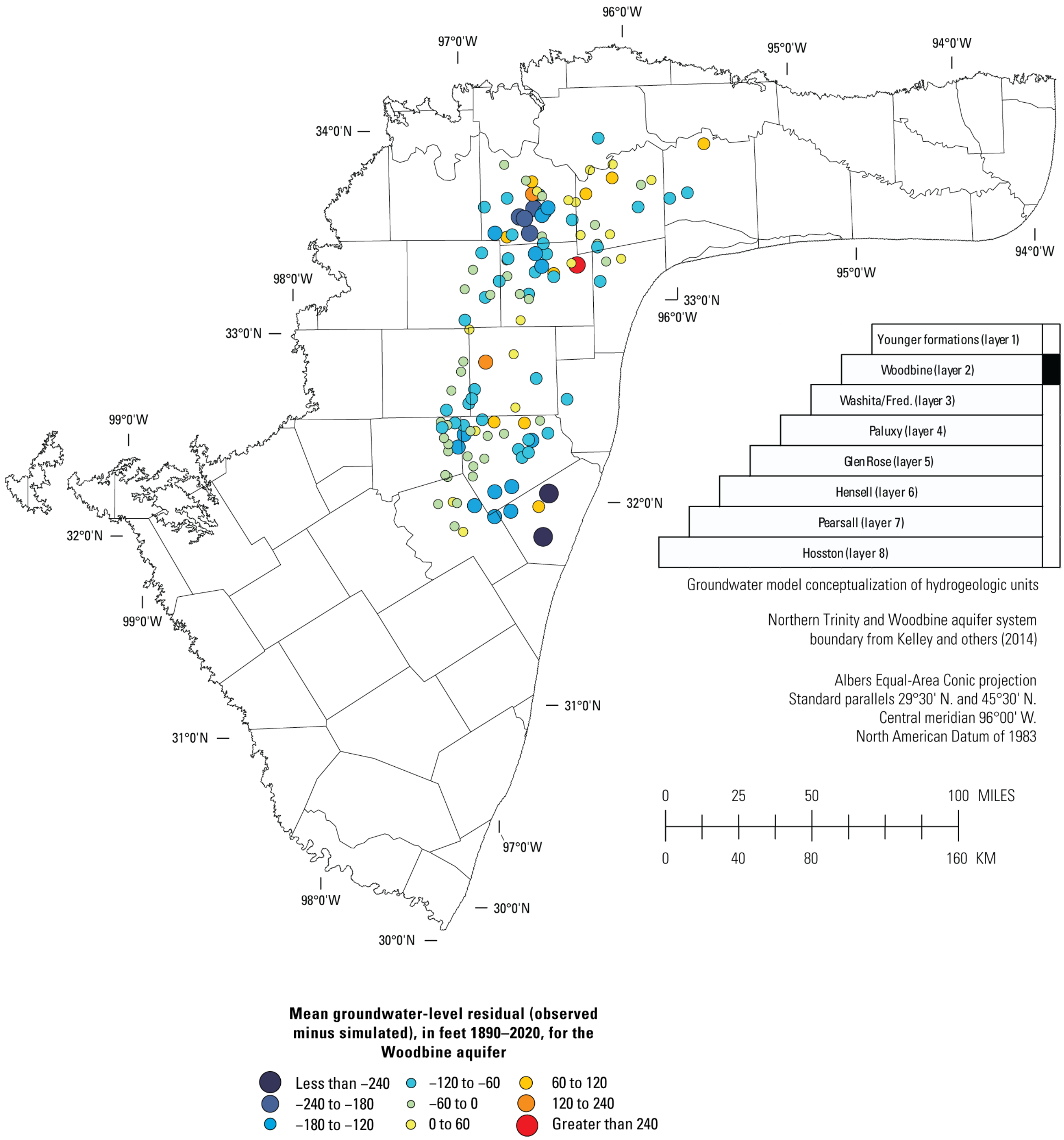

Figure 3-43. Spatial distribution of mean groundwater-level residuals for the Woodbine Aquifer (layer 2).

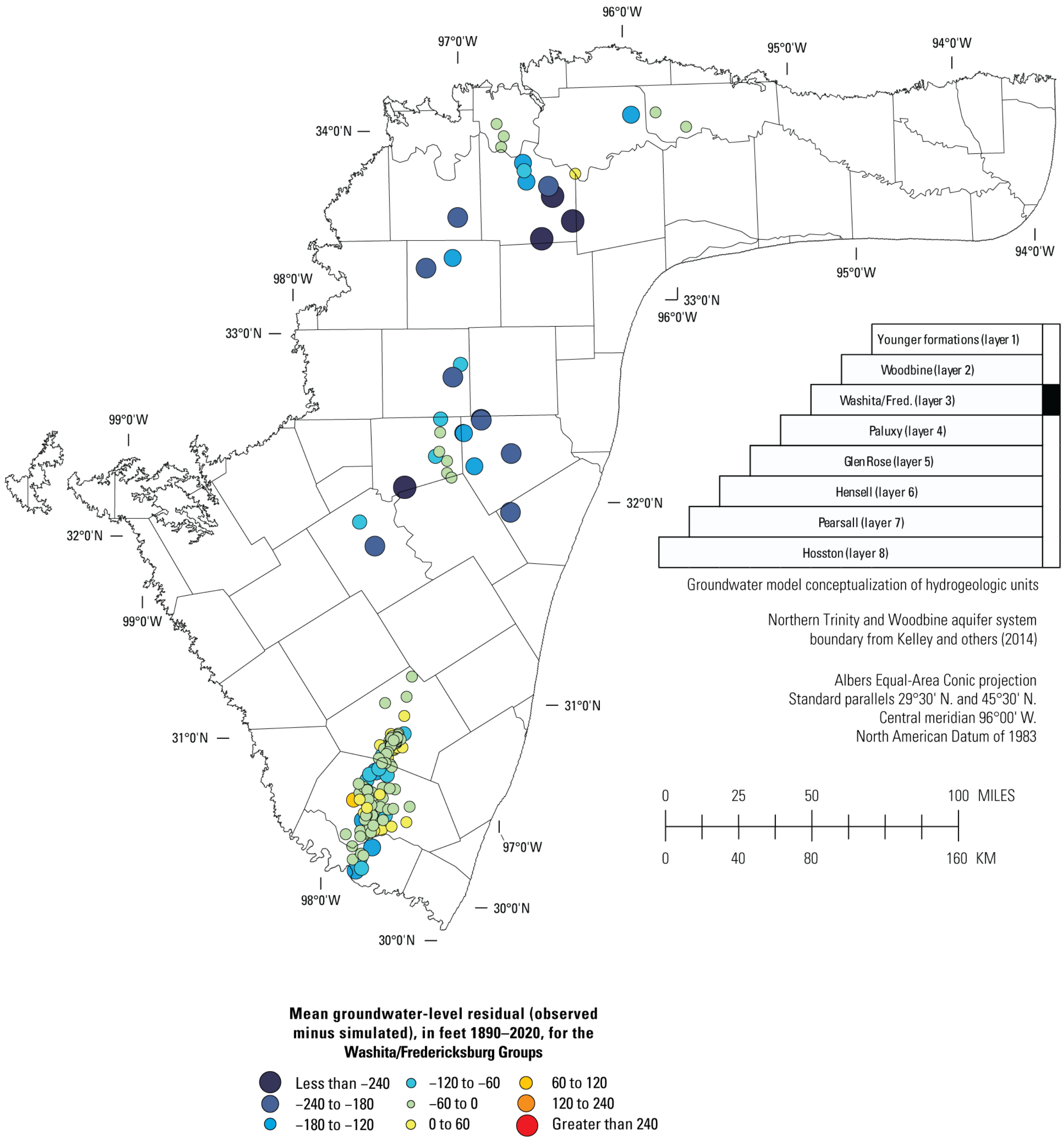

Figure 3-44. Spatial distribution of mean groundwater-level residuals for the Washita/Fredericksburg Groups (layer 3).

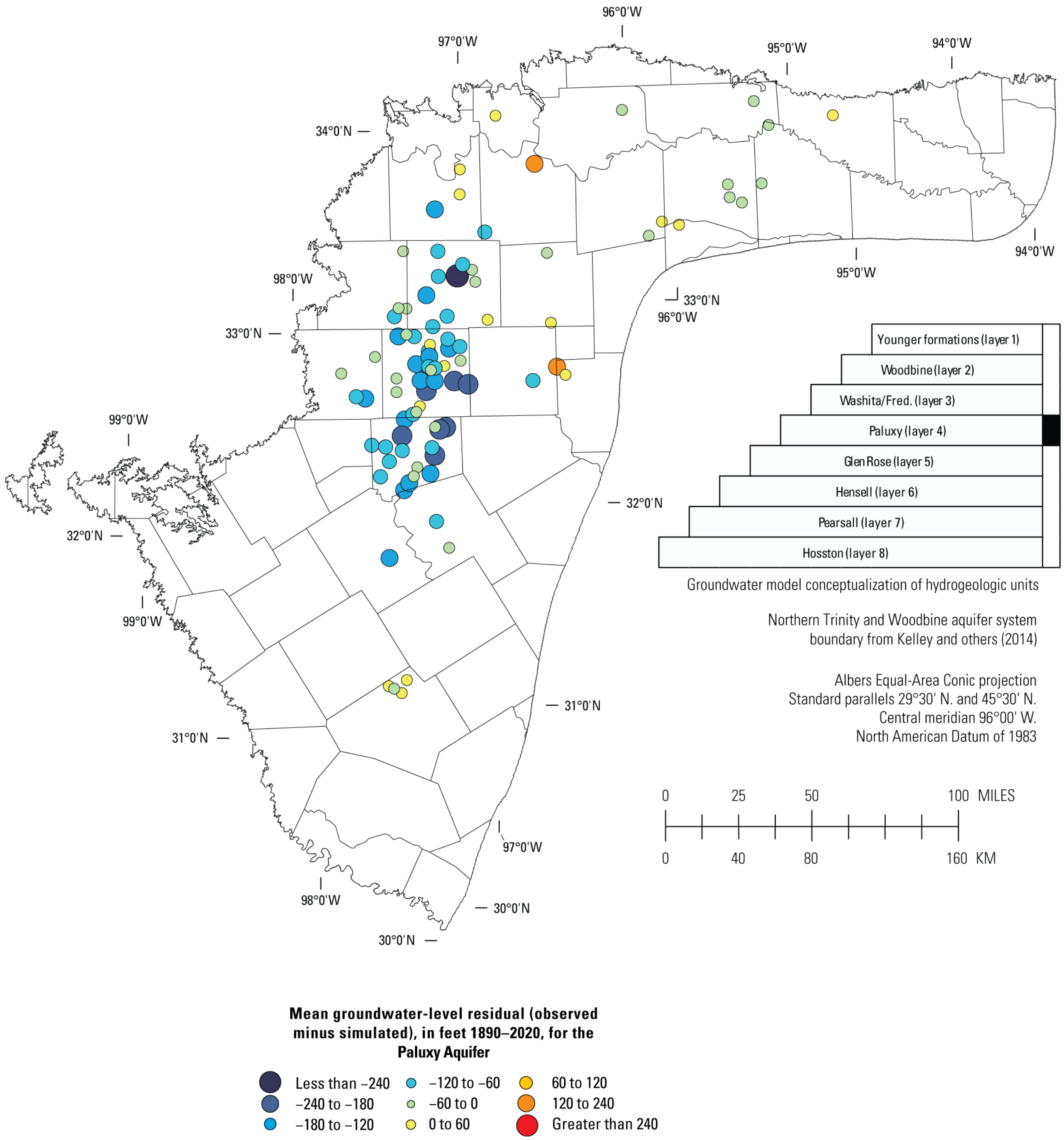

Figure 3-45. Spatial distribution of mean groundwater-level residuals for the Paluxy Aquifer (layer 4).

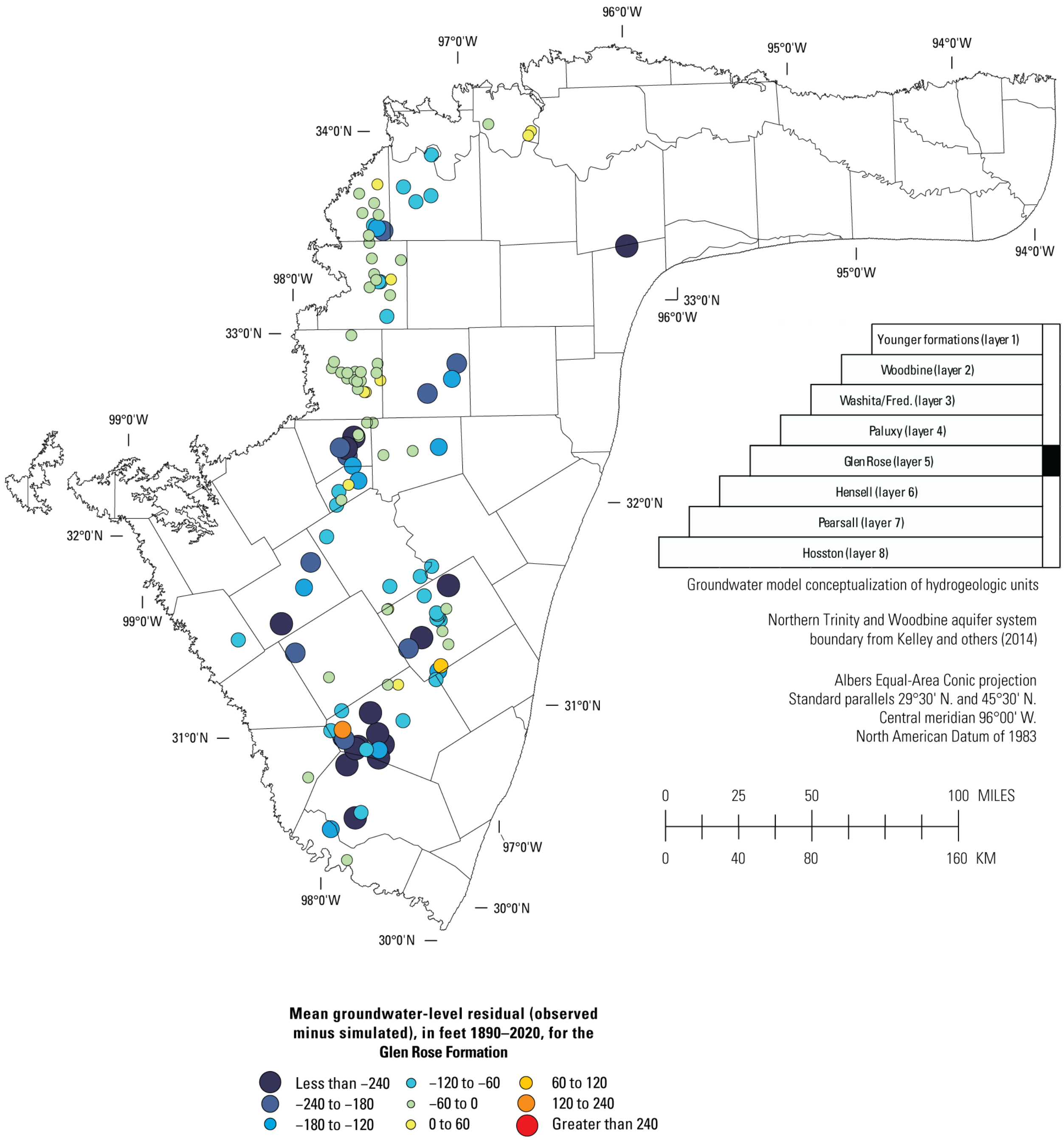

Figure 3-46. Spatial distribution of mean groundwater-level residuals for the Glen Rose Formation (layer 5).

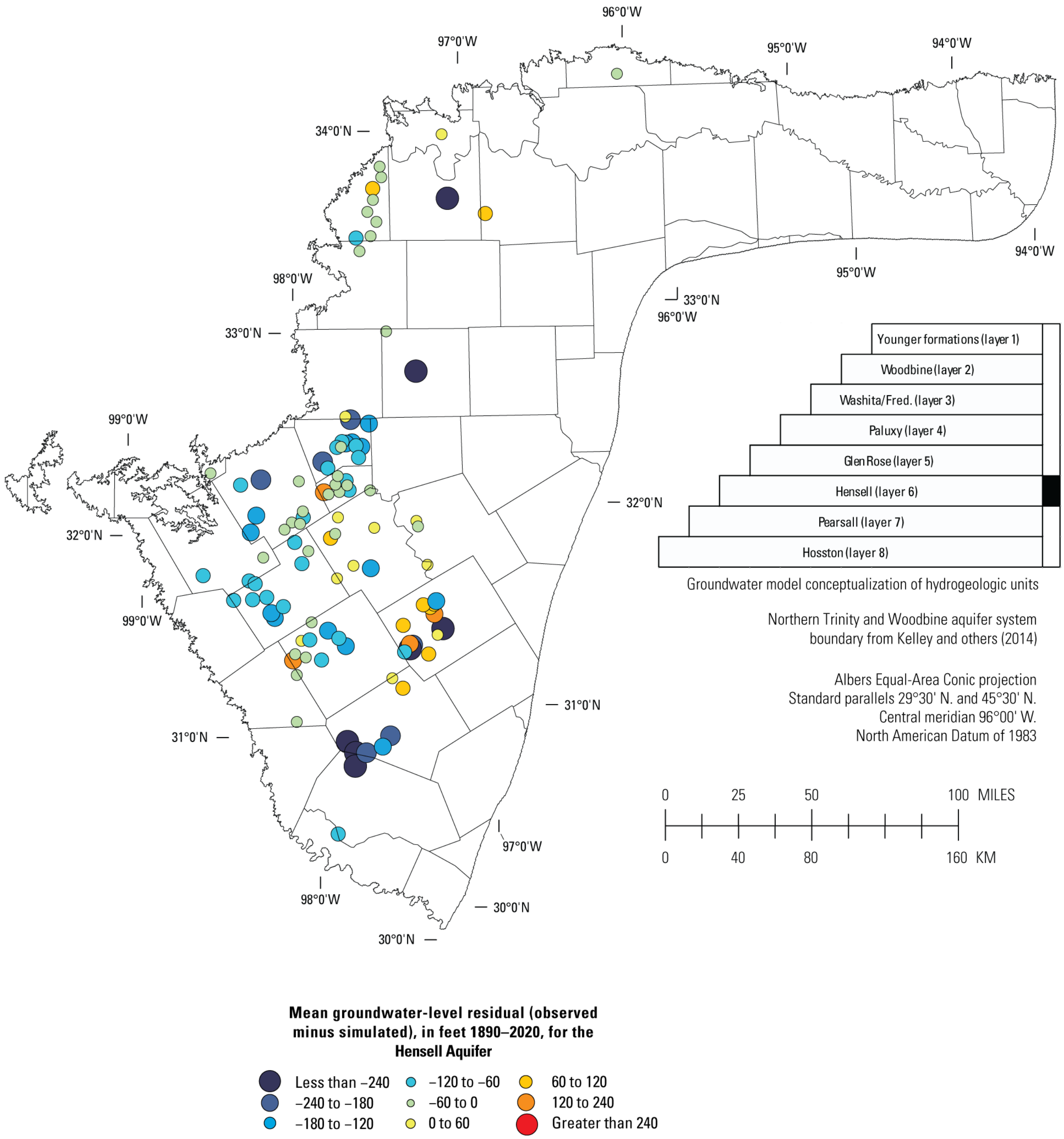

Figure 3-47. Spatial distribution of mean groundwater-level residuals for the Hensell Aquifer (layer 6).

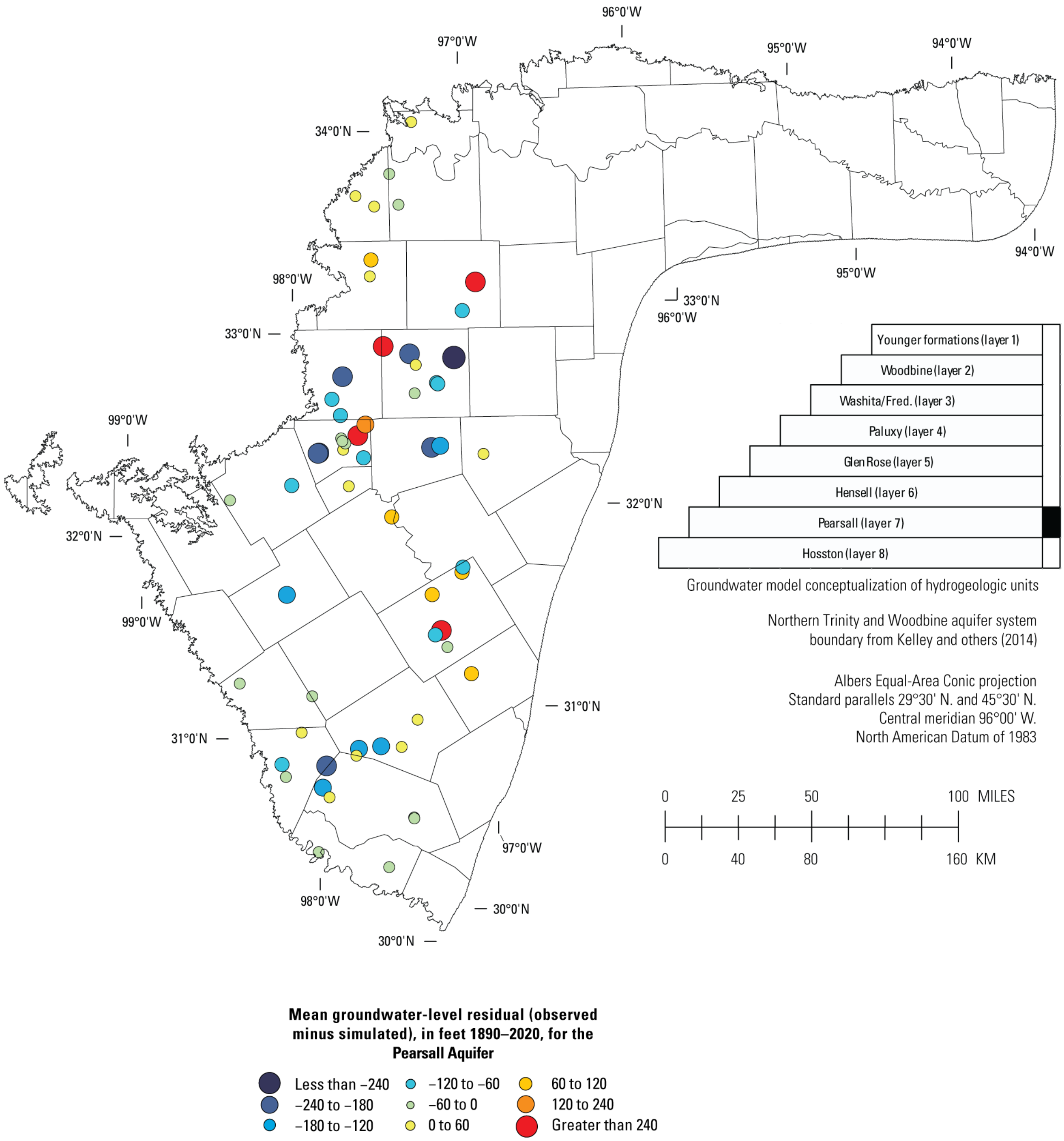

Figure 3-48. Spatial distribution of mean groundwater-level residuals for the Pearsall Formation (layer 7).

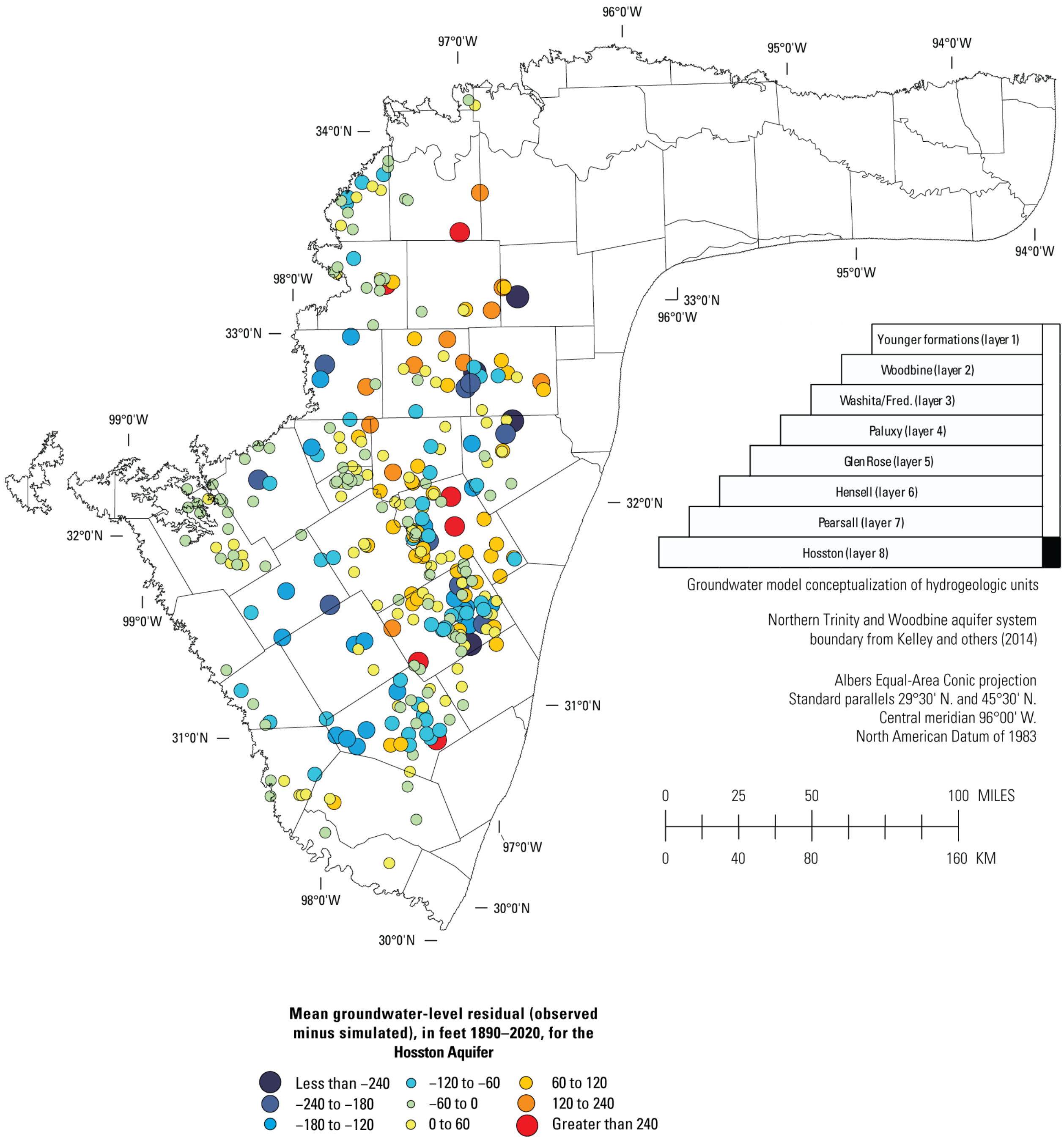

Figure 3-49. Spatial distribution of mean groundwater-level residuals for the Hosston Aquifer (layer 8).

Table 3-6 summarizes groundwater-level residual statistics on a layer basis. MAE values are below 10 percent of the measured ranges of groundwater elevations across the model domain for the entire transient period, although the MAE for some layers in 1980, 2000, and 2020 are above 10 percent. As shown in Figures 3-42 through 3-49, regional groundwater-level trends were reasonably matched. The most apparent deviations from observed trends are likely due to localized inaccuracies between simulated and actual groundwater production rates.

In the Glen Rose, only 34 of 118 observations had more than 20 years' worth of data and many wells did not have screening data as previously discussed. Additionally, the larger residuals in this layer occurred generally in the central to southern parts of the model domain where this unit is typically more confining, whereas the mean residuals in the Upper Trinity GCD were closer to zero (Figure 3-46). In the Washita/Fredericksburg, only 36 of the 162 single-layer observation wells were north of Bell County, and only 14 of the 36 wells had more than 20 years' worth of data; therefore, greater uncertainty exists in these simulated results. Whereas the remaining 126 observations in this layer were in the Edwards BFZ and had mean residuals closer to zero (Figure 3-44).

Figures 3-50 through 3-70 show observed and simulated groundwater levels across the model area. Most figures show declining water levels, although some areas, such as Upper Trinity GCD (Figures 3-55 and 3-56), include stable trends in measured and simulated water levels. Some areas such as Tarrant County (Northern Trinity GCD) (Figure 3-57), exhibit complex groundwater hydrograph patterns, which were generally well captured by the simulated trends. Some examples of difficulties in capturing measured water levels can be observed in parts D and F in Figure 3-64 for Middle Trinity GCD. In both cases, the base simulation (solid line) accurately captured measurements between 1960 and 1980, with simulated values deviating substantially from the measured trends from 1980 onwards—the time period for the recompleted groundwater use in this model. This type of discrepancy can be observed in other areas, suggesting that estimates of pumping distribution assigned to grid cells caused deviations between simulated and measured hydrographs. In the NTWGAM, municipal pumping was distributed between wells identified as municipal wells based on observed reductions in groundwater levels, which assist with matching observed water level data. In the NTGAM, this method was not used; rather, the spatial distribution of groundwater use was fixed at each well. This difference between the approaches taken in NTWGAM and NTGAM, combined with inaccuracies between simulated and actual pumping rates, probably accounts for much of the misfit in the simulated water level data vs the observed water level data.

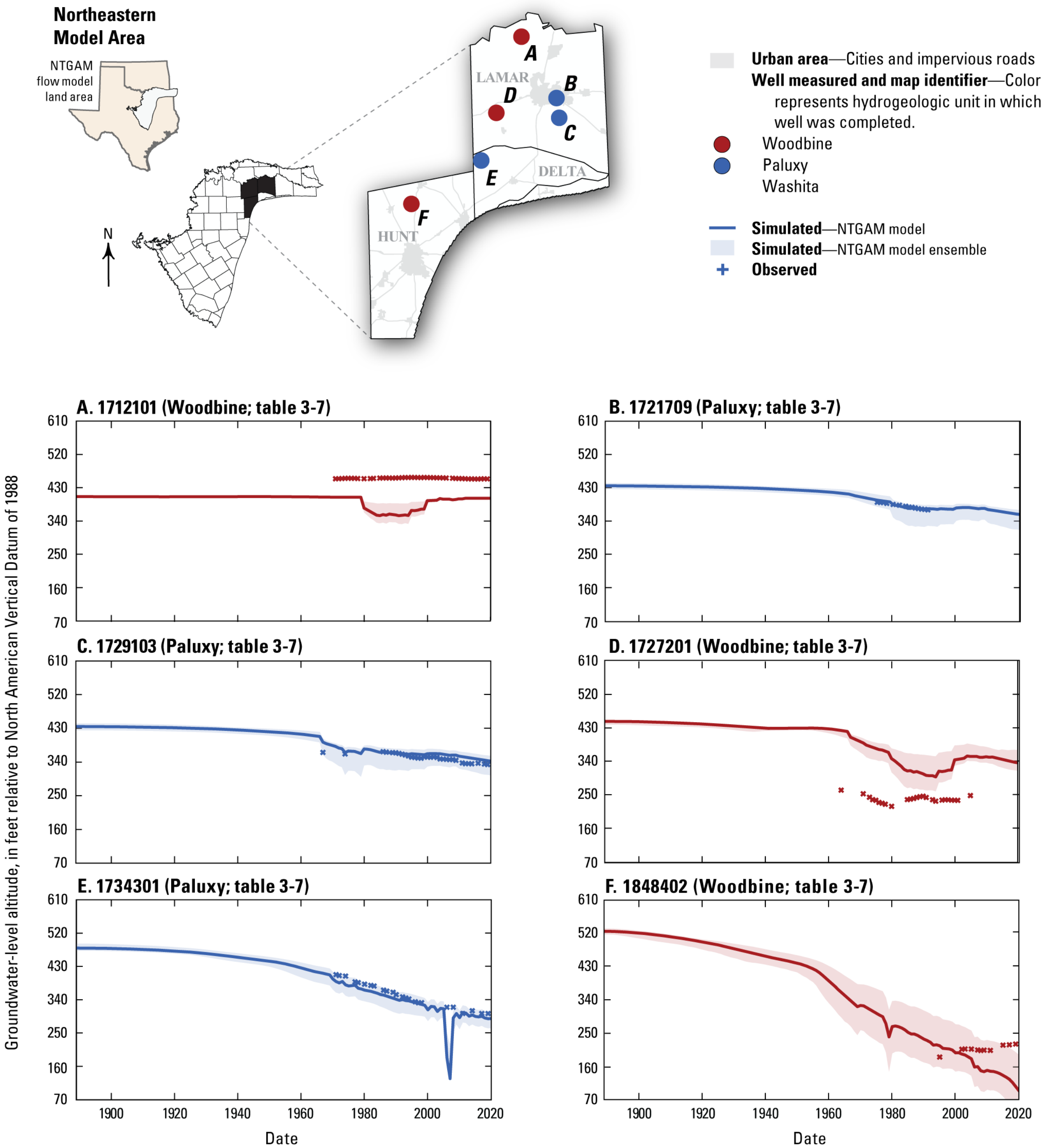

Figure 3-50. Locations and hydrographs of observed and simulated groundwater levels for selected wells in the northeastern part of the northern Trinity and Woodbine aquifer system.

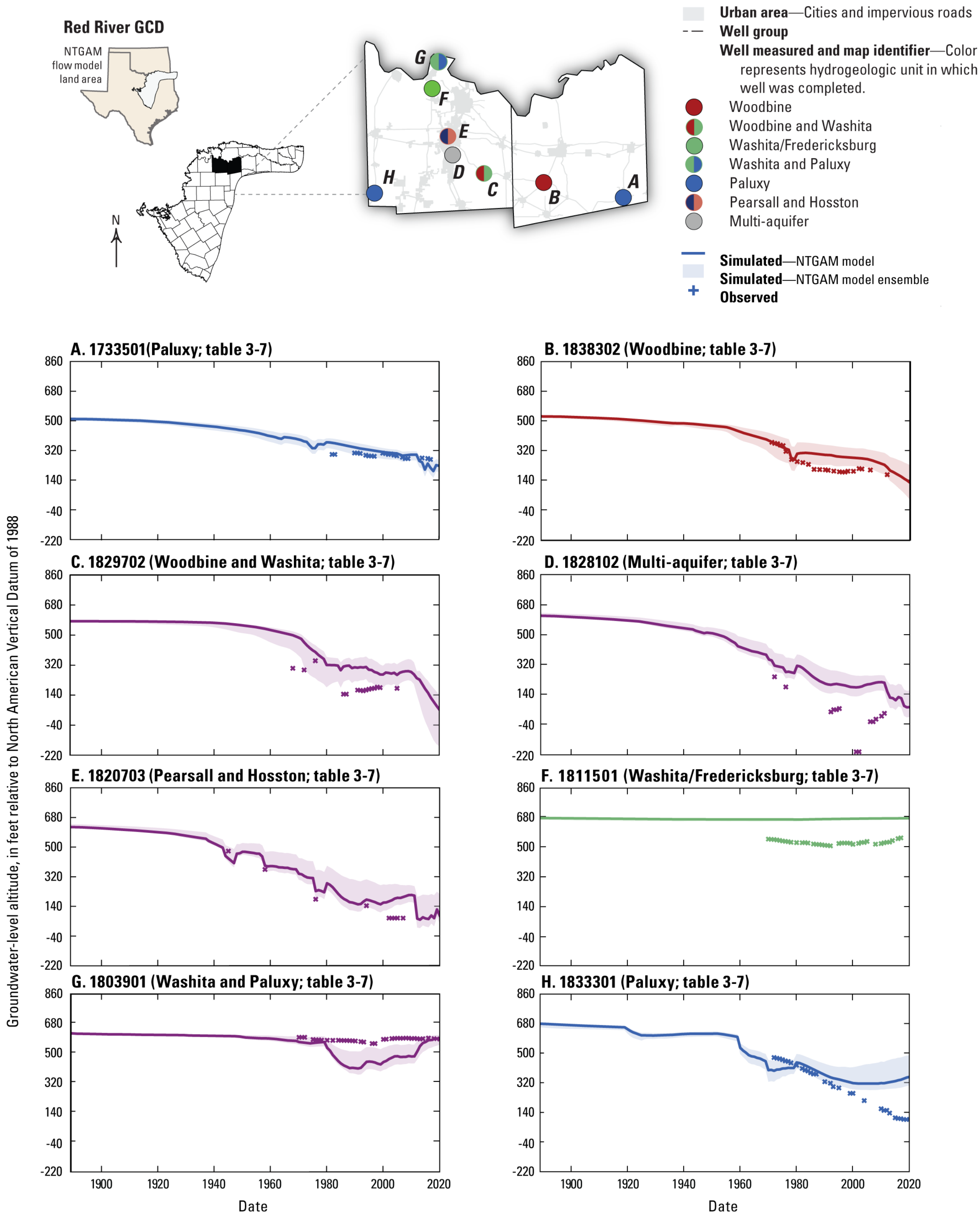

Figure 3-51. Locations and hydrographs of observed and simulated groundwater levels for selected wells in the Red River Groundwater Conservation District.

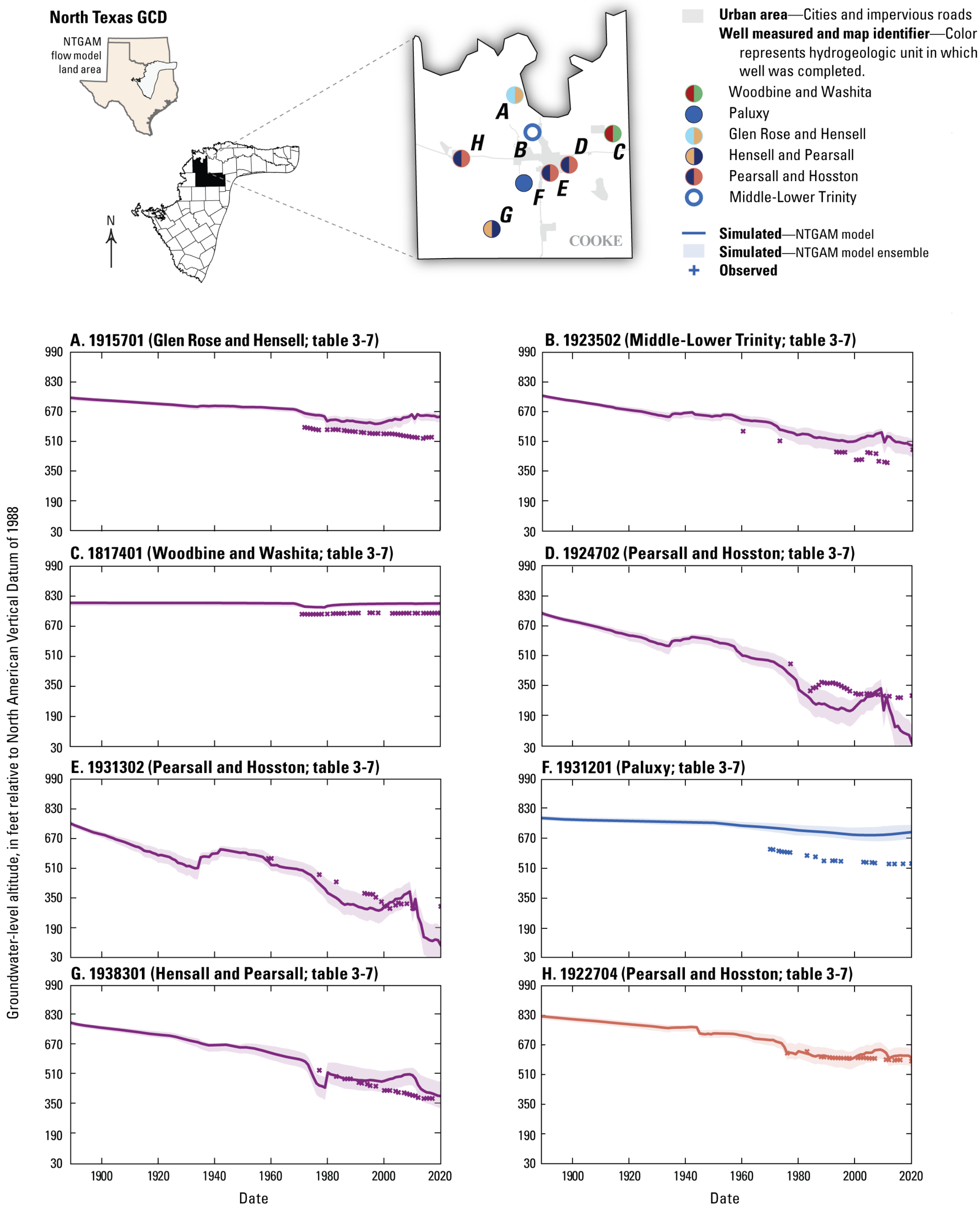

Figure 3-52. Locations and hydrographs of observed and simulated groundwater levels for selected wells in the North Texas Groundwater Conservation District in Cooke County.

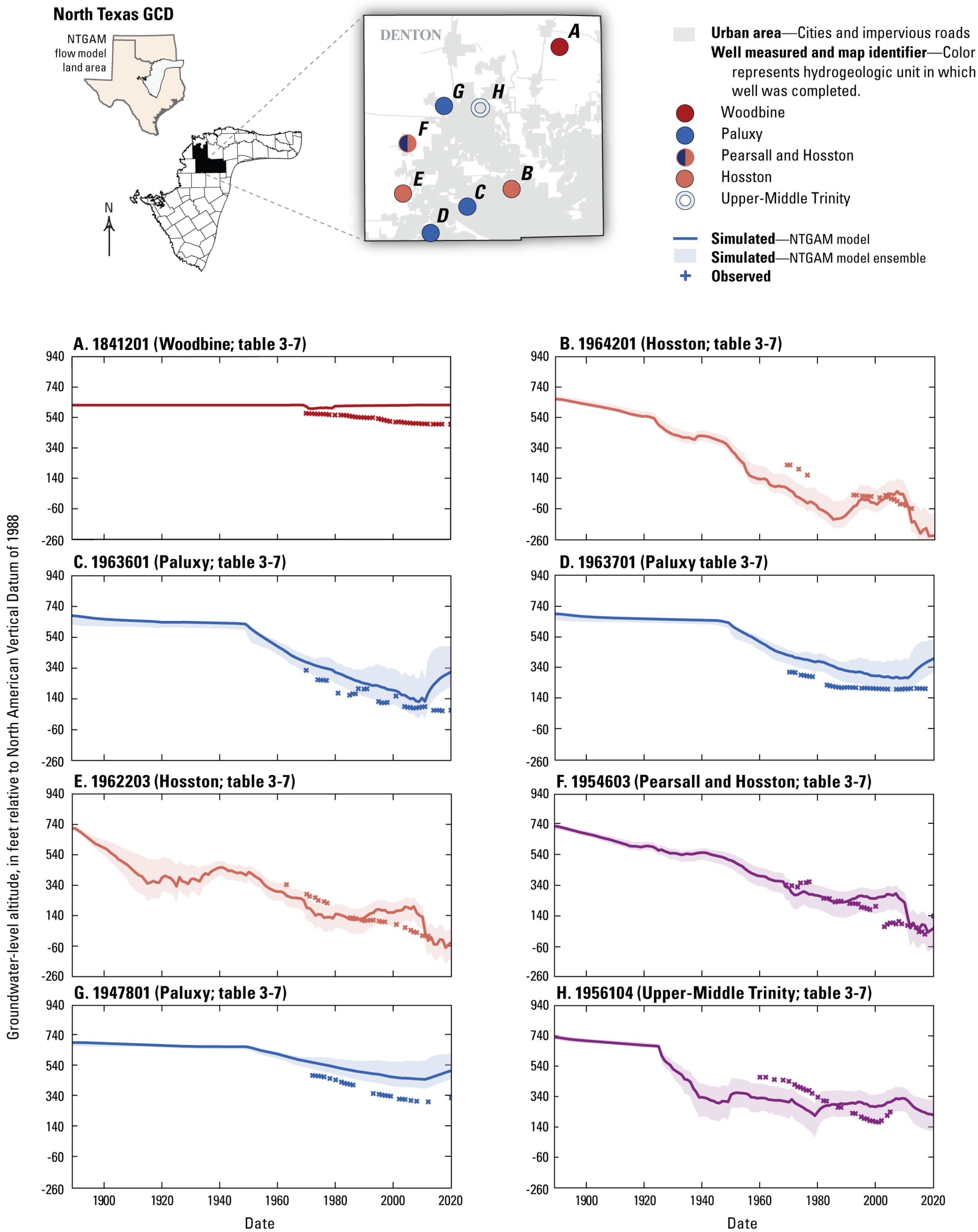

Figure 3-53. Locations and hydrographs of observed and simulated groundwater levels for selected wells in the North Texas Groundwater Conservation District in Denton County.

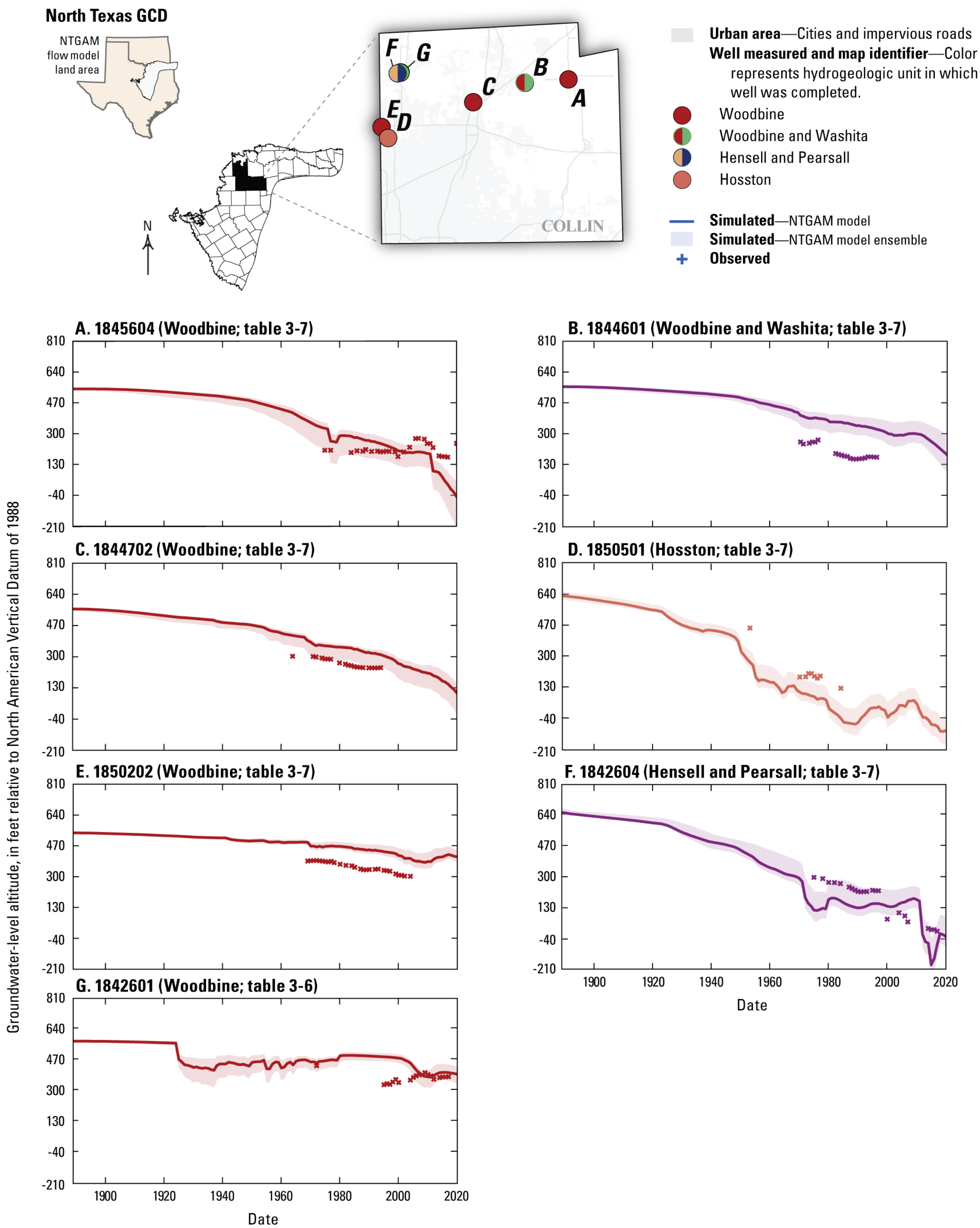

Figure 3-54. Locations and hydrographs of observed and simulated groundwater levels for selected wells in the North Texas Groundwater Conservation District in Collin County.

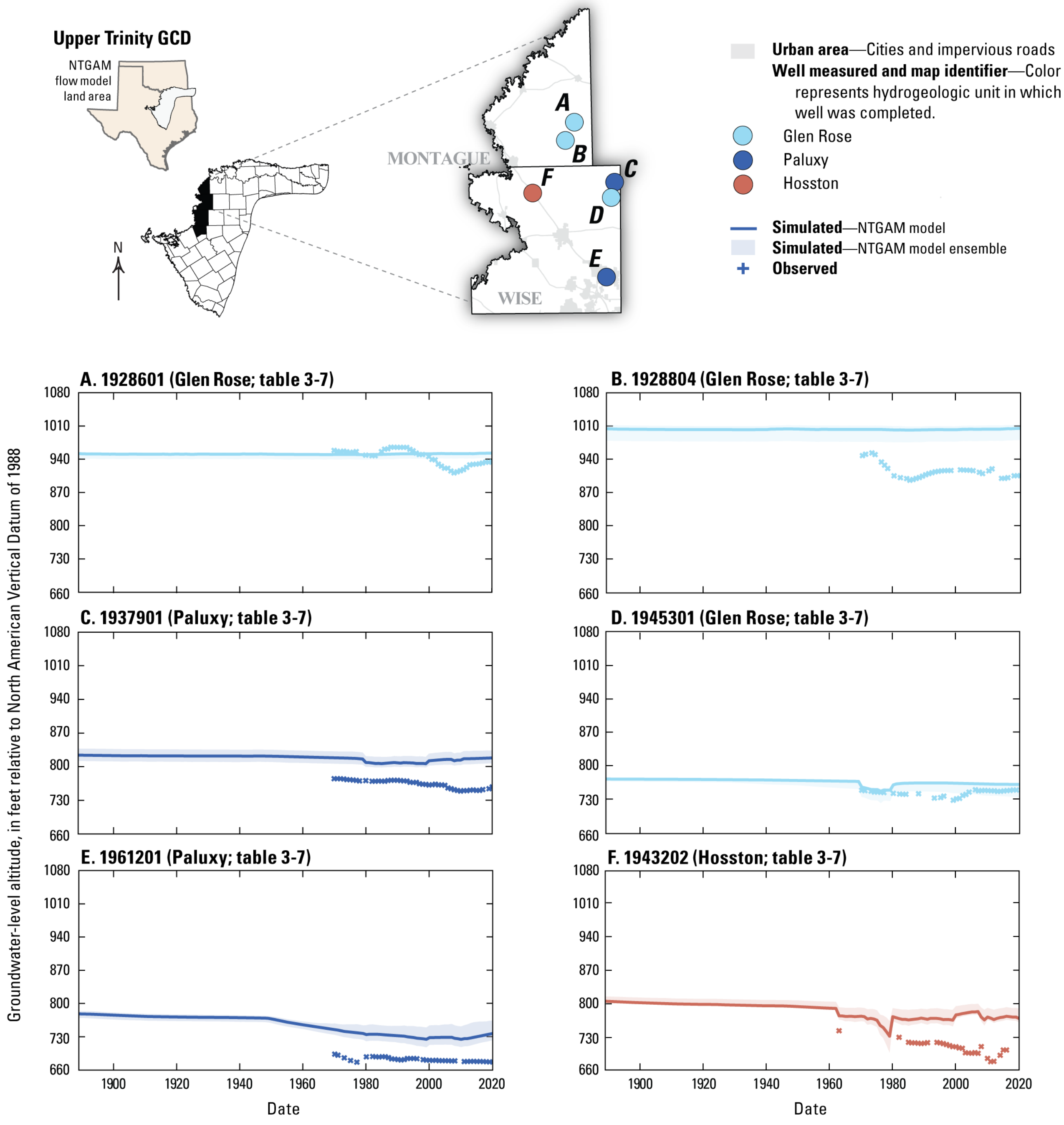

Figure 3-55. Locations and hydrographs of observed and simulated groundwater levels for selected wells in the Upper Trinity Groundwater Conservation District in Montague and Wise Counties.

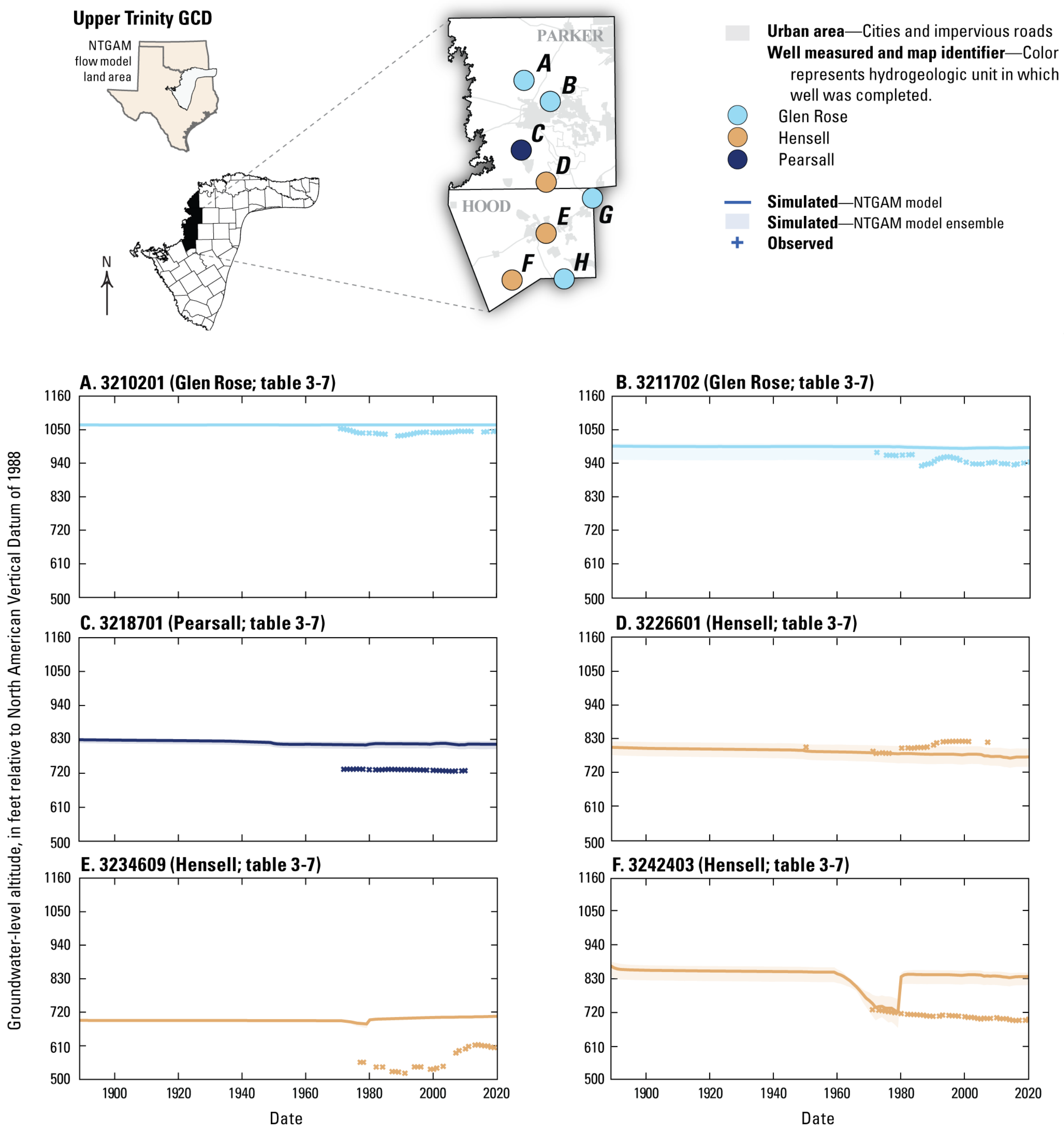

Figure 3-56. Locations and hydrographs of observed and simulated groundwater levels for selected wells in the Upper Trinity Groundwater Conservation District in Parker and Hood Counties.

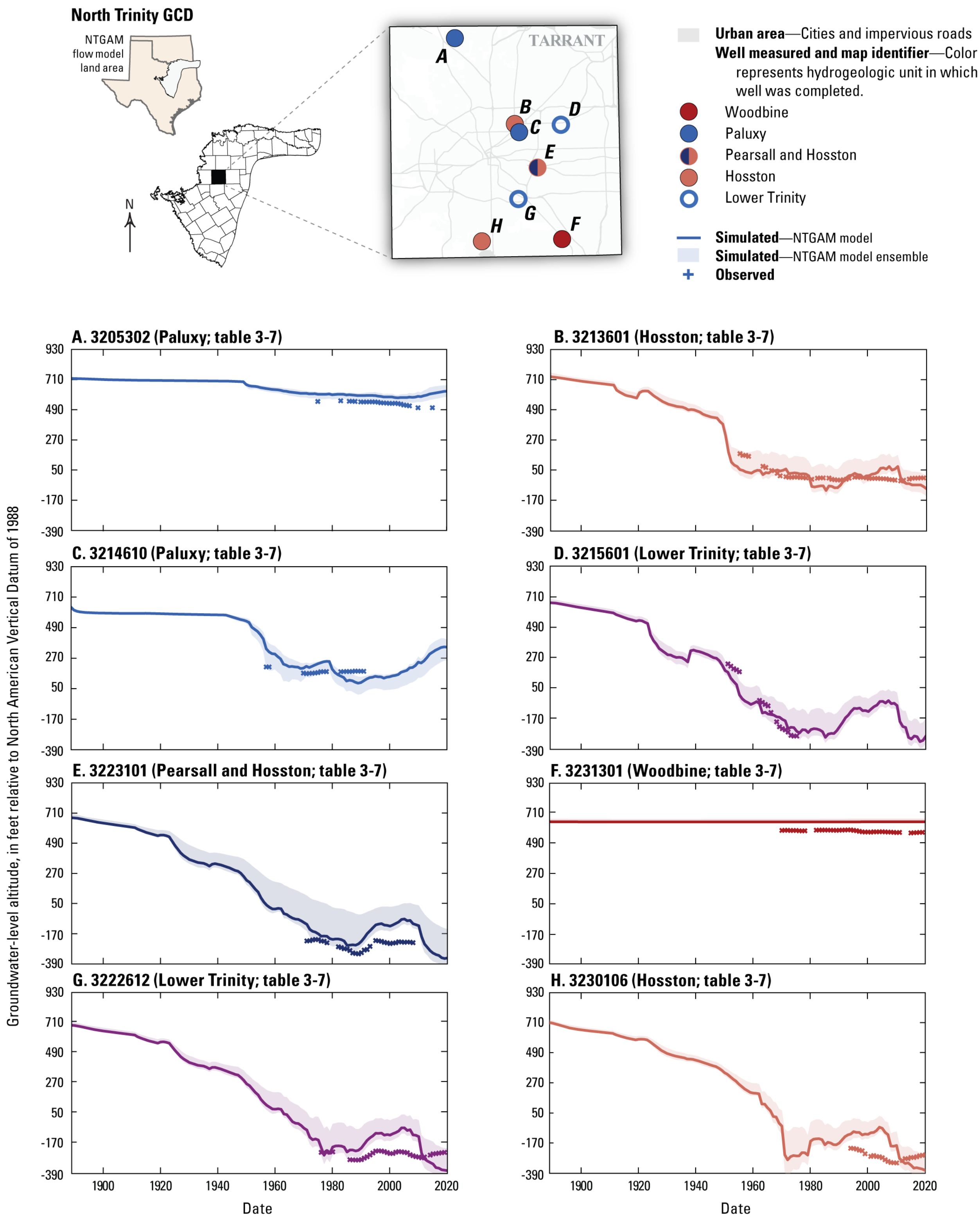

Figure 3-57. Locations and hydrographs of observed and simulated groundwater levels for selected wells in the Northern Trinity Groundwater Conservation District.

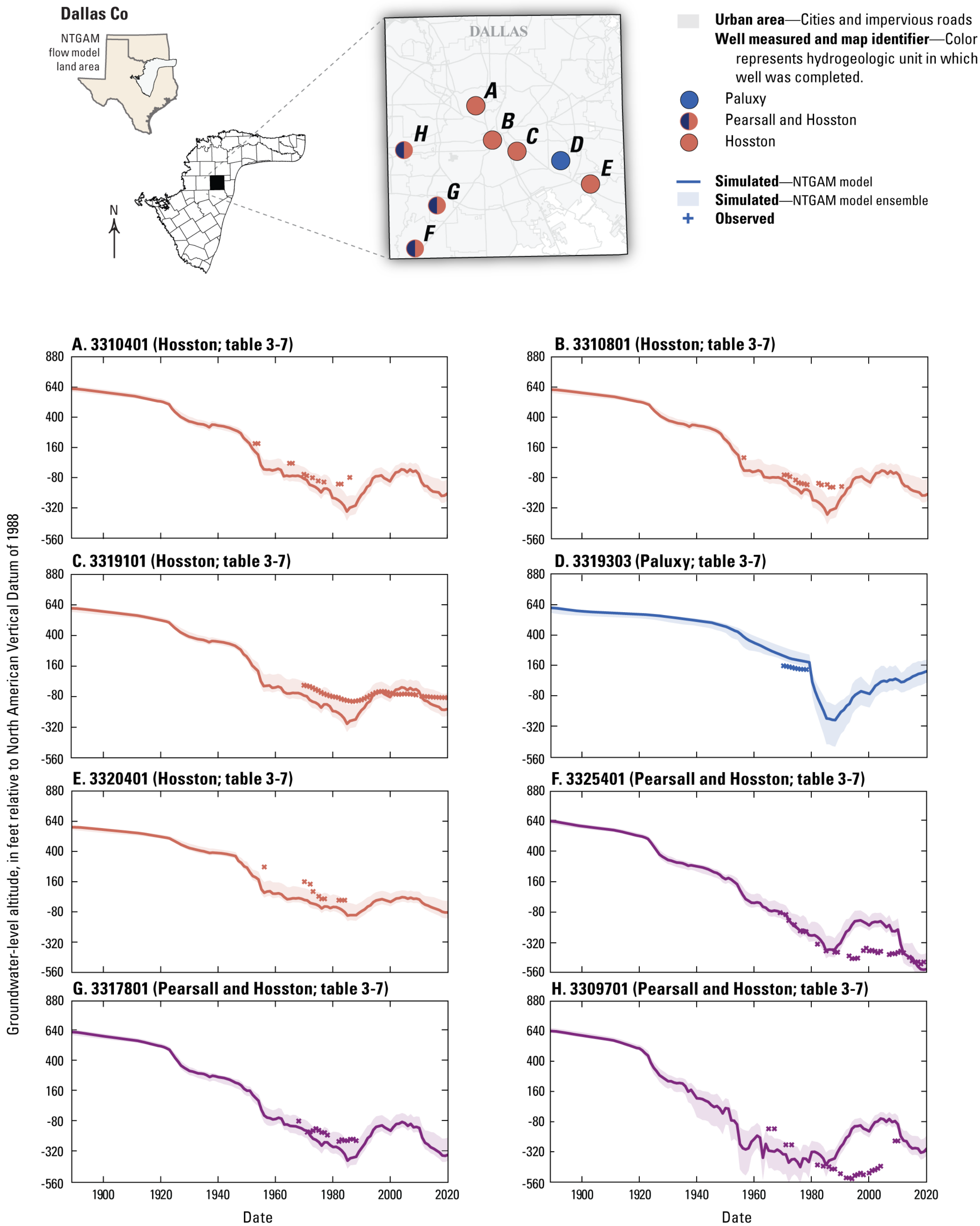

Figure 3-58. Locations and hydrographs of observed and simulated groundwater levels for selected wells in Dallas County.

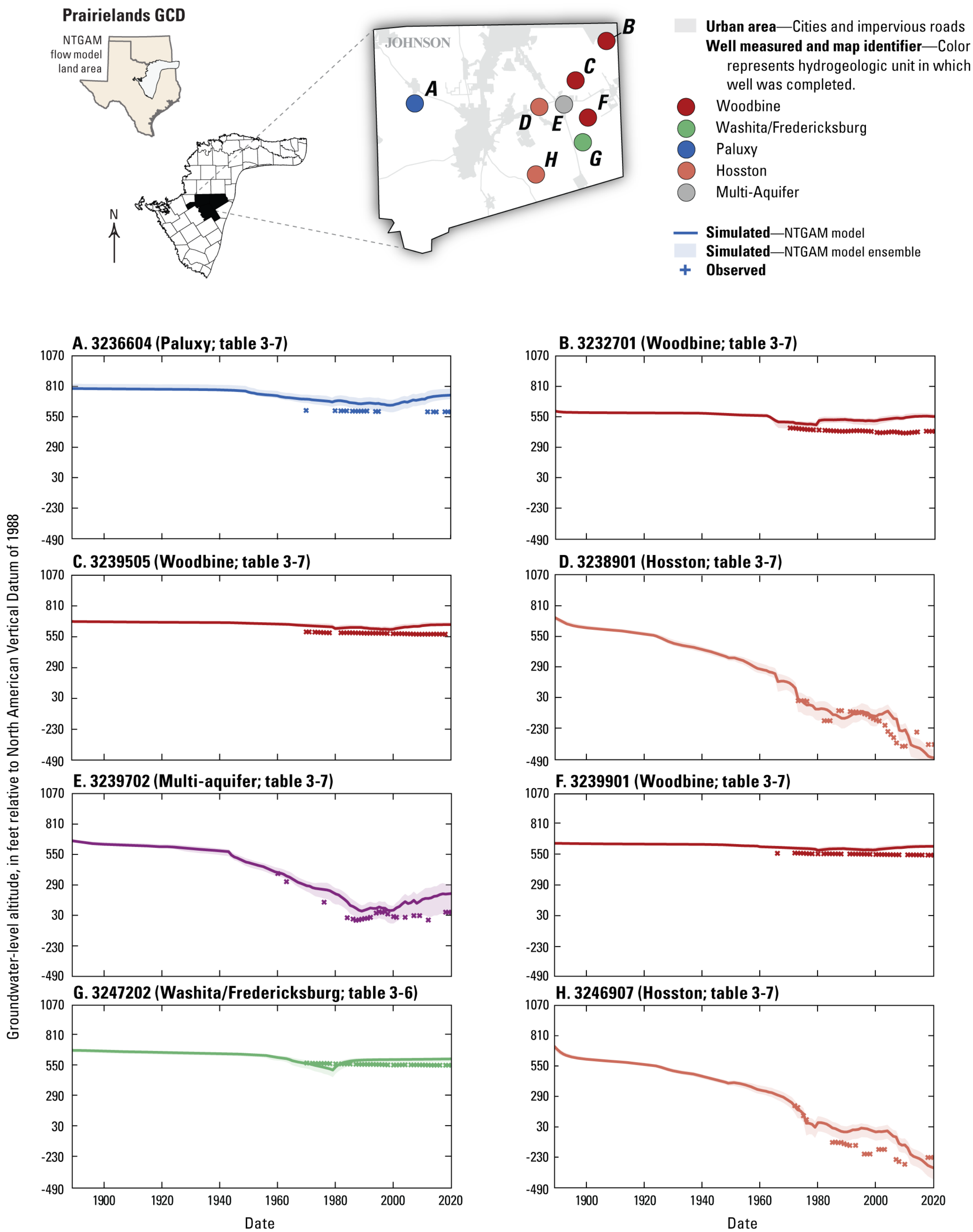

Figure 3-59. Locations and hydrographs of observed and simulated groundwater levels for selected wells in the Prairielands Groundwater Conservation District in Johnson County.

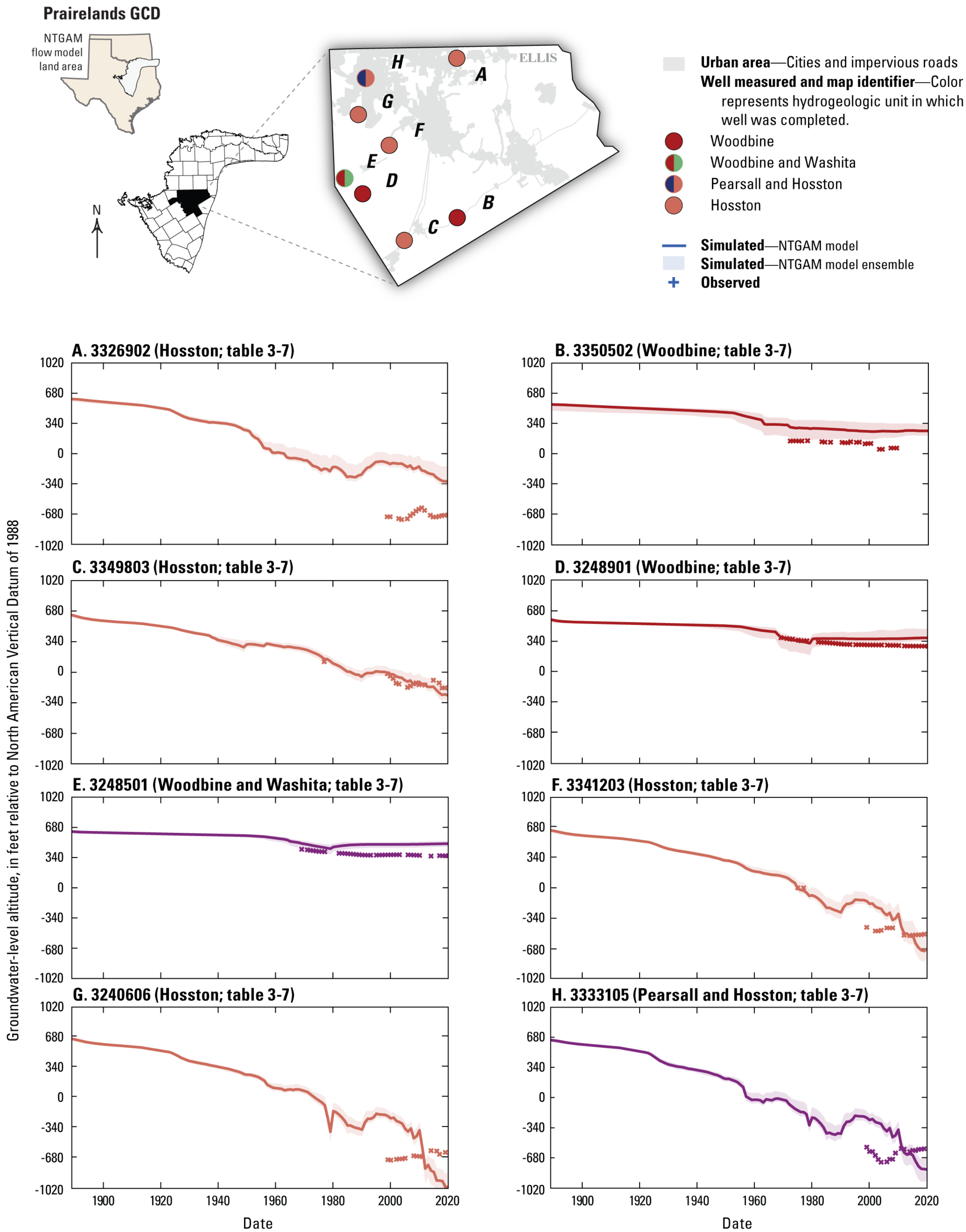

Figure 3-60. Locations and hydrographs of observed and simulated groundwater levels for selected wells in the Prairielands Groundwater Conservation District in Ellis County.

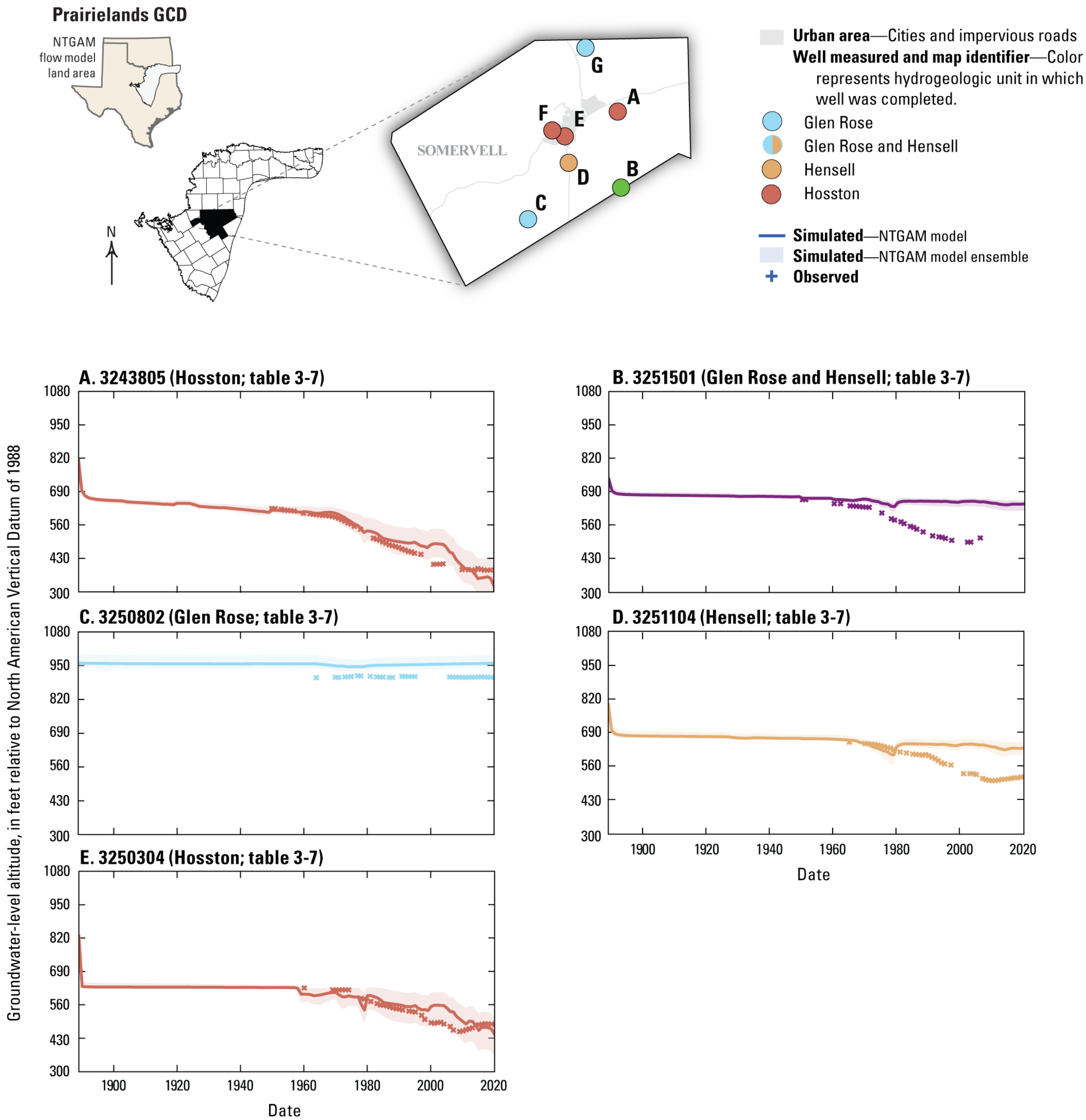

Figure 3-61. **Locations and hydrographs of observed and simulated groundwater levels for selected wells in the Prairielands Groundwater Conservation District in Somervell County.**

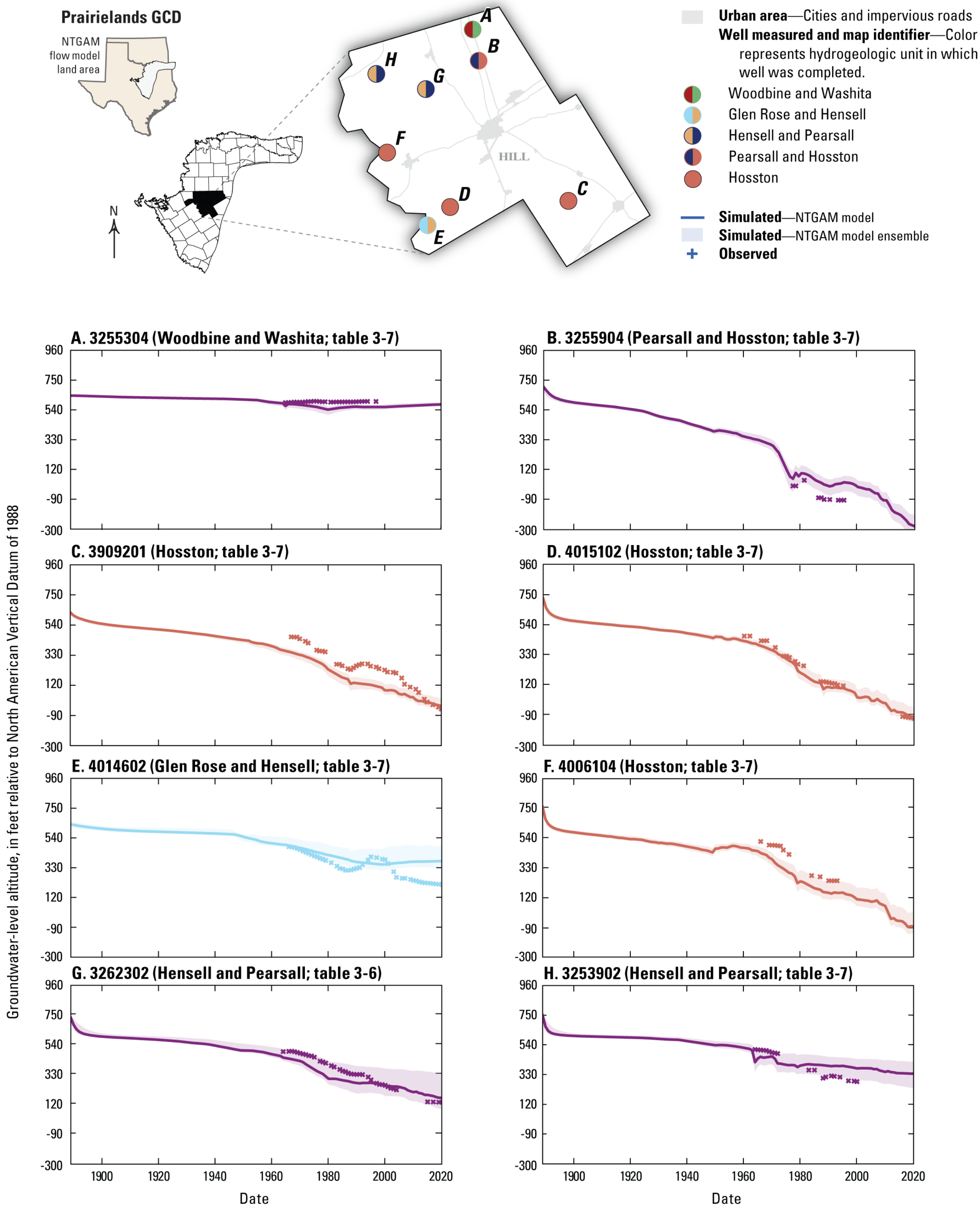

Figure 3-62. Locations and hydrographs of observed and simulated groundwater levels for selected wells in the Prairielands Groundwater Conservation District in Hill County.

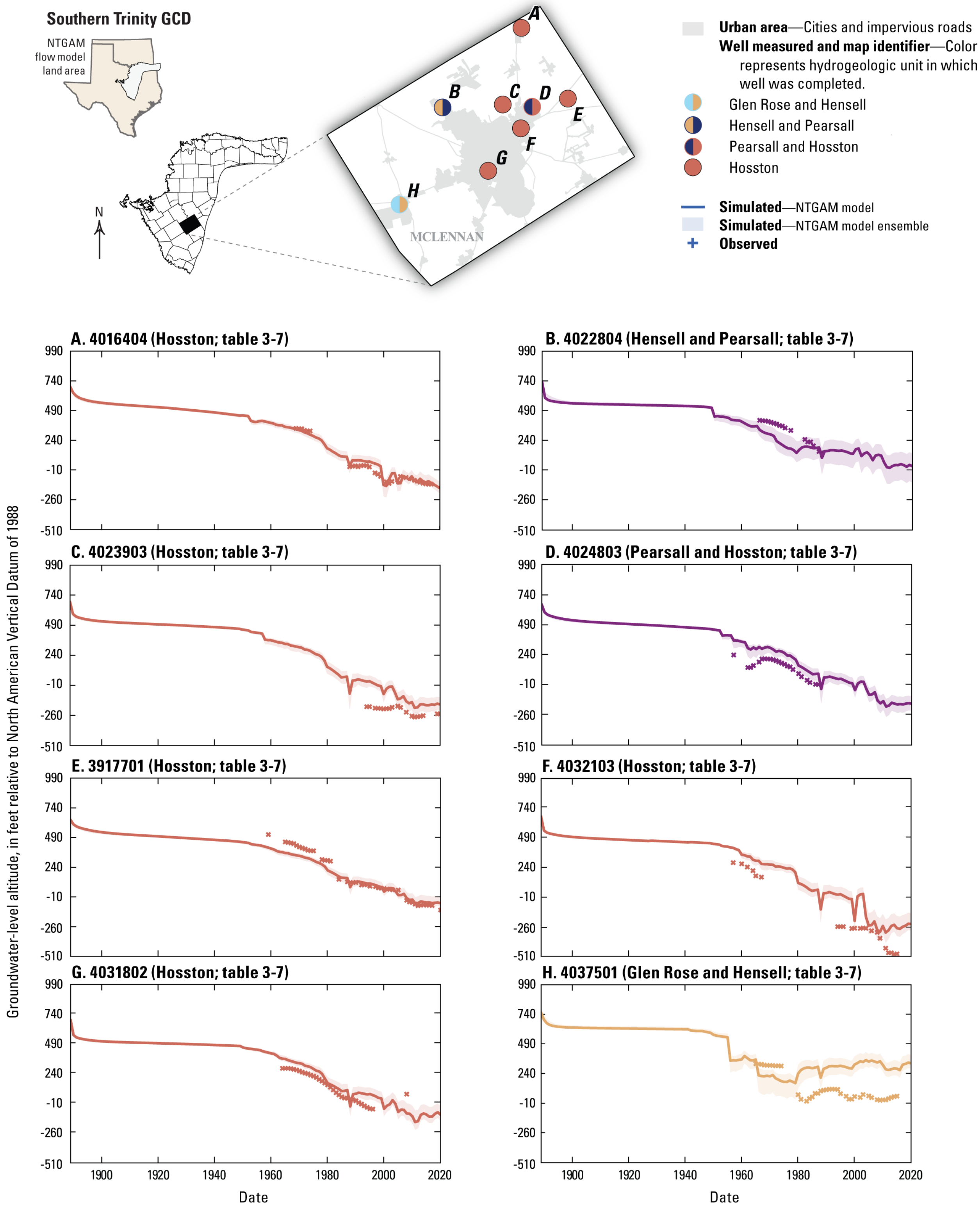

Figure 3-63. Locations and hydrographs of observed and simulated groundwater levels for selected wells in the Southern Trinity Groundwater Conservation District.

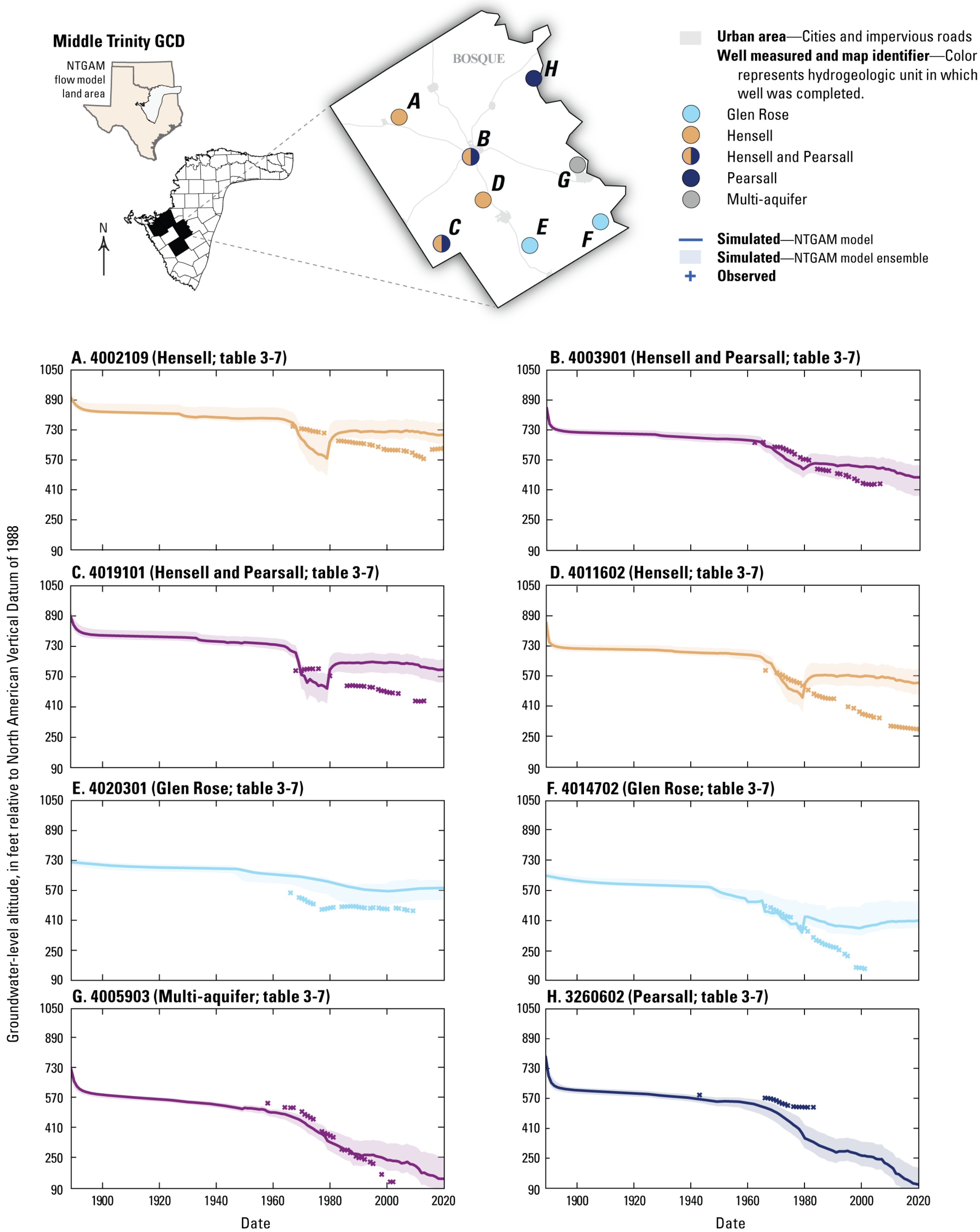

Figure 3-64. Locations and hydrographs of observed and simulated groundwater levels for selected wells in the Middle Trinity Groundwater Conservation District in Bosque County.

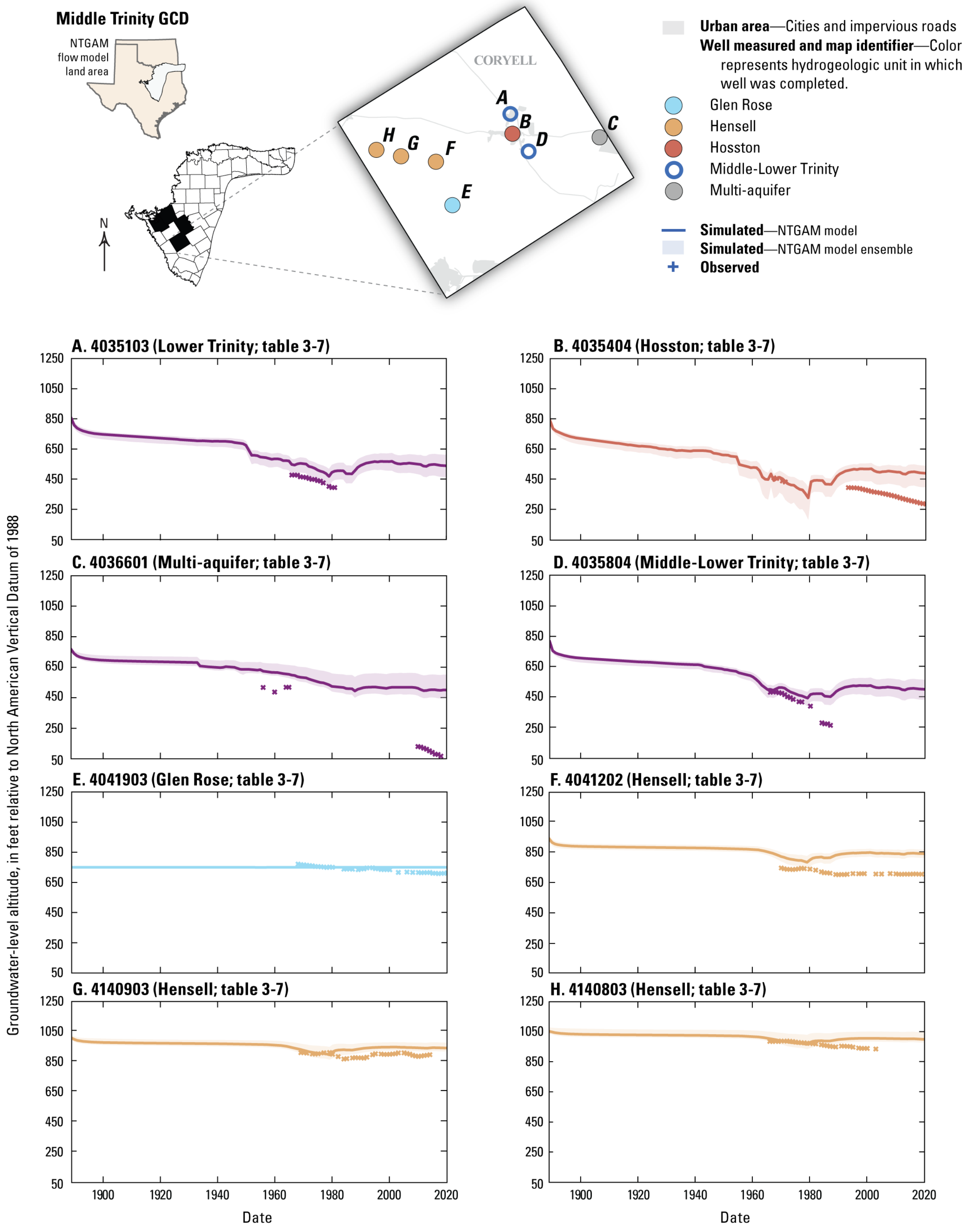

Figure 3-65. Locations and hydrographs of observed and simulated groundwater levels for selected wells in the Middle Trinity Groundwater Conservation District in Coryell County.

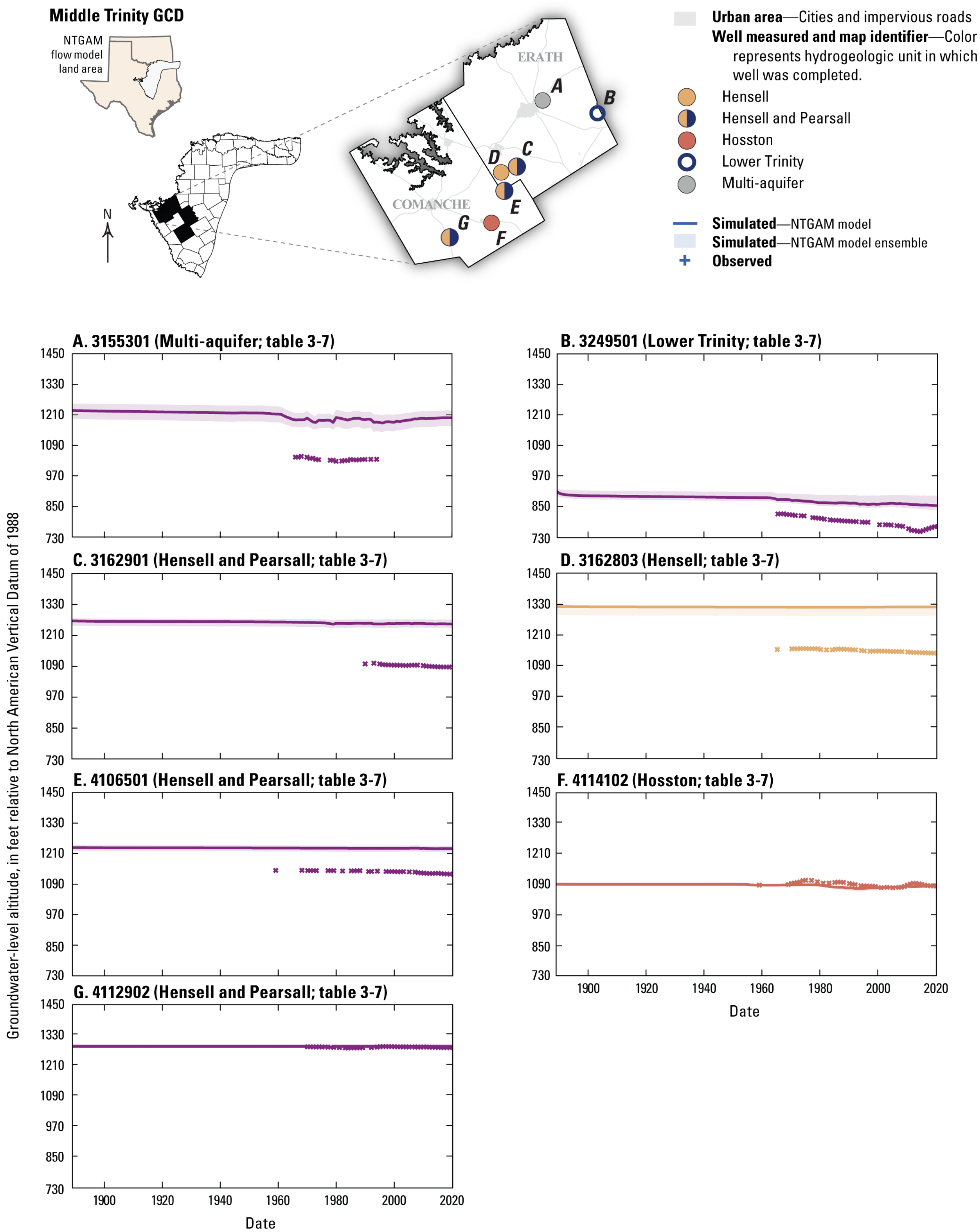

Figure 3-66. Locations and hydrographs of observed and simulated groundwater levels selected wells in the Middle Trinity Groundwater Conservation District in Erath and Commanche Counties.

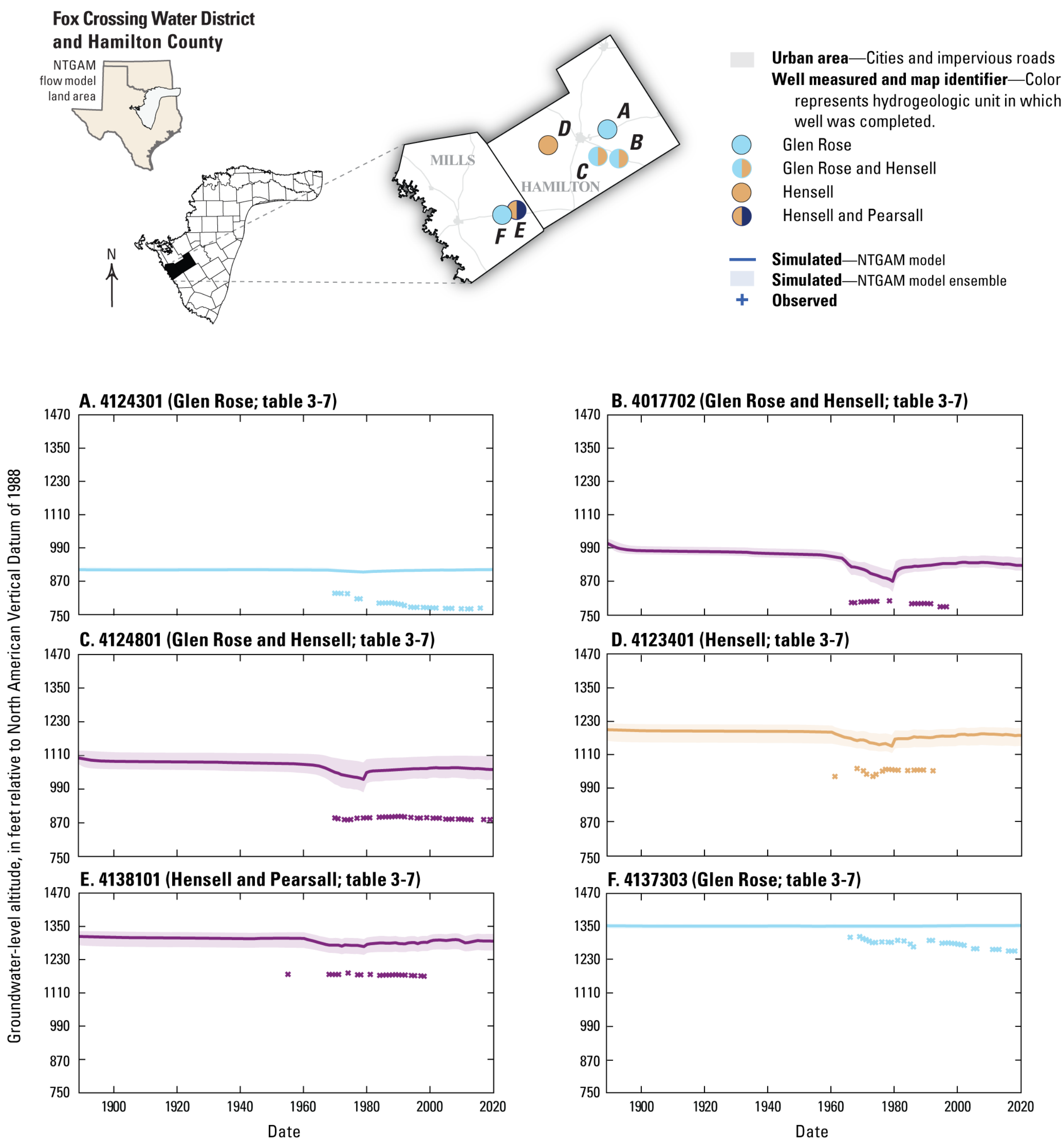

Figure 3-67. Locations and hydrographs of observed and simulated groundwater levels for selected wells in Mills and Hamilton Counties.

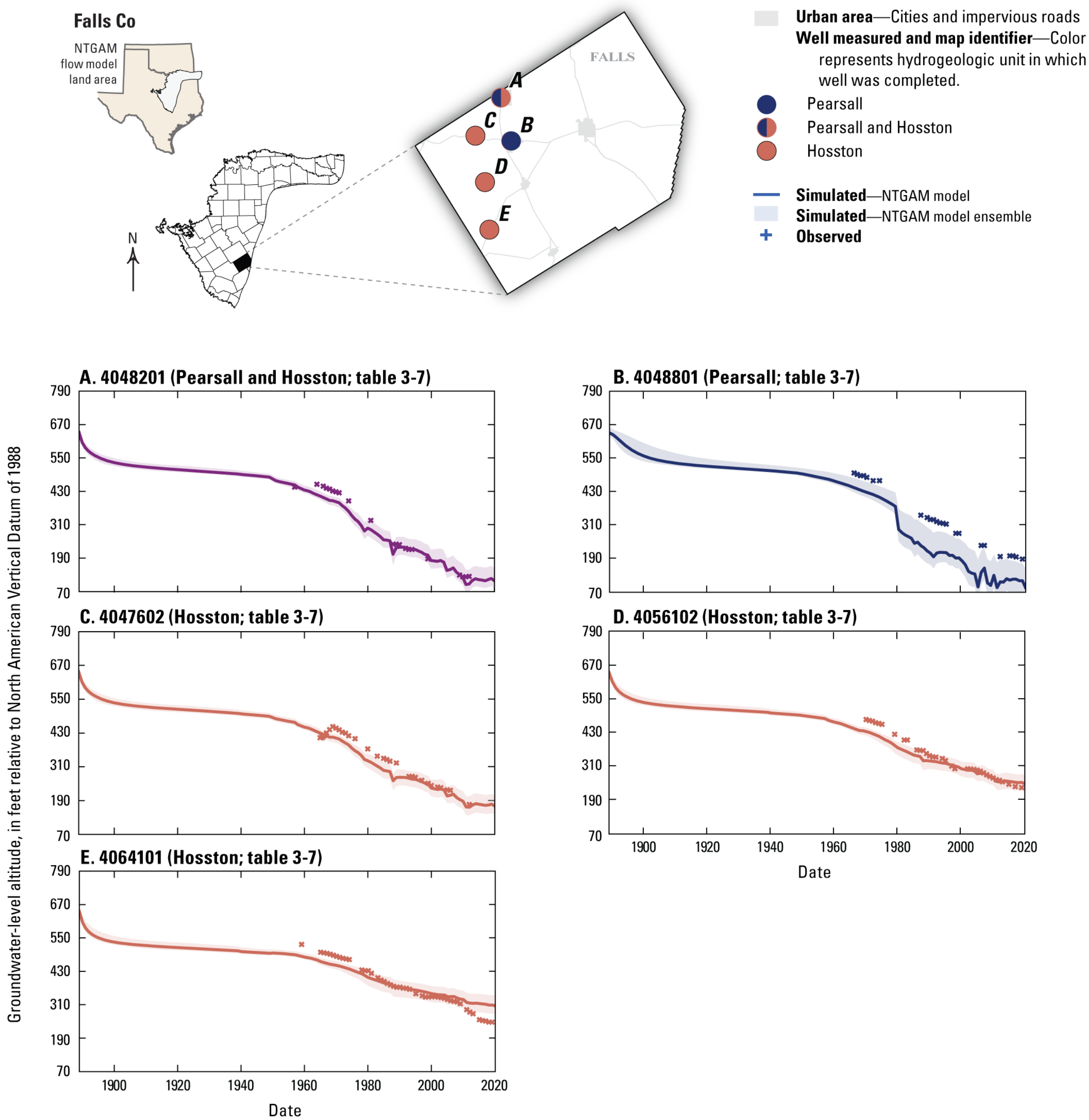

Figure 3-68. Locations and hydrographs of observed and simulated groundwater levels for selected wells in Falls County.

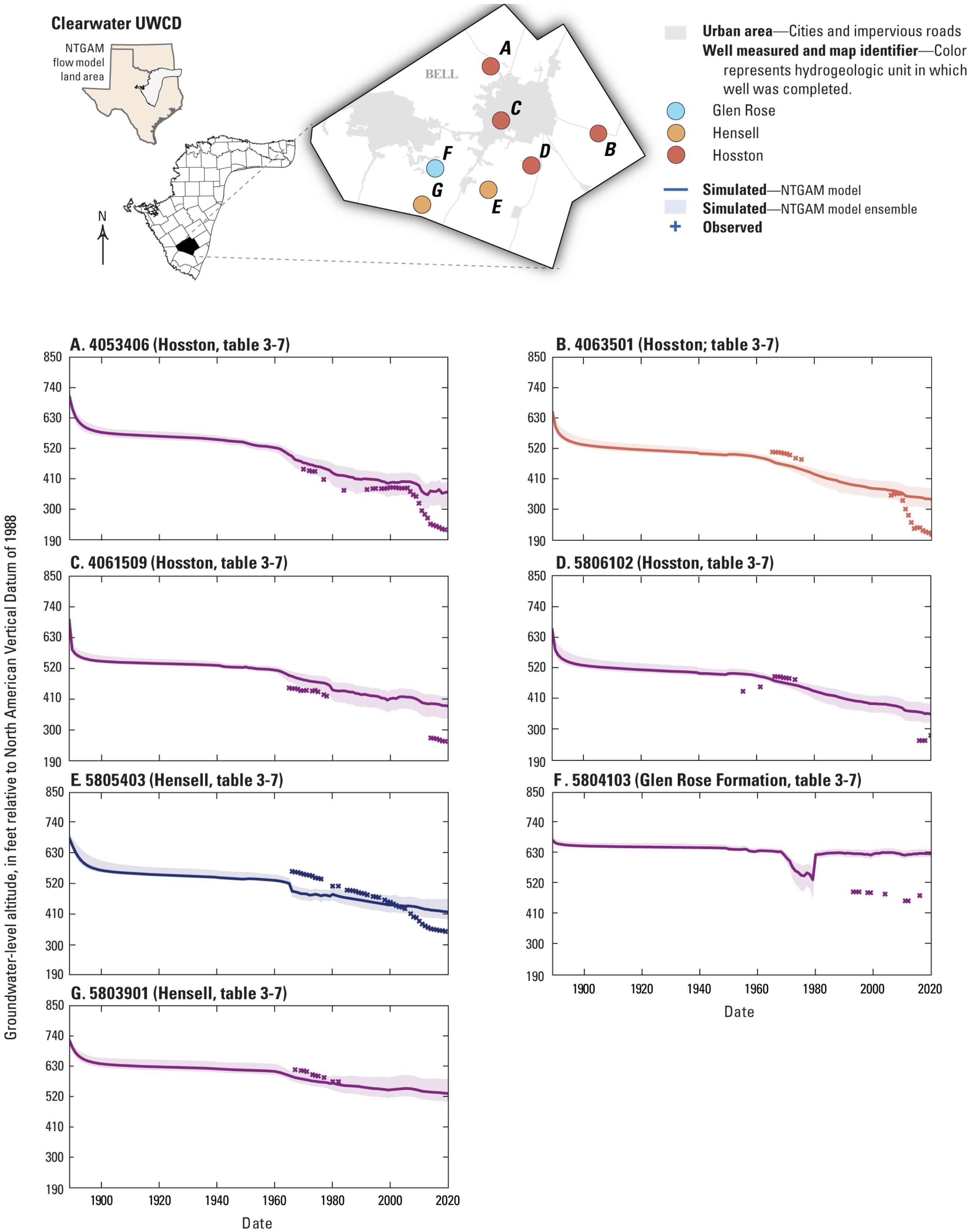

Figure 3-69. Locations and hydrographs of observed and simulated groundwater levels for selected wells in the Clearwater Underground Water Conservation District.

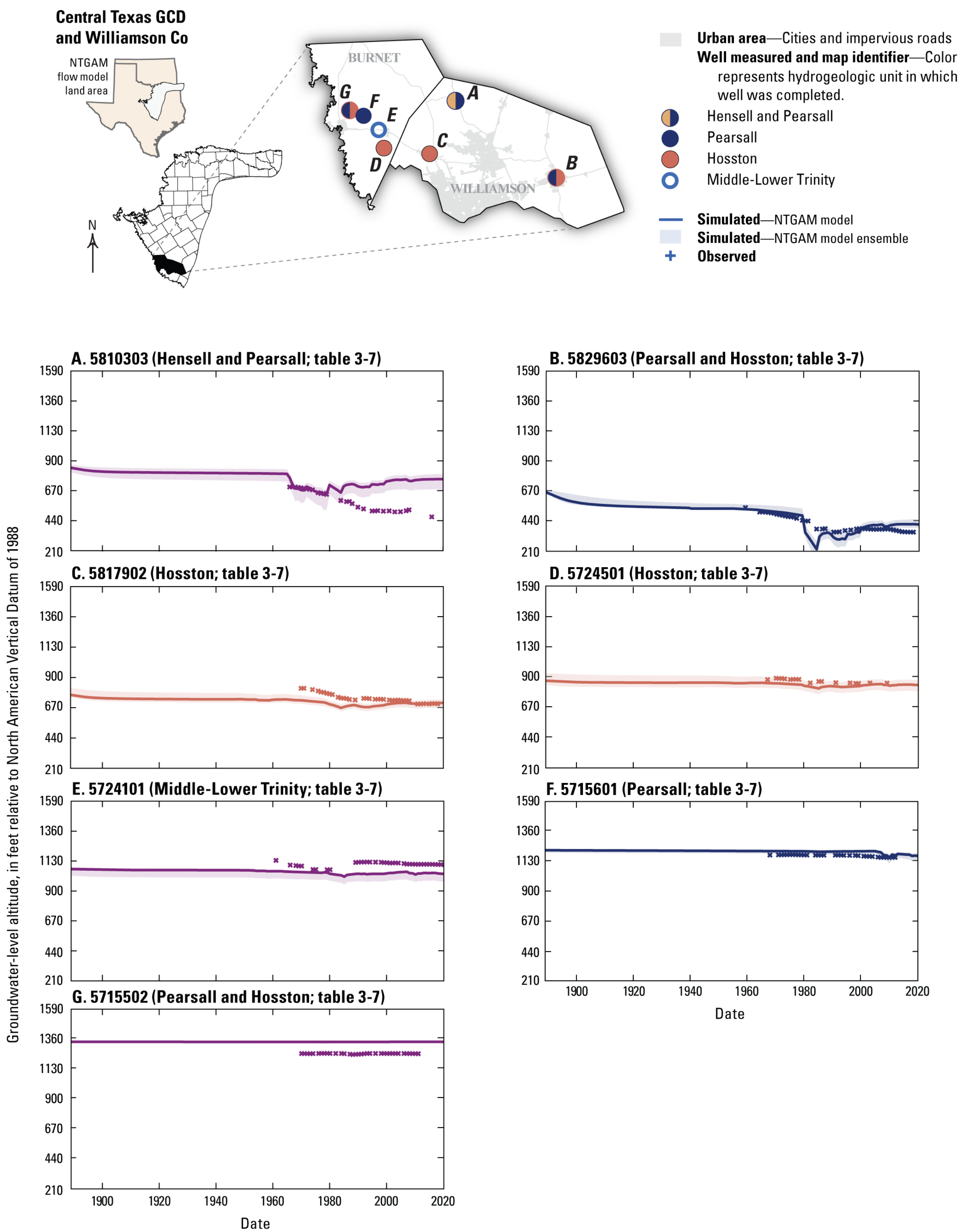

Figure 3-70. Locations and hydrographs of observed and simulated groundwater levels for selected wells in the Central Texas Groundwater Conservation District and Williamson County.

Table 3-6. Statistical summary of groundwater-level residuals.

Time period	Aquifer unit (model layer)	Observation count	Mean Error, in feet	MAE (ft)	RMSE, in feet	Range	Adjusted MAE[2]
Transient period (1890-2020)	All layers	16,510	-60.0	88.9	125	2,432	0.037
	Woodbine (layer 2)	1,741	-57.8	86.6	106	921	0.094
	Washita/Fredericksburg (layer 3)	1,557	-51.2	56.8	84.3	1,294	0.044
	Paluxy (layer 4)	1,135	-54.0	65.0	86.5	1,199	0.054
	Glen Rose (layer 5)	1,277	-72.7	81.8	120	1,449	0.056
	Hensell (layer 6)	1,561	-88.8	110	140	1,699	0.065
	Pearsall (layer 7)	633	-44.8	90.0	123	2,014	0.045
	Hosston (layer 8)	3,531	-21.9	69.6	102	2,273	0.031
	Multi-aquifer	5,075	-81.1	113	157	2,374	0.048
1980	All layers	257	-43.9	69.1	89.2	1,775	0.039
	Woodbine (layer 2)	28.0	-61.7	95.4	111	598	0.159
	Washita/Fredericksburg (layer 3)	38.0	-47.4	49.5	73.7	369	0.134
	Paluxy (layer 4)	24.0	-41.1	45.8	60.8	761	0.060
	Glen Rose (layer 5)	23.0	-58.8	66.1	90.0	928	0.071
	Hensell (layer 6)	26.0	-64.0	81.1	99.2	1,027	0.079
	Pearsall (layer 7)	9.0	20.1	102	122	1,569	0.065
	Hosston (layer 8)	34.0	0.0	51.1	59.4	1,317	0.039
	Multi-aquifer	75.0	-52.3	77.6	97.5	1,616	0.048
2000	All layers	226	-81.8	103	146	2,082	0.050
	Woodbine (layer 2)	32.0	-68.3	97.2	118	596	0.163
	Washita/Fredericksburg (layer 3)	19.0	-68.1	71.8	91.1	201	0.356
	Paluxy (layer 4)	15.0	-42.7	46.8	55.7	723	0.065
	Glen Rose (layer 5)	16.0	-72.9	89.3	130	1,325	0.067
	Hensell (layer 6)	18.0	-111	130	159	1,151	0.113
	Pearsall (layer 7)	6.0	-138	138	195	1,255	0.110
	Hosston (layer 8)	42.0	-50.3	86	139	2,082	0.042

Time period	Aquifer unit (model layer)	Observation count	Mean Error, in feet	MAE (ft)	RMSE, in feet	Range	Adjusted MAE[2]
	Multi-aquifer	78.0	-106.0	127	176	1,794	0.071
2020	All layers	461	-80.2	123	174	2,063	0.060
	Woodbine (layer 2)	21.0	-47.8	110	134	857	0.129
	Washita/Fredericksburg (layer 3)	33.0	-112	117	214	1,110	0.106
	Paluxy (layer 4)	24.0	-112	130	152	1,198	0.109
	Glen Rose (layer 5)	32.0	-96.4	100	157	1,255	0.079
	Hensell (layer 6)	50.0	-186	190	220	1,253	0.152
	Pearsall (layer 7)	16.0	-11.6	92	127	1,712	0.054
	Hosston (layer 8)	123	-20.8	84.0	111	2,063	0.041
	Multi-aquifer	162	-89.4	142	201	1,897	0.075

[1]Mean error is observed - simulated; therefore, a positive value denotes simulated values below observed values, and a negative value denotes simulated values above observed values.

[2]The Adjusted MAE is the MAE divided by the range in observed water level measurements

Table 3-7. Wells with groundwater-level observations used for model history matching.

Groundwater-well groups	TWDB state well number	Map ID (figs. 3-50 to 3-70)	County	Hydrogeologic unit (figure 3-1)[1]	Latitude, in decimal degrees	Longitude, in decimal degrees	Period of record (may contain gaps) (M/Y)[2]		Well depth, in feet below land surface[3]
							Begin	End	
Northeastern model area (figure 3-50)	1712101	A	Lamar	Woodbine	33.8639	-95.5928	10-1959	11-2023	165
	1721709	B	Lamar	Paluxy	33.6628	-95.4675	03-1965	01-1991	2,145
	1729103	C	Lamar	Paluxy	33.5992	-95.4603	02-1967	11-2023	2,563
	1727201	D	Lamar	Woodbine	33.6231	-95.7008	09-1964	12-2005	1,610
	1734301	E	Delta	Paluxy	33.4722	-95.7658	05-1971	11-2023	3,333
	1848402	F	Hunt	Woodbine	33.3119	-96.1089	10-1968	11-2022	2,388
Red River GCD (figure 3-51)	1733501	A	Fannin	Paluxy	33.4267	-95.9464	12-1970	11-2022	3,366
	1838302	B	Fannin	Woodbine	33.4844	-96.2542	07-1971	11-2012	1,297
	1829702	C	Grayson	Woodbine and Washita	33.5206	-96.4853	05-1968	03-2024	1,475
	1828102	D	Grayson	Multi-aquifer	33.5839	-96.6050	01-1959	04-2013	2,460
	1820703	E	Grayson	Pearsall and Hosston	33.6450	-96.6214	11-1945	04-2013	2,136
	1811501	F	Grayson	Washita/Fredericksburg	33.8017	-96.6775	10-1957	11-2021	317
	1833301	G	Grayson	Paluxy	33.4669	-96.9139	01-1960	01-2024	923
	1803901	H	Grayson	Washita and Paluxy	33.8892	-96.6486	09-1957	12-2023	290
North Texas GCD (figures 3-52, 3-53, 3-54)	1915701	A	Cooke	Glen Rose and Hensell	33.7758	-97.2236	09-1970	10-2017	348
	1923502	B	Cooke	Middle-Lower Trinity	33.6969	-97.1822	08-1942	01-2024	938
	1817401	C	Cooke	Woodbine and Washita	33.6878	-96.9786	09-1970	11-2021	235
	1924702	D	Cooke	Pearsall and Hosston	33.6271	-97.0912	03-1948	02-2020	1,238
	1931302	E	Cooke	Pearsall and Hosston	33.6083	-97.1397	03-1959	01-2024	997
	1931201	F	Cooke	Paluxy	33.5889	-97.2069	09-1970	11-2020	350
	1938301	G	Cooke	Hensell and Pearsall	33.4947	-97.2903	08-1963	10-2017	794
	1922704	H	Cooke	Pearsall and Hosston	33.6439	-97.3639	05-1971	01-2024	660
	1841201	A	Denton	Woodbine	33.3631	-96.9281	09-1970	03-2021	210

North Texas GCD (figures 3-52, 3-53, 3-54)	1964201	B	Denton	Hosston	33.0895	-97.0478	08-1969	10-2012	1,747
	1963601	C	Denton	Paluxy	33.0575	-97.1514	12-1967	04-2021	856
	1963701	D	Denton	Paluxy	33.0078	-97.2369	10-1970	03-2020	626
	1962203	E	Denton	Hosston	33.0872	-97.2983	08-1963	11-2012	1,003
	1954603	F	Denton	Pearsall and Hosston	33.1839	-97.2858	07-1969	02-2024	980
	1947801	G	Denton	Paluxy	33.2551	-97.1994	09-1970	03-2021	615
	1956104	H	Denton	Upper-Middle Trinity	33.2486	-97.1156	05-1957	11-2005	1,200
	1845604	A	Collin	Woodbine	33.2981	-96.4019	02-1975	02-2024	1,900
	1844601	B	Collin	Woodbine and Washita	33.2942	-96.5017	01-1970	02-2024	1,783
	1844702	C	Collin	Woodbine	33.2603	-96.6208	08-1964	11-1997	1,136
	1850501	D	Collin	Hosston	33.1967	-96.8172	09-1953	01-1984	2,694
	1850202	E	Collin	Woodbine	33.2181	-96.8314	07-1969	12-2005	640
	1842604	F	Collin	Hensell and Pearsall	33.3208	-96.7848	08-1967	10-2017	2,300
	1842601	G	Collin	Woodbine	33.3214	-96.7844	03-1928	10-2017	700
Upper Trinity GCD (figures 3-55, 3-56)	1928601	A	Montague	Glen Rose	33.5650	-97.5400	09-1970	06-2024	200
	1928804	B	Montague	Glen Rose	33.5114	-97.5733	09-1970	12-2023	250
	1937901	C	Wise	Paluxy	33.3847	-97.4022	10-1970	06-2024	335
	1961201	D	Wise	Paluxy	33.1036	-97.4386	10-1970	06-2024	360
	1945301	E	Wise	Glen Rose	33.3392	-97.4153	10-1967	11-2024	370
	1943202	F	Wise	Hosston	33.3578	-97.6933	01-1963	12-2016	381
	3210201	A	Parker	Glen Rose	32.8384	-97.8226	06-1971	11-2021	165
	3211702	B	Parker	Glen Rose	32.7825	-97.7429	08-1972	12-2023	220
	3218701	C	Parker	Pearsall	32.6578	-97.8353	02-1971	06-2011	204
	3226601	D	Parker	Hensell	32.5733	-97.7606	03-1950	02-2007	310
	3234609	E	Hood	Hensell	32.4408	-97.7640	07-1968	11-2019	222
	3242403	F	Hood	Hensell	32.3214	-97.8711	06-1971	07-2024	355
Northern Trinity GCD (figure 3-57)	3205302	A	Tarrant	Paluxy	32.9743	-97.3922	03-1972	11-2017	419
	3213601	B	Tarrant	Hosston	32.8017	-97.4117	04-1951	11-2021	967
	3214610	C	Tarrant	Paluxy	32.7953	-97.2547	01-1955	02-1991	425
	3215601	D	Tarrant	Lower Trinity	32.8067	-97.1586	11-1951	03-1982	1,483

	3223101	E	Tarrant	Pearsall and Hosston	32.7250	-97.2145	12-1947	01-2008	1,363
	3231301	F	Tarrant	Woodbine	32.5901	-97.1628	11-1970	08-2023	171
	3222612	G	Tarrant	Lower Trinity	32.6668	-97.2590	07-1962	12-2023	1,352
	3230106	H	Tarrant	Hosston	32.5881	-97.3449	11-1971	11-2021	1,220
Dallas Co (figure 3-58)	3310401	A	Dallas	Hosston	32.8314	-96.8364	07-1953	03-1986	2,689
	3310801	B	Dallas	Hosston	32.7681	-96.8025	05-1953	01-1990	2,797
	3319101	C	Dallas	Hosston	32.7464	-96.7503	05-1954	12-2024	3,076
	3319303	D	Dallas	Paluxy	32.7269	-96.6564	07-1948	04-1983	2,297
	3320401	E	Dallas	Hosston	32.6828	-96.5936	05-1956	03-1984	4,110
	3325401	F	Dallas	Pearsall and Hosston	32.5744	-96.9761	07-1969	11-2023	2,430
	3317801	G	Dallas	Pearsall and Hosston	32.6514	-96.9250	05-1960	01-1988	2,614
	3309701	H	Dallas	Pearsall and Hosston	32.7544	-96.9958	05-1965	06-2010	2,049
Prairielands GCD (figures 3-59, 3-60, 3-61, 3-62)	3236604	A	Johnson	Paluxy	32.4189	-97.5314	10-1966	02-2023	500
	3232701	B	Johnson	Woodbine	32.5247	-97.1147	10-1966	10-2023	240
	3239505	C	Johnson	Woodbine	32.4539	-97.1822	10-1966	10-2023	210
	3238901	D	Johnson	Hosston	32.4069	-97.2617	10-1964	11-2023	1,630
	3239702	E	Johnson	Multi-aquifer	32.4107	-97.2091	05-1947	11-2023	1,656
	3239901	F	Johnson	Woodbine	32.3856	-97.1575	10-1966	10-2023	220
Prairielands GCD (figures 3-59, 3-60, 3-61, 3-62)	3247202	G	Johnson	Washita/Fredericksburg	32.3400	-97.1703	08-1966	10-2023	216
	3246907	H	Johnson	Hosston	32.2842	-97.2733	04-1972	11-2023	1,560
	3326902	A	Ellis	Hosston	32.5317	-96.7819	02-1972	11-2023	3,178
	3350502	B	Ellis	Woodbine	32.2042	-96.7922	06-1965	11-2011	1,238
	3349803	C	Ellis	Hosston	32.1605	-96.9213	05-1968	12-2023	2,700
	3248901	D	Ellis	Woodbine	32.2586	-97.0186	06-1965	10-2023	384
	3248501	E	Ellis	Woodbine and Washita	32.2994	-97.0728	07-1963	10-2023	367
	3341203	F	Ellis	Hosston	32.3567	-96.9512	01-1975	01-2023	2,564
	3240606	G	Ellis	Hosston	32.4216	-97.0238	11-1970	12-2023	2,411
	3333105	H	Ellis	Pearsall and Hosston	32.4860	-96.9979	07-1968	11-2023	2,354
	3243805	A	Somervell	Hosston	32.2556	-97.6933	08-1950	10-2023	464
	3251501	B	Somervell	Glen Rose and Hensell	32.1845	-97.6914	09-1950	07-2006	370

Prairielands GCD (figures 3-59, 3-60, 3-61, 3-62)	3250802	C	Somervell	Glen Rose	32.1567	-97.7947	10-1964	11-2023	321
	3251104	D	Somervell	Hensell	32.2086	-97.7486	05-1965	10-2023	376
	3250304	E	Somervell	Hosston	32.2335	-97.7523	09-1960	11-2022	352
	3255304	A	Hill	Woodbine and Washita	32.2303	-97.1514	07-1964	01-1997	273
	3255904	B	Hill	Pearsall and Hosston	32.1622	-97.1406	06-1956	11-1995	1,856
	3909201	C	Hill	Hosston	31.8592	-96.9272	05-1960	11-2023	3,138
	4015102	D	Hill	Hosston	31.8537	-97.2180	01-1960	12-2024	1,485
	4014602	E	Hill	Glen Rose and Hensell	31.8180	-97.2778	03-1966	12-2024	1,102
	4006104	F	Hill	Hosston	31.9714	-97.3719	07-1958	02-1994	1,166
	3262302	G	Hill	Hensell and Pearsall	32.1058	-97.2700	01-1964	10-2023	1,213
	3253902	H	Hill	Hensell and Pearsall	32.1392	-97.3942	09-1964	11-2000	934
Southern Trinity GCD (figure 3-63)	4016404	A	McLennan	Hosston	31.8208	-97.0889	04-1969	10-2017	1,982
	4022804	B	McLennan	Hensell and Pearsall	31.6508	-97.3006	07-1962	04-1988	1,150
	4023903	C	McLennan	Hosston	31.6522	-97.1444	09-1958	10-2021	2,114
	4024803	D	McLennan	Pearsall and Hosston	31.6467	-97.0661	02-1953	01-2014	2,494
	3917701	E	McLennan	Hosston	31.6586	-96.9719	04-1959	10-2024	3,129
	4032103	F	McLennan	Hosston	31.5961	-97.0956	05-1957	12-2015	2,396
	4031802	G	McLennan	Hosston	31.5042	-97.1856	08-1947	04-2008	2,040
	4037501	H	McLennan	Glen Rose and Hensell	31.4350	-97.4194	04-1965	12-2015	1,050
Middle Trinity GCD (figures 3-64, 3-65, 3-66)	4002109	A	Bosque	Hensell	31.9961	-97.8358	03-1967	04-2022	364
	4003901	B	Bosque	Hensell and Pearsall	31.9108	-97.6622	07-1962	01-2006	570
	4019101	C	Bosque	Hensell and Pearsall	31.7292	-97.7369	11-1968	04-2013	540
	4011602	D	Bosque	Hensell	31.8194	-97.6333	08-1966	04-2024	631
	4020301	E	Bosque	Glen Rose	31.7219	-97.5211	05-1960	12-2011	650
	4005903	F	Bosque	Multi-aquifer	31.8883	-97.3989	02-1958	04-2024	1,135
	4014702	G	Bosque	Glen Rose	31.7681	-97.3461	04-1960	12-2001	1,010
	3260602	H	Bosque	Pearsall	32.0711	-97.5022	02-1943	03-1984	760
	4035103	A	Coryell	Lower Trinity	31.4756	-97.7353	07-1952	03-1984	771
	4035404	B	Coryell	Hosston	31.4322	-97.7308	07-1955	12-2024	755
	4036601	C	Coryell	Multi-aquifer	31.4200	-97.5067	04-1956	07-2024	1,170

Middle Trinity GCD (figures 3-64, 3-65, 3-66)	4035804	D	Coryell	Middle-Lower Trinity	31.3925	-97.6903	01-1943	04-1987	745
	4041903	E	Coryell	Glen Rose	31.2778	-97.8889	10-1968	07-2024	271
	4041202	F	Coryell	Hensell	31.3739	-97.9292	03-1970	07-2024	420
	4140903	G	Coryell	Hensell	31.3872	-98.0186	01-1969	07-2024	440
	4140803	H	Coryell	Hensell	31.4022	-98.0817	04-1966	01-2005	372
	3155301	A	Erath	Multi-aquifer	32.2470	-98.1583	12-1959	02-1995	520
	3249501	B	Erath	Lower Trinity	32.2008	-97.9425	10-1965	05-2024	512
	3162901	C	Erath	Hensell and Pearsall	32.0261	-98.2650	08-1972	05-2023	333
	3162803	D	Erath	Hensell	32.0083	-98.3267	10-1965	01-2023	265
	4106501	E	Commanche	Hensell and Pearsall	31.9467	-98.3117	10-1959	06-2024	250
	4114102	F	Commanche	Hosston	31.8397	-98.3678	10-1959	06-2024	179
	4112902	G	Commanche	Hensell and Pearsall	31.7900	-98.5311	03-1970	06-2024	112
Mills and Hamilton Co (figure 3-67)	4124301	A	Hamilton	Glen Rose	31.7264	-98.0209	04-1967	10-2016	177
	4017702	B	Hamilton	Glen Rose and Hensell	31.6403	-97.9822	09-1964	01-1999	327
	4124801	C	Hamilton	Glen Rose and Hensell	31.6475	-98.0581	05-1966	10-2024	432
	4123401	D	Hamilton	Hensell	31.6850	-98.2383	08-1961	01-1997	362
	4138101	E	Mills	Hensell and Pearsall	31.4831	-98.3567	06-1955	12-2003	325
	4137303	F	Mills	Glen Rose	31.4703	-98.4087	04-1966	10-2024	213
Falls Co (figure 3-68)	4048201	A	Falls	Pearsall and Hosston	31.3703	-97.0806	06-1957	10-2012	2,640
	4048801	B	Falls	Pearsall	31.2878	-97.0625	03-1966	10-2023	2,874
	4047602	C	Falls	Hosston	31.3019	-97.1403	08-1965	10-2012	2,609
	4056102	D	Falls	Hosston	31.2110	-97.1206	02-1968	10-2022	2,765
	4064101	E	Falls	Hosston	31.1199	-97.1150	05-1959	10-2024	3,060
Clearwater UWCD (figure 3-69)	4053406	A	Bell	Hosston	31.1967	-97.4594	01-1967	06-2024	1,192
	4063501	B	Bell	Hosston	31.0511	-97.1942	10-1965	06-2024	3,200
	4061509	C	Bell	Hosston	31.0798	-97.4364	03-1952	12-2024	1,261
	5806102	D	Bell	Hosston	30.9864	-97.3633	07-1955	12-2023	2,210
	5805403	E	Bell	Hensell	30.9328	-97.4717	03-1966	10-2023	1,630
	5804103	F	Bell	Glen Rose	30.9822	-97.6033	07-1960	10-2023	767
	5803901	G	Bell	Hensell	30.8997	-97.6336	06-1951	03-1984	857

Burnet and Williamson Co (figure 3-70)	5810303	A	Williamson	Hensell and Pearsall	30.8414	-97.7917	08-1966	10-2016	728
	5829603	B	Williamson	Pearsall and Hosston	30.5790	-97.4108	08-1946	12-2024	3,335
	5817902	C	Williamson	Hosston	30.6661	-97.8928	10-1967	10-2024	740
	5724501	D	Burnet	Hosston	30.6875	-98.0672	04-1967	02-2009	460
	5724101	E	Burnet	Middle-Lower Trinity	30.7479	-98.0859	01-1958	12-2024	480
	5715601	F	Burnet	Pearsall	30.7950	-98.1431	12-1968	02-2012	205
	5715502	G	Burnet	Pearsall and Hosston	30.8131	-98.1933	10-1968	02-2011	205

[1]The "Washita" listed here is a shortened form of "Washita/Fredericksburg". Note that the "Lower Trinity" designation is synonymous with the Twin Mountains and Travis Peak Formations.

[2]Well end dates are current as of December 2024.

[3]The hydrogeologic unit assigned to each well is based on the well's screened interval (reported or estimated); therefore, the well depth is listed to provide general information on well construction.

3.5.3.4.2 Transmissivity Estimates

Figures 3-71 to 3-73 show the residual distribution of transmissivity from the model history matching. Residuals pertaining to the Clearwater UWCD group (Figure 3-71 EF) showed a reasonable 1:1 agreement, indicating a balanced distribution between high and low transmissivity estimates captured by NTGAM within a relatively small area in Bell County. Difficulties in obtaining an accurate match within other transmissivity groups were primarily attributed to extreme localized variability in prior estimates, which cannot be well captured at a regional scale, especially if aquifer hydraulic tests do have associated well screen information that could be used for aquifer assignments of estimated values (e.g., Central Texas Groundwater Conservation District [CTGCD] group). Overall, the combined transmissivity residuals showed a normal Gaussian distribution of residuals (Figure 3-71AB), indicating an unbiased model representation of transmissivity estimates.

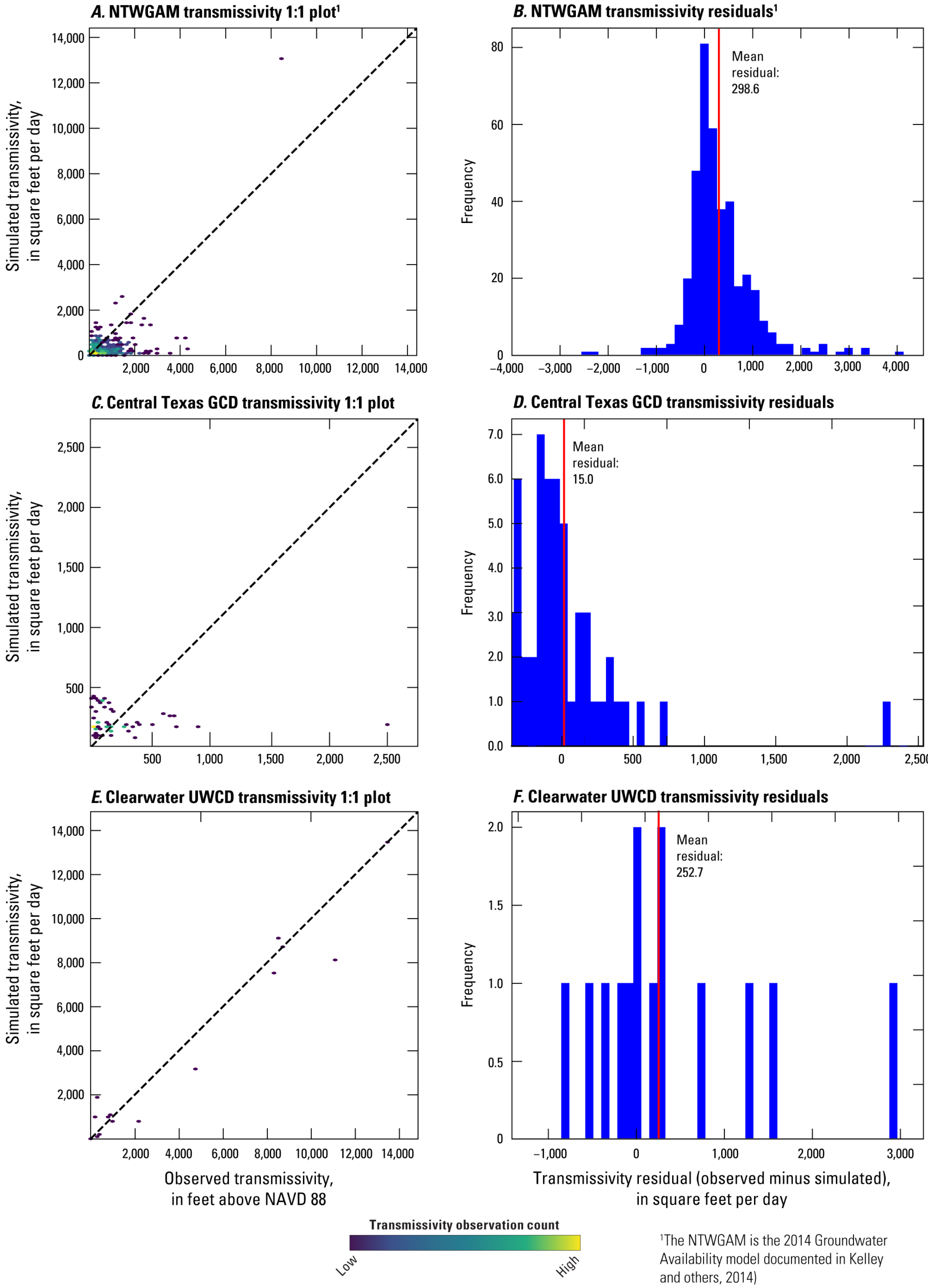

Figure 3-71. Observed and simulated transmissivity and transmissivity residual distributions for all aquifer units, for Central Texas GCD, and Clearwater UWCD.

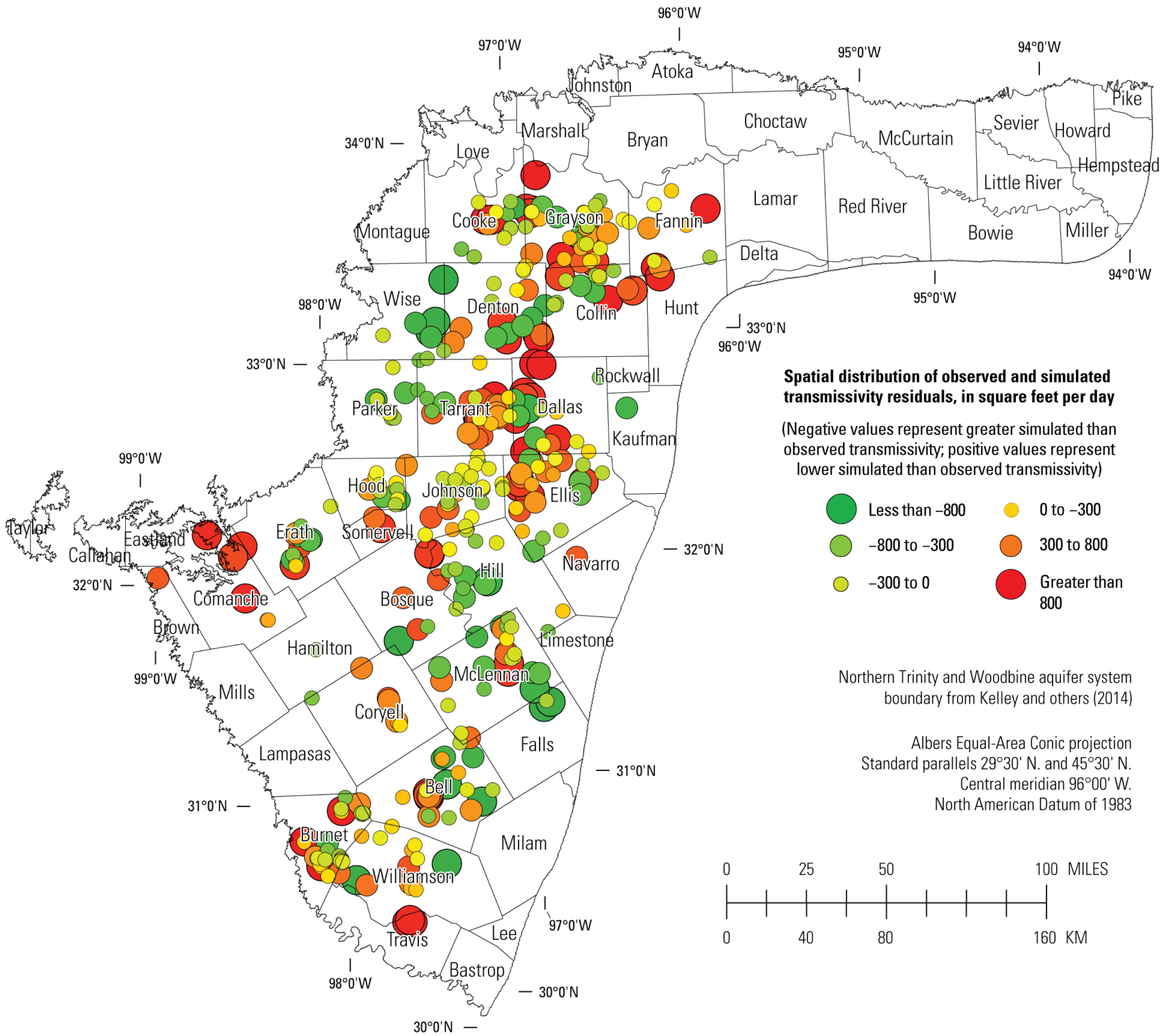

Figure 3-72. Spatial distribution of observed and simulated transmissivity for all model layers.

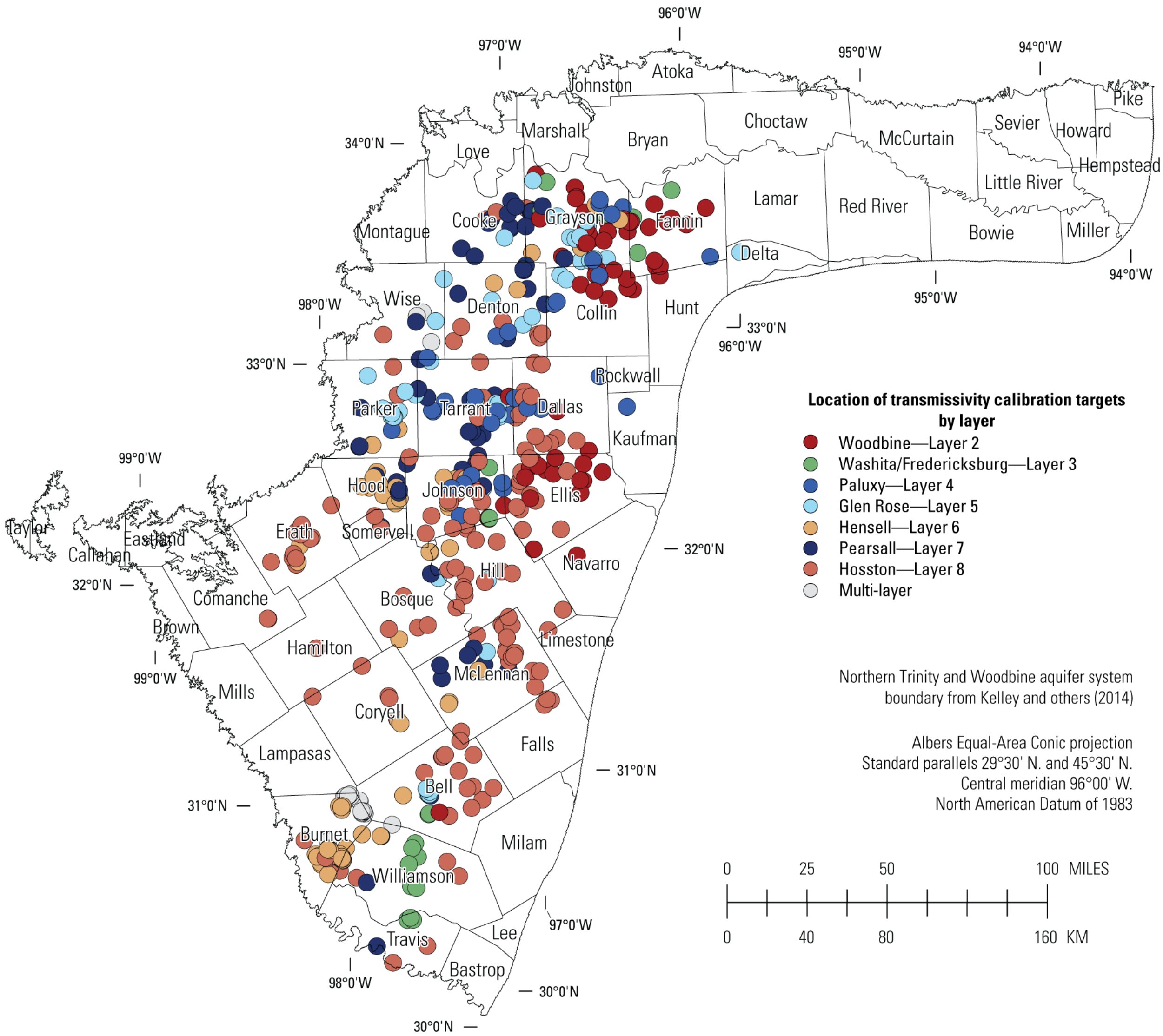

Figure 3-73. Location of transmissivity history matching targets by layer.

3.5.3.4.3 Stream Baseflow Targets

Almost all baseflow residuals shown in Figure 3-74 are distributed near the 1:1 line, suggesting a reasonable representation of time-averaged stream baseflow at the model scale. Figure 3-74B indicates a mean flux residual of -4,067 acre-ft per year, representing a general tendency for undersimulating groundwater flux contributions to perennial stream flows and riparian ET. However, as shown in Figure 3-75, over 50% of simulated fluxes at USGS stream-gage stations matched the measured orders of magnitude. Given that baseflow targets were the outcome of stream separation analysis (Kelley and others, 2014) and highly subject to model and measurement uncertainty, the NTGAM-simulated baseflows provide a reasonable order-of-magnitude representation of observed fluxes. Although more precise flux matching may have been attained through complex, spatially, and temporally correlated parameterization schemes of river stages, such effort would not guarantee a more robust representation of actual conditions at the regional model scale.

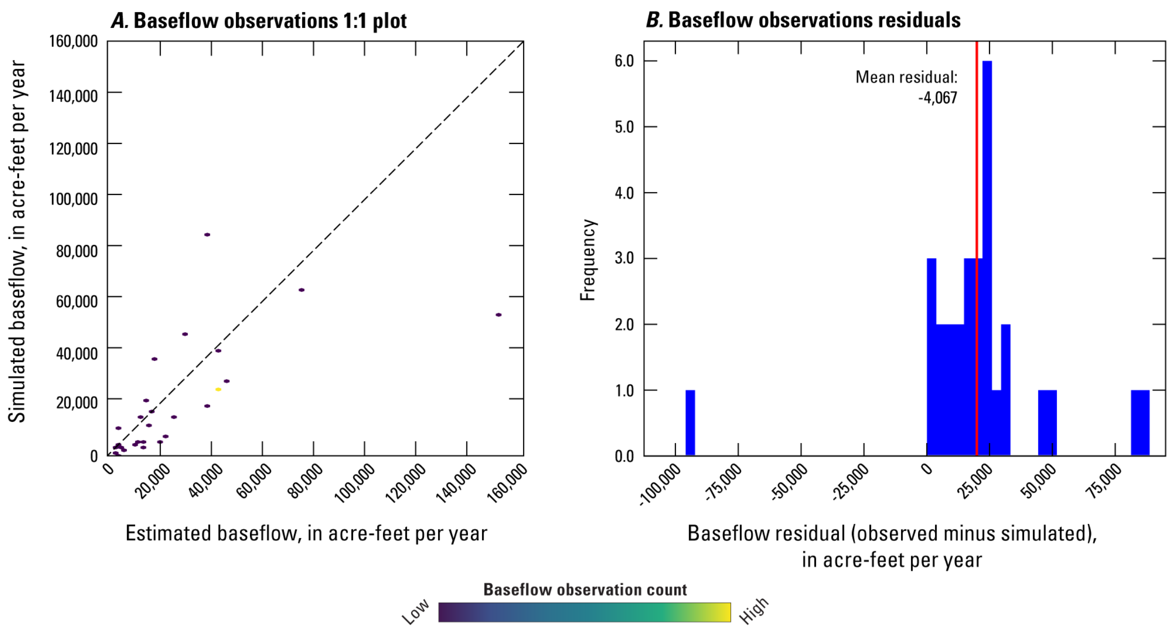

Figure 3-74. Observed and simulated stream base flow and base flow residual distributions.

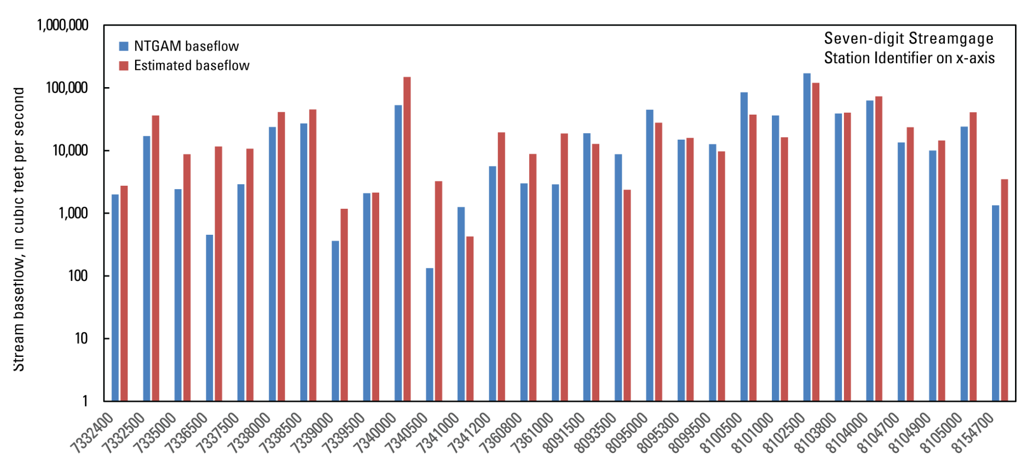

Figure 3-75. Observed and simulated stream base flow.

3.5.4 Water Budget

Summaries of the water budget for the steady-state model (1889) in terms of volume and percent of total inflow are presented in Tables 3-8 and 3-9, respectively. The overall percent discrepancy of the water balance for the steady-state model is 0 in the GWF model listing file, satisfying the GAM requirement of 1 percent. Recharge is the only boundary condition exhibiting net inflow to the model, with a total of 8,913 acre-ft per day. Water discharges the Northern Trinity and Woodbine aquifers through ephemeral streams (64.6 percent of net inflow), perennial streams (33.2 percent of net inflow), riparian ET (1.7 percent of net inflow), springs (0.1 of net inflow), and net upward cross-formational flow to the overlying younger formations (0.4 percent of net inflow).

Table 3-8. Water budget for the steady-state model (all rates reported in AFY).

Pre-Development	Cross-formational Flow			Recharge	Ephemeral Streams	Perennial Streams	Riparian Evapotranspiration	Springs	Younger
Formation	Surficial	Top	Bottom						
Younger Formations	0	0	8,475	3,953	0	39	0	0	-13,371
Woodbine Aquifer	1,832	-8,475	6,643	349,696	-229,035	-89,798	-14,071	-65	0
Wash/Fred Groups	2,049	-6,643	4,595	963,566	-578,331	-362,330	-8,236	-624	0
Paluxy Aquifer	2,337	-4,595	2,258	293,286	-162,558	-120,707	-5,049	-77	0
Glen Rose Formation	2,914	-2,258	-653	672,525	-348,091	-300,897	-8,373	-269	0
Hensell Aquifer	19,132	653	-19,784	377,500	-253,591	-93,204	-10,939	-152	0
Pearsall Formation	1,354	19,784	-21,137	109,000	-99,025	-31,751	-3,363	0	0
Hosston Aquifer	-21,101	21,137	0	483,126	-434,323	-77,903	-5,804	-710	0
Total	**8,517**	**19,603**	**-19,603**	**3,252,652**	**-2,104,954**	**-1,076,551**	**-55,835**	**-1,897**	**-13,371**

Table 3-9. Water budget for the steady-state model with values expressed as a percentage of total inflow

Pre-Development	Cross-formational Flow			Recharge	Ephemeral Streams	Perennial Streams	Riparian Evapotranspiration	Springs	Younger
Formation	Surficial	Top	Bottom						
Younger Formations	0.0%	0.0%	0.3%	0.1%	0.0%	0.0%	0.0%	0.0%	-0.4%
Woodbine Aquifer	0.1%	-0.3%	0.2%	10.8%	-7.0%	-2.8%	-0.4%	0.0%	0.0%
Wash/Fred Groups	0.1%	-0.2%	0.1%	29.6%	-17.8%	-11.1%	-0.3%	0.0%	0.0%
Paluxy Aquifer	0.1%	-0.1%	0.1%	9.0%	-5.0%	-3.7%	-0.2%	0.0%	0.0%
Glen Rose Formation	0.1%	-0.1%	0.0%	20.7%	-10.7%	-9.3%	-0.3%	0.0%	0.0%
Hensell Aquifer	0.6%	0.0%	-0.6%	11.6%	-7.8%	-2.9%	-0.3%	0.0%	0.0%
Pearsall Formation	0.0%	0.6%	-0.6%	3.4%	-3.0%	-1.0%	-0.1%	0.0%	0.0%
Hosston Aquifer	-0.6%	0.6%	0.0%	14.9%	-13.4%	-2.4%	-0.2%	0.0%	0.0%
Total	**0.3%**	**0.6%**	**-0.6%**	**100.0%**	**-64.7%**	**-33.1%**	**-1.7%**	**-0.1%**	**-0.4%**

A summary of the water budget averaged over the transient simulation period (1890-2020) is presented in Table 3-10 and Figure 3-76, including mean annual inflows, outflows, and the net change in storage. Recharge to the outcrop area was the largest inflow (88 percent), followed by diffuse recharge from the younger formations (12 percent), with minimal leakage inflows from reservoirs and perennial streams (less than 1 percent combined). Simulated outflows include leakage towards ephemeral streams (55 percent) and perennial streams (39 percent), groundwater production (3.4 percent), diffuse discharge to younger formations (<1 percent), and discharge to flowing wells, springs, and reservoirs (combining less than 1 percent). The sum of simulated outflows (3,585,354 AFY) minus the sum of inflows (3,581,805 AFY) and the numerical solver error (45 AFY) represents the average change in storage in the Northern Trinity and Woodbine aquifer system (3,504 AFY).

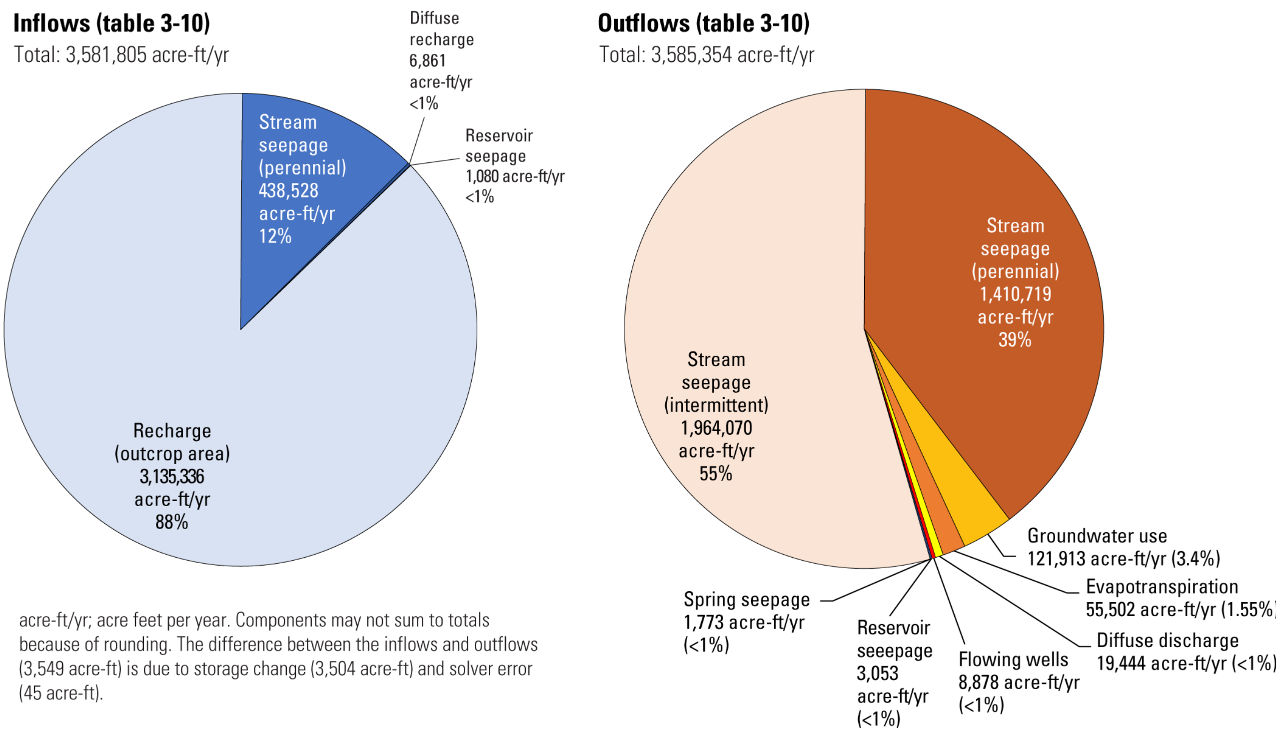

Figure 3-76. Mean annual water budget for the northern Trinity and Woodbine groundwater model.

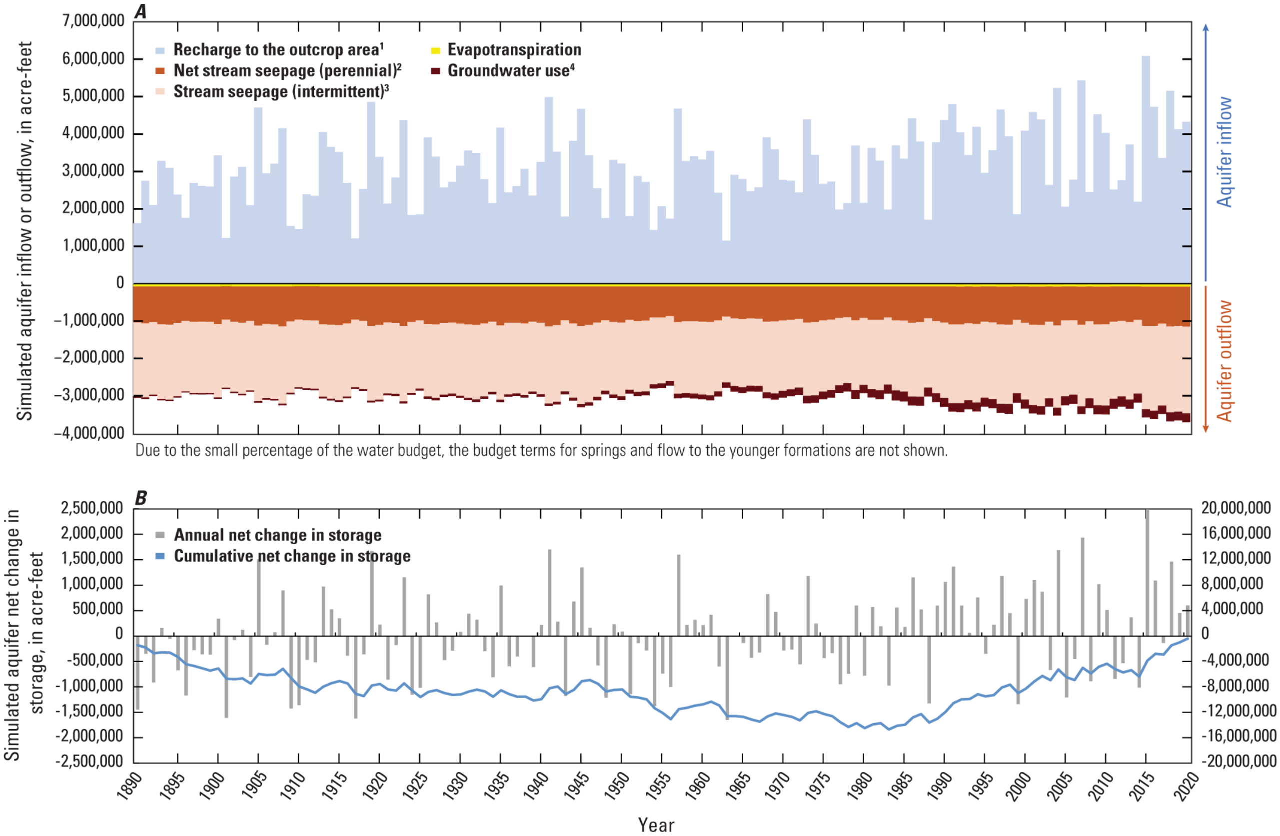

[1]Includes recharge to the shallow groundwater system, most of which does not infiltrate to underlying layers. Recharge from layer 1 to the underlying layers is shown on figure 3-37.
[2]Perennial rivers are simulated using the River Package. Note that the reservoir and younger formations also use the River Package and are identified in the MODFLOW name file
[3]Intermittent (and ephemerial) streams are simulated using the Drain Package. Note that evapotranspiration, flowing wells, and springs also use the Drain Package.
[4]Flowing wells are included in this budget term.

Figure 3-77. Simulated annual inflows and outflows for the northern Trinity and Woodbine groundwater model.

Table 3-10. Mean-annual water budget for the northern Trinity and Woodbine Aquifer groundwater model.

Water-budget category	Amount (in acre feet per year)	Percentage of the water budget
Inflow		
Recharge to the outcrop area[1]	3,135,336	88%
Stream seepage (perennial)[2]	438,528	12%
Diffuse recharge (Younger formations)	6,861	<1%
Reservoir seepage[3]	1,080	<1%
Total inflow	**3,581,805**	**100%**
Outflow		
Stream seepage (intermittent)[3]	1,964,070	55%
Stream seepage (perennial)[2]	1,410,719	39%
Groundwater use	121,913	3.40%
Evapotranspiration[3]	55,502	1.55%
Diffuse discharge	19,444	<1%
Flowing wells[3]	8,878	<1%
Reservoir seepage[2]	3,053	<1%
Spring seepage[3]	1,773	<1%
Total outflow	**3,585,354**	**100%**
Net change in storage		
Water derived from specific yield under unconfined conditions	2552	
Water derived from confined conditions	952	
Total storage change[4]	**3,504**	

[1]Includes recharge to the shallow groundwater system, most of which does not infiltrate to underlying layers. Recharge from layer 1 to the underlying layers is shown on Figure 3-37.

[2]Perennial streams and reservoirs are simulated using the River package

[3]Intermittent streams, evapotranspiration, flowing wells, and springs are simulated using the Drain package

[4]The difference between the outflows and the sum of the inflows and change in storage (-45 acre-ft/yr) corresponds to solver error.

Figure 3-77 shows the temporal variability of water budget components across NTGAM. Recharge exhibited the greatest variability throughout the simulation period, supporting relatively higher inflows during the last two decades. In contrast, groundwater production steadily increased approximately through the year 1980, with relatively steady outflows throughout the rest of the timeline. In general, both perennial and intermittent stream outflows remained consistent throughout the simulation timeline, suggesting that groundwater use was the primary mechanism driving a small fraction of recharge towards confined layers, despite groundwater use representing only 3.4 percent of the model outflows in the transient water budget on average. This also explains the model-wide stabilization of cumulative net change in storage around the year 1980 (Figure 3-77B) and the subsequent increase in the cumulative net change in storage through the year 2020. These results suggest that groundwater production rates of the last two decades support approximate storage equilibrium conditions within the northern Trinity aquifer system, which in turn are likely able to support surface water flows in the outcrop area.

Tables 3-11 through 3-13 summarize the water budget for the transient model in terms of net flow into or out of each of the aquifers/formations in the model for the years 1980, 2000, and 2020. Negative numbers indicate flow out of the aquifers/formations, while positive numbers indicate flow into the aquifers/formations. The first three columns detail cross-formational flow in each of the units. The surficial flow term represents flow across units within the surficial outcrop area of Layer 1, while the confined cross-formational flow is marked by the “Top” and “Bottom” fields, representing vertical flow across aquifers/formations deeper than Layer 1. “Top” indicates flow in or out of the top of aquifers/formations in the confined portion, while “Bottom” indicates flow in or out of the bottom of aquifers/formations that lie below the surficial layer. The water budgets in 2000 and 2020 by county and GCD are summarized in the appendix in the same way as Table 3-11.

Table 3-11. Water budget for the transient model in 1980.

1980	Cross-formational Flow			Recharge	Ephemeral Streams	Perennial Streams	Riparian	Springs	Flowing Wells	Reservoir	Younger	Wells	Storage
Unit	Surficial	Top	Bottom										
Younger Formations	0	0	304	3,963	0	38	0	0	0	0	-12,284	-3,625	10,965
Woodbine Aquifer	12,570	-304	-2,731	208,981	-188,552	-69,444	-13,611	-51	-739	-795	0	-17,729	97,023
Wash/Fred Groups	21,807	2,731	-14,291	622,471	-499,753	-288,611	-8,633	-540	-27	-1,559	0	-19,252	223,881
Paluxy Aquifer	22,386	14,291	-16,711	174,843	-139,442	-89,427	-4,877	-71	-150	449	0	-33,046	87,978
Glen Rose Formation	21,348	16,711	-32,328	490,083	-301,856	-264,341	-7,971	-238	-29	142	0	-19,831	132,527
Hensell Aquifer	51,236	32,328	-61,421	250,730	-212,843	-62,618	-10,603	-137	-395	78	0	-17,571	85,519
Pearsall Formation	17,374	61,421	-73,750	73,279	-83,381	-24,832	-3,201	0	0	-35	0	-14,135	34,016
Hosston Aquifer	1,548	73,750	0	336,420	-374,995	-58,141	-5,345	-658	-185	-147	0	-83,312	97,889
Total	**148,269**	**200,928**	**-200,928**	**2,160,770**	**-1,800,822**	**-857,376**	**-54,241**	**-1,695**	**-1,525**	**-1,867**	**-12,284**	**-208,501**	**769,798**

Table 3-12. Water budget for the transient model in 2000.

2000	Cross-formational Flow			Recharge	Ephemeral Streams	Perennial Streams	Riparian	Springs	Flowing Wells	Reservoir	Younger	Wells	Storage
Unit	Surficial	Top	Bottom										
Younger Formations	0	0	-1,947	3,963	0	38	0	0	0	0	-11,800	-1,816	10,950
Woodbine Aquifer	15,910	1,947	-3,705	424,297	-226,875	-88,122	-14,105	-58	-759	-2,009	0	-22,675	-55,226
Wash/Fred Groups	34,472	3,705	-17,780	1,248,242	-586,463	-322,323	-9,411	-590	0	-3,122	0	-35,768	-263,168
Paluxy Aquifer	25,803	17,780	-19,297	352,002	-162,769	-106,582	-5,191	-75	-210	366	0	-32,508	-49,774
Glen Rose Formation	21,223	19,297	-31,713	887,607	-343,546	-298,383	-8,601	-262	0	114	0	-20,836	-191,068
Hensell Aquifer	54,584	31,713	-68,963	457,793	-237,868	-75,875	-11,469	-152	-492	46	0	-18,893	-74,081
Pearsall Formation	19,262	68,963	-74,176	134,991	-92,058	-28,494	-3,380	0	0	-29	0	-16,965	-22,102
Hosston Aquifer	7,269	74,176	0	579,585	-412,293	-68,565	-5,614	-684	-77	-100	0	-87,432	-91,517

2000	Cross-formational Flow			Recharge	Ephemeral Streams	Perennial Streams	Riparian	Springs	Flowing Wells	Reservoir	Younger	Wells	Storage
Unit	Surficial	Top	Bottom										
Total	**178,523**	**217,581**	**-217,581**	**4,088,480**	**-2,061,872**	**-988,306**	**-57,771**	**-1,821**	**-1,538**	**-4,734**	**-11,800**	**-236,893**	**-735,986**

Table 3-13. Water budget for the transient model in 2020.

2020	Cross-formational Flow			Recharge	Ephemeral Streams	Perennial Streams	Riparian	Springs	Flowin g Wells	Reservoir	Younger	Wells	Storage
Unit	Surficial	Top	Bottom										
Younger Formations	0	0	-3,695	3,963	0	38	0	0	0	0	-11,311	-8,246	18,680
Woodbine Aquifer	15,483	3,695	-5,401	492,374	-257,747	-99,145	-14,428	-66	-771	-2,043	0	-23,870	-78,134
Wash/Fred Groups	33,191	5,401	-18,920	1,280,252	-662,519	-348,014	-10,037	-631	0	-3,659	0	-35,776	-193,125
Paluxy Aquifer	25,250	18,920	-22,878	427,922	-186,081	-121,685	-5,513	-80	-247	231	0	-16,011	-90,367
Glen Rose Formation	21,983	22,878	-38,230	814,455	-380,728	-318,518	-9,086	-280	0	31	0	-19,768	-58,042
Hensell Aquifer	56,744	38,230	-78,938	505,731	-272,693	-85,509	-12,109	-152	-287	-40	0	-19,201	-74,009
Pearsall Formation	20,147	78,938	-79,806	144,823	-101,558	-32,183	-3,549	0	0	-39	0	-24,446	-17,093
Hosston Aquifer	1525	79,806	0	655,561	-464,743	-80,620	-5,971	-718	-22	-122	0	-84,589	-108,419
Total	**174,323**	**247,868**	**-247,868**	**4,325,081**	**-2,326,069**	**-1,085,636**	**-60,693**	**-1,927**	**-1,327**	**-5,641**	**-11,311**	**-231,907**	**-600,509**

4.0 Model Uses, Limitation, and Assumptions

Every groundwater model, including numerical models, is a simplified representation of a real, more complex GWF system (Anderson and Woessner, 1992; Domenico, 1972). As such, many assumptions are required in model development. These assumptions result in model limitations, which should be carefully considered when evaluating the results of modeling studies. Model limitations include an overall understanding of the aquifer system, the quality and quantity of supporting data, and assumptions used to construct the model. Additional details regarding the limitations of this model are discussed in the following subsections.

By maintaining the underlying conceptual model of the Northern Trinity and Woodbine Aquifer system, updating NTGAM properties on the basis of previously unavailable data improves the reliability of its role as a regional groundwater planning tool within GMA 8. Unlike in previous model versions, history-matching of historical observations using hundreds of "calibrated" models provides the GCDs within GMA 8 with an opportunity to perform groundwater management analyses considering a probabilistic framework. Examples of such usage include quantifying the uncertainty variance of drawdown induced by groundwater production scenarios driven by the parameter uncertainty encapsulated in the history-matched (posterior) ensemble. The ensemble approach also provides an order-of-magnitude approximation of plausible variability in water sources and sinks represented by various boundary conditions in NTGAM. The representation of different hydrological processes in NTGAM remains the same as in the previous NTGWAM model despite the conversion to MODFLOW 6. Thus, the structural uncertainty inherent to the choice of model packages for representing complex hydrologic mechanisms, such as diffuse groundwater exchange between the Woodbine Aquifer and Younger Formations, remains the same as in NTWGAM.

An important limitation to matching complex groundwater level trends lies in data gaps, particularly regarding the spatiotemporal distribution of historical groundwater production rates. Sources of pumping uncertainty include a lack of completion information on wells intersecting multiple model layers and the grouping of extraction rate estimates within individual grid cells. The assignment of monitoring wells to model grid cells can also be problematic in cases where no detailed information exists on the completion of wells that span multiple model layers. The ensemble approach for history matching undertaken in this work acknowledges such uncertainties through the generation of ensemble realizations of model parameters and observations, minimizing potential bias arising from a single calibrated model. The observation weighting strategy and incorporation of data noise were applied in this effort, including groundwater level observations and aquifer hydraulic tests were designed to minimize bias in aquifer hydraulic parameters derived from highly uncertain data.

Additional uncertainties exist for input data used to estimate recharge for using the SWB code. Soil and land-cover properties, such as available water capacity and root-zone depth, influence model results but are not precisely known at the model scale. This includes the spatiotemporal distribution of climate stations and associated data, which was interpolated to estimate recharge. Likewise, the SWB code may not provide accurate estimates of recharge where the water table is near the land surface, potentially driving recharge overestimation in some areas. However, the SWB-constructed recharge applied in this work provides a more rigorous approach than the previous, smoothed recharge model developed for the NTWGAM. Here, uncertainty in the SWB model was incorporated into the NTGAM history matching process, although with a lesser degree of variability in comparison to aquifer hydraulic properties.

Previous assumptions regarding model construction and history matching of the NTWGAM (Kelley and others, 2014) remain in the NTGAM. Usage of the Well Package in MODFLOW 6 was not modified with respect to MODFLOW-NWT. Because of the computationally intensive history-matching process resulting from the NTGAM grid resolution, neither a dynamic apportioning of groundwater production rates on the basis of hydraulic transmissivity nor the usage of the more sophisticated multi-aquifer well (MAW) package was considered. This resulted in a non-uniform vertical distribution of extraction rates that were constrained by history matching but not necessarily by aquifer hydraulic properties. However, given that the latter is uncertain in any case, the final vertical distribution of pumping rates is likely reasonable given the input data quality and overall capturing of historical groundwater level trends in the history-matched model. Similar remaining model simplifications include the usage of the drain package to represent flowing wells and the river package to represent the hydraulic interaction between the Woodbine Aquifer and the overlying Younger Formations. The diffuse groundwater interactions with the Younger Formations encompass the previous conceptual understanding of a large model area that has not been thoroughly characterized (Kelly and others, 2014).

Although the spatial distribution of groundwater-level observations was reasonable, fewer observations were available for the northeastern area of the model—particularly in Red River, McCurtain, Sevier, Little River, Bowie, Pike, Howard, Hempstead, and Miller Counties; therefore, more uncertainty exists in the northeastern parts of the modeled area than in the central part where more observations are available. Additionally, layer 1 did not contain any groundwater-level observations and was not history-matched. Although the simulated water table in the northeastern area of the model was in an expected range, more site-specific and local history-matching target data would facilitate an improved characterization of GWF in this area.

A simplified approach to the simulation of surface-water/groundwater exchange through the use of the River and Drain packages is an important simplification in NTGAM. Although temporally averaged stream baseflow observations were part of the history-matching process, maintaining constant River and Drain stages was a limiting factor in simulating baseflow at some stream gage locations. Furthermore, NTGAM does not simulate surface-water diversions, connections with simulated lakes and reservoirs, and overland runoff, which may be better represented by the Streamflow-Routing package constrained by appropriate data. Thus, simulated surface water-groundwater interactions at streams, reservoirs, and springs provide order-of-magnitude flux estimates of actual conditions, warranting caution in the usage of NTGAM for surface water availability calculations.

As in the NTWGAM, the primary function of layer 1 in the NTGAM is to distribute recharged water within the outcrop zone of the model layers. The greater magnitude in the SWB-derived, history-matched recharge fluxes in certain years resulted in increased discharge to stream flows, with a relatively small fraction of recharge water entering the deeper aquifer system. Therefore, care should be taken when adding simulated groundwater production to simulated storage in layer 1. This is because much of the water captured by production wells in layer 1 may correspond to groundwater movement from recharge sources towards surface water sinks, primarily intermittent streams present throughout the entire outcrop zone, or diffuse discharge throughout the Younger Formations represented by a River boundary condition. While the simulation of groundwater extraction in layer 1 is consistent with well-completion details, caution is advised when using layer 1 to estimate groundwater availability.

5.0 Summary

This report describes an update to the Northern Trinity and Woodbine GAM, which includes a variety of recent hydrogeological datasets and state-of-the-art modeling techniques for improved decision support capabilities. The previous MODFLOW-NWT version of NTWGAM was converted to MODFLOW 6, increasing the computational efficiency and numerical accuracy supported by the iterative model solution (IMS) package and vertical passthrough grid cells. Applying passthrough cells allowed for a direct flow connectivity between the confined aquifer system and the shallow outcrop areas, providing a better representation of the aquifer system conceptualization, which was preserved from NTWGAM. Using MODFLOW 6 also allowed for the creation of different hydrologic stress packages representing various water sources and sinks simulated with the same numerical package. For example, the river package was split into three packages representing different features, namely perennial streams, reservoirs, and riparian ET, facilitating the history-matching and stochastic data assimilation process used to update the NTGAM hydrologic properties.

Although the previous hydrogeological understanding of the Northern Trinity aquifer system was not modified, the thickness of model layers was updated per newly acquired data. Specifically, a number of geophysical borehole logs were used to modify the model grid in areas that were previously unconstrained by geological information. Important updates to aquifer properties, such as hydraulic transmissivity and storativity, were primarily guided by stochastic assimilation of historical groundwater-level measurements, including data collected between 2012 and 2020. This time interval corresponds to the extended simulation period with respect to NTWGAM. Likewise, hydraulic transmissivity was modified via history-matching to prior estimates derived from aquifer hydraulic tests, including values that had been previously used by Kelly and others (2014) to define the initial NTWGAM conceptual model and more recent test data provided by GCDs.

Another important modification was the implementation of the SWB model constrained by hydro-climatic data. Implementing a detailed SWB recharge model did not significantly modify the fraction of precipitation water entering the deep groundwater system but generally increased surficial water outflows in the outcrop area. Despite these modifications, the overall water balance of the aquifer system remained consistent with the previous NTGWAM, including cross-formational GWFs with a primarily downward direction across the confined system. Estimates of groundwater production rates prior to the year 1980 were preserved from NTWGAM, while post-1980 rates and locations were updated by detailed production data. Specifically, post-1980 rural domestic use was updated on the basis of population census data, while post-1980 metered/estimated use provided by GCDs was incorporated as provided. Additional post-1980 groundwater use exceeding GCD rates was also incorporated in NTGAM from the TWDB database.

On average, groundwater production updates did not result in a significant modification with respect to NTWGAM. Yet localized, recent changes occurred at the GCD and county scales. Furthermore, all estimates of groundwater production were minimally adjusted by the history-matching process, resulting in a groundwater-level data mismatch at a few monitoring locations with respect to simulated levels. This outcome reflects numerical modeling challenges in capturing the intricacies of spatiotemporal groundwater trends at a regional level with grid-scale averaging of uncertain groundwater use estimates despite the quarter-mile resolution of NTGAM and favorable model history matching statistics meeting GAM standards. In turn, localized mismatches of groundwater level trends do not preclude the regional-scale decision support capabilities of NTGAM, which are supported by a water balance consistent with the conceptual understanding of the regional system and previous NTWGAM results, while including a hydraulic property distribution much closer to aquifer test data. Although these are critical improvements for estimating regional groundwater availability, highly detailed calculations of groundwater drawdown should be performed with analytical or numerical inset models leveraging NTGAM properties and simulated system states.

Similar to NTWGAM, groundwater use was shown to be the primary driver of the temporal variability in aquifer storage despite representing only about 3.5 percent of the simulated groundwater outflows on average. The updated, post-1980 groundwater use estimates and SWB-simulated recharge induced aquifer storage recovery throughout the last two decades, supporting surface water outflows towards perennial and intermittent streams across the outcrop region. Furthermore, the net GWF analysis suggested that the aquifer system was fully saturated under predevelopment conditions, with a fraction of recharge water being diverted back towards some shallow areas of the outcrop region during the first half of the last century. This result is consistent with previous NTWGAM findings, indicating a change in system dynamics driven by the development of the aquifers as a groundwater resource. Likewise, NTGAM results suggest that only a small percentage of recharge in the outcrop region reaches the confined downdip areas considering the overall, temporally averaged water balance.

Although the approximate groundwater recharge reaching confined aquifer units represents a minuscule increase with respect to the previous NTWGAM results, updates to NTGAM hydraulic properties and highly constrained groundwater production estimates were deemed responsible for an overall yet unbiased tendency for overstimulating measured groundwater levels by about 50 ft. Moreover, future system characterization efforts may be able to further constrain the conceptual understanding of the Northern Trinity aquifer water sources and sinks, including the poorly characterized diffuse interactions with Younger Formations, deep underlying Paleozoic-age strata, and lateral interactions with other systems such as the Cross Timber Aquifer. Similarly, stochastic methods for representing spatiotemporal uncertainties of groundwater use with respect to the model grid may allow for greater precision in matching complex groundwater-level trends, which could have implications for initial aquifer conditions of predictive groundwater availability and desired future condition analyses. In addition to incorporating recent hydrogeologic data, the history-matched distribution of NTGAM hydraulic properties consisting of 522 calibrated models provides GMA 8 and GCDs with a novel planning tool for groundwater management efforts.

6.0 References

Adkins, W.S., 1923, Geology and mineral resources of McLennan County, Texas: Bureau of Economic Geology, The University of Texas at Austin, Bulletin 2430, Austin, TX.

Adkins, W.S., 1933, The Mesozoic Systems in Texas: in Sellards, E.H., Adkins, W.S., and Plummer, F.B., The geology of Texas, Bureau of Economic Geology, The University of Texas at Austin, Bulletin 3232, Austin, TX.

Adkins, W.S., and Lozo, F.E., 1951, Stratigraphy of the Woodbine and Eagle Ford, Waco area: in The Woodbine and adjacent strata of the Waco area of central Texas, Fondren Science Series 4, Southern Methodist University, Dallas, TX

Allen, R.G., Pereira, L.S., Raes, D., and Smith, M., 1998, Crop evapotranspiration (ET) – Guidelines for computing crop water requirements: Food and Agriculture Organization of the United Nations (FAO), FAO Irrigation and drainage paper 56, Rome, Italy, http://www.fao.org/docrep/X0490E/X0490E00.htm.

Ambrose, M.L., 1990, Ground-water protection and management strategies for north-central Texas: A Critical Area Ground-Water Study: Texas Water Commission Critical Area File Report, March 1990.

Anderson, M.P., and Woessner, W.W., 1992, Applied groundwater modeling: Academic Press, San Diego, California.

Atlee, W.A., 1962, The lower Cretaceous Paluxy Sand in central Texas: Baylor Geological Studies, Bulletin 2, Baylor University, Waco, TX.

Back, W., 1966, Hydrochemical facies and groundwater flow patterns in northern part of the Atlantic Coastal Plain: USGS, Professional Paper 498-A.

Bain, J.S., 1973, The nature of the Cretaceous-PreCretaceous contact, north-central Texas: Baylor Geological Studies, Bulletin 25, Baylor University, Waco, TX.

Baker, E.T., Jr., 1960, Geology and ground-water resources of Grayson County, Texas: TWDB, Bulletin 6013, Austin, TX.

Baker, B.B., 1971, Occurrence and availability of ground water in the vicinity of Commerce, Texas: TWDB, unnumbered report, Austin, TX.

Baker, B.B., Dillard, J.W., Souders, V.L., and Peckham, R.C., 1963a, Reconnaissance investigation of the ground-water resources of the Sabine River basin, Texas: Texas Water Commission, Bulletin 6307, Austin, TX.

Baker, E.T., Jr., Long, A.T., Jr., Reeves, R.D., and Wood, L.A., 1963b, Reconnaissance investigation of the ground-water resources of the Red River, Sulphur River, and Cypress Creek basins, Texas: Texas Water Commission, Bulletin 6306, Austin, TX.

Baker, B., Duffin, G., Flores, R., and Lynch, T., 1990a, Evaluation of water resources in part of central Texas: TWDB, Report 319, Austin, TX.

Baker, B., Duffin, G., Flores, R., and Lynch, T., 1990b, Evaluation of water resources in part of north-central Texas: TWDB, Report 318, Austin, TX.

Bené, J., Harden, B., O'Rourke, D., Donnelly, A., and Yelderman, J., 2004, Northern Trinity/Woodbine groundwater availability model: Prepared for the TWDB by R.W. Harden & Associates, Inc., with Freese and Nichols, Inc, HDR Engineering, Inc., LBG Guyton Associates, USGS, and Dr. Joe Yelderman, Jr., http://www.twdb.state.tx.us/groundwater/models/gam/trnt_n/TRNT_N_Model_Report.pdf.

Bennett, R.R., 1942, Memorandum on ground-water resources in the area about 8 miles north of Belton: U.S. Department of the Interior, Geological Survey, Open-File Report.

Boone, P.A., 1968, Stratigraphy of the basal Trinity (Lower Cretaceous) sands of central Texas: Baylor Geological Studies, Bulletin No. 15, Baylor University.

Bradley, R.G., 1999, Updated evaluation of water resources within the Trinity Aquifer area, central Texas: TWDB, Open-File Report 99-03, Austin, TX.

Brown, Jr., L.F., Solis-Iriarte, R.F., and Johns, D.A., 1990, Regional depositional systems tracts, paleogeography, and sequence stratigraphy, upper Pennsylvanian and lower Permian strata, north- and west-Central Texas: Bureau of Economic Geology, The University of Texas at Austin, Report of Investigations 197, Austin, TX.

Bryan, F., 1951, The Grand Prairies of Texas: in The Woodbine and adjacent strata of the Waco area of central Texas, Fondren Science Series 4, Southern Methodist University, Dallas, TX.

Bullard, F.M., 1925, Geology of Love County Oklahoma: Oklahoma Geological Survey, Bulletin 33, University of Oklahoma, Norman, OK.

Bullard, F.M., 1926, Geology of Marshall County Oklahoma, Oklahoma Geological Survey, Bulletin No. 39, The University of Oklahoma, Norman, OK.

Caughey, C.A., 1977, Depositional systems in the Paluxy Formation (Lower Cretaceous), northeast Texas-oil, gas, and groundwater resources: Bureau of Economic Geology, The University of Texas at Austin, Geological Circular 77-8, Austin, TX.

Chaudhuri, S., and Ale, S., 2013, Characterization of groundwater resources in the Trinity and Woodbine aquifers in Texas: Science of the Total Environment, p. 452-453; 338-348.

Chebotarev, I.I., 1955, Metamorphism of natural waters in the crust of weathering:. Geochimica et Cosmochimica Acta, vol. 8, 22-48, 137-170, 198-212.

Cooper, H.H. and C.E. Jacob, 1946. A generalized graphical method for evaluating formation constants and summarizing well field history, Am. Geophys. Union Trans., vol. 27, 526-534.

Cronin, J.G., Follett, C.R., Shafer, G.H., and Rettman, P.L., 1973, Reconnaissance investigation of the ground-water resources of the Brazos River Basin, Texas: Texas Water Commission, Bulletin 6310, Austin, TX.

Cumley, J.C., 1943, Records of wells and springs, drillers' logs, water analyses, and map showing locations of wells and springs, Dallas County, Texas: Texas State Board of Water Engineers, Miscellaneous Report 66, Austin, TX.

Cumley, J.C., Cromack, G.H., and Follett, C.R., 1942, Records of wells and springs, drillers' logs, water analyses, and map showing locations of wells and springs, Williamson County, Texas: Texas State Board of Water Engineers, Miscellaneous Report 298, Austin, TX.

Dane, C.H., 1929, Upper Cretaceous formations of southwestern Arkansas: Arkansas Geological Survey, Bulletin 1, Little Rock, AR.

Davis, D.A., 1938, Records of wells, drillers' logs, and water analyses, and map showing location of wells, Brown County, Texas: Texas State Board of Water Engineers, Miscellaneous Report 23, Austin, TX.

Davis, L.V., 1960, Geology and ground-water resources of southern McCurtain County, Oklahoma: Oklahoma Geological Survey, Bulletin 86, University of Oklahoma, Norman, OK.

Davis, K.W., 1974, Stratigraphy and depositional environments of the Glen Rose Formation, north-central Texas,: Baylor Geological Studies, Bulletin 26, Baylor University, Waco, TX.

Davis, R.E., and Hart, D.L., 1978, Hydrologic data for the Antlers Aquifer, southeastern Oklahoma: USGS, Open-File Report 78-1038.

Diehl, M.L., 2011, Intra-aquifer characterization and potential management impacts: Trinity Aquifer, Central Texas: M.S. Thesis, Baylor University, Waco, TX.

Dodge, C.F., 1952, Stratigraphy of the Woodbine Formation in the Arlington Area, Tarrant County, Texas: Field & Laboratory, vol. 20, no. 2, p. 66-78.

Doherty, J.E., 2015, Calibration and uncertainty analysis for complex environmental models: Brisbane, Australia, Watermark Numerical Computing, 237 p.

Domenico, P.A., 1972, Concepts and models in groundwater hydrology: McGraw-Hill, New York, NY.

Duffin, G.L, and Musick, S.P., 1991, Evaluation of water resources in Bell, Burnet, Travis, Williamson and parts of adjacent counties, Texas: TWDB, Report 326, Austin, TX.

Dutton, A.R., Mace, R.E., Nance, H.S., and Blüm, M., 1996, Geologic hydrogeologic framework of regional aquifers in the Twin Mountains, Paluxy, and Woodbine formations near the SSC site, north-central Texas: Topical Report prepared for the Texas National Research Laboratory Commission by the Bureau of Economic Geology, The University of Texas at Austin, Austin, TX.

Fiedler, A.G., 1934, Artesian water in Somervell County Texas: U.S. Department of the Interior, Water-Supply Paper 660, Washington, DC.

Fienen, M.N., Corson-Dosch, N.T., White, J.T., Leaf, A.T., and Hunt, R.J., 2021, Risk-based wellhead protection decision support—A repeatable workflow approach: Groundwater, v. 60, no. 1, p. 71–86, accessed March 23, 2022, at https://doi.org/10.1111/gwat.13129.

Fisher, W.L., and Rodda, P.U., 1966, Nomenclature revision of the basal Cretaceous rocks between the Colorado and Red Rivers, Texas: Bureau of Economic Geology, The University of Texas at Austin, Report of Investigations 58, Austin, TX.

Gard, C. 1957, Records of wells producing water from the Travis Peak Formation in the Dallas area, Texas: Texas Board of Water Engineers

George, W.O., 1942, Ground water in the vicinity of Burnet and Bertram, Burnet County, Texas: U.S. Department of the Interior, Geological Survey, Open-File Report.

George, W.O., and Barnes, B.A., 1945, Results of tests on wells at Waco, Texas: TWDB, Report M288, Austin, TX.

George, W.O., and Rose, N.A., 1942, Ground water resources of Fort Worth and vicinity, Texas: TWDB, Report M087, Austin, TX.

George, P.G., Mace, R.E. and Petrossian, R., 2011, Aquifers of Texas: TWDB, Report 380, Austin, TX.

Griffith, G.E., Bryce, S.B., Omernik, J.M., and Rogers, A., 2007, Ecoregions of Texas: TCEQ, Austin, TX. 125p.

Guyton, W.F., and George, W.O., 1943, Results of pumping test of wells at Camp Hood, Texas:

U.S. Department of the Interior, Geological Survey, Open-File Report, TWDB, Report M031, Austin, TX.

Hall, W.D., 1976, Hydrogeologic significance of depositional systems and facies in lower Cretaceous sandstones, north-central Texas: Bureau of Economic Geology, The University of Texas at Austin, Geological Circular 76-1, Austin, TX.

Hamman, R.R., 2001, High resolution sequence stratigraphy of the Cretaceous Woodbine Formation, Henderson and Navarro counties, Texas: M.S. Thesis, The University of Texas at Austin, Austin, TX.

Harden, R.W., 1960, Report of preliminary investigation of the occurrence of ground water in the Trinity Group near Gainesville, Cooke County, Texas: Texas Board of Water Engineers.

Hart, D.L., Jr., 1974, Reconnaissance of the water resources of the Ardmore and Sherman quadrangles, southern Oklahoma: Oklahoma Geological Survey, Map HA-3, prepared in cooperation with the USGS, The University of Oklahoma, Norman, OK.

Hayward, O.T., and Brown, L.F., Jr., 1967, Comanchean (Cretaceous) rocks of central Texas: Society of Economic Paleontologists and Mineralogists, Permian Basin Section, Publication 67-8.

Healy, R.W., 2010, Estimating groundwater recharge: Cambridge University Press, 256 p.

Heitmuller, F.T., and Reece, B.D., 2003, Database of historically documented springs and spring flow measurements in Texas: USGS, Open-File Report 03-315, http://pubs.usgs.gov/of/2003/ofr03-315/.

Hill, R.T., 1901, Geography and geology of the Black and Grand Prairies, Texas with detailed descriptions of the Cretaceous formations and special reference to artesian waters: USGS, 21st Annual Report, Washington, DC, part 7.

Huffman, G.G., Alfonsi, P.P., Dalton, R.C., Duarte-Vivas, A., and Jeffries, E.L., 1975, Geology and mineral resources of Choctaw County, Oklahoma: Oklahoma Geological Survey, Bulletin 120, The University of Oklahoma, Norman, OK.

Huffman, G.G., Hart, T.A., Olson, L.J., Currier, J.D., and Ganser, R.W., 1978, Geology and mineral resources of Bryan County, Oklahoma: Oklahoma Geological Survey, Bulletin 126, The University of Oklahoma, Norman, OK.

Huffman, G.G., Bridges, K.F., Ganser, R.W., Holtzman, A.M., Jr., and Merritt, M.L., 1987, Geology and mineral resources of Marshall County, Oklahoma: Oklahoma Geological Survey, Bulletin 142, The University of Oklahoma, Norman, OK.

Jones, I.C., 2003, Groundwater availability modeling: northern segment of the Edwards Aquifer, Texas: TWDB, Report 358,

http://www.twdb.state.tx.us/publications/reports/numbered_reports/doc/R358/Report%20358%20Northern%20Edwards.pdf.

Keese, K.E., Scanlon, B.R., and Reedy R.C., 2005, Assessing controls on diffuse groundwater recharge using unsaturated flow modeling: Water Resources Research, vol. 41, W06010, doi:06010.01029/02004WR003841.

Kelley, Van A., John Ewing, Toya L. Jones, Steven C. Young, and Neil Deeds, eds. 2014, Updated Groundwater Availability Model of the Northern Trinity and Woodbine Aquifers: Final Report. Austin, TX: INTERA Incorporated and Bureau of Economic Geology, The University of Texas at Austin, August 2014.

Kelley, V.K., and Ewing, J.E., 2014, Northern Trinity and Woodbine aquifers GAM overhaul project – predictive simulations to support the GMA-8 joint-planning process: technical memorandum to Bill Mullican, Contract Manager for the Northern Trinity and Woodbine aquifers GAM Overhaul Project, dated August 29, 2014.

Klemt, W.R., Perkins, R.D., and Alvarez, H.J., 1975, Ground-water resources of part of central Texas with emphasis on the Antlers and Travis Peak formations, Volume 1: TWDB, Report 195, Austin, TX.

Langley, L., 1999, Updated evaluation of water resources in part of north-central Texas, 1990- 1999: TWDB, Report 349, Austin, TX.

Larkin, T.J., and Bomar, G.W., 1983, Climatic Atlas of Texas: Texas Department of Water Resources. LP-192, Austin, Texas.

Lee, H.L., 1958, Woodbine strata of northwest Hill County, Texas: M.S. Thesis, The University of Texas at Austin, Austin, TX.

Leggat, E.R., 1957, Geology and ground-water resources of Tarrant County, Texas: TWDB, Bulletin 5709, Austin, TX.

Livingston, P., 1945, Ground-water resources at Sherman, Texas: TWDB, Report M249, Austin, TX.

Livingston, P., and Bennett, R., 1942, Ground water in the vicinity of McGregor, McLennan County, Texas: U.S. Department of the Interior, Geological Survey, Open-File Report.

Livingston, P., and Hastings, W.W., 1942, Test well at proposed army camp 5 miles southeast of Gatesville, Texas: U.S. Department of the Interior, Geological Survey, Open-File Report.

Ludwig, A.M., 1973, Water resources of Hempstead, Lafayette, Little River, Miller, and Nevada counties, Arkansas: USGS, Water Supply Paper 1998.

Mace, R.E., Dutton, A.R. and Nance, H.S., 1994. Water-level declines in the Woodbine, Paluxy, and Trinity aquifers of north-central Texas.

Marcher, M.V., and Bergman, D.L., 1983, Reconnaissance of the water resources of the McAlester and Texarkana quadrangles, southeastern Oklahoma: Oklahoma Geological Survey, Map HA-9, prepared in cooperation with the USGS, The University of Oklahoma, Norman, OK.

Meyers, B. N., 1969, Compilation of Results of Aquifer Tests in Texas: Prepared by the U.S. Geological Survcey in cooperation with the Texas Water Development Board, Report 98. Austin, TX.

Moore, C., and Doherty, J., 2005, Role of the calibration process in reducing model predictive error: Water Resources Research, v. 41, no. 5, 14 p., at https://agupubs.onlinelibrary.wiley.com/doi/full/10.1029/2004WR003501.

Morton, R.B., 1992, Simulation of ground-water flow in the Antlers Aquifer in southeastern Oklahoma and northeastern Texas: USGS, Water-Resources Investigations Report 88-4208.

Mosteller, M.A., 1970, Subsurface stratigraphy of the Comanchean series in east central Texas: Baylor Geological Studies, Bulletin 19, Baylor University, Waco, TX.

Mount, J.R., 1962, Ground-water conditions in the vicinity of Burnet, Texas: Texas Water Commission, Memorandum Report 62-01, Austin, TX.

Mount, J.R., 1963, Ground-water availability at Whitney, Hill County, Texas: Texas Water Commission, LD-0263-MR, Austin, TX.

Niswonger, R.G., Panday, S., and Ibaraki, M., 2011, MODFLOW-NWT, a Newton formulation for MODFLOW-2005: USGS, Techniques and Methods 6-A37, 44 p.

Nordstrom, P.L., 1982, Occurrence, availability, and chemical quality of ground water in the Cretaceous aquifers of north-central Texas: Texas Department of Water Resources, Report 269, Austin, TX.

Nordstrom, P.L., 1987, Ground-water resources of the Antlers and Travis Peak Formations in the outcrop area of north central Texas: Texas Water Commission, Report 298, Austin, TX.

Oklahoma Water Resources Board [OWRB], 2023, Water Rights: Oklahoma Water Resources Board, available at https://www.owrb.ok.gov/maps/pmg/owrbdata_wr.html

Oliver, W.B., 1971, Depositional systems in the Woodbine Formation (Upper Cretaceous), northeast Texas: Bureau of Economic Geology, The University of Texas at Austin, Report of Investigations 73, Austin, TX.

Oliver, W., Harding, J., and Lupton, D., 2013, Development of a groundwater model for the Antlers Aquifer in southeastern Oklahoma: Prepared for The Choctaw and Chickasaw Nations by INTERA Incorporated.

Ophori, D. U., & Tóth, J., 1989. Patterns of Ground-Water Chemistry, Ross Creek Basin, Alberta, Canada. *Ground Water*, 27(1), 20–26.

Owen, M.T., 1979, The Paluxy Sand in north-central Texas: Baylor Geological Studies, Bulletin 36, Baylor

University, Waco, TX.

Peckham, R.C., Souders, V.L., Dillard, J.W., and Baker, B.B., 1963, Reconnaissance investigation of the ground-water resources of the Trinity River Basin, Texas: Texas Water Commission, Bulletin 6309, Austin, TX.

Price, J.C., 1951, The south Bosque oil field: in The Woodbine and adjacent strata of the Waco area of central Texas, Fondren Science Series 4, Southern Methodist University, Dallas, TX.

Raynor, F.A., 1959, Records of Water-Level Measurements in Bell, McLennan, and Somervell

Counties, Texas, 1930 Through 1957: Texas Water Commission Bulletin 5902.

Robinson, M.C., Deeds, N.E., & Lupton, D.M.. 2019. Identification of Potential Brackish Groundwater Production Areas – Northern Trinity Aquifer, Texas. Texas Water Development Board Technical Note 19-01.

Rodgers, R.W., 1967, Stratigraphy of Glen Rose Limestone, central Texas: in Comanchean (lower Cretaceous) stratigraphy and paleontology of Texas, Society of Economic Paleontologists and Mineralogists, Permian Basin Section, Midland, TX.

Rose, N.A., 1943, Results of pumping test of wells at Tank Destroyer Center, north Camp Hood, near Gatesville, Texas: U.S. Department of the Interior, Geological Survey, Open-File Report.

Rose, N.A., and George, W.O., 1942, Ground-water resources in selected areas in Erath, Hood and Hamilton counties, Texas: Texas State Board of Water Engineers, duplicated report.

Shuler, E.W., 1918, The Geology of Dallas County: Bureau of Economic Geology, The University of Texas at Austin, Bulletin 1818, Austin, TX.

Shumard, B.F., 1860, Observations upon the Cretaceous strata of Texas: St. Louis Academy of Science, Transactions, vol. 1, St. Louis, MO.

Stricklin, Jr., F.L., Smith, C.I., and Lozo, F.E., 1971, Stratigraphy of lower Cretaceous Trinity deposits of central Texas: Bureau of Economic Geology, The University of Texas at Austin, Report of Investigations 71, Austin, TX.

Sundstrom, R.W., 1948, Results of pumping tests on the city wells at Waxahachie, Texas: TWDB, Report M292, Austin, TX.

Sundstrom, R.W., and Barnes, B.A., 1942, Ground-water resources in the vicinity of Gatesville, Texas: USGS, Open-File Report.

Taff, J.A., 1892, Reports on the Cretaceous area north of the Colorado River: Third Annual Report of the Geological Survey of Texas, 1891, Austin, TX.

Thompson, G.L., 1967, Ground-water resources of Ellis County, Texas: TWDB, Report 62, Austin, TX.

Thompson, G.L., 1969, Ground-water Resources of Johnson County, Texas: TWDB, Report 94, Austin, TX.

Thompson, G.L., 1972, Ground-water resources of Navarro County, Texas: TWDB, Report 160, Austin, TX.

Thornton, T.S., 1992, Geohydrology of Pike and Howard counties, Arkansas: M.S. Thesis, Department of Geology, The University of Arkansas.

TWDB, 2023, TWDB groundwater database: http://www.twdb.state.tx.us/groundwater/data/gwdbrpt.asp, accessed October, 2023.

U.S. Geological Survey [USGS], 2023a, USGS water data for the Nation: U.S. Geological Survey National Water Information System database, at http://doi.org/10.5066/F7P55KJN.

U.S. Geological Survey (USGS), 2023b, National Hydrography Dataset, http://nhd.usgs.gov/.

Westenbroek, S.M., Kelson, V.A., Dripps, W.R., Hunt, R.J. and Bradbury, K.R., 2010. SWB--a modified Thornthwaite-Mather Soil-Water-Balance Code for estimating groundwater recharge (Vol. 6). Reston, VA: US Department of the Interior, US Geological Survey, Ground Resources Program.

Winslow, A.G., and Kister, L.R., 1956, Saline-water resources of Texas: USGS, Water-Supply Paper 1365.

Winston, R.B., 2020. GWChart: A program for creating specialized graphs used in groundwater studies. U.S. Geological Survey. Available at: https://www.usgs.gov/software/gwchart-a-program-creating-specialized-graphs-used-groundwater-studies

Winton, W.M., and Scott, G., 1922, The geology of Johnson County, Texas: Bureau of Economic Geology, The University of Texas at Austin, Bulletin 229, Austin, TX.

Yelderman, J.C., Casteel, W.M., Wong, S.S., 2018. The trinity Oasis LLC Aquifer Test; Hosston Formation.

7.0 Appendices

7.1 Model Temporal Discretization

The NTGAM groundwater model simulation period was temporally discretized into 132 annual stress periods with one time step each, representing the period from 1889 to 2020 (Appendix Table 7-1). This annual stress period approach was similar to the NTWGAM but extended the calibration period by 10 years from 2010 to 2020. The first stress period (1889) is considered steady-state, representing long-term average predevelopment conditions in the aquifer before 1890, which marked the beginning of a period of significant development. Although historical data indicate some development prior to 1890, water level records suggest that the aquifer remained largely in its natural, predevelopment state in many locations outside of the present-day metropolitan areas.

Appendix Table 7-1. Listing of stress periods for the northern Trinity and Woodbine Groundwater-Flow model.

Stress period[1]	Start date	End date	Stress period length, in days	NSTP	TSMULT
1	1889	1889	1	1	1
2	1/1/1890	12/31/1890	365	1	1
3	1/1/1891	12/31/1891	365	1	1
4	1/1/1892	12/31/1892	366	1	1
5	1/1/1893	12/31/1893	365	1	1
6	1/1/1894	12/31/1894	365	1	1
7	1/1/1895	12/31/1895	365	1	1
8	1/1/1896	12/31/1896	366	1	1
9	1/1/1897	12/31/1897	365	1	1
10	1/1/1898	12/31/1898	365	1	1
11	1/1/1899	12/31/1899	365	1	1
12	1/1/1900	12/31/1900	366	1	1
13	1/1/1901	12/31/1901	365	1	1
14	1/1/1902	12/31/1902	365	1	1
15	1/1/1903	12/31/1903	365	1	1
16	1/1/1904	12/31/1904	366	1	1
17	1/1/1905	12/31/1905	365	1	1
18	1/1/1906	12/31/1906	365	1	1
19	1/1/1907	12/31/1907	365	1	1
20	1/1/1908	12/31/1908	366	1	1
21	1/1/1909	12/31/1909	365	1	1
22	1/1/1910	12/31/1910	365	1	1
23	1/1/1911	12/31/1911	365	1	1

Stress period[1]	Start date	End date	Stress period length, in days	NSTP	TSMULT
24	1/1/1912	12/31/1912	366	1	1
25	1/1/1913	12/31/1913	365	1	1
26	1/1/1914	12/31/1914	365	1	1
27	1/1/1915	12/31/1915	365	1	1
28	1/1/1916	12/31/1916	366	1	1
29	1/1/1917	12/31/1917	365	1	1
30	1/1/1918	12/31/1918	365	1	1
31	1/1/1919	12/31/1919	365	1	1
32	1/1/1920	12/31/1920	366	1	1
33	1/1/1921	12/31/1921	365	1	1
34	1/1/1922	12/31/1922	365	1	1
35	1/1/1923	12/31/1923	365	1	1
36	1/1/1924	12/31/1924	366	1	1
37	1/1/1925	12/31/1925	365	1	1
38	1/1/1926	12/31/1926	365	1	1
39	1/1/1927	12/31/1927	365	1	1
40	1/1/1928	12/31/1928	366	1	1
41	1/1/1929	12/31/1929	365	1	1
42	1/1/1930	12/31/1930	365	1	1
43	1/1/1931	12/31/1931	365	1	1
44	1/1/1932	12/31/1932	366	1	1
45	1/1/1933	12/31/1933	365	1	1
46	1/1/1934	12/31/1934	365	1	1
47	1/1/1935	12/31/1935	365	1	1
48	1/1/1936	12/31/1936	366	1	1
49	1/1/1937	12/31/1937	365	1	1
50	1/1/1938	12/31/1938	365	1	1
51	1/1/1939	12/31/1939	365	1	1
52	1/1/1940	12/31/1940	366	1	1
53	1/1/1941	12/31/1941	365	1	1
54	1/1/1942	12/31/1942	365	1	1
55	1/1/1943	12/31/1943	365	1	1
56	1/1/1944	12/31/1944	366	1	1
57	1/1/1945	12/31/1945	365	1	1
58	1/1/1946	12/31/1946	365	1	1
59	1/1/1947	12/31/1947	365	1	1
60	1/1/1948	12/31/1948	366	1	1
61	1/1/1949	12/31/1949	365	1	1

Stress period[1]	Start date	End date	Stress period length, in days	NSTP	TSMULT
62	1/1/1950	12/31/1950	365	1	1
63	1/1/1951	12/31/1951	365	1	1
64	1/1/1952	12/31/1952	366	1	1
65	1/1/1953	12/31/1953	365	1	1
66	1/1/1954	12/31/1954	365	1	1
67	1/1/1955	12/31/1955	365	1	1
68	1/1/1956	12/31/1956	366	1	1
69	1/1/1957	12/31/1957	365	1	1
70	1/1/1958	12/31/1958	365	1	1
71	1/1/1959	12/31/1959	365	1	1
72	1/1/1960	12/31/1960	366	1	1
73	1/1/1961	12/31/1961	365	1	1
74	1/1/1962	12/31/1962	365	1	1
75	1/1/1963	12/31/1963	365	1	1
76	1/1/1964	12/31/1964	366	1	1
77	1/1/1965	12/31/1965	365	1	1
78	1/1/1966	12/31/1966	365	1	1
79	1/1/1967	12/31/1967	365	1	1
80	1/1/1968	12/31/1968	366	1	1
81	1/1/1969	12/31/1969	365	1	1
82	1/1/1970	12/31/1970	365	1	1
83	1/1/1971	12/31/1971	365	1	1
84	1/1/1972	12/31/1972	366	1	1
85	1/1/1973	12/31/1973	365	1	1
86	1/1/1974	12/31/1974	365	1	1
87	1/1/1975	12/31/1975	365	1	1
88	1/1/1976	12/31/1976	366	1	1
89	1/1/1977	12/31/1977	365	1	1
90	1/1/1978	12/31/1978	365	1	1
91	1/1/1979	12/31/1979	365	1	1
92	1/1/1980	12/31/1980	366	1	1
93	1/1/1981	12/31/1981	365	1	1
94	1/1/1982	12/31/1982	365	1	1
95	1/1/1983	12/31/1983	365	1	1
96	1/1/1984	12/31/1984	366	1	1
97	1/1/1985	12/31/1985	365	1	1
98	1/1/1986	12/31/1986	365	1	1
99	1/1/1987	12/31/1987	365	1	1
100	1/1/1988	12/31/1988	366	1	1

Stress period[1]	Start date	End date	Stress period length, in days	NSTP	TSMULT
101	1/1/1989	12/31/1989	365	1	1
102	1/1/1990	12/31/1990	365	1	1
103	1/1/1991	12/31/1991	365	1	1
104	1/1/1992	12/31/1992	366	1	1
105	1/1/1993	12/31/1993	365	1	1
106	1/1/1994	12/31/1994	365	1	1
107	1/1/1995	12/31/1995	365	1	1
108	1/1/1996	12/31/1996	366	1	1
109	1/1/1997	12/31/1997	365	1	1
110	1/1/1998	12/31/1998	365	1	1
111	1/1/1999	12/31/1999	365	1	1
112	1/1/2000	12/31/2000	366	1	1
113	1/1/2001	12/31/2001	365	1	1
114	1/1/2002	12/31/2002	365	1	1
115	1/1/2003	12/31/2003	365	1	1
116	1/1/2004	12/31/2004	366	1	1
117	1/1/2005	12/31/2005	365	1	1
118	1/1/2006	12/31/2006	365	1	1
119	1/1/2007	12/31/2007	365	1	1
120	1/1/2008	12/31/2008	366	1	1
121	1/1/2009	12/31/2009	365	1	1
122	1/1/2010	12/31/2010	365	1	1
123	1/1/2011	12/31/2011	365	1	1
124	1/1/2012	12/31/2012	366	1	1
125	1/1/2013	12/31/2013	365	1	1
126	1/1/2014	12/31/2014	365	1	1
127	1/1/2015	12/31/2015	365	1	1
128	1/1/2016	12/31/2016	366	1	1
129	1/1/2017	12/31/2017	365	1	1
130	1/1/2018	12/31/2018	365	1	1
131	1/1/2019	12/31/2019	365	1	1
132	1/1/2020	12/31/2020	366	1	1

[1]Model time is discretized into time steps within stress periods. The stress period length is the finest resolution at which temporally varying inflows and outflows can be represented and varied

7.2 Model Observations

Appendix Table 7-2. Model wells with groundwater-level measurements within the model area.

TWDB or OWRB state well number[1]	Map ID (figures 3-50 to 3-70)	County	Hydrogeologic unit	Period of record (may contain gaps) (M/Y)[2]		Layer (zero-based indexing)[3]	Well depth, in feet below land surface[4]	Row	Column
				Begin	End				
1712101	A	Lamar	Woodbine	2/1971	2/2019	1	165	673	1,124
1721709	B	Lamar	Paluxy	2/1975	2/1991	3	2,145	724	1,088
1729103	C	Lamar	Paluxy	2/1967	2/2019	3	2,563	734	1,073
1727201	D	Lamar	Woodbine	3/1964	2/2005	1	1,610	681	1,054
1734301	E	Delta	Paluxy	2/1971	2/2019	3	3,333	687	1,010
1848402	F	Hunt	Woodbine	2/1995	2/2019	1	2,388	637	934
1733501	A	Fannin	Paluxy	2/1982	2/2017	3	3,366	656	979
1838302	B	Fannin	Woodbine	2/1971	3/2012	1	1,297	585	961
1829702	C	Grayson	Woodbine and Washita/Fredericksburg	3/1968	2/2005	[1, 2]	1,475	533	946
1828102	D	Grayson	Multi-aquifer	3/1972	2/2011	[3, 4, 5, 6, 7]	2,460	501	949
1820703	E	Grayson	Pearsall and Hosston	2/1945	2/2007	[6, 7]	2,136	490	963
1811501	F	Grayson	Washita/Fredericksburg	2/1970	2/2017	2	317	459	996
1833301	G	Grayson	Paluxy	3/1972	3/2020	3	923	451	889
1803901	H	Grayson	Washita/Fredericksburg and Paluxy	2/1970	3/2020	[2, 3]	290	454	1,020
1915701	A	Cooke	Glen and Rose and Hensell	3/1972	2/2017	[4, 5]	348	350	933
1923502	B	Cooke	Middle-Lower and Trinity	3/1960	3/2020	[4, 5, 6, 7]	938	368	918
1817401	C	Cooke	Woodbine and Washita/Fredericksburg	2/1971	3/2020	[1, 2]	235	411	936
1924702	D	Cooke	Pearsall and Hosston	2/1977	3/2020	[6, 7]	1,238	395	910
1931302	E	Cooke	Pearsall and Hosston	2/1959	3/2020	[6, 7]	997	387	900
1931201	F	Cooke	Paluxy	2/1970	3/2020	3	350	376	888
1938301	G	Cooke	Hensell and Pearsall	2/1977	2/2017	[5, 6]	794	370	857

TWDB or OWRB state well number[1]	Map ID (figures 3-50 to 3-70)	County	Hydrogeologic unit	Period of record (may contain gaps) (M/Y)[2]		Layer (zero-based indexing)[3]	Well depth, in feet below land surface[4]	Row	Column
				Begin	End				
1922704	H	Cooke	Hosston	3/1976	3/2020	7	660	337	886
1841201	A	Denton	Woodbine	2/1970	3/2020	1	210	461	861
1964201	B	Denton	Hosston	2/1969	3/2012	7	1,747	470	781
1963601	C	Denton	Paluxy	2/1970	3/2020	3	856	453	763
1963701	D	Denton	Paluxy	2/1970	2/2017	3	626	441	742
1962203	E	Denton	Hosston	2/1963	3/2012	7	1,003	419	755
1954603	F	Denton	Pearsall and Hosston	2/1969	3/2020	[6, 7]	980	409	780
1947801	G	Denton	Paluxy	3/1972	3/2020	3	615	419	807
1956104	H	Denton	Upper-Middle and Trinity	3/1960	2/2005	[3, 4, 5, 6]	1,200	437	814
1845604	A	Collin	Woodbine	2/1975	3/2020	1	1,900	578	900
1844601	B	Collin	Woodbine and Washita/Fredericksburg	2/1970	3/1996	[1, 2]	1,783	558	889
1844702	C	Collin	Woodbine	3/1964	2/1994	1	1,136	538	868
1850501	D	Collin	Hosston	2/1953	3/1984	7	2,694	505	832
1850202	E	Collin	Woodbine	2/1969	3/2004	1	640	499	836
1842604	F	Collin	Hensell and Pearsall	2/1975	2/2017	[5, 6]	2,300	496	866
1842601	G	Collin	Woodbine	3/1972	2/2017	1	700	496	866
1928601	A	Montague	Glen Rose	2/1970	3/2020	4	200	310	848
1928804	B	Montague	Glen Rose	2/1970	3/2020	4	250	310	832
1937901	C	Wise	Paluxy	2/1970	3/2020	3	335	361	818
1961201	D	Wise	Paluxy	2/1970	3/2020	3	360	388	745
1945301	E	Wise	Glen Rose	2/1950	2/2019	4	370	364	805
1943202	F	Wise	Hosston	2/1963	3/2016	7	381	304	782
3210201	A	Parker	Glen Rose	2/1971	3/2020	4	165	340	640
3211702	B	Parker	Glen Rose	3/1972	3/2020	4	220	363	634
3218701	C	Parker	Pearsall	3/1972	2/2010	6	204	359	594

TWDB or OWRB state well number[1]	Map ID (figures 3-50 to 3-70)	County	Hydrogeologic unit	Period of record (may contain gaps) (M/Y)[2]		Layer (zero-based indexing)[3]	Well depth, in feet below land surface[4]	Row	Column
				Begin	End				
3226601	D	Parker	Hensell	2/1950	2/2007	5	310	385	580
3234609	E	Hood	Hensell	2/1977	2/2019	5	222	401	547
3242403	F	Hood	Hensell	2/1971	3/2020	5	355	393	506
3205302	A	Tarrant	Paluxy	2/1975	2/2015	3	419	413	717
3213601	B	Tarrant	Hosston	2/1955	2/2019	7	967	430	673
3214610	C	Tarrant	Paluxy	2/1957	2/1991	3	425	464	687
3215601	D	Tarrant	Lower and Trinity	2/1951	2/1975	[5, 6, 7]	1,483	482	700
3223101	E	Tarrant	Pearsall	2/1971	3/2008	6	1,363	481	674
3231301	F	Tarrant	Woodbine	2/1970	2/2019	1	171	508	646
3222612	G	Tarrant	Lower and Trinity	3/1976	2/2019	[5, 6, 7]	1,352	479	655
3230106	H	Tarrant	Hosston	2/1994	3/2020	7	1,220	470	627
3310401	A	Dallas	Hosston	2/1953	2/1986	7	2,689	546	740
3310801	B	Dallas	Hosston	3/1956	2/1990	7	2,797	561	728
3319101	C	Dallas	Hosston	2/1970	3/2020	7	3,076	575	728
3319303	D	Dallas	Paluxy	2/1970	2/1978	3	2,297	596	733
3320401	E	Dallas	Hosston	3/1956	3/1984	7	4,110	615	728
3325401	F	Dallas	Pearsall and Hosston	2/1969	2/2019	[6, 7]	2,430	549	662
3317801	G	Dallas	Pearsall and Hosston	3/1968	3/1988	[6, 7]	2,614	550	686
3309701	H	Dallas	Pearsall and Hosston	2/1965	2/2010	[6, 7]	2,049	523	704
3236604	A	Johnson	Paluxy	2/1970	3/2020	3	500	452	566
3232701	B	Johnson	Woodbine	2/1970	3/2020	1	240	526	635
3239505	C	Johnson	Woodbine	2/1970	2/2018	1	210	521	610
3238901	D	Johnson	Hosston	2/1973	3/2020	7	1,630	510	591
3239702	E	Johnson	Paluxy and Pearsall	3/1960	3/2020	[3, 6]	1,656	520	597
3239901	F	Johnson	Woodbine	2/1966	3/2020	1	220	534	596

TWDB or OWRB state well number[1]	Map ID (figures 3-50 to 3-70)	County	Hydrogeologic unit	Period of record (may contain gaps) (M/Y)[2]		Layer (zero-based indexing)[3]	Well depth, in feet below land surface[4]	Row	Column
				Begin	End				
3247202	G	Johnson	Washita/Fredericksburg	2/1970	3/2020	2	216	537	584
3246907	H	Johnson	Hosston	3/1972	3/2020	7	1,560	523	559
3326902	A	Ellis	Hosston	2/1999	3/2020	7	3,178	595	671
3350502	B	Ellis	Woodbine	3/1972	2/2009	1	1,238	633	589
3349803	C	Ellis	Hosston	2/1977	2/2019	7	2,700	611	565
3248901	D	Ellis	Woodbine	2/1969	3/2020	1	384	579	579
3248501	E	Ellis	Woodbine and Washita/Fredericksburg	2/1969	3/2020	[1, 2]	367	563	584
3341203	F	Ellis	Hosston	2/1975	2/2019	7	2,564	581	611
3240606	G	Ellis	Hosston	2/1999	2/2019	7	2,411	558	619
3333105	H	Ellis	Pearsall and Hosston	2/1999	2/2019	[6, 7]	2,354	555	638
3243805	A	Somervell	Hosston	2/1950	2/2019	7	464	438	508
3251501	B	Somervell	Glen and Rose and Hensell	2/1950	2/2006	[4, 5]	370	447	491
3250802	C	Somervell	Glen Rose	3/1964	3/2020	4	321	429	473
3251104	D	Somervell	Hensell	2/1965	3/2020	5	376	432	491
3250304	E	Somervell	Hosston	3/1960	3/2020	7	352	428	497
3255304	A	Hill	Woodbine and Washita/Fredericksburg	2/1965	2/1997	[1, 2]	273	555	558
3255904	B	Hill	Pearsall and Hosston	2/1977	2/1995	[6, 7]	1,856	565	543
3909201	C	Hill	Hosston	2/1967	3/2020	7	3,138	647	490
4015102	D	Hill	Hosston	3/1960	3/2020	7	1,485	587	458
4014602	E	Hill	Glen Rose	2/1966	3/2020	4	1,102	579	443
4006104	F	Hill	Hosston	2/1966	2/1993	7	1,166	540	471

TWDB or OWRB state well number[1]	Map ID (figures 3-50 to 3-70)	County	Hydrogeologic unit	Period of record (may contain gaps) (M/Y)[2]		Layer (zero-based indexing)[3]	Well depth, in feet below land surface[4]	Row	Column
				Begin	End				
3262302	G	Hill	Hensell and Pearsall	3/1964	3/2020	[5, 6]	1,213	545	515
3253902	H	Hill	Hensell and Pearsall	3/1964	3/2000	[5, 6]	934	515	511
4016404	A	McLennan	Hosston	2/1969	2/2017	7	1,982	618	464
4022804	B	McLennan	Hensell and Pearsall	2/1966	3/1988	[5, 6]	1,150	595	400
4023903	C	McLennan	Hosston	2/1994	3/2020	7	2,114	627	416
4024803	D	McLennan	Pearsall and Hosston	2/1957	2/1987	[6, 7]	2,494	644	423
3917701	E	McLennan	Hosston	2/1959	3/2020	7	3,129	663	436
4032103	F	McLennan	Hosston	2/1957	2/2015	7	2,396	645	407
4031802	G	McLennan	Hosston	3/1964	3/2008	7	2,040	637	375
4037501	H	McLennan	Hensell	2/1965	2/2015	5	1,050	596	334
4002109	A	Bosque	Hensell	2/1967	3/2020	5	364	440	429
4003901	B	Bosque	Hensell and Pearsall	2/1962	2/2006	[5, 6]	570	487	426
4019101	C	Bosque	Hensell and Pearsall	3/1968	2/2013	[5, 6]	540	493	373
4011602	D	Bosque	Hensell	2/1966	3/2020	5	631	504	407
4020301	E	Bosque	Glen Rose	2/1966	2/2009	4	650	539	394
4005903	F	Bosque	Multi-aquifer	2/1958	2/2002	[2, 3, 4, 5, 6, 7]	1,135	545	448
4014702	G	Bosque	Glen Rose	2/1966	2/2001	4	1,010	571	424
3260602	H	Bosque	Pearsall	2/1943	2/1983	6	760	501	483
4035103	A	Coryell	Lower and Trinity	2/1966	2/1981	[5, 6, 7]	771	524	311
4035404	B	Coryell	Hosston	2/1967	3/2020	7	755	530	301
4036601	C	Coryell	Multi-aquifer	3/1956	2/2018	[2, 3, 4, 5, 6, 7]	1,170	579	321
4035804	D	Coryell	Middle-Lower and Trinity	2/1966	2/1987	[4, 5, 6, 7]	745	544	295
4041903	E	Coryell	Glen Rose	3/1968	3/2020	4	271	516	246
4041202	F	Coryell	Hensell	2/1970	2/2019	5	420	496	265

TWDB or OWRB state well number[1]	Map ID (figures 3-50 to 3-70)	County	Hydrogeologic unit	Period of record (may contain gaps) (M/Y)[2]		Layer (zero-based indexing)[3]	Well depth, in feet below land surface[4]	Row	Column
				Begin	End				
4140903	G	Coryell	Hensell	2/1969	2/2014	5	440	475	259
4140803	H	Coryell	Hensell	2/1966	2/2003	5	372	460	257
3155301	A	Erath	Hensell and Hosston	2/1966	2/1994	[5, 7]	520	341	459
3249501	B	Erath	Lower and Trinity	2/1965	3/2020	[5, 6, 7]	512	392	469
3162901	C	Erath	Hensell and Pearsall	2/1990	3/2020	[5, 6]	333	346	393
3162803	D	Erath	Hensell	2/1965	2/2019	5	265	335	382
4106501	E	Comanche	Hensell and Pearsall	2/1959	2/2019	[5, 6]	250	345	368
4114102	F	Comanche	Hosston	2/1959	3/2020	7	179	346	336
4112902	G	Comanche	Hensell and Pearsall	2/1970	3/2020	[5, 6]	112	318	307
4124301	A	Hamilton	Glen Rose	2/1970	3/2016	4	177	433	343
4017702	B	Hamilton	Glen and Rose and Hensell	2/1966	3/1996	[4, 5]	327	452	326
4124801	C	Hamilton	Glen and Rose and Hensell	2/1970	2/2019	[4, 5]	432	435	320
4123401	D	Hamilton	Hensell	2/1961	3/1992	5	362	392	311
4138101	E	Mills	Hensell and Pearsall	2/1955	2/1998	[5, 6]	325	392	248
4137303	F	Mills	Glen Rose	2/1966	2/2018	4	213	382	240
4048201	A	Falls	Pearsall and Hosston	2/1957	3/2012	[6, 7]	2,640	676	353
4048801	B	Falls	Pearsall	2/1966	2/2019	6	2,874	690	335
4047602	C	Falls	Hosston	2/1965	3/2012	7	2,609	671	330
4056102	D	Falls	Hosston	2/1970	2/2019	7	2,765	687	310
4064101	E	Falls	Hosston	2/1959	3/2020	7	3,060	699	288
4053406	A	Bell	Pearsall and Hosston	2/1970	3/2020	[6, 7]	1,192	617	270
4063501	B	Bell	Hosston	2/1965	3/2020	7	3,200	691	262
4061509	C	Bell	Pearsall and Hosston	2/1965	3/2020	[6, 7]	1,261	636	244
5806102	D	Bell	Pearsall and Hosston	2/1955	3/2020	[6, 7]	2,210	663	229

TWDB or OWRB state well number[1]	Map ID (figures 3-50 to 3-70)	County	Hydrogeologic unit	Period of record (may contain gaps) (M/Y)[2]		Layer (zero-based indexing)[3]	Well depth, in feet below land surface[4]	Row	Column
				Begin	End				
4061703	E	Bell	Pearsall and Hosston	2/1965	2/1989	[6, 7]	1,293	634	231
5805403	F	Bell	Pearsall	2/1966	2/2019	6	1,630	646	204
5804103	G	Bell	Multi-aquifer	2/1993	3/2016	[3, 4, 5]	767	612	202
5803901	H	Bell	Middle-Lower and Trinity	2/1967	2/1982	[4, 5, 6, 7]	857	616	179
5810303	A	Williamson	Hensell and Pearsall	2/1966	3/2016	[5, 6]	728	589	148
5829603	B	Williamson	Pearsall	2/1959	2/2018	6	3,335	703	123
5817902	C	Williamson	Hosston	2/1970	2/2018	7	740	589	94
5724501	D	Burnet	Hosston	2/1967	2/2009	7	460	549	81
5724101	E	Burnet	Middle-Lower and Trinity	2/1961	3/2020	[4, 5, 6, 7]	480	538	94
5715601	F	Burnet	Pearsall	3/1968	3/2012	6	205	520	100
5715502	G	Burnet	Pearsall and Hosston	2/1970	2/2011	[6, 7]	205	507	99
1000013344	--	Atoka	Hensell	2/1994	2/2018	5	145	523	1,161
4052802	--	Bell	Washita/Fredericksburg	2/1950	2/1954	2	44	600	249
5804617	--	Bell	Washita/Fredericksburg	2/1971	2/1971	2	78	632	200
5804612	--	Bell	Washita/Fredericksburg	2/1977	2/1977	2	82	631	200
5804502	--	Bell	Washita/Fredericksburg	2/1978	3/2020	2	90	629	201
5804306	--	Bell	Washita/Fredericksburg	2/1977	2/1977	2	92	630	206
5804504	--	Bell	Washita/Fredericksburg	2/1974	2/1974	2	97	625	192
5804310	--	Bell	Washita/Fredericksburg	3/1972	3/1972	2	103	633	207
5804602	--	Bell	Washita/Fredericksburg	3/1968	2/2019	2	105	632	199
5804311	--	Bell	Washita/Fredericksburg	3/1980	2/1985	2	108	627	205

TWDB or OWRB state well number[1]	Map ID (figures 3-50 to 3-70)	County	Hydrogeologic unit	Period of record (may contain gaps) (M/Y)[2]		Layer (zero-based indexing)[3]	Well depth, in feet below land surface[4]	Row	Column
				Begin	End				
5804604	--	Bell	Washita/Fredericksburg	3/1972	3/1972	2	113	631	203
5804307	--	Bell	Washita/Fredericksburg	2/1970	2/1970	2	125	632	208
5804408	--	Bell	Washita/Fredericksburg	2/2009	3/2020	2	140	618	194
5804704	--	Bell	Washita/Fredericksburg	2/2018	3/2020	2	140	624	177
5805109	--	Bell	Washita/Fredericksburg	2/2018	3/2020	2	140	637	208
4060914	--	Bell	Washita/Fredericksburg	2/2019	2/2019	2	141	625	214
5804302	--	Bell	Washita/Fredericksburg	2/1973	2/1985	2	148	628	212
5804316	--	Bell	Washita/Fredericksburg	3/2020	3/2020	2	150	636	208
5805102	--	Bell	Washita/Fredericksburg	2/1971	2/1971	2	152	634	214
5805103	--	Bell	Washita/Fredericksburg	2/1971	2/1971	2	157	635	213
5804319	--	Bell	Washita/Fredericksburg	3/2020	3/2020	2	160	633	213
5804634	--	Bell	Washita/Fredericksburg	2/2015	3/2020	2	173	637	207
5804806	--	Bell	Washita/Fredericksburg	2/1978	2/1978	2	175	627	183
5804801	--	Bell	Washita/Fredericksburg	2/1966	2/2011	2	175	631	182
5804803	--	Bell	Washita/Fredericksburg	2/1967	2/1985	2	180	631	187
5804802	--	Bell	Washita/Fredericksburg	2/1967	2/1985	2	180	632	190
5804317	--	Bell	Washita/Fredericksburg	2/2010	3/2020	2	180	633	215
5804363	--	Bell	Washita/Fredericksburg	3/2020	3/2020	2	180	637	206
5804807	--	Bell	Washita/Fredericksburg	2/1978	2/1978	2	182	629	181
4053501	--	Bell	Washita/Fredericksburg	2/1950	2/1967	2	190	623	269
5804305	--	Bell	Washita/Fredericksburg	2/2017	3/2020	2	190	629	206
4061201	--	Bell	Washita/Fredericksburg	2/1951	2/1962	2	190	631	244
5804325	--	Bell	Washita/Fredericksburg	2/2015	2/2015	2	190	635	211
4061710	--	Bell	Washita/Fredericksburg	3/2020	3/2020	2	190	641	222
5804324	--	Bell	Washita/Fredericksburg	2/2001	2/2001	2	200	628	209

TWDB or OWRB state well number[1]	Map ID (figures 3-50 to 3-70)	County	Hydrogeologic unit	Period of record (may contain gaps) (M/Y)[2]		Layer (zero-based indexing)[3]	Well depth, in feet below land surface[4]	Row	Column
				Begin	End				
4061714	--	Bell	Washita/Fredericksburg	2/2013	2/2013	2	200	634	219
4057903	--	Bell	Glen Rose	2/2006	2/2019	4	200	549	181
5805106	--	Bell	Washita/Fredericksburg	2/2013	3/2020	2	210	640	213
4052301	--	Bell	Paluxy	2/1950	2/1953	3	220	602	272
5805108	--	Bell	Washita/Fredericksburg	2/2011	3/2020	2	240	634	217
5804811	--	Bell	Washita/Fredericksburg	2/1990	2/1990	2	250	631	181
4052202	--	Bell	Paluxy	2/1950	2/1953	3	265	594	272
4045901	--	Bell	Washita/Fredericksburg	2/1950	2/1950	2	274	618	297
5804808	--	Bell	Washita/Fredericksburg	2/1974	2/1974	2	275	632	180
4052201	--	Bell	Glen Rose	2/1950	2/1953	4	300	593	271
4053402	--	Bell	Paluxy	2/1950	2/1950	3	308	614	271
5804640	--	Bell	Washita/Fredericksburg	2/2019	3/2020	2	320	638	198
4057904	--	Bell	Glen and Rose and Hensell	3/2020	3/2020	[4, 5]	320	542	185
5802101	--	Bell	Glen and Rose and Hensell	3/2016	3/2020	[4, 5]	328	562	180
5804641	--	Bell	Washita/Fredericksburg	2/2019	2/2019	2	350	638	196
5804701	--	Bell	Glen Rose	3/1976	3/1976	4	350	620	185
5802203	--	Bell	Glen Rose	2/2014	3/2020	4	380	568	179
5812203	--	Bell	Washita/Fredericksburg	3/2012	3/2020	2	400	634	175
4045803	--	Bell	Paluxy	2/1951	2/1951	3	400	613	290
5803801	--	Bell	Glen Rose	3/1976	3/1996	4	402	604	178
4053101	--	Bell	Glen Rose	2/1951	2/1951	4	402	606	277
5804809	--	Bell	Washita/Fredericksburg	2/1978	2/1978	2	404	635	183
5805406	--	Bell	Washita/Fredericksburg	2/2015	2/2015	2	420	641	201
5805404	--	Bell	Washita/Fredericksburg	2/2002	3/2020	2	420	642	202
4058201	--	Bell	Glen Rose	2/2010	2/2019	4	435	551	212

TWDB or OWRB state well number[1]	Map ID (figures 3-50 to 3-70)	County	Hydrogeologic unit	Period of record (may contain gaps) (M/Y)[2]		Layer (zero-based indexing)[3]	Well depth, in feet below land surface[4]	Row	Column
				Begin	End				
5812204	--	Bell	Washita/Fredericksburg	3/2020	3/2020	2	450	635	175
5802304	--	Bell	Hensell	3/2020	3/2020	5	467	575	179
4057601	--	Bell	Multi-aquifer	2/2009	3/2020	[4, 5, 6]	469	538	192
5802202	--	Bell	Glen Rose	3/2016	3/2020	4	470	571	178
4058802	--	Bell	Glen Rose	2/1969	2/1969	4	490	563	186
4058801	--	Bell	Glen Rose	2/1969	2/1969	4	490	563	189
5812206	--	Bell	Washita/Fredericksburg	3/2000	3/2000	2	500	636	177
5803402	--	Bell	Glen Rose	3/2004	2/2007	4	500	592	177
5802504	--	Bell	Glen and Rose and Hensell	3/2020	3/2020	[4, 5]	510	578	168
4059803	--	Bell	Hensell and Pearsall	2/2017	3/2020	[5, 6]	595	594	206
5802103	--	Bell	Hosston	3/2004	2/2015	7	600	560	177
4058903	--	Bell	Multi-aquifer	2/2006	3/2020	[4, 5, 6]	600	573	197
5803505	--	Bell	Multi-aquifer	2/2017	3/2020	[4, 5, 6]	600	595	184
4059302	--	Bell	Glen Rose	2/2018	3/2020	4	605	588	226
4057602	--	Bell	Hosston	2/2009	3/2020	7	629	538	192
5803405	--	Bell	Glen Rose	3/2020	3/2020	4	630	590	173
5802501	--	Bell	Middle-Lower and Trinity	2/1983	2/1983	[4, 5, 6, 7]	630	577	169
5802505	--	Bell	Hensell and Pearsall	3/2020	3/2020	[5, 6]	632	575	172
5802303	--	Bell	Hosston	3/2020	3/2020	7	637	575	179
4059701	--	Bell	Multi-aquifer	2/1967	3/1996	[4, 5, 6]	640	584	201
5812305	--	Bell	Washita/Fredericksburg	3/1996	3/1996	2	650	642	176
5803404	--	Bell	Pearsall	2/2019	3/2020	6	685	594	177
4059301	--	Bell	Multi-aquifer	3/1964	3/1984	[2, 3, 4, 5, 6]	708	583	230
5804104	--	Bell	Glen Rose	3/2008	3/2020	4	720	609	204
5803408	--	Bell	Hosston	3/2020	3/2020	7	730	592	175

TWDB or OWRB state well number[1]	Map ID (figures 3-50 to 3-70)	County	Hydrogeologic unit	Period of record (may contain gaps) (M/Y)[2]		Layer (zero-based indexing)[3]	Well depth, in feet below land surface[4]	Row	Column
				Begin	End				
5803804	--	Bell	Washita/Fredericksburg and Paluxy	2/1993	3/1996	[2, 3]	735	604	178
5805401	--	Bell	Washita/Fredericksburg	2/1953	2/1953	2	740	647	204
5803506	--	Bell	Lower and Trinity	2/2018	3/2020	[5, 6, 7]	760	602	179
4059102	--	Bell	Multi-aquifer	2/1941	2/1967	[4, 5, 7]	772	568	223
4060402	--	Bell	Hensell and Pearsall	2/2006	3/2020	[5, 6]	780	604	220
5803704	--	Bell	Hensell	2/2007	3/2020	5	787	592	170
5803805	--	Bell	Hensell	3/1996	3/2004	5	787	605	176
5804406	--	Bell	Multi-aquifer	2/2001	3/2020	[4, 5, 6]	820	618	185
5804514	--	Bell	Glen Rose	2/2001	3/2020	4	860	622	194
4053707	--	Bell	Glen and Rose and Hensell	3/2016	3/2020	[4, 5]	860	616	257
5803809	--	Bell	Multi-aquifer	2/2001	2/2001	[4, 5, 6]	860	604	170
5803504	--	Bell	Pearsall and Hosston	2/2013	3/2020	[6, 7]	873	603	186
5804707	--	Bell	Glen Rose	3/2020	3/2020	4	880	624	175
4061404	--	Bell	Glen Rose	2/1965	3/1984	4	890	633	235
5804411	--	Bell	Hensell	2/2017	3/2020	5	890	622	193
5804405	--	Bell	Pearsall	2/2005	3/2020	6	895	620	193
5804706	--	Bell	Glen and Rose and Hensell	3/2020	3/2020	[4, 5]	910	624	178
4053102	--	Bell	Hensell	2/1963	3/2012	5	917	613	277
4061407	--	Bell	Glen and Rose and Hensell	2/2014	3/2020	[4, 5]	955	630	241
4061408	--	Bell	Hensell and Pearsall	3/2004	3/2020	[5, 6]	960	630	238
5804314	--	Bell	Glen and Rose and Hensell	3/2008	3/2020	[4, 5]	960	629	205
5804313	--	Bell	Hensell	2/2015	2/2019	5	980	625	211
4044901	--	Bell	Hensell	2/1966	2/1990	5	990	594	283
5804315	--	Bell	Glen and Rose and Hensell	2/2015	3/2020	[4, 5]	1,010	633	215

TWDB or OWRB state well number[1]	Map ID (figures 3-50 to 3-70)	County	Hydrogeologic unit	Period of record (may contain gaps) (M/Y)[2]		Layer (zero-based indexing)[3]	Well depth, in feet below land surface[4]	Row	Column
				Begin	End				
4045701	--	Bell	Hosston	2/2005	3/2012	7	1,014	607	283
4061105	--	Bell	Hosston	2/1965	2/1989	7	1,080	623	249
4053302	--	Bell	Hensell and Pearsall	3/1988	3/1996	[5, 6]	1,080	623	284
4061107	--	Bell	Hosston	3/1960	3/1960	7	1,093	619	249
4053405	--	Bell	Hosston	2/1974	3/2020	7	1,100	610	267
4060907	--	Bell	Hosston	2/1966	3/1996	7	1,110	622	224
4061104	--	Bell	Middle-Lower and Trinity	2/1942	2/1967	[4, 5, 6, 7]	1,186	627	241
4059802	--	Bell	Hosston	2/2006	3/2020	7	1,260	594	201
5804203	--	Bell	Pearsall and Hosston	2/2015	3/2020	[6, 7]	1,331	624	211
4053902	--	Bell	Hosston	2/1966	2/1981	7	1,355	632	264
4046901	--	Bell	Glen Rose	2/1966	2/1966	4	1,600	650	305
4054701	--	Bell	Hosston	3/1968	3/2020	7	1,669	643	263
4061601	--	Bell	Pearsall	2/1955	2/1955	6	1,685	650	247
4054501	--	Bell	Hosston	2/1934	2/1967	7	1,735	649	289
5805202	--	Bell	Hosston	2/1969	3/2020	7	1,740	649	220
5805402	--	Bell	Hosston	2/1951	2/1954	7	1,827	645	203
4054502	--	Bell	Hosston	2/1978	2/1978	7	1,828	648	283
4061901	--	Bell	Hosston	3/1964	2/2002	7	1,850	652	238
5805901	--	Bell	Upper-Middle and Trinity	2/1995	3/2020	[3, 4, 5, 6]	1,993	667	197
4062101	--	Bell	Hosston	2/1951	2/1969	7	2,136	651	262
4062501	--	Bell	Hosston	2/1966	3/2020	7	2,236	662	248
5804601	--	Bell	Hosston	2/1966	2/1994	7	2,300	633	196
4062401	--	Bell	Hosston	3/1944	3/2020	7	2,323	656	253
4062801	--	Bell	Pearsall and Hosston	2/1965	2/1990	[6, 7]	2,366	670	244
5805902	--	Bell	Hosston	2/1966	2/1999	7	2,420	666	197

TWDB or OWRB state well number[1]	Map ID (figures 3-50 to 3-70)	County	Hydrogeologic unit	Period of record (may contain gaps) (M/Y)[2]		Layer (zero-based indexing)[3]	Well depth, in feet below land surface[4]	Row	Column
				Begin	End				
5805502	--	Bell	Hosston	2/2013	3/2020	7	2,585	656	207
4055701	--	Bell	Hosston	2/1961	2/1974	7	2,652	675	283
5806201	--	Bell	Hosston	2/2013	3/2020	7	2,845	678	228
5806202	--	Bell	Hosston	3/2016	3/2020	7	2,850	671	231
5806601	--	Bell	Hosston	2/1966	2/1966	7	3,163	687	229
5806301	--	Bell	Hosston	2/2011	3/2020	7	3,247	685	243
3259501	--	Bosque	Washita/Fredericksburg	3/1960	2/1969	2	146	464	458
4001302	--	Bosque	Glen Rose	2/1966	2/1970	4	290	432	419
4004401	--	Bosque	Washita/Fredericksburg	3/1960	2/1985	2	347	497	437
3251601	--	Bosque	Hensell	2/1967	2/1975	5	375	458	503
4002108	--	Bosque	Hensell	2/1970	2/1982	5	397	437	421
4012301	--	Bosque	Paluxy	3/1968	2/1981	3	433	521	431
4014701	--	Bosque	Washita/Fredericksburg and Paluxy	3/1960	2/1967	[2, 3]	450	570	422
4011401	--	Bosque	Hensell	3/1964	2/1985	5	478	481	400
3258502	--	Bosque	Hensell	2/1967	3/1976	5	515	434	451
3259402	--	Bosque	Glen and Rose and Hensell	2/1970	2/1974	[4, 5]	611	452	452
4002111	--	Bosque	Multi-aquifer	2/2010	3/2020	[4, 6, 7]	640	436	420
4012802	--	Bosque	Lower and Trinity	3/1948	2/1983	[5, 6, 7]	646	521	405
3260701	--	Bosque	Hensell	2/1943	2/1975	5	675	485	459
4011403	--	Bosque	Hosston	2/2006	3/2020	7	686	487	391
4012804	--	Bosque	Lower and Trinity	3/1960	3/2020	[5, 6, 7]	702	521	404
4020602	--	Bosque	Glen and Rose and Hensell	3/1964	3/1972	[4, 5]	715	547	381
3261703	--	Bosque	Hensell and Pearsall	3/1964	2/1982	[5, 6]	746	509	470
4003604	--	Bosque	Hosston	2/1973	2/2011	7	758	483	432

TWDB or OWRB state well number[1]	Map ID (figures 3-50 to 3-70)	County	Hydrogeologic unit	Period of record (may contain gaps) (M/Y)[2]		Layer (zero-based indexing)[3]	Well depth, in feet below land surface[4]	Row	Column
				Begin	End				
4003601	--	Bosque	Hosston	2/1949	3/1976	7	759	486	430
4003603	--	Bosque	Hosston	2/1963	2/2011	7	838	488	432
3260201	--	Bosque	Hosston	2/2010	3/2012	7	860	484	488
4012201	--	Bosque	Glen and Rose and Hensell	2/1970	3/1992	[4, 5]	875	516	425
4010103	--	Bosque	Hosston	2/1989	2/1989	7	890	453	397
3260704	--	Bosque	Multi-aquifer	2/2006	3/2020	[2, 3, 4, 5, 6, 7]	906	485	460
4019202	--	Bosque	Multi-aquifer	2/1995	3/2020	[2, 3, 4, 5, 6, 7]	910	506	381
3261709	--	Bosque	Hosston	3/1988	3/2020	7	932	509	470
4003702	--	Bosque	Hosston	2/1978	2/2006	7	980	475	415
4003703	--	Bosque	Multi-aquifer	2/1995	3/2020	[2, 3, 4, 5, 6]	980	477	415
4020704	--	Bosque	Hosston	2/1982	3/2020	7	1,020	535	363
4022103	--	Bosque	Lower and Trinity	2/1999	3/2020	[5, 6, 7]	1,232	575	417
4022203	--	Bosque	Multi-aquifer	3/2016	3/2020	[2, 3, 4]	1,234	578	421
4014508	--	Bosque	Hensell	2/1966	2/1970	5	1,262	572	444
1000013976	--	Bryan	Washita/Fredericksburg	3/2000	2/2015	2	175	530	1,013
1000027985	--	Bryan	Woodbine	2/1994	2/2014	1	294	539	1,070
1000009131	--	Bryan	Washita/Fredericksburg	2/1977	2/2019	2	400	565	1,118
1000039489	--	Bryan	Woodbine and Washita/Fredericksburg	3/2000	2/2006	[1, 2]	400	501	1,050
1000156700	--	Bryan	Paluxy	2/2015	2/2019	3	500	550	1,119
5715702	--	Burnet	Hosston	2/1961	3/2020	7	78	505	83
5715903	--	Burnet	Glen and Rose and Hensell	2/2009	3/2020	[4, 5]	90	522	99
5723402	--	Burnet	Hosston	2/1957	2/1974	7	200	514	63
4164801	--	Burnet	Pearsall	2/1961	2/1975	6	270	514	164

TWDB or OWRB state well number[1]	Map ID (figures 3-50 to 3-70)	County	Hydrogeologic unit	Period of record (may contain gaps) (M/Y)[2]		Layer (zero-based indexing)[3]	Well depth, in feet below land surface[4]	Row	Column
				Begin	End				
5715302	--	Burnet	Pearsall	2/2019	3/2020	6	288	508	113
5708301	--	Burnet	Hensell and Pearsall	3/1968	2/1986	[5, 6]	317	526	155
5716901	--	Burnet	Glen Rose	2/1966	2/1986	4	330	548	110
5715804	--	Burnet	Pearsall and Hosston	2/1966	2/1998	[6, 7]	356	517	84
5715901	--	Burnet	Hosston	2/2010	2/2019	7	425	522	90
5716201	--	Burnet	Lower and Trinity	3/2012	3/2020	[5, 6, 7]	425	535	124
5724801	--	Burnet	Pearsall and Hosston	2/1961	2/1970	[6, 7]	456	551	73
5724202	--	Burnet	Pearsall and Hosston	2/1966	2/1966	[6, 7]	469	546	96
5723603	--	Burnet	Middle-Lower and Trinity	2/2009	3/2020	[4, 5, 6, 7]	500	532	69
5801801	--	Burnet	Multi-aquifer	2/1966	2/1974	[4, 5, 6]	508	554	145
5809201	--	Burnet	Lower and Trinity	2/2011	3/2020	[5, 6, 7]	540	560	132
5809702	--	Burnet	Hosston	2/2019	3/2020	7	545	556	116
5724601	--	Burnet	Hosston	3/2016	3/2020	7	545	557	86
5809701	--	Burnet	Pearsall and Hosston	2/2017	2/2019	[6, 7]	550	555	108
5809304	--	Burnet	Pearsall	3/2020	3/2020	6	620	564	137
5801202	--	Burnet	Pearsall and Hosston	2/2009	3/2020	[6, 7]	700	542	167
5809303	--	Burnet	Hensell and Hosston	2/2009	3/2020	[5, 7]	780	563	141
5724503	--	Burnet	Hosston	2/2009	3/2020	7	800	552	82
1000050341	--	Carter	Hosston	2/2015	2/2015	7	235	354	1,046
1000076706	--	Choctaw	Washita/Fredericksburg	2/2015	2/2019	2	142	640	1,135
1000148110	--	Choctaw	Paluxy	2/2017	2/2019	3	200	708	1,206
1000024990	--	Choctaw	Washita/Fredericksburg and Paluxy	2/2019	2/2019	[2, 3]	320	629	1,147
1000009174	--	Choctaw	Washita/Fredericksburg	3/1976	2/2019	2	370	594	1,135

TWDB or OWRB state well number[1]	Map ID (figures 3-50 to 3-70)	County	Hydrogeologic unit	Period of record (may contain gaps) (M/Y)[2]		Layer (zero-based indexing)[3]	Well depth, in feet below land surface[4]	Row	Column
				Begin	End				
1842603	--	Collin	Woodbine	2/1970	3/1980	1	771	497	869
1850301	--	Collin	Woodbine	3/1996	3/2008	1	958	506	847
1859702	--	Collin	Woodbine	2/1971	2/1971	1	980	548	800
1850901	--	Collin	Woodbine and Washita/Fredericksburg	2/1963	2/1977	[1, 2]	1,050	516	825
1851701	--	Collin	Woodbine	2/1970	2/1986	1	1,104	532	832
1851901	--	Collin	Woodbine	2/1970	2/1985	1	1,209	546	831
1843204	--	Collin	Woodbine and Washita/Fredericksburg	2/1971	2/1997	[1, 2]	1,216	517	885
1851902	--	Collin	Woodbine	2/1970	2/1998	1	1,415	543	837
1836803	--	Collin	Woodbine	3/1980	2/2017	1	1,450	532	908
1844804	--	Collin	Woodbine	2/2010	2/2017	1	1,450	543	879
1844803	--	Collin	Woodbine	2/1993	2/2009	1	1,506	544	879
1844202	--	Collin	Woodbine	2/1977	2/1977	1	1,557	542	897
1852301	--	Collin	Woodbine	2/1970	2/1977	1	1,577	564	873
1850802	--	Collin	Paluxy and Glen and Rose	2/1973	2/1999	[3, 4]	1,632	510	820
1850205	--	Collin	Paluxy and Glen and Rose	2/1993	3/2012	[3, 4]	1,656	504	843
1858803	--	Collin	Paluxy and Glen and Rose	2/1975	2/1978	[3, 4]	1,744	525	790
1852302	--	Collin	Woodbine	3/2020	3/2020	1	1,784	562	877
1845301	--	Collin	Woodbine and Washita/Fredericksburg	3/2020	3/2020	[1, 2]	1,927	573	910
1846701	--	Collin	Woodbine	3/2020	3/2020	1	2,008	586	901
1844204	--	Collin	Paluxy	2/1993	3/2020	3	2,288	540	899

TWDB or OWRB state well number[1]	Map ID (figures 3-50 to 3-70)	County	Hydrogeologic unit	Period of record (may contain gaps) (M/Y)[2]		Layer (zero-based indexing)[3]	Well depth, in feet below land surface[4]	Row	Column
				Begin	End				
1842302	--	Collin	Hensell and Pearsall	2/1993	3/2020	[5, 6]	2,398	499	872
1850502	--	Collin	Hosston	3/1980	2/2007	7	2,662	507	833
1860901	--	Collin	Paluxy	2/1971	2/1989	3	2,790	585	815
1850803	--	Collin	Multi-aquifer	2/1993	2/2001	[2, 5, 6, 7]	2,796	510	820
1851702	--	Collin	Hosston	2/2007	2/2015	7	3,105	529	829
4105801	--	Comanche	Hosston	2/1959	2/1974	7	85	328	342
3152503	--	Comanche	Hosston	2/1965	2/1974	7	93	264	398
4103206	--	Comanche	Hosston	2/1997	3/2020	7	95	260	333
3153721	--	Comanche	Hosston	2/1965	2/1974	7	105	283	403
3153414	--	Comanche	Hosston	3/1968	3/2000	7	115	279	405
4105902	--	Comanche	Hosston	2/1959	2/1971	7	118	339	347
3151907	--	Comanche	Hosston	2/1971	2/1995	7	123	253	386
3152214	--	Comanche	Hosston	3/1964	2/1973	7	125	261	419
3160106	--	Comanche	Hosston	2/1971	2/1974	7	129	262	376
4104603	--	Comanche	Hosston	2/1959	2/1970	7	130	302	342
3161816	--	Comanche	Hosston	2/1965	2/1987	7	130	306	372
4106901	--	Comanche	Hensell	2/1965	2/1973	5	150	365	358
4114303	--	Comanche	Lower and Trinity	2/1966	2/1982	[5, 6, 7]	150	371	346
3161210	--	Comanche	Hosston	2/1971	2/1974	7	152	296	393
4105503	--	Comanche	Hosston	2/1965	2/1975	7	156	322	356
4113201	--	Comanche	Hosston	2/1965	3/1992	7	160	329	331
4112304	--	Comanche	Hosston	2/1965	2/1986	7	165	314	331
3151805	--	Comanche	Hosston	2/1965	2/1974	7	170	244	376
4113302	--	Comanche	Hosston	2/1969	2/1974	7	185	338	333
3151309	--	Comanche	Hensell and Pearsall	3/1968	3/1988	[5, 6]	200	246	402

TWDB or OWRB state well number[1]	Map ID (figures 3-50 to 3-70)	County	Hydrogeologic unit	Period of record (may contain gaps) (M/Y)[2]		Layer (zero-based indexing)[3]	Well depth, in feet below land surface[4]	Row	Column
				Begin	End				
4115401	--	Comanche	Hosston	3/1968	3/1988	7	205	374	347
4112401	--	Comanche	Hensell	2/1970	3/1988	5	278	301	301
4114702	--	Comanche	Hensell	2/1966	2/1982	5	300	361	321
4111412	--	Comanche	Pearsall and Hosston	2/1970	3/1988	[6, 7]	482	277	295
1913703	--	Cooke	Pearsall	2/2013	3/2020	6	180	300	906
1913403	--	Cooke	Hosston	2/2001	3/2020	7	180	293	916
1921601	--	Cooke	Glen Rose	2/1970	2/1986	4	220	325	897
1930701	--	Cooke	Paluxy and Glen and Rose	2/1970	3/1980	[3, 4]	260	354	853
1930201	--	Cooke	Glen Rose	2/1970	2/1989	4	305	349	886
1915101	--	Cooke	Glen Rose	2/1970	3/1984	4	342	341	953
1913103	--	Cooke	Hosston	2/2011	3/2020	7	355	290	924
1923701	--	Cooke	Glen Rose	2/1970	2/1991	4	380	364	902
1932801	--	Cooke	Washita/Fredericksburg	2/1973	2/1983	2	550	410	891
1924801	--	Cooke	Paluxy	2/1970	2/1978	3	580	398	921
1930702	--	Cooke	Hensell and Pearsall	3/1972	2/1993	[5, 6]	604	354	858
1922707	--	Cooke	Multi-aquifer	2/2015	3/2020	[3, 4, 5]	625	338	886
1921902	--	Cooke	Hosston	2/1953	3/2020	7	683	333	886
1921901	--	Cooke	Hensell and Pearsall	2/1957	2/1970	[5, 6]	712	333	888
1916802	--	Cooke	Paluxy	2/1970	2/1986	3	730	384	952
1939301	--	Cooke	Multi-aquifer	3/1944	3/2020	[2, 3, 4, 5, 6]	817	397	868
1923901	--	Cooke	Hensell	2/1993	2/2011	5	904	385	909
1923503	--	Cooke	Lower and Trinity	2/1942	3/2020	[5, 6, 7]	912	365	919
1923805	--	Cooke	Pearsall and Hosston	2/1977	3/2020	[6, 7]	927	375	904
1923903	--	Cooke	Pearsall and Hosston	2/1941	3/1996	[6, 7]	931	382	903
1923906	--	Cooke	Pearsall and Hosston	2/1977	3/2020	[6, 7]	982	381	909

TWDB or OWRB state well number[1]	Map ID (figures 3-50 to 3-70)	County	Hydrogeologic unit	Period of record (may contain gaps) (M/Y)[2]		Layer (zero-based indexing)[3]	Well depth, in feet below land surface[4]	Row	Column
				Begin	End				
1929201	--	Cooke	Pearsall	2/1977	3/1996	6	1,040	329	873
1932803	--	Cooke	Multi-aquifer	3/1980	2/1995	[4, 5, 6]	1,300	413	886
1932302	--	Cooke	Lower and Trinity	2/1977	3/2016	[5, 6, 7]	1,301	414	907
1825201	--	Cooke	Multi-aquifer	2/1998	2/1998	[4, 5, 6]	1,400	431	916
1940201	--	Cooke	Hosston	3/1972	3/2020	7	1,422	420	876
1924904	--	Cooke	Lower and Trinity	3/2020	3/2020	[5, 6, 7]	1,430	405	925
4027401	--	Coryell	Washita/Fredericksburg and Paluxy	2/1961	2/1999	[2, 3]	217	512	329
4033102	--	Coryell	Hensell	2/1970	2/2005	5	297	470	283
4140801	--	Coryell	Glen Rose	3/2016	3/2020	4	315	460	257
4140203	--	Coryell	Hensell	3/1968	2/1985	5	320	460	277
4019803	--	Coryell	Washita/Fredericksburg and Paluxy	2/1965	2/1974	[2, 3]	334	508	359
4025404	--	Coryell	Hensell	3/1968	3/1972	5	337	462	306
4041702	--	Coryell	Multi-aquifer	3/1968	3/1980	[4, 5, 6]	364	496	228
4028402	--	Coryell	Paluxy and Glen and Rose	3/1964	3/1984	[3, 4]	410	540	340
4025902	--	Coryell	Hensell	3/1968	3/1988	5	417	487	305
4139307	--	Coryell	Multi-aquifer	2/2010	3/2020	[4, 5, 6]	425	438	270
4033603	--	Coryell	Glen and Rose and Hensell	2/1970	3/1992	[4, 5]	430	493	280
4049601	--	Coryell	Hensell and Pearsall	2/1993	3/2020	[5, 6]	440	521	224
4034201	--	Coryell	Hensell	2/1970	3/1988	5	445	505	302
4148101	--	Coryell	Hensell	2/1966	2/1969	5	455	461	248
4041201	--	Coryell	Hensell and Pearsall	3/1968	2/1982	[5, 6]	455	494	253
4139303	--	Coryell	Hosston	2/1965	3/1984	7	486	436	268
4049403	--	Coryell	Pearsall	2/1967	2/1999	6	496	506	215

TWDB or OWRB state well number[1]	Map ID (figures 3-50 to 3-70)	County	Hydrogeologic unit	Period of record (may contain gaps) (M/Y)[2]		Layer (zero-based indexing)[3]	Well depth, in feet below land surface[4]	Row	Column
				Begin	End				
4139305	--	Coryell	Hensell and Pearsall	2/1970	2/1995	[5, 6]	505	437	268
4034604	--	Coryell	Hensell	3/1964	2/1974	5	524	518	296
4057303	--	Coryell	Lower and Trinity	2/1951	2/1969	[5, 6, 7]	573	533	206
4041601	--	Coryell	Middle-Lower and Trinity	2/1963	2/1974	[4, 5, 6, 7]	613	513	257
4026102	--	Coryell	Hosston	2/1965	2/1974	7	622	478	331
4035401	--	Coryell	Middle-Lower and Trinity	2/1933	3/1964	[4, 5, 6, 7]	680	527	301
4019901	--	Coryell	Glen and Rose and Hensell	2/1970	2/1978	[4, 5]	792	516	365
4035701	--	Coryell	Hosston	3/1964	2/1982	7	821	537	297
4026201	--	Coryell	Lower and Trinity	2/1990	3/2020	[5, 6, 7]	908	493	340
4043603	--	Coryell	Hosston	2/1965	2/1974	7	990	568	280
4027102	--	Coryell	Lower and Trinity	2/1963	2/1995	[5, 6, 7]	1,003	507	345
4045402	--	Coryell	Multi-aquifer	2/1967	3/1996	[2, 3, 4, 5, 6, 7]	1,030	599	300
4035502	--	Coryell	Hosston	3/1992	3/2020	7	1,054	540	311
4028404	--	Coryell	Pearsall and Hosston	2/1970	3/1996	[6, 7]	1,076	539	339
4036301	--	Coryell	Pearsall and Hosston	3/1988	3/2008	[6, 7]	1,103	569	330
4044902	--	Coryell	Pearsall and Hosston	3/1968	2/1974	[6, 7]	1,126	593	286
4036603	--	Coryell	Lower and Trinity	2/2001	3/2020	[5, 6, 7]	1,160	577	320
3317401	--	Dallas	Woodbine	2/1971	2/1971	1	250	531	688
3208301	--	Dallas	Woodbine	2/1951	2/1965	1	269	490	759
3232301	--	Dallas	Woodbine	2/1970	2/1978	1	314	532	667
3309506	--	Dallas	Woodbine	2/1971	2/1986	1	325	529	728
3224901	--	Dallas	Woodbine	2/1971	2/1993	1	356	533	675
3224302	--	Dallas	Multi-aquifer	3/1956	2/1978	[2, 3, 4]	1,151	524	698
3310301	--	Dallas	Woodbine	3/1968	2/1978	1	1,154	559	754
3326303	--	Dallas	Woodbine	2/1950	2/1977	1	1,200	592	689

TWDB or OWRB state well number[1]	Map ID (figures 3-50 to 3-70)	County	Hydrogeologic unit	Period of record (may contain gaps) (M/Y)[2]		Layer (zero-based indexing)[3]	Well depth, in feet below land surface[4]	Row	Column
				Begin	End				
3319301	--	Dallas	Woodbine	3/1956	2/1991	1	1,600	601	737
3309704	--	Dallas	Hosston	2/2010	2/2010	7	2,001	520	710
3224305	--	Dallas	Multi-aquifer	2/2010	2/2010	[1, 2, 3, 4, 5, 6]	2,047	519	698
3224908	--	Dallas	Multi-aquifer	3/1988	2/2010	[2, 3, 4, 5, 6, 7]	2,060	529	674
3224307	--	Dallas	Hosston	2/1974	2/2010	7	2,062	521	694
3309402	--	Dallas	Hosston	2/1965	2/2010	7	2,084	516	716
3317116	--	Dallas	Pearsall and Hosston	2/1971	2/2010	[6, 7]	2,084	529	697
3309703	--	Dallas	Hosston	2/2010	2/2010	7	2,163	529	708
3325202	--	Dallas	Hosston	3/2000	2/2019	7	2,568	551	667
3310705	--	Dallas	Hosston	2/1941	3/1956	7	2,634	551	719
3318205	--	Dallas	Pearsall and Hosston	2/1934	3/1956	[6, 7]	2,745	562	720
3303901	--	Dallas	Middle-Lower and Trinity	3/1952	3/1984	[4, 5, 6, 7]	3,689	578	780
3320102	--	Dallas	Hosston	2/1969	2/1977	7	4,084	608	736
1956602	--	Denton	Woodbine	3/1976	3/2020	1	60	461	806
1841708	--	Denton	Woodbine	3/2008	3/2020	1	145	460	835
1946601	--	Denton	Washita/Fredericksburg	2/1970	2/1991	2	249	400	810
1964901	--	Denton	Woodbine	2/1970	2/2003	1	260	479	768
1849901	--	Denton	Woodbine	2/1970	2/1974	1	275	496	814
1964306	--	Denton	Woodbine and Washita/Fredericksburg	2/1974	2/2001	[1, 2]	308	477	790
1948101	--	Denton	Washita/Fredericksburg	2/1970	3/1980	2	350	427	838
1939801	--	Denton	Paluxy	2/1970	3/1984	3	366	404	838
1849801	--	Denton	Woodbine	2/1970	3/1992	1	420	491	808
1954901	--	Denton	Paluxy	2/1969	3/1984	3	450	415	777
3207106	--	Denton	Paluxy and Glen and Rose	2/1941	2/1963	[3, 4]	615	444	740

TWDB or OWRB state well number[1]	Map ID (figures 3-50 to 3-70)	County	Hydrogeologic unit	Period of record (may contain gaps) (M/Y)[2]		Layer (zero-based indexing)[3]	Well depth, in feet below land surface[4]	Row	Column
				Begin	End				
1948501	--	Denton	Paluxy	2/1973	2/2003	3	641	442	836
1948711	--	Denton	Paluxy	2/2014	3/2020	3	710	442	819
1946701	--	Denton	Multi-aquifer	2/1987	2/2011	[2, 3, 4]	816	387	797
1849101	--	Denton	Paluxy	2/1970	3/1996	3	915	468	822
1841706	--	Denton	Paluxy	2/1983	3/1992	3	957	457	835
1947201	--	Denton	Pearsall and Hosston	2/1970	2/1986	[6, 7]	968	411	836
1946702	--	Denton	Lower and Trinity	3/2012	3/2016	[5, 6, 7]	970	387	797
1947901	--	Denton	Multi-aquifer	2/1953	2/1983	[4, 5, 6]	1,200	433	814
1956101	--	Denton	Hensell and Pearsall	3/1952	2/1983	[5, 6]	1,214	442	806
1857802	--	Denton	Washita/Fredericksburg and Paluxy	2/2010	3/2020	[2, 3]	1,245	502	780
1857901	--	Denton	Paluxy	2/1970	2/1995	3	1,308	505	782
1955302	--	Denton	Multi-aquifer	2/1951	2/1958	[3, 4, 5]	1,333	431	801
1857601	--	Denton	Paluxy and Glen and Rose	3/2020	3/2020	[3, 4]	1,432	505	797
1833801	--	Denton	Hensell and Pearsall	2/1966	2/1985	[5, 6]	1,489	453	865
1849102	--	Denton	Pearsall	2/1970	3/1988	6	1,542	469	822
1964406	--	Denton	Lower and Trinity	2/2006	3/2020	[5, 6, 7]	1,600	463	773
1964505	--	Denton	Pearsall	2/1986	3/2012	6	1,652	469	779
1964211	--	Denton	Lower and Trinity	2/1997	3/2012	[5, 6, 7]	1,664	464	778
1964308	--	Denton	Hosston	3/1976	3/2012	7	1,770	472	783
1964506	--	Denton	Multi-aquifer	3/1992	3/2012	[1, 2, 3, 4, 5]	1,778	472	777
1857602	--	Denton	Hosston	2/1974	3/2020	7	2,405	505	797
3151215	--	Eastland	Hosston	2/1965	2/1974	7	96	232	398
3144502	--	Eastland	Hensell	2/1965	2/1974	5	115	251	432
3151306	--	Eastland	Pearsall and Hosston	2/1966	2/1975	[6, 7]	269	239	410

TWDB or OWRB state well number[1]	Map ID (figures 3-50 to 3-70)	County	Hydrogeologic unit	Period of record (may contain gaps) (M/Y)[2]		Layer (zero-based indexing)[3]	Well depth, in feet below land surface[4]	Row	Column
				Begin	End				
3248202	--	Ellis	Woodbine	2/1985	3/2020	1	347	561	601
3232803	--	Ellis	Woodbine	2/1971	2/1982	1	355	538	637
3240207	--	Ellis	Washita/Fredericksburg	3/2020	3/2020	2	405	541	628
3248602	--	Ellis	Woodbine	3/1956	3/2020	1	410	574	592
3240209	--	Ellis	Washita/Fredericksburg	3/2020	3/2020	2	417	542	628
3240208	--	Ellis	Woodbine	3/2020	3/2020	1	419	544	626
3248605	--	Ellis	Washita/Fredericksburg	3/2020	3/2020	2	462	574	593
3240305	--	Ellis	Woodbine	2/1971	2/1995	1	543	550	634
3333103	--	Ellis	Woodbine	3/1940	3/1956	1	699	556	637
3341202	--	Ellis	Woodbine	2/1965	3/1972	1	727	583	608
3325901	--	Ellis	Woodbine	2/1959	2/1971	1	735	574	659
3240612	--	Ellis	Woodbine and Washita/Fredericksburg	2/2019	2/2019	[1, 2]	740	558	619
3333501	--	Ellis	Woodbine	3/1968	3/1984	1	780	574	638
3325409	--	Ellis	Washita/Fredericksburg	3/2020	3/2020	2	840	555	655
3341403	--	Ellis	Woodbine and Washita/Fredericksburg	2/2018	3/2020	[1, 2]	840	581	601
3341404	--	Ellis	Woodbine and Washita/Fredericksburg	2/2018	3/2020	[1, 2]	840	581	602
3325803	--	Ellis	Woodbine	3/2012	3/2020	1	874	558	655
3325712	--	Ellis	Washita/Fredericksburg	3/2020	3/2020	2	880	556	654
3357202	--	Ellis	Woodbine and Washita/Fredericksburg	3/1964	3/2020	[1, 2]	900	611	554
3349602	--	Ellis	Woodbine	2/1957	2/1977	1	935	615	573
3334209	--	Ellis	Woodbine	3/1988	3/2020	1	1,120	593	650
3326822	--	Ellis	Woodbine and Washita/Fredericksburg	2/1985	3/2020	[1, 2]	1,178	587	669
3342201	--	Ellis	Washita/Fredericksburg	2/1965	2/1982	2	1,285	612	630

TWDB or OWRB state well number[1]	Map ID (figures 3-50 to 3-70)	County	Hydrogeologic unit	Period of record (may contain gaps) (M/Y)[2]		Layer (zero-based indexing)[3]	Well depth, in feet below land surface[4]	Row	Column
				Begin	End				
3335702	--	Ellis	Woodbine	3/1964	2/1977	1	1,321	620	639
3328703	--	Ellis	Woodbine	2/1971	2/1978	1	1,350	630	687
3343101	--	Ellis	Woodbine	2/1983	2/1983	1	1,365	629	631
3335504	--	Ellis	Woodbine	2/1985	2/1995	1	1,440	627	657
3327801	--	Ellis	Woodbine	2/1965	3/1972	1	1,447	612	675
3343204	--	Ellis	Woodbine	2/1985	3/1996	1	1,448	634	641
3335503	--	Ellis	Woodbine	3/1964	2/1977	1	1,522	631	658
3336201	--	Ellis	Woodbine	3/1960	2/1997	1	1,982	647	676
3248606	--	Ellis	Pearsall and Hosston	3/1992	3/2020	[6, 7]	2,066	574	592
3256603	--	Ellis	Hosston	2/2005	2/2019	7	2,245	585	565
3256301	--	Ellis	Hosston	2/1999	2/2019	7	2,400	588	570
3333203	--	Ellis	Pearsall and Hosston	2/1986	3/2020	[6, 7]	2,530	563	645
3341207	--	Ellis	Pearsall	2/2019	2/2019	6	2,566	578	614
3341501	--	Ellis	Hosston	2/1965	2/1975	7	2,606	588	605
3325802	--	Ellis	Hosston	2/1974	2/1977	7	2,662	564	654
3333304	--	Ellis	Pearsall and Hosston	3/2020	3/2020	[6, 7]	2,790	579	647
3334703	--	Ellis	Hosston	2/1973	2/1981	7	2,950	600	627
3334702	--	Ellis	Hosston	2/1913	2/1978	7	2,950	600	628
3326817	--	Ellis	Hosston	2/1977	3/2020	7	3,065	587	669
3334210	--	Ellis	Hosston	3/1984	2/2006	7	3,085	594	651
3334207	--	Ellis	Hosston	2/2011	3/2020	7	3,088	593	650
3350202	--	Ellis	Hosston	2/1977	3/2020	7	3,204	630	592
3146101	--	Erath	Hosston	2/1970	3/2020	7	59	286	469
3138602	--	Erath	Hosston	2/1990	3/2020	7	115	295	493
3153403	--	Erath	Pearsall and Hosston	2/1965	2/1978	[6, 7]	161	279	412

TWDB or OWRB state well number[1]	Map ID (figures 3-50 to 3-70)	County	Hydrogeologic unit	Period of record (may contain gaps) (M/Y)[2]		Layer (zero-based indexing)[3]	Well depth, in feet below land surface[4]	Row	Column
				Begin	End				
3153503	--	Erath	Pearsall	2/1965	2/1971	6	177	291	410
3161301	--	Erath	Hensell and Pearsall	2/1959	2/1986	[5, 6]	188	302	402
3163301	--	Erath	Multi-aquifer	3/1968	2/1991	[4, 5, 6]	202	360	422
3147302	--	Erath	Hensell and Pearsall	2/1993	3/2020	[5, 6]	240	329	484
3148901	--	Erath	Hensell	2/1970	2/1974	5	274	365	473
3147501	--	Erath	Hensell and Pearsall	2/1970	3/1988	[5, 6]	275	329	467
3164402	--	Erath	Hensell	2/1971	2/1986	5	281	380	418
3163901	--	Erath	Hensell	2/1966	2/1986	5	289	375	405
3162303	--	Erath	Hensell	2/1993	2/2019	5	297	332	406
3139502	--	Erath	Hosston	2/1965	2/1987	7	308	310	497
3153601	--	Erath	Pearsall and Hosston	2/1967	2/2003	[6, 7]	317	304	416
3146907	--	Erath	Hensell	2/2007	3/2020	5	330	317	453
3155504	--	Erath	Pearsall and Hosston	3/2000	3/2020	[6, 7]	332	343	444
3164607	--	Erath	Hensell	3/2000	2/2003	5	333	391	431
3164301	--	Erath	Hensell	3/1968	2/1973	5	353	387	438
3155803	--	Erath	Lower and Trinity	2/1963	3/2020	[5, 6, 7]	360	344	432
3155107	--	Erath	Hensell and Hosston	2/1966	2/1990	[5, 7]	364	333	447
3153303	--	Erath	Hensell	3/1964	2/1974	5	365	295	435
3146207	--	Erath	Lower and Trinity	2/1995	2/1995	[5, 6, 7]	380	300	468
3154801	--	Erath	Hosston	2/1965	2/1975	7	387	321	421
3155807	--	Erath	Lower and Trinity	2/1993	3/2020	[5, 6, 7]	396	347	427
3156201	--	Erath	Pearsall	2/1995	2/2005	6	405	359	464
3164101	--	Erath	Hensell and Pearsall	3/1968	2/1978	[5, 6]	405	373	425
3146901	--	Erath	Hosston	2/1963	2/1971	7	435	315	451
3155201	--	Erath	Pearsall and Hosston	3/1960	3/1980	[6, 7]	440	337	455

TWDB or OWRB state well number[1]	Map ID (figures 3-50 to 3-70)	County	Hydrogeologic unit	Period of record (may contain gaps) (M/Y)[2]		Layer (zero-based indexing)[3]	Well depth, in feet below land surface[4]	Row	Column
				Begin	End				
3164602	--	Erath	Hensell	2/1970	2/1982	5	454	391	421
3162104	--	Erath	Hensell and Pearsall	2/1967	2/1981	[5, 6]	469	320	401
3155208	--	Erath	Hosston	2/1918	2/1971	7	519	331	453
3164305	--	Erath	Pearsall and Hosston	3/2016	3/2020	[6, 7]	550	385	434
4056301	--	Falls	Pearsall and Hosston	3/1940	2/1974	[6, 7]	3,300	704	320
3933604	--	Falls	Hosston	2/1965	2/1975	7	3,651	705	383
1822801	--	Fannin	Woodbine	2/1970	2/2019	1	179	556	994
1814906	--	Fannin	Woodbine	3/1960	2/2019	1	220	547	1,026
1815902	--	Fannin	Woodbine	2/1970	2/2017	1	489	572	1,046
1830102	--	Fannin	Woodbine	3/1936	2/1977	1	528	548	978
1823301	--	Fannin	Woodbine	2/1970	2/1995	1	800	579	1,029
1717602	--	Fannin	Woodbine	2/1971	3/1988	1	1,208	629	1,049
1717401	--	Fannin	Woodbine	2/1970	3/1984	1	1,236	619	1,037
1831602	--	Fannin	Woodbine and Washita/Fredericksburg	2/1965	2/1983	[1, 2]	1,480	598	996
1839501	--	Fannin	Woodbine	2/1959	3/2016	1	1,595	609	958
1847101	--	Fannin	Woodbine	3/1944	2/1970	1	1,605	601	935
1838402	--	Fannin	Woodbine	2/1969	3/1988	1	1,606	573	940
1725302	--	Fannin	Woodbine and Washita/Fredericksburg	2/1963	3/2020	[1, 2]	1,660	642	1,026
1839701	--	Fannin	Woodbine	2/1957	3/1960	1	1,690	599	939
1725401	--	Fannin	Woodbine	3/1936	3/1984	1	1,691	628	1,008
1734101	--	Fannin	Paluxy	2/1965	2/1993	3	3,063	664	1,004
1810601	--	Grayson	Woodbine	2/1970	2/1982	1	234	438	983

TWDB or OWRB state well number[1]	Map ID (figures 3-50 to 3-70)	County	Hydrogeologic unit	Period of record (may contain gaps) (M/Y)[2]		Layer (zero-based indexing)[3]	Well depth, in feet below land surface[4]	Row	Column
				Begin	End				
1825301	--	Grayson	Woodbine	3/1972	2/2017	1	280	438	919
1812401	--	Grayson	Paluxy	2/1970	2/2007	3	295	473	1,002
1821901	--	Grayson	Woodbine and Washita/Fredericksburg	2/1965	2/1977	[1, 2]	301	536	989
1811801	--	Grayson	Washita/Fredericksburg	2/1970	3/2020	2	375	465	987
1834601	--	Grayson	Woodbine	2/1957	2/1990	1	387	483	895
1818901	--	Grayson	Woodbine	2/1970	2/1985	1	390	461	943
1834101	--	Grayson	Woodbine	2/1970	3/2004	1	400	466	893
1810201	--	Grayson	Washita/Fredericksburg and Paluxy	2/1970	2/1989	[2, 3]	490	425	993
1811805	--	Grayson	Woodbine and Washita/Fredericksburg	2/1962	2/1990	[1, 2]	496	464	983
1820101	--	Grayson	Woodbine	2/1970	2/1971	1	630	482	978
1829301	--	Grayson	Woodbine	3/1936	3/2020	1	709	538	976
1820707	--	Grayson	Woodbine	3/1992	2/2013	1	786	490	963
1819301	--	Grayson	Washita/Fredericksburg	2/1969	3/2020	2	788	474	975
1819302	--	Grayson	Woodbine	2/1970	2/2018	1	790	474	976
1835406	--	Grayson	Woodbine	3/1960	2/1971	1	838	488	901
1827801	--	Grayson	Woodbine	2/1973	2/2013	1	950	487	927
1820901	--	Grayson	Washita/Fredericksburg	3/2020	3/2020	2	950	515	972
1820711	--	Grayson	Woodbine	2/1957	2/1997	1	955	494	969
1820401	--	Grayson	Woodbine and Washita/Fredericksburg	3/1992	2/2013	[1, 2]	1,012	490	971

TWDB or OWRB state well number[1]	Map ID (figures 3-50 to 3-70)	County	Hydrogeologic unit	Period of record (may contain gaps) (M/Y)[2]		Layer (zero-based indexing)[3]	Well depth, in feet below land surface[4]	Row	Column
				Begin	End				
1828103	--	Grayson	Woodbine	3/1992	2/2013	1	1,023	501	949
1835601	--	Grayson	Woodbine	3/2020	3/2020	1	1,023	509	913
1820801	--	Grayson	Woodbine	2/1966	2/2013	1	1,025	499	966
1820804	--	Grayson	Woodbine	2/1977	3/2008	1	1,044	503	966
1828402	--	Grayson	Woodbine	2/1970	2/2013	1	1,050	500	946
1820604	--	Grayson	Washita/Fredericksburg	2/1977	2/1977	2	1,050	504	982
1827804	--	Grayson	Woodbine	3/1992	3/2008	1	1,061	494	928
1820609	--	Grayson	Washita/Fredericksburg and Paluxy	3/2020	3/2020	[2, 3]	1,130	501	985
1828705	--	Grayson	Woodbine and Washita/Fredericksburg	2/1977	3/2020	[1, 2]	1,134	504	934
1829902	--	Grayson	Woodbine	2/1938	3/2020	1	1,189	554	954
1828504	--	Grayson	Woodbine	3/1992	2/2013	1	1,202	515	948
1828802	--	Grayson	Woodbine	2/1982	2/2013	1	1,207	514	942
1828605	--	Grayson	Woodbine	2/1983	3/2008	1	1,265	517	955
1829904	--	Grayson	Washita/Fredericksburg	2/1973	3/2020	2	1,388	554	953
1836502	--	Grayson	Washita/Fredericksburg	2/1955	2/1995	2	1,401	526	913
1836504	--	Grayson	Woodbine	3/1968	2/1985	1	1,425	526	916
1825603	--	Grayson	Hensell	2/1965	2/1977	5	1,460	441	912
1825604	--	Grayson	Hensell and Pearsall	2/1971	2/2010	[5, 6]	1,474	440	912
1817902	--	Grayson	Hensell and Pearsall	2/1935	2/1977	[5, 6]	1,518	430	936
1828901	--	Grayson	Woodbine and Washita/Fredericksburg	2/1989	3/2020	[1, 2]	1,520	529	943
1817908	--	Grayson	Pearsall and Hosston	2/1978	3/2020	[6, 7]	1,522	429	934

TWDB or OWRB state well number[1]	Map ID (figures 3-50 to 3-70)	County	Hydrogeologic unit	Period of record (may contain gaps) (M/Y)[2]		Layer (zero-based indexing)[3]	Well depth, in feet below land surface[4]	Row	Column
				Begin	End				
1836602	--	Grayson	Woodbine and Washita/Fredericksburg	2/1995	3/2020	[1, 2]	1,527	540	922
1819306	--	Grayson	Glen and Rose and Hensell	2/1945	2/1977	[4, 5]	1,570	473	976
1817502	--	Grayson	Hosston	2/1983	2/1983	7	1,595	422	937
1829302	--	Grayson	Paluxy and Glen and Rose	2/1959	3/1992	[3, 4]	1,600	538	976
1820802	--	Grayson	Multi-aquifer	2/1967	2/2013	[2, 3, 4, 5, 6, 7]	2,231	499	966
1827803	--	Grayson	Multi-aquifer	3/1976	2/2013	[2, 3, 4, 5, 6]	2,250	487	927
1820713	--	Grayson	Multi-aquifer	2/1957	2/1993	[2, 3, 4, 5, 6, 7]	2,295	497	963
1836503	--	Grayson	Paluxy and Glen and Rose	2/1971	3/1984	[3, 4]	2,300	525	913
1828101	--	Grayson	Multi-aquifer	3/1972	2/2013	[3, 4, 5, 6, 7]	2,380	497	954
1836601	--	Grayson	Paluxy and Glen and Rose	2/1983	3/1992	[3, 4]	2,432	541	922
1827901	--	Grayson	Upper-Middle and Trinity	2/1975	2/2013	[3, 4, 5, 6]	2,460	498	933
1827802	--	Grayson	Washita/Fredericksburg and Paluxy	2/1975	2/2013	[2, 3]	2,480	494	928
1828404	--	Grayson	Upper-Middle and Trinity	3/1972	3/2004	[3, 4, 5, 6]	2,500	505	942
1835603	--	Grayson	Glen and Rose and Hensell	3/2020	3/2020	[4, 5]	2,520	512	906
1828606	--	Grayson	Paluxy and Glen and Rose	2/1983	2/2013	[3, 4]	2,582	517	955
1828505	--	Grayson	Upper-Middle and Trinity	2/1987	2/2013	[3, 4, 5, 6]	2,600	515	948
1828803	--	Grayson	Upper-Middle and Trinity	3/1992	2/2013	[3, 4, 5, 6]	2,643	514	942
4009203	--	Hamilton	Washita/Fredericksburg and Paluxy	3/1968	2/1978	[2, 3]	204	437	386
4115501	--	Hamilton	Lower and Trinity	2/1966	2/2019	[5, 6, 7]	210	387	345
4122502	--	Hamilton	Hensell	2/1963	2/1982	5	230	376	300
4116801	--	Hamilton	Glen and Rose and Hensell	3/1960	3/1984	[4, 5]	235	419	349
4131202	--	Hamilton	Hensell	3/1960	2/1969	5	250	414	290

TWDB or OWRB state well number[1]	Map ID (figures 3-50 to 3-70)	County	Hydrogeologic unit	Period of record (may contain gaps) (M/Y)[2]		Layer (zero-based indexing)[3]	Well depth, in feet below land surface[4]	Row	Column
				Begin	End				
4108201	--	Hamilton	Glen and Rose and Hensell	2/1963	2/1982	[4, 5]	264	392	400
4114801	--	Hamilton	Hensell	2/1966	2/1982	5	273	370	321
4138301	--	Hamilton	Hensell and Pearsall	2/1966	3/1996	[5, 6]	273	406	256
4121501	--	Hamilton	Hensell	2/1969	3/1984	5	286	353	288
4123901	--	Hamilton	Hensell	2/1970	3/1996	5	323	418	309
4131602	--	Hamilton	Glen Rose	2/1966	3/1976	4	324	426	285
4131102	--	Hamilton	Hensell	2/1970	2/1974	5	327	407	294
4108502	--	Hamilton	Hensell	2/1966	2/1970	5	358	395	395
4132501	--	Hamilton	Glen and Rose and Hensell	3/1968	2/1979	[4, 5]	390	443	297
4009103	--	Hamilton	Glen Rose	2/1966	3/1968	4	400	427	378
4108308	--	Hamilton	Lower and Trinity	2/1975	2/2009	[5, 6, 7]	400	401	406
4116301	--	Hamilton	Hensell	2/1969	2/1974	5	423	416	373
4124406	--	Hamilton	Pearsall	3/1964	2/1974	6	439	416	326
4130201	--	Hamilton	Hosston	2/2006	3/2020	7	450	383	281
4001701	--	Hamilton	Hensell	2/1966	2/1995	5	473	417	392
4009901	--	Hamilton	Glen and Rose and Hensell	2/1961	2/1975	[4, 5]	505	449	369
4010801	--	Hamilton	Hensell	2/1962	2/1982	5	549	468	375
4108301	--	Hamilton	Hosston	2/1965	2/1989	7	600	400	407
4124401	--	Hamilton	Hosston	2/1965	3/1976	7	601	414	328
4018703	--	Hamilton	Hosston	2/2006	3/2020	7	620	476	336
4009201	--	Hamilton	Hosston	2/1966	2/1994	7	760	439	387
3255701	--	Hill	Woodbine	3/1968	2/1974	1	166	552	525
3263912	--	Hill	Woodbine	3/1960	3/1992	1	237	585	507

TWDB or OWRB state well number[1]	Map ID (figures 3-50 to 3-70)	County	Hydrogeologic unit	Period of record (may contain gaps) (M/Y)[2]		Layer (zero-based indexing)[3]	Well depth, in feet below land surface[4]	Row	Column
				Begin	End				
3255305	--	Hill	Woodbine and Washita/Fredericksburg	2/2019	3/2020	[1, 2]	265	556	557
3247903	--	Hill	Washita/Fredericksburg	3/2020	3/2020	2	278	552	566
3255909	--	Hill	Woodbine	3/1968	3/1968	1	289	569	536
3255601	--	Hill	Woodbine and Washita/Fredericksburg	2/1965	2/1974	[1, 2]	305	560	552
3256703	--	Hill	Woodbine	2/1966	2/1966	1	353	575	537
3254701	--	Hill	Paluxy and Glen and Rose	2/1965	2/1974	[3, 4]	428	518	516
3253603	--	Hill	Multi-aquifer	2/2018	3/2020	[2, 3, 4]	460	506	517
3254401	--	Hill	Paluxy and Glen and Rose	2/2019	2/2019	[3, 4]	460	512	530
4008101	--	Hill	Woodbine	3/1968	2/1973	1	480	599	505
3263403	--	Hill	Paluxy	2/1965	2/1991	3	667	558	503
3264301	--	Hill	Woodbine	2/1963	2/1973	1	676	598	544
4007801	--	Hill	Paluxy	3/1960	2/1970	3	796	589	478
3357601	--	Hill	Woodbine	2/1930	2/1974	1	832	629	542
3253701	--	Hill	Hosston	2/1963	2/1981	7	835	497	502
3263910	--	Hill	Paluxy and Glen and Rose	2/1941	2/1974	[3, 4]	845	583	506
3261201	--	Hill	Hosston	3/1964	2/1974	7	1,002	506	502
3262701	--	Hill	Hensell	2/1966	2/1985	5	1,007	538	486
3262401	--	Hill	Hensell	2/1966	2/1975	5	1,020	533	492
4006701	--	Hill	Multi-aquifer	2/2018	2/2019	[2, 3, 4, 5, 6]	1,100	556	458

TWDB or OWRB state well number[1]	Map ID (figures 3-50 to 3-70)	County	Hydrogeologic unit	Period of record (may contain gaps) (M/Y)[2]		Layer (zero-based indexing)[3]	Well depth, in feet below land surface[4]	Row	Column
				Begin	End				
4005306	--	Hill	Hosston	3/1988	2/2018	7	1,130	535	476
4005309	--	Hill	Hosston	2/1963	2/2018	7	1,132	534	477
4014102	--	Hill	Hosston	3/1956	2/1979	7	1,145	554	447
3261905	--	Hill	Hosston	2/1990	3/2020	7	1,160	524	485
3261903	--	Hill	Hosston	3/1980	2/2018	7	1,183	533	479
4005310	--	Hill	Hosston	2/2019	2/2019	7	1,183	540	467
3262703	--	Hill	Pearsall and Hosston	2/2018	2/2019	[6, 7]	1,202	537	482
4006703	--	Hill	Hosston	2/1989	2/2018	7	1,210	558	455
3253904	--	Hill	Hosston	3/2020	3/2020	7	1,216	516	510
4014201	--	Hill	Hosston	2/1966	2/1974	7	1,225	563	450
4006107	--	Hill	Hosston	2/1982	2/2018	7	1,235	541	475
4006105	--	Hill	Hosston	2/2018	2/2019	7	1,238	541	472
3262403	--	Hill	Pearsall and Hosston	2/2001	3/2020	[6, 7]	1,250	532	493
4014203	--	Hill	Multi-aquifer	2/2006	3/2020	[2, 3, 4, 5, 6]	1,255	565	453
4006102	--	Hill	Hosston	2/1966	2/2018	7	1,260	542	477
4006801	--	Hill	Hosston	2/1966	3/1976	7	1,275	559	460
4006507	--	Hill	Pearsall and Hosston	2/2018	2/2019	[6, 7]	1,276	557	465
4006501	--	Hill	Pearsall and Hosston	3/1960	3/2020	[6, 7]	1,283	554	471
4014903	--	Hill	Hosston	3/2020	3/2020	7	1,324	582	431
4006201	--	Hill	Hosston	2/2002	3/2020	7	1,360	554	480
4014610	--	Hill	Hosston	2/1978	2/1998	7	1,360	579	443
3262801	--	Hill	Hosston	2/2006	3/2020	7	1,396	547	489
3262503	--	Hill	Hosston	3/1988	2/2009	7	1,446	540	497
4006601	--	Hill	Hosston	2/2002	3/2020	7	1,470	561	473
4006302	--	Hill	Hosston	2/2002	3/2020	7	1,477	558	479

TWDB or OWRB state well number[1]	Map ID (figures 3-50 to 3-70)	County	Hydrogeologic unit	Period of record (may contain gaps) (M/Y)[2]		Layer (zero-based indexing)[3]	Well depth, in feet below land surface[4]	Row	Column
				Begin	End				
3262201	--	Hill	Hosston	3/1988	3/2020	7	1,485	535	511
3254802	--	Hill	Hosston	3/1988	3/2020	7	1,490	532	516
4015403	--	Hill	Lower and Trinity	3/2020	3/2020	[5, 6, 7]	1,525	587	450
4006602	--	Hill	Multi-aquifer	2/2015	2/2019	[2, 3, 4, 5, 6, 7]	1,550	570	470
3254602	--	Hill	Hosston	2/1991	3/2020	7	1,570	540	534
3254603	--	Hill	Hosston	3/2020	3/2020	7	1,590	539	535
3255702	--	Hill	Hosston	3/1988	3/2020	7	1,680	554	529
4015201	--	Hill	Hosston	2/1965	2/1982	7	1,700	596	466
3263908	--	Hill	Hosston	2/1941	2/1990	7	1,810	585	506
3255902	--	Hill	Hosston	2/1965	2/1974	7	1,835	563	541
3264702	--	Hill	Lower and Trinity	2/1962	2/1981	[5, 6, 7]	1,876	586	512
4008801	--	Hill	Hosston	3/1960	3/2020	7	2,103	614	481
3264803	--	Hill	Multi-aquifer	3/2020	3/2020	[1, 2, 3, 4, 5]	2,196	603	513
3264802	--	Hill	Pearsall and Hosston	2/1979	3/2020	[6, 7]	2,215	599	515
3357402	--	Hill	Hosston	2/1966	3/2020	7	2,652	617	532
3901602	--	Hill	Hosston	2/1965	3/2020	7	2,988	647	508
3909901	--	Hill	Hosston	3/1964	2/1994	7	3,458	670	470
3910201	--	Hill	Hosston	3/1960	2/1970	7	3,555	676	501
3910203	--	Hill	Hosston	2/2002	3/2020	7	3,750	678	500
3235206	--	Hood	Glen Rose	2/1985	3/2020	4	113	414	562
3226703	--	Hood	Hosston	2/1973	3/2020	7	150	373	557
3235202	--	Hood	Glen Rose	2/1978	2/2019	4	160	412	564
3234608	--	Hood	Hensell	2/1971	2/1973	5	160	395	547
3234629	--	Hood	Hensell	3/2020	3/2020	5	180	397	540

TWDB or OWRB state well number[1]	Map ID (figures 3-50 to 3-70)	County	Hydrogeologic unit	Period of record (may contain gaps) (M/Y)[2]		Layer (zero-based indexing)[3]	Well depth, in feet below land surface[4]	Row	Column
				Begin	End				
3234113	--	Hood	Pearsall and Hosston	2/1970	3/2020	[6, 7]	190	380	552
3234516	--	Hood	Hensell and Pearsall	3/2020	3/2020	[5, 6]	202	388	544
3234614	--	Hood	Pearsall	2/1974	3/2020	6	225	396	548
3234306	--	Hood	Pearsall	2/1993	3/2020	6	240	393	551
3243418	--	Hood	Glen Rose	2/2015	3/2020	4	255	423	522
3234627	--	Hood	Pearsall	2/2010	2/2019	6	255	401	547
3234211	--	Hood	Hosston	3/2020	3/2020	7	258	390	551
3241301	--	Hood	Hensell	2/1971	2/1978	5	285	383	511
3235104	--	Hood	Glen Rose	2/1971	2/1971	4	292	408	558
3234814	--	Hood	Glen Rose	3/1988	3/2020	4	310	397	537
3234917	--	Hood	Hosston	3/1968	3/2020	7	310	399	538
3234903	--	Hood	Pearsall	2/2010	3/2020	6	317	402	538
3234517	--	Hood	Hensell	3/2020	3/2020	5	320	392	537
3226903	--	Hood	Pearsall and Hosston	2/1981	3/2020	[6, 7]	320	390	569
3235502	--	Hood	Hensell	2/1974	2/2019	5	330	415	550
3242303	--	Hood	Glen Rose	2/1971	2/1977	4	350	411	531
3235406	--	Hood	Hensell	2/2010	3/2020	5	350	408	552
3243103	--	Hood	Glen and Rose and Hensell	2/1971	2/1978	[4, 5]	360	418	523
3234911	--	Hood	Glen Rose	2/1977	2/2018	4	364	405	540
3243202	--	Hood	Hensell	2/1974	2/2010	5	371	425	537
3233402	--	Hood	Hosston	2/1971	2/1975	7	380	362	522
3234624	--	Hood	Hensell and Pearsall	2/1973	3/2020	[5, 6]	386	404	546
3235501	--	Hood	Hensell	2/2010	2/2010	5	395	422	552
3227903	--	Hood	Glen Rose	2/2010	3/2020	4	400	416	584
3234907	--	Hood	Hensell and Hosston	2/1986	2/2010	[5, 7]	410	405	540

TWDB or OWRB state well number[1]	Map ID (figures 3-50 to 3-70)	County	Hydrogeologic unit	Period of record (may contain gaps) (M/Y)[2]		Layer (zero-based indexing)[3]	Well depth, in feet below land surface[4]	Row	Column
				Begin	End				
3235407	--	Hood	Multi-aquifer	2/1969	3/2020	[4, 5, 6]	415	410	547
3233806	--	Hood	Pearsall	2/2010	3/2020	6	422	373	519
3243417	--	Hood	Hosston	2/2010	3/2020	7	425	423	522
3234702	--	Hood	Hensell and Pearsall	2/1995	3/2020	[5, 6]	425	388	532
3233810	--	Hood	Hosston	2/2011	3/2020	7	450	373	516
3233809	--	Hood	Pearsall	2/2007	2/2017	6	455	374	520
3235508	--	Hood	Multi-aquifer	2/2010	2/2019	[4, 6, 7]	465	415	550
3234912	--	Hood	Multi-aquifer	2/1987	3/2020	[4, 5, 7]	490	402	536
3243206	--	Hood	Glen and Rose and Pearsall	2/1994	3/2020	[4, 6]	500	430	533
3235906	--	Hood	Hosston	2/1997	2/2010	7	534	432	544
3235201	--	Hood	Pearsall	2/1979	3/2020	6	540	412	564
3235205	--	Hood	Hosston	2/1985	2/2019	7	577	414	562
3243303	--	Hood	Lower and Trinity	2/1993	2/2010	[5, 6, 7]	578	438	540
3235509	--	Hood	Pearsall and Hosston	3/2016	3/2020	[6, 7]	580	423	551
3243304	--	Hood	Pearsall	2/2010	2/2010	6	597	432	540
3235806	--	Hood	Pearsall and Hosston	2/1985	2/2010	[6, 7]	600	424	551
3235505	--	Hood	Hosston	2/2010	2/2010	7	620	420	558
3227906	--	Hood	Pearsall	2/2009	2/2019	6	745	415	582
3227907	--	Hood	Hensell	2/2009	2/2017	5	765	418	585
3227905	--	Hood	Pearsall and Hosston	2/2010	3/2020	[6, 7]	780	415	583
3227902	--	Hood	Pearsall and Hosston	2/2010	3/2020	[6, 7]	827	417	584
1847502	--	Hunt	Woodbine	2/1971	2/1975	1	2,015	620	922
1855401	--	Hunt	Woodbine	2/1995	2/1998	1	2,400	624	894
1848201	--	Hunt	Glen Rose	2/1971	2/1983	4	3,300	636	953
3236402	--	Johnson	Paluxy	2/1966	2/1983	3	105	434	560

TWDB or OWRB state well number[1]	Map ID (figures 3-50 to 3-70)	County	Hydrogeologic unit	Period of record (may contain gaps) (M/Y)[2]		Layer (zero-based indexing)[3]	Well depth, in feet below land surface[4]	Row	Column
				Begin	End				
3231808	--	Johnson	Woodbine	3/2020	3/2020	1	110	508	628
3247107	--	Johnson	Washita/Fredericksburg	2/1977	3/2020	2	163	520	583
3247815	--	Johnson	Woodbine	3/2016	3/2020	1	180	548	564
3231511	--	Johnson	Washita/Fredericksburg	3/2020	3/2020	2	195	505	632
3244806	--	Johnson	Washita/Fredericksburg and Paluxy	3/2000	3/2020	[2, 3]	210	468	523
3231906	--	Johnson	Woodbine	2/2014	3/2020	1	224	518	628
3247814	--	Johnson	Washita/Fredericksburg	2/2019	2/2019	2	228	544	569
3231802	--	Johnson	Woodbine	2/1966	2/1987	1	240	513	622
3239602	--	Johnson	Woodbine	2/1971	2/1998	1	250	530	605
3239705	--	Johnson	Washita/Fredericksburg	2/1966	2/1975	2	251	522	591
3239201	--	Johnson	Washita/Fredericksburg	2/1966	3/2004	2	270	512	615
3244804	--	Johnson	Paluxy	2/2017	3/2020	3	320	463	526
3247813	--	Johnson	Woodbine	3/2008	2/2017	1	341	544	565
3240704	--	Johnson	Woodbine	3/2020	3/2020	1	367	544	607
3228702	--	Johnson	Glen Rose	2/1966	2/1983	4	375	423	587
3253203	--	Johnson	Washita/Fredericksburg	2/2018	3/2020	2	400	500	527
3253502	--	Johnson	Paluxy	2/2018	2/2019	3	400	500	523
3253305	--	Johnson	Paluxy	2/2018	2/2019	3	400	502	535
3244302	--	Johnson	Paluxy	2/1970	2/1970	3	449	465	550
3244206	--	Johnson	Glen Rose	2/1986	3/2020	4	468	455	553

TWDB or OWRB state well number[1]	Map ID (figures 3-50 to 3-70)	County	Hydrogeologic unit	Period of record (may contain gaps) (M/Y)[2]		Layer (zero-based indexing)[3]	Well depth, in feet below land surface[4]	Row	Column
				Begin	End				
3237702	--	Johnson	Paluxy and Glen and Rose	2/1966	3/2020	[3, 4]	478	461	568
3236611	--	Johnson	Paluxy and Glen and Rose	3/2004	3/2020	[3, 4]	480	449	573
3245406	--	Johnson	Paluxy and Glen and Rose	2/2019	2/2019	[3, 4]	500	477	539
3253302	--	Johnson	Washita/Fredericksburg and Glen and Rose	3/1960	2/1970	[2, 4]	510	506	537
3246702	--	Johnson	Paluxy	2/1970	3/1984	3	537	504	546
3229602	--	Johnson	Paluxy	2/1986	3/2020	3	549	460	611
3237802	--	Johnson	Paluxy	2/1985	3/2020	3	563	475	571
3229902	--	Johnson	Paluxy and Glen and Rose	2/1970	2/1990	[3, 4]	584	470	610
3237404	--	Johnson	Paluxy and Glen and Rose	2/1985	3/2020	[3, 4]	590	462	582
3237207	--	Johnson	Paluxy	3/2020	3/2020	3	600	466	589
3246402	--	Johnson	Paluxy	2/1966	2/1982	3	640	503	559
3237204	--	Johnson	Paluxy and Glen and Rose	2/1986	3/2020	[3, 4]	645	471	588
3230805	--	Johnson	Paluxy and Glen and Rose	2/1970	2/1982	[3, 4]	657	486	610
3246405	--	Johnson	Paluxy and Glen and Rose	2/1986	3/2020	[3, 4]	670	506	554
3252506	--	Johnson	Hosston	2/2018	3/2020	7	680	472	507
3238701	--	Johnson	Glen Rose	2/1966	3/1972	4	700	489	575
3247105	--	Johnson	Paluxy and Glen and Rose	3/1972	3/2020	[3, 4]	754	520	583
3231702	--	Johnson	Paluxy	2/1966	2/1970	3	762	502	619

TWDB or OWRB state well number[1]	Map ID (figures 3-50 to 3-70)	County	Hydrogeologic unit	Period of record (may contain gaps) (M/Y)[2]		Layer (zero-based indexing)[3]	Well depth, in feet below land surface[4]	Row	Column
				Begin	End				
3247106	--	Johnson	Paluxy	2/1970	3/2020	3	770	518	584
3246908	--	Johnson	Paluxy	3/1988	3/2020	3	800	523	559
3230607	--	Johnson	Paluxy and Glen and Rose	2/1986	3/2020	[3, 4]	818	492	625
3239714	--	Johnson	Paluxy and Glen and Rose	2/1982	3/2020	[3, 4]	818	516	589
3230912	--	Johnson	Washita/Fredericksburg and Paluxy	2/2018	3/2020	[2, 3]	820	495	619
3238907	--	Johnson	Paluxy	2/1986	2/2014	3	823	510	592
3231708	--	Johnson	Paluxy	2/1982	3/2020	3	835	509	619
3238312	--	Johnson	Paluxy and Glen and Rose	2/1981	3/2020	[3, 4]	855	501	605
3239701	--	Johnson	Glen Rose	3/1960	2/1983	4	861	519	595
3239407	--	Johnson	Multi-aquifer	2/1998	3/2020	[2, 3, 4]	880	513	600
3231807	--	Johnson	Paluxy	2/1983	2/2019	3	907	515	625
3228703	--	Johnson	Hosston	2/1963	3/2020	7	910	421	584
3228707	--	Johnson	Multi-aquifer	2/2017	3/2020	[3, 5, 6, 7]	915	422	584
3252202	--	Johnson	Pearsall and Hosston	2/1965	2/1982	[6, 7]	926	469	521
3239805	--	Johnson	Paluxy and Glen and Rose	2/1989	3/2020	[3, 4]	950	526	601
3253202	--	Johnson	Hensell and Pearsall	2/2018	3/2020	[5, 6]	980	492	525
3240703	--	Johnson	Washita/Fredericksburg and Paluxy	3/2020	3/2020	[2, 3]	1,039	544	607
3244205	--	Johnson	Hosston	2/1969	3/2020	7	1,061	455	553
3245707	--	Johnson	Hosston	2/2019	3/2020	7	1,125	477	538
3245307	--	Johnson	Middle-Lower and Trinity	2/1941	2/1977	[4, 5, 6, 7]	1,206	490	563

TWDB or OWRB state well number[1]	Map ID (figures 3-50 to 3-70)	County	Hydrogeologic unit	Period of record (may contain gaps) (M/Y)[2]		Layer (zero-based indexing)[3]	Well depth, in feet below land surface[4]	Row	Column
				Begin	End				
3245902	--	Johnson	Hosston	2/1966	3/2020	7	1,215	500	541
3254101	--	Johnson	Hosston	2/1966	3/2020	7	1,215	508	536
3237801	--	Johnson	Multi-aquifer	2/1981	3/2020	[4, 5, 7]	1,224	475	571
3253304	--	Johnson	Hosston	2/1987	3/2020	7	1,232	506	537
3238109	--	Johnson	Hensell and Pearsall	3/2020	3/2020	[5, 6]	1,240	476	601
3245601	--	Johnson	Lower and Trinity	2/1955	2/1974	[5, 6, 7]	1,266	492	557
3237203	--	Johnson	Lower and Trinity	2/1982	2/2010	[5, 6, 7]	1,283	471	588
3230813	--	Johnson	Lower and Trinity	3/2020	3/2020	[5, 6, 7]	1,320	485	618
3237905	--	Johnson	Lower and Trinity	2/1977	3/2020	[5, 6, 7]	1,330	485	580
3237315	--	Johnson	Lower and Trinity	3/1980	3/2020	[5, 6, 7]	1,363	476	594
3246404	--	Johnson	Lower and Trinity	2/2007	3/2020	[5, 6, 7]	1,384	506	554
3238408	--	Johnson	Multi-aquifer	2/1983	3/2020	[4, 5, 7]	1,390	488	588
3230602	--	Johnson	Lower and Trinity	2/1970	3/2020	[5, 6, 7]	1,400	490	622
3246403	--	Johnson	Hosston	3/1968	3/2020	7	1,425	504	560
3238206	--	Johnson	Lower and Trinity	2/2018	3/2020	[5, 6, 7]	1,460	488	607
3238512	--	Johnson	Lower and Trinity	2/1999	3/2020	[5, 6, 7]	1,475	497	598
3238507	--	Johnson	Lower and Trinity	3/1984	3/2020	[5, 6, 7]	1,486	496	599
3238309	--	Johnson	Lower and Trinity	3/1976	3/2020	[5, 6, 7]	1,490	495	609
3254204	--	Johnson	Multi-aquifer	2/2018	3/2020	[2, 3, 4, 5, 6]	1,490	521	546
3246201	--	Johnson	Pearsall and Hosston	2/1983	2/1983	[6, 7]	1,518	503	571
3254203	--	Johnson	Hosston	3/1984	3/2020	7	1,555	524	543
3231709	--	Johnson	Lower and Trinity	2/1985	3/2020	[5, 6, 7]	1,557	501	621
3230606	--	Johnson	Lower and Trinity	2/1985	3/2020	[5, 6, 7]	1,562	492	625
3239408	--	Johnson	Multi-aquifer	2/2018	3/2020	[1, 4, 5]	1,564	515	602
3230908	--	Johnson	Lower and Trinity	3/1972	3/2020	[5, 6, 7]	1,568	499	615

TWDB or OWRB state well number[1]	Map ID (figures 3-50 to 3-70)	County	Hydrogeologic unit	Period of record (may contain gaps) (M/Y)[2]		Layer (zero-based indexing)[3]	Well depth, in feet below land surface[4]	Row	Column
				Begin	End				
3238904	--	Johnson	Hosston	2/1970	3/2020	7	1,590	509	592
3238905	--	Johnson	Pearsall	3/1976	2/2014	6	1,597	510	592
3239713	--	Johnson	Pearsall and Hosston	3/1980	3/2020	[6, 7]	1,606	516	589
3239715	--	Johnson	Multi-aquifer	2/2018	3/2020	[1, 4, 5]	1,635	517	596
3239711	--	Johnson	Hosston	2/1986	3/2020	7	1,636	522	594
3231706	--	Johnson	Pearsall and Hosston	3/1976	3/2020	[6, 7]	1,640	509	619
3247108	--	Johnson	Pearsall and Hosston	2/1981	3/2020	[6, 7]	1,660	527	581
3239507	--	Johnson	Pearsall	2/1985	3/2020	6	1,668	520	599
3231805	--	Johnson	Hosston	3/1976	3/2020	7	1,721	515	625
3239804	--	Johnson	Pearsall and Hosston	2/1977	3/2020	[6, 7]	1,778	526	601
1000013766	--	Johnston	Glen and Rose and Hensell	3/2016	2/2017	[4, 5]	125	430	1,111
3321801	--	Kaufman	Woodbine	2/1961	2/1987	1	2,340	651	729
3312601	--	Kaufman	Paluxy	2/1975	3/1992	3	2,843	618	764
3313701	--	Kaufman	Paluxy	2/1971	2/1974	3	3,195	633	759
1726202	--	Lamar	Woodbine	3/1964	2/1983	1	1,673	662	1,037
1729601	--	Lamar	Paluxy	2/1971	2/2010	3	2,644	752	1,074
4164501	--	Lampasas	Hensell	2/1969	2/1977	5	125	501	174
4162902	--	Lampasas	Hosston	2/1961	2/1982	7	200	466	149
4154401	--	Lampasas	Pearsall and Hosston	3/1968	2/1985	[6, 7]	290	424	173
4153330	--	Lampasas	Hensell and Pearsall	2/2006	3/2020	[5, 6]	310	414	179
4154801	--	Lampasas	Hosston	2/1966	2/1969	7	311	439	168
4145902	--	Lampasas	Pearsall	2/1959	2/1974	6	318	409	189
4153309	--	Lampasas	Hosston	2/1966	2/1970	7	335	416	178
4153322	--	Lampasas	Hensell and Pearsall	3/1968	2/1979	[5, 6]	350	417	178
4153319	--	Lampasas	Hensell and Pearsall	2/1966	2/1969	[5, 6]	384	416	181

TWDB or OWRB state well number[1]	Map ID (figures 3-50 to 3-70)	County	Hydrogeologic unit	Period of record (may contain gaps) (M/Y)[2]		Layer (zero-based indexing)[3]	Well depth, in feet below land surface[4]	Row	Column
				Begin	End				
4148503	--	Lampasas	Hensell	2/1965	2/1974	5	450	474	232
4163401	--	Lampasas	Hosston	2/1993	3/2020	7	585	470	155
1000114133	--	Love	Pearsall	2/2015	2/2015	6	200	297	983
1000157335	--	Love	Hensell	2/2015	2/2019	5	400	341	985
1000013791	--	Marshall	Paluxy	2/1994	3/2004	3	125	397	1,039
1000121866	--	Marshall	Washita/Fredericksburg	2/2015	2/2015	2	150	420	1,018
1000184834	--	Marshall	Washita/Fredericksburg	2/2019	2/2019	2	151	404	1,029
1000028539	--	Marshall	Washita/Fredericksburg	2/1994	2/2019	2	160	423	1,003
1000013794	--	Marshall	Glen Rose	2/2015	2/2019	4	218	394	1,024
1000112142	--	Marshall	Hosston	2/2015	2/2015	7	235	365	1,043
1000009588	--	Marshall	Glen Rose	2/1978	2/2019	4	503	450	1,033
1000122829	--	Marshall	Glen Rose	2/2015	3/2016	4	566	451	1,040
1000139141	--	McCurtain	Paluxy	2/2015	2/2015	3	140	814	1,234
1000017381	--	McCurtain	Washita/Fredericksburg and Paluxy	2/1994	2/2002	[2, 3]	315	795	1,212
4028202	--	McLennan	Glen Rose	3/1968	3/1968	4	477	549	364
4028301	--	McLennan	Glen Rose	2/1965	2/1965	4	500	550	365
4021702	--	McLennan	Glen and Rose and Hensell	2/1965	2/1978	[4, 5]	761	558	383
4029105	--	McLennan	Glen and Rose and Hensell	2/1973	2/1973	[4, 5]	940	563	367
4029805	--	McLennan	Hensell	2/1965	2/2015	5	941	577	355
4021703	--	McLennan	Multi-aquifer	2/1997	3/2020	[2, 3, 6, 7]	970	558	383

INTERA

TWDB or OWRB state well number[1]	Map ID (figures 3-50 to 3-70)	County	Hydrogeologic unit	Period of record (may contain gaps) (M/Y)[2]		Layer (zero-based indexing)[3]	Well depth, in feet below land surface[4]	Row	Column
				Begin	End				
4029201	--	McLennan	Glen and Rose and Hensell	2/1993	3/2020	[4, 5]	975	569	378
4029702	--	McLennan	Hensell and Pearsall	2/1985	2/1985	[5, 6]	981	570	349
4037803	--	McLennan	Glen Rose	2/1949	2/1949	4	1,009	596	324
4022807	--	McLennan	Hensell	2/1962	2/1962	5	1,010	590	392
4037603	--	McLennan	Hensell	2/1958	2/1958	5	1,018	596	336
4037606	--	McLennan	Glen and Rose and Hensell	2/2006	3/2020	[4, 5]	1,020	600	343
4037806	--	McLennan	Glen Rose	2/1991	2/1991	4	1,025	598	328
4037607	--	McLennan	Hensell	3/2012	3/2020	5	1,040	600	336
4037608	--	McLennan	Hensell	3/1988	3/2020	5	1,050	599	330
4030201	--	McLennan	Hensell	2/1962	2/1962	5	1,060	600	393
4037804	--	McLennan	Hensell	2/1965	2/1965	5	1,062	594	323
4038101	--	McLennan	Glen Rose	3/1988	3/2020	4	1,066	608	349
4021704	--	McLennan	Hosston	3/1988	3/2020	7	1,066	558	382
4022501	--	McLennan	Glen Rose	2/1967	2/1967	4	1,076	587	402
4029104	--	McLennan	Lower and Trinity	2/1974	2/1974	[5, 6, 7]	1,080	565	373
4037805	--	McLennan	Glen and Rose and Hensell	2/1989	2/1989	[4, 5]	1,081	596	325
4029401	--	McLennan	Hosston	3/1976	3/1976	7	1,120	565	364
4021604	--	McLennan	Hosston	3/1980	3/1980	7	1,125	571	397
4030301	--	McLennan	Glen Rose	2/1966	2/1966	4	1,126	612	388
4030602	--	McLennan	Glen Rose	3/1960	3/1960	4	1,127	616	381
4030302	--	McLennan	Hensell	2/1966	2/1966	5	1,140	609	387
4022702	--	McLennan	Hosston	2/1981	2/1981	7	1,140	581	394
4030603	--	McLennan	Glen and Rose and Hensell	2/1966	2/1989	[4, 5]	1,146	608	378

TWDB or OWRB state well number[1]	Map ID (figures 3-50 to 3-70)	County	Hydrogeologic unit	Period of record (may contain gaps) (M/Y)[2]		Layer (zero-based indexing)[3]	Well depth, in feet below land surface[4]	Row	Column
				Begin	End				
4028902	--	McLennan	Hosston	2/1981	3/2020	7	1,165	567	343
4030604	--	McLennan	Glen Rose	2/1966	2/1966	4	1,171	614	387
4031402	--	McLennan	Glen Rose	2/1966	2/1966	4	1,184	621	381
4021901	--	McLennan	Hosston	3/1956	3/1956	7	1,186	578	385
4022701	--	McLennan	Pearsall and Hosston	3/2012	3/2012	[6, 7]	1,190	582	398
4031403	--	McLennan	Glen Rose	2/1966	2/1966	4	1,192	617	384
4028302	--	McLennan	Pearsall and Hosston	3/2012	3/2020	[6, 7]	1,194	551	367
4022902	--	McLennan	Hensell	2/1965	2/1965	5	1,200	603	399
4022905	--	McLennan	Hensell	3/2012	3/2020	5	1,200	604	404
4029601	--	McLennan	Hosston	2/1966	3/1988	7	1,206	588	366
4022503	--	McLennan	Pearsall and Hosston	3/2012	3/2012	[6, 7]	1,206	590	412
4022810	--	McLennan	Pearsall and Hosston	2/1982	3/2020	[6, 7]	1,211	590	394
4037602	--	McLennan	Lower and Trinity	2/1942	2/1942	[5, 6, 7]	1,250	597	337
4030803	--	McLennan	Lower and Trinity	2/1978	2/1978	[5, 6, 7]	1,252	611	365
4022504	--	McLennan	Hosston	2/1995	2/1995	7	1,254	584	405
4030101	--	McLennan	Lower and Trinity	2/1993	2/2009	[5, 6, 7]	1,274	589	380
4022606	--	McLennan	Pearsall	2/1977	2/1977	6	1,275	596	410
4031210	--	McLennan	Glen Rose	2/1962	2/1962	4	1,285	622	399
4030802	--	McLennan	Middle-Lower and Trinity	2/2013	2/2013	[4, 5, 6, 7]	1,294	606	367
4022605	--	McLennan	Hensell and Pearsall	2/1995	2/1995	[5, 6]	1,296	595	410
4022811	--	McLennan	Hosston	2/1985	2/1985	7	1,302	597	394
4038202	--	McLennan	Multi-aquifer	2/1993	3/2020	[4, 6, 7]	1,306	614	355
4030502	--	McLennan	Pearsall and Hosston	3/1988	3/1988	[6, 7]	1,320	601	382
4023201	--	McLennan	Glen Rose	2/1987	2/1987	4	1,322	611	429

TWDB or OWRB state well number[1]	Map ID (figures 3-50 to 3-70)	County	Hydrogeologic unit	Period of record (may contain gaps) (M/Y)[2]		Layer (zero-based indexing)[3]	Well depth, in feet below land surface[4]	Row	Column
				Begin	End				
4022607	--	McLennan	Multi-aquifer	2/1993	3/2020	[2, 3, 4, 5, 7]	1,322	600	411
4022812	--	McLennan	Pearsall and Hosston	2/2013	2/2013	[6, 7]	1,325	592	399
4038203	--	McLennan	Multi-aquifer	3/1988	2/2019	[2, 3, 4, 5, 6, 7]	1,328	617	359
4030901	--	McLennan	Hosston	2/1961	2/1974	7	1,360	613	370
4022802	--	McLennan	Hosston	2/1943	2/1943	7	1,400	595	400
4045601	--	McLennan	Hosston	2/1978	2/1978	7	1,406	616	309
4038303	--	McLennan	Pearsall	2/1965	2/1965	6	1,440	623	362
4038801	--	McLennan	Hensell	2/1965	2/1982	5	1,460	625	334
4031103	--	McLennan	Hosston	3/1988	3/1988	7	1,475	610	396
4038302	--	McLennan	Hensell	2/1938	2/1965	5	1,485	625	363
4046402	--	McLennan	Pearsall and Hosston	2/1985	2/2002	[6, 7]	1,494	625	309
4046101	--	McLennan	Hosston	2/1995	2/1995	7	1,500	619	316
4047403	--	McLennan	Glen Rose	2/1967	2/1967	4	1,535	648	325
4031102	--	McLennan	Middle-Lower and Trinity	2/1942	2/1982	[4, 5, 6, 7]	1,540	616	397
4031211	--	McLennan	Hensell and Pearsall	3/1972	3/1972	[5, 6]	1,540	623	405
4039502	--	McLennan	Glen Rose	2/1965	3/1988	4	1,560	645	356
4046403	--	McLennan	Hosston	2/1957	2/1983	7	1,561	625	308
4046602	--	McLennan	Glen Rose	3/1964	2/2018	4	1,565	648	317
4039103	--	McLennan	Glen Rose	2/1950	2/1966	4	1,570	630	369
4046801	--	McLennan	Pearsall and Hosston	2/1994	3/2020	[6, 7]	1,680	637	309
4031708	--	McLennan	Pearsall	2/1985	3/2020	6	1,790	628	371
4039109	--	McLennan	Lower and Trinity	2/1986	3/2020	[5, 6, 7]	1,805	627	367
4039402	--	McLennan	Lower and Trinity	2/1986	2/1986	[5, 6, 7]	1,806	634	351
4031707	--	McLennan	Hensell	2/1985	2/2014	5	1,820	628	374

TWDB or OWRB state well number[1]	Map ID (figures 3-50 to 3-70)	County	Hydrogeologic unit	Period of record (may contain gaps) (M/Y)[2]		Layer (zero-based indexing)[3]	Well depth, in feet below land surface[4]	Row	Column
				Begin	End				
4031801	--	McLennan	Hosston	2/1965	2/1965	7	1,828	632	374
4039101	--	McLennan	Hosston	2/1965	2/1965	7	1,865	631	371
4039104	--	McLennan	Hosston	2/1965	2/1965	7	1,872	630	370
4039702	--	McLennan	Hensell and Pearsall	3/1964	2/1990	[5, 6]	1,881	645	343
4030203	--	McLennan	Multi-aquifer	3/2016	3/2020	[2, 3, 4, 5, 6]	1,900	596	392
4039204	--	McLennan	Lower and Trinity	2/2001	3/2020	[5, 6, 7]	1,914	639	363
4016405	--	McLennan	Pearsall	2/1999	2/1999	6	1,924	618	462
4031702	--	McLennan	Hosston	2/1965	2/1965	7	1,936	631	372
4015905	--	McLennan	Multi-aquifer	2/1994	2/2015	[1, 2, 3, 4, 5, 6]	1,959	614	446
4039503	--	McLennan	Pearsall	3/1968	3/1968	6	1,960	645	354
4039504	--	McLennan	Middle-Lower and Trinity	3/1988	2/2010	[4, 5, 6, 7]	1,969	638	362
4015904	--	McLennan	Hosston	3/1988	3/1988	7	1,980	614	452
4016402	--	McLennan	Hosston	2/1949	3/1976	7	2,008	620	458
4039802	--	McLennan	Pearsall and Hosston	2/1982	3/2020	[6, 7]	2,008	646	347
4016401	--	McLennan	Glen and Rose and Hensell	2/1926	2/1969	[4, 5]	2,010	620	458
4031805	--	McLennan	Pearsall and Hosston	3/2012	2/2015	[6, 7]	2,041	641	377
4016703	--	McLennan	Pearsall	3/1988	3/1988	6	2,069	620	455
4039302	--	McLennan	Hosston	3/1952	3/1976	7	2,096	646	370
4039301	--	McLennan	Pearsall and Hosston	2/1957	3/2020	[6, 7]	2,100	646	367
4031604	--	McLennan	Pearsall and Hosston	2/1959	2/1991	[6, 7]	2,122	642	392
4031504	--	McLennan	Hosston	2/1942	2/1966	7	2,150	633	388
4031614	--	McLennan	Hosston	2/1945	2/1966	7	2,151	633	393
4031612	--	McLennan	Hosston	3/1960	2/1994	7	2,194	640	400

TWDB or OWRB state well number[1]	Map ID (figures 3-50 to 3-70)	County	Hydrogeologic unit	Period of record (may contain gaps) (M/Y)[2]		Layer (zero-based indexing)[3]	Well depth, in feet below land surface[4]	Row	Column
				Begin	End				
4039304	--	McLennan	Hosston	3/2012	3/2012	7	2,241	651	369
4024101	--	McLennan	Hosston	2/1959	2/1995	7	2,269	625	435
4024401	--	McLennan	Hosston	3/1960	3/1964	7	2,270	634	425
4016803	--	McLennan	Hosston	3/1996	2/2015	7	2,278	625	456
4032403	--	McLennan	Hosston	3/1964	3/1964	7	2,312	645	400
4024103	--	McLennan	Hosston	3/1988	3/1988	7	2,350	627	440
4024104	--	McLennan	Multi-aquifer	2/1994	2/2005	[1, 2, 3, 4, 5, 6]	2,376	625	434
4040101	--	McLennan	Hosston	3/1960	3/1960	7	2,391	655	374
4032107	--	McLennan	Pearsall and Hosston	2/1994	2/2014	[6, 7]	2,410	642	414
4024501	--	McLennan	Hosston	2/1967	2/1967	7	2,414	638	426
4032813	--	McLennan	Hosston	2/1983	2/1983	7	2,417	660	391
4039305	--	McLennan	Hosston	3/1960	3/2000	7	2,450	651	379
4032202	--	McLennan	Hosston	2/1993	2/2011	7	2,464	646	412
4032501	--	McLennan	Hosston	2/1965	2/1987	7	2,493	650	405
4040401	--	McLennan	Hosston	2/1966	3/2012	7	2,500	658	370
4024805	--	McLennan	Pearsall and Hosston	2/2007	2/2007	[6, 7]	2,500	649	419
4040703	--	McLennan	Hosston	2/1991	2/2018	7	2,514	666	354
4040701	--	McLennan	Hosston	2/1993	2/2003	7	2,550	667	363
4024201	--	McLennan	Hosston	3/1980	3/1980	7	2,670	638	448
4040517	--	McLennan	Hosston	3/2004	3/2004	7	2,710	673	368
3933101	--	McLennan	Pearsall and Hosston	2/1966	2/1966	[6, 7]	2,820	684	386
4024301	--	McLennan	Hosston	2/1966	2/2002	7	2,863	644	449
3933102	--	McLennan	Pearsall and Hosston	3/1952	3/1952	[6, 7]	2,898	684	388
3925102	--	McLennan	Hosston	3/1964	2/1974	7	2,905	669	417
3925103	--	McLennan	Hosston	2/2011	2/2011	7	2,907	669	419

TWDB or OWRB state well number[1]	Map ID (figures 3-50 to 3-70)	County	Hydrogeologic unit	Period of record (may contain gaps) (M/Y)[2]		Layer (zero-based indexing)[3]	Well depth, in feet below land surface[4]	Row	Column
				Begin	End				
3925402	--	McLennan	Hosston	2/1969	2/1969	7	2,950	675	416
3925702	--	McLennan	Hosston	2/2010	2/2010	7	3,010	677	401
3925401	--	McLennan	Hosston	2/1967	2/1967	7	3,035	674	416
3933104	--	McLennan	Hosston	2/1967	2/1967	7	3,115	684	396
3925201	--	McLennan	Hosston	2/1994	3/2020	7	3,148	676	429
3925501	--	McLennan	Hosston	2/1965	2/2015	7	3,181	682	418
3917702	--	McLennan	Hosston	2/1983	2/1983	7	3,250	662	426
3925801	--	McLennan	Hosston	2/1966	2/1966	7	3,370	692	403
3917901	--	McLennan	Hosston	2/1966	2/2017	7	3,375	680	437
3933202	--	McLennan	Hosston	3/1964	3/2020	7	3,531	696	397
5807901	--	Milam	Pearsall and Hosston	2/1966	2/1999	[6, 7]	3,448	726	226
4119702	--	Mills	Lower and Trinity	2/2010	3/2020	[5, 6, 7]	250	298	250
4145401	--	Mills	Hosston	2/1966	3/1976	7	315	386	195
4137802	--	Mills	Middle-Lower and Trinity	3/1968	2/1977	[4, 5, 6, 7]	320	385	217
4136205	--	Mills	Hensell and Pearsall	3/1968	2/1986	[5, 6]	345	347	226
4136201	--	Mills	Hensell and Pearsall	2/1955	2/1967	[5, 6]	478	350	228
1920201	--	Montague	Glen Rose	2/1970	2/1995	4	128	291	885
1927602	--	Montague	Glen Rose	2/2011	3/2020	4	160	289	841
1928202	--	Montague	Glen Rose	3/2008	2/2017	4	160	298	860
1936101	--	Montague	Glen Rose	2/2010	3/2020	4	160	310	817
1912608	--	Montague	Hensell	2/2013	3/2020	5	160	283	909
1912901	--	Montague	Hensell	2/2011	3/2020	5	200	291	897
1928301	--	Montague	Glen and Rose and Hensell	3/2000	3/2020	[4, 5]	200	306	862
1912903	--	Montague	Hosston	3/2012	3/2020	7	210	292	904

TWDB or OWRB state well number[1]	Map ID (figures 3-50 to 3-70)	County	Hydrogeologic unit	Period of record (may contain gaps) (M/Y)[2]		Layer (zero-based indexing)[3]	Well depth, in feet below land surface[4]	Row	Column
				Begin	End				
1936103	--	Montague	Hensell	2/2011	3/2020	5	220	312	818
1919803	--	Montague	Pearsall	2/2014	2/2018	6	220	271	859
1935501	--	Montague	Hensell	2/2014	2/2015	5	235	295	807
1919601	--	Montague	Glen Rose	2/2014	2/2017	4	240	274	863
1918901	--	Montague	Hosston	2/1971	3/1996	7	243	255	847
1920502	--	Montague	Hensell	2/2011	3/2020	5	250	287	878
1919702	--	Montague	Hosston	2/1971	3/1996	7	260	261	855
1919902	--	Montague	Hosston	2/2015	2/2015	7	260	272	860
1920802	--	Montague	Hensell	2/2011	3/2020	5	300	294	864
1928101	--	Montague	Hensell and Pearsall	2/2010	3/2020	[5, 6]	320	288	854
1920204	--	Montague	Hosston	2/2014	3/2020	7	340	285	883
1927102	--	Montague	Hosston	3/2012	2/2014	7	350	270	836
1927801	--	Montague	Hosston	2/2011	2/2017	7	360	286	818
1936204	--	Montague	Glen Rose	2/2014	3/2020	4	380	316	831
1919303	--	Montague	Hosston	3/2012	2/2017	7	400	270	882
1936308	--	Montague	Glen Rose	3/2016	3/2020	4	420	325	831
1928104	--	Montague	Hensell	3/2012	3/2020	5	420	294	846
1928902	--	Montague	Multi-aquifer	3/2004	3/2020	[4, 5, 6]	420	322	838
1920601	--	Montague	Hosston	2/2011	3/2020	7	430	298	883
1928806	--	Montague	Multi-aquifer	2/2011	3/2020	[3, 4, 6]	430	315	837
1928803	--	Montague	Hensell	3/1964	3/2020	5	456	311	839
1919707	--	Montague	Hosston	2/2014	3/2020	7	460	263	847
1928203	--	Montague	Pearsall	2/2013	3/2020	6	480	300	857
1926902	--	Montague	Hosston	3/2016	3/2020	7	500	269	816
1936305	--	Montague	Pearsall and Hosston	2/2011	3/2020	[6, 7]	620	325	831
1920602	--	Montague	Multi-aquifer	2/1945	3/2020	[4, 5, 6]	700	298	883

TWDB or OWRB state well number[1]	Map ID (figures 3-50 to 3-70)	County	Hydrogeologic unit	Period of record (may contain gaps) (M/Y)[2]		Layer (zero-based indexing)[3]	Well depth, in feet below land surface[4]	Row	Column
				Begin	End				
3358502	--	Navarro	Washita/Fredericksburg	2/1971	2/1971	2	1,290	645	557
3358503	--	Navarro	Woodbine	2/1973	2/2018	1	1,300	646	558
3359301	--	Navarro	Woodbine	2/1958	2/1997	1	1,650	678	580
3352801	--	Navarro	Woodbine	3/1956	2/1977	1	1,750	683	602
3904401	--	Navarro	Woodbine	3/1968	2/1985	1	1,750	701	545
3211701	--	Parker	Glen Rose	2/1971	2/1975	4	120	366	627
3211832	--	Parker	Glen Rose	2/2011	3/2020	4	125	372	640
3210915	--	Parker	Paluxy	2/2015	3/2020	3	147	355	631
3212108	--	Parker	Paluxy	2/2015	3/2020	3	197	387	671
3219902	--	Parker	Paluxy	2/2015	3/2020	3	197	399	614
3212208	--	Parker	Paluxy and Glen and Rose	3/2016	3/2020	[3, 4]	197	395	668
3203104	--	Parker	Glen Rose	2/2018	3/2020	4	205	346	683
3211813	--	Parker	Glen Rose	2/1986	3/2012	4	217	375	633
3210916	--	Parker	Glen Rose	2/2015	3/2020	4	220	355	631
3211910	--	Parker	Glen Rose	2/2006	3/2020	4	220	379	643
3219207	--	Parker	Glen Rose	2/1990	2/2013	4	220	380	629
3226204	--	Parker	Hensell and Pearsall	2/1978	2/2019	[5, 6]	220	371	585
3219604	--	Parker	Glen Rose	2/1971	3/1988	4	228	395	620
3212502	--	Parker	Glen Rose	3/1984	3/1988	4	240	395	663
3210406	--	Parker	Glen Rose	2/1994	3/2020	4	250	341	631
3219303	--	Parker	Glen Rose	3/1984	2/2009	4	250	384	632
3212506	--	Parker	Paluxy and Glen and Rose	3/2016	3/2020	[3, 4]	258	394	659
3219502	--	Parker	Glen Rose	3/2020	3/2020	4	260	385	620
3217302	--	Parker	Lower and Trinity	2/2010	3/2020	[5, 6, 7]	260	338	599

TWDB or OWRB state well number[1]	Map ID (figures 3-50 to 3-70)	County	Hydrogeologic unit	Period of record (may contain gaps) (M/Y)[2]		Layer (zero-based indexing)[3]	Well depth, in feet below land surface[4]	Row	Column
				Begin	End				
3219301	--	Parker	Paluxy and Glen and Rose	2/1986	3/2020	[3, 4]	260	392	636
3219218	--	Parker	Glen Rose	2/2007	2/2015	4	275	376	629
3220802	--	Parker	Paluxy and Glen and Rose	3/2012	3/2020	[3, 4]	280	415	620
3226203	--	Parker	Lower and Trinity	3/1984	3/2020	[5, 6, 7]	280	371	587
3219501	--	Parker	Paluxy	3/2020	3/2020	3	300	387	611
3219611	--	Parker	Glen Rose	2/2006	3/2020	4	300	397	621
3220203	--	Parker	Glen Rose	2/1997	2/2011	4	300	408	644
3226605	--	Parker	Pearsall	3/2020	3/2020	6	300	379	579
3211829	--	Parker	Glen Rose	2/1997	3/2016	4	310	379	632
3227403	--	Parker	Hensell	2/1971	2/1995	5	358	393	579
3203212	--	Parker	Pearsall and Hosston	2/1991	3/2020	[6, 7]	364	356	685
3209908	--	Parker	Hosston	3/2020	3/2020	7	370	333	612
3212805	--	Parker	Glen Rose	2/2006	2/2019	4	440	399	651
3227405	--	Parker	Hosston	2/1993	3/2020	7	440	393	579
3203103	--	Parker	Hosston	2/2018	3/2020	7	450	346	683
3210203	--	Parker	Lower and Trinity	2/1975	3/2020	[5, 6, 7]	454	339	641
3210914	--	Parker	Pearsall	2/2007	2/2019	6	460	359	628
3209601	--	Parker	Hosston	3/2020	3/2020	7	460	330	633
3204510	--	Parker	Lower and Trinity	2/2010	3/2020	[5, 6, 7]	500	387	689
3204505	--	Parker	Pearsall and Hosston	3/1988	3/2020	[6, 7]	520	386	688
3219222	--	Parker	Pearsall and Hosston	3/2012	3/2020	[6, 7]	642	381	631
3211911	--	Parker	Middle-Lower and Trinity	2/2019	2/2019	[4, 5, 6, 7]	660	387	636
3219308	--	Parker	Hosston	2/2006	3/2020	7	680	394	629
3220105	--	Parker	Pearsall and Hosston	3/2000	2/2010	[6, 7]	680	401	630

TWDB or OWRB state well number[1]	Map ID (figures 3-50 to 3-70)	County	Hydrogeologic unit	Period of record (may contain gaps) (M/Y)[2]		Layer (zero-based indexing)[3]	Well depth, in feet below land surface[4]	Row	Column
				Begin	End				
3219311	--	Parker	Pearsall and Hosston	3/2012	3/2020	[6, 7]	722	392	636
3220204	--	Parker	Hosston	3/2020	3/2020	7	800	404	638
1000014046	--	Pushmataha	Hensell and Pearsall	2/2015	2/2015	[5, 6]	125	712	1,236
1707402	--	Red River	Paluxy	2/1971	2/1998	3	406	740	1,185
1722902	--	Red River	Paluxy	2/1975	3/2000	3	2,025	765	1,109
3313103	--	Rockwall	Paluxy and Glen and Rose	2/2011	2/2019	[3, 4]	3,180	619	781
3305401	--	Rockwall	Paluxy and Glen and Rose	2/1961	2/1983	[3, 4]	3,342	612	803
3250305	--	Somervell	Glen Rose	2/1950	2/1985	4	120	429	496
3250201	--	Somervell	Hensell	2/1950	3/2020	5	176	412	490
3250307	--	Somervell	Hensell	2/1950	2/1962	5	177	427	496
3250801	--	Somervell	Glen Rose	3/1960	2/1977	4	225	426	464
3251210	--	Somervell	Glen Rose	2/2019	2/2019	4	260	439	507
3242906	--	Somervell	Hensell	2/2015	3/2020	5	281	423	501
3241902	--	Somervell	Lower and Trinity	3/1960	3/1984	[5, 6, 7]	288	397	488
3250501	--	Somervell	Glen Rose	2/1946	2/1963	4	297	421	482
3250202	--	Somervell	Hosston	2/1950	2/1995	7	297	412	491
3249601	--	Somervell	Hensell	3/1960	2/1974	5	345	402	474
3250503	--	Somervell	Hensell	2/1965	2/1977	5	347	421	483
3242801	--	Somervell	Hensell	3/1964	2/1986	5	352	410	502
3250208	--	Somervell	Hosston	3/1984	3/2020	7	354	413	494
3250402	--	Somervell	Hensell	3/1964	2/1995	5	372	409	474
3243703	--	Somervell	Middle-Lower and Trinity	2/1930	2/1986	[4, 5, 6, 7]	374	432	509
3243419	--	Somervell	Hensell and Pearsall	2/2018	3/2020	[5, 6]	400	425	521
3251108	--	Somervell	Hosston	2/2006	3/2020	7	410	431	503

TWDB or OWRB state well number[1]	Map ID (figures 3-50 to 3-70)	County	Hydrogeologic unit	Period of record (may contain gaps) (M/Y)[2]		Layer (zero-based indexing)[3]	Well depth, in feet below land surface[4]	Row	Column
				Begin	End				
3242604	--	Somervell	Hosston	2/2001	3/2020	7	470	412	515
3251105	--	Somervell	Pearsall	2/2006	3/2020	6	484	430	496
3242907	--	Somervell	Hosston	2/2015	3/2020	7	500	420	503
3242904	--	Somervell	Hosston	2/1991	3/2020	7	500	425	504
3243502	--	Somervell	Hosston	2/2018	3/2020	7	500	430	520
3250505	--	Somervell	Hensell and Pearsall	2/2006	2/2017	[5, 6]	500	427	478
3250302	--	Somervell	Hosston	2/1950	2/1953	7	567	419	495
3250507	--	Somervell	Hosston	2/2014	3/2020	7	600	427	478
3243905	--	Somervell	Hosston	2/2018	3/2020	7	640	447	520
3250803	--	Somervell	Pearsall and Hosston	2/1989	2/2019	[6, 7]	714	428	474
3223601	--	Tarrant	Woodbine	2/1970	3/1992	1	135	503	673
3213702	--	Tarrant	Paluxy	2/1950	2/1958	3	201	426	657
3228301	--	Tarrant	Paluxy and Glen and Rose	2/1973	2/2019	[3, 4]	210	426	614
3216801	--	Tarrant	Woodbine	2/1970	2/2001	1	217	504	702
3221501	--	Tarrant	Paluxy	2/1950	3/1980	3	227	434	640
3216503	--	Tarrant	Woodbine	3/1952	3/1952	1	267	501	716
3206102	--	Tarrant	Paluxy	2/1950	3/1984	3	325	424	719
3221505	--	Tarrant	Paluxy and Glen and Rose	2/1967	2/2017	[3, 4]	348	434	645
3204304	--	Tarrant	Hensell	2/2017	2/2018	5	360	386	709
3222201	--	Tarrant	Paluxy	2/1954	2/1962	3	380	457	668
3214603	--	Tarrant	Paluxy	2/1951	2/1954	3	385	461	686
3205207	--	Tarrant	Paluxy	3/2020	3/2020	3	390	404	710
3214403	--	Tarrant	Paluxy	2/1950	2/1958	3	400	442	686
3206103	--	Tarrant	Paluxy and Glen and Rose	2/1989	3/2020	[3, 4]	460	424	720

TWDB or OWRB state well number[1]	Map ID (figures 3-50 to 3-70)	County	Hydrogeologic unit	Period of record (may contain gaps) (M/Y)[2]		Layer (zero-based indexing)[3]	Well depth, in feet below land surface[4]	Row	Column
				Begin	End				
3214606	--	Tarrant	Paluxy	2/1943	2/1982	3	482	459	690
3214301	--	Tarrant	Paluxy	2/1951	2/1955	3	500	454	703
3230401	--	Tarrant	Paluxy	3/1956	2/1977	3	500	467	622
3215406	--	Tarrant	Paluxy	3/1952	2/2019	3	500	468	692
3230202	--	Tarrant	Paluxy	2/1970	2/1974	3	500	471	636
3204609	--	Tarrant	Pearsall	2/2018	2/2019	6	500	392	689
3206901	--	Tarrant	Paluxy	2/1954	2/1966	3	503	450	709
3214111	--	Tarrant	Multi-aquifer	2/1977	2/1995	[2, 3, 4]	525	429	695
3230110	--	Tarrant	Paluxy	2/1994	3/2020	3	550	470	627
3222603	--	Tarrant	Paluxy	3/1940	2/1950	3	550	470	659
3206607	--	Tarrant	Paluxy	2/1978	2/2011	3	625	448	718
3215504	--	Tarrant	Paluxy	2/1973	3/2012	3	667	478	700
3222604	--	Tarrant	Glen Rose	2/1950	2/1951	4	690	474	655
3223105	--	Tarrant	Paluxy	2/1954	2/1955	3	700	475	676
3216701	--	Tarrant	Washita/Fredericksburg	2/1954	2/1954	2	720	496	691
3214704	--	Tarrant	Hensell	2/1902	2/1954	5	728	446	677
3208801	--	Tarrant	Paluxy	2/1954	2/1957	3	788	486	733
3207607	--	Tarrant	Paluxy	3/1980	2/2014	3	802	467	735
3223318	--	Tarrant	Multi-aquifer	2/2017	2/2019	[2, 3, 4]	803	494	678
3207914	--	Tarrant	Paluxy	2/2010	2/2018	3	825	474	724
3221504	--	Tarrant	Multi-aquifer	2/1967	2/2019	[2, 5, 6, 7]	830	434	645
3213902	--	Tarrant	Pearsall and Hosston	3/1948	2/1958	[6, 7]	834	436	667
3216502	--	Tarrant	Washita/Fredericksburg	2/1951	2/1955	2	863	498	711
3214803	--	Tarrant	Hensell and Pearsall	2/1950	2/1953	[5, 6]	887	455	671

TWDB or OWRB state well number[1]	Map ID (figures 3-50 to 3-70)	County	Hydrogeologic unit	Period of record (may contain gaps) (M/Y)[2]		Layer (zero-based indexing)[3]	Well depth, in feet below land surface[4]	Row	Column
				Begin	End				
3224104	--	Tarrant	Paluxy	2/1953	3/1956	3	900	499	687
3216401	--	Tarrant	Glen Rose	2/1953	2/1965	4	900	493	709
3214722	--	Tarrant	Pearsall and Hosston	2/1913	3/1944	[6, 7]	938	446	677
3223301	--	Tarrant	Glen Rose	2/1961	2/1961	4	950	496	687
3216201	--	Tarrant	Paluxy	2/1961	2/1993	3	959	495	716
3214110	--	Tarrant	Pearsall	3/1976	2/2006	6	1,041	429	695
3214401	--	Tarrant	Hosston	3/1912	2/1958	7	1,053	441	684
3214405	--	Tarrant	Pearsall	2/1921	2/1954	6	1,055	443	685
3224301	--	Tarrant	Paluxy	2/1953	3/1956	3	1,060	518	691
3206406	--	Tarrant	Hosston	2/2019	2/2019	7	1,070	426	717
3222204	--	Tarrant	Hosston	2/1937	2/1954	7	1,080	454	667
3222401	--	Tarrant	Pearsall	2/1950	2/1958	6	1,083	458	649
3214502	--	Tarrant	Pearsall and Hosston	3/1956	2/1969	[6, 7]	1,108	451	686
3214102	--	Tarrant	Pearsall and Hosston	2/1959	2/1998	[6, 7]	1,112	433	692
3214901	--	Tarrant	Hosston	2/1950	2/1955	7	1,160	458	683
3222602	--	Tarrant	Pearsall and Hosston	3/1948	2/1954	[6, 7]	1,288	472	656
3222903	--	Tarrant	Lower and Trinity	2/1971	2/2005	[5, 6, 7]	1,346	475	653
3223106	--	Tarrant	Hosston	3/1948	2/1954	7	1,376	478	675
3223103	--	Tarrant	Pearsall	2/1914	2/1969	6	1,432	479	675
3223304	--	Tarrant	Hosston	2/1977	2/2019	7	1,552	494	678
3215201	--	Tarrant	Hosston	3/1964	2/1977	7	1,588	472	712
3207602	--	Tarrant	Hosston	3/1972	2/2019	7	1,610	467	735
3216101	--	Tarrant	Pearsall	2/1970	3/2000	6	1,690	486	716
3224101	--	Tarrant	Pearsall and Hosston	2/1953	2/1957	[6, 7]	1,775	499	687
3216504	--	Tarrant	Hosston	2/1951	2/1957	7	1,846	501	716
3224501	--	Tarrant	Hosston	2/1974	2/2010	7	1,968	518	685

TWDB or OWRB state well number[1]	Map ID (figures 3-50 to 3-70)	County	Hydrogeologic unit	Period of record (may contain gaps) (M/Y)[2]		Layer (zero-based indexing)[3]	Well depth, in feet below land surface[4]	Row	Column
				Begin	End				
3224805	--	Tarrant	Multi-aquifer	3/1988	2/2010	[1, 2, 3, 4, 5, 6, 7]	2,048	523	672
5835723	--	Travis	Washita/Fredericksburg	2/2005	3/2012	2	100	657	49
5842201	--	Travis	Glen Rose	2/1949	3/1952	4	132	644	30
5834901	--	Travis	Washita/Fredericksburg	3/1940	3/1952	2	150	650	37
5825907	--	Travis	Glen Rose	3/1996	2/2006	4	247	606	59
5835201	--	Travis	Woodbine and Washita/Fredericksburg	3/1940	3/1996	[1, 2]	270	656	63
5842602	--	Travis	Washita/Fredericksburg	2/1949	2/1965	2	330	660	25
5833407	--	Travis	Multi-aquifer	2/2011	2/2011	[4, 5, 6]	450	598	24
5843101	--	Travis	Washita/Fredericksburg	2/1941	2/1951	2	458	666	31
5833403	--	Travis	Pearsall	2/1967	3/1988	6	459	604	26
5825201	--	Travis	Middle-Lower and Trinity	2/1975	3/1984	[4, 5, 6, 7]	520	588	73
5835906	--	Travis	Woodbine and Washita/Fredericksburg	2/1978	3/1996	[1, 2]	600	672	56
5835607	--	Travis	Woodbine and Washita/Fredericksburg	2/1935	2/1985	[1, 2]	609	672	67
5835701	--	Travis	Washita/Fredericksburg	2/1942	2/2011	2	610	659	42
5835811	--	Travis	Washita/Fredericksburg	3/2004	2/2013	2	610	661	48

TWDB or OWRB state well number[1]	Map ID (figures 3-50 to 3-70)	County	Hydrogeologic unit	Period of record (may contain gaps) (M/Y)[2]		Layer (zero-based indexing)[3]	Well depth, in feet below land surface[4]	Row	Column
				Begin	End				
5836402	--	Travis	Woodbine and Washita/Fredericksburg	2/1949	2/2005	[1, 2]	610	677	71
5833217	--	Travis	Hosston	2/1973	3/2020	7	615	603	49
5825901	--	Travis	Middle-Lower and Trinity	2/1966	2/1978	[4, 5, 6, 7]	630	604	51
5835601	--	Travis	Washita/Fredericksburg	2/1949	2/1957	2	690	667	63
5825916	--	Travis	Lower and Trinity	2/1994	3/2020	[5, 6, 7]	940	607	64
5842302	--	Travis	Multi-aquifer	3/1956	2/1989	[2, 3, 4]	1,135	656	31
5834603	--	Travis	Multi-aquifer	3/1960	3/2020	[4, 5, 6]	1,253	640	48
5835721	--	Travis	Multi-aquifer	3/1988	3/2020	[2, 3, 4]	1,265	658	43
5835803	--	Travis	Multi-aquifer	3/1940	3/1992	[1, 2, 3, 4]	1,400	666	50
5843303	--	Travis	Multi-aquifer	2/1941	2/1981	[1, 2, 3, 4]	1,456	676	46
5844201	--	Travis	Hosston	2/1941	3/2008	7	3,001	700	48
5844204	--	Travis	Pearsall	2/1974	3/2020	6	3,086	700	48
5819505	--	Williamson	Washita/Fredericksburg	2/1978	2/1994	2	90	632	125
5819626	--	Williamson	Washita/Fredericksburg	3/1984	2/2018	2	105	633	127
5819522	--	Williamson	Washita/Fredericksburg	2/2005	3/2012	2	125	632	116
5819204	--	Williamson	Washita/Fredericksburg	3/1976	2/1985	2	126	628	131
5819205	--	Williamson	Washita/Fredericksburg	3/1980	3/1988	2	126	628	132

TWDB or OWRB state well number[1]	Map ID (figures 3-50 to 3-70)	County	Hydrogeologic unit	Period of record (may contain gaps) (M/Y)[2]		Layer (zero-based indexing)[3]	Well depth, in feet below land surface[4]	Row	Column
				Begin	End				
5835110	--	Williamson	Washita/Fredericksburg	3/1980	2/1985	2	131	646	70
5818605	--	Williamson	Washita/Fredericksburg	2/2005	3/2012	2	135	617	111
5819105	--	Williamson	Washita/Fredericksburg	2/2005	3/2012	2	137	620	123
5811704	--	Williamson	Washita/Fredericksburg	3/1980	2/1985	2	138	614	134
5811803	--	Williamson	Washita/Fredericksburg	2/2011	2/2019	2	140	622	143
5827829	--	Williamson	Washita/Fredericksburg	2/1979	2/2005	2	140	646	78
5826808	--	Williamson	Washita/Fredericksburg	2/2005	3/2012	2	141	627	64
5827224	--	Williamson	Washita/Fredericksburg	2/1987	3/1996	2	160	642	100
5819206	--	Williamson	Washita/Fredericksburg	3/1980	2/1985	2	162	622	133
5819910	--	Williamson	Washita/Fredericksburg	3/1992	2/2007	2	165	642	115
5827519	--	Williamson	Washita/Fredericksburg	3/1972	2/1981	2	165	642	93
5811602	--	Williamson	Washita/Fredericksburg	2/1981	2/1981	2	174	622	152
5819303	--	Williamson	Washita/Fredericksburg	2/1978	2/1998	2	175	635	131
5827203	--	Williamson	Washita/Fredericksburg	3/1940	2/1962	2	175	641	99

TWDB or OWRB state well number[1]	Map ID (figures 3-50 to 3-70)	County	Hydrogeologic unit	Period of record (may contain gaps) (M/Y)[2]		Layer (zero-based indexing)[3]	Well depth, in feet below land surface[4]	Row	Column
				Begin	End				
5834621	--	Williamson	Washita/Fredericksburg	2/2005	3/2012	2	175	642	53
5827610	--	Williamson	Washita/Fredericksburg	2/2005	3/2012	2	175	653	87
5819412	--	Williamson	Washita/Fredericksburg	2/2005	3/2012	2	180	624	115
5819503	--	Williamson	Washita/Fredericksburg	2/1971	2/1983	2	180	633	123
5819612	--	Williamson	Washita/Fredericksburg	3/1976	2/1985	2	180	638	126
5819901	--	Williamson	Washita/Fredericksburg	2/1971	2/2005	2	184	642	116
5819511	--	Williamson	Washita/Fredericksburg	2/1993	3/1996	2	185	635	120
5819811	--	Williamson	Washita/Fredericksburg	3/1968	3/1996	2	185	638	117
5819803	--	Williamson	Washita/Fredericksburg	3/1952	2/2005	2	186	638	109
5827202	--	Williamson	Washita/Fredericksburg	2/1959	2/1974	2	200	641	94
5819615	--	Williamson	Washita/Fredericksburg	3/1980	3/1996	2	207	636	127
5827715	--	Williamson	Washita/Fredericksburg	2/1978	2/1981	2	212	643	77
5827228	--	Williamson	Washita/Fredericksburg	2/2005	3/2012	2	215	637	101
5827814	--	Williamson	Washita/Fredericksburg	2/1978	2/2019	2	222	649	77

TWDB or OWRB state well number[1]	Map ID (figures 3-50 to 3-70)	County	Hydrogeologic unit	Period of record (may contain gaps) (M/Y)[2]		Layer (zero-based indexing)[3]	Well depth, in feet below land surface[4]	Row	Column
				Begin	End				
5827801	--	Williamson	Washita/Fredericksburg	2/1957	2/1969	2	222	655	77
5827517	--	Williamson	Washita/Fredericksburg	2/1973	2/1985	2	260	649	89
5811603	--	Williamson	Washita/Fredericksburg	2/1981	2/1985	2	262	628	159
5819610	--	Williamson	Washita/Fredericksburg	2/1973	3/1996	2	270	638	129
5827531	--	Williamson	Washita/Fredericksburg	2/1987	3/1996	2	300	646	94
5819902	--	Williamson	Washita/Fredericksburg	2/1971	3/1996	2	300	650	113
5827607	--	Williamson	Washita/Fredericksburg	2/1987	3/1996	2	300	654	95
5827810	--	Williamson	Washita/Fredericksburg	2/1979	2/1979	2	302	654	79
5827526	--	Williamson	Washita/Fredericksburg	2/1987	3/1996	2	304	640	91
5827303	--	Williamson	Washita/Fredericksburg	2/1978	3/1996	2	306	649	108
5820703	--	Williamson	Washita/Fredericksburg	2/1970	3/1996	2	311	649	119
5827305	--	Williamson	Washita/Fredericksburg	3/1980	2/2015	2	314	647	101
5812101	--	Williamson	Washita/Fredericksburg	2/2019	2/2019	2	330	631	173
5827304	--	Williamson	Washita/Fredericksburg	2/1979	3/1996	2	340	650	99

TWDB or OWRB state well number[1]	Map ID (figures 3-50 to 3-70)	County	Hydrogeologic unit	Period of record (may contain gaps) (M/Y)[2]		Layer (zero-based indexing)[3]	Well depth, in feet below land surface[4]	Row	Column
				Begin	End				
5827502	--	Williamson	Washita/Fredericksburg	2/1941	2/1954	2	350	643	92
5820701	--	Williamson	Washita/Fredericksburg	3/1976	2/2007	2	351	654	118
5820413	--	Williamson	Washita/Fredericksburg	2/1987	3/1996	2	360	646	133
5827307	--	Williamson	Washita/Fredericksburg	2/1987	3/1996	2	360	649	103
5835204	--	Williamson	Woodbine and Washita/Fredericksburg	3/1964	2/2002	[1, 2]	370	657	73
5827603	--	Williamson	Washita/Fredericksburg	2/1973	3/1996	2	380	656	91
5827916	--	Williamson	Washita/Fredericksburg	2/1981	2/1985	2	380	657	81
5817401	--	Williamson	Multi-aquifer	3/1968	3/2004	[4, 5, 6]	380	565	92
5817201	--	Williamson	Pearsall	3/1972	2/2019	6	390	572	108
5812404	--	Williamson	Washita/Fredericksburg	2/1967	3/1980	2	400	630	164
5827901	--	Williamson	Woodbine and Washita/Fredericksburg	2/1966	2/1985	[1, 2]	425	663	80
5820403	--	Williamson	Washita/Fredericksburg	2/1973	3/2020	2	440	652	130
5820501	--	Williamson	Woodbine and Washita/Fredericksburg	3/1976	3/1988	[1, 2]	446	658	128

TWDB or OWRB state well number[1]	Map ID (figures 3-50 to 3-70)	County	Hydrogeologic unit	Period of record (may contain gaps) (M/Y)[2]		Layer (zero-based indexing)[3]	Well depth, in feet below land surface[4]	Row	Column
				Begin	End				
5817802	--	Williamson	Multi-aquifer	2/1966	3/1984	[4, 5, 6]	450	583	90
5817803	--	Williamson	Hensell and Pearsall	2/1965	2/1997	[5, 6]	450	583	91
5817601	--	Williamson	Pearsall	2/1970	2/2003	6	492	586	100
5817504	--	Williamson	Pearsall and Hosston	3/2004	3/2020	[6, 7]	500	580	98
5827902	--	Williamson	Washita/Fredericksburg	3/1956	3/1996	2	504	660	85
5828706	--	Williamson	Washita/Fredericksburg	2/1978	2/2019	2	520	669	90
5826604	--	Williamson	Multi-aquifer	3/1984	2/2009	[2, 3, 4]	550	629	87
5820201	--	Williamson	Woodbine and Washita/Fredericksburg	2/1973	2/2019	[1, 2]	565	653	140
5825303	--	Williamson	Multi-aquifer	2/1975	3/1980	[4, 5, 6]	580	595	79
5820204	--	Williamson	Washita/Fredericksburg	3/1984	2/2019	2	590	655	146
5820102	--	Williamson	Washita/Fredericksburg	2/1957	2/2019	2	603	646	143
5812502	--	Williamson	Washita/Fredericksburg	3/1968	2/1990	2	610	644	161
5820803	--	Williamson	Washita/Fredericksburg	2/1986	2/2019	2	610	665	119

TWDB or OWRB state well number[1]	Map ID (figures 3-50 to 3-70)	County	Hydrogeologic unit	Period of record (may contain gaps) (M/Y)[2]		Layer (zero-based indexing)[3]	Well depth, in feet below land surface[4]	Row	Column
				Begin	End				
5820502	--	Williamson	Woodbine and Washita/Fredericksburg	2/1973	2/1990	[1, 2]	612	659	137
5828401	--	Williamson	Washita/Fredericksburg	3/1976	3/2020	2	630	665	103
5810702	--	Williamson	Multi-aquifer	2/1966	3/1980	[4, 5, 6]	634	584	127
5828201	--	Williamson	Washita/Fredericksburg	2/1977	2/2019	2	640	665	110
5802901	--	Williamson	Glen and Rose and Hensell	2/2013	3/2020	[4, 5]	647	587	165
5812302	--	Williamson	Washita/Fredericksburg	2/1989	2/1989	2	665	645	174
5810805	--	Williamson	Glen and Rose and Hensell	2/1995	2/2011	[4, 5]	673	591	126
5810302	--	Williamson	Glen Rose	2/1966	3/1976	4	685	589	148
5826102	--	Williamson	Pearsall and Hosston	2/1971	2/1986	[6, 7]	695	601	83
5818701	--	Williamson	Hosston	2/1966	2/1967	7	700	596	92
5826406	--	Williamson	Pearsall and Hosston	2/1969	2/1986	[6, 7]	709	608	75
5820901	--	Williamson	Washita/Fredericksburg	2/1966	2/2019	2	745	671	123
5811102	--	Williamson	Hensell	2/2019	2/2019	5	760	599	153
5826401	--	Williamson	Multi-aquifer	2/1954	2/1969	[2, 3, 4, 5, 6, 7]	780	608	76

TWDB or OWRB state well number[1]	Map ID (figures 3-50 to 3-70)	County	Hydrogeologic unit	Period of record (may contain gaps) (M/Y)[2]		Layer (zero-based indexing)[3]	Well depth, in feet below land surface[4]	Row	Column
				Begin	End				
5828601	--	Williamson	Washita/Fredericksburg	3/1940	2/2011	2	790	679	100
5818906	--	Williamson	Multi-aquifer	3/1984	2/2007	[2, 3, 4]	797	616	105
5820302	--	Williamson	Washita/Fredericksburg	2/1987	2/2019	2	840	662	148
5826705	--	Williamson	Hensell	2/1966	3/1988	5	850	617	59
5826605	--	Williamson	Glen Rose	2/2011	2/2017	4	880	630	87
5803701	--	Williamson	Glen and Rose and Hensell	2/2014	3/2020	[4, 5]	880	602	167
5819405	--	Williamson	Multi-aquifer	2/1986	2/1999	[2, 3, 4]	890	625	114
5803707	--	Williamson	Pearsall	2/1994	2/2018	6	902	595	167
5811801	--	Williamson	Multi-aquifer	3/1968	2/1999	[2, 3, 4]	905	616	144
5806708	--	Williamson	Glen and Rose and Pearsall	2/2017	3/2020	[4, 6]	940	596	167
5812601	--	Williamson	Multi-aquifer	2/1967	3/2020	[1, 2, 3, 4]	1,041	652	171
5821802	--	Williamson	Washita/Fredericksburg	2/1987	2/1993	2	1,080	690	135
5829501	--	Williamson	Washita/Fredericksburg	2/1969	2/1994	2	1,115	695	114
5827101	--	Williamson	Glen Rose	2/1965	3/1976	4	1,224	634	97

TWDB or OWRB state well number[1]	Map ID (figures 3-50 to 3-70)	County	Hydrogeologic unit	Period of record (may contain gaps) (M/Y)[2]		Layer (zero-based indexing)[3]	Well depth, in feet below land surface[4]	Row	Column
				Begin	End				
5813502	--	Williamson	Multi-aquifer	2/2005	3/2020	[2, 3, 4]	1,595	672	174
5821202	--	Williamson	Hosston	2/1965	2/1989	7	2,607	678	154
5813503	--	Williamson	Hosston	2/1958	2/1987	7	2,617	672	174
5829602	--	Williamson	Pearsall	2/1934	2/1975	6	3,308	702	124
5829608	--	Williamson	Hosston	2/1986	2/2017	7	3,383	708	118
1942801	--	Wise	Hosston	2/1969	2/1990	7	70	292	753
1952401	--	Wise	Glen Rose	2/1970	2/1989	4	115	341	753
1942506	--	Wise	Hosston	2/1999	3/2020	7	123	287	754
1936402	--	Wise	Glen Rose	2/2013	3/2020	4	125	315	808
1942614	--	Wise	Hosston	2/1981	3/2020	7	135	289	762
1944801	--	Wise	Glen Rose	2/1970	2/1977	4	148	339	772
1953101	--	Wise	Glen Rose	2/1970	2/1985	4	178	363	775
1944102	--	Wise	Glen Rose	2/2015	3/2020	4	180	327	790
1960604	--	Wise	Glen Rose	2/1998	3/2020	4	200	379	727
1952603	--	Wise	Paluxy and Glen and Rose	3/2020	3/2020	[3, 4]	200	355	757
1935902	--	Wise	Hensell	2/2013	3/2020	5	210	307	793
1953702	--	Wise	Glen Rose	3/2020	3/2020	4	220	371	755
1960401	--	Wise	Pearsall and Hosston	2/1970	3/1988	[6, 7]	226	352	720
1958401	--	Wise	Pearsall and Hosston	2/1973	3/2008	[6, 7]	240	308	691
1952206	--	Wise	Glen Rose	3/2016	3/2020	4	300	345	766
1952205	--	Wise	Glen Rose	2/2013	2/2019	4	340	349	765

TWDB or OWRB state well number[1]	Map ID (figures 3-50 to 3-70)	County	Hydrogeologic unit	Period of record (may contain gaps) (M/Y)[2]		Layer (zero-based indexing)[3]	Well depth, in feet below land surface[4]	Row	Column
				Begin	End				
1952301	--	Wise	Glen Rose	2/2013	2/2019	4	340	351	766
1960702	--	Wise	Hosston	3/2020	3/2020	7	340	367	710
1961409	--	Wise	Paluxy	2/2018	3/2020	3	380	388	732
1960201	--	Wise	Hensell and Hosston	2/1970	2/2010	[5, 7]	394	364	729
1961301	--	Wise	Paluxy	2/1971	3/2020	3	415	398	749
1944103	--	Wise	Pearsall	2/2015	3/2020	6	430	327	789
1944702	--	Wise	Pearsall	3/2016	3/2020	6	500	335	768
1952106	--	Wise	Hosston	2/2013	3/2020	7	500	337	753
1944902	--	Wise	Hosston	3/2016	3/2020	7	560	348	773
1944901	--	Wise	Hosston	3/2016	3/2020	7	643	354	775
1952604	--	Wise	Hosston	3/2020	3/2020	7	676	355	757
1952302	--	Wise	Hosston	3/2016	3/2020	7	733	354	773
1952306	--	Wise	Multi-aquifer	3/2020	3/2020	[3, 4, 5, 6, 7]	770	360	764
1952303	--	Wise	Hosston	3/2016	2/2019	7	810	359	768
1952304	--	Wise	Hosston	3/2016	3/2020	7	817	349	770
1953102	--	Wise	Hosston	3/2016	3/2020	7	825	366	775
1961411	--	Wise	Lower and Trinity	3/2020	3/2020	[5, 6, 7]	860	385	735

1The OWRB well IDs were standardized by using "1" followed by a sequence of zeros to ensure all well IDs were the same length

2Well end dates are current as of December 2024

3To obtain a model layer number that corresponds to the layering presented in Figure 3-1, add one to each value on this column. Values within brackets indicate that the well was completed in more than one model layer.

4The hydrogeologic unit assigned to each well is based on the well's screened interval (reported or estimated); therefore, the well depth is listed to provide general information on well construction.

7.3 Water Budgets

Appendix Table 7-3. Water budget for the transient model in 2020 by county for the Northern Trinity and Woodbine aquifer system.

County	Unit	Cross-formational Flow			Recharge	Ephemeral	Perennial	Riparian	Springs	Flowing	Reservoirs	Younger	Wells	Storage
		Surficial	Top	Bottom		Streams	Streams	ET		Wells				
Bastrop	Younger Formations	0	0	50	78	0	0	0	0	0	0	-467	0	234
Bastrop	Woodbine Aquifer	0	-50	49	0	0	0	0	0	0	0	0	0	1
Bastrop	Wash/Fred Groups	0	-49	29	0	0	0	0	0	0	0	0	0	4
Bastrop	Paluxy Aquifer	0	-29	26	0	0	0	0	0	0	0	0	0	2
Bastrop	Glen Rose Formation	0	-26	-15	0	0	0	0	0	0	0	0	0	14
Bastrop	Hensell Aquifer	0	15	-16	0	0	0	0	0	0	0	0	0	0
Bastrop	Pearsall Formation	0	16	-28	0	0	0	0	0	0	0	0	0	10
Bastrop	Hosston Aquifer	0	28	0	0	0	0	0	0	0	0	0	0	16
Bastrop	total	0	-95	95	78	0	0	0	0	0	0	-467	0	281
Bell	Younger Formations	0	0	36	119	0	-20	0	0	0	0	139	0	52
Bell	Woodbine Aquifer	-1	-36	26	30	0	70	0	0	0	0	0	0	2
Bell	Wash/Fred Groups	2,659	-26	-343	50,328	-26,002	-17,076	-25	-362	0	-55	0	-2,769	-4,863
Bell	Paluxy Aquifer	307	343	-409	1,038	-1,044	-26	0	0	-247	-17	0	0	-135
Bell	Glen Rose Formation	1,107	409	-1,810	27,413	-12,317	-15,325	-6	-26	0	-15	0	-219	2,029
Bell	Hensell Aquifer	0	1,810	-1,737	0	0	0	0	0	-21	0	0	-409	3
Bell	Pearsall Formation	0	1,737	-1,926	0	0	0	0	0	0	0	0	0	73
Bell	Hosston Aquifer	0	1,926	0	0	0	0	0	0	0	0	0	-1,147	118
Bell	total	4,072	6,163	-6,163	78,928	-39,363	-32,377	-31	-388	-268	-87	139	-4,544	-2,721
Bosque	Younger Formations	0	0	0	0	0	0	0	0	0	0	0	0	0
Bosque	Woodbine Aquifer	0	0	0	0	0	0	0	0	0	0	0	0	0
Bosque	Wash/Fred Groups	2,306	0	-2,319	138,984	-87,313	-21,024	-223	-8	0	13	0	-688	-19,432
Bosque	Paluxy Aquifer	-775	2,319	-1,421	22,435	-13,308	-10,101	0	0	0	0	0	-335	-2,521
Bosque	Glen Rose Formation	-234	1,421	-686	29,257	-12,784	-20,280	0	0	0	0	0	-648	-2,992

Bosque	Hensell Aquifer	0	686	-931	0	0	0	0	0	0	0	0	-1,102	-12
Bosque	Pearsall Formation	0	931	-807	0	0	0	0	0	0	0	0	-309	75
Bosque	Hosston Aquifer	0	807	0	0	0	0	0	0	0	0	0	-2,069	82
Bosque	total	1,297	6,164	-6,164	190,676	-113,405	-51,405	-223	-8	0	13	0	-5,151	-24,800
Bowie	Younger Formations	0	0	474	171	0	0	0	0	0	0	-701	0	83
Bowie	Woodbine Aquifer	0	-474	458	0	0	0	0	0	0	0	0	0	11
Bowie	Wash/Fred Groups	0	-458	440	0	0	0	0	0	0	0	0	0	11
Bowie	Paluxy Aquifer	0	-440	411	0	0	0	0	0	0	0	0	0	12
Bowie	Glen Rose Formation	0	-411	362	0	0	0	0	0	0	0	0	0	11
Bowie	Hensell Aquifer	0	-362	361	0	0	0	0	0	0	0	0	0	0
Bowie	Pearsall Formation	0	-361	356	0	0	0	0	0	0	0	0	0	10
Bowie	Hosston Aquifer	0	-356	0	0	0	0	0	0	0	0	0	0	31
Bowie	total	0	-2,862	2,862	171	0	0	0	0	0	0	-701	0	169
Brown	Younger Formations	0	0	0	0	0	0	0	0	0	0	0	0	0
Brown	Woodbine Aquifer	0	0	0	0	0	0	0	0	0	0	0	0	0
Brown	Wash/Fred Groups	0	0	0	0	0	0	0	0	0	0	0	0	0
Brown	Paluxy Aquifer	0	0	0	0	0	0	0	0	0	0	0	0	0
Brown	Glen Rose Formation	-12	0	-1	158	0	0	0	0	0	0	0	0	-10
Brown	Hensell Aquifer	318	1	-322	3,235	-844	0	0	0	0	0	0	-23	-225
Brown	Pearsall Formation	1,013	322	-1,214	7,296	-8,812	0	0	0	0	0	0	-72	-940
Brown	Hosston Aquifer	1,325	1,214	0	45,165	-33,681	0	0	-268	0	0	0	-652	-5,949
Brown	total	2,644	1,537	-1,537	55,854	-43,337	0	0	-268	0	0	0	-747	-7,124
Burnet	Younger Formations	0	0	0	0	0	0	0	0	0	0	0	0	0
Burnet	Woodbine Aquifer	0	0	0	0	0	0	0	0	0	0	0	0	0
Burnet	Wash/Fred Groups	0	0	0	0	0	0	0	0	0	0	0	0	0
Burnet	Paluxy Aquifer	0	0	0	0	0	0	0	0	0	0	0	0	0
Burnet	Glen Rose Formation	3,144	0	-2,646	36,979	-25,747	-6,870	-687	0	0	0	0	-329	6,226
Burnet	Hensell Aquifer	96	2,646	-1,843	6,760	-4,386	-4,521	0	0	0	0	0	-195	649
Burnet	Pearsall Formation	2,488	1,843	-3,887	2,476	-1,327	0	0	0	0	0	0	-218	217
Burnet	Hosston Aquifer	653	3,887	0	12,759	-10,282	-223	-78	-44	0	-31	0	-858	-753
Burnet	total	6,381	8,376	-8,376	58,974	-41,742	-11,614	-765	-44	0	-31	0	-1,600	6,339

Callahan	Younger Formations	0	0	0	0	0	0	0	0	0	0	0	0	0
Callahan	Woodbine Aquifer	0	0	0	0	0	0	0	0	0	0	0	0	0
Callahan	Wash/Fred Groups	0	0	0	0	0	0	0	0	0	0	0	0	0
Callahan	Paluxy Aquifer	0	0	0	0	0	0	0	0	0	0	0	0	0
Callahan	Glen Rose Formation	0	0	0	0	0	0	0	0	0	0	0	0	0
Callahan	Hensell Aquifer	7	0	-7	481	-226	0	0	0	0	0	0	0	-93
Callahan	Pearsall Formation	105	7	-111	777	-645	0	0	0	0	0	0	-1	-143
Callahan	Hosston Aquifer	931	111	0	56,036	-41,583	0	0	-46	0	0	0	-1,170	-11,663
Callahan	total	1,043	118	-118	57,294	-42,454	0	0	-46	0	0	0	-1,171	-11,899
Collin	Younger Formations	0	0	-180	207	0	0	0	0	0	0	-153	-332	494
Collin	Woodbine Aquifer	0	180	88	0	0	0	0	0	0	0	0	-3,434	1,710
Collin	Wash/Fred Groups	0	-88	-186	0	0	0	0	0	0	0	0	-71	76
Collin	Paluxy Aquifer	0	186	83	0	0	0	0	0	0	0	0	-1,379	133
Collin	Glen Rose Formation	0	-83	-200	0	0	0	0	0	0	0	0	-53	391
Collin	Hensell Aquifer	0	200	-162	0	0	0	0	0	0	0	0	-150	28
Collin	Pearsall Formation	0	162	-111	0	0	0	0	0	0	0	0	-150	66
Collin	Hosston Aquifer	0	111	0	0	0	0	0	0	0	0	0	-376	-8
Collin	total	0	668	-668	207	0	0	0	0	0	0	-153	-5,945	2,890
Comanche	Younger Formations	0	0	0	0	0	0	0	0	0	0	0	0	0
Comanche	Woodbine Aquifer	0	0	0	0	0	0	0	0	0	0	0	0	0
Comanche	Wash/Fred Groups	0	0	0	0	0	0	0	0	0	0	0	0	0
Comanche	Paluxy Aquifer	0	0	0	0	0	0	0	0	0	0	0	0	0
Comanche	Glen Rose Formation	-60	0	-121	4,972	-1,397	0	0	0	0	0	0	-9	-178
Comanche	Hensell Aquifer	11,114	121	-10148	44,853	-27,266	-2,779	-37	0	0	0	0	-1,715	461
Comanche	Pearsall Formation	4,463	10,148	-10346	19,319	-12,411	-6,330	-244	0	0	0	0	-4,093	488
Comanche	Hosston Aquifer	3,262	10,346	0	103,901	-74,507	-28,603	-2,398	-39	0	-60	0	- 14447	-10,199
Comanche	total	18,779	20,615	-20615	173,045	-115,581	-37,712	-2,679	-39	0	-60	0	- 20264	-9,428
Cooke	Younger Formations	0	0	0	0	0	0	0	0	0	0	0	0	0
Cooke	Woodbine Aquifer	509	0	-123	30,095	-20,235	0	0	-28	0	-888	0	-554	-5,605
Cooke	Wash/Fred Groups	1,670	123	-209	119,359	-58,451	-23,158	-692	-23	0	-777	0	-1,047	-31,108

Cooke	Paluxy Aquifer	2,440	209	-1,280	42,190	-18,431	-11,012	-834	0	0	-66	0	-260	-11,889
Cooke	Glen Rose Formation	302	1,280	-1,584	23,922	-5,922	-15,164	-892	0	0	-1	0	-642	-4,825
Cooke	Hensell Aquifer	658	1,584	-1,638	5,491	-2,538	925	-605	0	0	0	0	-241	-1,129
Cooke	Pearsall Formation	110	1,638	-551	1,241	-1,574	-1,746	-64	0	0	0	0	-3,164	331
Cooke	Hosston Aquifer	-577	551	0	2,934	-692	-2,390	-182	0	0	0	0	-1,614	-392
Cooke	total	5,112	5,385	-5,385	225,232	-107,843	-52,545	-3,269	-51	0	-1,732	0	-7,522	-54,617
Coryell	Younger Formations	0	0	0	0	0	0	0	0	0	0	0	0	0
Coryell	Woodbine Aquifer	0	0	0	0	0	0	0	0	0	0	0	0	0
Coryell	Wash/Fred Groups	2,128	0	-1,184	68,322	-36,643	-18,848	-447	-42	0	0	0	-507	-6,641
Coryell	Paluxy Aquifer	-251	1,184	-758	3,764	-2,074	-2,739	0	0	0	0	0	-39	-301
Coryell	Glen Rose Formation	1,044	758	-1,639	119,375	-57,467	-61,258	0	0	0	0	0	-788	-3,527
Coryell	Hensell Aquifer	0	1,639	-1,514	0	0	0	0	0	-171	0	0	-256	4
Coryell	Pearsall Formation	0	1,514	-1,396	0	0	0	0	0	0	0	0	-104	72
Coryell	Hosston Aquifer	0	1,396	0	0	0	0	0	0	0	0	0	-523	60
Coryell	total	2,921	6,491	-6,491	191,461	-96,184	-82,845	-447	-42	-171	0	0	-2,217	-10,333
Dallas	Younger Formations	0	0	-205	211	0	0	0	0	0	0	-282	0	206
Dallas	Woodbine Aquifer	31	205	113	1,581	0	-2,066	0	0	0	0	0	-1,836	-229
Dallas	Wash/Fred Groups	0	-113	-319	0	0	0	0	0	0	0	0	0	24
Dallas	Paluxy Aquifer	0	319	17	0	0	0	0	0	0	0	0	-682	-200
Dallas	Glen Rose Formation	0	-17	-169	0	0	0	0	0	0	0	0	-74	11
Dallas	Hensell Aquifer	0	169	-375	0	0	0	0	0	0	0	0	0	24
Dallas	Pearsall Formation	0	375	184	0	0	0	0	0	0	0	0	-9	-67
Dallas	Hosston Aquifer	0	-184	0	0	0	0	0	0	0	0	0	-943	-100
Dallas	total	31	754	-754	1,792	0	-2,066	0	0	0	0	-282	-3,544	-331
Delta	Younger Formations	0	0	-162	63	0	0	0	0	0	0	-585	0	374
Delta	Woodbine Aquifer	0	162	-150	0	0	0	0	0	0	0	0	0	61
Delta	Wash/Fred Groups	0	150	-304	0	0	0	0	0	0	0	0	0	11
Delta	Paluxy Aquifer	0	304	-361	0	0	0	0	0	0	0	0	-30	17
Delta	Glen Rose Formation	0	361	-469	0	0	0	0	0	0	0	0	-30	39
Delta	Hensell Aquifer	0	469	-499	0	0	0	0	0	0	0	0	0	2
Delta	Pearsall Formation	0	499	-328	0	0	0	0	0	0	0	0	0	17

Delta	Hosston Aquifer	0	328	0	0	0	0	0	0	0	0	0	-15	10
Delta	total	0	2,273	-2,273	63	0	0	0	0	0	0	-585	-75	531
Denton	Younger Formations	0	0	-5	45	0	0	0	0	0	0	-158	0	11
Denton	Woodbine Aquifer	3,984	5	-274	51,457	-28,950	-490	0	-38	0	-634	0	-3,175	-11,314
Denton	Wash/Fred Groups	-2,414	274	-222	137,691	-64,437	-48,024	-743	-61	0	-1,166	0	-2,234	-28,301
Denton	Paluxy Aquifer	-127	222	29	7,129	-141	-8,274	0	0	0	0	0	-1,635	-2,465
Denton	Glen Rose Formation	0	-29	-482	0	0	0	0	0	0	0	0	-983	1,079
Denton	Hensell Aquifer	0	482	-635	0	0	0	0	0	0	0	0	-1,859	194
Denton	Pearsall Formation	0	635	-231	0	0	0	0	0	0	0	0	-3,077	257
Denton	Hosston Aquifer	0	231	0	0	0	0	0	0	0	0	0	-4,505	-24
Denton	total	1,443	1,820	-1,820	196,322	-93,528	-56,788	-743	-99	0	-1,800	-158	-17468	-40,563
Eastland	Younger Formations	0	0	0	0	0	0	0	0	0	0	0	0	0
Eastland	Woodbine Aquifer	0	0	0	0	0	0	0	0	0	0	0	0	0
Eastland	Wash/Fred Groups	0	0	0	0	0	0	0	0	0	0	0	0	0
Eastland	Paluxy Aquifer	0	0	0	0	0	0	0	0	0	0	0	0	0
Eastland	Glen Rose Formation	0	0	0	0	0	0	0	0	0	0	0	0	0
Eastland	Hensell Aquifer	389	0	-171	6,994	-5,254	0	0	0	0	0	0	-215	-399
Eastland	Pearsall Formation	160	171	-88	4,162	-3,666	0	0	0	0	0	0	-249	-646
Eastland	Hosston Aquifer	1,815	88	0	78,040	-67,132	0	0	0	0	0	0	-2,746	-12,250
Eastland	total	2,364	259	-259	89,196	-76,052	0	0	0	0	0	0	-3,210	-13,295
Ellis	Younger Formations	0	0	-331	223	0	0	0	0	0	0	-9	0	308
Ellis	Woodbine Aquifer	0	331	85	0	0	0	0	0	0	0	0	-1,560	-159
Ellis	Wash/Fred Groups	0	-85	-245	0	0	0	0	0	0	0	0	-39	127
Ellis	Paluxy Aquifer	0	245	-87	0	0	0	0	0	0	0	0	-99	-22
Ellis	Glen Rose Formation	0	87	-361	0	0	0	0	0	0	0	0	-88	43
Ellis	Hensell Aquifer	0	361	-595	0	0	0	0	0	0	0	0	0	33
Ellis	Pearsall Formation	0	595	-2,440	0	0	0	0	0	0	0	0	-41	133
Ellis	Hosston Aquifer	0	2,440	0	0	0	0	0	0	0	0	0	-10136	202
Ellis	total	0	3,974	-3,974	223	0	0	0	0	0	0	-9	-11963	665
Erath	Younger Formations	0	0	0	0	0	0	0	0	0	0	0	0	0

Erath	Woodbine Aquifer	0	0	0	0	0	0	0	0	0	0	0	0	0
Erath	Wash/Fred Groups	0	0	0	167	0	0	0	0	0	0	0	0	-38
Erath	Paluxy Aquifer	414	0	-358	9,516	-8,691	0	0	0	0	0	0	-40	-434
Erath	Glen Rose Formation	744	358	-384	52,101	-27,851	-16,981	-17	0	0	0	0	-712	513
Erath	Hensell Aquifer	18,303	384	-13516	78,165	-42,460	-2,152	0	0	0	0	0	-3,230	-585
Erath	Pearsall Formation	-564	13,516	-10086	9,558	-9,196	20	0	0	0	0	0	-1,966	-931
Erath	Hosston Aquifer	183	10,086	0	22,476	-22,601	-5,484	0	0	0	0	0	-7,888	-2,609
Erath	total	19,080	24,344	-24344	171,983	-110,799	-24,597	-17	0	0	0	0	-13836	-4,084
Falls	Younger Formations	0	0	-143	173	0	0	0	0	0	0	-768	-7,478	7,988
Falls	Woodbine Aquifer	0	143	-153	0	0	0	0	0	0	0	0	0	9
Falls	Wash/Fred Groups	0	153	-592	0	0	0	0	0	0	0	0	0	31
Falls	Paluxy Aquifer	0	592	-599	0	0	0	0	0	0	0	0	0	4
Falls	Glen Rose Formation	0	599	-765	0	0	0	0	0	0	0	0	-176	36
Falls	Hensell Aquifer	0	765	-768	0	0	0	0	0	0	0	0	0	1
Falls	Pearsall Formation	0	768	-715	0	0	0	0	0	0	0	0	-95	127
Falls	Hosston Aquifer	0	715	0	0	0	0	0	0	0	0	0	-857	140
Falls	total	0	3,735	-3,735	173	0	0	0	0	0	0	-768	-8,606	8,336
Fannin	Younger Formations	0	0	-134	178	0	0	0	0	0	0	-136	-235	340
Fannin	Woodbine Aquifer	2,019	134	55	35,098	-7,969	-7,627	-2,257	0	0	38	0	-3,976	-4,671
Fannin	Wash/Fred Groups	60	-55	-32	983	0	-449	-84	0	0	0	0	-298	-87
Fannin	Paluxy Aquifer	0	32	46	0	0	0	0	0	0	0	0	-315	114
Fannin	Glen Rose Formation	0	-46	-144	0	0	0	0	0	0	0	0	-121	820
Fannin	Hensell Aquifer	0	144	-113	0	0	0	0	0	0	0	0	-17	15
Fannin	Pearsall Formation	0	113	-411	0	0	0	0	0	0	0	0	-127	17
Fannin	Hosston Aquifer	0	411	0	0	0	0	0	0	0	0	0	-331	11
Fannin	total	2,079	733	-733	36,259	-7,969	-8,076	-2,341	0	0	38	-136	-5,420	-3,441
Franklin	Younger Formations	0	0	26	5	0	0	0	0	0	0	-97	0	38
Franklin	Woodbine Aquifer	0	-26	21	0	0	0	0	0	0	0	0	0	5
Franklin	Wash/Fred Groups	0	-21	16	0	0	0	0	0	0	0	0	0	1
Franklin	Paluxy Aquifer	0	-16	3	0	0	0	0	0	0	0	0	0	2
Franklin	Glen Rose Formation	0	-3	0	0	0	0	0	0	0	0	0	0	1

Franklin	Hensell Aquifer	0	0	0	0	0	0	0	0	0	0	0	0	0
Franklin	Pearsall Formation	0	0	-3	0	0	0	0	0	0	0	0	0	1
Franklin	Hosston Aquifer	0	3	0	0	0	0	0	0	0	0	0	0	0
Franklin	total	0	-63	63	5	0	0	0	0	0	0	-97	0	48
Grayson	Younger Formations	0	0	-174	134	0	0	0	0	0	0	76	-24	148
Grayson	Woodbine Aquifer	4,639	174	-181	56,975	-40,680	0	0	0	-771	-614	0	-7,495	-8,538
Grayson	Wash/Fred Groups	967	181	-346	24,118	-6,266	-9,199	-4	0	0	-341	0	-1,206	-7,448
Grayson	Paluxy Aquifer	616	346	-45	220	0	676	0	0	0	-40	0	-913	-526
Grayson	Glen Rose Formation	0	45	-198	0	0	0	0	0	0	0	0	-2,492	1,551
Grayson	Hensell Aquifer	0	198	-154	0	0	0	0	0	0	0	0	-747	45
Grayson	Pearsall Formation	0	154	-7	0	0	0	0	0	0	0	0	-1,413	370
Grayson	Hosston Aquifer	0	7	0	0	0	0	0	0	0	0	0	-486	140
Grayson	total	6,222	1,105	-1,105	81,447	-46,946	-8,523	-4	0	-771	-995	76	-14776	-14,258
Hamilton	Younger Formations	0	0	0	0	0	0	0	0	0	0	0	0	0
Hamilton	Woodbine Aquifer	0	0	0	0	0	0	0	0	0	0	0	0	0
Hamilton	Wash/Fred Groups	351	0	-363	15,644	-12,047	615	0	0	0	0	0	-33	258
Hamilton	Paluxy Aquifer	-72	363	-225	2,071	-629	-269	0	0	0	0	0	-12	59
Hamilton	Glen Rose Formation	2,943	225	-2,847	111,192	-45,758	-58,268	-28	0	0	0	0	-465	1,481
Hamilton	Hensell Aquifer	769	2,847	-2,084	7,538	-3,484	-10,815	-2	0	0	0	0	-453	512
Hamilton	Pearsall Formation	0	2,084	-1,605	0	0	0	0	0	0	0	0	-384	74
Hamilton	Hosston Aquifer	0	1,605	0	0	0	0	0	0	0	0	0	-1,023	48
Hamilton	total	3,991	7,124	-7,124	136,445	-61,918	-68,737	-30	0	0	0	0	-2,370	2,432
Henderson	Younger Formations	0	0	-81	10	0	0	0	0	0	0	-206	0	204
Henderson	Woodbine Aquifer	0	81	-118	0	0	0	0	0	0	0	0	0	30
Henderson	Wash/Fred Groups	0	118	-251	0	0	0	0	0	0	0	0	0	25
Henderson	Paluxy Aquifer	0	251	-256	0	0	0	0	0	0	0	0	0	1
Henderson	Glen Rose Formation	0	256	-263	0	0	0	0	0	0	0	0	0	2
Henderson	Hensell Aquifer	0	263	-262	0	0	0	0	0	0	0	0	0	1
Henderson	Pearsall Formation	0	262	-252	0	0	0	0	0	0	0	0	0	2
Henderson	Hosston Aquifer	0	252	0	0	0	0	0	0	0	0	0	0	8
Henderson	total	0	1,483	-1,483	10	0	0	0	0	0	0	-206	0	273

Hill	Younger Formations	0	0	-142	146	0	0	0	0	0	0	7	0	98
Hill	Woodbine Aquifer	213	142	-87	3,809	-1,395	-834	-247	0	0	-7	0	-85	-87
Hill	Wash/Fred Groups	902	87	-637	62,403	-36,638	-19,648	-1,120	0	0	63	0	-910	-5,143
Hill	Paluxy Aquifer	0	637	-362	0	0	0	0	0	0	0	0	-4	-26
Hill	Glen Rose Formation	0	362	-397	0	0	0	0	0	0	0	0	-2	3
Hill	Hensell Aquifer	0	397	-860	0	0	0	0	0	0	0	0	-12	16
Hill	Pearsall Formation	0	860	-1,003	0	0	0	0	0	0	0	0	-181	177
Hill	Hosston Aquifer	0	1,003	0	0	0	0	0	0	0	0	0	-3,686	103
Hill	total	1,115	3,488	-3,488	66,358	-38,033	-20,482	-1,367	0	0	56	7	-4,880	-4,859
Hood	Younger Formations	0	0	0	0	0	0	0	0	0	0	0	0	0
Hood	Woodbine Aquifer	0	0	0	0	0	0	0	0	0	0	0	0	0
Hood	Wash/Fred Groups	0	0	0	0	0	0	0	0	0	0	0	0	0
Hood	Paluxy Aquifer	24	0	-142	5,816	-3,459	0	0	0	0	0	0	-38	-1,090
Hood	Glen Rose Formation	1,759	142	-1,110	41,429	-14,023	-16,523	-252	-95	0	11	0	-1,070	-5,258
Hood	Hensell Aquifer	7,594	1,110	-5,730	21,233	-7,773	-6,884	-606	0	0	-44	0	-3,108	-2,325
Hood	Pearsall Formation	-637	5,730	-3,721	3,687	-624	-3,189	-326	0	0	-8	0	-2,106	-464
Hood	Hosston Aquifer	30	3,721	0	18,623	-14,106	-266	0	0	-22	-18	0	-2,445	-2,293
Hood	total	8,770	10,703	-10703	90,788	-39,985	-26,862	-1,184	-95	-22	-59	0	-8,767	-11,430
Hopkins	Younger Formations	0	0	-23	14	0	0	0	0	0	0	-153	0	151
Hopkins	Woodbine Aquifer	0	23	-33	0	0	0	0	0	0	0	0	0	10
Hopkins	Wash/Fred Groups	0	33	-43	0	0	0	0	0	0	0	0	0	4
Hopkins	Paluxy Aquifer	0	43	-68	0	0	0	0	0	0	0	0	0	7
Hopkins	Glen Rose Formation	0	68	-77	0	0	0	0	0	0	0	0	0	5
Hopkins	Hensell Aquifer	0	77	-72	0	0	0	0	0	0	0	0	0	0
Hopkins	Pearsall Formation	0	72	-55	0	0	0	0	0	0	0	0	0	4
Hopkins	Hosston Aquifer	0	55	0	0	0	0	0	0	0	0	0	0	2
Hopkins	total	0	371	-371	14	0	0	0	0	0	0	-153	0	183
Hunt	Younger Formations	0	0	-830	158	0	0	0	0	0	0	-449	0	1,131
Hunt	Woodbine Aquifer	0	830	-757	0	0	0	0	0	0	0	0	-493	657
Hunt	Wash/Fred Groups	0	757	-1,591	0	0	0	0	0	0	0	0	0	48
Hunt	Paluxy Aquifer	0	1,591	-1,634	0	0	0	0	0	0	0	0	0	81

Hunt	Glen Rose Formation	0	1,634	-2,103	0	0	0	0	0	0	0	0	0	352
Hunt	Hensell Aquifer	0	2,103	-2,128	0	0	0	0	0	0	0	0	0	12
Hunt	Pearsall Formation	0	2,128	-2,296	0	0	0	0	0	0	0	0	0	38
Hunt	Hosston Aquifer	0	2,296	0	0	0	0	0	0	0	0	0	0	28
Hunt	total	0	11,339	-11339	158	0	0	0	0	0	0	-449	-493	2,347
Jack	Younger Formations	0	0	0	0	0	0	0	0	0	0	0	0	0
Jack	Woodbine Aquifer	0	0	0	0	0	0	0	0	0	0	0	0	0
Jack	Wash/Fred Groups	0	0	0	0	0	0	0	0	0	0	0	0	0
Jack	Paluxy Aquifer	0	0	0	0	0	0	0	0	0	0	0	0	0
Jack	Glen Rose Formation	0	0	0	0	0	0	0	0	0	0	0	0	0
Jack	Hensell Aquifer	-26	0	-4	183	-120	0	0	0	0	0	0	0	-63
Jack	Pearsall Formation	132	4	-163	1,005	-676	0	0	0	0	0	0	0	-251
Jack	Hosston Aquifer	15	163	0	13,114	-8,413	0	0	0	0	0	0	-21	-3,810
Jack	total	121	167	-167	14,302	-9,209	0	0	0	0	0	0	-21	-4,124
Johnson	Younger Formations	0	0	-84	33	0	0	0	0	0	0	115	0	0
Johnson	Woodbine Aquifer	923	84	-214	22,245	-16,892	-205	-32	0	0	0	0	-910	-2,628
Johnson	Wash/Fred Groups	3,653	214	-1,553	97,559	-73,744	-249	0	-55	0	59	0	-1,974	-14,335
Johnson	Paluxy Aquifer	1,615	1,553	-291	3,575	-220	-493	-1	0	0	0	0	-1,269	-592
Johnson	Glen Rose Formation	711	291	-517	2,672	-12	-300	0	0	0	0	0	-224	-254
Johnson	Hensell Aquifer	0	517	-1,136	0	0	0	0	0	0	0	0	-312	16
Johnson	Pearsall Formation	0	1,136	-1,525	0	0	0	0	0	0	0	0	-795	93
Johnson	Hosston Aquifer	0	1,525	0	0	0	0	0	0	0	0	0	-3,122	71
Johnson	total	6,902	5,320	-5,320	126,084	-90,868	-1,247	-33	-55	0	59	115	-8,606	-17,629
Kaufman	Younger Formations	0	0	-782	149	0	0	0	0	0	0	-886	0	1,369
Kaufman	Woodbine Aquifer	0	782	-1,007	0	0	0	0	0	0	0	0	0	169
Kaufman	Wash/Fred Groups	0	1,007	-2,130	0	0	0	0	0	0	0	0	0	136
Kaufman	Paluxy Aquifer	0	2,130	-2,229	0	0	0	0	0	0	0	0	-29	22
Kaufman	Glen Rose Formation	0	2,229	-2,353	0	0	0	0	0	0	0	0	-17	74
Kaufman	Hensell Aquifer	0	2,353	-2,342	0	0	0	0	0	0	0	0	0	10
Kaufman	Pearsall Formation	0	2,342	-2,216	0	0	0	0	0	0	0	0	0	36
Kaufman	Hosston Aquifer	0	2,216	0	0	0	0	0	0	0	0	0	-6	71

Kaufman	total	0	13,059	-13059	149	0	0	0	0	0	0	-886	-52	1,887
Lamar	Younger Formations	0	0	-4	200	0	0	0	0	0	0	-85	0	32
Lamar	Woodbine Aquifer	134	4	8	21,630	-3,874	-9,652	-466	0	0	0	0	-96	-4,444
Lamar	Wash/Fred Groups	3	-8	-10	177	0	60	-33	0	0	0	0	0	12
Lamar	Paluxy Aquifer	0	10	-18	0	0	0	0	0	0	0	0	-84	59
Lamar	Glen Rose Formation	0	18	-59	0	0	0	0	0	0	0	0	-22	66
Lamar	Hensell Aquifer	0	59	-84	0	0	0	0	0	0	0	0	-2	1
Lamar	Pearsall Formation	0	84	-83	0	0	0	0	0	0	0	0	-22	7
Lamar	Hosston Aquifer	0	83	0	0	0	0	0	0	0	0	0	-102	8
Lamar	total	137	250	-250	22,007	-3,874	-9,592	-499	0	0	0	-85	-328	-4,259
Lampasas	Younger Formations	0	0	0	0	0	0	0	0	0	0	0	0	0
Lampasas	Woodbine Aquifer	0	0	0	0	0	0	0	0	0	0	0	0	0
Lampasas	Wash/Fred Groups	0	0	0	0	0	0	0	0	0	0	0	0	0
Lampasas	Paluxy Aquifer	0	0	0	0	0	0	0	0	0	0	0	0	0
Lampasas	Glen Rose Formation	1,321	0	-741	22,680	-6,636	-7,842	0	0	0	0	0	-234	-1,128
Lampasas	Hensell Aquifer	-347	741	-122	43,280	-21,942	-32,413	0	0	0	0	0	-403	-4,561
Lampasas	Pearsall Formation	1,175	122	-1,260	10,311	-5,069	0	0	0	0	0	0	-160	-1,301
Lampasas	Hosston Aquifer	-945	1,260	0	22,155	-18,407	0	0	-255	0	0	0	-309	-3,390
Lampasas	total	1,204	2,123	-2,123	98,426	-52,054	-40,255	0	-255	0	0	0	-1,106	-10,380
Lee	Younger Formations	0	0	16	33	0	0	0	0	0	0	-359	0	230
Lee	Woodbine Aquifer	0	-16	15	0	0	0	0	0	0	0	0	0	0
Lee	Wash/Fred Groups	0	-15	-57	0	0	0	0	0	0	0	0	0	2
Lee	Paluxy Aquifer	0	57	-58	0	0	0	0	0	0	0	0	0	1
Lee	Glen Rose Formation	0	58	-132	0	0	0	0	0	0	0	0	0	5
Lee	Hensell Aquifer	0	132	-133	0	0	0	0	0	0	0	0	0	0
Lee	Pearsall Formation	0	133	-134	0	0	0	0	0	0	0	0	0	1
Lee	Hosston Aquifer	0	134	0	0	0	0	0	0	0	0	0	0	4
Lee	total	0	483	-483	33	0	0	0	0	0	0	-359	0	243
Limestone	Younger Formations	0	0	-911	92	0	0	0	0	0	0	-406	0	1,513
Limestone	Woodbine Aquifer	0	911	-1,064	0	0	0	0	0	0	0	0	0	138
Limestone	Wash/Fred Groups	0	1,064	-1,372	0	0	0	0	0	0	0	0	0	18

Limestone	Paluxy Aquifer	0	1,372	-1,396	0	0	0	0	0	0	0	0	0	4
Limestone	Glen Rose Formation	0	1,396	-2,013	0	0	0	0	0	0	0	0	0	33
Limestone	Hensell Aquifer	0	2,013	-2,006	0	0	0	0	0	0	0	0	0	2
Limestone	Pearsall Formation	0	2,006	-2,070	0	0	0	0	0	0	0	0	0	132
Limestone	Hosston Aquifer	0	2,070	0	0	0	0	0	0	0	0	0	0	43
Limestone	total	0	10,832	-10832	92	0	0	0	0	0	0	-406	0	1,883
McLennan	Younger Formations	0	0	-18	150	0	22	0	0	0	0	-65	-178	208
McLennan	Woodbine Aquifer	0	18	-46	85,170	-21,968	-53,787	-383	0	0	157	0	-1,452	-12,119
McLennan	Wash/Fred Groups	-21	46	-646	0	0	0	0	0	0	0	0	0	9
McLennan	Paluxy Aquifer	0	646	-749	0	0	0	0	0	0	0	0	0	-1
McLennan	Glen Rose Formation	0	749	-307	0	0	0	0	0	0	0	0	-1,453	49
McLennan	Hensell Aquifer	0	307	-413	0	0	0	0	0	0	0	0	-1,200	31
McLennan	Pearsall Formation	0	413	262	0	0	0	0	0	0	0	0	-1,626	197
McLennan	Hosston Aquifer	0	-262	0	0	0	0	0	0	0	0	0	-9,778	182
McLennan	total	-21	1,917	-1,917	85,320	-21,968	-53,765	-383	0	0	157	-65	- 15687	-11,444
Milam	Younger Formations	0	0	137	189	0	0	0	0	0	0	-1,666	0	894
Milam	Woodbine Aquifer	0	-137	134	0	0	0	0	0	0	0	0	0	2
Milam	Wash/Fred Groups	0	-134	-529	0	0	0	0	0	0	0	0	0	18
Milam	Paluxy Aquifer	0	529	-532	0	0	0	0	0	0	0	0	0	2
Milam	Glen Rose Formation	0	532	-677	0	0	0	0	0	0	0	0	0	20
Milam	Hensell Aquifer	0	677	-681	0	0	0	0	0	0	0	0	0	1
Milam	Pearsall Formation	0	681	-666	0	0	0	0	0	0	0	0	0	15
Milam	Hosston Aquifer	0	666	0	0	0	0	0	0	0	0	0	0	70
Milam	total	0	2,814	-2,814	189	0	0	0	0	0	0	-1,666	0	1,022
Mills	Younger Formations	0	0	0	0	0	0	0	0	0	0	0	0	0
Mills	Woodbine Aquifer	0	0	0	0	0	0	0	0	0	0	0	0	0
Mills	Wash/Fred Groups	921	0	-878	6,905	-3,347	-1,640	-286	0	0	0	0	-18	862
Mills	Paluxy Aquifer	-63	878	-795	606	-128	209	-25	0	0	0	0	-6	26
Mills	Glen Rose Formation	1,019	795	-1,111	34,971	-31,104	152	-18	0	0	0	0	-135	2,201
Mills	Hensell Aquifer	3,411	1,111	-3,273	25,578	-18,650	0	0	0	0	0	0	-335	4,685
Mills	Pearsall Formation	3,033	3,273	-5,787	4,182	-4,481	0	0	0	0	0	0	-304	225

Mills	Hosston Aquifer	-3,768	5,787	0	12,718	-22,605	0	0	0	0	0	0	-753	934
Mills	total	4,553	11,844	-11844	84,960	-80,315	-1,279	-329	0	0	0	0	-1,551	8,933
Montague	Younger Formations	0	0	0	0	0	0	0	0	0	0	0	0	0
Montague	Woodbine Aquifer	0	0	0	0	0	0	0	0	0	0	0	0	0
Montague	Wash/Fred Groups	0	0	0	0	0	0	0	0	0	0	0	0	0
Montague	Paluxy Aquifer	605	0	-349	4,008	-1,174	0	0	0	0	0	0	-17	-1,264
Montague	Glen Rose Formation	194	349	-256	38,881	-14,146	-10,916	-804	0	0	0	0	-108	-8,731
Montague	Hensell Aquifer	1,906	256	-1,043	23,686	-11,077	-1,804	-1,960	0	0	0	0	-133	-3,918
Montague	Pearsall Formation	4,082	1,043	-3,094	14,710	-10,191	-1,584	-135	0	0	0	0	-118	-1,819
Montague	Hosston Aquifer	73	3,094	0	33,890	-24,145	-6,183	-24	0	0	0	0	-387	-3,112
Montague	total	6,860	4,742	-4,742	115,175	-60,733	-20,487	-2,923	0	0	0	0	-763	-18,844
Navarro	Younger Formations	0	0	-848	171	0	0	0	0	0	0	-1,468	0	1,824
Navarro	Woodbine Aquifer	0	848	-1,520	0	0	0	0	0	0	0	0	0	466
Navarro	Wash/Fred Groups	0	1,520	-2,141	0	0	0	0	0	0	0	0	0	197
Navarro	Paluxy Aquifer	0	2,141	-2,242	0	0	0	0	0	0	0	0	0	18
Navarro	Glen Rose Formation	0	2,242	-2,675	0	0	0	0	0	0	0	0	-91	60
Navarro	Hensell Aquifer	0	2,675	-2,680	0	0	0	0	0	0	0	0	0	9
Navarro	Pearsall Formation	0	2,680	-2,633	0	0	0	0	0	0	0	0	0	198
Navarro	Hosston Aquifer	0	2,633	0	0	0	0	0	0	0	0	0	-28	176
Navarro	total	0	14,739	-14739	171	0	0	0	0	0	0	-1,468	-119	2,948
Palo Pinto	Younger Formations	0	0	0	0	0	0	0	0	0	0	0	0	0
Palo Pinto	Woodbine Aquifer	0	0	0	0	0	0	0	0	0	0	0	0	0
Palo Pinto	Wash/Fred Groups	0	0	0	0	0	0	0	0	0	0	0	0	0
Palo Pinto	Paluxy Aquifer	0	0	0	0	0	0	0	0	0	0	0	0	0
Palo Pinto	Glen Rose Formation	0	0	0	0	0	0	0	0	0	0	0	0	0
Palo Pinto	Hensell Aquifer	0	0	0	0	0	0	0	0	0	0	0	0	0
Palo Pinto	Pearsall Formation	0	0	0	0	0	0	0	0	0	0	0	0	0
Palo Pinto	Hosston Aquifer	88	0	0	4,067	-3,098	0	0	0	0	0	0	-29	-358
Palo Pinto	total	88	0	0	4,067	-3,098	0	0	0	0	0	0	-29	-358
Parker	Younger Formations	0	0	0	0	0	0	0	0	0	0	0	0	0
Parker	Woodbine Aquifer	0	0	0	0	0	0	0	0	0	0	0	0	0

Parker	Wash/Fred Groups	205	0	-3	2,795	-1,352	0	0	0	0	0	0	-21	-157
Parker	Paluxy Aquifer	3,787	3	-1,405	59,630	-33,529	-8,325	-7	0	0	0	0	-1,558	-7,083
Parker	Glen Rose Formation	4,406	1,405	-3,487	61,940	-34,681	-14,126	-242	-17	0	4	0	-2,937	-9,132
Parker	Hensell Aquifer	2,052	3,487	-4,146	16,132	-7,540	-476	-2	0	0	0	0	-522	-3,527
Parker	Pearsall Formation	2,570	4,146	-5,462	10,286	-3,825	-3,060	-200	0	0	0	0	-937	-2,080
Parker	Hosston Aquifer	-2,555	5,462	0	37,491	-30,060	-7,004	-63	0	0	0	0	-2,178	-6,294
Parker	total	10,465	14,503	-14503	188,274	-110,987	-32,991	-514	-17	0	4	0	-8,153	-28,273
Red River	Younger Formations	0	0	232	225	0	9	0	0	0	0	-708	0	162
Red River	Woodbine Aquifer	51	-232	144	19,418	-10,450	-1,261	-673	0	0	0	0	-19	-3,687
Red River	Wash/Fred Groups	10	-144	53	3,830	-730	-2,386	-275	0	0	0	0	-3	-421
Red River	Paluxy Aquifer	0	-53	-31	0	0	0	0	0	0	0	0	-756	25
Red River	Glen Rose Formation	0	31	-100	0	0	0	0	0	0	0	0	0	4
Red River	Hensell Aquifer	0	100	-106	0	0	0	0	0	0	0	0	0	-4
Red River	Pearsall Formation	0	106	-214	0	0	0	0	0	0	0	0	0	-3
Red River	Hosston Aquifer	0	214	0	0	0	0	0	0	0	0	0	-421	-7
Red River	total	61	22	-22	23,473	-11,180	-3,638	-948	0	0	0	-708	-1,199	-3,931
Robertson	Younger Formations	0	0	-2	8	0	0	0	0	0	0	-216	0	220
Robertson	Woodbine Aquifer	0	2	-2	0	0	0	0	0	0	0	0	0	0
Robertson	Wash/Fred Groups	0	2	-45	0	0	0	0	0	0	0	0	0	1
Robertson	Paluxy Aquifer	0	45	-45	0	0	0	0	0	0	0	0	0	0
Robertson	Glen Rose Formation	0	45	-99	0	0	0	0	0	0	0	0	0	2
Robertson	Hensell Aquifer	0	99	-99	0	0	0	0	0	0	0	0	0	0
Robertson	Pearsall Formation	0	99	-108	0	0	0	0	0	0	0	0	0	3
Robertson	Hosston Aquifer	0	108	0	0	0	0	0	0	0	0	0	0	5
Robertson	total	0	400	-400	8	0	0	0	0	0	0	-216	0	231
Rockwall	Younger Formations	0	0	-6	35	0	0	0	0	0	0	-31	0	9
Rockwall	Woodbine Aquifer	0	6	1	0	0	0	0	0	0	0	0	0	49
Rockwall	Wash/Fred Groups	0	-1	-16	0	0	0	0	0	0	0	0	0	9
Rockwall	Paluxy Aquifer	0	16	3	0	0	0	0	0	0	0	0	0	4
Rockwall	Glen Rose Formation	0	-3	-9	0	0	0	0	0	0	0	0	0	33
Rockwall	Hensell Aquifer	0	9	-8	0	0	0	0	0	0	0	0	0	2

Rockwall	Pearsall Formation	0	8	4	0	0	0	0	0	0	0	0	0	8
Rockwall	Hosston Aquifer	0	-4	0	0	0	0	0	0	0	0	0	0	1
Rockwall	total	0	31	-31	35	0	0	0	0	0	0	-31	0	115
Shackelford	Younger Formations	0	0	0	0	0	0	0	0	0	0	0	0	0
Shackelford	Woodbine Aquifer	0	0	0	0	0	0	0	0	0	0	0	0	0
Shackelford	Wash/Fred Groups	0	0	0	0	0	0	0	0	0	0	0	0	0
Shackelford	Paluxy Aquifer	0	0	0	0	0	0	0	0	0	0	0	0	0
Shackelford	Glen Rose Formation	0	0	0	0	0	0	0	0	0	0	0	0	0
Shackelford	Hensell Aquifer	0	0	0	0	0	0	0	0	0	0	0	0	0
Shackelford	Pearsall Formation	0	0	0	0	0	0	0	0	0	0	0	0	0
Shackelford	Hosston Aquifer	1	0	0	4	0	0	0	0	0	0	0	0	-2
Shackelford	total	1	0	0	4	0	0	0	0	0	0	0	0	-2
Somervell	Younger Formations	0	0	0	0	0	0	0	0	0	0	0	0	0
Somervell	Woodbine Aquifer	0	0	0	0	0	0	0	0	0	0	0	0	0
Somervell	Wash/Fred Groups	-48	0	-1	168	-5	0	0	0	0	0	0	-3	-49
Somervell	Paluxy Aquifer	581	1	-317	6,178	-1,712	0	0	0	0	0	0	-52	-1,339
Somervell	Glen Rose Formation	-327	317	-151	25,339	-6,637	-22,765	0	0	0	104	0	-566	-1,758
Somervell	Hensell Aquifer	144	151	-709	1,458	0	-2,599	0	0	-36	0	0	-97	176
Somervell	Pearsall Formation	0	709	-714	0	0	0	0	0	0	0	0	-75	44
Somervell	Hosston Aquifer	0	714	0	0	0	0	0	0	0	0	0	-822	67
Somervell	total	350	1,892	-1,892	33,143	-8,354	-25,364	0	0	-36	104	0	-1,615	-2,859
Tarrant	Younger Formations	0	0	-64	21	0	3	0	0	0	0	161	0	1
Tarrant	Woodbine Aquifer	1,907	64	-116	36,034	-17,966	-9,356	0	0	0	62	0	-239	-5,696
Tarrant	Wash/Fred Groups	1,651	116	-449	109,099	-57,392	-39,318	-387	-52	0	-25	0	-756	-9,552
Tarrant	Paluxy Aquifer	3,722	449	-559	17,877	-11,105	-5,197	-269	-80	0	368	0	-4,968	-2,098
Tarrant	Glen Rose Formation	0	559	-987	0	0	0	0	0	0	0	0	-461	-41
Tarrant	Hensell Aquifer	0	987	-1,804	0	0	0	0	0	0	0	0	-22	18
Tarrant	Pearsall Formation	0	1,804	-1,889	0	0	0	0	0	0	0	0	-215	-72
Tarrant	Hosston Aquifer	0	1,889	0	0	0	0	0	0	0	0	0	-4,582	-112
Tarrant	total	7,280	5,868	-5,868	163,031	-86,463	-53,868	-656	-132	0	405	161	-11,243	-17,552
Taylor	Younger Formations	0	0	0	0	0	0	0	0	0	0	0	0	0

Taylor	Woodbine Aquifer	0	0	0	0	0	0	0	0	0	0	0	0	0
Taylor	Wash/Fred Groups	0	0	0	0	0	0	0	0	0	0	0	0	0
Taylor	Paluxy Aquifer	0	0	0	0	0	0	0	0	0	0	0	0	0
Taylor	Glen Rose Formation	0	0	0	0	0	0	0	0	0	0	0	0	0
Taylor	Hensell Aquifer	0	0	0	0	0	0	0	0	0	0	0	0	0
Taylor	Pearsall Formation	38	0	-38	76	0	0	0	0	0	0	0	0	-24
Taylor	Hosston Aquifer	415	38	0	6,414	-3,012	0	0	0	0	0	0	-47	-1,855
Taylor	total	453	38	-38	6,490	-3,012	0	0	0	0	0	0	-47	-1,879
Titus	Younger Formations	0	0	52	7	0	0	0	0	0	0	-151	0	35
Titus	Woodbine Aquifer	0	-52	46	0	0	0	0	0	0	0	0	0	5
Titus	Wash/Fred Groups	0	-46	40	0	0	0	0	0	0	0	0	0	1
Titus	Paluxy Aquifer	0	-40	26	0	0	0	0	0	0	0	0	0	1
Titus	Glen Rose Formation	0	-26	13	0	0	0	0	0	0	0	0	0	1
Titus	Hensell Aquifer	0	-13	12	0	0	0	0	0	0	0	0	0	0
Titus	Pearsall Formation	0	-12	-4	0	0	0	0	0	0	0	0	0	0
Titus	Hosston Aquifer	0	4	0	0	0	0	0	0	0	0	0	0	1
Titus	total	0	-185	185	7	0	0	0	0	0	0	-151	0	44
Travis	Younger Formations	0	0	-78	76	0	0	0	0	0	0	-54	0	178
Travis	Woodbine Aquifer	0	78	-96	9	0	0	0	0	0	0	0	0	82
Travis	Wash/Fred Groups	2,476	96	-58	7,165	-2,117	-1,764	-107	-26	0	-1	0	-5,175	974
Travis	Paluxy Aquifer	1	58	-94	44	-29	-7	0	0	0	-2	0	-2	-9
Travis	Glen Rose Formation	619	94	-690	7,756	-6,137	-638	-139	0	0	-61	0	-983	64
Travis	Hensell Aquifer	-160	690	-455	2,229	-698	73	-252	0	-4	-16	0	-525	-2,957
Travis	Pearsall Formation	175	455	-247	417	0	-27	0	0	0	-9	0	-542	-512
Travis	Hosston Aquifer	-206	247	0	379	0	-109	0	0	0	-11	0	-597	-461
Travis	total	2,905	1,718	-1,718	18,075	-8,981	-2,472	-498	-26	-4	-100	-54	-7,824	-2,641
Williamson	Younger Formations	0	0	-37	145	0	1	0	0	0	0	187	0	153
Williamson	Woodbine Aquifer	0	37	-92	33,217	-13,344	-11,411	-21	-2	0	11	0	-565	7,323
Williamson	Wash/Fred Groups	15,239	92	-147	432	-306	-19	0	0	0	0	0	-15,732	147
Williamson	Paluxy Aquifer	29	147	-144	19,699	-7,684	-13,951	0	-51	0	0	0	-1,136	4,830
Williamson	Glen Rose Formation	3,173	144	-1,571	0	0	0	0	0	0	0	0	-584	4

Williamson	Hensell Aquifer	0	1,571	-1,264	0	0	0	0	0	-54	0	0	-191	3
Williamson	Pearsall Formation	0	1,264	-990	0	0	0	0	0	0	0	0	-233	51
Williamson	Hosston Aquifer	0	990	0	0	0	0	0	0	0	0	0	-286	78
Williamson	total	18,441	4,245	-4,245	53,493	-21,334	-25,380	-21	-53	-54	11	187	-18,727	12,589
Wise	Younger Formations	0	0	0	0	0	0	0	0	0	0	0	0	0
Wise	Woodbine Aquifer	0	0	0	0	0	0	0	0	0	0	0	0	0
Wise	Wash/Fred Groups	605	0	-14	19,935	-11,462	-118	0	0	0	0	0	-297	-2,891
Wise	Paluxy Aquifer	5,110	14	-1,435	43,667	-23,173	-3,579	-647	0	0	4	0	-800	-8,559
Wise	Glen Rose Formation	334	1,435	-860	53,284	-24,703	-15,539	-919	-48	0	11	0	-1,249	-13,351
Wise	Hensell Aquifer	2,754	860	-2,720	41,246	-25,389	-1,193	-931	-61	0	0	0	-902	-10,089
Wise	Pearsall Formation	2,252	2,720	-3,936	21,089	-15,278	-3,405	-186	0	0	0	0	-706	-4,258
Wise	Hosston Aquifer	-706	3,936	0	44,477	-34,482	-2,194	-129	-67	0	0	0	-1,928	-8,607
Wise	total	10,349	8,965	-8,965	223,698	-134,487	-26,028	-2,812	-176	0	15	0	-5,882	-47,755

Appendix Table 7-4. Water budget for the transient model in 2020 by Groundwater Conservation District for the Northern Trinity and Woodbine aquifer system.

County	Unit	Cross-formational Flow			Recharge	Ephemeral	Perennial	Riparian	Springs	Flowing	Reservoirs	Younger	Wells	Storage
		Surficial	Top	Bottom		Streams	Streams	ET		Wells				
Brazos Valley GCD	Younger Formations	0	0	-2	8	0	0	0	0	0	0	-216	0	220
Brazos Valley GCD	Woodbine Aquifer	0	2	-2	0	0	0	0	0	0	0	0	0	0
Brazos Valley GCD	Wash/Fred Groups	0	2	-45	0	0	0	0	0	0	0	0	0	1
Brazos Valley GCD	Paluxy Aquifer	0	45	-45	0	0	0	0	0	0	0	0	0	0
Brazos Valley GCD	Glen Rose Formation	0	45	-99	0	0	0	0	0	0	0	0	0	2
Brazos Valley GCD	Hensell Aquifer	0	99	-99	0	0	0	0	0	0	0	0	0	0
Brazos Valley GCD	Pearsall Formation	0	99	-108	0	0	0	0	0	0	0	0	0	3
Brazos Valley GCD	Hosston Aquifer	0	108	0	0	0	0	0	0	0	0	0	0	5
Brazos Valley GCD	total	0	400	-400	8	0	0	0	0	0	0	-216	0	231
Central Texas GCD	Younger Formations	0	0	0	0	0	0	0	0	0	0	0	0	0
Central Texas GCD	Woodbine Aquifer	0	0	0	0	0	0	0	0	0	0	0	0	0
Central Texas GCD	Wash/Fred Groups	0	0	0	0	0	0	0	0	0	0	0	0	0
Central Texas GCD	Paluxy Aquifer	0	0	0	0	0	0	0	0	0	0	0	0	0
Central Texas GCD	Glen Rose Formation	3,144	0	-2,646	36,979	-25,747	-6,870	-687	0	0	0	0	-329	6,226
Central Texas GCD	Hensell Aquifer	96	2,646	-1,843	6,760	-4,386	-4,521	0	0	0	0	0	-195	649
Central Texas GCD	Pearsall Formation	2,488	1,843	-3,887	2,476	-1,327	0	0	0	0	0	0	-218	217
Central Texas GCD	Hosston Aquifer	653	3,887	0	12,759	-10,282	-223	-78	-44	0	-31	0	-858	-753
Central Texas GCD	total	6,381	8,376	-8,376	58,974	-41,742	-11,614	-765	-44	0	-31	0	-1,600	6,339
Clearwater UWCD	Younger Formations	0	0	36	119	0	-20	0	0	0	0	139	0	52
Clearwater UWCD	Woodbine Aquifer	-1	-36	26	30	0	70	0	0	0	0	0	0	2
Clearwater UWCD	Wash/Fred Groups	2,659	-26	-343	50,328	-26,002	-17,076	-25	-362	0	-55	0	-2,769	-4,863
Clearwater UWCD	Paluxy Aquifer	307	343	-409	1,038	-1,044	-26	0	0	-247	-17	0	0	-135

Clearwater UWCD	Glen Rose Formation	1,107	409	-1,810	27,413	-12,317	-15,325	-6	-26	0	-15	0	-219	2,029
Clearwater UWCD	Hensell Aquifer	0	1,810	-1,737	0	0	0	0	0	-21	0	0	-409	3
Clearwater UWCD	Pearsall Formation	0	1,737	-1,926	0	0	0	0	0	0	0	0	0	73
Clearwater UWCD	Hosston Aquifer	0	1,926	0	0	0	0	0	0	0	0	0	-1,147	118
Clearwater UWCD	total	4,072	6,163	-6,163	78,928	-39,363	-32,377	-31	-388	-268	-87	139	-4,544	-2,721
Lost Pines GCD	Younger Formations	0	0	65	111	0	0	0	0	0	0	-826	0	464
Lost Pines GCD	Woodbine Aquifer	0	-65	64	0	0	0	0	0	0	0	0	0	1
Lost Pines GCD	Wash/Fred Groups	0	-64	-27	0	0	0	0	0	0	0	0	0	6
Lost Pines GCD	Paluxy Aquifer	0	27	-32	0	0	0	0	0	0	0	0	0	3
Lost Pines GCD	Glen Rose Formation	0	32	-148	0	0	0	0	0	0	0	0	0	19
Lost Pines GCD	Hensell Aquifer	0	148	-149	0	0	0	0	0	0	0	0	0	0
Lost Pines GCD	Pearsall Formation	0	149	-162	0	0	0	0	0	0	0	0	0	11
Lost Pines GCD	Hosston Aquifer	0	162	0	0	0	0	0	0	0	0	0	0	20
Lost Pines GCD	total	0	389	-389	111	0	0	0	0	0	0	-826	0	524
Middle Trinity GCD	Younger Formations	0	0	0	0	0	0	0	0	0	0	0	0	0
Middle Trinity GCD	Woodbine Aquifer	0	0	0	0	0	0	0	0	0	0	0	0	0
Middle Trinity GCD	Wash/Fred Groups	4,434	0	-3,503	207,473	-123,957	-39,872	-670	-50	0	13	0	-1,195	-26,112
Middle Trinity GCD	Paluxy Aquifer	-612	3,503	-2,537	35,715	-24,073	-12,839	0	0	0	0	0	-415	-3,255
Middle Trinity GCD	Glen Rose Formation	1,495	2,537	-2,830	205,706	-99,499	-98,519	-17	0	0	0	0	-2,156	-6,183
Middle Trinity GCD	Hensell Aquifer	29,418	2,830	-26,109	123,018	-69,726	-4,931	-37	0	-171	0	0	-6,303	-133
Middle Trinity GCD	Pearsall Formation	3,900	26,109	-22,636	28,877	-21,607	-6,310	-244	0	0	0	0	-6,472	-296
Middle Trinity GCD	Hosston Aquifer	3,445	22,636	0	126,378	-97,108	-34,087	-2,398	-39	0	-60	0	-24,927	-12,665
Middle Trinity GCD	total	42,080	57,615	-57,615	727,167	-435,970	-196,558	-3,366	-89	-171	-47	0	-41,468	-48,644
Neches & Trinity Valleys GCD	Younger Formations	0	0	-81	10	0	0	0	0	0	0	-206	0	204
Neches & Trinity Valleys GCD	Woodbine Aquifer	0	81	-118	0	0	0	0	0	0	0	0	0	30

Neches & Trinity Valleys GCD	Wash/Fred Groups	0	118	-251	0	0	0	0	0	0	0	0	0	25
Neches & Trinity Valleys GCD	Paluxy Aquifer	0	251	-256	0	0	0	0	0	0	0	0	0	1
Neches & Trinity Valleys GCD	Glen Rose Formation	0	256	-263	0	0	0	0	0	0	0	0	0	2
Neches & Trinity Valleys GCD	Hensell Aquifer	0	263	-262	0	0	0	0	0	0	0	0	0	1
Neches & Trinity Valleys GCD	Pearsall Formation	0	262	-252	0	0	0	0	0	0	0	0	0	2
Neches & Trinity Valleys GCD	Hosston Aquifer	0	252	0	0	0	0	0	0	0	0	0	0	8
Neches & Trinity Valleys GCD	total	0	1,483	-1,483	10	0	0	0	0	0	0	-206	0	273
North Texas GCD	Younger Formations	0	0	-184	252	0	0	0	0	0	0	-311	-332	505
North Texas GCD	Woodbine Aquifer	4,493	184	-309	81,553	-49,185	-490	0	-66	0	-1,522	0	-7,163	-15,209
North Texas GCD	Wash/Fred Groups	-745	309	-617	257,050	-122,887	-71,182	-1,435	-84	0	-1,943	0	-3,352	-59,332
North Texas GCD	Paluxy Aquifer	2,313	617	-1,168	49,319	-18,572	-19,285	-834	0	0	-66	0	-3,274	-14,222
North Texas GCD	Glen Rose Formation	302	1,168	-2,266	23,922	-5,922	-15,164	-892	0	0	-1	0	-1,679	-3,355
North Texas GCD	Hensell Aquifer	658	2,266	-2,434	5,491	-2,538	925	-605	0	0	0	0	-2,250	-907
North Texas GCD	Pearsall Formation	110	2,434	-893	1,241	-1,574	-1,746	-64	0	0	0	0	-6,391	653
North Texas GCD	Hosston Aquifer	-577	893	0	2,934	-692	-2,390	-182	0	0	0	0	-6,495	-423
North Texas GCD	total	6,554	7,871	-7,871	421,762	-201,370	-109,332	-4,012	-150	0	-3,532	-311	-30,936	-92,290
Northern Trinity GCD	Younger Formations	0	0	-64	21	0	3	0	0	0	0	161	0	1
Northern Trinity GCD	Woodbine Aquifer	1,907	64	-116	36,034	-17,966	-9,356	0	0	0	62	0	-239	-5,696
Northern Trinity GCD	Wash/Fred Groups	1,651	116	-449	109,099	-57,392	-39,318	-387	-52	0	-25	0	-756	-9,552
Northern Trinity GCD	Paluxy Aquifer	3,722	449	-559	17,877	-11,105	-5,197	-269	-80	0	368	0	-4,968	-2,098
Northern Trinity GCD	Glen Rose Formation	0	559	-987	0	0	0	0	0	0	0	0	-461	-41
Northern Trinity GCD	Hensell Aquifer	0	987	-1,804	0	0	0	0	0	0	0	0	-22	18

Northern Trinity GCD	Pearsall Formation	0	1,804	-1,889	0	0	0	0	0	0	0	0	-215	-72
Northern Trinity GCD	Hosston Aquifer	0	1,889	0	0	0	0	0	0	0	0	0	-4,582	-112
Northern Trinity GCD	total	7,280	5,868	-5,868	163,031	-86,463	-53,868	-656	-132	0	405	161	-11,243	-17,552
Post Oak Savannah GCD	Younger Formations	0	0	137	189	0	0	0	0	0	0	-1,666	0	894
Post Oak Savannah GCD	Woodbine Aquifer	0	-137	134	0	0	0	0	0	0	0	0	0	2
Post Oak Savannah GCD	Wash/Fred Groups	0	-134	-529	0	0	0	0	0	0	0	0	0	18
Post Oak Savannah GCD	Paluxy Aquifer	0	529	-532	0	0	0	0	0	0	0	0	0	2
Post Oak Savannah GCD	Glen Rose Formation	0	532	-677	0	0	0	0	0	0	0	0	0	20
Post Oak Savannah GCD	Hensell Aquifer	0	677	-681	0	0	0	0	0	0	0	0	0	1
Post Oak Savannah GCD	Pearsall Formation	0	681	-666	0	0	0	0	0	0	0	0	0	15
Post Oak Savannah GCD	Hosston Aquifer	0	666	0	0	0	0	0	0	0	0	0	0	70
Post Oak Savannah GCD	total	0	2,814	-2,814	189	0	0	0	0	0	0	-1,666	0	1,022
Prairielands GCD	Younger Formations	0	0	-557	402	0	0	0	0	0	0	113	0	406
Prairielands GCD	Woodbine Aquifer	1,137	557	-216	26,054	-18,287	-1,039	-279	0	0	-7	0	-2,554	-2,873
Prairielands GCD	Wash/Fred Groups	4,508	216	-2,436	160,130	-110,387	-19,896	-1,120	-55	0	122	0	-2,927	-19,400
Prairielands GCD	Paluxy Aquifer	2,196	2,436	-1,057	9,753	-1,932	-493	-1	0	0	0	0	-1,424	-1,979
Prairielands GCD	Glen Rose Formation	383	1,057	-1,425	28,011	-6,649	-23,065	0	0	0	104	0	-880	-1,966
Prairielands GCD	Hensell Aquifer	144	1,425	-3,300	1,458	0	-2,599	0	0	-36	0	0	-420	241
Prairielands GCD	Pearsall Formation	0	3,300	-5,683	0	0	0	0	0	0	0	0	-1,092	446
Prairielands GCD	Hosston Aquifer	0	5,683	0	0	0	0	0	0	0	0	0	-17,765	442
Prairielands GCD	total	8,368	14,674	-14,674	225,808	-137,255	-47,092	-1,400	-55	-36	219	113	-27,062	-24,683
Red River GCD	Younger Formations	0	0	-308	312	0	0	0	0	0	0	-60	-259	488
Red River GCD	Woodbine Aquifer	6,658	308	-125	92,073	-48,648	-7,627	-2,257	0	-771	-576	0	-11,471	-13,208
Red River GCD	Wash/Fred Groups	1,027	125	-378	25,101	-6,266	-9,648	-87	0	0	-341	0	-1,504	-7,536

Red River GCD	Paluxy Aquifer	616	378	1	220	0	676	0	0	0	-40	0	-1,228	-413
Red River GCD	Glen Rose Formation	0	-1	-342	0	0	0	0	0	0	0	0	-2,613	2,371
Red River GCD	Hensell Aquifer	0	342	-266	0	0	0	0	0	0	0	0	-764	60
Red River GCD	Pearsall Formation	0	266	-418	0	0	0	0	0	0	0	0	-1,540	387
Red River GCD	Hosston Aquifer	0	418	0	0	0	0	0	0	0	0	0	-816	151
Red River GCD	total	8,301	1,836	-1,836	117,706	-54,914	-16,599	-2,344	0	-771	-957	-60	-20,195	-17,700
Saratoga UWCD	Younger Formations	0	0	0	0	0	0	0	0	0	0	0	0	0
Saratoga UWCD	Woodbine Aquifer	0	0	0	0	0	0	0	0	0	0	0	0	0
Saratoga UWCD	Wash/Fred Groups	0	0	0	0	0	0	0	0	0	0	0	0	0
Saratoga UWCD	Paluxy Aquifer	0	0	0	0	0	0	0	0	0	0	0	0	0
Saratoga UWCD	Glen Rose Formation	1,321	0	-741	22,680	-6,636	-7,842	0	0	0	0	0	-234	-1,128
Saratoga UWCD	Hensell Aquifer	-347	741	-122	43,280	-21,942	-32,413	0	0	0	0	0	-403	-4,561
Saratoga UWCD	Pearsall Formation	1,175	122	-1,260	10,311	-5,069	0	0	0	0	0	0	-160	-1,301
Saratoga UWCD	Hosston Aquifer	-945	1,260	0	22,155	-18,407	0	0	-255	0	0	0	-309	-3,390
Saratoga UWCD	total	1,204	2,123	-2,123	98,426	-52,054	-40,255	0	-255	0	0	0	-1,106	-10,380
Southern Trinity GCD	Younger Formations	0	0	-18	150	0	22	0	0	0	0	-65	-178	208
Southern Trinity GCD	Woodbine Aquifer	0	18	-46	85,170	-21,968	-53,787	-383	0	0	157	0	-1,452	-12,119
Southern Trinity GCD	Wash/Fred Groups	-21	46	-646	0	0	0	0	0	0	0	0	0	9
Southern Trinity GCD	Paluxy Aquifer	0	646	-749	0	0	0	0	0	0	0	0	0	-1
Southern Trinity GCD	Glen Rose Formation	0	749	-307	0	0	0	0	0	0	0	0	-1,453	49
Southern Trinity GCD	Hensell Aquifer	0	307	-413	0	0	0	0	0	0	0	0	-1,200	31
Southern Trinity GCD	Pearsall Formation	0	413	262	0	0	0	0	0	0	0	0	-1,626	197
Southern Trinity GCD	Hosston Aquifer	0	-262	0	0	0	0	0	0	0	0	0	-9,778	182
Southern Trinity GCD	total	-21	1,917	-1,917	85,320	-21,968	-53,765	-383	0	0	157	-65	-15,687	-11,444

Upper Trinity GCD	Younger Formations	0	0	0	0	0	0	0	0	0	0	0	0	0
Upper Trinity GCD	Woodbine Aquifer	0	0	0	0	0	0	0	0	0	0	0	0	0
Upper Trinity GCD	Wash/Fred Groups	809	0	-17	22,730	-12,813	-118	0	0	0	0	0	-319	-3,049
Upper Trinity GCD	Paluxy Aquifer	9,526	17	-3,330	113,120	-61,336	-11,904	-654	0	0	4	0	-2,413	-17,997
Upper Trinity GCD	Glen Rose Formation	6,693	3,330	-5,713	195,535	-87,553	-57,104	-2,217	-160	0	26	0	-5,364	-36,474
Upper Trinity GCD	Hensell Aquifer	14,306	5,713	-13,639	102,297	-51,779	-10,357	-3,499	-61	0	-44	0	-4,665	-19,861
Upper Trinity GCD	Pearsall Formation	8,268	13,639	-16,213	49,771	-29,918	-11,238	-847	0	0	-8	0	-3,866	-8,621
Upper Trinity GCD	Hosston Aquifer	-3,158	16,213	0	134,481	-102,793	-15,648	-216	-67	-22	-18	0	-6,938	-20,306
Upper Trinity GCD	total	36,444	38,912	-38,912	617,934	-346,192	-106,369	-7,433	-288	-22	-40	0	-23,565	-106,308